IMPACT OF IMPURITIES ON THERMO-PHYSICAL PROPERTIES OF CO_2-RICH SYSTEMS: EXPERIMENTAL AND MODELLING

by

Mahmoud Nazeri Ghojogh

Submitted for the degree of Doctor of Philosophy

In

Petroleum Engineering

Heriot-Watt University

Institute of Petroleum Engineering

May 2015

ABSTRACT

Numerous industrial and academic communities have directed their efforts into developing technologies for reducing the emission of CO_2 in the atmosphere. Carbon dioxide capture and storage (CCS) is one of the most promising technologies that can eliminate/reduce global warming, helping the world to move towards a low-carbon society. The process comprises of the separation of CO_2 from industrial sources, transport to a storage location and then long-term isolation from the atmosphere. CO_2-rich pipelines are a key part of any carbon capture and storage projects. Modelling of these types of pipelines are challenging due to the lack of thermo-physical properties of CO_2 in presence of impurities. As these properties, particularly density and viscosity, have a significant impact on the sizing of equipment, therefore, it is crucial to investigate the impact of different impurities on the thermo-physical properties of CO_2-rich systems.

Densities and viscosities of pure CO_2, two $CO_2 – H_2$ binary systems (with 5 and with 10 mol% H_2), and 6 multi-component mixtures (MIX 1 with 5 mol% impurity, MIX 2 with 10 mol % impurity, MIX 3 with 30 mol % impurity, MIX 4 with 50 mol % impurity, MIX 5 with 4 mol % impurity and MIX 6 with 30 mol % impurity) were measured at pressures ranging from 10 to 1,400 bar (1 to 140 MPa) and six different temperatures, 0, 10, 25, 50, 100, 150 °C (273.15, 283.15, 298.15, 323.15, 373.15 and 423.15 K) in the gas, liquid, and supercritical regions using an Anton Paar densitometer and capillary tube technique for density and viscosity measurements, respectively. The experimental density data then were applied to evaluate the models using CO_2 correction volume, Peneloux shift parameter and original equation of states (PR and SRK). Also, the obtained viscosity data were employed to tune the correlative Lohrenz-Bray-Clark (LBC) and CO_2-LBC models and to evaluate the predictive models. The predictive models in this work are based on corresponding states (CS) theory models. The "*One reference fluid*" corresponding states model is based on the approach developed by Pedersen et al. and modified for CO_2-rich fluids; the "*two reference fluids*" corresponding states models are based on the model proposed by Aasberg-Petersen (CS2) and CO_2-CS2 models. Two models based on the extended corresponding states (ECS) theory, SUPERTRAP and CO_2-SUPERTRAP models were also tested.

The densities of 95%CO_2-5%H_2S and 95%CO_2-5%SO_2 systems were measured continuously using a high temperature and pressure Vibrating Tube Densitometer (VTD), Anton Paar DMA 512 at pressures up to 400 bar (40 MPa) at five different temperatures, 0, 10, 25, 50 and 80 °C (273.15, 283.15, 298.15, 323.15 and 353.15 K) in the gas, liquid and supercritical regions at Mines Paristech, France. The experimental data then were used to evaluate the new CO_2 volume correction model by comparing to the original PR and PR-Peneloux equations of state.

A good understanding of vapour-solid / vapour-liquid-solid / liquid-solid equilibrium of CO_2 and CO_2-mixtures at low temperature is an important issue regarding the safety assessment of CO_2 pipelines and the possibility of solid or 'dry ice' discharge during an accidental release or rapid decompression. The frost points of some of the above systems were measured using the SETARAM BT 2.15 calorimeter at various pressures.

Dedicated to my wife and son Azimeh and Aran

ACKNOWLEDGMENTS

This thesis is submitted in partial fulfilment of the requirements for the PhD degree at Heriot-Watt University. This work has been conducted at the Institute of Petroleum Engineering (IPE) from December 2010 to May 2015 under the supervision of Professor Bahman Tohidi and Dr Antonin Chapoy.

I would like to express my sincere gratitude to Professor Bahman Tohidi for providing me the opportunity to work with such a scientifically interesting project in the Hydrates, Flow Assurance & Phase Equilibria Group. As second supervisor, Dr Antonin Chapoy has taken a great deal of interest in my PhD project and I am extremely grateful to him for reading my draft thesis, his constructive advice and the support and confidence that he instilled in me throughout the process. Also in this regard, I would like to thank Dr Rod Burgess for his collaboration and experimental work support. Additionally, I greatly appreciate the help from Professor Christophe Coquelet at Mines Paristech for his generous support during the internship. I am also grateful to all the colleagues as well as friends in the Institute of Petroleum Engineering making my stay in Edinburgh very pleasant and provided me with any help needed.

I also would like to be grateful to my internal examiner, Professor Mercedes Maroto-Valer, for her great patient and support, particularly during the corrections. A great appreciate goes to the external examiners, Professor Martin Trusler from Imperial College London and Dr Norman Glen from TUV NEL, for their precise comments to improve the quality of my thesis.

Last but by no means least I am especially grateful for the patience and understanding shown by my wife Azimeh for her moral support, patience and encouragement.

The project has been financed by grants by a Joint Industrial Project (JIP) “Impact of Common Impurities on Carbon Dioxide Capture, Transport and Storage” conducted at the Institute of Petroleum Engineering, Heriot-Watt University. The JIP is supported by Chevron, Total, Statoil, National Grid, OMV, Petroleum Experts, Linde Group and Galp Energia which is gratefully acknowledged.

ACADEMIC REGISTRY
Research Thesis Submission

Name*:*	**MAHMOUD NAZERI GHOJOGH**		
School/PGI:	**Institute of Petroleum Engineering**		
Version: *(i.e. First, Resubmission, Final)*	Final	Degree Sought (Award **and** Subject area)	**PhD in Petroleum Engineering**

Declaration

In accordance with the appropriate regulations I hereby submit my thesis and I declare that:

1) the thesis embodies the results of my own work and has been composed by myself
2) where appropriate, I have made acknowledgement of the work of others and have made reference to work carried out in collaboration with other persons
3) the thesis is the correct version of the thesis for submission and is the same version as any electronic versions submitted*.
4) my thesis for the award referred to, deposited in the Heriot-Watt University Library, should be made available for loan or photocopying and be available via the Institutional Repository, subject to such conditions as the Librarian may require
5) I understand that as a student of the University I am required to abide by the Regulations of the University and to conform to its discipline.

* *Please note that it is the responsibility of the candidate to ensure that the correct version of the thesis is submitted.*

Signature of Candidate*:*		Date:	

Submission

Submitted By *(name in capitals):*	**MAHMOUD NAZERI GHOJGH**
Signature of Individual Submitting:	
Date Submitted:	

For Completion in the Student Service Centre (SSC)

Received in the SSC by *(name in capitals):*			
Method of Submission *(Handed in to SSC; posted through internal/external mail):*			
E-thesis Submitted (mandatory for final theses)			
Signature:		Date:	

TABLE OF CONTENTS

LIST OF TABLES

LIST OF FIGURES

LIST OF PUBLICATIONS

Chapoy, A., Nazeri, M., Kapateh, M. H., Burgass, R. W., Coquelet, C. & Tohidi Kalorazi, B. "*Effect of impurities on thermophysical properties and phase behaviour of a CO_2-rich system in CCS*", Int. J. of Greenhouse Gas Control, Vol. 19, Nov. 2013, Pages 92–100
http://dx.doi.org/10.1016/j.ijggc.2013.08.019

Chapoy, A., Nazeri, M., Kapateh, M., Burgass, R. W., Tohidi Kalorazi, B. & Coquelet, C. "*Thermophysical Properties and Phase Behaviour of a CO_2-Rich Natural Gas*", 1 Jan 2014 GPA Annual Convention Proceedings, Gas Processors Association, p. 601-628

Nazeri, M., Tohidi, B., Chapoy, A., "*An Evaluation of Risk of Hydrate Formation at the Top of a Pipeline*", SPE-160404-PA, Oil and Gas Facilities SPE Journal, Vol. 3, No. 2, 67-72, April 2014

Papers in preparation:

Density measurement and modelling of CO_2-rich mixtures in CCS

Viscosity measurement and modelling of CO_2-rich mixtures in CCS

Measurements of the thermodynamic properties of CO_2+H_2S and CO_2+SO_2 at pressures up to 40 MPa

Frost point measurements of CO_2-rich mixtures in CCS using calorimeter

Density measurements of sulphur dioxide at pressures up to 22 MPa

LIST OF MAIN SYMBOLS

A	Densitometer calibration parameter
AAD	Absolute Average Deviation
B	Densitometer calibration parameter
BIN	Binary
C	Unit conversion factor
CCS	Carbon Capture and Storage
CO_2-CS2	Aasberg-Petersen model modified for CO_2 systems
CO_2-LBC	LBC tuned for CO_2 systems
CO_2-Ped	Pedersen model modified for CO_2 systems
CO_2-ST	SUPERTRAP model modified for CO_2 systems
C_p	Specific heat capacity
CS	Corresponding States
CS2	Aasberg-Petersen
D	Diameter
ECS	Extended Corresponding States
EoS	Equation of State
EXP	Experimental
f_i	Reducing ratio
f	Fugacity
h_i	Reducing ratio
K_{cs}	Interpolation parameter function
L	Length
LBC	Lohrenz-Bray-Clark
M	Molecular Weight
mBWR	modified Benedict-Webb-Rubin
MIX	Mixture
MW	Molecular Weight
P	Pressure
Ped	Pedersen
PR	Peng-Robinson
Q	Flow rate
SC	Supercritical
SRK	Soave-Redlich-Kwong
ST	SUPERTRAP
T	Temperature
TCF	Trillion Cubic Feet
V	Volume
VTD	Vibrating Tube Densitometer
xi	Composition of component i
ΔP	Pressure Differential

Greek Letters

ρ	Density
τ	Period of oscillation
η	Viscosity
η^*	Dilute gas viscosity
ξ	Viscosity reducing parameter
ω	Acentric factor
φ	Shape factor
θ	Shape factor
σ	hard-sphere diameter
ν	Molar volume
ϕ	Fugacity coefficient

Subscripts

0	Reference component
c	Critical
i	Component i
j	Component j
k	Component k
m	Mixture
mix	Mixture
r	Reduced
R	Reference fluid
sub	Sublimation
x	pure compound x

CHAPTER 1: INTRODUCTION

The Power and other industry sectors account for more than 60% of the total carbon dioxide emissions. In these sectors, the carbon dioxide emissions are being generated by burning fossil fuels in boilers and furnaces. These large scale stationary sources are potential targets for equipping with capture technologies for reducing CO_2 emissions. These large emission sources, emitting above 0.1 $MtCO_2/yr$, can be divided to three main groups: fuel combustion processes, industrial units and natural gas processing. The fossil fuel for burning in the power plants can be coal, natural gas and oil. Hydro power, nuclear and renewables also is considered for power generation. Currently, coal is the dominant fuel accounting for 38% of the electricity generation, while the natural gas is 17.3% and oil is 9% in the world [1]. Carbon dioxide emissions from industrial processes can be from the fuel used in petrochemical processes [2], metal production from ores, calcination of dolomite and limestone in cement industry, converting sugar to alcohol and a combination of chemical combustion activities like aluminium production [3]. CO_2 is also known as a common impurity in natural gas which should be removed from the gas stream to avoid corrosion, meeting the transport pipeline criteria and improving the heating value of the gas [4].

1.1 Carbon capture and storage (CCS)

Climate change mitigation encompasses the actions to limit or prevent emission of greenhouse gases (GHGs). It can include using renewable energies, improving energy efficiency of older equipment, switching to less carbon-intensive fuels, changing consumer behaviour or management practices, or using new technologies to capture and store carbon dioxide [5]. Efforts around the world can be as complex as a plan for a new city, protecting natural carbon sinks like forests and oceans, or creating new sinks

through green agriculture, or as simple as improvements to a cool stove design, creating bicycling paths and walkways [6].

Carbon dioxide capture and storage (CCS) is one of the most promising technologies for the reduction of CO_2 emissions from industries, energy-related sources and human activities, so that global warming effect can be reduced/eliminated and helping the world to move towards a low-carbon society. The process comprises of the separation of CO_2 from the industrial sources, transport to a storage location and then long-term isolation from the atmosphere. CCS has the potential to reduce the total CAPEX of mitigation and increase flexibility in reduction of greenhouse gas emissions [5]. Figure 1.1 illustrates the overview of the CCS chain from power plants or industrial processes to the storage formation.

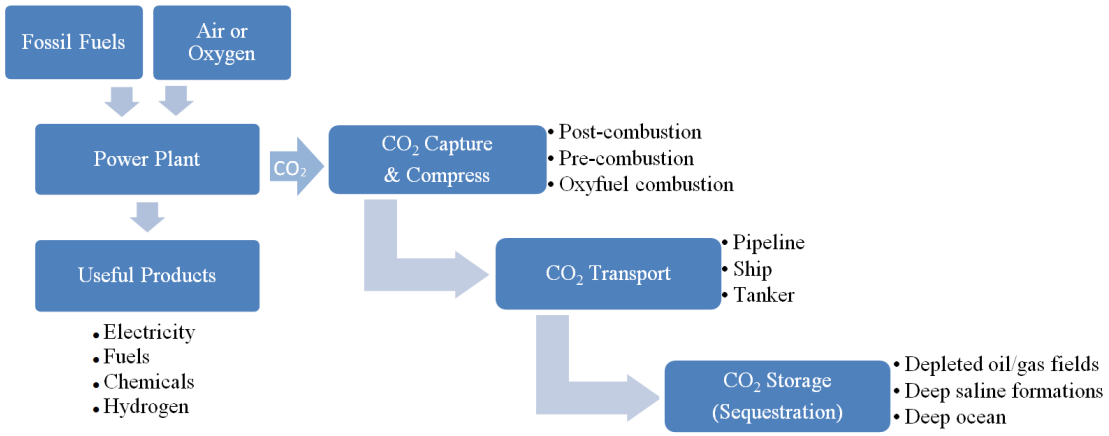

Figure 1.1 Schematic view of CCS chain: CO_2 capture from CO_2-generating processes, transport and storage

1.1.1 CO_2 capture

To reduce the emission of CO_2, the carbon dioxide in flue gas of the feedstock in industrial processes must be captured and separated to produce the high-purity CO_2 for the storage purposes or enhanced oil recovery. There are various technologies available to capture and separate emitted CO_2 from the flue gas in the industrial scale. Figure 1.2 shows the technical options available for capturing carbon dioxide.

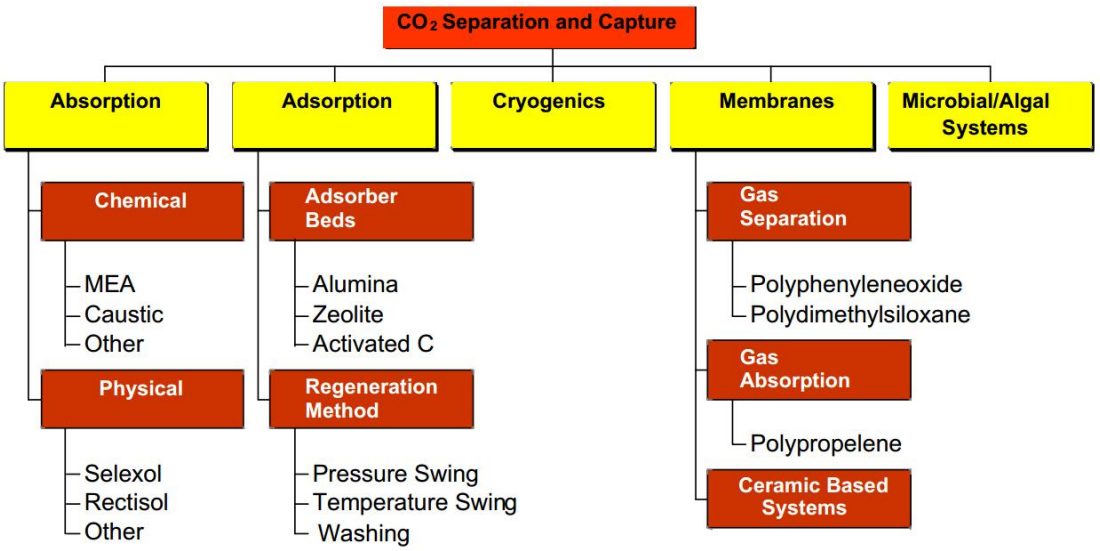

Figure 1.2 Available technologies for capturing CO_2 [7]

1.1.1.1 Pre-combustion capture process

This process captures the CO_2 from the synthesis gas (syngas) prior to the combustion of the fuel as the name suggested. At the first step of this process, after separating nitrogen from oxygen in the air separation unit, partial oxidation process combust coal at high temperature to provide the heat of gasification reactions in gasifier. During this process, the coal is chemically broken apart and converted to syngas [8]. The syngas is mainly composed of hydrogen, carbon dioxide and carbon monoxide. However, the composition depends on the gasifier conditions and the coal characteristics. After producing the syngas, a fixed-bed reactor with shift catalysts uses steam to transform carbon monoxide into a mixture of H_2 and CO_2.

Water Gas Shift Reaction: $CO + H_2O \leftrightarrow CO_2 + H_2$ (2-1)

The concentration of the CO_2 in this CO_2-rich mixture ranges from 15% to 60% (dry basis) which is higher compared to post-combustion process [9]. The total pressure of the system can be ranged from 2-7 MPa [10]. Following the shift reactor, CO_2 and sulphur compounds are separated from hydrogen in an acid gas removal unit. The remained H_2 can be used as a fuel to generate electricity in a combined-cycle gas turbine (CCGT) or other applications in chemical or oil and gas industry. The captured CO_2 can be compressed and transported to the storage site. The novel pre-combustion capture process can be applied to IGCC systems, such as the glycol-based Selexol and methanol-based Rectisol processes, by employing physical solvents to absorb CO_2 from

the syngas. For instance, the Dakota Gasification Company's substitute natural gas plant in North Dakota uses the Rectisol system to remove 1.5 million tons of CO_2 per annum from the syngas. Then, the captured CO_2 is transported through 320-kilometer pipeline after purification to be injected into the Weyburn oilfield in Canada [8]. The strong points of pre-combustion process include [11]:

- Capturing CO_2 from the CO_2-H_2 mixture due to the higher partial pressure of CO_2 is easier than capturing it from the flue gas after combustion
- Most advanced capture technology
- Low overall emissions, low fresh-water consumption and high CO_2 purity
- Hydrogen fuel can be used in other applications or stored

Also the weaknesses of this process are [11]:

- Complex equipment with many individual processes
- Unsuitable for retrofit onto existing conventional power plants
- Improved thermal efficiency only possible through greater plant complexity
- High complex systems limit operational flexibility

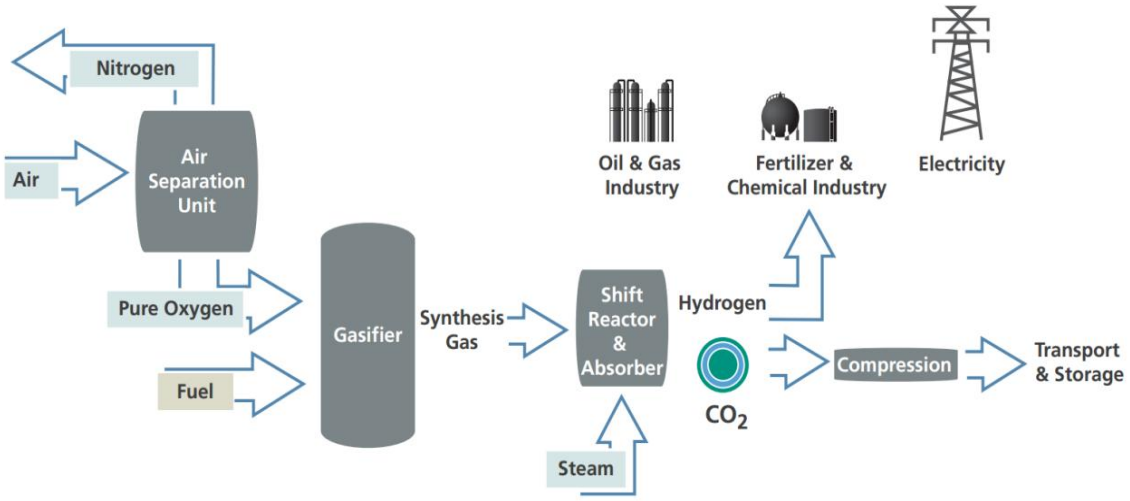

Figure 1.3 Pre-combustion process [12]

1.1.1.2 Post-combustion capture process

This capture process is a technology widely used to capture CO_2 for use in the food and beverage industry as well as in the gas processing units in gas field development projects. In this process, the flue gas produced by conventional coal combustion in air at atmospheric pressure has a CO_2 concentration of 10-15 volume % [13]. To capture the CO_2, the exhaust gas from the boiler enters to the bottom of the column to expose to a solvent, e.g., amines, to absorb the CO_2. The CO_2-rich solvent then is piped into a second fractionating column and heated with steam until the CO_2 is separated. The regenerated solvent then is recycled to the first column, resulting a closed scrubbing cycle. The key research area in this process is to minimise the energy to heat-up the CO_2-rich solvent and thus reduce the operating costs.

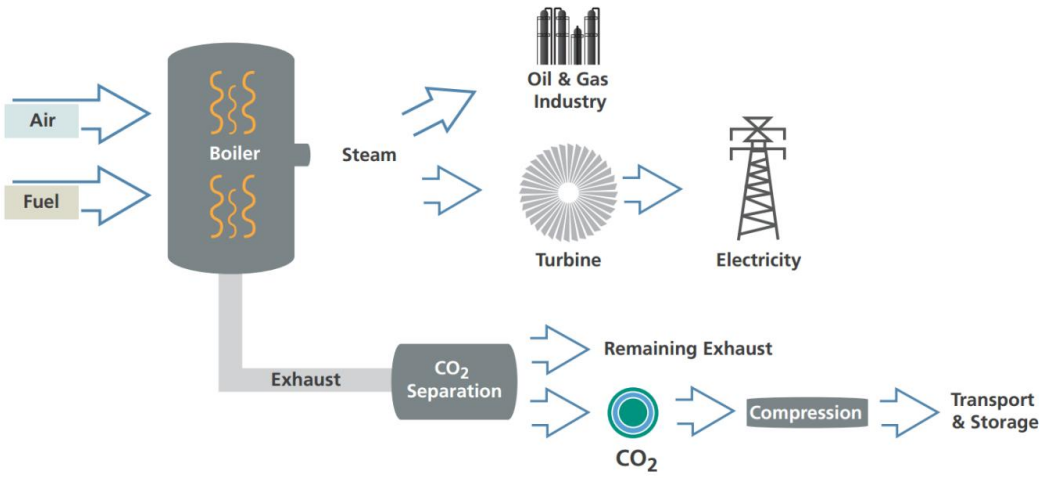

Figure 1.4 Post-combustion process [12]

The strengths of post-combustion process include [14]:

- Good prospects for retrofitting
- Robust process with only limited impact on plant availability
- Significant potential for technical optimisation
- Energy required for carbon capture can be offset by advances in the thermal efficiency of conventional generation
- Flexible operating characteristics
- High degree of CO_2 purity (>99.5 vol%)
- Commercial rollout likely by 2020

- Can be used in conventional power plants
- Several equipment suppliers conducting R&D

The weaknesses of the process are [14]:

- Significantly increases operating costs
- Capture equipment requires considerable additional space and cooling water
- Large amounts of chemicals must be handled
- Only limited experience worldwide with capturing carbon from the flue gas of coal-fired power plants

1.1.1.3 Oxyfuel capturing process

In addition to the pre- and post-combustion processes, the oxyfuel capture process is another promising technology for coal fired power plants. This process has been investigated in literature by many researchers [8-16]. In the oxyfuel technology, the combustion would be with pure oxygen comes from an air separation unit (ASU) and instead of the air, the flue gas recirculated [24]. This eliminates the nitrogen from the flue gas. Then after removing the fly ash, only water vapour, CO_2 and small quantity of SO_x and NO_x will remain in the flue gas [7]. Figure 1.5 shows the schematic view of the oxyfuel process.

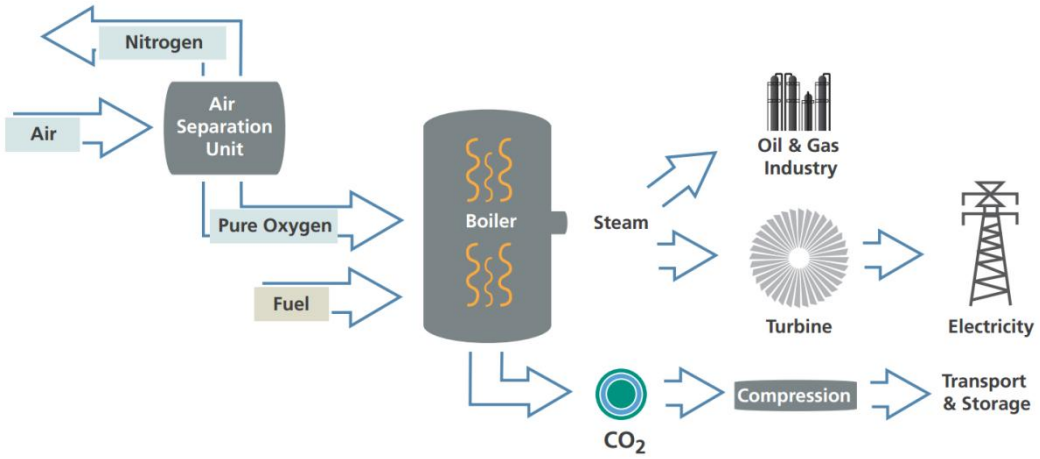

Figure 1.5 Oxyfuel process [12]

The concentration of CO_2 in the flue gas of oxyfuel process can reach the values about 80-90 vol% on a dry basis which assist the separation of CO_2 from the flue gas. The quality of the separated CO_2 is influenced by the oxygen purity coming from the air

separation unit, fuel composition and combustion stoichiometry. CO_2 purities of 85 vol% to high purity of 99.9 vol% are achievable from power plants with oxyfuel capture process. The amount of the impurity will influence the cost and the capture rate of the CO_2. The acceptable amount of the impurities will depends on the pipeline design specifications and the geology of the storage formation in each project.

Different scenarios have been developed for the oxyfuel process in the COORAL project [25]. The target of the project is to determine and estimate the CO_2 purity and possible impurities in the oxyfuel, pre- and post-combustion processes.

In the first scenario, oxyfuel I - zero emission, it is assumed that the whole flue gas without any vent gas to the atmosphere is compressed and transported to the storage formation. In this case, the CO_2 purity accounts to 85 vol% with the full capture rate.

In the second scenario, oxyfuel II - concentration, the CO_2 purity will be increased to 98 vol% by liquefaction. In this case, the concentration of impurities like oxygen, nitrogen and argon are reduced while the concentrations of impurities like carbon monoxide, nitrous oxides, sulphur oxides and water remains the same as the first scenario.

To increase the CO_2 purity further, the third scenario, oxyfuel III - distillation, can be applied by an additional distillation of the separated CO_2 stream. In this case, the CO_2 purity can be more than 99.9% and the concentrations of the nitrogen, oxygen and argon are further reduced. The concentrations of NO_x and SO_x in the oxyfuel process in all scenarios can be reduced more by cleaning the flue gas before liquefaction. The concentrations of the possible impurities at different scenarios of the oxyfuel process can be found below in Table 1.1.

The strong points of oxyfuel process are [26]:

- Incorporates known, commonly used technologies and processes
- Modifications to power plants are primarily required on the flue gas side
- No solvents needed
- Little space required for additional equipment at power plant site

The weaknesses of this process include [26]:

- Separation of air into pure oxygen and CO_2 scrubbing are energy intensive

- Low CO_2 purity; achieving higher levels of purities requires significantly more energy
- Development phase would require complete pilot and demonstration power plant
- Limited operational flexibility

Table 1.1 Impurity percentage in different scenarios of oxyfuel at COORAL

Impurities	Oxyfuel I Zero emission	Oxyfuel II Concentration	Oxyfuel III Distillation
CO_2 (vol%)	85.0	98.0	99.94
O_2 (vol%)	4.70	0.67	0.01
N_2 (vol%)	5.80	0.71	0.01
Ar (vol%)	4.47	0.59	0.01
NO_x (ppm)	100	100	100
SO_2 (ppm)	50	50	50
SO_3 (ppm)	20	20	20
H_2O (ppm)	100	100	100
CO (ppm)	50	50	50

1.1.2 CO_2 transport

The safe transport of CO_2 from the capture point to the storage location is a crucial step in the carbon capture and storage chain. Transporting CO_2 takes place daily in many parts of the world by truck and ship, however, for CO_2 captured from large scale power plants or chemical processes significant investment in transportation infrastructure such as construction of CO_2 pipeline networks are required.

For small amounts of CO_2, transporting to a nearby storage site by truck or rail can be a safe and possible option. Also ship transportation can be an alternative option for medium quantities (around 1,000 tonnes) [27]. Carbon capture is a continuous process at the plant on land while the ship transportation cycle is discrete. Thus, the temporary land storage and loading facilities should be considered. Ship transportation of CO_2 has large similarities to the liquefied petroleum gas (LPG) transportation by ship which is widely in use in the oil and gas industry [10].

The desirable condition to transport CO_2 in pipelines is to transport in supercritical or dense phase as a combination of relatively high density with a relatively low viscosity of CO_2 systems can be found in this state. CO_2 transport in the gaseous state is inefficient due to the low density of the CO_2 and comparatively high pressure drop in

the pipeline per unit length [28]. However, transporting CO_2 in the gaseous phase would be unavoidable when using some of existing infrastructures. To transport the low-pressure CO_2 in the gas phase, the operating pressure should not exceed the maximum pressure of 4.8 MPa at temperature above 20 °C (293 K). Operating CO_2 pipeline at pressures above the critical pressure of CO_2 of 7.38 MPa, i.e. at supercritical phase, will eliminate the phase changes and two-phase flow formation with temperature variations along the pipeline. The operating temperature of CO_2 pipelines will depends on the environment temperature. The maximum temperature at the inlet of the pipeline or at the discharge of the compressor station required to be controlled by the allowable temperature rating for the pipeline coating of flange temperature rating. The existing CO_2 pipelines in USA operates at pressures from 8.6 MPa to 20 MPa [29] with ambient temperature ranging from 4 °C to 38 °C (277 to 311 K). Table 1.2 shows the list of existing long distance CO_2 pipelines.

Table 1.2 Existing long-distance CO_2 pipelines [10]

Pipeline	Location	Operator	Capacity $MtCO_2/yr$	Length km	Diameter in	Year finished
Cortez	USA	Kinder Morgan	19.3	808	30	1984
Sheep Mountain	USA	BP Amoco	9.5	660	24	-
Bravo	USA	BP Amoco	7.3	350	20	1984
Canyon Reef	USA	Kinder Morgan	5.2	225		1972
Val Verde	USA	Petrosource	2.5	130		1998
Bati Raman	Turkey	Turkish Petroleum	1.1	90		1983
Weyburn	USA	North Dakota Gasification Co.	5	328	12-14	2000
Total			49.9	2591		

The quality specifications for composition of CO_2 pipelines given for Canyon Reef project are [10]:

- Carbon Dioxide: The CO_2 stream shall contain minimum 95 mol% of CO_2
- Water: The stream shall not contain free water
- Hydrogen sulphide: The stream shall not contain more than 1500 ppmw H_2S
- Total Sulphur: Not more than 1450 ppmw of total sulphur
- Temperature: Not more than 48.9 °C
- Nitrogen: Not more than 4 mol%

- Hydrocarbons: Not more than 5 mol%
- Dew point: Shall not exceed -28.9 °C in the presence of hydrocarbons
- Oxygen: Not more than 10 ppmw

1.1.3 CO_2 storage

The captured and transported CO_2 would be effective to the climate protection only if the CO_2 can be stored permanently and safely underground. A practical geological storage location should consist of a porous rock formation and one impermeable cap rock on top of the formation to prevent the release of stored CO_2. Over the next few millennia, most of the CO_2 would dissolve in the water among the rock formation. The dense CO_2-rich water then would sink to the formation's floor and the CO_2 would be bound to the rock formation after crystallisation by mineral processes.

Saline aquifers with typically more than 800 meters below the surface are suitable for permanent carbon storage. Depleted natural gas reservoirs also can be suitable option for storage [30].

1.2 This work

This work is a part of the joint industrial project titled "Impact of Common Impurities on Carbon Dioxide Capture, Transport and Storage" [31]. The physical properties to be investigated during the project are phase equilibira, hydrates, solid formation, density, viscosity, interfacial tension, solubility in brine and pH. The first phase of the project has been conducted from October 2011 to October 2014. The companies sponsored the project, which is acknowledged, are Chevron, Total, Statoil, National Grid, OMV, Petroleum Experts, Linde Group and Galp Energia.

The aim of this work is to investigate the effect of common impurities such as methane, ethane$^+$, nitrogen, oxygen, hydrogen, argon, carbon monoxide, hydrogen sulphide and sulphur dioxide on the thermos-physical properties, particularly density and viscosity, of CO_2-rich systems.

In chapter 2, different types of impurities in capture processes and specifications for the transport of CO_2 systems in pipelines would be reviewed. Then, the different CO_2 streams containing impurities, which were investigated in this work, will be introduced.

To understand the thermodynamic properties of different CO_2-mixtures, study of Equations of State (EoS) is extremely important. In literature several references are available on CO_2 and CO_2 mixture EoS, nevertheless a suitable equation of state for mixtures in appropriate conditions for pipeline transport, in particular with a high CO_2 concentration, has not been clearly defined. The aim of chapter 3 and chapter 5 is to investigate the density of CO_2 streams containing impurities. In chapter 3, the densities of pure CO_2, for calibration purposes, binary systems and multi-component mixtures were measured. Then, the generated experimental data were employed to evaluate the equation of states with new volume correction for CO_2 systems in our in-house software package. In chapter 5, the densities of acid gases and liquids, CO_2 containing H_2S and SO_2 have been measured.

Estimation of transport properties is of crucial interest to understand and estimate flow and heat transfer behaviour of fluids. Viscosity is a key transport property for pipeline systems as well as sub-surface and process systems. There are some methods to predict the viscosity of fluids in each system. A widely used method to calculate the transport properties of fluids, particularly viscosity, is based on the corresponding states (CS) and extended corresponding states (ECS) concepts. Another common concept to determine the viscosity of fluids is the residual viscosity concept. The aim of chapter 4 is to investigate the viscosity of CO_2-rich systems by measuring the viscosity using classical capillary tube technique. The modified predictive models and correlative models then would be evaluated using the measured viscosity data.

A good understanding of vapour-solid / vapour-liquid-solid / liquid-solid equilibrium of CO_2 and CO_2-mixtures at low temperature is an important issue regarding the safety assessment of CO_2 pipelines and the possibility of solid or 'dry ice' discharge during an accidental release or rapid decompression. In chapter 6, the frost points of some of the mixtures were measured using a SETARAM BT 2.15 calorimeter at various pressures.

REFERENCES

[1] J. Gale, "IPCC Special Report on Carbon dioxide Capture and Storage," *Chapter 2 Sources CO_2*, Jun. .

[2] T. S. Christensen and I. I. (Haldor T. C. (Denmark)) Primdahl, "Improve syngas production using autothermal reforming," *Hydrocarb. Process. (United States)*, vol. 73:3, Mar. 1994.

[3] IEA-GHG-2000, "Greenhouse Gas Emissions from Major Industrial Sources - IV, the Aluminium Industry," *IEA GHG, 2000 Greenh. Gas Emiss. from Major Ind. Sources - IV, Alum. Ind.*, Feb. 2000.

[4] R. Maddox, "Gas Conditioning and Processing: Gas and Liquid Sweetening," *Campbell Petroleum Series, OK, USA, 498 pp.*, 1998. [Online]. Available: http://www.amazon.com/Gas-Conditioning-Processing-Liquid-Sweetening/dp/9991205896. [Accessed: 24-Feb-2015].

[5] H. Rubin, E., de Coninck, "IPCC Special Report on Carbon Dioxide Capture and Storage," *Cambridge University Press, Cambridge*, 2005. [Online]. Available: http://www.cmu.edu/epp/iecm/rubin/PDF files/2006/2006a Rubin, Intl Wkshp on CO2 Geo Storage (Feb).pdf. [Accessed: 14-Jan-2015].

[6] U. N. E. P. (UNEP), "Climate Change Mitigation," *http://www.unep.org/climatechange/mitigation/Default.aspx*. [Online]. Available: http://www.unep.org/climatechange/mitigation/Default.aspx. [Accessed: 14-Jan-2015].

[7] E. S. Rubin, H. Mantripragada, A. Marks, P. Versteeg, and J. Kitchin, "The outlook for improved carbon capture technology," *Prog. Energy Combust. Sci.*, vol. 38, no. 5, pp. 630–671, Oct. 2012.

[8] "Pre-Combustion CO_2 Control | netl.doe.gov." [Online]. Available: http://www.netl.doe.gov/research/coal/carbon-capture/pre-combustion. [Accessed: 25-Feb-2015].

[9] "Pre-Combustion Carbon Capture Research | Department of Energy." [Online]. Available: http://energy.gov/fe/science-innovation/carbon-capture-and-storage-research/carbon-capture-rd/pre-combustion-carbon. [Accessed: 25-Feb-2015].

[10] IPCC-2005, *IPCC,2005: Special Report on CARBON DIOXIDE CAPTURE AND STORAGE*. 2005.

[11] "Pre-Combustion Capture - E.ON SE." [Online]. Available: http://www.eon.com/en/business-areas/power-generation/coal/carbon-capture-and-storage/pre-combustion-capture.html. [Accessed: 25-Feb-2015].

[12] "Carbon Capture & Storage | Graphics | ICO2N," *http://www.ico2n.com/library/graphics*. [Online]. Available: http://www.ico2n.com/library/graphics. [Accessed: 25-Feb-2015].

[13] "Post-Combustion CO_2 Control | netl.doe.gov." [Online]. Available: http://www.netl.doe.gov/research/coal/carbon-capture/post-combustion. [Accessed: 27-Feb-2015].

[14] "Post-Combustion Capture Technology - E.ON SE." [Online]. Available: http://www.eon.com/en/business-areas/power-generation/coal/carbon-capture-and-storage/post-combustion-capture-technology.html. [Accessed: 25-Feb-2015].

[15] G. Cléon, D. Honoré, C. Lacour, and A. Cessou, "Experimental investigation of structure and stabilization of spray oxyfuel flames diluted by carbon dioxide," *Proc. Combust. Inst.*, vol. 35, no. 3, pp. 3565–3572, 2015.

[16] J. Dickmeis and A. Kather, "The Coal-fired Oxyfuel-process with Additional Gas Treatment of the Ventgas for Increased Capture Rates," *Energy Procedia*, vol. 63, pp. 332–341, 2014.

[17] J. Dickmeis and A. Kather, "Integration of Oxygen-containing Exhaust Gas into the Air Separation Unit of an Oxyfuel Power Plant," *Energy Procedia*, vol. 51, pp. 99–108, 2014.

[18] A. Komaki, T. Gotou, T. Uchida, T. Yamada, T. Kiga, and C. Spero, "Operation Experiences of Oxyfuel Power Plant in Callide Oxyfuel Project," *Energy Procedia*, vol. 63, pp. 490–496, 2014.

[19] X. Liang, H. Zhao, and X. Pei, "Technical Issues in Financing and Managing Risk of Large-scale Oxyfuel CO_2 Capture Power Plant in China," *Energy Procedia*, vol. 63, pp. 7234–7241, 2014.

[20] X. Liang, H. Zhao, and X. Pei, "Assessing the Option Value of Retrofitting a 200MW Power Plant to Oxyfuel CO_2 Capture," *Energy Procedia*, vol. 63, pp. 7330–7336, 2014.

[21] P. Markewitz, J. Marx, A. Schreiber, and P. Zapp, "Ecological Evaluation of Coal-fired Oxyfuel Power Plants -cryogenic Versus Membrane-based Air Separation-," *Energy Procedia*, vol. 37, pp. 2864–2876, 2013.

[22] S. C. Pickard, S. S. Daood, M. Pourkashanian, and W. Nimmo, "Co-firing coal with biomass in oxygen- and carbon dioxide-enriched atmospheres for CCS applications," *Fuel*, vol. 137, pp. 185–192, Dec. 2014.

[23] M. C. Romano, "Ultra-high CO_2 capture efficiency in CFB oxyfuel power plants by calcium looping process for CO_2 recovery from purification units vent gas," *Int. J. Greenh. Gas Control*, vol. 18, pp. 57–67, Oct. 2013.

[24] A. Kather and S. Kownatzki, "Assessment of the different parameters affecting the CO2 purity from coal fired oxyfuel process," *Int. J. Greenh. Gas Control*, vol. 5, pp. S204–S209, Jun. 2011.

[25] "BGR - Project website: COORAL - CO_2 Purity for Capture and Storage." [Online]. Available:

http://www.bgr.bund.de/EN/Themen/CO2Speicherung/COORAL/Home/cooral_node_en.html. [Accessed: 25-Feb-2015].

[26] "Oxyfuel Combustion - E.ON SE." [Online]. Available: http://www.eon.com/en/business-areas/power-generation/coal/carbon-capture-and-storage/oxyfuel-combustion.html. [Accessed: 25-Feb-2015].

[27] "How CCS works - transport | Global Carbon Capture and Storage Institute." [Online]. Available: http://www.globalccsinstitute.com/content/how-ccs-works-transport. [Accessed: 27-Feb-2015].

[28] S. MCCOY and E. RUBIN, "An engineering-economic model of pipeline transport of CO_2 with application to carbon capture and storage," *Int. J. Greenh. Gas Control*, vol. 2, no. 2, pp. 219–229, Apr. 2008.

[29] J. R. and M. D. Patricia Seevam, "Carbon dioxide pipelines for sequestration in the UK: an engineering gap analysis," *J. Pipeline Eng.*, 2007.

[30] Storage - E.ON SE, "http://www.eon.com/en/business-areas/power-generation/coal/carbon-capture-and-storage/storage.html." [Online]. Available: http://www.eon.com/en/business-areas/power-generation/coal/carbon-capture-and-storage/storage.html. [Accessed: 27-Feb-2015].

[31] "Impact of Common Impurities on Carbon Dioxide Capture, Transport and Storage." [Online]. Available: http://www.pet.hw.ac.uk/research/co2cts/. [Accessed: 28-Feb-2015].

CHAPTER 2: IMPURITIES IN THE CO_2 STREAM

2.1 Introduction

The main sources of the CO_2 emissions are power plants in the CCS chain. The produced CO_2 in the flue gases before or after the fuel combustion should be captured. The captured carbon dioxide from the power plants or any other sources may contain impurities which would have practical impacts on the design and also potential impacts on health, safety and environmental issues during the transport and storage of the carbon dioxide. In the CCS chain, the types and concentrations of the impurities will depend on the type of capture process. Table 2.1 shows the types and quantities of the possible impurities from different capture technologies. As seen in this table, the post-combustion process has the lowest impurity content in comparison to the other two capture technologies. There are many post-combustion capture plants which produce high purity CO_2 for use in the food industry.

In a pre-combustion process, CO_2 capture by physical solvent usually contains 1-2 mol% hydrogen, carbon monoxide and traces of hydrogen sulphide. In other pre-combustion processes impurities like nitrogen, methane, hydrogen and carbon monoxide may be found. The CO_2 stream captured by oxyfuel processes contains argon, oxygen, nitrogen, sulphur dioxide and nitrous oxides. Further reduction of the impurities in this capture process can be implemented by liquefaction of the flue gas and distillation process which will increase the cost of capturing process [1].

Apart from the CCS chain, some natural accumulation of CO_2 can happen naturally in geological structures. Some natural gas reservoirs have a large CO_2 content up to 70 mol% or more; the higher the concentration of CO_2, the less possibility the field to be commercialised. For instance the Natuna gas field in Indonesia with more than 46 trillion cubic feet (TCF) of natural gas reserves is the biggest natural gas field in the South-East Asia. However, the field gas contains about 70% CO_2. Thus, the field may never be exploited for its natural gas without finding a solution for re-injecting for

enhanced oil recovery or geological storage of the CO_2. These types of natural accumulations of CO_2 also can be found in Italy, Western United States, and Southern Australia [2].

Table 2.1 Concentrations of impurities in CO_2 in vol% (Source: IEA GHG 2003, 2004 and 2005)

	SO_2	NO	H_2S	H_2	CO	CH_4	$N_2/Ar/O_2$	Total
COAL FIRED PLANTS								
Post-combustion process	<0.01	<0.01	0	0	0	0	0.01	0.01
Pre-combustion process	0	0	0.01-0.6	0.8-0.2	0.03-0.4	0.01	0.03-0.6	2.1-2.7
Oxyfuel	0.5	0.01	0	0	0	0	3.7	4.2
GAS FIRED PLANTS								
Post-combustion process	<0.01	<0.01	0	0	0	0	0.01	0.01
Pre-combustion process	0	0	<0.01	1.0	0.04	2.0	1.3	4.4
Oxyfuel	<0.01	<0.01	0	0	0	0	4.1	4.1

Some technical specifications should be considered for safe and economic transport of the contaminated CO_2 with impurities. Nowadays, there are no widely accepted standards for CO_2 purity and composition of CO_2-rich stream for pipeline transportation. Only few trade agreements and business guidelines are available in some specific projects in the United States. Table 2.2 shows CO_2 specifications from pipeline operators [3]. It is mentioned in these guidelines that the amount of the non-condensable gases shall not exceed 5 mol% in the design basis and shall not be more than 3 mol% during pipeline operation.

The techno-economic studies by Yan et al. [4] about the impact of non-condensable gases produced in the oxyfuel process on CO_2 transportation shows that the reasonable purification limit in terms of cost is limited to 4 volume percent. However, for short distance applications, purification level could be raised up to 10 volume percent. Also in Dynamis CO_2 quality recommendations [5] the limit of 4 volume percent for non-condensable gases is set to minimise their impact on the pipeline capacity and compression costs for the hydraulic behaviour of CO_2 transport in presence of impurities.

Table 2.2 CO_2 specifications from the pipeline operators and business agreements

Component		Kinder Morgan	Weyburn	Sleipner
Type of project		EOR	EOR	
CO_2	vol%	95%	96%	93-96%
CH_4	ppm		0.70%	
C_2H_6	ppm			
C_3^+	ppm			
Total hydrocarbons	vol%	<5%	2.30%	0.5 - 2.0%
H_2	ppm			
CO	ppm		1000	
N_2	vol%	<4%	<300 ppm	
Other inerts	ppm			
Total inerts	vol%			3-5%
O_2	ppm	10	<50	
H_2S	ppm	10-200	9000	<150
SO_x	ppm			
Total sulphur	ppm			
H_2O	lbs/MMcf	30	<20 ppm	saturated
Glycol	gal/MMcf	0.3		

2.2 Materials in this work

The materials include pure CO_2, CO_2-hydrogen binary systems, CO_2-toxic gases binaries and multi-component mixtures. The mixtures supplied by BOC were certified on the basis of gravimetry in accordance with ISO 6142 with analytical validation. The volume of the cylinders is about 2 cubic meters. It is recommended by supplier not to use the product below 5% of actual contents. According to the suppliers' instructions to prevent condensation, the cylinders were kept in the laboratory area with a temperature of about 20 °C. The reported expanded uncertainties in each table are based on a standard uncertainty multiplied by a coverage factor k = 2, providing a level of confidence of approximately 95%. The following pure compounds and mixtures were used to conduct the density, viscosity and melting point measurement tests.

2.2.1 Pure carbon dioxide

Pure CO_2 used to conduct the tests has been supplied by Air Products in research grade (N4.5). Table 2.3 shows the maximum level of impurities in the CO_2 used in this work.

Table 2.3 Impurities of Pure CO_2

Impurities	Quantity (ppm)
O_2	< 10
H_2O	< 7
CO	< 2
THC (as CH_4)	< 5
N_2	< 25

2.2.2 Binary systems

Two carbon dioxide binary systems with approximately 5% and 10% hydrogen as the impurity have been studied.

- Hydrogen-CO_2 binary system 1, BINARY 1, Supplied by BOC, Research Grade, uncertainty < 2%, with approximately 5% impurity
- Hydrogen-CO_2 binary system 2, BINARY 2, Supplied by BOC, Research Grade, uncertainty < 2%, with approximately 10% impurity

The following chemicals have been used to prepare binary mixtures using gravimetry technique in the tests conducted in Mines Paristech, Fontainbleau, France. The compositions of the binary systems are given in Table 2.4.

- Hydrogen Sulphide binary system
  - CO_2, used in experiments was 99.995% pure, supplied by Air Liquide
  - H_2S, used in experiments was 99.5% pure, supplied by Air Liquide
- Sulphur Dioxide binary system
  - CO_2, used in experiments was 99.995% pure, supplied by Air Liquide
  - SO_2, used in experiments was 99.5% pure, supplied by Air Liquide

Table 2.4 and Figure 2.1 show the compositions and phase envelopes of the binary mixtures, respectively.

Table 2.4 Compositions of the binary systems (% mole)

Components	BINARY 1	BINARY 2	$CO_2 + H_2S$	$CO_2 + SO_2$ At 25 °C	$CO_2 + SO_2$
Carbon Dioxide	Balance 94.82	Balance 89.67	95.05 (±0.143%)	94.78 (±0.180%)	95.03 (±0.181%)
Hydrogen	5.18 (±0.104%)	10.33 (±0.207%)	---	---	---
Hydrogen Sulphide	---	---	4.95 (±0.004%)	---	---
Sulphur Dioxide	---	---		5.22 (±0.010%)	4.97 (±0.010%)
Total	**100**	**100**	**100**	**100**	**100**

2.2.3 Multi-component mixture systems

Varieties of multi-component mixtures with diverse impurities and different percentages have been prepared. Each mixture represents the composition of gas from a specific source. MIX 1 with approximately 4.4% impurities such as methane, nitrogen, hydrogen, argon, oxygen and carbon monoxide can show a proper behaviour of the streams suitable for the carbon capture, transport and storage. MIX 2 with a wider range of approximately 10% of non-condensable gases, i.e., nitrogen, oxygen and argon, has been prepared to denote the CCS stream fluids. Mixture 3 with 30% light hydrocarbons and 70% CO_2 represents the Natuna gas field composition in Indonesia which is the biggest gas field in the South East Asia.

- Multi-component mixture 1, MIX 1, supplied by BOC, Research Grade, uncertainty < 5%, with approximately 4.4% impurities
- Multi-component mixture 2, MIX 2, supplied by BOC, Research Grade, with approximately 10% impurities of non-condensable gases
- Multi-component mixture 3, MIX 3, supplied by BOC, Research Grade, with approximately 30% impurities of hydrocarbons, Natuna natural gas offshore field, South East Asia, Indonesia
- Multi-component mixture 4, MIX 4, supplied by BOC, Research Grade, with approximately 50% impurities of hydrocarbons
- Multi-component mixture 5, MIX 5, supplied by BOC, Research Grade, uncertainty < 2%, with approximately 4% of non-condensable gases
- Multi-component mixture 6, MIX 6, supplied by BOC, Research Grade, with approximately 30% impurities of hydrocarbons and nitrogen

The compositions of the multi-component mixtures are given in Table 2.5. Also, Table 2.6 shows the molecular weights, critical points, cricondentherm and cricondenbar for the studied binaries and multi-component mixture systems.

Table 2.5 Compositions of the multi-component mixture (mole%)

Components	MIX 1	MIX 2	MIX 3	MIX 4	MIX 5	MIX 6
Carbon Dioxide	Balance 95.64	Balance 89.83	Balance 69.99	Balance 49.93	Balance 95.97	Balance 69.99
Methane	0.6261 (±0.031%)	0	20.02 (±0.11%)	39.99 (±0.20%)	0	7.901 (±0.040%)
Ethane	0	0	6.612 (±0.034%)	3.510 (±0.018%)	0	7.015 (±0.036%)
Propane	0	0	2.58 (±0.013%)	1.530 (±0.008%)	0	4.968 (±0.025%)
n-Butane	0	0	0.3997 (±40 ppm)	0.501 (±0.006%)	0	2.067 (±0.0011%)
i-Butane	0	0	0.3998 (±40 ppm)	0.499 (±0.005%)	0	2.049 (±0.0011%)
n-Pentane	0	0	0	0.513 (±0.006%)	0	0
Nitrogen	1.41 (±0.071%)	5.05 (±0.04%)	0	3.524 (±0.018%)	2.028 (±0.041%)	6.009 (±0.031%)
Hydrogen	0.8175 (±0.041%)	0	0	0	0.605 (±0.012%)	0
Oxygen	0.08 (±0.004%)	3.07 (±0.10%)	0	0	0.783 (±0.016%)	0
Argon	1.21 (±0.061%)	2.05 (±0.06%)	0	0	0.611 (±0.012%)	0
Carbon Monoxide	0.2127 (±0.011%)	0	0	0	0	0
Total	**100**	**100**	**100**	**100**	**100**	**100**

Table 2.6 Properties of binaries and multi-component mixture systems using modified PR EoS

Material	MW	Critical Point		Cricondentherm		Cricondenbar	
		T / K	P / MPa	T / K	P / MPa	T / K	P / MPa
CO_2+H_2S	43.5	304.95	7.700	306.36	7.056	304.95	7.700
CO_2+SO_2	45.0	313.25	7.893	313.45	7.861	313.25	7.893
MIX 1	43.6	301.35	7.982	301.46	7.922	301.17	8.119
MIX 2	42.8	295.03	8.938	297.43	8.587	295.03	8.938
MIX 3	37.6	284.96	7.640	286.33	7.501	284.79	7.667
MIX 4	32.1	264.32	8.781	272.30	7.348	263.20	8.800
MIX 5	43.3	301.58	7.969	301.74	7.950	301.46	8.081
MIX 6	40.4	296.09	7.932	298.59	7.388	295.95	7.969

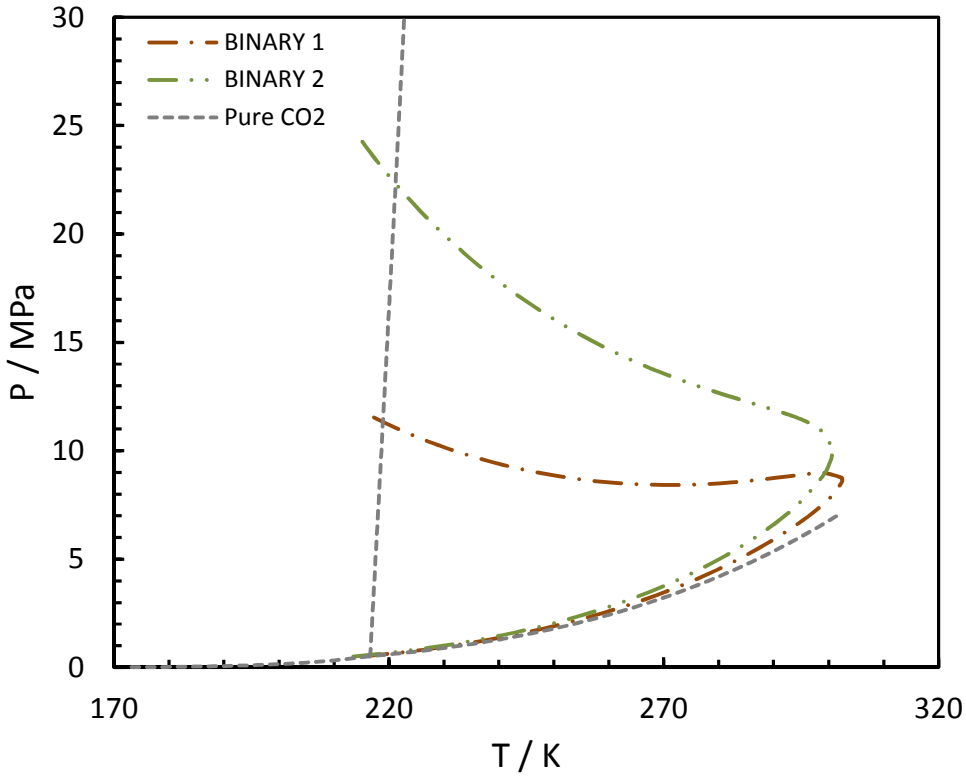

Figure 2.1 Phase envelopes for hydrogen-CO_2 binary systems

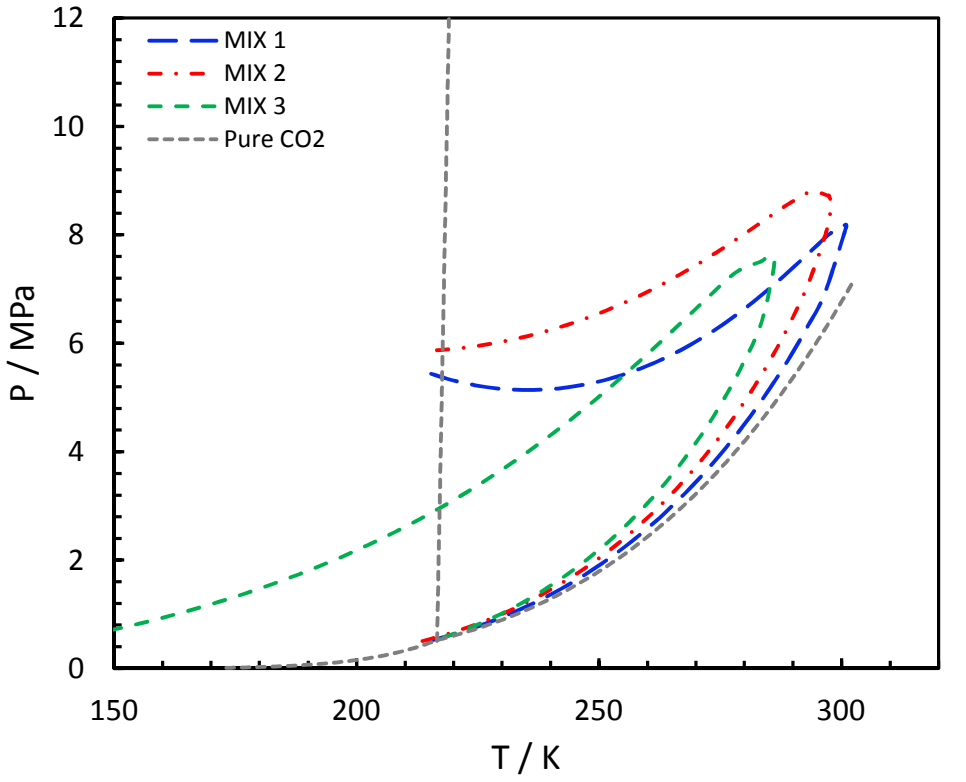

Figure 2.2 Phase envelopes for multi-component mixture systems 1, 2 and 3

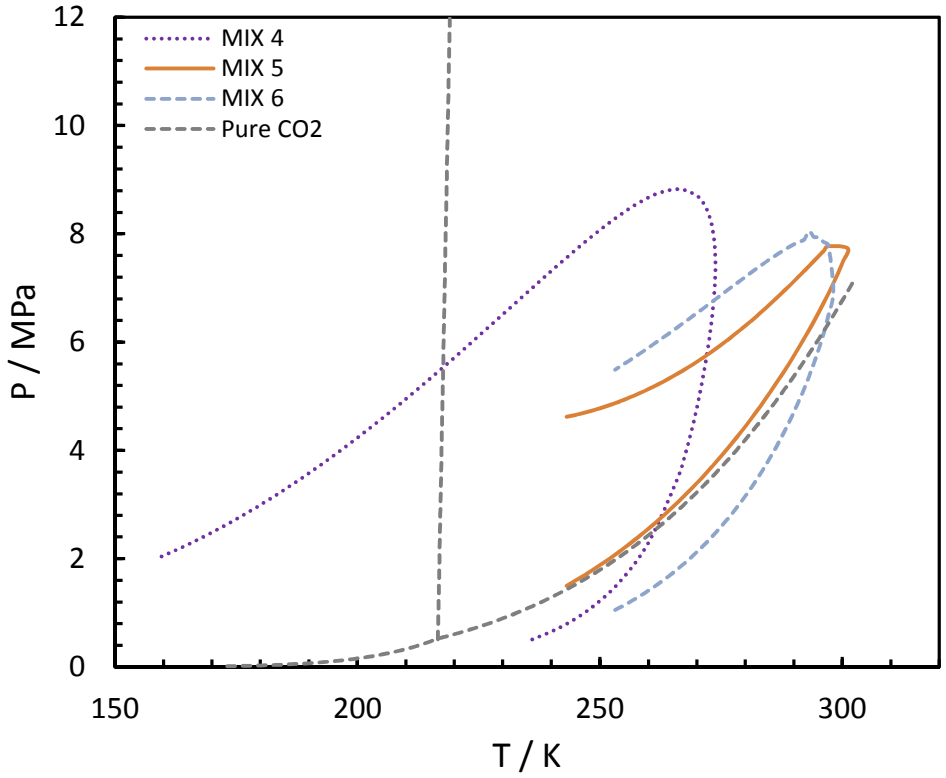

Figure 2.3 Phase envelopes for multi-component mixture systems 4, 5 and 6

REFERENCES

[1] *IPCC,2005: Special Report on CARBON DIOXIDE CAPTURE AND STORAGE*. 2005.

[2] Peter Cook, *Clean Energy, Climate and Carbon*. CO2CRC Limited, 2012.

[3] E. de Visser, C. Hendriks, M. Barrio, M. J. Mølnvik, G. de Koeijer, S. Liljemark, and Y. Le Gallo, "Dynamis CO_2 quality recommendations," *Int. J. Greenhouse Gas Control*, vol. 2, no. 4, pp. 478–484, Oct. 2008.

[4] C. B. Jinying Yan, Marie Anheden, "Impacts of Non-condensable Components on CCS," 2008.

[5] B. Wetenhall, H. Aghajani, H. Chalmers, S. D. Benson, M.-C. Ferrari, J. Li, J. M. Race, P. Singh, and J. Davison, "Impact of CO_2 impurity on CO_2 compression, liquefaction and transportation," *Energy Procedia*, vol. 63, pp. 2764–2778, 2014.

CHAPTER 3: DENSITY MEASUREMENTS AND MODELLING

The aim of this chapter is to investigate the densities of the CO_2-rich systems. The densities of pure CO_2, two CO_2-H_2 binary systems (with 5 and with 10 mol% H_2), and 6 multi-component mixtures (MIX 1 with 5 mol% impurity, MIX 2 with 10 mol% impurity, MIX 3 with 30 mol% impurity, MIX 4 with 50 mol% impurity, MIX 5 with 4 mol% impurity and MIX 6 with 30 mol% impurity) were measured at pressures ranging from 1 to 120 MPa at six different temperatures, 273.15, 283.15, 298.15, 323.15, 373.15 and 423.15 K (0, 10, 25, 50, 100, 150 °C) in the gas, liquid and supercritical regions using an Anton Paar densitometer. The experimental data then were used to evaluate a new CO_2 volume correction model as well as classical cubic equation of states (PR and SRK) with and without Peneloux shift parameters.

3.1 Introduction

The application of carbon capture and storage becomes increasingly important, from both scientific and industrial points of view, the overall aim being to reduce CO_2 emissions. CCS technology can provide a potential to cut/reduce the large scale release of CO_2 emissions to the atmosphere. The process comprises three main steps: capture, transport and storage. Three capturing technologies are under development: pre-combustion, post-combustion and oxy-fuel combustion. The aim of each capturing technology is to capture CO_2, preventing it from release to the atmosphere, following this to transport it to a suitable place of storage. However, the CO_2 coming from capture processes will contain a range of impurities as none of the technologies are efficient enough to produce pure CO_2. The concentration and type of the impurities will depends on many factors like fuel type, capture technology and the design of the plant. [1] Between the capture and storage, the CO_2 has to be transported by one or a combination of different means of transport, i.e. road, rail, sea or pipeline. Transport by pipeline is the preferred option when transporting large quantities of carbon dioxide over longer distances.[2] Carbon dioxide transport pipelines play a key role in linking the capture

and storage of CO_2 systems. Technically, CO_2 can be transported through pipelines in the form of a gas, a supercritical fluid or in the sub-cooled liquid state. Operationally, the most efficient CO_2 pipelines used for enhanced oil recovery transport the CO_2 as a supercritical fluid. [3] As the critical point of CO_2 (7.38 at 31.1 °C) and triple point (0.518 MPa at -56.6 °C) are very different from conventional fluids present in transport pipelines in oil and gas industry, the modelling of these pipelines poses new challenges. [4] It has been proposed that the operating pressure of CO_2 transport pipelines should be above 8.6 MPa to make sure that the fluid will be always in the single super critical phase over a range of temperatures that the pipeline may encounter. [5] The captured CO_2 from the power plants or other energy sources is not pure and contains impurities depending on the capture technology. The main effect of the presence of impurities, particularly if hydrogen or nitrogen is present, is to change physical properties of the stream such as critical pressure, which can have a significant effect on the hydraulic behaviour of the CO_2 stream. In addition both the density and viscosity of the fluid will change. [6]

To understand thermodynamic properties of different CO_2-mixtures, study of Equations of State (EoS) is extremely important. In literature several references are available on EoS suitable/used for CO_2 and CO_2 mixtures [7] [8] [9] [10], nevertheless a suitable equation of state for mixtures in appropriate conditions for pipeline transport, in particular with a high CO_2 concentration, has not been clearly defined [11].

3.2 Literature review

According to the requirements of engineering applications for design and operation of CO_2 capture and storage systems, cubic equation of states are preferable to predict VLE properties and density calculations [9] due to the simplicity and availability in the oil and gas industry as well as commercial software packages. The systems to be studied may contain a wide range of components including pure CO_2, and mixtures with other gases, amines, ionic liquids, water, and brines. Some studies have been conducted to investigate thermodynamic properties of CO_2 and CO_2-mixture systems using equations of state.

The SRK EoS was investigated by Frey et al. [12] for density and phase equilibria of mixtures, including the CO_2-H_2O and CO_2-CH_4 binary systems. They applied a density and temperature dependant volume translation function on SRK EoS. They found that selection of mixing rules has a significant influence on the results of their method, which is abbreviated as DMT. Also, Thiery et al. [13] evaluated the SRK EoS for VLE

and volume calculations of CO_2-N_2, CO_2-CH_4 and CO_2-CH_4-N_2. Their results showed that with the SRK EoS, the average deviation for the saturated pressures is around 1% in the temperature range of 208.45-270 K for the CO_2-CH_4 system, 4% in the temperature range of 218.15-273.15 K for the CO_2-N_2 system, and 2-3% for the CO_2-CH_4-N_2 system.

The PR and Patel-Teja (PT) EoS were investigated by Al-Sahhaf et al. [14] for VLE of the N_2-CO_2-CH_4ternary system. Also, Boyle and Carroll [15] investigated PR, SRK, PT, PR-Peneloux, SRK-Peneloux and PR-Mathias EoS for density calculations of CO_2-H_2S. The results showed that PT is the most accurate EoS in liquid region, supercritical region, and overall, with an Absolute Average Deviation (AAD) of 2.16%, 2.26% and 1.82% respectively; while SRK is the most accurate EoS in the vapour region with an AAD of 0.51%. Seven cubic equations of state were evaluated with respect to VLE and density of CO_2 mixtures including CH_4, N_2, O_2, H_2S, SO_2 and Ar using many of the experimental data presented by Li et al. [9] [11] [16]. The EoS evaluated were PR, RK, SRK, PT, PR-Peneloux, SRK-Peneloux and the improved SRK. The binary interaction parameters, k_{ij}, were calibrated with respect to VLE data.

Mantovani et al. [17] presented experimental data for supercritical CO_2 binary systems of nitrogen, oxygen and argon used in oxy-fuel capture process with almost 5% and 10% impurities. They have used vibrating tube densimeter (VTD) for pressures ranging from 1 MPa to 20 MPa at different temperatures from 303 to 383 K. They also have tuned the binary interaction parameters against experimental data using PR, SRK-Peneloux and BWRS equations of state. For the CO_2-N_2 systems, they have reported an AAD of 2.10%, 3.05% and 1.71% for PR, SRKP and BWRS, respectively. Also, the AAD of 2.37%, 3.92% and 1.97% for those of CO_2-O_2 systems and 2.56%, 4.07% and 1.75% for those of CO_2-Ar systems. All the AADs reported using the new regressed k_{ij} parameters. It can be seen that for each case, BWRS can predicts better than cubic equation of states. Sanchez-Vicente et al. [1] presented the density data for three CO_2-H_2 mixtures, as the main impurity of pre-combustion capturing process, with 2%, 7.5% and 10% as the impurity at 288.15–333.15 K and pressures between 1.5 and 23 MPa. Then, they have compared their density data with the values calculated by the GERG-2004 equation of state using the original parameters provided by Kunz et al. [8]. The deviations between the experimental and calculated density are also calculated and analysed in the critical and liquid regions of the mixtures. They have concluded that 2% hydrogen can reduces the molar density of CO_2 up to 25% in the critical region which can significantly affect the compression and transportation developments for CCS. They

also have found that the GERG-2004 EoS can accurately predict the density of CO_2-rich systems with low H_2 concentration (2%) with an AAD of 0.6% while for the high H_2 concentrations, AADs of up to 4% and 14% were observed for the liquid phase and supercritical phase, respectively.

Rivas et al. [18] measured density of CO_2-CH_4 and CO_2-CO systems at T = 304.21 and 308.14 K and pressures ranging from 0.1 MPa to 20 MPa and $x_{CO2} > 0.97$. Then, they modelled the volumetric behaviour of these systems using the PR, PC-SAFT and GERG equations of state. The deviations were reported less than 3.5% for PR, 2.8% for rescaled PC-SAFT and 1.0% for GERG.

3.3 Experiments

3.3.1 Equipment description

The densities of CO_2-rich systems were measured using a high temperature and pressure oscillating U-tube densitometer, Anton Paar DMA-HPM, which consists of a measuring cell and an evaluation unit. A schematic view of the apparatus is shown in Figure 3.1. The measuring cell includes a U-shaped Hastelloy C-276 tube that is excited to vibrate at its characteristic frequency electronically. The DMA-HPM is connected to an mPDS 2000V3 evaluation unit which measures the oscillation period. The resolution of the unit is seven significant digits.

The temperature of densitometer is controlled by an oven, manufactured by BINDER GmbH, which can be used at temperatures between -70 ˚C to 200 ˚C (203 K to 473 K). The measuring U-shaped cell is insulated from the environment keeping the temperature stable to ±0.01 °C. A built-in thermometer which is connected to the mPDS 2000V3 unit can show the temperature of vibrating tube cell. A hand pump which can inject or withdraw the mercury to the set-up is used to control the system pressure. Two Quartzdyne pressure transducer (model: QS 30K-B) with the design pressure up to 207 MPa and standard uncertainty of ±0.02 MPa [19] were connected to record the system pressure.

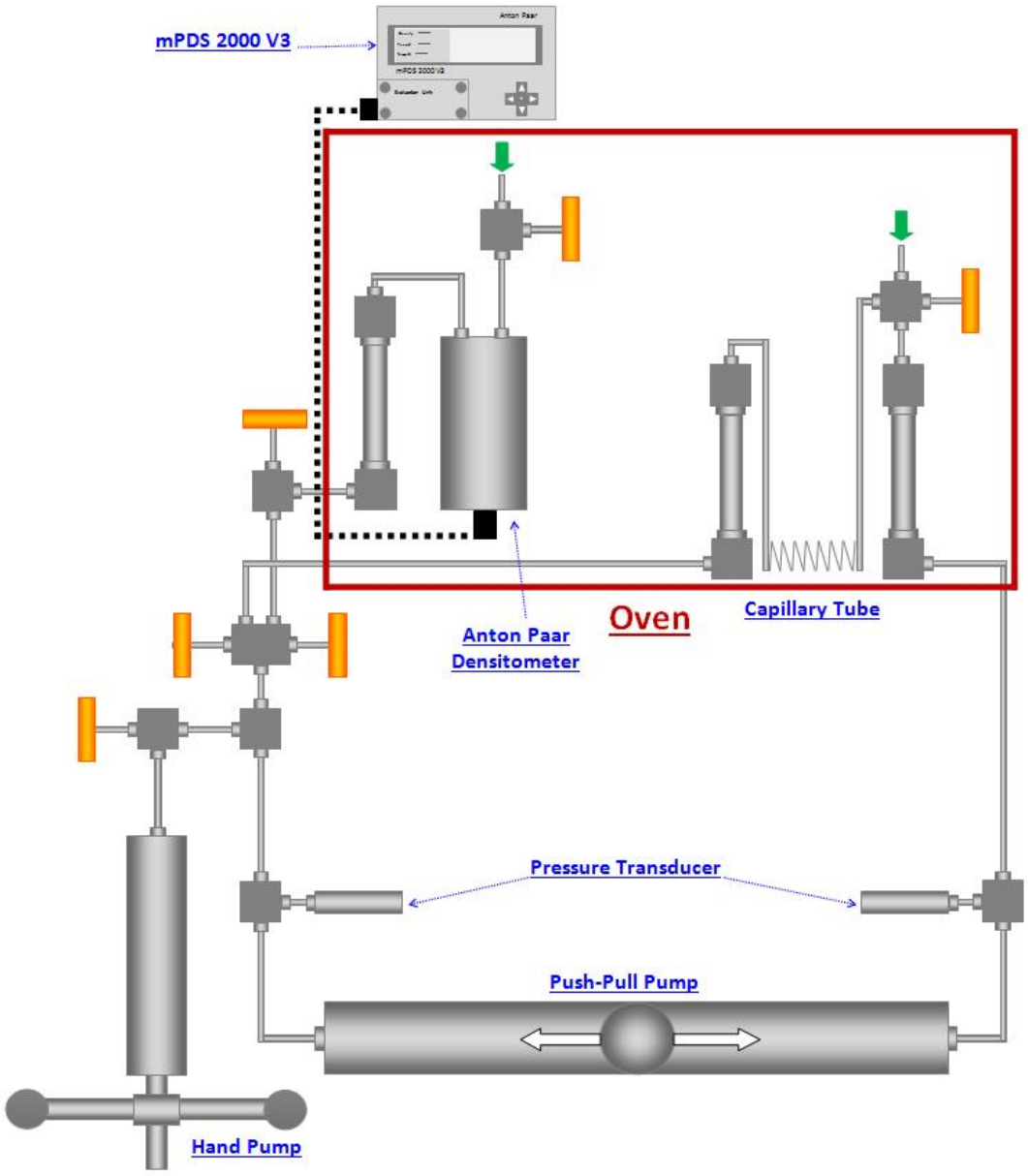

Figure 3.1 Schematic diagram of the densitometer apparatus

3.3.2 Measurement and calibration procedures

All the experiments were conducted using the Anton Paar densitometer. In each test, after applying vacuum to the entire system, the sample was injected through the injection point on top of the densitometer. It should be pointed out that the sample fluid during the injection must be kept in single phase to avoid composition change due to flashing. Then after disconnecting the sample cylinder from the system, it was allowed to stabilise at the desired temperature. When the temperature of the vibrating tube is stable, the desired pressure was set using the hand pump. Once conditions had

stabilized, the oscillation period of the U-tube is determined from the interface mPDS 2000V3 evaluation unit.

The measurement of density with a vibrating tube densitometer is not absolute, thus, the raw data (period of oscillation) should be further treated to obtain the densities. The relationship between them is:

$$\rho(T,P) = A(T,P)\tau^2(T,P) - B(T,P) \tag{3-1}$$

where $\rho(T,P)$ is the sample density at temperature T and pressure P, $\tau(T,P)$ is the period of oscillation at temperature and pressure, $A(T,P)$ and $B(T,P)$ are the apparatus parameters depending on temperature and pressure, and they must be determined from calibration measurements. For calibration, CO_2 density can be used as a reference substance at two different pressures (the lowest and the highest desired pressures in the system at the same temperature) in gas, liquid and supercritical phases. The apparatus parameters then were defined as follows:

$$A(T,P) = \frac{\rho(T,P_1) - \rho(T,P_2)}{\tau^2(T,P_1) - \tau^2(T,P_2)} \tag{3-2}$$

$$B(T,P) = \frac{\tau^2(T,P_2)\rho(T,P_1) - \tau^2(T,P_1)\rho(T,P_2)}{\tau^2(T,P_1) - \tau^2(T,P_2)} \tag{3-3}$$

During our calibration, the density of pure CO_2 have been measured at different desired pressures for each isotherm. The density data used for calibration were calculated with REFPROP v8.0 using the Span and Wagner multi-parameters equation of state [20]. Then, the parameters A and B were calculated by plotting the linear trend line for density versus squared oscillation period measured at different desired pressures at each isotherm. The procedure has been repeated for each isotherm once at low pressures, i.e. gas phase, then at higher pressures, i.e. dense liquid / supercritical phases. Figure 3.2 and Figure 3.3 show the procedure to determine A and B parameters at 373.15 K (100 ºC) at low and high pressures, respectively. All calibration data for each isotherm at low pressures (gas phase) and high pressures (dense phase) can be seen in Table 3.1 and Table 3.2, respectively.

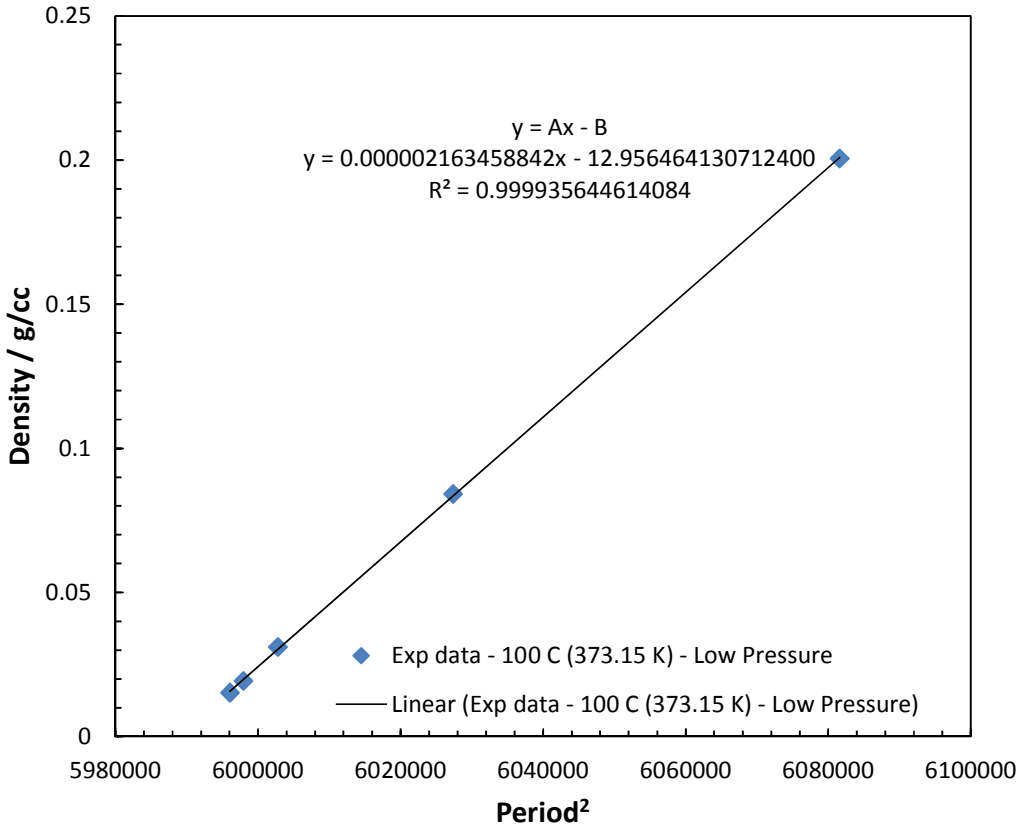

Figure 3. 2 Calibration procedure using pure CO_2 at 373.15 K at low pressures (gas phase)

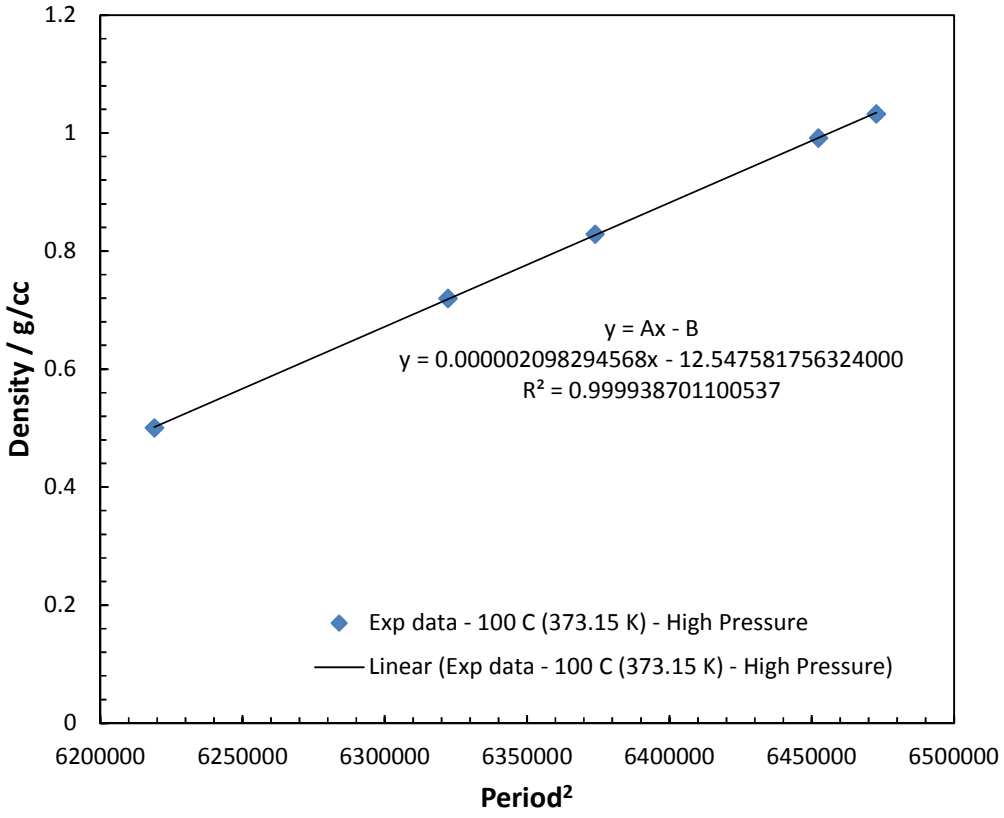

Figure 3. 3 Calibration procedure using pure CO_2 at 373.15 K at high pressures (dense phase)

Table 3. 1 Calibration data using pure CO_2 at low pressures (gas phase)

No	T K (±0.1)	P MPa (±0.02)	Period μs (±0.005)	ρ REFPROP g/cc	Period^2 μs^2
1	273.27	1.276	2417.372	0.0272	5843687.4
2	273.27	2.075	2419.303	0.0477	5853027.0
3	273.27	3.287	2423.028	0.0887	5871064.7
4	283.32	0.967	2420.026	0.0192	5856525.8
5	283.32	2.085	2422.275	0.0451	5867416.2
6	283.31	3.809	2427.179	0.0999	5891197.9
7	283.29	0.745	2419.422	0.0146	5853602.8
8	283.31	0.986	2419.942	0.0196	5856119.3
9	283.32	2.034	2422.182	0.0438	5866965.6
10	283.30	4.109	2428.783	0.1133	5898986.9
11	298.36	0.669	2423.921	0.0123	5875393.0
12	298.36	1.034	2424.438	0.0194	5877899.6
13	298.37	2.080	2426.469	0.0415	5887751.8
14	298.36	5.168	2435.391	0.1387	5931129.3
15	323.46	1.040	2432.229	0.0177	5915737.9
16	323.45	1.705	2433.385	0.0299	5921362.6
17	323.46	2.095	2434.084	0.0374	5924764.9
18	323.47	5.232	2440.921	0.1112	5958095.3
19	323.48	6.923	2446.297	0.1682	5984369.0
20	373.55	1.050	2448.685	0.0153	5996058.2
21	373.55	1.320	2449.071	0.0193	5997948.8
22	373.55	2.082	2450.061	0.0310	6002798.9
23	373.56	5.199	2455.071	0.0842	6027373.6
24	373.56	10.492	2466.093	0.2006	6081614.7
25	423.46	1.314	2465.475	0.0167	6078567.0
26	423.46	2.079	2466.363	0.0268	6082946.4
27	423.46	4.985	2470.217	0.0671	6101972.0
28	423.47	10.376	2478.314	0.1517	6142040.3
29	423.48	20.820	2497.709	0.3415	6238550.2

Table 3. 2 Calibration data using pure CO_2 at high pressures (dense phase)

No	T K (±0.1)	P MPa (±0.02)	Period µs (±0.005)	ρ REFPROP g/cc	Period^2 µs^2
1	273.07	3.615	2500.031	0.9292	6250155.0
2	273.07	4.958	2500.974	0.9407	6254870.9
3	273.09	10.763	2504.517	0.9786	6272605.4
4	273.10	20.937	2508.752	1.0243	6293836.6
5	273.10	52.060	2516.628	1.1088	6333416.5
6	273.10	103.634	2524.503	1.1907	6373115.4
7	273.10	125.170	2527.011	1.2161	6385784.6
8	283.03	4.597	2497.442	0.8637	6237216.5
9	283.03	5.196	2497.982	0.8724	6239914.1
10	283.03	10.484	2502.835	0.9249	6264183.0
11	283.01	21.329	2508.552	0.9868	6292833.1
12	283.00	51.444	2517.232	1.0803	6336456.9
13	283.03	104.127	2525.886	1.1707	6380100.1
14	283.02	125.563	2528.511	1.1973	6393367.9
15	298.49	4.993	2434.706	0.1304	5927793.3
16	298.48	12.337	2500.926	0.8472	6254630.9
17	298.49	20.395	2507.222	0.9152	6286162.2
18	298.50	50.955	2518.404	1.0358	6342358.7
19	298.50	76.410	2523.778	1.0928	6369455.4
20	298.49	103.645	2528.125	1.1380	6391416.0
21	298.49	124.914	2530.945	1.1668	6405682.6
22	298.50	22.902	2508.612	0.9302	6293134.2
23	323.67	40.117	2516.382	0.9221	6332178.4
24	323.66	25.518	2508.396	0.8361	6292050.5
25	323.66	76.897	2526.968	1.0352	6385567.3
26	323.65	104.173	2531.985	1.0878	6410948.0
27	323.66	125.526	2535.163	1.1205	6427051.4
28	323.66	125.526	2535.163	1.1205	6427051.4
29	373.45	17.162	2489.108	0.3984	6195658.6
30	373.46	20.837	2493.806	0.5002	6219068.4
31	373.48	35.627	2514.401	0.7198	6322212.4
32	373.49	52.121	2524.656	0.8286	6373887.9
33	373.49	104.283	2540.168	0.9914	6452453.5
34	373.49	125.860	2544.158	1.0325	6472739.9
35	423.37	26.990	2506.068	0.4470	6280376.8
36	423.38	51.343	2529.613	0.6953	6398941.9
37	423.38	75.907	2541.127	0.8158	6457326.4
38	423.38	104.243	2549.567	0.9024	6500291.9
39	423.39	124.656	2554.176	0.9487	6523815.0

Finally, the A and B calibration parameters at low and high pressures at different measuring temperatures can be found below in Table 3.3.

Table 3. 3 Calibration Parameters for Anton Paar DMA-HPM Densitometer using pure CO_2

		Gas Phase		Liquid or Supercritical Phase	
T / ºC	T / K	A	B	A	B
0	273.15	2.2489E-06	13.1148729	2.11433E-06	12.28403271
10	283.15	2.22815E-06	13.02872592	2.13096E-06	12.42475544
25	298.15	2.25362E-06	13.22771299	2.11904E-06	12.40548964
50	323.15	2.19724E-06	12.98059669	2.10897E-06	12.43289764
100	373.15	2.16346E-06	12.95646413	2.09829E-06	12.54758176
150	423.15	2.02721E-06	12.30358989	2.06409E-06	12.51471964

3.3.3 Density validation

The measured density for pure CO_2 and MIX 1 has been compared to the density data measured by Al-Siyabi et al. Figure 3.4 shows the deviations between the pure CO_2 density data calculated using the PR-CO_2 model and the data from Al-Siyabi et al [21] and this work at different isotherms. The densities measured by Al-Siyabi et al. [21] are only in the dense liquid / supercritical phase while in this work, the densities were measured in both gas and dense phases. Also, the deviations of the measured density of multi component mixture, MIX 1, from the PR-CO_2 equation of state can be seen at two isotherms 283.15 K and 323.15 K. The comparisons demonstrate that the density measurements are in good agreement with experimental data in literature as well as with predicted results by equation of state.

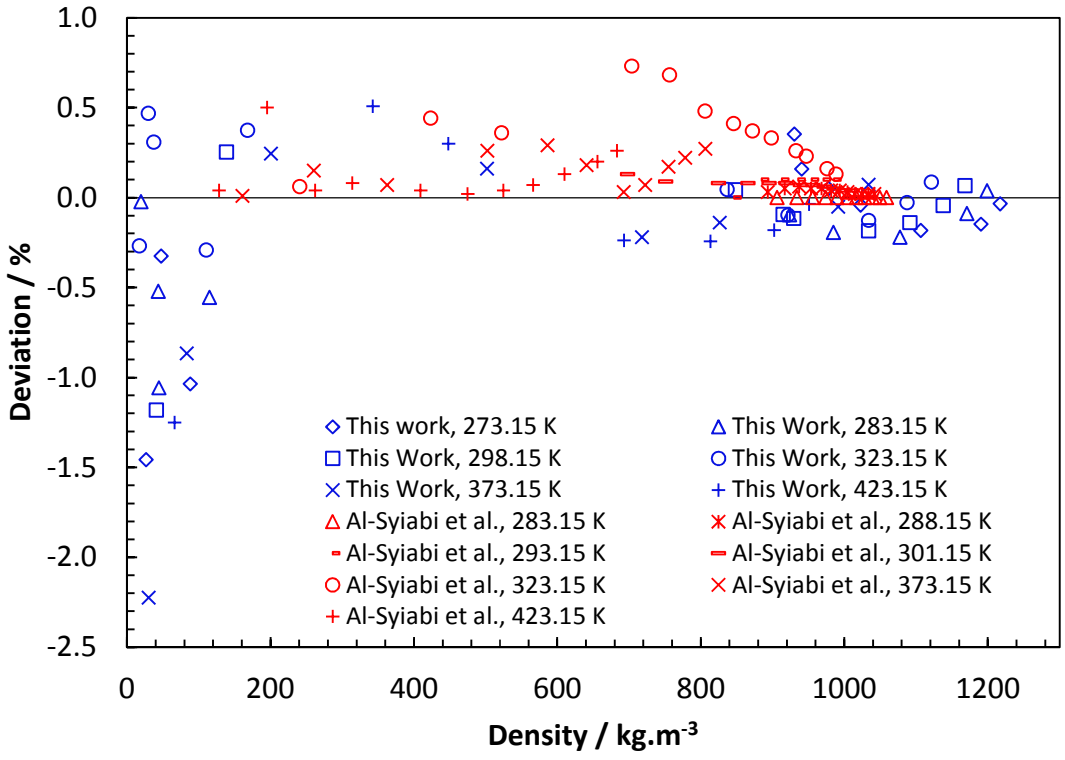

Figure 3. 4 Validation data of pure CO_2 density at different isotherms

3.3.4 Density measurement uncertainties

The combined standard uncertainties [22] of density measurements for each measured quantity have been calculated using the root sum of the squares of uncertainties as shown in the following equation.

$$u_c(\rho) = \sqrt{u_1(T)^2 + u_2(p)^2 + u_3(\tau)^2} \quad (3\text{-}4)$$

where, $u_1(T)$ is the estimated uncertainties due to the temperature, $u_2(p)$ the estimated uncertainties due to pressure and $u_3(\tau)$ the estimated uncertainties of oscillation period. The estimated uncertainties due to temperature variations, $u_1(T)$, has been calculated from the equation below:

$$u_1(T) = \sqrt{\left(\frac{\partial \rho}{\partial T}\right)^2 . u(T)^2} \quad (3\text{-}5)$$

In the above equation, *u(T)* is the standard estimated uncertainty of temperature probe and is considered to be ±0.1 K [23]. The density gradient due to the temperature variations, $\left(\frac{\partial \rho}{\partial T}\right)$, has been calculated from the equation below.

$$\left(\frac{\partial \rho}{\partial T}\right) = \frac{1}{2u(T)}\left(\rho_{T+u(T)} - \rho_{T-u(T)}\right) \quad (3\text{-}6)$$

The upper and lower limits of densities due to temperature effect, $\rho_{T+u(T)}$ *and* $\rho_{T-u(T)}$, were estimated from REFPROP v8.0 [20].

The similar procedures have been followed to estimate the uncertainties due to the pressure and period of oscillations. The standard uncertainty of high pressure Quartzdyne pressure transducer (model: QS 30K-B), *u(p)*, is determined ±0.02 MPa [19] and standard uncertainty of oscillation period, *u(τ)*, is ±0.005 µs [24].

$$u_2(p) = \sqrt{\left(\frac{\partial \rho}{\partial p}\right)^2 . u(p)^2} \quad (3\text{-}7)$$

$$\left(\frac{\partial \rho}{\partial p}\right) = \frac{1}{2u(p)}\left(\rho_{T+u(p)} - \rho_{T-u(p)}\right) \quad (3\text{-}8)$$

$$u_3(\tau) = \sqrt{\left(\frac{\partial \rho}{\partial \tau}\right)^2 . u(\tau)^2} \quad (3\text{-}9)$$

$$\left(\frac{\partial \rho}{\partial \tau}\right) = \frac{1}{2u(\tau)}\left(\rho_{T+u(\tau)} - \rho_{T-u(\tau)}\right) \quad (3\text{-}10)$$

Finally, the expanded uncertainty of each measured density, *U(ρ)*, were calculated by multiplying to coverage factor, *k*. In this work, the coverage factor K = 2 has been used to give a level of confidence of 95% for uncertainty of measurements.

$$U(\rho) = k\, u_c(\rho) \quad (3\text{-}11)$$

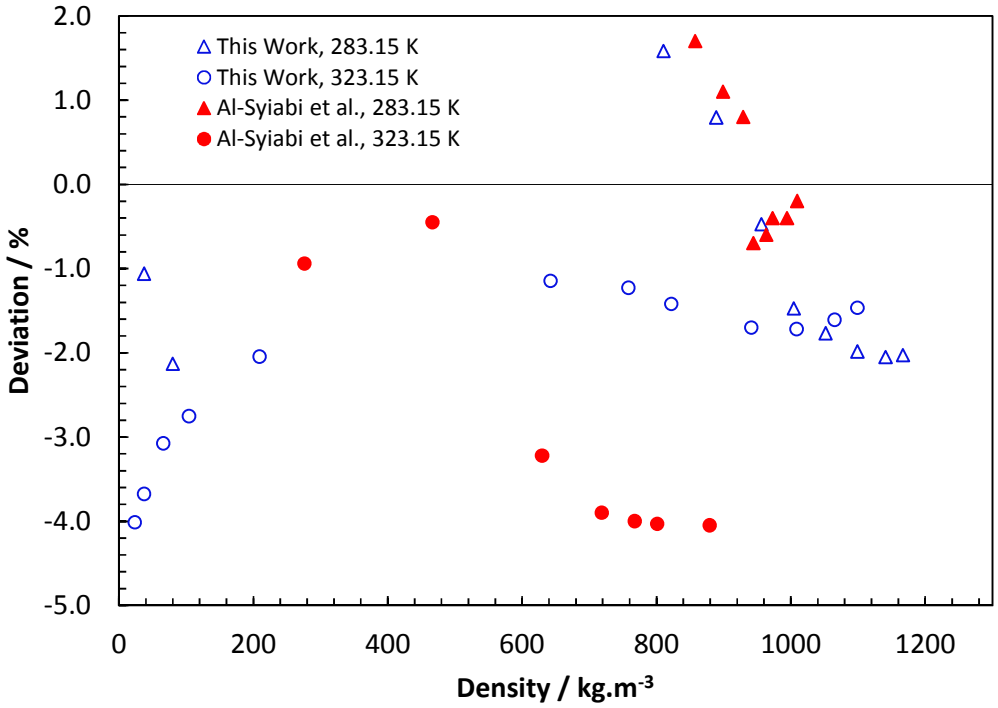

Figure 3. 5 Density validation data at two isotherms for MIX 1

3.4 Modelling

Density prediction using classical cubic equations of state are normally lower than the real density of fluid particularly in the liquid phase. This is due to the unrealistic critical compressibility assumption for all compounds in the cubic equations of state [25]. To improve this underestimation in the density, Peneloux, Rauzy, and Freze [26] introduced volume translation parameter to the overestimated molar volume predicted by equations of state. In this work, to improve the overestimation of molar volume by equations of state, a new volume correction parameter, called CO_2 volume correction parameter, were subtracted from the molar volume of carbon dioxide and mixtures containing high CO_2 concentrations calculated by the cubic equations of state.

$$V^{new} = V^{EoS} - V^{c} \qquad (3\text{-}12)$$

where V^{EoS} is the molar volume calculated by the desired equation of state. The volume correction parameter in the Equation (3-12), V^{c}, is given below:

$$V^{c} = \sum_{i}^{NComp} x_i V_i^{c} \qquad (3\text{-}13)$$

z_i in the above equation is the composition of component i and V^c is the molar volume predicted by Equation of state for each composition in the same phase. As this volume

correction parameter is applicable for the CO_2-rich mixtures, the molar volume of CO_2, V_i^c is defined by:

$$V_{CO_2}^c = V_{\text{Pure } CO_2}^{\text{Eos}} - V_{\text{Pure } CO_2}^{\text{mBWR}} \tag{3-14}$$

The molar volume for pure CO_2 by mBWR equation of state can be calculated from the equation proposed by McCarty [27] below.

$$P = \sum_{n=1}^{9} a_n(T)\rho^n + \sum_{n=10}^{15} a_n(T)\rho^{2n-17} e^{-\gamma\rho^2} \tag{3-15}$$

Or in more detailed form:

$$\begin{aligned}
P &= \rho RT + \rho^2\left[G(1)T + G(2)T^{1/2} + G(3) + G(4)/T + G(5)/T^2\right] \\
&+\rho^3\left[G(6)T + G(7) + G(8)/T + G(9)/T^2\right] + \rho^4\left[G(10)T + G(11) + G(12)/T\right] \\
&+\rho^5\left[G(13)\right] + \rho^6\left[G(14)/T + G(15)/T^2\right] + \rho^7\left[G(16)/T\right] \\
&+\rho^8\left[G(17)/T + G(18)/T^2\right] + \rho^9\left[G(19)/T^2\right] \\
&+\rho^3\left[G(20)/T^2 + G(21)/T^3\right]\exp\left(\gamma\rho^2\right) + \rho^5\left[G(22)/T^2 + G(23)/T^4\right]\exp\left(\gamma\rho^2\right) \\
&+\rho^7\left[G(24)/T^2 + G(25)/T^3\right]\exp\left(\gamma\rho^2\right) + \rho^9\left[G(26)/T^2 + G(27)/T^4\right]\exp\left(\gamma\rho^2\right) \\
&+\rho^{11}\left[G(28)/T^2 + G(29)/T^3\right]\exp\left(\gamma\rho^2\right) \\
&+\rho^{13}\left[G(30)/T^2 + G(31)/T^3 + G(32)/T^4\right]\exp\left(\gamma\rho^2\right)
\end{aligned} \tag{3-16}$$

where,

$$\gamma = \frac{-1}{\rho_c^{\,2}} \tag{3-17}$$

The parameters G(1) to G(32) in the equation (3-16) can be found from Table 3.4.

In this work, PR and SRK equations of states were employed to predict the densities. The properties of components in this work are summarised below in Table 3.5. The modified binary interaction parameters, k_{ij}, shown in Table 3.6 and Table 3.7 for PR and SRK equations of state, have been employed to improve the phase equilibrium predictions.

Table 3. 4 Parameters G(1) – G(32) in the mBWR equation of state

G	CO_2 [28]	CH_4 [29]	C_3H_8 [29]
G(1)	-0.981851065838x10^{-03}	0.9898937956 x10^{-05}	-0.2804337729 x10^{-03}
G(2)	0.995062267309 x10^{-01}	0.2199608275 x10^{-01}	0.1180666107 x10^{+00}
G(3)	-0.228380160313 x10^{+01}	-0.5322788000 x10^{+00}	-0.3756325860 x10^{+01}
G(4)	0.281827634529 x10^{+03}	0.2021657962 x10^{+02}	0.5624374521 x10^{+03}
G(5)	-0.347001262699 x10^{+05}	-0.2234398926 x10^{+04}	-0.9354759605 x10^{+05}
G(6)	0.394706709102 x10^{-04}	0.1067940280 x10^{-04}	-0.4557405505 x10^{-04}
G(7)	-0.325550000110 x10^{-01}	0.1457922469 x10^{-03}	0.1530044332 x10^{+00}
G(8)	0.484320083063 x10^{+00}	-0.9265816666 x10^{+00}	-0.1078107476 x10^{+03}
G(9)	-0.352181542995 x10^{+05}	0.2915364732 x10^{+03}	0.2218072099 x10^{+05}
G(10)	-0.324053603343 x10^{-05}	0.2313546209 x10^{-06}	0.6629473971 x10^{-05}
G(11)	0.468596684665 x10^{+00}	0.1387214274 x10^{-03}	-0.6199354447 x10^{-02}
G(12)	-0.754547012075 x10^{+00}	0.4780467451 x10^{-02}	0.6754207966 x10^{+01}
G(13)	-0.381894354016 x10^{-05}	0.1176103833 x10^{-04}	0.6472837570 x10^{-03}
G(14)	-0.442192933859 x10^{-02}	-0.1982096730 x10^{-03}	-0.6804325262 x10^{-01}
G(15)	0.516925168095 x10^{+01}	-0.2512887756 x10^{-01}	-0.9726162355 x10^{+01}
G(16)	0.212450985237 x10^{-03}	0.9748899826 x10^{-05}	0.5097956459 x10^{-02}
G(17)	-0.261009474785 x10^{-05}	-0.1202192137 x10^{-06}	-0.1004655900 x10^{-03}
G(18)	-0.888533388977 x10^{-02}	0.4128353939 x10^{-04}	0.4363693352 x10^{-01}
G(19)	0.155226179403 x10^{-03}	-0.7215842918 x10^{-06}	-0.1249351947 x10^{-02}
G(20)	0.415091004940 x10^{+05}	0.5081738255 x10^{+03}	0.2644755879 x10^{+05}
G(21)	-0.110173967489 x10^{+07}	-0.9198903192 x10^{+05}	-0.7944237270 x10^{+07}
G(22)	0.291990583344 x10^{+03}	-0.2732264677 x10^{+01}	-0.7299920845 x10^{+03}
G(23)	0.143254606508 x10^{+07}	0.7499024351 x10^{+05}	0.5381095003 x10^{+08}
G(24)	0.108574207533 x10^{+01}	0.1114060908 x10^{-02}	0.3450217377 x10^{+01}
G(25)	-0.247799657039 x10^{+02}	0.1083955159 x10^{+01}	0.9936666689 x10^{+03}
G(26)	0.199293590763 x10^{-02}	-0.4490960312 x10^{-04}	-0.2166699036 x10^{+00}
G(27)	0.102749908059 x10^{+02}	-0.1380337847 x10^{+01}	-0.1612103424 x10^{+05}
G(28)	0.377618865158 x10^{-05}	-0.2371902232 x10^{-07}	-0.3633126990 x10^{-03}
G(29)	-0.332276512346 x10^{-03}	0.3761652197 x10^{-04}	0.1108612343 x10^{+01}
G(30)	0.179196707121 x10^{-08}	-0.2375166954 x10^{-09}	-0.1330932838 x10^{-04}
G(31)	0.945076627807 x10^{-06}	-0.1237640790 x10^{-07}	-0.3157701101 x10^{-02}
G(32)	-0.123400943061 x10^{-03}	0.6766926453 x10^{-06}	0.1423083811 x10^{+00}

Table 3. 5 Properties of the components in this work [30]

Compound	MW g/mol	T_c K	R_{oc} mol/L	Z_c	W	P_c MPa
CO_2	44.01	304.128	10.600	0.274	0.225	7.374
CH_4	16.04	190.530	10.150	0.286	0.011	4.599
C_2H_6	30.07	305.340	6.875	0.279	0.099	4.898
C_3H_8	44.10	369.850	5.000	0.276	0.152	3.398
i- C_4H_{10}	58.12	407.810	3.880	0.278	0.186	3.494
n-C_4H_{10}	58.12	425.125	3.923	0.274	0.201	3.796
n-C_5H_{12}	72.15	469.700	3.215	0.268	0.252	3.370
CO	28.01	132.800	10.850	0.292	0.050	4.872
Ar	39.95	150.687	13.407	0.291	-0.002	4.248
N_2	28.01	126.192	11.184	0.289	0.037	3.640
H_2	2.02	33.145	15.508	0.303	-0.217	1.293
O_2	32.00	154.580	13.630	0.288	0.022	5.043
n-$C_{10}H_{22}$	142.29	617.700	1.603	0.256	0.490	2.110

Table 3. 6 Modified binary interaction parameters in this work for PR EoS [31]

	CO_2	CO	N_2	O_2	Ar	H_2	CH_4	C_2H_6	C_3H_8	SO_2	H_2S
CO_2		-0.079	-0.014	0.111	0.129	0.089	0.099	0.129	0.131	0.02	0.082
CO			0.005	0[a]	0.007	0[a]	0.022	-0.003	0[a]	0.024	0.085
N_2				-0.013	-0.007	0[a]	0.032	0.039	0.083	0.128	0.174
O_2					0[a]	0[a]	0[a]	0[a]	0.112	0.222	0[a]
Ar						0[a]	0.026	0.054	0[a]	0[a]	0[a]
H_2							0[a]	0[a]	0[a]	0[a]	0[a]
CH_4								0.001	0.016	0.129	0.084
C_2H_6									-0.006	0.11	0.084
C_3H_8										0[a]	0.082
SO_2											0[a]
H_2S											

a: The EoS was not tuned for this binary system

Table 3. 7 Modified binary interaction parameters in this work for SRK EoS [31]

	CO_2	CO	N_2	O_2	Ar	H_2	CH_4	C_2H_6	C_3H_8	SO_2	H_2S
CO_2		-0.062	-0.046	0.106	0.123	0.2	0.100	0.137	0.139	0.020	0.096
CO			0.006	0[a]	0.008	0[a]	0.030	-0.022	0[a]	0.000	0.061
N_2				-0.014	-0.008	0[a]	0.030	0.032	0.078	0.091	0.157
O_2					0[a]	0[a]	0[a]	0[a]	0.113	0.219	0[a]
Ar						0[a]	0.028	0.053	0[a]	0[a]	0[a]
H_2							0[a]	0[a]	0[a]	0[a]	0[a]
CH_4								-0.003	0.010	0.119	0.077
C_2H_6									-0.005	0.11	0.087
C_3H_8										0[a]	0.087
SO_2											0[a]
H_2S											

a: The EoS was not tuned for this binary system

3.5 Experimental and modelling results and discussions

Densities of pure CO_2 (for calibration purposes), two hydrogen binary systems, BINARY 1 with 5% and BINARY 2 with 10% hydrogen, multi-component mixtures, MIX 1 with 5% impurity, MIX 2 with 10% impurity, MIX 3 with 30% impurity, MIX 4 with 50% impurity, MIX 5 with 4% impurity and MIX 6 with 30% impurity were measured at pressures ranging from 1 MPa to 120 MPa at six different temperatures, 273.15, 283.15, 298.15, 323.15, 373.15 and 423.15 K in gas, liquid and supercritical regions. Both experimental and modelling results, using CO_2 correction volume, Peneloux shift parameter and original equation of states (PR and SRK), are shown in Table 3.8 through Table 3.15 and Figure 3.6 through Figure 3.23. In each table, the measured densities as well as the estimated uncertainties of measurements are shown at the corresponding pressure, temperature and phase. Also, the calculated density using CO_2 correction volume, Peneloux shift parameter and original equation of state (PR) are presented in these tables. Finally, corresponding deviations of the models from experimental density for each measurement are also shown in each table. In addition, the Absolute Average Deviations (AADs) for all data are listed in the tables.

Table 3.16 shows the average and maximum estimated expanded uncertainties of density measurements in this work. The expanded uncertainties were reported with a level of confidence of 95% by multiplying the calculated combined standard uncertainty, $u_c(\rho)$, by coverage factor of K = 2 [22]. The average expanded uncertainties, $U(\rho)$, in the gas phase is 1.7% while in the dense phase is 0.1%. The maximum expanded uncertainty in the gas phase were reported 4.5% for MIX 1 at very low pressure and temperature while that in the dense phase is 0.7%. Generally, the uncertainty of the measurements are higher at very low pressures in the gas phase as well as at points close to the two-phase area in either the gas phase or liquid phase.

Table 3.17 summarises the AAD and maximum deviation of the models with PR and SRK equations of state using CO_2 volume correction, original and Peneloux shift parameters, from experimental data for each material at different regions. As can be seen, both SRK and PR equation of states using CO_2 volume correction are in good agreement with experimental density data. The AADs for PR and SRK using CO_2 volume correction are 2.2% and 2.3%, respectively. The original PR also can predict well compared to the original SRK. The AADs for PR and SRK are 4.4% and 4.9%, respectively. Using the Peneloux shift parameters to predict the density of CO_2 systems

can result in an AAD of 3.0% and 4.0% for PR and SRK, respectively. By comparing the AADs, it is clear that CO_2 volume correction with PR and SRK equations of state can predict well compared to original of EoSs or those using Peneloux shift parameters for CO_2-rich mixtures.

Increasing the density of CO_2 fluids will reduce the pipeline size and the running cost. However, the presence of common impurities in CO_2 stream will reduce the density of pure CO_2. The amount of reduction is function of the mixture composition, pipeline operating pressure and temperature. The lighter components will reduce the density more. Also, the amount of reduction could be high at pressures and temperatures close to the critical pressure and temperature of the mixture. In order to investigate this effect, spline interpolation is implemented to the modelling and experimental data. Table 3.18 and Figure 3.24 show the reduction in CO_2 density for tests conducted at 323.15 K (50 °C). A maximum reduction of the CO_2 density at a certain pressure for a given temperature is observed for the CO_2 mixtures. The maximum reduction is 29.2% in BIN 1 (MW = 41.84), 40.3% in BIN 2 (MW = 39.67), 21.7% in MIX 1 (MW = 43.64), 33.9% in MIX 2 (MW = 42.75), 38.5% in MIX 3 (MW = 37.60), 51.9% in MIX 4 (MW = 32.06), 21.1% in MIX 5 (MW = 43.31) and 31.4% in MIX 6 (MW = 40.45). The maximum reduction occurs at pressure around 11 MPa (1600 psia) for BIN 1, BIN2, MIX 1, MIX 2 and MIX 5, and 12.4 MPa (1800 psia) for MIX 3, MIX 4 and MIX 6.

3.6 Conclusions

Evaluation of the new volume correction model based on EoSs using our in-house software package and the measured experimental data for binary systems and multi-component mixtures show that the model is in good agreement with the experimental data.

A maximum reduction of the density at a certain pressure for a given temperature, 323.15 K (50 °C), at supercritical region was found for CO_2 in the presence of impurities. Overall, the lighter molecular weight impurities tend to reduce CO_2 density much more than those with a molecular weight close to pure CO_2.

Table 3. 8 Experimental and modelling results of BINARY 1

No	Phase	Temp.	Press.				Density (kg/m^3)			Absolute Deviation (%)		
		K (±0.1)	MPa (±0.02)	Exp.	$U(\rho)$ kg/m^3	$U(\rho)$ %	PR-CO_2	PR	PR Pen	PR-CO_2	PR	PR Pen
1	Gas	273.28	1.425	29.9	0.91	3.0	29.1	29.1	29.0	2.6	2.7	3.0
2	Gas	273.28	2.106	46.9	1.03	2.2	45.6	45.6	45.4	2.7	2.9	3.3
3	Liq.	273.28	10.730	910.1	1.14	0.1	876.8	887.8	851.8	3.7	2.4	6.4
4	Liq.	273.28	21.025	968.9	0.81	0.1	946.3	977.1	933.5	2.3	0.8	3.7
5	Liq.	273.28	51.473	1,062.2	0.61	0.1	1,048.9	1,107.2	1,051.4	1.3	4.2	1.0
6	Liq.	273.28	103.269	1,151.9	0.43	0.0	1,141.6	1,213.8	1,147.0	0.9	5.4	0.4
7	Liq.	273.28	124.556	1,179.3	0.33	0.0	1,168.3	1,242.3	1,172.5	0.9	5.3	0.6
8	Gas	283.35	1.438	28.9	0.85	3.0	27.8	28.0	27.9	3.7	3.0	3.3
9	Gas	283.33	2.099	41.7	0.94	2.3	42.6	42.9	42.8	2.4	3.1	2.7
10	Gas	283.32	4.515	115.9	1.75	1.5	119.0	118.2	117.2	2.7	2.0	1.2
11	Liq.	283.31	10.220	855.3	1.47	0.2	800.4	796.9	767.8	6.4	6.8	10.2
12	Liq.	283.31	20.702	934.3	0.87	0.1	900.4	922.0	883.1	3.6	1.3	5.5
13	Liq.	283.32	51.487	1,042.2	0.55	0.1	1,020.6	1,076.0	1,023.2	2.1	3.2	1.8
14	Liq.	283.31	105.354	1,139.5	0.33	0.0	1,123.1	1,196.3	1,131.3	1.4	5.0	0.7
15	Liq.	283.31	124.983	1,161.9	0.41	0.0	1,149.0	1,224.3	1,156.4	1.1	5.4	0.5
16	Gas	298.38	2.189	43.5	0.86	2.0	41.3	41.7	41.6	5.2	4.2	4.6
17	Gas	298.38	5.203	126.3	1.50	1.2	123.1	126.0	125.0	2.5	0.3	1.1
18	Liq.	298.37	10.096	654.1	3.05	0.5	634.6	612.0	594.6	3.0	6.4	9.1
19	Liq.	298.37	20.440	841.7	1.00	0.1	824.9	831.8	799.8	2.0	1.2	5.0
20	Liq.	298.38	51.445	986.1	0.55	0.1	977.6	1,027.4	979.1	0.9	4.2	0.7
21	Liq.	298.39	103.469	1,096.2	0.41	0.0	1,088.7	1,161.6	1,100.2	0.7	6.0	0.4
22	Liq.	298.38	124.467	1,127.4	0.33	0.0	1,119.0	1,195.4	1,130.5	0.7	6.0	0.3
23	Gas	323.44	2.051	36.5	0.74	2.0	34.4	34.8	34.6	5.7	4.8	5.2
24	Gas	323.47	5.251	104.1	1.02	1.0	102.1	104.3	103.6	1.9	0.3	0.4
25	Gas	323.48	10.358	298.8	2.74	0.9	306.7	297.1	292.2	2.7	0.6	2.2
26	SC	323.46	20.557	702.7	1.28	0.2	685.7	670.3	649.1	2.4	4.6	7.6
27	SC	323.44	51.982	914.3	0.57	0.1	907.4	946.7	905.4	0.8	3.5	1.0
28	SC	323.45	102.822	1,041.4	0.41	0.0	1,036.3	1,106.6	1,050.6	0.5	6.3	0.9
29	SC	323.45	125.382	1,078.7	0.41	0.0	1,072.9	1,149.2	1,089.0	0.5	6.5	1.0
30	Gas	373.54	1.996	27.8	0.60	2.2	28.1	28.3	28.2	1.2	1.8	1.4
31	Gas	373.54	5.210	77.6	0.70	0.9	78.9	79.9	79.5	1.8	3.0	2.4
32	Gas	373.54	10.392	178.6	0.91	0.5	179.4	181.4	179.4	0.4	1.5	0.4
33	Gas	373.55	17.543	356.2	1.20	0.3	356.9	346.5	340.2	0.2	2.7	4.5
34	SC	373.54	29.181	589.9	0.89	0.2	580.8	564.6	549.0	1.5	4.3	6.9
35	SC	373.55	52.182	777.9	0.55	0.1	769.1	787.0	757.8	1.1	1.2	2.6
36	SC	373.55	103.531	948.7	0.37	0.0	941.9	1,001.9	955.6	0.7	5.6	0.7
37	SC	373.55	124.391	991.2	0.34	0.0	984.0	1,052.9	1,001.9	0.7	6.2	1.1
38	Gas	423.45	2.065	28.0	0.51	1.8	25.2	25.3	25.3	9.7	9.4	9.7
39	Gas	423.45	5.231	67.1	0.56	0.8	66.7	67.1	66.7	0.6	0.0	0.5
40	Gas	423.45	10.475	139.6	0.64	0.5	142.7	143.3	142.0	2.2	2.6	1.7
41	Gas	423.45	20.833	302.1	0.74	0.2	310.9	305.2	300.2	2.9	1.0	0.6
42	SC	423.43	48.610	629.5	0.53	0.1	625.5	625.5	606.4	0.6	0.6	3.7
43	SC	423.45	104.123	859.4	0.34	0.0	857.7	905.2	866.9	0.2	5.3	0.9
44	SC	423.46	124.288	907.1	0.32	0.0	905.7	963.4	920.3	0.2	6.2	1.5
Absolute Average Deviation (AAD)										**2.1**	**3.6**	**2.8**

Table 3.9 Experimental and modelling results of BINARY 2

No	Phase	Temp.	Press.				Density (kg/m^3)			Absolute Deviation (%)		
		K (±0.1)	MPa (±0.02)	Exp.	$U(\rho)$ kg/m^3	$U(\rho)$ %	PR-CO_2	PR	PR Pen	PR-CO_2	PR	PR Pen
1	Gas	273.29	1.177	24.7	0.81	3.3	22.2	22.1	22.1	10.2	10.3	10.6
2	Gas	273.27	2.078	43.0	0.93	2.2	41.8	41.7	41.6	2.9	3.0	3.4
3	Gas	273.28	3.916	93.1	1.40	1.5	93.4	93.3	92.7	0.3	0.2	0.5
4	Liq.	273.26	20.564	829.8	0.85	0.1	860.5	885.4	844.6	3.7	6.7	1.8
5	Liq.	273.27	52.306	973.2	0.52	0.1	990.6	1,042.5	986.0	1.8	7.1	1.3
6	Liq.	273.27	103.290	1,076.7	0.33	0.0	1,089.7	1,155.1	1,086.0	1.2	7.3	0.9
7	Liq.	273.26	124.687	1,106.6	0.41	0.0	1,118.0	1,185.4	1,112.8	1.0	7.1	0.6
8	Gas	283.29	1.383	26.0	0.79	3.0	25.1	25.2	25.1	3.4	2.8	3.1
9	Gas	283.28	2.106	39.7	0.86	2.2	39.9	40.2	40.0	0.6	1.3	0.9
10	Gas	283.31	4.900	115.7	1.53	1.3	119.0	118.3	117.3	2.8	2.2	1.4
11	Liq.	283.30	14.412	794.4	1.28	0.2	741.1	747.2	718.3	6.7	5.9	9.6
12	Liq.	283.30	20.241	809.1	0.93	0.1	808.0	824.7	789.3	0.1	1.9	2.5
13	Liq.	283.32	52.629	899.0	0.52	0.1	962.8	1,012.1	958.7	7.1	12.6	6.6
14	Liq.	283.32	103.634	992.8	0.41	0.0	1,068.8	1,134.7	1,068.0	7.7	14.3	7.6
15	Liq.	283.32	124.467	1,022.9	0.33	0.0	1,098.0	1,166.5	1,096.1	7.3	14.0	7.1
16	Gas	298.38	2.058	39.4	0.78	2.0	36.1	36.4	36.3	8.5	7.6	8.0
17	Gas	298.37	5.210	113.8	1.22	1.1	110.2	112.5	111.6	3.1	1.1	1.9
18	Liq.	298.37	52.278	773.9	0.52	0.1	918.4	962.4	914.0	18.7	24.4	18.1
19	Liq.	298.37	102.842	936.9	0.38	0.0	1,036.0	1,101.6	1,038.6	10.6	17.6	10.8
20	Liq.	298.38	124.735	979.5	0.41	0.0	1,069.3	1,138.7	1,071.5	9.2	16.3	9.4
21	Gas	323.44	2.058	34.6	0.69	2.0	32.5	32.8	32.6	6.2	5.4	5.7
22	Gas	323.47	5.237	94.6	0.90	0.9	93.2	95.1	94.4	1.5	0.5	0.2
23	Gas	323.45	10.447	247.7	1.75	0.7	254.7	247.5	243.9	2.8	0.1	1.6
24	SC	323.44	26.518	531.2	0.94	0.2	673.8	673.6	649.5	26.8	26.8	22.3
25	SC	323.45	52.306	746.6	0.53	0.1	846.5	880.7	839.8	13.4	18.0	12.5
26	SC	323.46	104.136	913.2	0.37	0.0	987.5	1,051.0	993.3	8.1	15.1	8.8
27	SC	323.47	125.148	956.3	0.34	0.0	1,023.2	1,092.1	1,030.0	7.0	14.2	7.7
28	Gas	373.54	2.271	28.6	0.57	2.0	30.3	30.5	30.4	5.8	6.5	6.1
29	Gas	373.53	5.251	72.2	0.64	0.9	74.2	75.1	74.7	2.8	4.0	3.4
30	Gas	373.54	10.392	161.8	0.80	0.5	163.2	164.8	163.0	0.9	1.9	0.8
31	Gas	373.54	18.513	332.8	0.99	0.3	335.7	325.7	319.4	0.9	2.1	4.0
32	SC	373.53	36.462	528.3	0.68	0.1	597.9	593.5	574.1	13.2	12.4	8.7
33	SC	373.54	52.423	649.3	0.51	0.1	712.5	728.0	699.4	9.7	12.1	7.7
34	SC	373.52	104.880	861.1	0.35	0.0	895.6	949.8	902.2	4.0	10.3	4.8
35	SC	373.54	125.024	906.0	0.32	0.0	937.4	999.5	947.0	3.5	10.3	4.5
36	Gas	423.42	2.058	25.9	0.48	1.9	23.8	23.8	23.8	8.4	8.1	8.4
37	Gas	423.42	5.224	62.2	0.52	0.8	62.5	62.8	62.5	0.5	1.1	0.5
38	Gas	423.41	10.379	128.0	0.58	0.4	131.1	131.5	130.3	2.4	2.8	1.8
39	Gas	423.41	20.420	267.9	0.64	0.2	277.3	272.9	268.2	3.5	1.9	0.1
40	SC	423.41	38.906	464.4	0.55	0.1	499.8	492.2	478.3	7.6	6.0	3.0
41	SC	423.43	52.113	565.4	0.46	0.1	600.2	603.4	583.0	6.2	6.7	3.1
42	SC	423.45	103.999	783.9	0.32	0.0	810.9	853.1	814.0	3.4	8.8	3.8
43	SC	423.46	124.659	836.2	0.30	0.0	860.9	912.8	868.4	3.0	9.2	3.8
Absolute Average Deviation (AAD)										**5.8**	**8.1**	**5.3**

Table 3.10 Experimental and modelling results of MIX 1

No	Phase	Temp.	Press.	Density (kg/m^3)						Abs Deviation (%)		
		K (±0.1)	MPa (±0.02)	Exp.	$U(\rho)$ kg/m^3	$U(\rho)$ %	PR-CO_2	PR	PR-Pen	PR-CO_2	PR	PR-Pen
1	Gas	273.39	1.714	38.4	0.99	2.6	37.7	37.6	37.6	2.0	2.1	2.2
2	Gas	273.41	2.072	47.4	1.07	2.3	47.1	47.0	46.9	0.6	0.7	0.9
3	Gas	273.41	2.732	66.4	1.26	1.9	66.6	66.5	66.3	0.3	0.2	0.1
4	Liq.	273.40	6.710	888.0	1.40	0.2	894.0	893.8	859.8	0.7	0.6	3.2
5	Liq.	273.42	11.308	927.8	1.08	0.1	937.2	950.6	912.3	1.0	2.5	1.7
6	Liq.	273.41	21.803	983.9	0.81	0.1	997.9	1,032.0	987.0	1.4	4.9	0.3
7	Liq.	273.42	36.270	1,034.2	0.62	0.1	1,051.3	1,102.1	1,050.8	1.7	6.6	1.6
8	Liq.	273.42	51.734	1,073.6	0.52	0.0	1,092.6	1,153.9	1,097.9	1.8	7.5	2.3
9	Liq.	273.43	76.401	1,121.7	0.41	0.0	1,142.2	1,212.6	1,150.9	1.8	8.1	2.6
10	Liq.	273.41	104.377	1,164.4	0.43	0.0	1,185.1	1,260.3	1,193.8	1.8	8.2	2.5
11	Liq.	273.42	126.015	1,192.1	0.41	0.0	1,211.9	1,288.9	1,219.4	1.7	8.1	2.3
12	Gas	283.32	1.810	36.5	0.94	2.5	38.0	38.0	38.0	4.0	4.1	3.9
13	Gas	283.32	3.365	78.3	1.29	1.6	82.1	81.6	81.3	5.0	4.3	3.9
14	Liq.	283.28	6.359	810.8	1.63	0.2	797.9	778.3	752.4	1.6	4.0	7.2
15	Liq.	283.27	11.679	888.9	1.26	0.1	881.9	882.9	849.7	0.8	0.7	4.4
16	Liq.	283.28	22.567	956.3	0.84	0.1	960.9	987.7	946.4	0.5	3.3	1.0
17	Liq.	283.27	36.414	1,004.6	0.72	0.1	1,019.4	1,065.2	1,017.3	1.5	6.0	1.3
18	Liq.	283.28	54.129	1,052.1	0.52	0.0	1,070.7	1,130.6	1,076.8	1.8	7.5	2.3
19	Liq.	283.27	77.997	1,099.3	0.52	0.0	1,121.2	1,191.4	1,131.8	2.0	8.4	3.0
20	Liq.	283.27	105.093	1,141.3	0.43	0.0	1,164.8	1,240.9	1,176.3	2.1	8.7	3.1
21	Liq.	283.29	124.852	1,167.1	0.33	0.0	1,190.8	1,269.0	1,201.6	2.0	8.7	3.0
22	Gas	298.29	1.679	32.1	0.84	2.6	32.3	32.6	32.5	0.6	1.4	1.3
23	Gas	298.29	1.961	38.6	0.87	2.3	38.3	38.7	38.6	0.7	0.3	0.1
24	Gas	298.29	2.760	57.0	0.97	1.7	56.7	57.5	57.4	0.5	0.9	0.6
25	Gas	298.29	3.076	64.8	1.02	1.6	64.6	65.6	65.4	0.3	1.3	1.0
26	Liq.	298.33	12.553	778.4	1.68	0.2	784.9	767.0	741.9	0.8	1.5	4.7
27	Liq.	298.37	20.262	865.2	1.02	0.1	876.0	883.0	849.8	1.2	2.1	1.8
28	Liq.	298.36	50.117	999.6	0.59	0.1	1,016.8	1,068.2	1,020.0	1.7	6.9	2.0
29	Liq.	298.38	75.616	1,061.8	0.41	0.0	1,080.1	1,147.4	1,092.0	1.7	8.1	2.8
30	Liq.	298.38	103.393	1,111.8	0.43	0.0	1,130.0	1,206.0	1,144.9	1.6	8.5	3.0
31	Liq.	298.40	126.332	1,145.6	0.33	0.0	1,162.8	1,242.5	1,177.8	1.5	8.5	2.8
32	Gas	323.35	1.452	24.0	0.73	3.0	24.9	25.1	25.1	4.0	4.7	4.6
33	Gas	323.35	2.189	37.4	0.77	2.1	38.8	39.1	39.1	3.7	4.7	4.5
34	Gas	323.34	3.599	66.0	0.89	1.3	68.0	69.1	68.9	3.1	4.7	4.4
35	Gas	323.34	5.217	104.6	1.07	1.0	107.4	109.9	109.3	2.8	5.1	4.6
36	Gas	323.35	8.266	209.5	1.92	0.9	213.8	219.1	217.0	2.0	4.5	3.5
37	SC	323.37	15.884	642.4	2.03	0.3	649.7	617.0	600.7	1.1	3.9	6.5
38	SC	323.36	22.595	758.5	1.15	0.2	767.8	756.9	732.3	1.2	0.2	3.4
39	SC	323.36	29.518	822.1	0.88	0.1	833.7	840.6	810.5	1.4	2.3	1.4
40	SC	323.38	54.067	941.5	0.57	0.1	957.5	1,001.4	958.9	1.7	6.4	1.9
41	SC	323.35	77.970	1,008.7	0.52	0.1	1,026.1	1,088.4	1,038.4	1.7	7.9	2.9
42	SC	323.35	106.001	1,065.5	0.43	0.0	1,082.7	1,157.1	1,100.8	1.6	8.6	3.3
43	SC	323.37	126.462	1,099.1	0.33	0.0	1,115.2	1,194.9	1,135.0	1.5	8.7	3.3
44	Gas	373.53	2.120	28.0	0.62	2.1	31.3	31.5	31.4	11.8	12.5	12.4
45	Gas	373.53	2.753	38.0	0.64	1.6	41.3	41.6	41.5	8.5	9.3	9.1
46	Gas	373.53	3.517	50.3	0.66	1.3	53.7	54.2	54.1	6.6	7.7	7.4
47	Gas	373.53	5.244	79.9	0.73	0.9	83.6	84.7	84.4	4.6	6.0	5.6
48	Gas	373.53	10.613	191.4	1.00	0.5	196.2	198.3	196.6	2.5	3.6	2.7
49	SC	373.47	26.160	568.5	1.04	0.2	576.2	554.8	541.5	1.3	2.4	4.7
50	SC	373.53	53.565	805.3	0.57	0.1	815.5	836.6	806.8	1.3	3.9	0.2
51	SC	373.54	77.942	900.8	0.45	0.0	912.6	959.0	920.0	1.3	6.5	2.1
52	SC	373.55	104.584	970.6	0.38	0.0	982.9	1,046.3	1,000.1	1.3	7.8	3.0
53	SC	373.55	123.180	1,008.7	0.41	0.0	1,020.6	1,092.1	1,041.7	1.2	8.3	3.3
54	Gas	423.40	0.950	11.4	0.51	4.5	11.9	25.8	12.0	4.6	125.3	4.7

No	Phase	Temp.	Press.				Density (kg/m^3)			Abs Deviation (%)		
		K (±0.1)	**MPa (±0.02)**	**Exp.**	***U(ρ)*** **kg/m^3**	***U(ρ)*** **%**	**PR-CO$_2$**	**PR**	**PR-Pen**	**PR-CO$_2$**	**PR**	**PR-Pen**
55	Gas	423.41	2.085	25.3	0.53	2.1	26.7	47.4	26.7	5.2	87.2	5.4
56	Gas	423.41	3.593	44.5	0.55	1.2	46.9	70.8	47.1	5.4	59.2	5.7
57	Gas	423.41	5.279	66.8	0.58	0.9	70.6	152.4	70.8	5.6	128.1	5.9
58	Gas	423.41	7.743	101.7	0.62	0.6	107.2	152.4	107.4	5.4	50.0	5.6
59	SC	423.41	34.178	521.3	0.68	0.1	527.1	514.5	503.0	1.1	1.3	3.5
60	SC	423.42	53.524	682.4	0.51	0.1	692.0	697.6	676.7	1.4	2.2	0.8
61	SC	423.42	76.139	791.7	0.41	0.1	803.6	832.9	803.3	1.5	5.2	1.5
62	SC	423.42	104.164	880.1	0.36	0.0	894.1	944.2	906.3	1.6	7.3	3.0
63	SC	423.42	121.851	922.5	0.33	0.0	937.2	996.5	954.5	1.6	8.0	3.5
Absolute Average Deviation (AAD)										**2.1**	**4.9**	**3.0**

Table 3.11 Experimental and modelling results of MIX 2

No	Phase	Temp.	Press.				Density (kg/m^3)			Abs Deviation (%)		
		K (±0.1)	MPa (±0.02)	Exp.	$U(\rho)$ kg/m^3	$U(\rho)$ %	PR-CO_2	PR	PR Pen	PR-CO_2	PR	PR Pen
1	Gas	273.18	1.789	38.4	0.97	2.5	38.4	38.3	38.2	0.2	0.3	0.7
2	Gas	273.18	2.244	49.8	1.05	2.1	50.0	50.0	49.7	0.5	0.3	0.1
3	Liq.	273.27	8.796	841.6	1.62	0.2	837.4	842.8	810.0	0.5	0.1	3.8
4	Liq.	273.28	10.922	867.7	1.36	0.2	865.7	876.1	840.8	0.2	1.0	3.1
5	Liq.	273.28	20.998	941.0	0.89	0.1	947.2	975.8	932.2	0.7	3.7	0.9
6	Liq.	273.29	52.044	1,048.9	0.62	0.1	1,064.0	1,119.6	1,062.7	1.4	6.7	1.3
7	Liq.	273.29	104.164	1,145.6	0.41	0.0	1,163.2	1,232.4	1,163.9	1.5	7.6	1.6
8	Liq.	273.29	125.705	1,174.9	0.41	0.0	1,191.4	1,262.6	1,190.8	1.4	7.5	1.4
9	Gas	283.31	1.741	37.0	0.90	2.4	35.0	35.3	35.2	5.4	4.6	5.0
10	Gas	283.30	2.278	46.5	0.97	2.1	48.3	48.0	47.8	3.8	3.2	2.7
11	Liq.	283.31	10.674	803.7	1.85	0.2	783.5	781.6	753.2	2.5	2.7	6.3
12	Liq.	283.31	20.840	895.0	0.97	0.1	899.0	919.2	880.4	0.5	2.7	1.6
13	Liq.	283.32	52.457	1,012.6	0.62	0.1	1,036.0	1,089.0	1,035.1	2.3	7.5	2.2
14	Liq.	283.32	104.116	1,114.4	0.43	0.0	1,141.3	1,211.2	1,144.9	2.4	8.7	2.7
15	Liq.	283.31	125.258	1,145.3	0.41	0.0	1,170.9	1,243.1	1,173.4	2.2	8.5	2.5
16	Gas	298.38	2.078	39.2	0.85	2.2	39.7	40.1	39.9	1.1	2.1	1.7
17	Gas	298.38	3.531	75.3	1.03	1.4	73.5	74.7	74.3	2.4	0.8	1.4
18	SC	298.38	12.581	702.1	2.38	0.3	684.0	670.9	649.5	2.6	4.4	7.5
19	SC	298.39	20.805	827.0	1.12	0.1	820.8	827.7	795.9	0.7	0.1	3.8
20	SC	298.40	51.342	979.9	0.59	0.1	988.3	1,035.2	986.3	0.9	5.6	0.7
21	SC	298.40	104.102	1,097.0	0.43	0.0	1,108.9	1,178.7	1,115.9	1.1	7.5	1.7
22	SC	298.38	125.877	1,130.3	0.43	0.0	1,141.8	1,215.2	1,148.5	1.0	7.5	1.6
23	Gas	323.49	2.574	45.3	0.78	1.7	45.0	45.4	45.3	0.7	0.4	0.0
24	Gas	323.50	3.703	67.5	0.86	1.3	67.8	68.8	68.4	0.3	1.9	1.3
25	SC	323.45	12.271	409.1	2.78	0.7	406.6	383.8	375.8	0.6	6.2	8.1
26	SC	323.45	20.908	687.5	1.39	0.2	677.9	665.0	643.9	1.4	3.3	6.3
27	SC	323.48	51.555	909.3	0.60	0.1	914.3	950.9	909.3	0.5	4.6	0.0
28	SC	323.50	105.058	1,047.7	0.41	0.0	1,058.2	1,126.1	1,068.5	1.0	7.5	2.0
29	SC	323.49	125.478	1,082.4	0.43	0.0	1,092.9	1,166.0	1,104.4	1.0	7.7	2.0
30	Gas	373.57	1.528	20.7	0.59	2.9	21.7	21.8	21.8	4.7	5.2	4.9
31	Gas	373.58	2.567	34.5	0.62	1.8	37.3	37.6	37.4	8.1	8.8	8.4
32	SC	373.49	17.220	353.9	1.12	0.3	346.3	337.6	331.6	2.2	4.6	6.3
33	SC	373.50	21.005	439.7	1.12	0.3	435.9	419.7	410.7	0.9	4.6	6.6
34	SC	373.53	52.560	777.7	0.57	0.1	776.8	794.1	764.6	0.1	2.1	1.7
35	SC	373.55	103.937	951.8	0.39	0.0	958.3	1,015.8	968.5	0.7	6.7	1.8
36	SC	373.55	125.148	996.1	0.36	0.0	1,003.1	1,069.3	1,017.1	0.7	7.4	2.1
37	Gas	423.48	2.395	30.4	0.52	1.7	30.0	30.1	30.0	1.2	0.8	1.2
38	Gas	423.49	3.414	43.6	0.54	1.2	43.3	43.5	43.3	0.6	0.1	0.5
39	SC	423.38	18.472	283.7	0.71	0.2	273.7	270.5	266.5	3.5	4.7	6.1
40	SC	423.38	21.748	335.5	0.72	0.2	327.0	320.8	315.4	2.5	4.4	6.0
41	SC	423.41	52.787	660.6	0.51	0.1	657.9	662.1	641.3	0.4	0.2	2.9
42	SC	423.42	102.774	862.5	0.35	0.0	867.4	912.0	873.5	0.6	5.7	1.3
43	SC	423.42	124.646	915.9	0.33	0.0	922.2	977.5	933.5	0.7	6.7	1.9
Absolute Average Deviation (AAD)										**1.6**	**4.3**	**2.9**

Table 3.12 Experimental and modelling results of MIX 3

No	Phase	Temp.	Press.				Density (kg/m^3)			Abs Deviation (%)		
		K (±0.1)	MPa (±0.02)	Exp.	$U(\rho)$ kg/m^3	$U(\rho)$ %	PR-CO_2	PR	PR Pen	PR-CO_2	PR	PR Pen
1	Gas	273.28	1.067	20.0	0.77	3.8	19.0	19.0	19.0	4.8	4.8	5.0
2	Gas	273.26	2.127	41.6	0.91	2.2	41.3	41.3	41.1	0.6	0.7	1.1
3	Liq.	273.23	12.712	685.5	1.05	0.2	667.5	674.7	641.7	2.6	1.6	6.4
4	Liq.	273.20	20.895	740.2	0.72	0.1	738.5	753.7	712.7	0.2	1.8	3.7
5	Liq.	273.20	52.278	838.1	0.44	0.1	858.1	889.7	833.2	2.4	6.2	0.6
6	Liq.	273.18	103.765	920.2	0.33	0.0	947.6	987.6	918.5	3.0	7.3	0.2
7	Liq.	273.20	124.501	944.3	0.30	0.0	971.3	1,012.6	940.1	2.9	7.2	0.5
8	Gas	283.32	1.122	18.7	0.73	3.9	19.1	19.2	19.2	2.1	2.5	2.3
9	Gas	283.32	2.085	36.8	0.84	2.3	38.0	38.2	38.0	3.3	3.8	3.5
10	Gas	283.28	4.873	110.8	1.60	1.4	117.7	117.1	116.1	6.2	5.6	4.7
11	Liq.	283.31	9.518	564.7	2.41	0.4	531.5	529.3	508.8	5.9	6.3	9.9
12	Liq.	283.32	20.633	701.4	0.77	0.1	697.0	707.5	671.3	0.6	0.9	4.3
13	Liq.	283.34	51.893	814.3	0.44	0.1	834.0	864.0	810.6	2.4	6.1	0.5
14	Liq.	283.34	103.365	902.8	0.32	0.0	930.4	970.8	903.9	3.1	7.5	0.1
15	Liq.	283.32	125.368	929.6	0.30	0.0	957.1	999.1	928.5	3.0	7.5	0.1
16	Gas	298.36	1.101	18.6	0.68	3.7	17.6	17.7	17.7	5.4	5.0	5.1
17	Gas	298.36	2.085	36.0	0.76	2.1	35.2	35.4	35.3	2.3	1.6	1.8
18	Gas	298.38	5.175	108.2	1.23	1.1	108.0	109.9	108.9	0.2	1.5	0.7
19	SC	298.40	10.964	462.0	2.84	0.6	438.7	431.4	417.7	5.0	6.6	9.6
20	SC	298.29	20.833	642.9	0.86	0.1	636.7	640.5	610.7	1.0	0.4	5.0
21	SC	298.30	51.734	779.9	0.44	0.1	799.4	826.4	777.5	2.5	6.0	0.3
22	SC	298.29	102.106	873.8	0.32	0.0	904.2	944.7	881.2	3.5	8.1	0.9
23	SC	298.30	124.969	903.9	0.30	0.0	934.4	977.3	909.6	3.4	8.1	0.6
24	Gas	323.44	1.218	19.3	0.62	3.2	17.8	17.9	17.9	7.6	7.2	7.3
25	Gas	323.45	2.113	32.7	0.66	2.0	32.0	32.2	32.1	2.3	1.6	1.8
26	Gas	323.44	5.231	90.6	0.88	1.0	90.9	92.3	91.7	0.3	1.9	1.2
27	SC	323.47	11.810	316.8	1.83	0.6	308.5	296.1	289.6	2.6	6.5	8.6
28	SC	323.49	20.227	531.8	1.05	0.2	520.9	513.0	493.7	2.0	3.5	7.2
29	SC	323.41	49.821	718.0	0.45	0.1	735.2	755.2	714.1	2.4	5.2	0.5
30	SC	323.43	103.427	837.2	0.31	0.0	866.4	906.0	847.5	3.5	8.2	1.2
31	SC	323.45	124.838	868.2	0.29	0.0	898.0	940.9	878.0	3.4	8.4	1.1
32	Gas	373.54	2.099	24.5	0.54	2.2	26.6	26.8	26.7	8.8	9.3	9.0
33	Gas	373.55	5.237	68.9	0.62	0.9	71.3	72.0	71.6	3.5	4.5	3.9
34	Gas	373.55	10.427	156.3	0.77	0.5	159.4	160.7	158.7	1.9	2.8	1.5
35	SC	373.56	20.730	364.2	0.84	0.2	359.6	349.7	340.6	1.2	4.0	6.5
36	SC	373.57	46.524	601.3	0.46	0.1	608.4	614.1	586.6	1.2	2.1	2.4
37	SC	373.53	63.338	668.4	0.38	0.1	684.5	701.9	666.2	2.4	5.0	0.3
38	SC	373.54	63.159	667.7	0.38	0.1	683.8	701.1	665.5	2.4	5.0	0.3
39	SC	373.55	103.400	767.8	0.30	0.0	792.4	826.6	777.6	3.2	7.7	1.3
40	SC	373.55	122.278	800.7	0.28	0.0	826.6	865.5	812.0	3.2	8.1	1.4
41	SC	373.56	125.292	804.9	0.27	0.0	831.4	871.0	816.8	3.3	8.2	1.5
42	Gas	423.43	2.120	23.2	0.46	2.0	23.3	23.4	23.3	0.7	1.0	0.8
43	Gas	423.43	5.224	58.2	0.50	0.9	59.8	60.1	59.8	2.8	3.3	2.8
44	Gas	423.43	10.358	120.5	0.55	0.5	125.9	126.2	125.0	4.5	4.8	3.8
45	Gas	423.44	20.943	258.3	0.59	0.2	271.3	267.7	262.3	5.0	3.6	1.6
46	SC	423.45	29.078	371.6	0.54	0.1	370.1	363.0	353.3	0.4	2.3	4.9
47	SC	423.45	49.869	527.2	0.40	0.1	534.5	535.3	514.3	1.4	1.5	2.4
48	SC	423.46	103.359	704.5	0.27	0.0	725.8	753.1	712.3	3.0	6.9	1.1
49	SC	423.47	124.804	746.2	0.25	0.0	770.1	803.8	757.4	3.2	7.7	1.5
Absolute Average Deviation (AAD)										**3.0**	**5.0**	**2.9**

Table 3.13 Experimental and modelling results of MIX 4

No	Phase	Temp.	Press.				Density (kg/m^3)			Abs Deviation (%)		
		K (±0.1)	MPa (±0.02)	Exp.	$U(\rho)$ kg/m^3	$U(\rho)$ %	PR-CO_2	PR	PR Pen	PR-CO_2	PR	PR Pen
1	SC	273.24	1.872	30.5	0.69	2.3	29.3	29.3	29.2	3.8	3.9	4.2
2	SC	273.24	2.085	33.7	0.71	2.1	33.1	33.1	33.0	1.6	1.7	2.0
3	SC	273.24	2.767	45.9	0.78	1.7	45.9	45.9	45.7	0.0	0.1	0.6
4	SC	273.25	3.469	60.3	0.86	1.4	60.5	60.4	60.1	0.4	0.3	0.4
5	SC	273.25	5.279	104.9	1.21	1.1	107.1	107.0	105.8	2.0	2.0	0.8
6	SC	273.25	7.467	189.7	2.25	1.2	194.8	194.9	190.9	2.7	2.8	0.6
7	SC	273.25	11.404	403.0	1.96	0.5	392.5	394.2	378.2	2.6	2.2	6.2
8	SC	273.27	15.719	509.7	1.05	0.2	487.3	491.5	466.9	4.4	3.6	8.4
9	SC	273.26	20.730	560.0	0.75	0.1	548.0	554.9	523.6	2.2	0.9	6.5
10	SC	273.26	27.591	601.7	0.58	0.1	601.2	611.3	573.6	0.1	1.6	4.7
11	SC	273.28	31.094	627.0	0.53	0.1	621.7	633.1	592.8	0.9	1.0	5.5
12	SC	273.29	54.783	699.3	0.38	0.1	710.8	728.9	676.0	1.6	4.2	3.3
13	SC	273.30	78.362	744.3	0.31	0.0	762.8	784.4	723.4	2.5	5.4	2.8
14	SC	273.29	104.556	781.5	0.28	0.0	802.9	826.7	759.2	2.7	5.8	2.8
15	SC	273.26	124.102	804.3	0.26	0.0	826.1	850.8	779.5	2.7	5.8	3.1
16	SC	283.28	1.796	26.4	0.65	2.5	26.7	26.7	26.6	1.1	1.1	0.9
17	SC	283.29	2.072	30.4	0.67	2.2	31.2	31.3	31.1	2.4	2.7	2.4
18	SC	283.27	3.462	54.6	0.78	1.4	56.7	56.5	56.2	3.9	3.6	2.9
19	SC	283.27	5.217	91.9	1.00	1.1	96.0	95.7	94.7	4.4	4.1	3.0
20	SC	283.27	9.050	221.5	1.99	0.9	228.2	227.7	222.3	3.0	2.8	0.4
21	SC	283.28	14.522	434.3	1.33	0.3	414.1	415.4	397.6	4.7	4.3	8.4
22	SC	283.28	20.791	518.4	0.79	0.2	510.1	514.9	487.9	1.6	0.7	5.9
23	SC	283.29	27.908	569.2	0.60	0.1	572.4	580.7	546.6	0.6	2.0	4.0
24	SC	283.30	35.210	604.3	0.49	0.1	615.9	627.2	587.6	1.9	3.8	2.8
25	SC	283.29	41.941	629.1	0.43	0.1	646.5	660.2	616.4	2.8	4.9	2.0
26	SC	283.28	50.048	653.5	0.39	0.1	676.0	692.0	644.1	3.4	5.9	1.4
27	SC	283.32	78.169	724.8	0.32	0.0	745.7	767.1	708.7	2.9	5.8	2.2
28	SC	283.32	104.370	764.1	0.28	0.0	788.3	812.3	747.1	3.2	6.3	2.2
29	SC	283.33	122.650	786.7	0.26	0.0	811.3	836.3	767.3	3.1	6.3	2.5
30	SC	298.37	2.595	39.0	0.64	1.6	37.2	37.4	37.2	4.7	4.1	4.5
31	SC	298.37	5.403	89.5	0.83	0.9	88.3	89.2	88.4	1.4	0.3	1.3
32	SC	298.34	7.626	141.1	1.08	0.8	143.7	142.1	140.0	1.9	0.7	0.8
33	SC	298.35	10.929	251.1	1.47	0.6	241.9	240.0	234.0	3.7	4.4	6.8
34	SC	298.30	16.173	399.1	1.15	0.3	379.6	378.9	364.1	4.9	5.1	8.8
35	SC	298.33	20.908	468.6	0.83	0.2	455.7	457.3	435.9	2.8	2.4	7.0
36	SC	298.36	20.661	465.9	0.85	0.2	452.3	453.8	432.7	2.9	2.6	7.1
37	SC	298.35	36.311	583.3	0.49	0.1	583.1	592.3	556.9	0.0	1.5	4.5
38	SC	298.32	51.246	630.3	0.38	0.1	648.7	663.3	619.2	2.9	5.2	1.8
39	SC	298.36	54.288	646.5	0.37	0.1	658.9	674.4	628.9	1.9	4.3	2.7
40	SC	298.36	77.619	699.0	0.31	0.0	719.8	740.4	685.9	3.0	5.9	1.9
41	SC	298.38	99.036	734.7	0.28	0.0	758.8	782.3	721.6	3.3	6.5	1.8
42	SC	298.40	124.026	768.1	0.26	0.0	793.3	818.8	752.6	3.3	6.6	2.0
43	SC	323.40	2.443	32.3	0.56	1.7	31.3	31.4	31.3	3.3	2.8	3.1
44	SC	323.44	5.203	73.0	0.66	0.9	72.5	73.3	72.7	0.7	0.4	0.4
45	SC	323.42	9.243	146.2	0.84	0.6	147.8	148.3	146.0	1.1	1.5	0.1
46	SC	323.44	20.736	385.6	0.81	0.2	373.4	370.3	356.2	3.2	4.0	7.6
47	SC	323.45	28.224	465.3	0.60	0.1	459.8	460.6	438.9	1.2	1.0	5.7
48	SC	323.45	35.306	513.8	0.50	0.1	515.7	520.2	492.7	0.4	1.2	4.1
49	SC	323.48	53.923	599.8	0.37	0.1	608.9	621.2	582.3	1.5	3.6	2.9
50	SC	323.47	78.534	663.5	0.31	0.0	681.9	700.9	651.8	2.8	5.6	1.8
51	SC	323.48	104.652	710.6	0.27	0.0	733.1	756.5	699.6	3.2	6.5	1.5
52	SC	323.47	119.209	731.9	0.25	0.0	755.2	780.3	719.9	3.2	6.6	1.6
53	SC	373.54	2.388	24.2	0.46	1.9	25.7	25.8	25.7	6.0	6.4	5.9
54	SC	373.37	5.182	55.1	0.50	0.9	58.4	58.8	58.3	6.0	6.7	5.8

No	Phase	Temp.	Press.				Density (kg/m^3)			Abs Deviation (%)		
		K (±0.1)	MPa (±0.02)	Exp.	$U(\rho)$ kg/m^3	$U(\rho)$ %	PR-CO_2	PR	PR Pen	PR-CO_2	PR	PR Pen
55	SC	373.42	11.239	134.4	0.58	0.4	138.1	138.7	136.3	2.8	3.2	1.4
56	SC	373.55	19.931	266.5	0.59	0.2	260.7	256.2	248.6	2.2	3.9	6.7
57	SC	373.56	28.032	354.5	0.52	0.1	352.9	348.0	334.6	0.5	1.8	5.6
58	SC	373.57	34.563	407.9	0.45	0.1	409.4	407.0	389.0	0.4	0.2	4.6
59	SC	373.57	41.397	452.3	0.41	0.1	456.6	457.4	435.0	1.0	1.1	3.8
60	SC	373.56	56.015	525.3	0.33	0.1	531.3	538.3	508.8	1.1	2.5	3.1
61	SC	373.56	73.579	581.5	0.29	0.1	594.4	607.3	570.1	2.2	4.4	2.0
62	SC	373.47	105.754	651.5	0.25	0.0	671.9	692.4	644.4	3.1	6.3	1.1
63	SC	373.47	124.350	682.0	0.23	0.0	704.2	727.6	674.9	3.3	6.7	1.0
64	SC	423.42	2.512	25.5	0.39	1.5	23.5	23.6	23.4	7.7	7.5	7.9
65	SC	423.39	3.104	30.7	0.40	1.3	29.2	29.3	29.1	5.0	4.7	5.2
66	SC	423.41	5.217	50.4	0.41	0.8	50.0	50.2	49.8	0.6	0.3	1.1
67	SC	423.42	10.599	103.2	0.43	0.4	105.8	106.0	104.6	2.5	2.7	1.3
68	SC	423.41	20.372	216.5	0.44	0.2	209.8	208.1	202.9	3.1	3.9	6.3
69	SC	423.41	28.004	285.7	0.42	0.1	283.5	279.9	270.8	0.8	2.0	5.2
70	SC	423.42	34.618	335.8	0.38	0.1	337.6	334.0	321.4	0.5	0.6	4.3
71	SC	423.42	41.507	379.9	0.35	0.1	384.9	382.7	366.5	1.3	0.7	3.5
72	SC	423.32	46.676	413.5	0.34	0.1	415.1	414.5	396.8	0.4	0.2	4.0
73	SC	423.42	47.983	414.9	0.33	0.1	422.2	421.9	403.6	1.7	1.7	2.7
74	SC	423.37	73.971	521.1	0.27	0.1	531.6	540.1	510.5	2.0	3.6	2.0
75	SC	423.40	103.957	594.0	0.24	0.0	612.2	628.3	588.6	3.1	5.8	0.9
76	SC	423.42	124.742	659.2	0.22	0.0	653.0	673.0	627.6	0.9	2.1	4.8
	Absolute Average Deviation (AAD)									**2.4**	**3.4**	**3.5**

Table 3.14 Experimental and modelling results of MIX 5

No	Phase	Temp.	Press.	Density (kg/m^3)						Abs Deviation (%)		
		K (±0.1)	MPa (±0.02)	Exp.	*U(ρ)* kg/m^3	*U(ρ)* %	PR-CO_2	PR	PR Pen	PR-CO_2	PR	PR-Pen
1	Gas	273.28	1.666	35.3	0.99	2.8	36.2	36.2	36.1	2.6	2.4	2.3
2	Gas	273.28	2.127	47.7	1.09	2.3	48.3	48.2	48.1	1.3	1.1	0.9
3	Gas	273.29	2.815	67.8	1.30	1.9	68.9	68.8	68.6	1.6	1.4	1.1
4	Gas	273.28	3.503	93.5	1.67	1.8	94.1	94.0	93.6	0.6	0.5	0.1
5	Liq.	273.28	6.084	896.7	1.47	0.2	884.7	882.4	849.3	1.3	1.6	5.3
6	Liq.	273.28	10.344	932.4	1.13	0.1	926.2	937.3	900.1	0.7	0.5	3.5
7	Liq.	273.28	20.310	986.4	0.84	0.1	985.8	1,017.7	973.9	0.1	3.2	1.3
8	Liq.	273.29	34.907	1,038.1	0.72	0.1	1,040.7	1,090.2	1,040.1	0.3	5.0	0.2
9	Liq.	273.29	52.168	1,082.1	0.52	0.0	1,086.5	1,147.9	1,092.5	0.4	6.1	1.0
10	Liq.	273.30	77.158	1,130.2	0.41	0.0	1,135.7	1,206.1	1,145.1	0.5	6.7	1.3
11	Liq.	273.30	100.984	1,166.9	0.41	0.0	1,172.0	1,246.6	1,181.5	0.4	6.8	1.3
12	Liq.	273.30	120.234	1,192.3	0.41	0.0	1,196.5	1,272.8	1,205.1	0.4	6.8	1.1
13	Liq.	273.29	123.957	1,196.8	0.43	0.0	1,200.8	1,277.4	1,209.2	0.3	6.7	1.0
14	Gas	283.27	1.094	20.7	0.85	4.1	21.5	21.6	21.6	3.9	4.4	4.3
15	Gas	283.28	1.473	29.0	0.90	3.1	29.7	29.9	29.9	2.5	3.2	3.1
16	Gas	283.29	2.085	43.0	0.99	2.3	44.2	44.5	44.4	2.8	3.5	3.3
17	Gas	283.29	2.836	63.3	1.14	1.8	65.1	64.7	64.5	2.9	2.2	2.0
18	Gas	283.29	3.544	84.9	1.37	1.6	87.8	87.2	86.9	3.4	2.8	2.4
19	Liq.	283.27	6.538	807.8	1.17	0.1	802.8	783.8	757.5	0.6	3.0	6.2
20	Liq.	283.29	10.606	877.0	1.35	0.2	866.9	864.3	832.5	1.2	1.5	5.1
21	Liq.	283.30	21.108	951.4	0.88	0.1	947.6	971.7	931.7	0.4	2.1	2.1
22	Liq.	283.32	36.559	1,013.5	0.64	0.1	1,013.3	1,059.1	1,011.7	0.0	4.5	0.2
23	Liq.	283.26	52.450	1,056.1	0.62	0.1	1,059.3	1,118.0	1,065.5	0.3	5.9	0.9
24	Liq.	283.29	77.915	1,106.5	0.52	0.0	1,113.0	1,183.0	1,124.3	0.6	6.9	1.6
25	Liq.	283.33	106.490	1,151.7	0.41	0.0	1,158.1	1,234.1	1,170.3	0.6	7.2	1.6
26	Liq.	283.31	126.256	1,178.1	0.43	0.0	1,183.7	1,261.7	1,195.1	0.5	7.1	1.4
27	Gas	298.31	1.211	22.7	0.80	3.5	22.5	22.7	22.6	1.0	0.4	0.5
28	Gas	298.30	1.652	31.3	0.84	2.7	31.5	31.7	31.7	0.6	1.5	1.3
29	Gas	298.30	2.106	41.0	0.89	2.2	41.2	41.7	41.6	0.7	1.7	1.5
30	Gas	298.30	3.503	75.1	1.10	1.5	75.5	76.8	76.5	0.4	2.2	1.9
31	Liq.	298.29	10.964	753.4	2.11	0.3	751.4	726.6	704.0	0.3	3.6	6.6
32	Liq.	298.31	20.268	869.1	1.03	0.1	872.3	879.4	846.5	0.4	1.2	2.6
33	Liq.	298.32	34.198	946.6	0.73	0.1	953.1	986.8	945.6	0.7	4.3	0.1
34	Liq.	298.32	52.409	1,008.9	0.62	0.1	1,016.9	1,070.1	1,021.8	0.8	6.1	1.3
35	Liq.	298.31	77.509	1,068.4	0.52	0.0	1,076.5	1,144.4	1,089.3	0.8	7.1	2.0
36	Liq.	298.30	105.024	1,117.2	0.43	0.0	1,124.5	1,200.5	1,140.1	0.7	7.5	2.0
37	Liq.	298.30	126.008	1,148.0	0.33	0.0	1,154.0	1,233.4	1,169.7	0.5	7.4	1.9
38	Gas	323.55	1.239	21.8	0.72	3.3	20.9	21.0	21.0	4.0	3.5	3.6
39	Gas	323.57	2.113	36.9	0.77	2.1	37.0	37.3	37.3	0.3	1.3	1.1
40	Gas	323.62	2.822	50.7	0.82	1.6	51.0	51.6	51.5	0.5	1.8	1.5
41	Gas	323.36	3.572	65.8	0.89	1.4	66.9	68.0	67.8	1.7	3.3	3.0
42	Gas	323.36	5.327	108.1	1.11	1.0	109.7	112.3	111.7	1.5	3.9	3.4
43	Gas	323.37	7.323	170.5	1.56	0.9	173.4	178.2	176.8	1.7	4.5	3.7
44	SC	323.37	15.864	647.3	2.04	0.3	648.7	615.6	599.3	0.2	4.9	7.4
45	SC	323.36	21.294	747.2	1.25	0.2	748.6	733.6	710.6	0.2	1.8	4.9
46	SC	323.38	36.910	871.5	0.74	0.1	876.9	898.1	863.8	0.6	3.1	0.9
47	SC	323.38	52.884	939.9	0.59	0.1	947.1	989.7	948.2	0.8	5.3	0.9
48	SC	323.39	77.288	1,009.5	0.52	0.1	1,017.2	1,079.0	1,029.9	0.8	6.9	2.0
49	SC	323.35	104.522	1,065.4	0.43	0.0	1,072.3	1,146.0	1,090.8	0.6	7.6	2.4
50	SC	323.35	124.019	1,097.9	0.33	0.0	1,103.5	1,182.4	1,123.8	0.5	7.7	2.4
51	Gas	373.53	1.363	19.0	0.60	3.2	19.6	19.7	19.7	3.1	3.5	3.4
52	Gas	373.53	2.099	29.4	0.62	2.1	30.7	30.9	30.9	4.6	5.3	5.1
53	Gas	373.53	3.496	50.9	0.67	1.3	53.0	53.5	53.3	4.1	5.1	4.9
54	Gas	373.54	5.389	81.8	0.73	0.9	85.7	86.8	86.4	4.7	6.1	5.7

No	Phase	Temp.	Press.		Density (kg/m^3)					Abs Deviation (%)		
		K (±0.1)	MPa (±0.02)	Exp.	*U(ρ)* kg/m^3	*U(ρ)* %	PR-CO_2	PR	PR Pen	PR-CO_2	PR	PR-Pen
55	Gas	373.53	7.756	127.3	0.84	0.7	131.4	133.4	132.6	3.2	4.8	4.1
56	Gas	373.54	10.454	187.1	0.99	0.5	191.2	193.4	191.8	2.2	3.4	2.5
57	SC	373.53	27.743	595.8	1.00	0.2	597.6	577.8	563.4	0.3	3.0	5.4
58	SC	373.53	31.452	644.0	0.88	0.1	645.6	631.2	614.0	0.3	2.0	4.7
59	SC	373.54	43.544	750.3	0.67	0.1	751.8	758.1	733.5	0.2	1.0	2.2
60	SC	373.54	55.747	818.9	0.55	0.1	821.2	845.0	814.6	0.3	3.2	0.5
61	SC	373.55	76.325	898.1	0.46	0.1	901.2	946.2	908.2	0.3	5.4	1.1
62	SC	373.55	101.411	965.6	0.40	0.0	968.7	1,030.4	985.5	0.3	6.7	2.1
63	SC	373.55	116.022	996.6	0.37	0.0	999.6	1,068.1	1,020.0	0.3	7.2	2.3
64	SC	373.56	125.513	1,014.2	0.41	0.0	1,017.3	1,089.5	1,039.4	0.3	7.4	2.5
65	Gas	423.43	2.099	26.7	0.53	2.0	26.6	26.7	26.7	0.3	0.1	0.0
66	Gas	423.44	3.510	44.9	0.55	1.2	45.4	45.7	45.6	1.2	1.8	1.6
67	Gas	423.45	5.237	67.5	0.58	0.9	69.5	69.9	69.7	2.9	3.5	3.2
68	Gas	423.45	7.619	100.8	0.61	0.6	104.5	105.2	104.7	3.7	4.3	3.8
69	Gas	423.45	11.225	155.2	0.68	0.4	161.7	162.2	161.1	4.2	4.5	3.8
70	Gas	423.46	17.137	252.4	0.76	0.3	263.4	260.9	257.9	4.4	3.4	2.2
71	SC	423.39	43.778	614.5	0.59	0.1	618.1	612.8	596.6	0.6	0.3	2.9
72	SC	423.40	53.799	685.3	0.53	0.1	689.4	695.3	674.6	0.6	1.5	1.6
73	SC	423.41	78.142	800.3	0.42	0.1	805.9	836.9	807.1	0.7	4.6	0.8
74	SC	423.41	104.542	882.1	0.36	0.0	888.8	938.9	901.5	0.8	6.4	2.2
75	SC	423.41	104.845	883.1	0.36	0.0	889.6	939.8	902.4	0.7	6.4	2.2
76	SC	423.41	94.955	855.9	0.38	0.0	862.0	906.0	871.2	0.7	5.9	1.8
77	SC	423.42	126.442	933.8	0.33	0.0	940.3	1,001.5	959.0	0.7	7.2	2.7
Absolute Average Deviation (AAD)										**1.2**	**4.1**	**2.4**

Table 3.15 Experimental and modelling results of MIX 6

No	Phase	Temp.	Press.				Density (kg/m^3)			Abs Deviation (%)		
		K (±0.1)	MPa (±0.02)	Exp.	$U(\rho)$ kg/m^3	$U(\rho)$ %	PR-CO_2	PR	PR Pen	PR-CO_2	PR	PR-Pen
1	Gas	273.27	1.198	23.3	0.86	3.7	23.5	23.5	23.4	0.8	0.7	0.6
2	Gas	273.27	2.085	45.7	1.03	2.3	44.5	44.4	44.3	2.7	2.8	3.1
3	Liq.	273.29	10.523	714.8	1.08	0.2	690.2	695.1	662.2	3.4	2.7	7.3
4	Liq.	273.30	15.747	749.9	0.80	0.1	739.7	750.6	712.3	1.4	0.1	5.0
5	Liq.	273.30	21.610	777.8	0.66	0.1	777.3	793.4	750.8	0.1	2.0	3.5
6	Liq.	273.31	36.077	825.7	0.51	0.1	838.0	862.9	812.7	1.5	4.5	1.6
7	Liq.	273.31	53.620	866.2	0.42	0.0	885.7	917.0	860.6	2.2	5.9	0.7
8	Liq.	273.31	78.541	908.7	0.36	0.0	932.6	968.9	906.1	2.6	6.6	0.3
9	Liq.	273.31	104.852	943.8	0.33	0.0	968.7	1,007.5	939.8	2.6	6.8	0.4
10	Liq.	273.31	126.063	967.6	0.30	0.0	991.8	1,031.6	960.7	2.5	6.6	0.7
11	Gas	283.30	1.239	22.3	0.82	3.7	23.1	23.2	23.2	3.5	4.0	3.8
12	Gas	283.32	2.072	40.3	0.94	2.3	41.4	41.6	41.5	2.6	3.1	2.8
13	Gas	283.31	3.145	68.4	1.19	1.7	70.5	70.2	69.8	3.0	2.5	2.0
14	Liq.	283.29	10.461	658.2	1.39	0.2	628.7	627.4	600.4	4.5	4.7	8.8
15	Liq.	283.30	14.467	699.3	0.96	0.1	683.6	687.7	655.4	2.2	1.7	6.3
16	Liq.	283.31	21.445	743.3	0.70	0.1	741.4	753.1	714.6	0.3	1.3	3.9
17	Liq.	283.31	35.485	797.9	0.53	0.1	809.8	831.9	785.1	1.5	4.3	1.6
18	Liq.	283.32	53.131	843.2	0.43	0.1	863.1	893.1	839.4	2.4	5.9	0.4
19	Liq.	283.32	78.052	889.1	0.36	0.0	914.0	950.0	889.6	2.8	6.9	0.1
20	Liq.	283.31	105.836	928.1	0.32	0.0	954.4	993.8	927.8	2.8	7.1	0.0
21	Liq.	283.32	126.628	952.5	0.29	0.0	978.1	1,018.8	949.6	2.7	7.0	0.3
22	Gas	298.32	1.342	24.1	0.76	3.2	23.6	23.7	23.7	1.9	1.4	1.6
23	Gas	298.33	2.092	39.3	0.84	2.1	38.6	38.9	38.8	1.7	0.9	1.2
24	Gas	298.34	2.732	53.5	0.93	1.7	52.7	53.2	53.0	1.5	0.5	0.9
25	Gas	298.33	3.937	84.8	1.16	1.4	83.6	84.9	84.3	1.4	0.0	0.6
26	Gas	298.32	5.279	131.3	1.65	1.3	129.3	131.6	130.4	1.5	0.3	0.7
27	Gas	298.32	6.401	191.4	2.71	1.4	195.2	189.4	186.9	1.9	1.1	2.4
28	Liq.	298.37	9.498	489.8	3.29	0.7	470.9	459.7	445.1	3.9	6.1	9.1
29	Liq.	298.37	10.723	541.8	2.20	0.4	521.4	511.3	493.2	3.8	5.6	9.0
30	Liq.	298.36	14.632	621.3	1.19	0.2	608.8	604.4	579.3	2.0	2.7	6.8
31	Liq.	298.36	21.149	683.0	0.79	0.1	683.3	687.7	655.4	0.0	0.7	4.0
32	Liq.	298.36	34.804	751.8	0.55	0.1	766.6	783.7	742.1	2.0	4.2	1.3
33	Liq.	298.36	51.707	803.5	0.44	0.1	826.9	853.7	804.5	2.9	6.2	0.1
34	Liq.	298.36	75.320	853.4	0.36	0.0	882.1	916.7	860.3	3.4	7.4	0.8
35	Liq.	298.36	105.506	900.1	0.32	0.0	930.8	970.5	907.5	3.4	7.8	0.8
36	Liq.	298.36	126.373	926.2	0.29	0.0	956.6	998.2	931.6	3.3	7.8	0.6
37	Gas	323.36	1.500	25.0	0.69	2.8	24.1	24.2	24.2	3.6	3.1	3.3
38	Gas	323.36	2.113	35.9	0.73	2.0	34.9	35.1	35.0	3.0	2.3	2.6
39	Gas	323.33	3.138	55.8	0.80	1.4	54.4	55.0	54.8	2.6	1.6	1.9
40	Gas	323.34	4.184	77.0	0.91	1.2	76.7	77.7	77.3	0.4	0.9	0.4
41	Gas	323.34	5.292	103.2	1.04	1.0	103.5	105.2	104.4	0.3	2.0	1.2
42	Gas	323.33	7.681	177.0	1.54	0.9	177.1	180.6	178.3	0.0	2.0	0.7
43	Gas	323.34	9.904	285.7	2.20	0.8	277.3	274.2	268.9	3.0	4.0	5.9
44	SC	323.44	15.967	520.4	1.38	0.3	500.9	485.4	469.1	3.8	6.7	9.9
45	SC	323.44	18.906	569.8	1.07	0.2	554.0	543.1	522.8	2.8	4.7	8.3
46	SC	323.44	23.792	623.2	0.80	0.1	614.5	610.8	585.2	1.4	2.0	6.1
47	SC	323.44	37.591	706.5	0.54	0.1	712.9	724.3	688.6	0.9	2.5	2.5
48	SC	323.45	53.159	761.8	0.43	0.1	777.4	799.6	756.3	2.1	5.0	0.7
49	SC	323.46	78.541	822.0	0.36	0.0	844.7	877.4	825.6	2.8	6.7	0.4
50	SC	323.48	105.437	867.8	0.31	0.0	893.0	932.1	873.8	2.9	7.4	0.7
51	SC	323.47	127.061	897.5	0.29	0.0	922.9	965.0	902.6	2.8	7.5	0.6
52	Gas	373.53	3.152	42.7	0.62	1.4	44.5	44.8	44.7	4.4	5.0	4.7
53	Gas	373.53	4.191	58.3	0.65	1.1	60.9	61.4	61.1	4.4	5.2	4.8
54	Gas	373.53	5.237	74.6	0.69	0.9	78.2	78.9	78.5	4.8	5.8	5.2

No	Phase	Temp.	Press.				Density (kg/m^3)			Abs Deviation (%)		
		K (±0.1)	MPa (±0.02)	Exp.	$U(\rho)$ kg/m^3	$U(\rho)$ %	PR-CO_2	PR	PR Pen	PR-CO_2	PR	PR-Pen
55	Gas	373.53	7.626	116.8	0.78	0.7	121.4	122.7	121.6	3.9	5.0	4.1
56	SC	373.51	20.819	410.7	0.89	0.2	401.6	390.1	379.5	2.2	5.0	7.6
57	SC	373.51	27.632	502.7	0.70	0.1	498.8	487.8	471.3	0.8	3.0	6.2
58	SC	373.53	35.465	571.5	0.56	0.1	572.3	568.2	546.0	0.1	0.6	4.5
59	SC	373.54	52.787	663.7	0.42	0.1	673.4	684.2	652.3	1.5	3.1	1.7
60	SC	373.55	76.277	738.2	0.34	0.0	755.8	780.1	738.8	2.4	5.7	0.1
61	SC	373.55	104.529	798.6	0.30	0.0	820.6	854.8	805.5	2.8	7.0	0.9
62	SC	373.55	126.256	834.4	0.27	0.0	857.5	896.6	842.5	2.8	7.4	1.0
63	Gas	423.43	1.707	19.7	0.49	2.5	20.2	20.2	20.2	2.6	2.8	2.7
64	Gas	423.42	2.175	25.2	0.50	2.0	25.9	26.0	25.9	2.8	3.1	2.9
65	Gas	423.42	3.083	36.0	0.51	1.4	37.2	37.3	37.2	3.4	3.8	3.5
66	Gas	423.43	4.219	49.7	0.53	1.1	51.8	52.0	51.8	4.1	4.6	4.2
67	Gas	423.43	5.320	63.2	0.54	0.9	66.4	66.7	66.4	5.0	5.5	5.0
68	Gas	423.43	7.598	92.9	0.57	0.6	97.9	98.3	97.6	5.3	5.8	5.1
69	SC	423.41	19.243	282.0	0.65	0.2	273.3	270.3	265.2	3.1	4.2	6.0
70	SC	423.43	28.045	395.3	0.58	0.1	390.7	383.1	372.9	1.2	3.1	5.7
71	SC	423.43	38.644	491.0	0.48	0.1	492.6	486.8	470.4	0.3	0.8	4.2
72	SC	423.44	52.202	572.4	0.39	0.1	580.3	582.7	559.3	1.4	1.8	2.3
73	SC	423.45	76.882	665.9	0.31	0.0	682.1	698.8	665.5	2.4	4.9	0.1
74	SC	423.45	104.790	734.6	0.27	0.0	756.6	784.5	742.8	3.0	6.8	1.1
75	SC	423.45	125.292	783.4	0.25	0.0	797.2	830.8	784.1	1.8	6.0	0.1
Absolute Average Deviation (AAD)										**2.4**	**4.1**	**3.0**

Table 3. 16 Uncertainties of density measurements for each mixture with 95% level of confidence

			Average		Max	
			U(ρ)	*U(ρ)*	*U(ρ)*	*U(ρ)*
Material	Phase	No	kg/m^3	%	kg/m^3	%
BIN 1	Gas	18	1.01	1.5	2.74	3.0
	Liquid	15	0.82	0.1	3.05	0.5
	SC	11	0.55	0.1	1.28	0.2
	Total	44	0.83	0.6	3.05	3.0
BIN 2	Gas	19	0.89	1.4	1.75	3.3
	Liquid	12	0.58	0.1	1.28	0.2
	SC	12	0.47	0.1	0.94	0.2
	Total	43	0.68	0.7	1.75	3.3
MIX 1	Gas	24	0.88	1.8	1.92	4.5
	Liquid	22	0.75	0.1	1.68	0.2
	SC	17	0.65	0.1	2.03	0.3
	Total	63	0.77	0.7	2.03	4.5
MIX 2	Gas	12	0.81	1.9	1.05	2.9
	Liquid	11	0.87	0.1	1.85	0.2
	SC	20	0.84	0.1	2.78	0.7
	Total	43	0.84	0.6	2.78	2.9
MIX 3	Gas	18	0.76	1.9	1.60	3.9
	Liquid	10	0.71	0.1	2.41	0.4
	SC	21	0.62	0.1	2.84	0.6
	Total	49	0.69	0.7	2.84	3.9
MIX 4	Gas	25	0.85	1.3	2.25	2.5
	Liquid	0	2.00	3.0	0.00	0.0
	SC	51	0.48	0.1	1.47	0.6
	Total	76	0.60	0.5	2.25	2.5
MIX 5	Gas	33	0.90	1.8	1.67	4.1
	Liquid	24	0.75	0.1	2.11	0.3
	SC	22	0.62	0.1	2.04	0.3
	Total	79	0.77	0.8	2.11	4.1
MIX 6	Gas	30	0.95	1.7	2.71	3.7
	Liquid	27	0.76	0.1	3.29	0.7
	SC	22	0.53	0.1	1.38	0.3
	Total	79	0.76	0.7	3.29	3.7
Total	Gas	179	0.89	1.7	2.74	4.5
	Liquid	121	0.75	0.1	3.29	0.7
	SC	176	0.58	0.1	2.84	0.7
	Total	**476**	**0.74**	**0.7**	**3.29**	**4.5**

Table 3.17 AAD and Max. Deviations of this work using PR and SRK EoSs

			AAD						Max Dev.					
			PR	SRK	PR	SRK	PR	SRK	PR	SRK	PR	SRK	PR	SRK
Material	Phase	No	CO_2				Peneloux		CO_2				Peneloux	
Pure CO_2	Gas	19	0.7	0.7	1.5	1.4	1.3	1.1	2.2	2.1	2.9	8.7	3.8	5.8
	Liquid	19	0.1	0.2	4.3	7.1	2.3	4.2	0.4	0.4	7.1	13.0	6.0	7.6
	SC	15	0.1	0.5	4.5	6.1	2.6	4.5	0.3	1.6	7.4	12.0	6.6	8.5
	Total	53	0.3	0.4	3.4	4.8	2.0	3.2	2.2	2.1	7.4	13.0	6.6	8.5
BIN 1	Gas	18	2.8	2.7	2.5	4.0	2.7	3.2	9.7	10.0	9.4	10.3	9.7	10.1
	Liquid	15	2.1	2.5	4.3	8.4	3.1	4.3	6.4	6.9	6.8	16.2	10.2	11.6
	SC	11	0.8	1.6	4.6	6.5	2.5	4.4	2.4	3.2	6.5	13.0	7.6	8.6
	Total	44	2.1	2.3	3.6	6.1	2.8	3.9	9.7	10.0	9.4	16.2	10.2	11.6
BIN 2	Gas	19	3.6	3.3	3.3	4.3	3.3	3.7	10.2	10.6	10.3	11.0	10.6	10.9
	Liquid	12	6.3	5.7	11.3	5.6	6.4	8.6	18.7	17.7	24.4	14.8	18.1	19.8
	SC	12	8.8	7.7	12.5	3.4	7.6	9.5	26.8	25.6	26.8	16.0	22.3	21.7
	Total	43	5.8	5.2	8.1	4.4	5.3	6.7	26.8	25.6	26.8	16.0	22.3	21.7
MIX 1	Gas	24	3.1	3.2	3.8	2.8	3.5	3.0	7.7	7.6	8.4	10.2	8.3	7.7
	Liquid	22	1.5	1.2	5.9	5.4	2.7	4.6	2.1	1.9	8.7	13.8	7.2	9.3
	SC	17	1.4	0.7	5.3	5.0	2.8	4.8	1.7	1.2	8.7	12.0	6.5	7.9
	Total	63	2.1	1.8	4.9	4.3	3.0	4.1	7.7	7.6	8.7	13.8	8.3	9.3
MIX 2	Gas	12	2.4	2.3	2.4	2.5	2.3	2.4	8.1	7.8	8.8	7.5	8.4	7.8
	Liquid	11	1.4	1.2	5.2	5.9	2.5	4.4	2.5	3.3	8.7	12.0	6.3	7.4
	SC	20	1.2	1.3	5.1	6.6	3.5	5.4	3.5	4.4	7.7	12.4	8.1	9.4
	Total	43	1.6	1.6	4.3	5.3	2.9	4.3	8.1	7.8	8.8	12.4	8.4	9.4
MIX 3	Gas	18	3.5	3.0	3.6	2.9	3.2	2.8	8.8	8.2	9.3	8.0	9.0	8.2
	Liquid	10	2.6	2.8	5.2	6.4	2.6	4.3	5.9	8.7	7.5	14.0	9.9	10.8
	SC	21	2.6	1.9	5.7	5.5	2.8	4.7	5.0	7.2	8.4	13.0	9.6	10.3
	Total	49	3.0	2.4	5.0	4.6	2.9	3.9	8.8	8.7	9.3	14.0	9.9	10.8
MIX 4	Gas	0	0.0	0.0	0.0	0.0	0.0	0.0	0.0	0.0	0.0	0.0	0.0	0.0
	Liquid	0	0.0	0.0	0.0	0.0	0.0	0.0	0.0	0.0	0.0	0.0	0.0	0.0
	SC	76	2.4	3.6	3.4	5.4	3.5	3.2	7.7	8.7	7.5	11.4	8.8	9.1
	Total	76	2.4	3.6	3.4	5.4	3.5	3.2	7.7	8.7	7.5	11.4	8.8	9.1
MIX 5	Gas	33	2.3	2.0	2.9	1.5	2.6	1.7	4.7	4.5	6.1	4.3	5.7	4.6
	Liquid	24	0.5	0.4	4.9	6.5	2.1	4.1	1.3	1.7	7.5	13.0	6.6	8.3
	SC	22	0.5	0.4	4.8	5.7	2.5	4.4	0.8	1.0	7.7	12.9	7.4	8.9
	Total	79	1.2	1.0	4.1	4.2	2.4	3.2	4.7	4.5	7.7	13.0	7.4	8.9
MIX 6	Gas	30	2.7	3.0	2.9	2.8	2.8	2.7	5.3	10.4	5.8	9.2	5.9	7.2
	Liquid	27	2.4	3.0	4.9	6.9	2.9	4.2	4.5	7.9	7.8	13.5	9.1	9.4
	SC	22	2.0	2.7	4.6	6.6	3.2	4.6	3.8	6.5	7.5	13.7	9.9	10.3
	Total	79	2.4	2.9	4.1	5.3	3.0	3.8	5.3	10.4	7.8	13.7	9.9	10.3
Total	Gas	173	2.6	2.5	2.9	2.7	2.8	2.5	10.2	10.6	10.3	11.0	10.6	10.9
	Liquid	140	1.9	1.9	5.5	6.6	2.9	4.7	18.7	17.7	24.4	16.2	18.1	19.8
	SC	216	2.1	2.4	4.8	5.7	3.4	4.8	26.8	25.6	26.8	16.0	22.3	21.7
	Total	**529**	**2.2**	**2.3**	**4.4**	**4.9**	**3.0**	**4.0**	**26.8**	**25.6**	**26.8**	**16.2**	**22.3**	**21.7**

Table 3.18 Density reduction of pure CO_2 at supercritical area, temperature 323.15 K (50 °C)

Material	Min	Pressure	
	%	psia	MPa
BIN 1	-30.7	1600	11.01
BIN 2	-44.6	1600	11.01
MIX 1	-20.1	1600	11.01
MIX 2	-33.9	1600	11.01
MIX 3	-45.9	1800	12.39
MIX 4	-63.9	1800	12.39
MIX 5	-20.1	1600	11.01
MIX 6	-35.1	1800	12.39

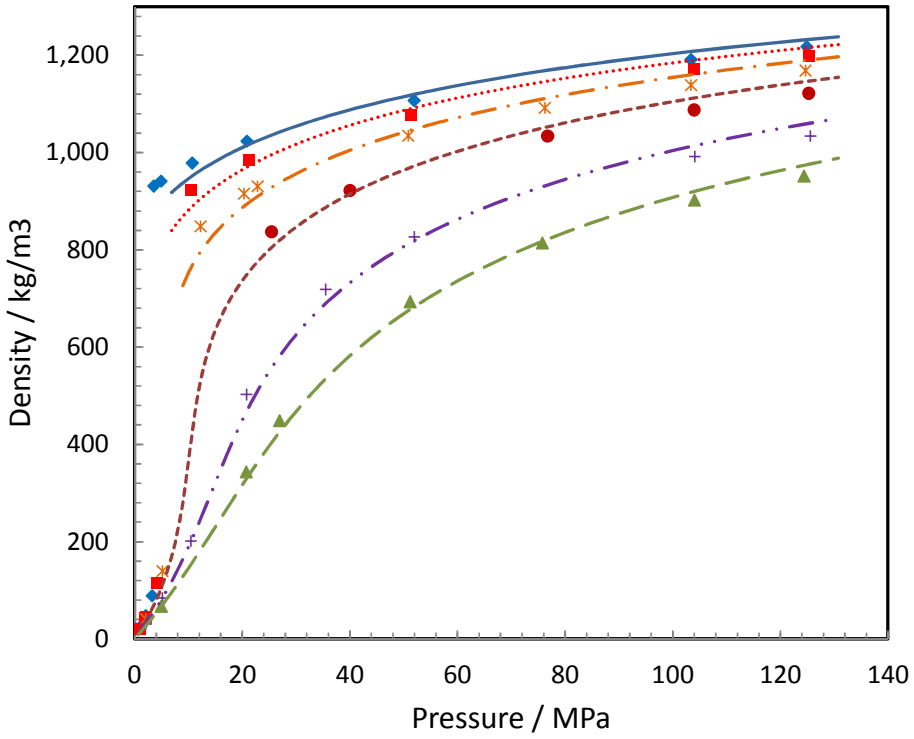

Figure 3.6 Experimental and modelling results of pure CO_2, experimental / modelling (PR-CO_2) results: (♦/——) at 273.15 K, (■/….) at 283.15 K, (x/—.—) at 298.15 K, (●/----) at 323.15 K, (+/—..—) at 373.15 K and (▲/— —) at 423.15 K

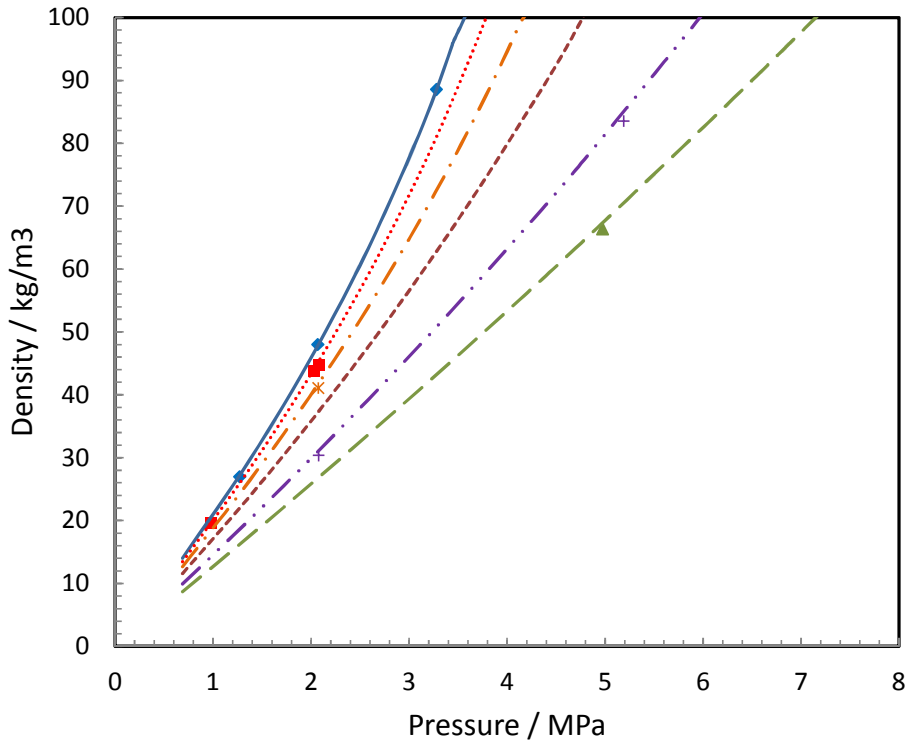

Figure 3.7 Experimental and modelling results of pure CO_2 at low pressures, experimental / modelling (PR-CO_2) results: (♦/——) at 273.15 K, (■/….) at 283.15 K, (x/—.—) at 298.15 K, (●/----) at 323.15 K, (+/—..—) at 373.15 K and (▲/— —) at 423.15 K

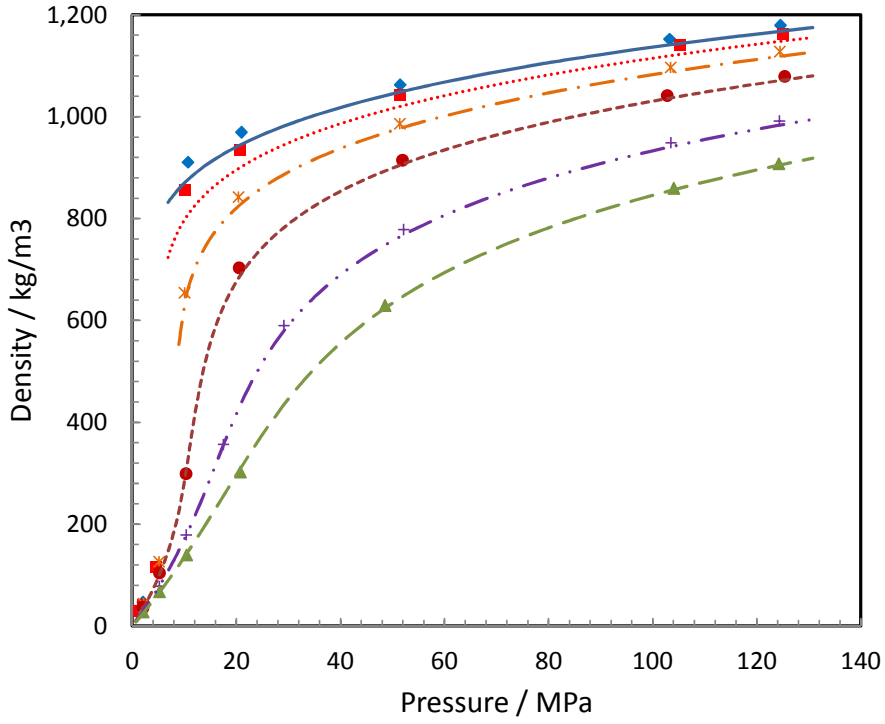

Figure 3.8 Experimental and modelling results of BINARY 1, experimental / modelling (PR-CO_2) results: (♦/——) at 273.15 K, (■/….) at 283.15 K, (x/—.—) at 298.15 K, (●/----) at 323.15 K, (+/—..—) at 373.15 K and (▲/— —) at 423.15 K

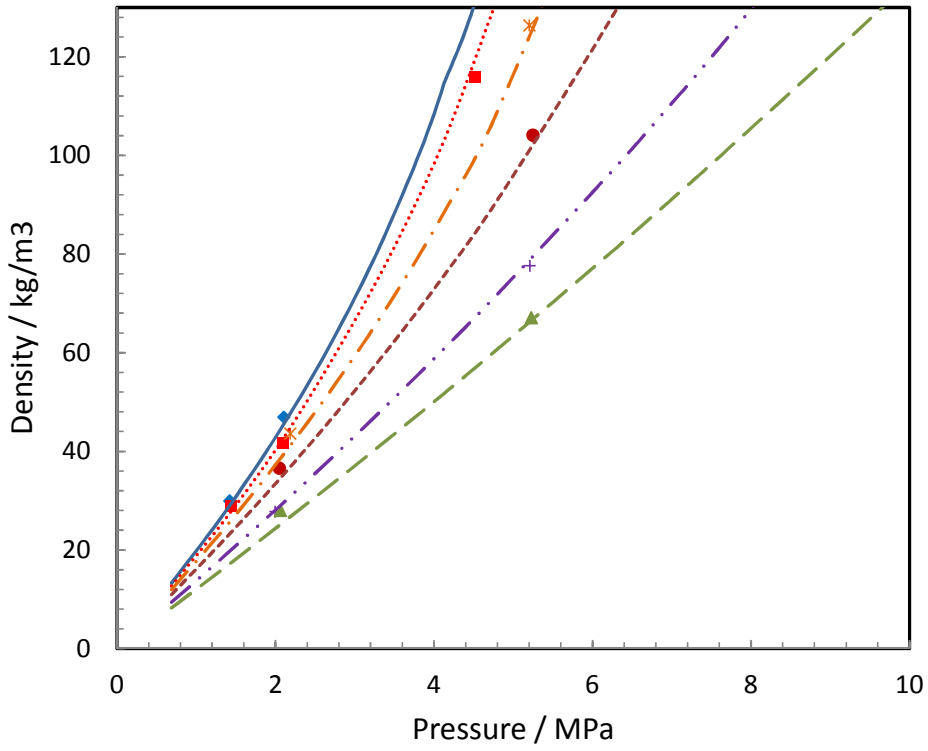

Figure 3.9 Experimental and modelling results of BINARY 1 at low pressures, experimental / modelling (PR-CO_2) results: (♦/——) at 273.15 K, (■/….) at 283.15 K, (x/—.—) at 298.15 K, (●/----) at 323.15 K, (+/—..—) at 373.15 K and (▲/— —) at 423.15 K

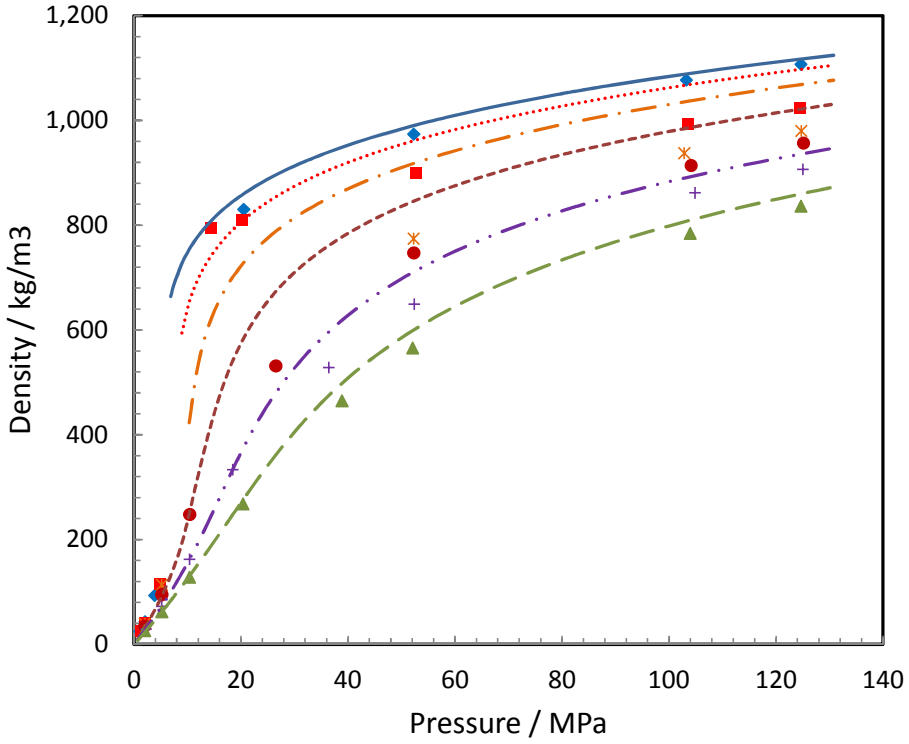

Figure 3.10 Experimental and modelling results of BINARY 2, experimental / modelling (PR-CO_2) results: (♦/——) at 273.15 K, (■/….) at 283.15 K, (x/—.—) at 298.15 K, (●/----) at 323.15 K, (+/—..—) at 373.15 K and (▲/— —) at 423.15 K

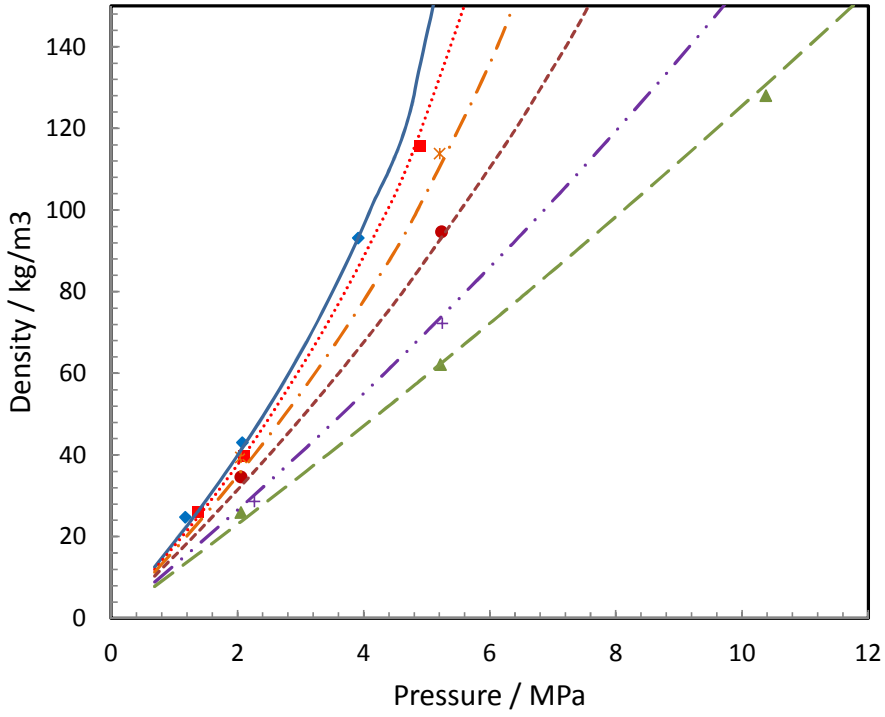

Figure 3.11 Experimental and modelling results of BINARY 2 at low pressures, experimental / modelling (PR-CO_2) results: (♦/——) at 273.15 K, (■/….) at 283.15 K, (x/—.—) at 298.15 K, (●/----) at 323.15 K, (+/—..—) at 373.15 K and (▲/— —) at 423.15 K

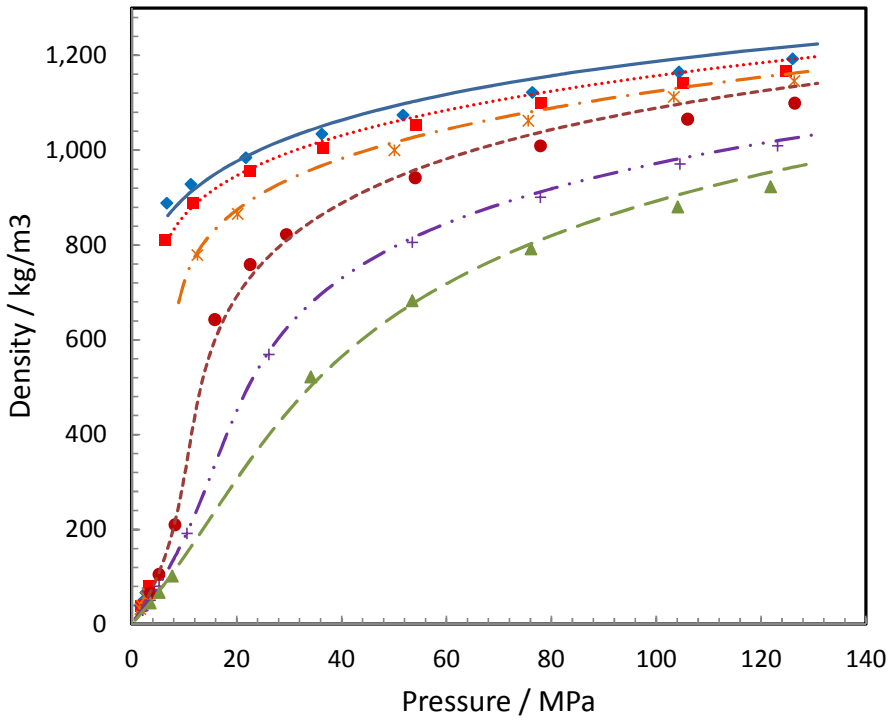

Figure 3.12 Experimental and modelling results of MIX 1, experimental / modelling (PR-CO_2) results: (♦/——) at 273.15 K, (■/….) at 283.15 K, (x/—.—) at 298.15 K, (●/----) at 323.15 K, (+/—..—) at 373.15 K and (▲/— —) at 423.15 K

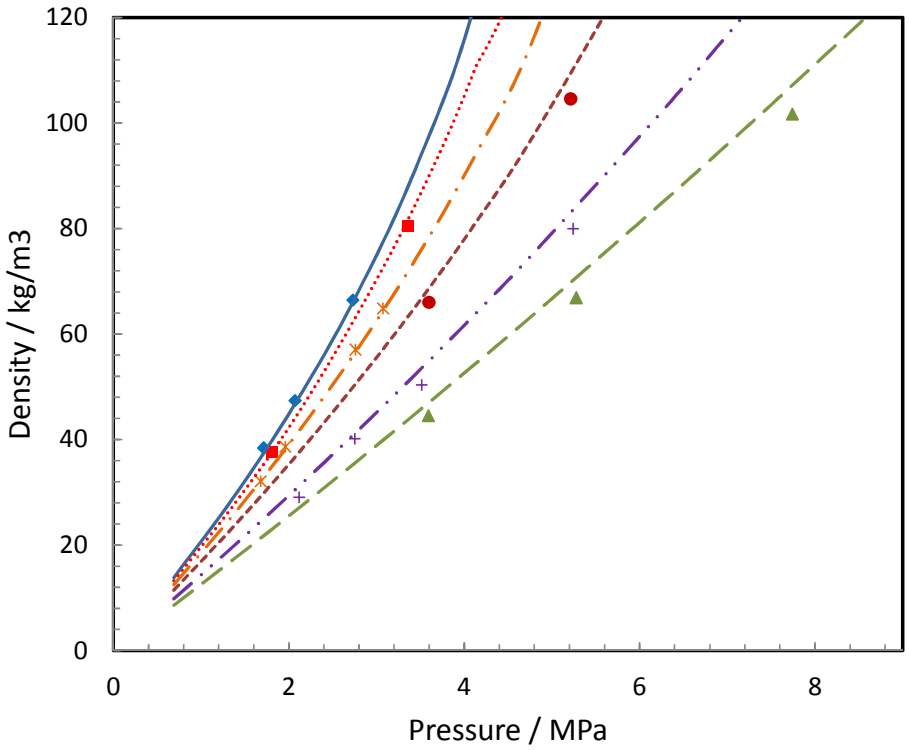

Figure 3.13 Experimental and modelling results of MIX 1 at low pressures, experimental / modelling (PR-CO_2) results: (♦/——) at 273.15 K, (■/….) at 283.15 K, (x/—.—) at 298.15 K, (●/----) at 323.15 K, (+/—..—) at 373.15 K and (▲/— —) at 423.15 K

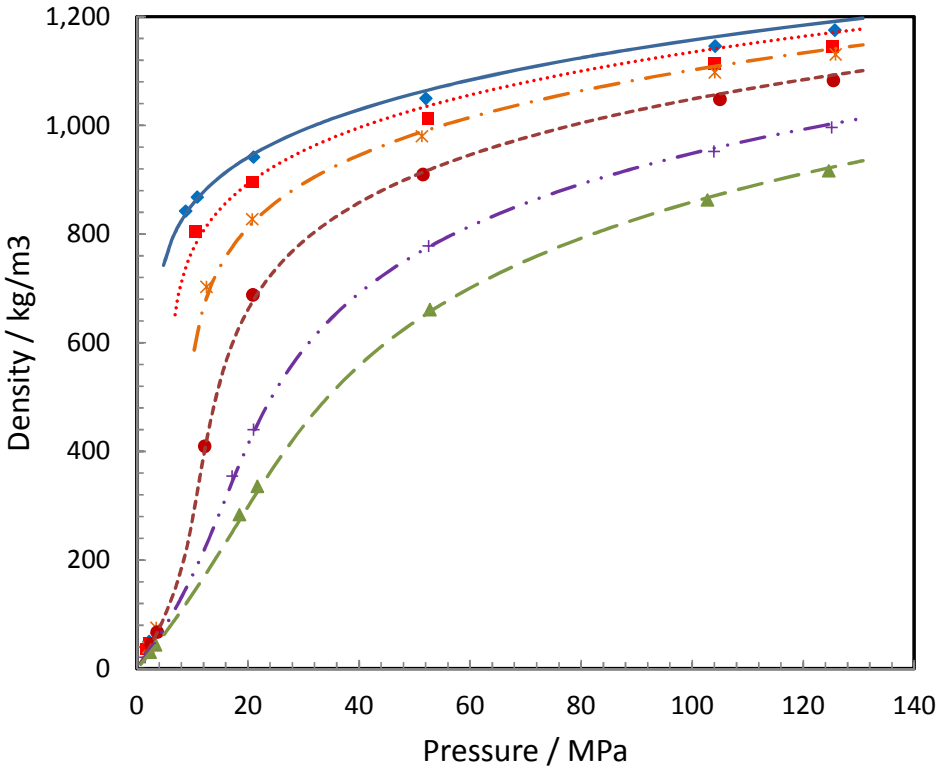

Figure 3.14 Experimental and modelling results of MIX 2, experimental / modelling (PR-CO_2) results: (♦/___) at 273.15 K, (■/….) at 283.15 K, (x/___.) at 298.15 K, (●/----) at 323.15 K, (+/___..) at 373.15 K and (▲/___ ___) at 423.15 K

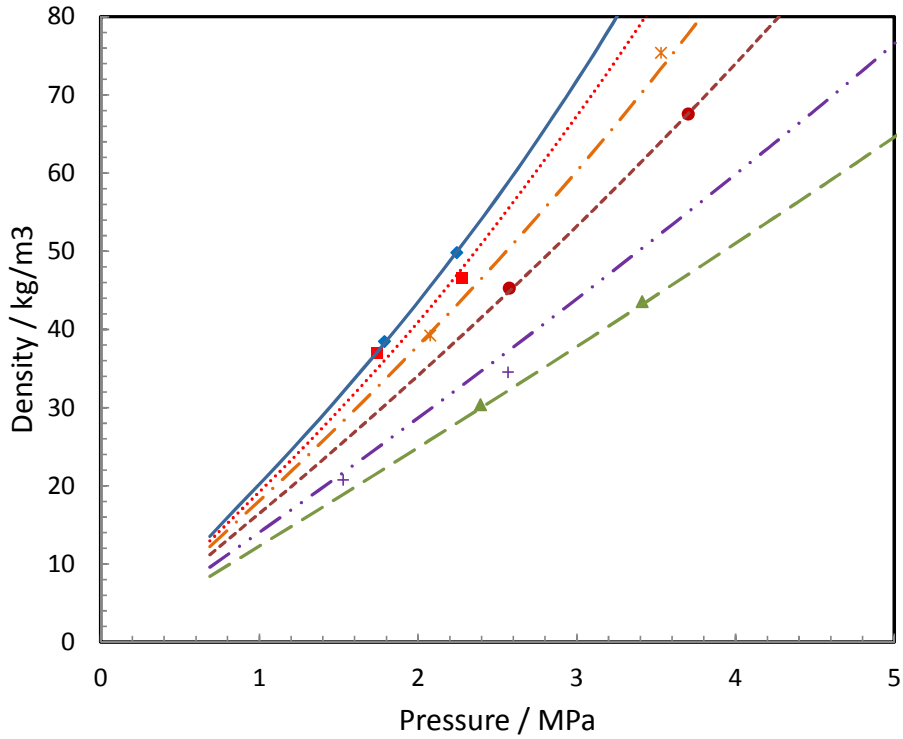

Figure 3.15 Experimental and modelling results of MIX 2 at low pressures, experimental / modelling (PR-CO_2) results: (♦/___) at 273.15 K, (■/….) at 283.15 K, (x/___.) at 298.15 K, (●/----) at 323.15 K, (+/___..) at 373.15 K and (▲/___ ___) at 423.15 K

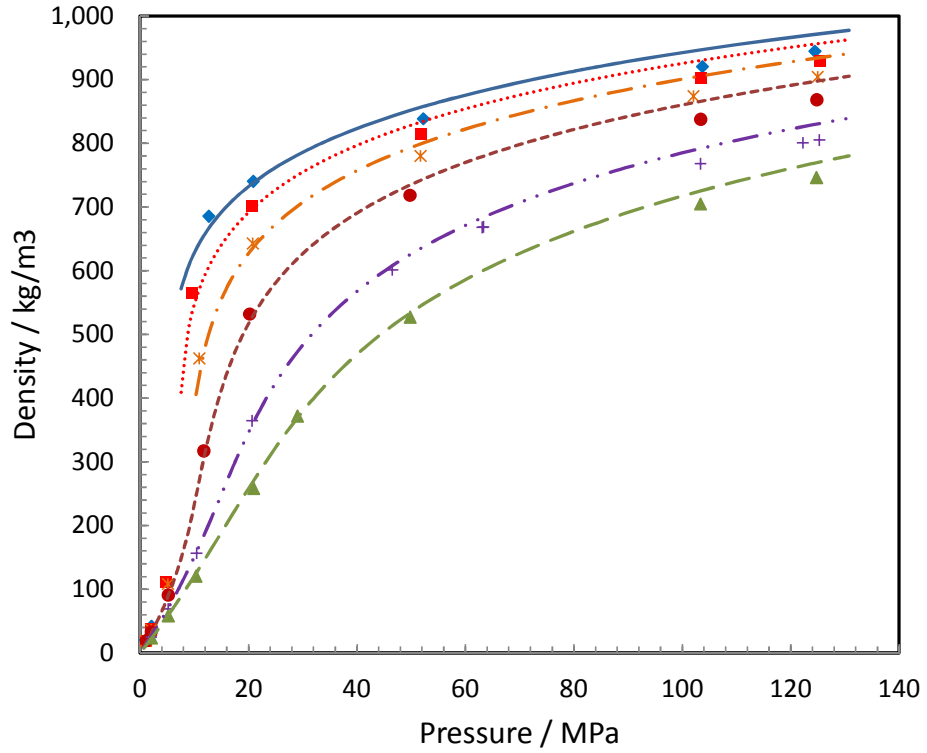

Figure 3. 16 Experimental and modelling results of MIX 3, experimental / modelling (PR-CO_2) results: (♦/___) at 273.15 K, (■/….) at 283.15 K, (x/___.) at 298.15 K, (●/----) at 323.15 K, (+/___..) at 373.15 K and (▲/___ ___) at 423.15 K

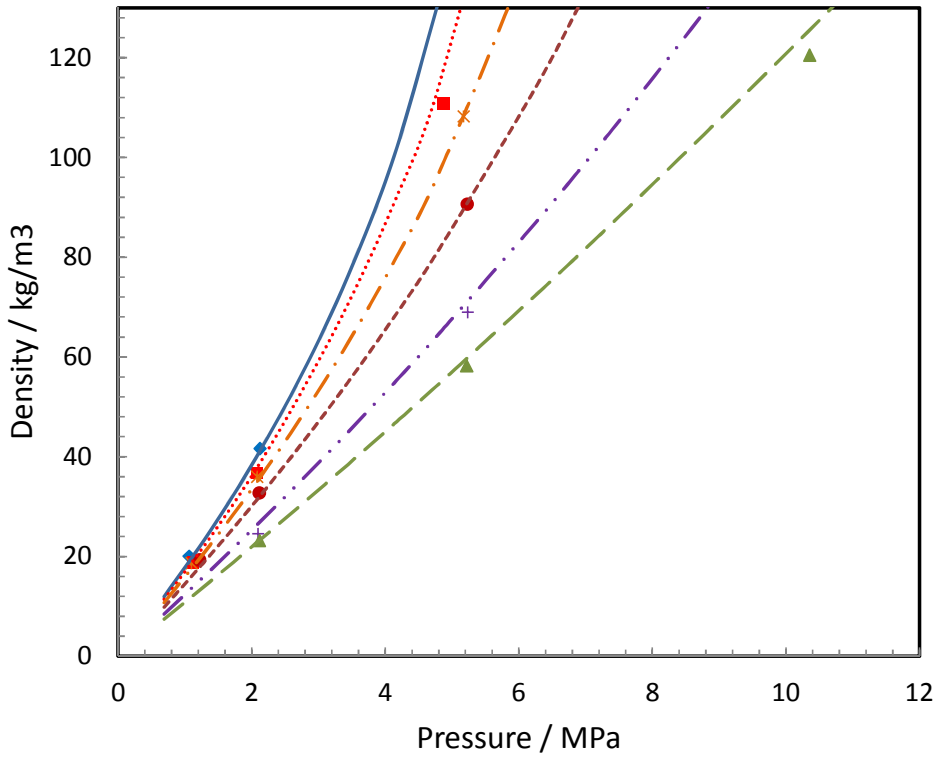

Figure 3.17 Experimental and modelling results of MIX 3 at low pressures, experimental / modelling (PR-CO_2) results: (♦/___) at 273.15 K, (■/….) at 283.15 K, (x/___.) at 298.15 K, (●/----) at 323.15 K, (+/___..) at 373.15 K and (▲/___ ___) at 423.15 K

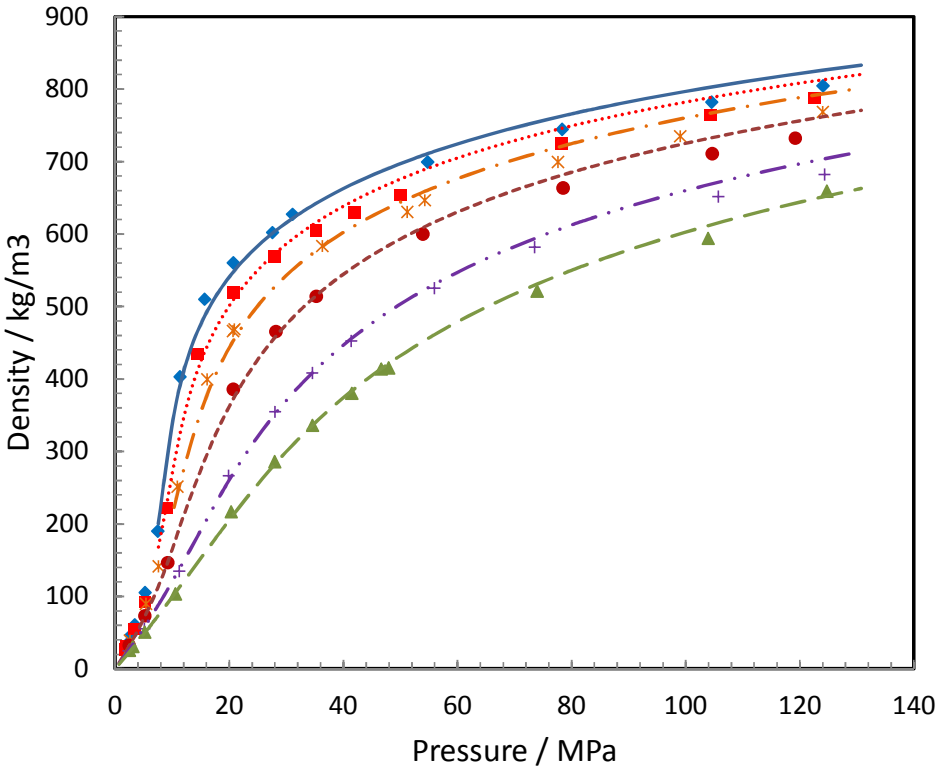

Figure 3.18 Experimental and modelling results of MIX 4, experimental / modelling (PR-CO_2) results: (♦/——) at 273.15 K, (■/….) at 283.15 K, (x/——.) at 298.15 K, (●/----) at 323.15 K, (+/——..) at 373.15 K and (▲/—— ——) at 423.15 K

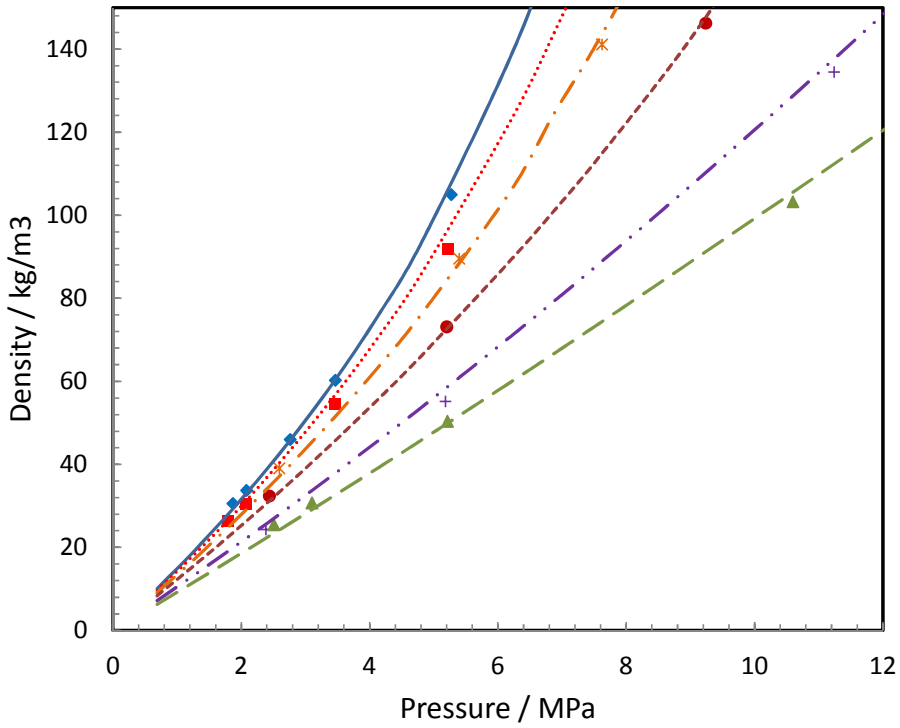

Figure 3.19 Experimental and modelling results of MIX 4 at low pressures, experimental / modelling (PR-CO_2) results: (♦/——) at 273.15 K, (■/….) at 283.15 K, (x/——.) at 298.15 K, (●/----) at 323.15 K, (+/——..) at 373.15 K and (▲/—— ——) at 423.15 K

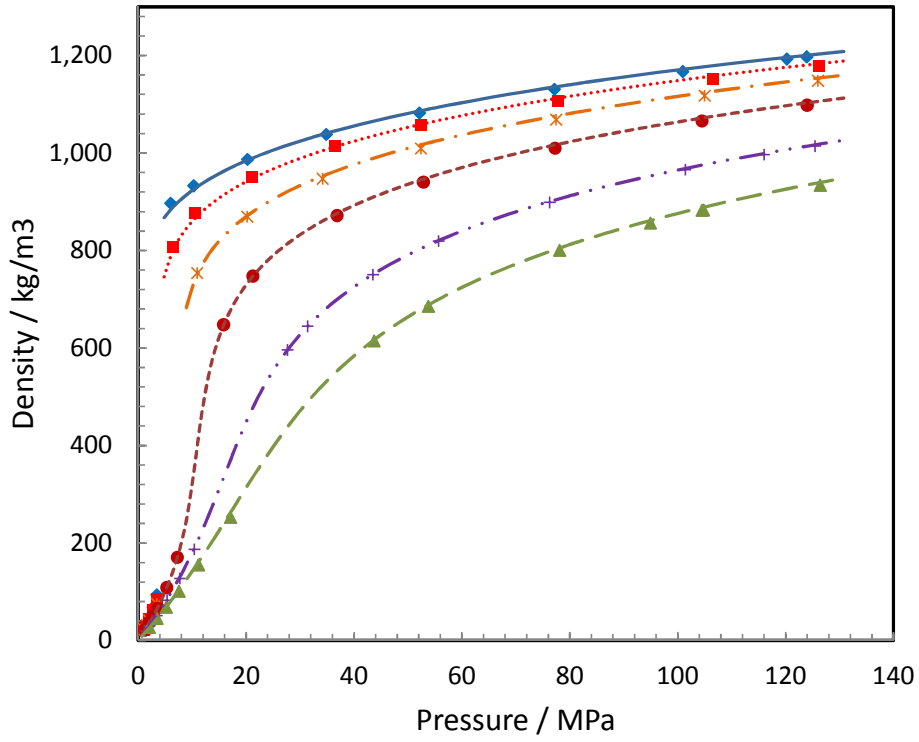

Figure 3.20 Experimental and modelling results of MIX 5, experimental / modelling (PR-CO_2) results: (♦/——) at 273.15 K, (■/….) at 283.15 K, (x/—.—) at 298.15 K, (●/----) at 323.15 K, (+/—..—) at 373.15 K and (▲/— —) at 423.15 K

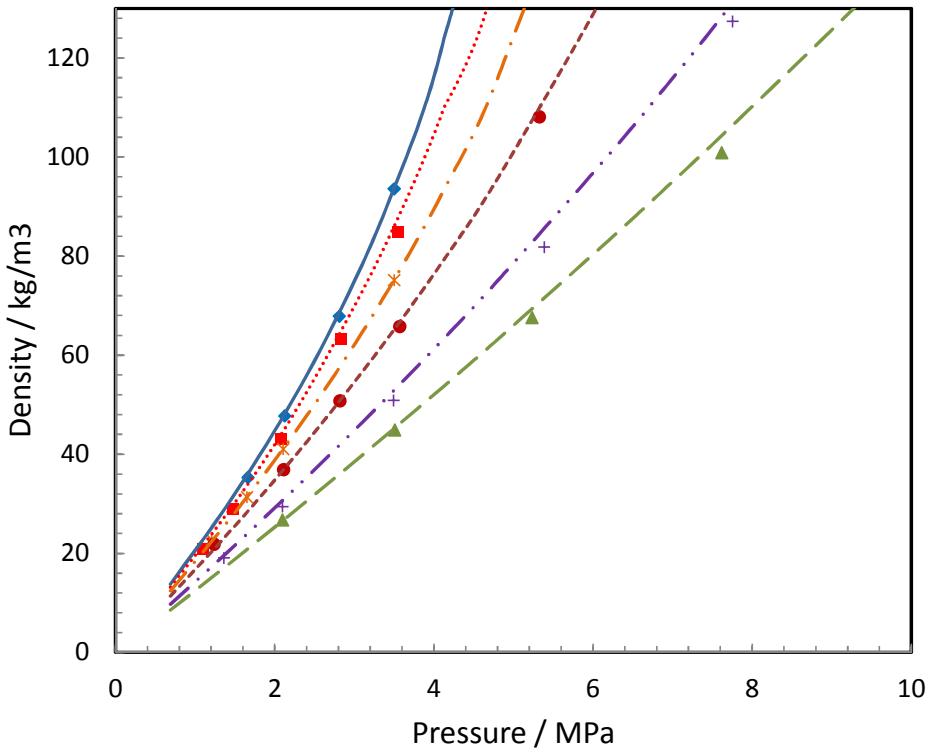

Figure 3.21 Experimental and modelling results of MIX 5 at low pressures, experimental / modelling (PR-CO_2) results: (♦/——) at 273.15 K, (■/….) at 283.15 K, (x/—.—) at 298.15 K, (●/----) at 323.15 K, (+/—..—) at 373.15 K and (▲/— —) at 423.15 K

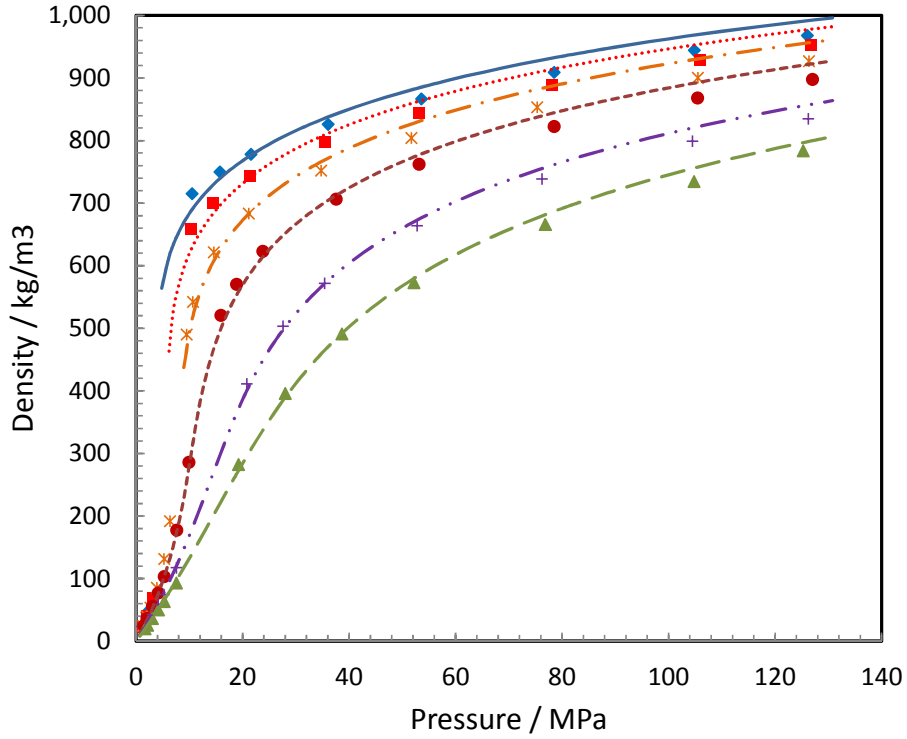

Figure 3.22 Experimental and modelling results of MIX 6, experimental / modelling (PR-CO_2) results: (♦/——) at 273.15 K, (■/….) at 283.15 K, (x/——.) at 298.15 K, (●/----) at 323.15 K, (+/——..) at 373.15 K and (▲/—— ——) at 423.15 K

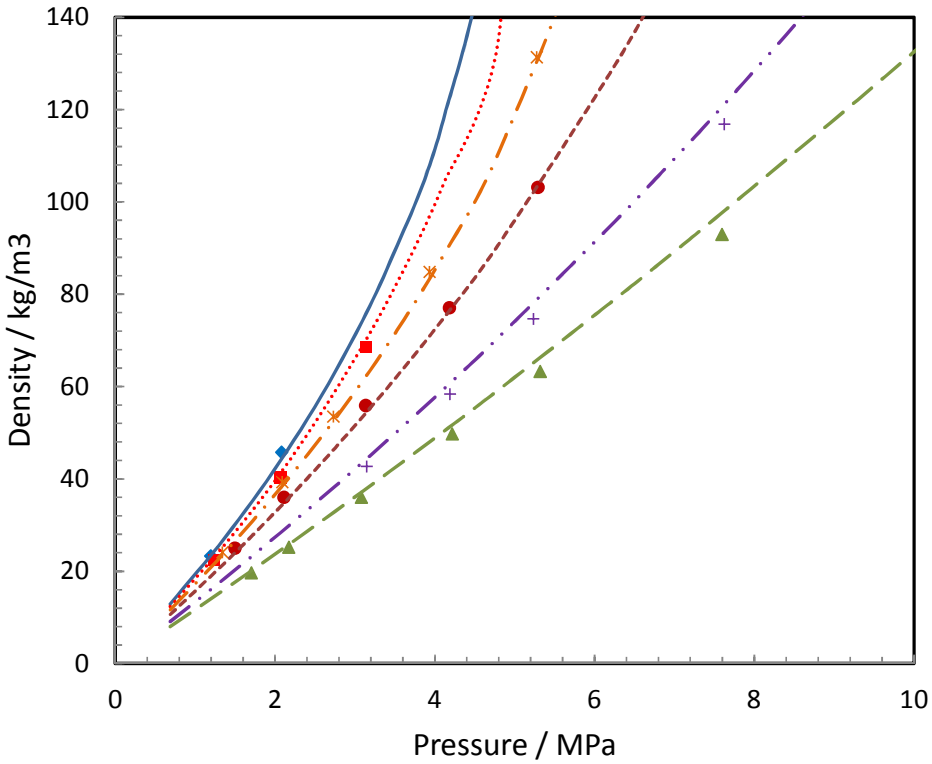

Figure 3.23 Experimental and modelling results of MIX 6 at low pressures, experimental / modelling (PR-CO_2) results: (♦/——) at 273.15 K, (■/….) at 283.15 K, (x/——.) at 298.15 K, (●/----) at 323.15 K, (+/——..) at 373.15 K and (▲/—— ——) at 423.15 K

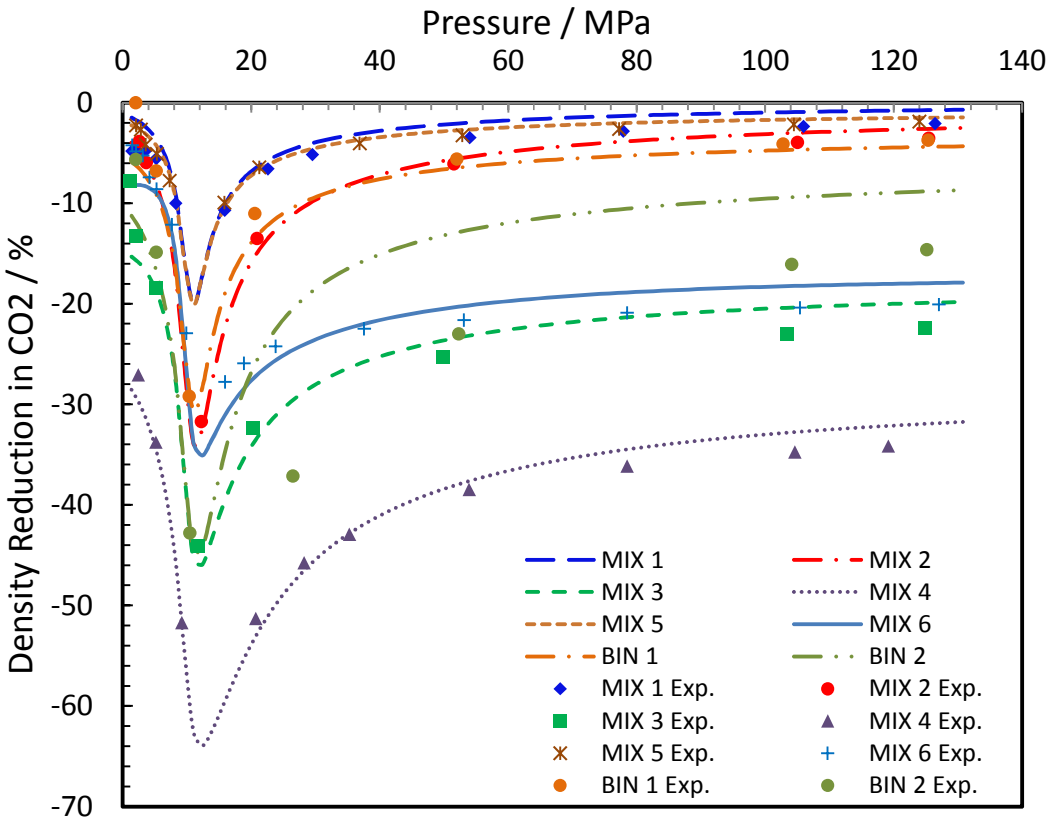

Figure 3.24 Density reduction of pure CO_2 at supercritical area, temperature 323.15 K (50 °C)

REFERENCES

[1] Y. Sanchez-Vicente, T. C. Drage, M. Poliakoff, J. Ke, and M. W. George, "Densities of the carbon dioxide+hydrogen, a system of relevance to carbon capture and storage," *Int. J. Greenh. Gas Control*, vol. 13, no. null, pp. 78–86, Mar. 2013.

[2] J. Koornneef, M. Spruijt, M. Molag, A. Ramirez, A. Faaij, and W. Turkenburg, "Uncertainties in risk assessment of CO2 pipelines," *Energy Procedia*, vol. 1, no. 1, pp. 1587–1594, Feb. 2009.

[3] Z. X. Zhang, G. X. Wang, P. Massarotto, and V. Rudolph, "Optimization of pipeline transport for CO2 sequestration," *Energy Convers. Manag.*, vol. 47, no. 6, pp. 702–715, Apr. 2006.

[4] P. Aursand, M. Hammer, S. T. Munkejord, and Ø. Wilhelmsen, "Pipeline transport of CO2 mixtures: Models for transient simulation," *Int. J. Greenh. Gas Control*, vol. 15, no. null, pp. 174–185, Jul. 2013.

[5] N. I. Diamantonis, G. C. Boulougouris, D. M. Tsangaris, M. J. El Kadi, H. Saadawi, S. Negahban, and I. G. Economou, "Thermodynamic and transport property models for carbon capture and sequestration (CCS) processes with emphasis on CO2 transport," *Chem. Eng. Res. Des.*, vol. null, no. null, Jul. 2013.

[6] C. A. Millat, J., Dymond, J.H., Nieto de Castro, "Transport of CO2 for carbon capture and storage — Pipelines International — The international pipeline magazine," *Cambridge University Press, IUPAC*, 2005. [Online]. Available: http://pipelinesinternational.com/news/transport_of_co2_for_carbon_capture_and_storage/040204/. [Accessed: 09-Sep-2013].

[7] R. Span and W. Wagner, "A New Equation of State for Carbon Dioxide Covering the Fluid Region from the Triple-Point Temperature to 1100 K at Pressures up to 800 MPa," *J. Phys. Chem. Ref. Data*, vol. 25, no. 6, p. 1509, Nov. 1996.

[8] M. J. O. Kunz, R. Klimeck, W. Wagner, "The GERG-2004 Wide-Range Equation of State for Natural Gases and Other Mixtures."

[9] H. Li and J. Yan, "Evaluating cubic equations of state for calculation of vapor–liquid equilibrium of CO2 and CO2-mixtures for CO2 capture and storage processes," *Appl. Energy*, vol. 86, no. 6, pp. 826–836, Jun. 2009.

[10] H. Li and J. Yan, "Impacts of equations of state (EOS) and impurities on the volume calculation of CO2 mixtures in the applications of CO2 capture and storage (CCS) processes," *Appl. Energy*, vol. 86, no. 12, pp. 2760–2770, Dec. 2009.

[11] H. Li, J. P. Jakobsen, Ø. Wilhelmsen, and J. Yan, "PVTxy properties of CO2 mixtures relevant for CO2 capture, transport and storage: Review of available experimental data and theoretical models," *Appl. Energy*, vol. 88, no. 11, pp. 3567–3579, Nov. 2011.

[12] K. Frey, M. Modell, and J. W. Tester, "Density-and-temperature-dependent volume translation for the SRK EOS: 2. Mixtures," *Fluid Phase Equilib.*, vol. 343, no. null, pp. 13–23, Apr. 2013.

[13] R. Thiery, J. Vidal, and J. Dubessy, "Phase equilibria modelling applied to fluid inclusions: Liquid-vapour equilibria and calculation of the molar volume in the CO2□CH4□N2 system," *Geochim. Cosmochim. Acta*, vol. 58, no. 3, pp. 1073–1082, Feb. 1994.

[14] T. A. Al-Sahhaf, "Vapor—liquid equilibria for the ternary system N2 + CO2 + CH4 at 230 and 250 K," *Fluid Phase Equilib.*, vol. 55, no. 1–2, pp. 159–172, Jan. 1990.

[15] C. J. Boyle TB, "Study determines best methods for calculating acid-gas density - Oil & Gas Journal." [Online]. Available: http://www.ogj.com/articles/print/volume-100/issue-2/drilling-production/study-determines-best-methods-for-calculating-acid-gas-density.html. [Accessed: 09-Sep-2013].

[16] H. Li , "Thermodynamic properties of CO2 mixtures and their applications in advanced power cycles with CO2 capture processes," Department of chemical engineering and technology, Royal institute of technology, Stockholm, 2008.

[17] M. Mantovani, P. Chiesa, G. Valenti, M. Gatti, and S. Consonni, "Supercritical pressure–density–temperature measurements on CO2–N2, CO2–O2 and CO2–Ar binary mixtures," *J. Supercrit. Fluids*, vol. 61, pp. 34–43, Jan. 2012.

[18] C. Rivas, S. T. Blanco, J. Fernández, M. Artal, and I. Velasco, "Influence of methane and carbon monoxide in the volumetric behaviour of the anthropogenic CO2: Experimental data and modelling in the critical region," *Int. J. Greenh. Gas Control*, vol. 18, pp. 264–276, Oct. 2013.

[19] B. Tohidi, R. W. Burgass, A. Danesh, and A. C. Todd, "Viscosity and Density of Methane + Methylcyclohexane from (323 to 423) K and Pressures to 140 MPa," *J. Chem. Eng. Data*, vol. 46, no. 2, pp. 385–390, Mar. 2001.

[20] M. M. Lemmon EW, Huber ML, "NIST standard reference database 23: reference fluid thermodynamic and transport properties – REFPROP version 8.0. Gaithersburg: National Institute of Standards and Technology, Standard Reference Data Program." 2007.

[21] I. Al-Siyabi, "Effect of Impurities on CO2 Stream Properties," Heriot-Watt University, 2013.

[22] S. Bell, *Measurement Good Practice Guide No. 11 (Issue 2), A Beginner's Guide to Uncertainty of Measurement*. National Physical Laboratory, 2001.

[23] K. Kashefi, A. Chapoy, K. Bell, and B. Tohidi, "Viscosity of binary and multicomponent hydrocarbon fluids at high pressure and high temperature conditions: Measurements and predictions," *J. Pet. Sci. Eng.*, vol. 112, pp. 153–160, Dec. 2013.

[24] E. C. Efika, R. Hoballah, X. Li, E. F. May, M. Nania, Y. Sanchez-Vicente, and J. P. Martin Trusler, "Saturated phase densities of (CO2 + H2O) at temperatures from (293 to 450) K and pressures up to 64 MPa," *J. Chem. Thermodyn.*, Jul. 2015.

[25] T. Ahmed, *Equations of State and PVT Analysis*. Elsevier, 2007.

[26] A. Péneloux, E. Rauzy, and R. Fréze, "A consistent correction for Redlich-Kwong-Soave volumes," *Fluid Phase Equilib.*, vol. 8, no. 1, pp. 7–23, Jan. 1982.

[27] R. D. McCarty, "A modified Benedict-Webb-Rubin equation of state for methane using recent experimental data," *Cryogenics (Guildf).*, vol. 14, no. 5, pp. 276–280, May 1974.

[28] W. M. Ely, James F. / Magee, J. W. / Haynes, *Thermophysical properties for special high CO2 content mixtures, Research Report RR-110, Gas Processors Association, Tulsa, OK*. 1987.

[29] B. a. Younglove and J. F. Ely, "Thermophysical Properties of Fluids. II. Methane, Ethane, Propane, Isobutane, and Normal Butane," *J. Phys. Chem. Ref. Data*, vol. 16. pp. 577–798, 1987.

[30] J. P. O. Bruce E. Poling, John M. Prausnitz, *Properties of Gases and Liquids, Fifth Edition*. McGraw-Hill Education, 2001.

[31] Chapoy, A.,Nazeri, M., Kapateh, M., Burgass, R., Tohidi, B., Coquelet, C., and Stringari, P."Impact of CommonImpurities on CO_2 Capture, Transport and Storage, 2011-2014 Programme, Final Report," 2015.

CHAPTER 4: VISCOSITY MEASUREMENTS AND MODELLING

In this chapter, the viscosities of CO_2-rich systems have been investigated. After a short introduction about the importance of transport properties, particularly viscosity, and a comprehensive literature review of the viscosity data available for CO_2-rich systems, the experimental apparatus and measurement procedures has been described and explained. The viscosities of various binary systems and multi-component mixtures were measured using the classical capillary tube technique. The tests were conducted at pressures from 1 MPa to pressure up to 140 MPa at various temperatures in gas, liquid and supercritical regions. In the modelling part, correlative and predictive models were evaluated using the measured experimental viscosity data. The correlative model, i.e., LBC model, then was tuned to match the experimental data and predictive models were modified by replacing the reference fluids. The predictive models in this work are based on corresponding states (CS) theory models. One reference fluid corresponding states models are Pedersen and CO_2-Pedersen; two reference fluid corresponding states models are Aasberg-Petersen (CS2) and CO_2-CS2 models and two models based on extended corresponding states (ECS) theory, SUPERTRAP and CO_2-SUPERTRAP models. The experimental and modelling results were reported. As the viscosity is a function of density, the effect of the mixture density on the mixture viscosity has been studied. Also, the viscosity reduction of pure CO_2 due to the presence of impurities in each system has been demonstrated. The main important conclusions were then summarised.

4.1 Introduction

The CCS process comprises of separating CO_2 from industrial sources, transporting to a storage location and then long-term isolation from the atmosphere. CCS has the potential to reduce the total CAPEX of mitigation and increase flexibility in reduction of greenhouse gas emissions [1].

Between the capture and storage, the CO_2 has to be transported by one or a combination of several transport media like truck, ship or pipelines. Transport by pipeline is preferred when transporting large quantities of carbon dioxide over longer distances [2]. Carbon dioxide transport pipelines play a key role in linking the capture and storage of CO_2 systems.

Existing CO_2 pipelines commonly contains 85-98% CO_2 with other impurities like methane, hydrogen sulphide, nitrogen, hydrogen, argon and ethane$^+$ light hydrocarbons depending on the capture technology employed for the CO_2 removal [3].

CO_2-rich pipelines are a key part of any carbon capture and storage (CCS) projects. Modelling phase behaviour, pressure drop and/or heat transfer in these pipelines are challenging due to the lack of thermo-physical properties of CO_2 in presence of impurities. As these properties have a significant impact on sizing of the equipment, therefore, it is crucial to investigate the impact of different impurities on the thermo-physical properties of CO_2-rich systems.

Accurate experimental data on the transport properties of the CO_2-rich systems are required to develop accurate predictive and correlative models in order to precisely design carbon capture, transport and storage processes. Transport properties have a major effect on the sizing of the equipment while the thermodynamic properties determine the feasibility of a given process. Accurate experimental data and models can lead to reduction in the CAPEX costs by cost-effective design and sizing of the equipment.

The importance of transport properties of CO_2-rich systems could be illustrated by considering the example of CO_2 transport pipelines. The power consumption and sizing of pumps/compressors to maintain flow through the pipelines is directly related to the pressure drop which is a function of Reynolds number and viscosity. In practice, if a viscosity model under-predicts viscosity by 20%, this will result in a 20% underestimation of the pump/compressor power consumption.

Another importance of the thermo-physical properties in CCS is the effect of them on flow measurements. The European Union Emission Trading Scheme (EU ETS) is an important plan to control the greenhouse gas emissions [49]. Regarding the safety concerns for leakage from the storage sites, measurement and monitoring would be a key element in CCS projects. The EU ETS regulations require an uncertainty of ±1.5% by mass on the quantity of stored CO_2 [50]. This requires a precise flow measurement of CO_2 stream with impurities. Unlike other transportable fluids by pipelines (e.g. natural gas, water and oil), the CO_2 critical point is very close to the ambient

temperature. On the other word, small gradients in pressure or temperature may have a significant change in the physical properties such as density, viscosity, compressibility and phase [51]. In this case, it will be difficult to achieve the ±1.5% uncertainty target. Also, there is a risk of phase change and multiphase flow can arise in the pipeline. Presence of both liquid and gas phases simultaneously may cause serious operational problems as well as great effect on the fluid physical properties and consequently flow measurement [52].

Since the CO_2 captured from power plants always contains impurities and the presence of these impurities will significantly change the transport properties compared to pure CO_2, therefore, the transport properties of CO_2-rich mixtures attract more attention in the industry [4].

Estimation of transport properties is of crucial interest to understand and estimate flow and heat transfer behaviour of fluids. Viscosity is a key transport property for pipeline systems as well as sub-surface and process systems. There are some methods to predict the viscosity of fluids. A widely used method to calculate the transport properties of fluids, particularly viscosity, is based on the predictions by using the corresponding states (CS) and extended corresponding states (ECS) concepts. The principle of corresponding states arises from the fact that properties of many fluids are functions of critical temperature and critical density. Extended corresponding states models modify the properties by employing extra shape factors, which are functions of reduced temperature, reduced density and the acentric factor, to account for deviations from the corresponding state principle and consequently to improve predictions [5].

Another common concept to determine the viscosity of fluids is the residual viscosity concept which is based on the observation that the difference between the dense phase viscosity and the dilute gas viscosity is function of density and approximately independent of temperature [6].

4.2 Literature review

Viscosity data for binary systems of carbon dioxide and other gases can be found in the open literature over different temperature ranges and CO_2 fractions; however most of the measurements were conducted at atmospheric pressure and in the gas phase. Furthermore, in the gas phase few data have been reported at pressures higher than 2.53 MPa.

Kestin and Leidenfrost [7] measured the viscosity of the CO_2-N_2 binary mixture using an in-house oscillating-disk viscometer at 20 °C (293.15 K) and pressure ranges of 1 to

21 atm (0.101 to 2.120 MPa). The estimated accuracy of 0.05% was reported for the measurements. Also, Kestin at al. [8] measured the viscosity of four binary gaseous mixture including CO_2-N_2 and CO_2-Ar at 20 °C and 30 °C (293.15 K and 303.15 K) and at pressures from 1 atm (0.101 MPa) to 25 atm (2.53 MPa). The measurements were performed using oscillating-disk viscometer with the accuracy of ±0.10%. Figure 4.1 and Figure 4.2 show the experimental viscosity of CO_2-N_2 and CO_2-Ar at various carbon dioxide concentrations and two temperatures, respectively.

Gururaja et al. [9] measured the viscosity of different CO_2 binary and ternary gas mixtures using the same method applied by Kestin et al. They have measured the viscosity of CO_2-O_2, CO_2-N_2 and CO_2-H_2 at atmospheric pressure (14.2 psia), ambient temperature (25 °C) and different CO_2 concentrations. They have also measured the viscosity of ternary systems CO_2-O_2-H_2 and CO_2-O_2-N_2 with different CO_2 mole percent all below 50% CO_2. Figure 4.3 shows the experimental viscosity of the binary gas mixtures.

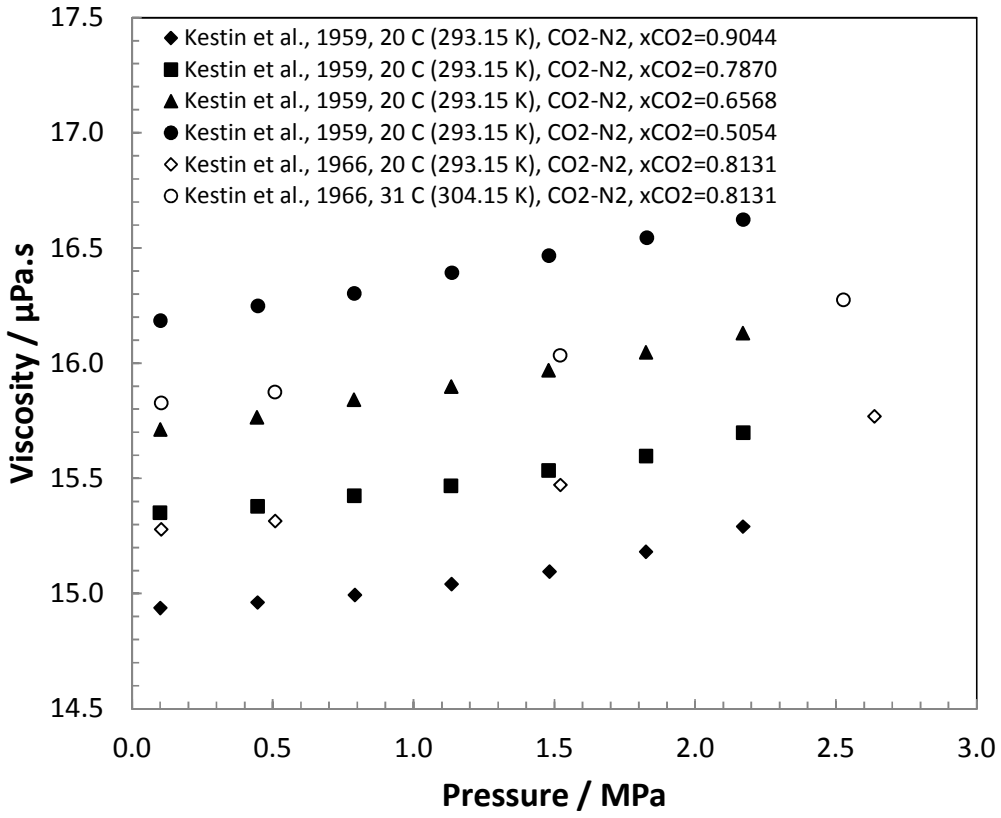

Figure 4.1 Viscosity of CO_2-N_2 measured by Kestin et al., at different mole fractions of CO_2

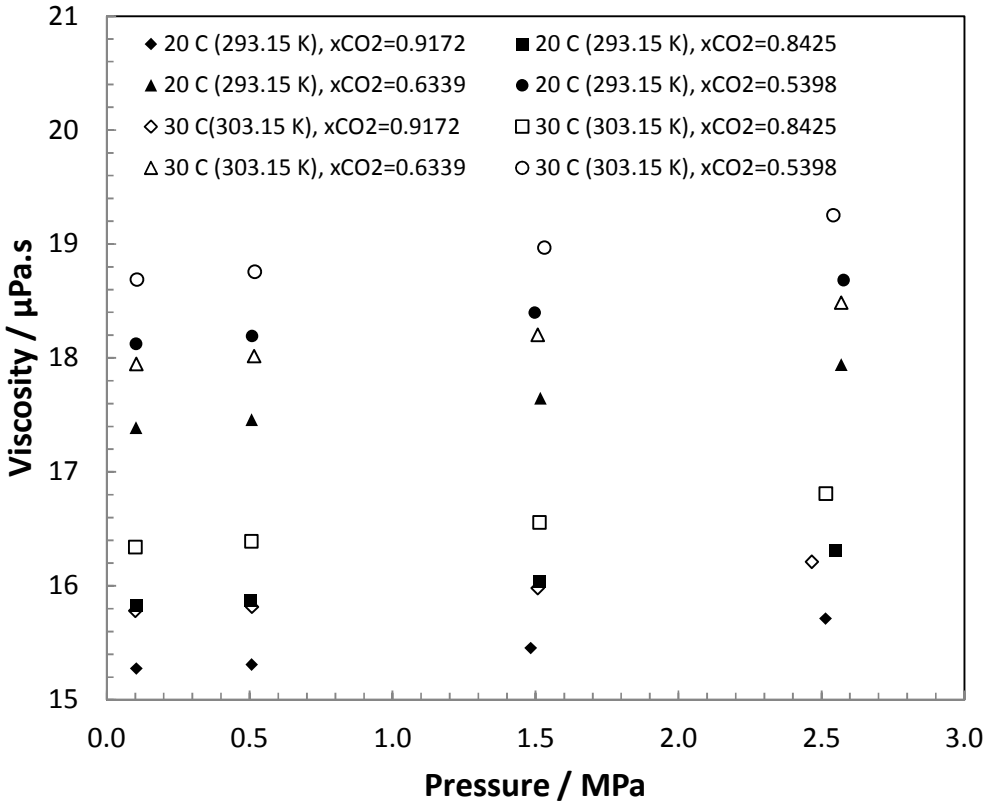

Figure 4.2 Viscosity of CO_2-Ar measured by Kestin et al., at different mole fractions of CO_2

Kestin and Ro [10] measured the viscosity of several binary systems including CO_2 with N_2, Ar, H_2 and CH_4 at atmospheric pressure and temperatures from 25 °C to 700 °C. They also have measured the viscosity of two ternary systems i.e.,CO_2-N_2-Ar and CO_2-N_2-CH_4. The accuracy of measurements was reported as ±0.10% at 25 °C and ±0.30% at 700 °C. Figure 4.4 shows the experimental results for high CO_2 content mixtures at various temperature ranges.

Kestin and Khalifa [11] performed measurements to obtain the viscosity of eighteen binary gas mixtures including CO_2-O_2 systems with high CO_2 contents. Figure 4.4 shows the results. The accuracy of the measurements was believed to be within ±0.10% - ±0.20% from room temperatures to 400 °C. Kestin and Ro [12] [13] also measured viscosity of CO_2-N_2O and CO_2-CO systems, and the results are shown on Figure 4.4, with an accuracy of ±0.30% for CO_2-N_2O and ±0.10% for CO_2-CO mixtures.

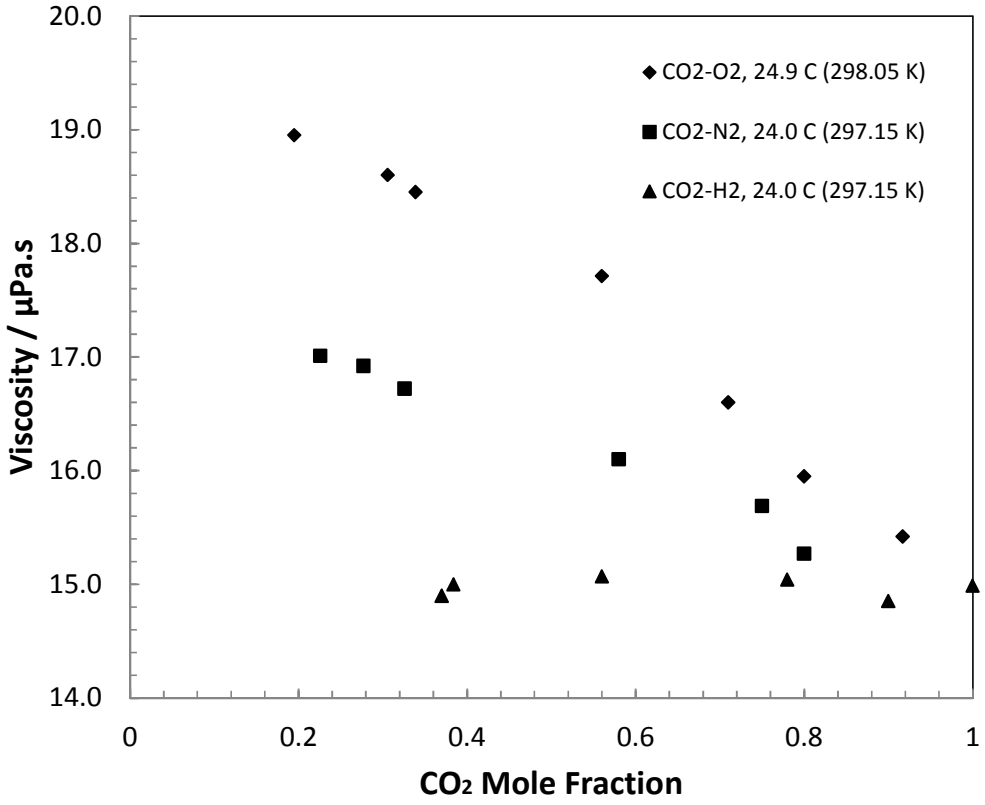

Figure 4.3 Viscosity of different CO_2 binary systems measured by Gururaja et al., 1967

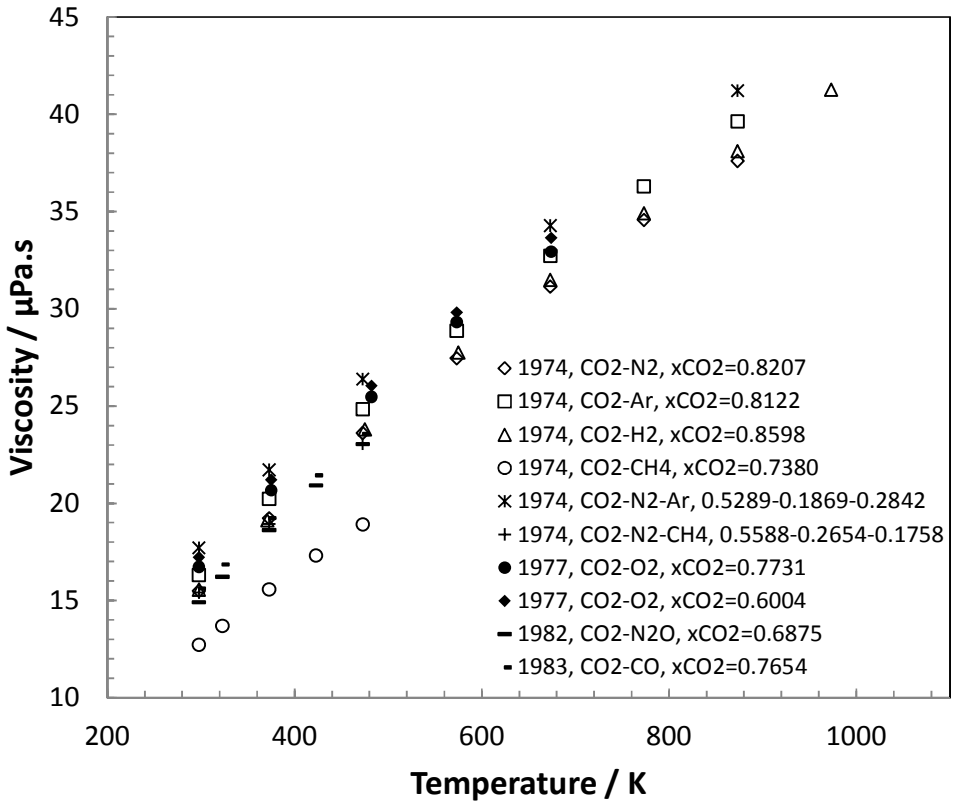

Figure 4.4 Viscosity of different high CO_2 content mixtures measured by Kestin et al., 1974 and 1977

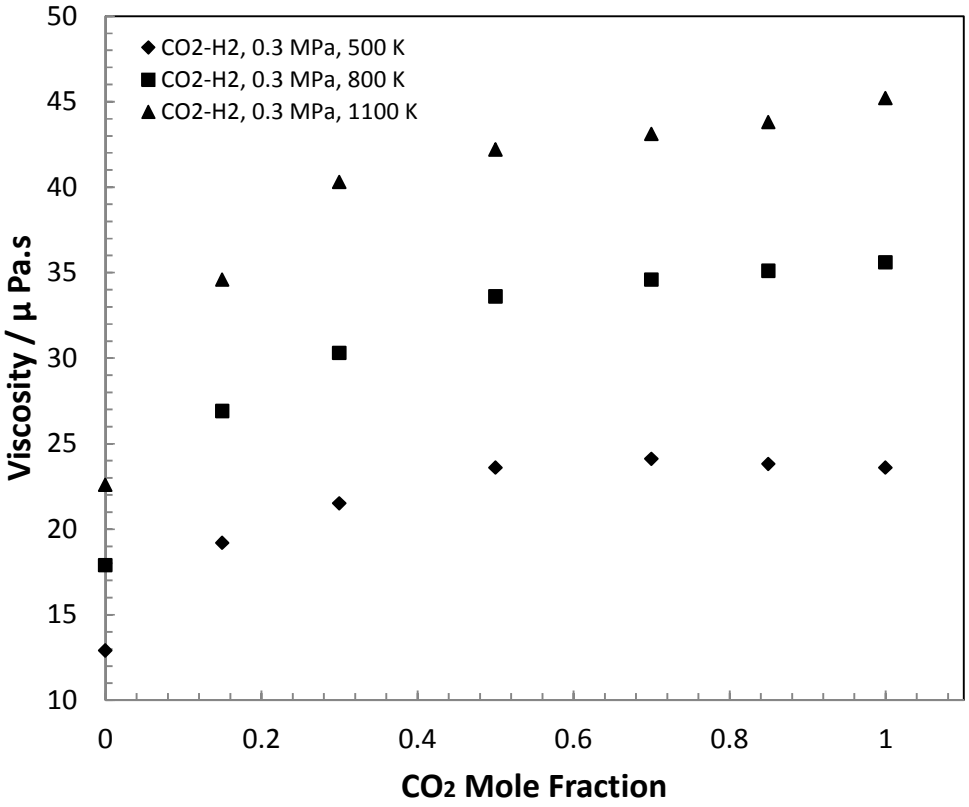

Figure 4.5 Viscosity of CO_2-H_2 measured by Mal'tsev et al., 2004

Mal'tsev et al. [14] carried out viscosity measurements on CO_2-H_2 mixtures at $3x10^5$ Pa at 500 K, 800 K and 1100 K with different CO_2 mole fractions with an accuracy of less than 3%. Figure 4.5 illustrates the results of their measurements.

Table 4.1 summarises the available experimental viscosity data of mixtures containing CO_2 in the literature. The ranges of temperature and pressure, CO_2 fraction, state of the fluid and uncertainty are listed in the table. As can be seen, most of the available viscosity data are in the gas phase and at atmospheric pressure.

Table 4.1 Available experimental viscosity data in the literature

Year	Phase	Substance	T (K)	P (MPa)	No. of Exp. Point	Uncertainty	Ref.
1936	G	CO_2-O_2-CO-H_2- CH_4-N_2	293.15-1287		17	---	[15]
1959	G	CO_2-N_2	293.15	0.101-2.12	45	±0.05%	[7]
1966	G	CO_2-N_2	293.15 & 303.15	0.101-2.53	12	±0.10%	[8]
		CO_2-Ar					
1967	G	CO_2-O_2	295.15-303.15	0.098	7	---	[9]
		CO_2-N_2			6		
		CO_2-H_2			5		
		CO_2-O_2-H_2			12		
		CO_2-O_2-N_2			11		
1968	G	CO_2-CH_4	293.15 & 303.15	0.101-2.53	32	±0.05%	[16]
		CO_2-Kr			24		
1974	G	CO_2-N_2	298.15-973.15	0.101	28	±0.1- ±0.3%	[10]
		CO_2-Ar			28		
		CO_2-He			56		
		CO_2-CH_4			20		
		CO_2-N_2-Ar			20		
		CO_2-N_2-CH_4			12		
1977	G	CO_2-O_2	298.15-674.15	0.101	15	±0.1- ±0.2%	[11]
1982	G	CO_2-N_2O	298.15-473.15	0.101	10	±0.3%	[12]
1983	G	CO_2-H_2	295.15-303.15	0.101	3	±0.10%	[17]
1983	G	CO_2-CO	298.15-473.15	0.101	10	±0.10%	[13]
1989	G	CO_2-Ar	310.15-521.15	0.101	19	±0.7%	[18]
2004	G	CO_2-H_2	500-800-1100	0.3	15	±3%	[14]

4.3 Experimental part

4.3.1 Experimental equipment

All viscosity measurements were conducted using an in-house designed and constructed set-up, a schematic view is shown in Figure 4.6 below. This setup has been designed to have a maximum working pressure of 200 MPa/29,000 psia and a maximum working temperature of 250 °C (523.15 K). The set-up is located inside an oven, manufactured by BINDER GmbH, capable of being used at temperatures from -70 °C to 200 °C (203.15 K to 473.15 K).

The set-up is comprised of two small cylinders, with volumes of 25 cm^3, connected to each other through a capillary tube with measured length of 14.78 metres and a temperature-dependent calibrated internal diameter. An oscillating U tube densitometer Anton Paar DMA-HPM is connected to the set-up. Two three-way valves, one on top of the cylinders connected to capillary tube and one on top of the densitometer, are installed to inject the sample inside the cylinders, tube system and densitometer. The base side of the two cylinders are connected to opposite sides of a push-pull, motor

driven mercury pump. This pump can move the sample fluid forwards and backwards between the two cylinders. There is also a hand pump connected to the system to control the pressure of the entire fluid system by injection and withdrawal of mercury. Two Quartzdyne pressure transducer (model: QS 30K-B) with the design pressure up to 207 MPa and standard uncertainty of ±0.02 MPa were connected to record the system pressure.

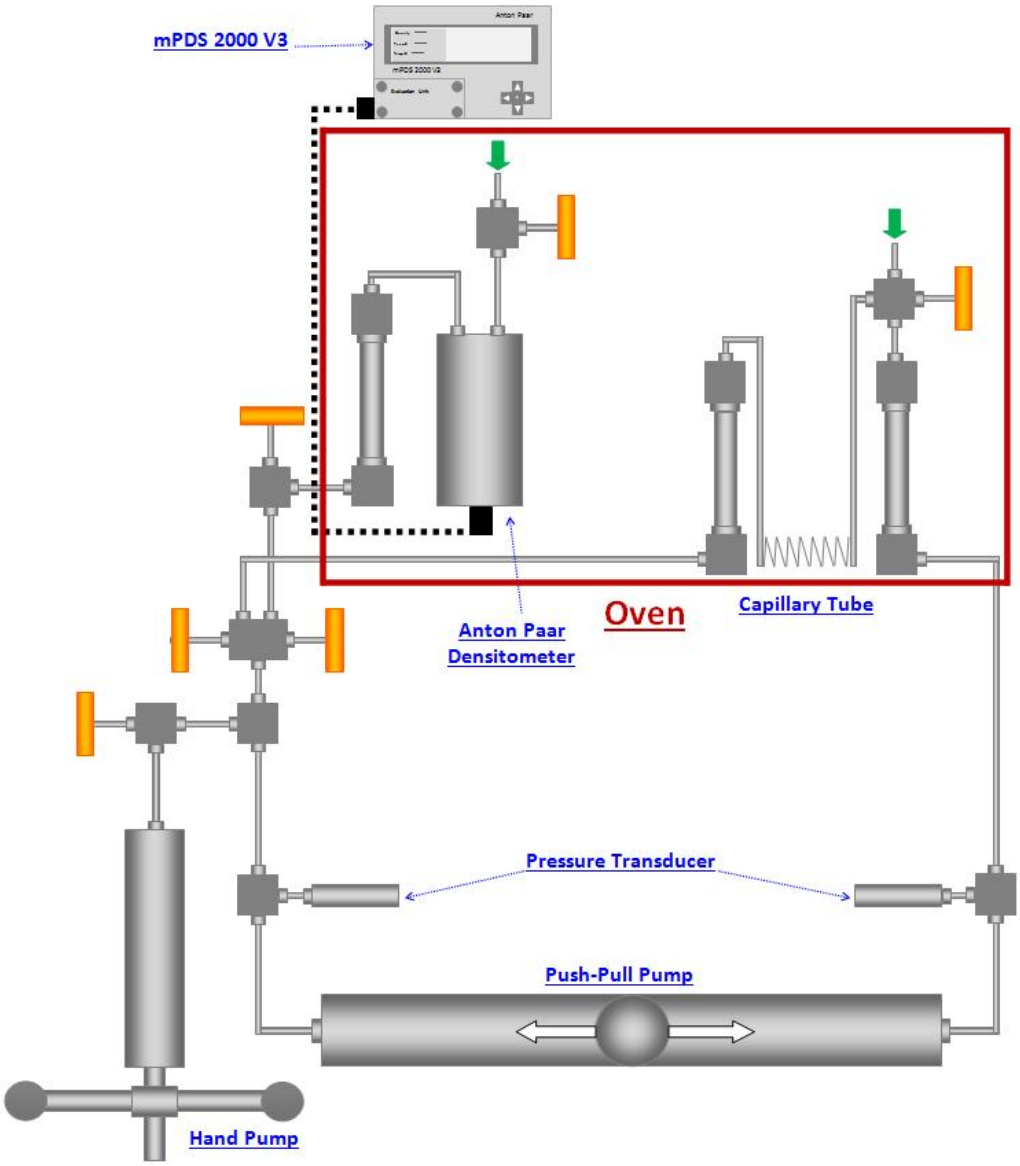

Figure 4.6 A schematic view of the viscosity experimental setup

4.3.2 Measurement procedure

The capillary tube viscosity measurement method has been employed to measure the viscosity of CO_2 systems with impurities. In each test, after applying vacuum to the entire system, the set-up was loaded with the sample mixtures through the injection

point at the top of the densitometer. Then after disconnecting the sample cylinder from the system, the sample fluid was pushed through the capillary tube into the other cylinder using the push-pull mercury pump. The temperature of the system was set to the desired condition and the desired pressure was achieved using the hand pump. Once conditions had stabilized, and after isolating the densitometer by closing the related valve, the sample was pumped through the capillary tube at a number of flow rates. To ensure the consistency of the measurements, at each pressure, viscosities were determined at two or three different flow rates and at each flow rate three readings were logged, so the reported viscosity data in this study are an average of at least six or nine separate readings.

Pumping the sample fluid through the capillary tube by piston pump resulted in a dynamic differential pressure that was monitored and recorded until stable. Then the pump was stopped to record the static differential pressure. The difference between the dynamic and static differential pressure was used as the pressure drop across the tube. To ensure laminar flow conditions, Reynolds numbers were checked for the flow rates in which the measurements were performed. Poiseuille equation, below, can relate the pressure drop across the capillary tube to the viscosity, tube characteristics and also flow rate for laminar flow:

$$\Delta P = \frac{128\ L\ Q\ \eta}{C\ \pi\ D^4} \qquad (4\text{-}01)$$

Where, ΔP is differential pressure across the capillary tube viscometer in psi, Q represents flow rate in cm^3/sec, L is length of the capillary tube in cm, D refers to internal diameter of the capillary tube in cm, η is viscosity of the flown fluid in cP and C is unit conversion factor equal to 6894757 if the above units are used.

The internal diameter of the tube was calibrated. The tube length changes with temperature but this had no noticeable influence on the measured viscosity. The set flow rate has no effect on the accuracy of the viscosity measurement. Only differential pressure as a variable in the above formulation can cause error in viscosity measurement. The usual variation in differential pressure measurement is 0.01 psi and this leads to ±1% of error in the calculated viscosity for those measured in this study.

4.3.3 Diameter calibration procedure

The diameter of the capillary tube were calibrated using the viscosity data of pure CO_2 from REFPROP v8.0 [19]. First, the pressure drop at desired pressures and temperatures were measured and the viscosity were calculated using assumed diameter and employing Hagen-Poiseuille equation. The assumed diameter, 0.29653 mm, were obtained from the previous experiments for the oil and gas fluids [20]. The new diameter for each isotherm were optimised by minimising the total deviations of experimental data from the viscosity data calculated by REFPROP v8.0 [19]. Then, a correlation were found by fitting a linear trend line on the optimised diameters versus temperature. Figure 4.7 shows the trend line which fitted optimised diameter on temperature. The calibrated diameter as a function of temperature can be found from Equation (4-01a). The results of diameter calibration can be found below in Table 4.2.

$$D = -1E\text{-}06\ T + 0.0298 \qquad (4\text{-}02)$$

where,

D is in cm and T is in K.

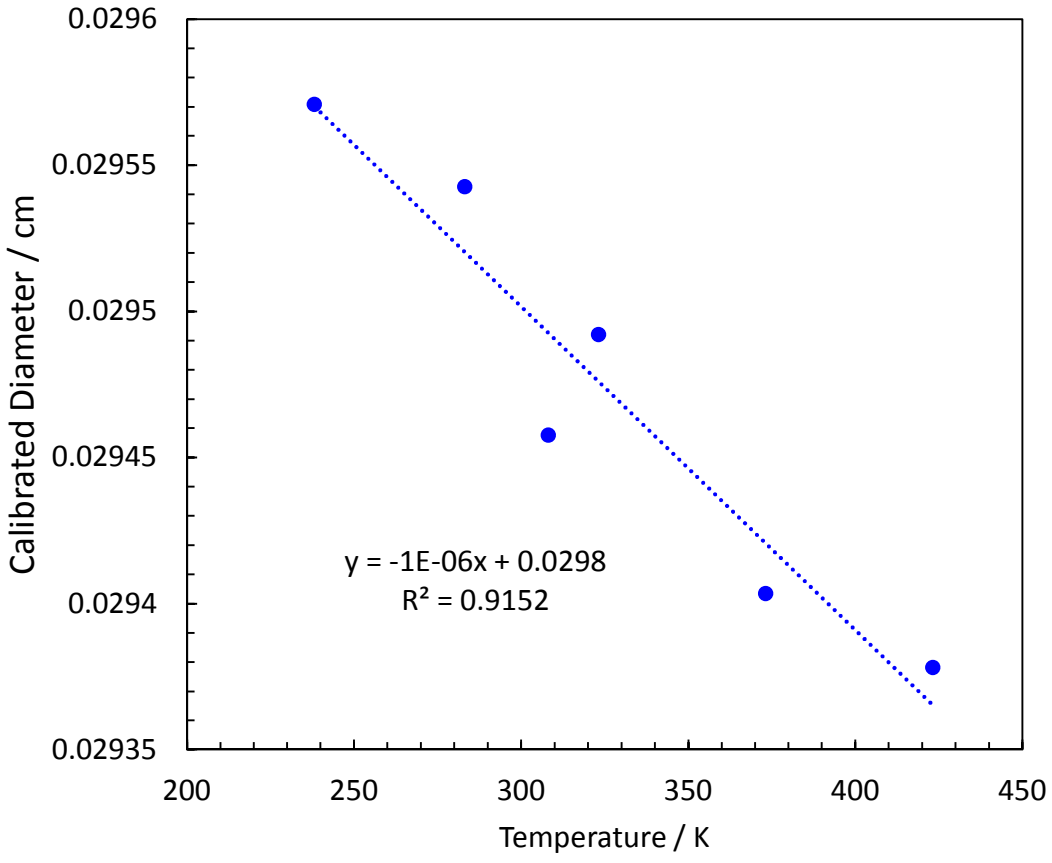

Figure 4. 7 Calibrating diameter versus temperature

Table 4. 2 Diameter calibration data using pure CO_2

					Viscosity (μPa.s)			Deviation (%)	
No	**Phase**	**T**	**P**	**Calib D**	**Exp. Old D**	**REFPROP**	**Exp.Calib D**	**Old D**	**Calib D**
		K	**MPa**	**cm**	**0.029653**				
		(±0.1)	**(±0.02)**						
1	Liq	238.2	10.22	0.02956	194.0	195.6	191.6	0.8	2.0
2	Liq	238.2	21.18	0.02956	212.0	214.7	209.4	1.2	2.4
3	Liq	238.2	51.70	0.02956	260.5	261.8	257.4	0.5	1.7
4	Liq	243.2	102.78	0.02956	320.4	313.7	316.3	2.2	0.8
5	Liq	243.2	126.15	0.02956	354.4	342.6	349.9	3.5	2.1
6	Liq	253.2	50.43	0.02955	218.2	216.9	215.0	0.6	0.9
7	Liq	253.2	102.56	0.02955	285.8	282.6	281.7	1.1	0.3
8	Liq	253.2	150.16	0.02955	348.7	337.7	343.8	3.3	1.8
9	Gas	273.2	1.05	0.02953	13.9	13.8	13.7	0.7	1.0
10	Gas	273.2	2.05	0.02953	14.1	14.1	13.9	0.5	1.2
11	Liq	273.2	10.47	0.02953	116.5	115.1	114.5	1.2	0.5
12	Liq	273.2	20.13	0.02953	134.0	132.0	131.7	1.5	0.2
13	Liq	273.2	52.05	0.02953	177.1	176.0	174.1	0.6	1.1
14	Liq	273.2	102.61	0.02953	234.5	234.0	230.5	0.2	1.5
15	Liq	273.2	150.44	0.02953	287.0	284.1	282.2	1.0	0.7
16	Gas	283.2	1.09	0.02952	14.6	14.3	14.3	2.1	0.2
17	Gas	283.2	2.07	0.02952	14.6	14.5	14.4	0.8	1.0
18	Liq	283.2	7.89	0.02952	93.1	92.5	91.4	0.7	1.2
19	Liq	283.2	23.07	0.02952	123.1	120.6	120.9	2.1	0.3
20	Liq	283.2	39.85	0.02952	146.5	143.9	143.8	1.8	0.1
21	Liq	283.2	59.01	0.02952	170.5	167.2	167.4	2.0	0.1
22	Liq	283.2	101.38	0.02952	216.6	213.2	212.7	1.6	0.2
23	Liq	283.2	151.26	0.02952	265.3	263.2	260.4	0.8	1.0
24	Gas	293.2	1.13	0.02951	14.9	14.8	14.6	0.7	1.3
25	Gas	293.2	2.05	0.02951	15.0	15.0	14.7	0.4	1.6
26	Liq	293.2	11.47	0.02951	88.3	85.4	86.5	3.3	1.3
27	Liq	293.2	20.37	0.02951	105.7	102.4	103.6	3.2	1.2
28	Liq	293.2	36.79	0.02951	132.0	125.9	129.5	4.9	2.8
29	Liq	293.2	68.99	0.02951	169.2	163.1	165.9	3.7	1.7
30	Liq	293.2	101.04	0.02951	199.2	196.0	195.3	1.6	0.3
31	Liq	293.2	141.60	0.02951	239.4	235.0	234.7	1.9	0.1
32	Gas	308.2	1.20	0.02949	15.7	15.5	15.3	0.9	1.3
33	Gas	308.2	2.07	0.02949	15.7	15.7	15.4	0.2	1.9
34	SC	308.2	11.33	0.02949	65.3	63.8	63.9	2.4	0.2
35	SC	308.2	22.09	0.02949	90.3	87.6	88.4	3.1	0.9
36	SC	308.2	34.97	0.02949	109.4	106.0	107.0	3.2	1.0
37	SC	308.2	68.93	0.02949	147.5	143.7	144.4	2.7	0.5
38	SC	308.2	101.20	0.02949	177.4	174.7	173.6	1.6	0.6
39	SC	308.2	150.52	0.02949	227.3	219.0	222.4	3.8	1.5
40	Gas	323.2	1.27	0.02948	16.5	16.3	16.1	1.6	0.7
41	Gas	323.2	2.05	0.02948	16.7	16.4	16.3	2.0	0.4
42	Gas	323.2	5.04	0.02948	17.8	17.4	17.4	2.2	0.2
43	SC	323.2	11.44	0.02948	40.7	41.2	39.8	1.1	3.4
44	SC	323.2	20.67	0.02948	72.8	70.5	71.1	3.3	0.8
45	SC	323.2	50.82	0.02948	114.7	109.9	111.9	4.4	1.9
46	SC	323.2	105.53	0.02948	164.5	160.8	160.6	2.3	0.1
47	SC	323.2	150.43	0.02948	200.0	198.6	195.3	0.7	1.6
48	Gas	373.2	1.48	0.02943	19.1	18.6	18.6	2.9	0.2
49	Gas	373.2	2.06	0.02943	19.3	18.7	18.7	3.3	0.2
50	Gas	373.2	5.15	0.02943	20.1	19.3	19.5	3.8	0.7

No	Phase	T	P	Calib D	Viscosity (µPa.s)			Deviation (%)	
					Exp. Old D	REFPROP	Exp.Calib D	Old D	Calib D
		K	MPa	cm	0.029653				
		(±0.1)	(±0.02)						
51	Gas	373.2	8.38	0.02943	21.6	20.8	21.0	4.1	1.0
52	SC	373.2	21.67	0.02943	41.5	41.0	40.2	1.2	1.8
53	SC	373.2	51.46	0.02943	80.7	78.0	78.3	3.4	0.3
54	SC	373.2	102.71	0.02943	122.9	117.8	119.2	4.3	1.2
55	SC	373.2	149.33	0.02943	154.8	149.9	150.1	3.2	0.1
56	Gas	423.2	1.71	0.02938	21.6	20.8	20.8	3.6	0.2
57	Gas	423.2	2.06	0.02938	21.6	20.9	20.8	3.6	0.2
58	Gas	423.2	5.13	0.02938	22.3	21.4	21.5	4.5	0.7
59	Gas	423.2	8.12	0.02938	23.1	22.2	22.3	4.3	0.4
60	SC	423.2	51.25	0.02938	61.7	60.6	59.4	1.9	1.8
61	SC	423.2	102.61	0.02938	98.6	94.5	95.0	4.4	0.5
62	SC	423.2	148.94	0.02938	125.6	121.0	121.0	3.8	0.0
Absolute Average Deviation (Total)								**2.2**	**1.0**
Total Deviations								**138.1**	**59.5**

4.3.4 Viscosity validation

The viscosities of pure CO_2 and MIX 1 have been measured at two isotherms to validate the experimental procedure by comparing to experimental data obtained by Al-Siyabi et al. [21] and Pensado et al [22]. They have measured the viscosity of pure CO_2 and MIX 1 at the desired temperatures at dense phase and at pressures up to 60 MPa. In this work, the viscosities of pure CO_2 and MIX 1 have been measured at two isotherms in gas, liquid and supercritical phases at pressures up to 150 MPa. The results are in good agreement with the literature. As can be seen, the accuracy of measurements for pure CO_2 is estimated to be ±2% in gas, liquid and supercritical phases.

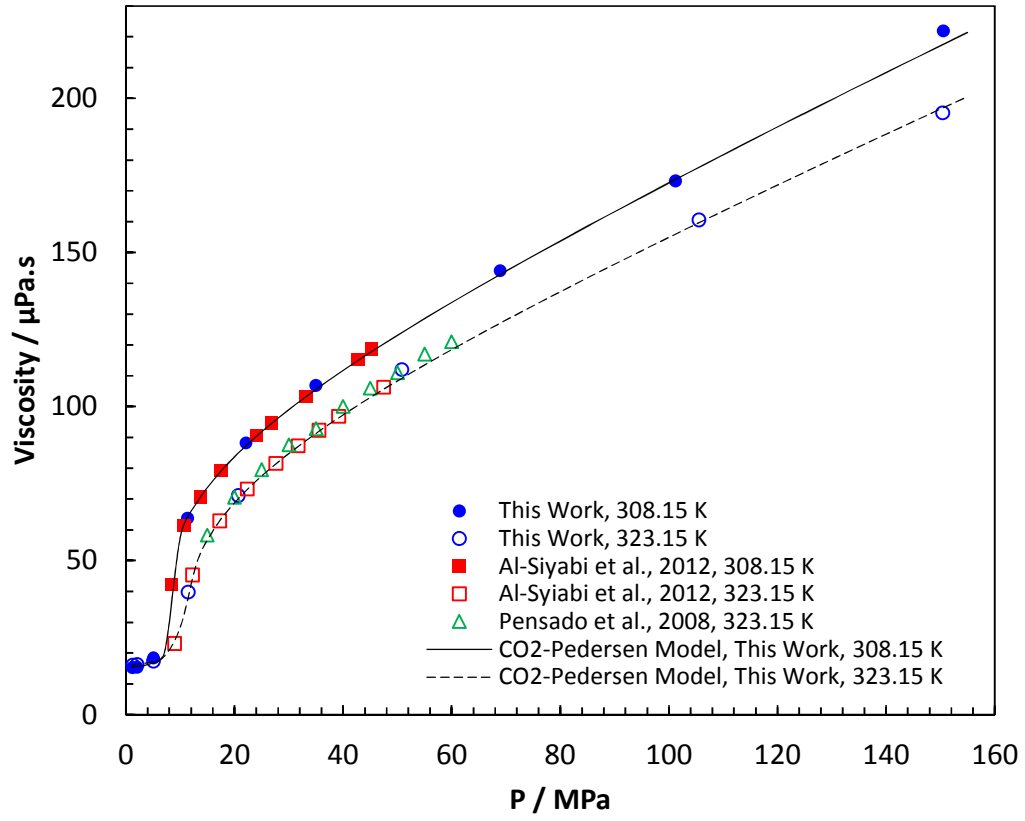

Figure 4. 8 Viscosity validation using pure CO_2

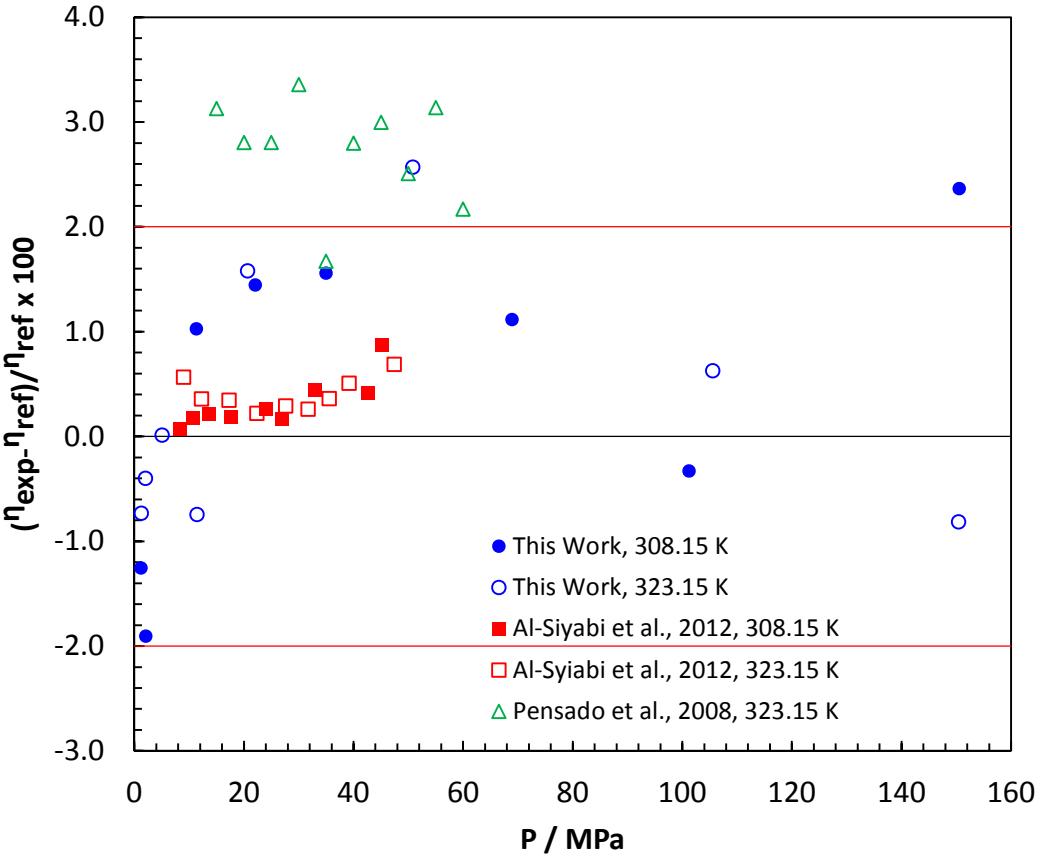

Figure 4. 9 Deviations of pure CO_2 viscosity at different isotherms

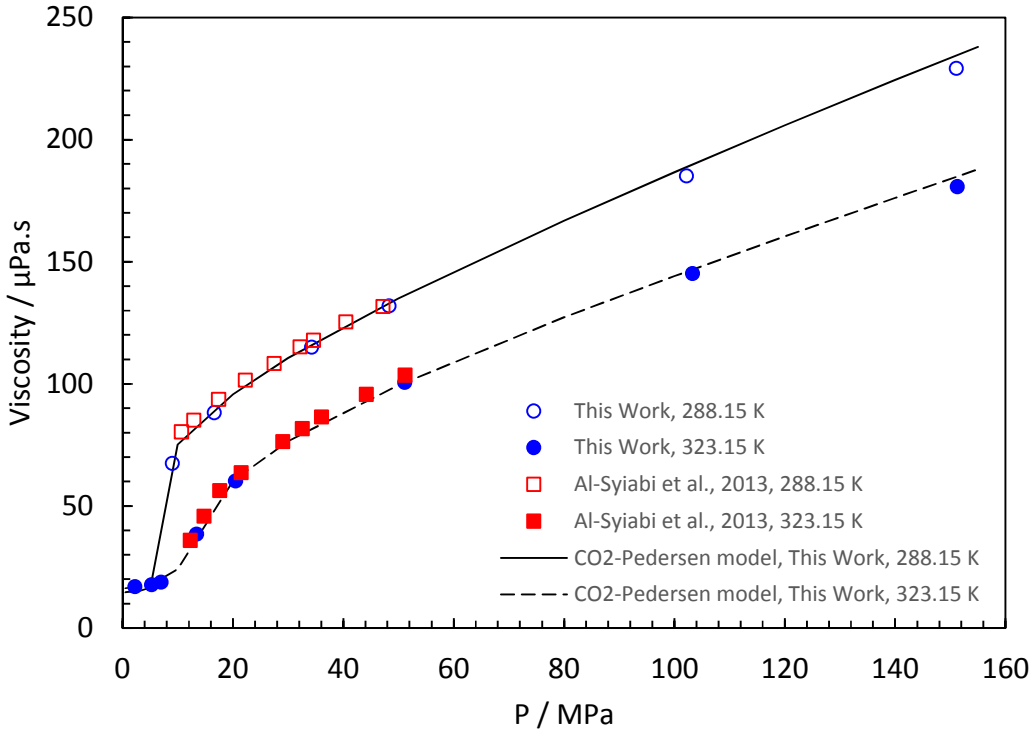

Figure 4. 10 Viscosity validation using MIX 1 at 2 different isotherms

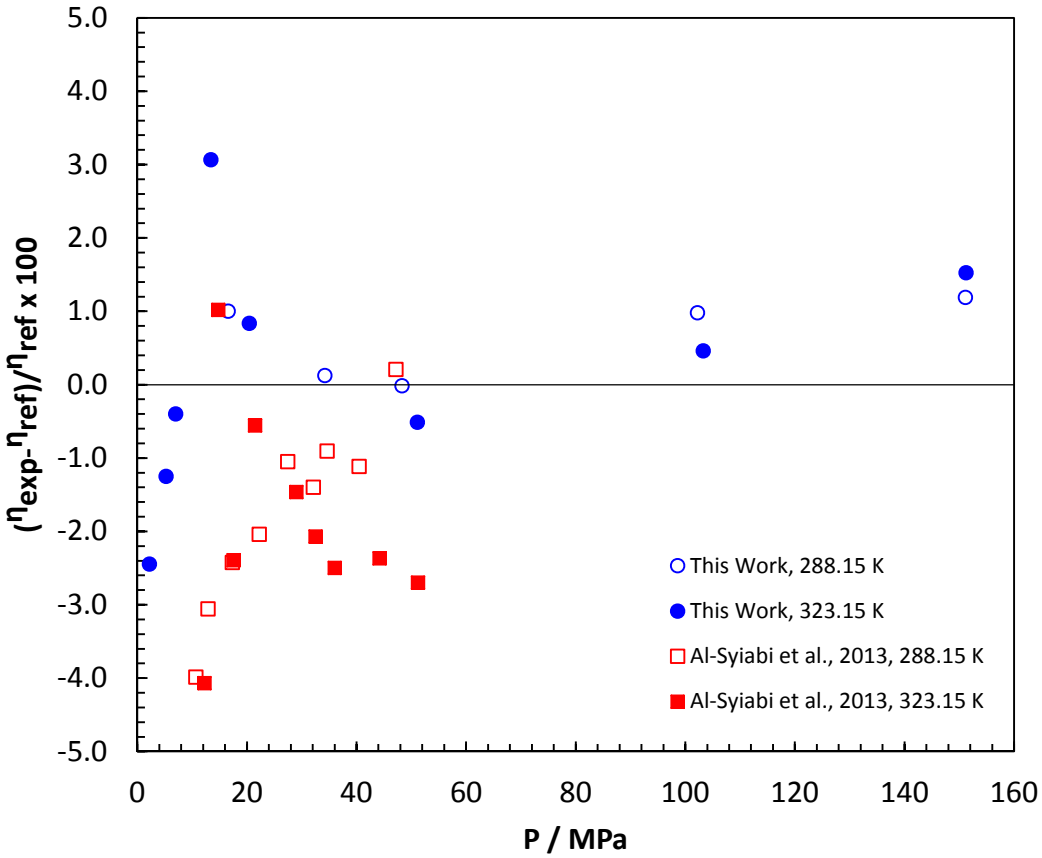

Figure 4. 11 Deviations of MIX 1 viscosity at two different isotherms

4.3.5 Viscosity measurement uncertainties

The type A and type B [23][24] uncertainty of each experimentally measured viscosity have been calculated. The type A uncertainties of the viscosity measurements, $u_A(\eta)$, have been calculated from the standard deviations of up to 9 independent measurements. In general, the uncertainties of viscosity measurements in the gas phase and at low temperatures are higher than the dense phase CO_2 mixtures.

$$u_A(\eta) = \frac{s}{\sqrt{n}} \quad (4\text{-}03)$$

$$s = \sqrt{\frac{\sum_{i=1}^{n}(x_i - \bar{x})^2}{n-1}} \quad (4\text{-}04)$$

where,

s: Estimated standard deviation

$\bar{x}$: The mean of viscosity readings

u_A: Estimated standard uncertainty type A

n: number of measurements

The type B uncertainty of viscosity measurements were calculated according to the random error propagation theory.

$$u_c(\eta) = \pm\sqrt{\left[\left(\frac{\partial\eta}{\partial\Delta p}\right).d\Delta p\right]^2 + \left[\left(\frac{\partial\eta}{\partial Q}\right).dQ\right]^2 + \left[\left(\frac{\partial\eta}{\partial D}\right).dD\right]^2 + \left[\left(\frac{\partial\eta}{\partial L}\right).dL\right]^2} \quad (4\text{-}05)$$

In the above equation, the uncertainty of viscosity due to each variable, $\left(\frac{\partial\eta}{\partial M}\right)$, can be calculated from the following equation. The variable M could be pressure drop, Δp, flow rate, Q, internal diameter, D, or tube length, L.

$$\left(\frac{\partial\eta}{\partial M}\right) = \frac{1}{2u(M)}\left(\eta_{M+u(M)} - \eta_{M-u(M)}\right) \quad (4\text{-}06)$$

The standard uncertainties for pressure drop, flow rate, diameter and tube length were estimated to be ±0.01 psi, ±0.02 cc/hr, ±0.00005 cm and ±5 cm, respectively. Standard uncertainties in temperature and pressure are $u(T)$ = ±0.1 K [20] and $u(p)$ = ±0.02 MPa [20] [25].

4.4 Viscosity modelling

Four models were tested and developed predict the viscosity of CO_2 dominated systems with impurities.

- Correlative models based on residual viscosity theory, i.e., Lohrenz–Bray–Clark (LBC) and Tuned CO_2-LBC
- Predictive models based on one-reference fluid corresponding states (CS) theory, i.e., Pedersen and CO_2-Pedersen
- Predictive models based on two-reference fluid corresponding states (CS) theory, i.e., Pedersen and CO_2-Pedersen
- Predictive models based on extended corresponding states (ECS) theory, i.e., SUPERTRAP and CO_2-SUPERTRAP

The LBC correlation is a fourth-degree polynomial equation in the reduced density which can be tuned to match experimental data. The CO_2-Pedersen model predicts the viscosity using the corresponding states theory, while the CO_2-TRAPP model predicts using the extended corresponding states theory by employing shape factors.

4.4.1 Residual viscosity theory

Due to the simplicity, flexibility and consistency, the most common empirical viscosity calculation method for both gases and liquids in petroleum industry which widely in use in compositional simulators, based on the residual viscosity concept, is a correlation derived by Jossi et al. (1962) [26] for pure fluids. The concept of residual viscosity is based on the experimental observation that the viscosity differences between the dense phase and dilute gas at a specific temperature is a function of its density [26]. This correlation is mostly referred as Lohrenz-Bray-Clark or LBC correlation in the oil and gas industry. Lohrenz et al. (1964) [27] extended the JST method [26] for calculating the viscosity of mixtures of naturally occurring hydrocarbons. The LBC correlation is a fourth-degree polynomial equation in the reduced density, $\rho_r = \frac{\rho}{\rho_c}$, presented in 1964. The equation is:

$$\left[\left(\eta - \eta^*\right)\xi + 10^{-4}\right]^{1/4} = a_1 + a_2\,\rho_r + a_3\rho_r^{\,2} + a_4\rho_r^{\,3} + a_5\rho_r^{\,4} \qquad (4\text{-}07)$$

where η^* is the viscosity of dilute gas, ξ the viscosity reducing parameter and ρ_r the reduced density. The constants a_1 to a_5, available from Table 4.3, were adjusted by Jossi et al. [26] using 11 pure compounds for reduced densities of 0.02 to 3.0. The

compounds were: carbon dioxide, sulphur dioxide, non-condensable gases (oxygen, argon, nitrogen) and hydrocarbons (methane, ethane, propane, i-butane, n-butane, and n-pentane). Also, these parameters can be tuned to match to the experimental data of CO_2 systems with impurities.

The following mixing rules were applied by Lohrenz et al. (1964) [27] in order to calculate the viscosity reducing parameter and dilute gas mixture viscosity. Low pressure mixture viscosity, η*, has been presented by Herning et al. (1936) [15].

Table 4.3 Parameters in the Original LBC Viscosity Correlation

LBC Parameters	Constants
a_1	0.10230
a_2	0.023364
a_3	0.058533
a_4	-0.040758
a_5	0.0093324

$$\xi = \frac{\left[\sum_{i=1}^{N} Z_i T_{ci}\right]^{1/6}}{\left[\sum_{i=1}^{N} Z_i M_i\right]^{1/2}\left[\sum_{i=1}^{N} Z_i P_{ci}\right]^{2/3}} \qquad (4\text{-}08)$$

$$\eta^* = \frac{\sum_{i=1}^{N} Z_i \eta_i^* \sqrt{M_i}}{\sum_{i=1}^{N} Z_i \sqrt{M_i}} \qquad (4\text{-}09)$$

N is the number of components in the mixture, T_{ci}, P_{ci}, M_i and Z_i are the critical temperature, critical pressure, molecular weight and mole fraction of component i, respectively. The critical density of mixtures can be determined from the critical molar volume.

$$\rho_c = \frac{1}{V_c} = \frac{1}{\sum_{i=1}^{N} Z_i V_{ci}} \qquad (4\text{-}10)$$

where, V_{ci} is the critical molar volume of component i in the mixture. The density of the mixture can be calculated by any equation of state. However, as the original model developed based on the experimental density, the accuracy of the model significantly depends on the input density. In this work, HydraFLASH 2.2.23 has been used to calculate the mixture density using the Peng-Robinson equation of state with the volume correction for CO_2 systems described in Chapter 3, Section 3.4.

The dilute component viscosity, η_i^*, for each component are expressed as a function of reduced temperature, T_r, by Stiel and Thodos, 1961 [28] as follows:

$$\eta_i^* = 34 \text{ x } 10^{-5} \frac{1}{\xi_i} T_{ri}^{0.94} \quad ; \quad \text{for } T_{ri} < 1.5 \tag{4-11}$$

$$\eta_i^* = 17.78 \text{ x } 10^{-5} \frac{1}{\xi_i} \left(4.58 T_{ri} - 1.67\right)^{5/8} \quad ; \quad \text{for } T_{ri} > 1.5 \tag{4-12}$$

where,

$$\xi_i = \frac{T_{ci}^{1/6}}{M_i^{1/2} P_{ci}^{2/3}} \tag{4-13}$$

It should be mentioned that the model predicts the natural gas and light hydrocarbons mixtures viscosity with a reasonable accuracy. This could be due to the fact that the parameters of the model were adjusted using light hydrocarbons. Dandekar et al. (1994) [29] showed that the model predicts the viscosity of hydrocarbon systems with a reasonable range of accuracy when the reduced densities are less than 2.5. The model under-predicts the fluid viscosity significantly for systems with reduced densities above 2.5. They also have modified the model for heavier hydrocarbon systems by introducing reduced temperature and molecular weight [29].

Furthermore, the residual viscosity in the main equation is supposed to be a function of reduced temperature. But, as shown by Vogel et al. (1998) [30] in the Figure 4.12 for propane, a temperature dependency can be observed for reduced densities above 3. A similar behaviour can be expected for other systems at higher reduced densities.

4.4.2 Corresponding states (CS) theory

One of the well-known semi-theoretical approaches to predict the transport property of fluids is corresponding states (CS) theory. The principle of corresponding states arises from the fact that properties of many fluids are similar as a function of critical temperature and critical density. [5]

4.4.2.1 One reference fluid

The model has been derived by Pedersen et al. (1987) [31] from the approach of Christensen and Fredenslund (1980) [32] presented for the thermal conductivity of gases and liquids. According to the corresponding states principles applied to viscosity,

the reduced viscosity, $\eta_r = \frac{\eta(P,T)}{\eta_c}$, for two components at the same reduced pressure, $P_r = \frac{P}{P_c}$, and reduced temperature, $T_r = \frac{T}{T_c}$, will be same.

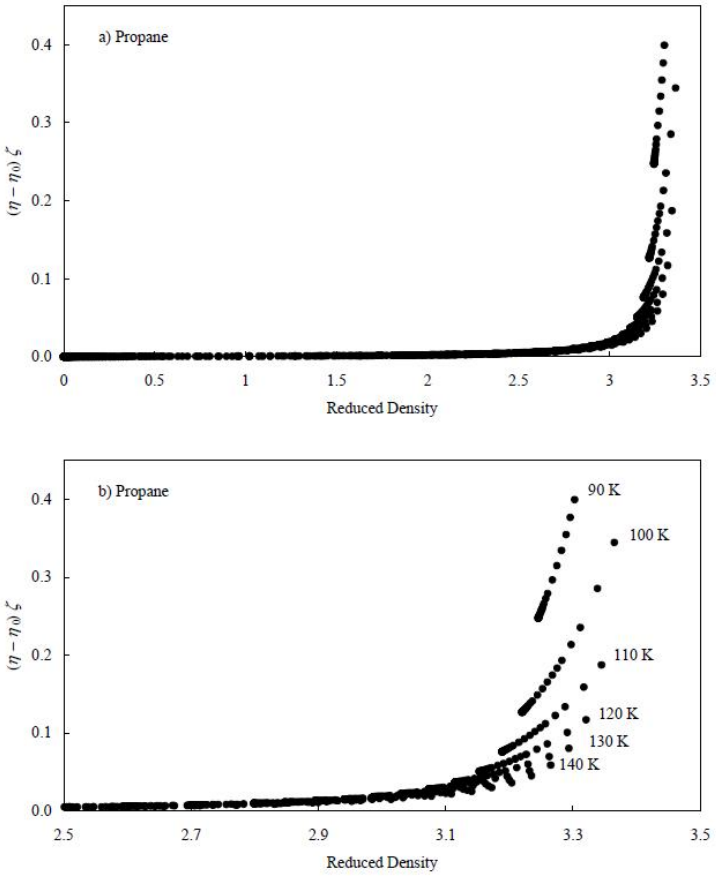

Figure 4.12 The reduced residual viscosity in the LBC model vs the reduced density for propane; a) Includes all data taken from Vogel et al. (1998) ranging from 90 K – 600 K and up to 1000 bar, b) Shows the temperature dependency at high reduced densities

$$\eta_r = f(P_r,\ T_r) \tag{4-14}$$

Based on the dilute gases considerations, viscosity at critical point can be approximated as:

$$\eta_c \approx \frac{P_c^{2/3} M^{1/2}}{T_c^{1/6}} \tag{4-15}$$

Where, M denotes the Molecular weight. Thus, the reduced viscosity can be expressed as:

$$\eta_r = \frac{\eta(P,T)}{\eta_c} = \frac{\eta(P,T)\ T_c^{1/6}}{P_c^{2/3} M^{1/2}} \tag{4-16}$$

For one component as a reference component if the function *f* in Equation (4-14) is known, it is possible to calculate the viscosity of any other components, such as component x, at any pressure and temperature. Thus,

$$\eta_x(P,T)=\frac{\left(\frac{P_{cx}}{P_{c0}}\right)^{\frac{2}{3}}\left(\frac{M_x}{M_0}\right)^{\frac{1}{2}}}{\left(\frac{T_{cx}}{T_{c0}}\right)^{\frac{1}{6}}}\eta_0\left(\frac{PP_{c0}}{P_{cx}},\frac{T\,T_{c0}}{T_{cx}}\right) \tag{4-17}$$

Where, 0 refers to the reference component. Methane with the viscosity data published by Hanley et al. (1975) [33] has been selected as the reference fluid in the original Pedersen Model.

Viscosity of methane as a function of temperature and density can be calculated from the equation below:

$$\eta(\rho,T)=\eta_0(T)+\eta_1(T)\rho+\Delta\eta'(\rho,T) \tag{4-18}$$

Where η_0, viscosity of the dilute gas, expressed as:

$$\eta_0(T)=\frac{GV(1)}{T}+\frac{GV(2)}{T^{2/3}}+\frac{GV(3)}{T^{1/3}}+GV(4)+GV(5)T^{1/3}+GV(6)T^{2/3}+GV(7)T+GV(8)T^{4/3}+GV(9)T^{5/3} \tag{4-19}$$

The following empirical equation is employed to obtain η_1:

$$\eta_1(T)=A+B\left(C-\ln\frac{T}{F}\right)^2 \tag{4-20}$$

Finally, the term $\Delta\eta'(\rho,T)$ is given by:

$$\Delta\eta'(\rho,T)=\exp\left(j_1+\frac{j_4}{T}\right)\left[\exp\left[\rho^{0.1}\left(j_2+\frac{j_3}{T^{3/2}}\right)+\theta\rho^{0.5}\left(j_5+\frac{j_6}{T}+\frac{j_7}{T^2}\right)\right]-1.0\right] \tag{4-21}$$

The density related parameter, θ, is:

$$\theta=\frac{\rho-\rho_c}{\rho_c} \tag{4-22}$$

The density of the reference fluid methane is calculated by a modified BWR equation in the 32 term form below.

$$P=\sum_{n=1}^{9}a_n(T)\rho^n+\sum_{n=10}^{15}a_n(T)\rho^{2n-17}e^{-\gamma\rho^2} \tag{4-23}$$

In the equations above, the constants GV(1) to GV(9), The constants A, B, C and F and j_1 to j_7 are given below in Table 4.4.

In this work, $CO_2$with the viscosity data published by Fenghour et al. [34] has been selected as the reference fluid for the CO_2 systems including impurities. The viscosity

of CO_2 as a function of density and temperature can be calculated from the following equation:

$$\eta(\rho,T) = \eta_0(T) + \Delta\eta(\rho,T) \tag{4-24}$$

Where, $\eta_0(T)$ is the zero-density viscosity and can be obtained from the following equation:

$$\eta_0(T) = \frac{1.00697\ T^{1/2}}{\Psi^*_\eta(T^*)} \tag{4-25}$$

Table 4.4 Constants in equations expressing corresponding states model for viscosities in 10^{-4} cP

Equation	Constant	Value
4-19	GV(1)	-2.090975 x 10^5
	GV(2)	2.647269 x 10^5
	GV(3)	-1.472818 x 10^5
	GV(4)	4.716740 x 10^4
	GV(5)	-9.491872 x 10^3
	GV(6)	1.219979 x 10^3
	GV(7)	-9.627993 x 10^1
	GV(8)	4.274152
	GV(9)	-8.141531 x 10^{-2}
4-20	A	1.696985927
	B	-0.133372346
	C	1.4
	F	168.0
4-21	j_1	-10.3506
	j_2	17.5716
	j_3	-3019.39
	j_4	188.73
	j_5	0.0429036
	j_6	145.29
	j_7	6127.68

In this equation, the zero-density viscosity is in units of μPa.s and temperature, T, in K. The reduced effective cross section, $\Psi^*_\eta(T^*)$, is represented by the empirical equation:

$$\ln\Psi^*_\eta(T^*) = \sum_{i=0}^{4} a_i (\ln T^*)^i \tag{4-26}$$

Where the reduced temperature, T^*, is given by

$$T^* = kT/\varepsilon \tag{4-27}$$

And the energy scaling parameter, $\frac{\varepsilon}{k} = 251.196$ K. The coefficients, a_i, are listed below in Table 4.5.

Table 4.5 Values of Coefficients a_i for CO_2

i	a_i
0	0.235156
1	-0.491266
2	5.211155×10^{-2}
3	5.347906×10^{-2}
4	-1.537102×10^{-2}

The second contribution in Equation (4-24) is the excess viscosity, $\Delta\eta(\rho,T)$, which describes how the viscosity can change as a function of density outside of the critical region. The excess viscosity correlation can be correlated as follows:

$$\Delta\eta(\rho,T) = d_{11}\rho + d_{21}\rho^2 + \frac{d_{64}\rho^6}{T^{*3}} + d_{81}\rho^8 + \frac{d_{82}\rho^8}{T^*} \qquad (4\text{-}28)$$

Where, the temperature is in Kelvin, the density in kg/m^3 and the excess viscosity in μPa.s. T* can be calculated from Equation (4-27). The coefficients are shown below in Table 4.6.

Table 4.6 Values of coefficients in d_{ij}

d_{ij}	Value
d_{11}	0.4071119×10^{-2}
d_{21}	0.7198037×10^{-4}
d_{64}	$0.2411697 \times 10^{-16}$
d_{81}	$0.2971072 \times 10^{-22}$
d_{82}	$-0.1627888 \times 10^{-22}$

The carbon dioxide density is calculated from a modified Benedict-Webb-Rubin equation of state, known as mBWR, in the form of 32 term equation presented by Younglove and Ely [35].

$$P = \sum_{n=1}^{9} a_n(T)\rho^n + \sum_{n=10}^{15} a_n(T)\rho^{2n-17}e^{-\gamma\rho^2} \qquad (4\text{-}29)$$

The corresponding states principle expressed in Equation (4-17) for the viscosity of pure components works well for mixtures. Pedersen et al. (1987) [31] have expressed the following expression to calculate the viscosity of mixtures at any pressure and temperature.

$$\eta_{mix}(P,T)=\frac{\left(\frac{P_{cmix}}{P_{c0}}\right)^{\frac{2}{3}}\left(\frac{M_{mix}}{M_0}\right)^{\frac{1}{2}}\left(\frac{\alpha_{mix}}{\alpha_0}\right)}{\left(\frac{T_{cmix}}{T_{c0}}\right)^{\frac{1}{6}}}\eta_0(P_0,T_0) \tag{4-30}$$

where

$$P_0=\frac{PP_{c0}}{P_{cmix}}\frac{\alpha_0}{\alpha_{mix}};\quad T_0=\frac{T\,T_{c0}}{T_{cmix}}\frac{\alpha_0}{\alpha_{mix}} \tag{4-31}$$

The critical temperature and pressure for mixtures, according to recommended mixing rules by Mo and Gubbins (1977) [36], can be found from

$$T_{cmix}=\frac{\sum_{i=1}^{N}\sum_{j=1}^{N}Z_iZ_j\left[\left(\frac{T_{ci}}{P_{ci}}\right)^{\frac{1}{3}}+\left(\frac{T_{cj}}{P_{cj}}\right)^{\frac{1}{3}}\right]^3\sqrt{T_{ci}T_{cj}}}{\sum_{i=1}^{N}\sum_{j=1}^{N}Z_iZ_j\left[\left(\frac{T_{ci}}{P_{ci}}\right)^{\frac{1}{3}}+\left(\frac{T_{cj}}{P_{cj}}\right)^{\frac{1}{3}}\right]^3} \tag{4-32}$$

$$P_{cmix}=\frac{8\sum_{i=1}^{N}\sum_{j=1}^{N}Z_iZ_j\left[\left(\frac{T_{ci}}{P_{ci}}\right)^{\frac{1}{3}}+\left(\frac{T_{cj}}{P_{cj}}\right)^{\frac{1}{3}}\right]^3\sqrt{T_{ci}T_{cj}}}{\left(\sum_{i=1}^{N}\sum_{j=1}^{N}Z_iZ_j\left[\left(\frac{T_{ci}}{P_{ci}}\right)^{\frac{1}{3}}+\left(\frac{T_{cj}}{P_{cj}}\right)^{\frac{1}{3}}\right]^3\right)^2} \tag{4-33}$$

The mixture molecular weight is found from

$$M_{mix}=1.304\ x10^{-4}\left(\bar{M}_w^{\,2.303}-\bar{M}_n^{\,2.303}\right)+\bar{M}_n \tag{4-34}$$

where $\bar{M}_w$ and $\bar{M}_n$ are the weight average and number average molecular weights, respectively.

$$\bar{M}_w=\frac{\sum_{i=1}^{N}Z_iM_i^{\,2}}{\sum_{i=1}^{N}Z_iM_i} \tag{4-35}$$

$$\bar{M}_n=\sum_{i=1}^{N}Z_iM_i \tag{4-36}$$

The parameter α for mixtures introduced by Pedersen et al. (1987) [31] to account for the effect of molecular size and density on viscosity. This parameter can be found in Equation (4-25) from:

$$\alpha_{mix} = 1.000 + 7.378 \text{ x } 10^{-3} \rho_r^{1.847} M_{mix}^{0.5173} \quad (4\text{-}37)$$

Also, α for the reference fluid can be found from the Equation (4-37) by replacing the molecular weight of the mixture with that of the reference fluid, carbon dioxide. The reduced density, ρ_r, is defined as:

$$\rho_r = \frac{\rho_0\left(\frac{PP_{c0}}{P_{cmix}}, \frac{T\,T_{c0}}{T_{cmix}}\right)}{\rho_{c0}} \quad (4\text{-}38)$$

The critical density of carbon dioxide, ρ_{c0}, is equal to 467.69 kg/m^3.

The modified Benedict–Webb–Rubin (mBWR) equation of state is applied for computing the reference fluid density, ρ_0, at the desired pressure and temperature of $\frac{PP_{c0}}{P_{cmix}}, \frac{T\,T_{c0}}{T_{cmix}}$. The mathematical equation of the MBWR has been presented by Younglove et al. [35].

The procedure below should be followed to calculate the viscosity of CO_2 systems with impurities by the corresponding state principle of Pedersen Model:

1 Calculate the T_{cmix}, P_{cmix} and M_{mix} from Equations (4-32), (4-33) and (4-34), respectively.

2 Obtain CO_2 density at $\frac{PP_{c0}}{P_{cmix}}, \frac{T\,T_{c0}}{T_{cmix}}$ from the MBWR EOS and calculate reduced density from Equation (4-38)

3 The mixture parameter, α_{mix}, and α_0 should be calculated from Equation (4-37)

4 The reference pressure and temperature, P_0 and T_0, should be calculated from Equation (4-31)

5 Calculate the CO_2 reference fluid, $\eta_0(P_0, T_0)$, in Equation (4-30) from Equation (4-24)

6 Calculate the mixture viscosity from Equation (4-30)

4.4.2.2 Two reference fluids

A viscosity model based on corresponding states theory with two reference fluids have been proposed by Aasberg-Petersen et al. [37] to predict the viscosity of both gases and liquid systems for hydrocarbons. They have selected methane and n-decane as the reference fluids.

$$\eta_{mix} = \eta_{C,mix} \frac{\eta_1(T_1,P_1)}{\eta_{C,1}} \left(\frac{\eta_2(T_2,P_2).\eta_{C,1}}{\eta_1(T_1,P_1).\eta_{C,2}} \right)^{K_{CS}} \quad (4\text{-}39)$$

where K_{CS} is an interpolation parameter function of molecular weights of the mixture and reference fluids.

$$K_{CS} = \frac{M_{w,mix} - M_{w,1}}{M_{w,2} - M_{w,1}} \quad (4\text{-}40)$$

Et-Tahir (1993) [38] investigated the effect of interpolation parameter, K_{CS}, by introducing other parameters, i.e., acentric factor, critical pressure and temperature, as shown on the equation below.

$$K_{CS} = \frac{1}{4} \left(\frac{M_{w,mix} - M_{w,1}}{M_{w,2} - M_{w,1}} + \frac{\omega_{mix} - \omega_1}{\omega_2 - \omega_1} + \frac{P_{C,mix} - P_{C,1}}{P_{C,2} - P_{C,1}} + \frac{T_{C,mix} - T_{C,1}}{T_{C,2} - T_{C,1}} \right) \quad (4\text{-}41)$$

4.4.3 Extended corresponding states (ECS) theory

The method was proposed by Hanley (1976) [39] and also by Mo & Gubbins (1974, 1976) [40] [41]. It led to a computer programme known as TRAPP (TRAnsport Properties Prediction) [42]. The method is also the basis for NIST Standard Reference Database 4 (SUPERTRAPP, [43]). The method can predict viscosity and thermal conductivity of pure fluids and their mixtures over the entire phase range from gas to dense liquid.

The original version of the TRAPP method [42] was used to estimate the viscosity and thermal conductivity of fluids and their mixtures and employed methane as a reference fluid. In the most recent version presented below for pure fluids, propane is the reference fluid. Other reference fluids can be chosen. For example, Huber and Ely (1992) [44] use R134a as the reference fluid to predict transport properties of refrigerants.

In the original TRAPP method, the residual viscosity of a pure fluid at density ρ and temperature T is related to the residual viscosity of the reference fluid, propane, at a corresponding state point of (ρ_0, T_0) [5]:

$$\Delta\eta_{mix}\left(\rho, T, \{x_i\}\right) \equiv \Delta\eta_x\left(\rho, T\right) \equiv \Delta\eta_R\left(\rho_0, T_0\right) F_\eta \quad (4\text{-}42)$$

The subscript x denotes the pure fluid of interest while the subscript R refers to the reference fluid. The state points T_0 and density ρ_0 are calculated by:

$$T_0 = \frac{T}{f_x} \quad (4\text{-}43)$$

$$\rho_0 = \rho h_x \tag{4-44}$$

and F_η

$$F_\eta = \left(\left(\frac{M_x}{M_R}\right)^{1/2}\right)\left(f_x^{1/2}\right)\left(h_x^{-2/3}\right) \tag{4-45}$$

Where f_x and h_x are reducing ratios function of critical parameters and can be calculated by the following equations:

$$f_x = \frac{T_{c,x}}{T_{c,R}} \quad \text{and} \quad h_x = \frac{\rho_{c,R}}{\rho_{c,x}} \tag{4-46}$$

Rowlinson and Watson (1969) [45] supplemented significantly the applicability range of the corresponding states by introducing the concept of extended corresponding states. In this concept, the reducing ratios are functions of critical temperature, critical density and acentric factor.

$$f_x = \frac{T_{c,x}}{T_{c,R}}\theta_x\left(\rho_{r,x}, T_{r,x}, \omega_x\right) \tag{4-47}$$

$$h_x = \frac{\rho_{c,R}}{\rho_{c,x}}\phi_x\left(\rho_{r,x}, T_{r,x}, \omega_x\right) \tag{4-48}$$

Where θ_x and ϕ_x are shape factors and functions of reduced temperature, reduced density and acentric factor. A simplified density independent correlation to determine the shape factors were presented [5].

$$\theta_x\left(\rho_{r,x}, T_{r,x}, \omega_x\right) = \left[1 + \left(\omega - \omega_R\right)\left(0.05203 - 0.7498 \ln T_{r,x}\right)\right] \tag{4-49}$$

$$\phi_x\left(\rho_{r,x}, T_{r,x}, \omega_x\right) = \frac{Z_{c,R}}{Z_{c,x}}\left[1 - \left(\omega - \omega_R\right)\left(0.1436 - 0.2822 \ln T_{r,x}\right)\right] \tag{4-50}$$

For propane Younglove and Ely [35] give:

$$\eta_R - \eta_{0R} = G_1 \exp\left[\rho_0^{0.1} G_2 + \rho_0^{0.5}\left(\rho_{r,R} - 1\right) G_3\right] - G_1 \tag{4-51}$$

Where

$$\rho_{r,R} = \frac{\rho_0}{\rho_{c,R}} \tag{4-52}$$

$\eta^R - \eta^{R0}$ is in μPa.s,

$\rho_{c,R}$ and ρ_0 are in mols/L

In Equation (4-51), η_R is the true viscosity of the reference fluid, propane, at temperature T_0 and density ρ_0, η_{0R} is the low pressure viscosity value for propane at

temperature T_0. The reference fluid values are evaluated at T_0 and density ρ_0 not T and ρ.

The parameters G_1, G_2 and G_3 can be calculated from:

$$G_1 = \exp\left(E_1 + \frac{E_2}{T}\right) \tag{4-53}$$

$$G_2 = E_3 + \frac{E_4}{T^{1.5}} \tag{4-54}$$

$$G_3 = E_5 + \frac{E_6}{T} + \frac{E_7}{T^2} \tag{4-55}$$

E-parameters for the propane are listed below in Table 4.7.

Table 4.7 E parameters for the Propane reference fluid

E Parameters	Value (-)
E1	-14.113294896
E2	968.22940153
E3	13.686545032
E4	-12511.628378
E5	0.01168910864
E6	43.527109444
E7	7659.4543472

4.4.3.1 CO_2-SUPERTRAPP model for mixtures

The residual viscosity of the mixture, which is related to the residual viscosity of the reference fluid, is given by:

$$\eta_m - \eta_m^0 = F_{\eta m}\left[\eta^R - \eta^{R0}\right] + \Delta\eta^{ENSKOG} \tag{4-56}$$

The term $\eta^R - \eta^{R0}$ is for the residual viscosity of the reference fluid which should be evaluated at temperature of T_0 and density ρ_0 (not at T and ρ). In the original SUPERTRAPP method, propane is the reference fluid which its residual viscosity can be determined from a method given by Younglove and Ely (Zaytsev and Aseyev, 1992) [46] as described above for pure components.

In this work, Carbon Dioxide with the viscosity data published by Fenghour et al. (1998) [34] has been used as the reference fluid. Thus, instead of Equations (4-51) to (4-55) for the propane viscosity calculation, the viscosity of CO_2 as a function of density and temperature can be calculated from the data published by Fenghour et al. [34], Equation (4-24).

The following mixing rules are applied to determine $F_{\eta m}$, T_0 and ρ_0 in the Equation (4-56):

$$h_m = \sum_i \sum_j y_i y_j h_{ij} \tag{4-57}$$

$$f_m h_m = \sum_i \sum_j y_i y_j f_{ij} h_{ij} \tag{4-58}$$

$$h_{ij} = \frac{\left[\left(h_i\right)^{1/3} + \left(h_j\right)^{1/3} \right]^3}{8} \tag{4-59}$$

$$f_{ij} = \left(f_i f_j\right)^{1/2} \tag{4-60}$$

Where f_i and h_i can be calculated by the following equations:

$$f_i = \frac{T_{ci}}{T_c^R}\left[1 + \left(\omega_i - \omega^R\right)\left(0.05203 - 0.7498 \ln T_{ri}\right)\right] \tag{4-61}$$

$$h_i = \frac{\rho_c^R}{\rho_{ci}} \frac{Z_c^R}{Z_{ci}}\left[1 - \left(\omega_i - \omega^R\right)\left(0.1436 - 0.2822 \ln T_{ri}\right)\right] \tag{4-62}$$

T_0 and ρ_0 are calculated by the following equations:

$$T_0 = \frac{T}{f_m} \tag{4-63}$$

$$\rho_0 = \rho h_m = \frac{h_m}{V} \tag{4-64}$$

Finally,

$$F_{\eta m} = \left(M_R\right)^{-1/2} \left(h_m^{-2}\right) \sum_i \sum_j y_i y_j \left(f_{ij} M_{ij}\right)^{1/2} \left(h_{ij}\right)^{4/3} \tag{4-65}$$

where

$$M_{ij} = \frac{2 M_i M_j}{M_i + M_j} \tag{4-66}$$

The term $\Delta\eta^{ENSKOG}$ accounts for size differences based on a hard sphere assumption (Ely, 1981) [42] and is calculated by:

$$\Delta\eta^{ENSKOG} = \eta_m^{ENSKOG} - \eta_x^{ENSKOG} \tag{4-67}$$

where

$$\eta_m^{ENSKOG} = \sum_i \beta_i Y_i + \alpha \rho^2 \sum_i \sum_j y_i y_j \sigma_{ij}^{\ 6} \eta_{ij}^0 g_{ij} \tag{4-68}$$

where

ρ is density in mols/L, σ is hard-sphere diameter in Å, and η_{ij}^0 and η^{ENSKOG} are in μP

$$\alpha = \frac{48}{25\pi}\left[\frac{2\pi}{3}\left(6.023 \times 10^{-4}\right)\right]^2 = 9.725 \times 10^{-7} \tag{4-69}$$

$$\sigma_i = 4.771 h_i^{1/3} \tag{4-70}$$

$$\sigma_{ij} = \frac{\sigma_i + \sigma_j}{2} \tag{4-71}$$

η^0 based on a rigid, non-attracting sphere assumed in the kinetic theory of Chapman and Enskog can be calculated from

$$\eta_i^0 = 26.69 \frac{(M_i T)^{1/2}}{\sigma_i^2} \tag{4-72}$$

where

η = viscosity, μP

σ = hard-sphere diameter, Å

For a binary system, the method of Wilke (1950) [47] simplified the kinetic theory approach. The viscosity of binary systems in this method can be calculated by:

$$\eta_{ij}^0 = \frac{y_i \eta_i^0}{y_i + y_j \phi_{ij}} + \frac{y_j \eta_j^0}{y_j + y_i \phi_{ji}} \tag{4-73}$$

where

$$\phi_{ij} = \frac{\left[1 + \left(\frac{\eta_i^0}{\eta_j^0}\right)^{1/2} \left(\frac{M_i}{M_j}\right)^{1/4}\right]^2}{\left[8\left(1 + \frac{M_i}{M_j}\right)\right]^2} \tag{4-74}$$

ϕ_{ji} is found by:

$$\phi_{ji} = \frac{\eta_j^0}{\eta_i^0} \frac{M_i}{M_j} \phi_{ij} \tag{4-75}$$

The radial distribution function, g_{ij}, is calculated by (Tham and Gubbins, 1971) [48]:

$$g_{ij} = (1-\xi)^{-1} + \frac{3\xi}{(1-\xi)^2}\theta_{ij} + \frac{2\xi^2}{(1-\xi)^3}\theta_{ij}^2 \tag{4-76}$$

$$\theta_{ij} = \frac{\sigma_i \sigma_j}{2\sigma_{ij}} \frac{\sum_k y_k \sigma_k^2}{\sum_k y_k \sigma_k^3} \tag{4-77}$$

$$Y_i = y_i \left[1 + \frac{8\pi}{15}(6.023 \times 10^{-4})\rho \sum_j y_j \left(\frac{M_j}{M_i + M_j}\right) \sigma_{ij}^3 g_{ij}\right] \tag{4-78}$$

The n values of βi can be calculated by solving the n linear equations of the form

$$\sum_j B_{ij} \beta_j = Y_i \tag{4-79}$$

where

$$B_{ij} = 2\sum_k y_i y_k \frac{g_{ik}}{\eta_{ik}^0} \left(\frac{M_k}{M_i + M_k}\right)^2 \left[\left(1 + \frac{5M_i}{3M_k}\right)\delta_{ij} - \frac{2M_i}{3M_k}\delta_{jk}\right] \tag{4-80}$$

The parameter η_x^{ENSKOG} in Equation (4-67) is for a pure hypothetical fluid with the same density as the mixture, which can be determined from the same equation for η_m^{ENSKOG} with parameters defined by:

$$\sigma_x = \left(\sum_i \sum_j y_i y_j \sigma_{ij}^{\ 3} \right)^{1/3} \tag{4-81}$$

$$M_x = \left[\sum_i \sum_j y_i y_j M_{ij}^{\ 1/2} \sigma_{ij}^{\ 4} \right]^2 \sigma_x^{\ -8} \tag{4-82}$$

4.5 Results and discussion

4.5.1 Experimental and modelling results

Most of the available viscosity data are in the gas phase and atmospheric pressure as discussed in the literature review. There are large gaps between the available experimental data and the requirements for the viscosity of CO_2-rich systems in carbon capture, transport and storage. As the operationally and economically preferred scenarios to transport captured carbon dioxide in CCS is by pipeline in the dense phase, liquid or supercritical phase, availability of robust viscosity data at higher pressure and in the dense phase is of crucial importance.

The viscosities of pure CO_2, multi-component mixtures of MIX 1 (with 5% impurity), MIX 2 (with 10% impurity), MIX 3 (with 30% impurity), MIX 4 (with 50% impurity) and binary systems of BINARY 1 (5% H_2 as impurity) and BINARY 2 (10% H_2 as impurity) have been measured using the capillary tube technique. For calibration purposes, viscosity of pure CO_2 has been measured over a wide range of pressure, temperature and fluid conditions (62 points). Totally, 329 viscosity data for pure CO_2, MIX 1, MIX 2, MIX 3, BIN 1, BIN 2 and MIX 4 have been measured which 108 points are in the gas phase, 115 points are in the liquid phase and 106 points are in the supercritical phase. Average and maximum of the type A and type B of estimated standard uncertainties of viscosity for each material has been reported in Table 4.22. A summary of the measurements is listed in Table 4.23.

The experimental data then were employed to tune the correlative LBC and CO_2-LBC models and to evaluate the predictive models. The predictive models in this work are based on the corresponding states (CS) theory models. One reference fluid models are Pedersen and CO_2-Pedersen; two reference fluid models are Aasberg-Petersen (CS2) and CO_2-CS2 models and two models base on extended corresponding states (ECS) theory, SUPERTRAP and CO_2-SUPERTRAP models. The experimental and modelling

results are shown in Table 4.8 to Table 4.21 and Figure 4.13 to Figure 4.22. The results of the correlative models, LBC and CO_2-LBC, are shown Table 4.8 to Table 4.14 while the results of the predictive models are shown in Table 4.15 to Table 4.21.

Tables of the correlative models, i.e., Table 4.8 to Table 4.14, include fifteen columns. In each table, columns 1 to 7, are showing the experimental conditions, number of measurements, phase, temperature, pressure, experimental viscosity data, type A and type B estimated standard uncertainty of measured viscosity, respectively. Columns 8 to 12 show the modelling results of the LBC and CO_2-LBC models with and without density correction term using the Peng-Robinson equation of state. The viscosity predicted by the LBC models is a strong function of the density of the mixture. Therefore, to compare the effect of density correction on the viscosity predicted by the LBC models, columns 8 and 9 show the results with density correction term and columns 10 and 11 show the results without density correction term. Finally, the last four columns, columns 12 to 15, show the corresponding deviations of the LBC models with and without density correction term from the experimental data.

Tables of the predictive models, i.e., Table 4.15 to Table 4.21, include 23 columns. Like the tables for the correlative models, in each table, columns 1 to 7, showing the experimental conditions, number of measurements, phase, temperature, , experimental viscosity data, type A ($u_A(\eta)$) and type B ($u_c(\eta)$) of estimated standard uncertainty of measured viscosity, respectively. Columns 8 to 15 show the predicted viscosity results by different predictive models. Columns 7 to 11 show the results of the models based on extended corresponding states (ECS) theory, i.e., SUPERTRAP and CO_2-SUPERTRAP models with and without density correction term using Peng-Robinson equation of states. The viscosity predicted by SUPERTRAP models, like LBC, is a strong function of the density of the mixture. Therefore, to compare the effect of density correction on the viscosity predicted by the SUPERTRAP models, columns 8 and 9 show the results with density correction term and columns 10 and 11 show the results without density correction term. Columns 11 and 12 show the results of the models based on two-reference fluid corresponding states theory, i.e., Aasberg-Petersen (CS2) and CO_2-CS2 models. Columns 14 and 15 show the results of the models based on one-reference fluid corresponding states (CS) theory, i.e., Pedersen and CO_2-Pedersen models. Finally, the last eight columns, columns 16 to 23, show the corresponding deviations of the predictive models from the experimental data.

The summary of the Absolute Average Deviations (AADs) for each mixture in gas, liquid and supercritical phases are presented in Table 4.23 and Table 4.24 for both correlative and predictive models, respectively.

4.5.2 Discussions on the correlative models

The LBC correlation based on the residual viscosity theory is one of the most common correlations in the oil and gas industry to calculate viscosity of fluids. CO_2-LBC model is the LBC correlation with new tuned parameters using the experimental viscosity data of CO_2-rich systems generated in this work. The LBC original parameters are available from Table 4.3. The new tuned parameters for the CO_2-LBC model are 0.10799, 0.035452, 0.021269, -0.013284 and 0.0034455 for a_1 to a_5, respectively.

As can be seen in Table 4.23, by comparing columns 8 and 9, the AAD for the original LBC correlation using original Peng-Robinson equation of state without density correction is 19.9 % while after tuning and applying the predicted mixture density using the same equation of state with CO_2 volume correction (CO_2-LBC) is 8.5%. The application of CO_2 volume correction has been discussed in chapter 3. The minimum and maximum AADs for the original LBC correlation are 7.3% and 13.6% for MIX 1 and MIX 3, respectively while those are 6.7% and 16.2% for MIX 1 and MIX 3, respectively, using the CO_2-LBC with density correction.

4.5.2.1 Effect of tuning parameters and mixture density

In part 4.4.1, Equation (4-07) is the main equation for the LBC correlation which is function of the mixture density and five constant parameters. The original parameters for the LBC correlation are presented in Table 4.3. There are two methods to improve the prediction of the LBC correlation. One of the most common methods for this purpose is to tune the parameters to match to experimental data. Improving the mixture density prediction can be another method. The effect of tuning can be analysed from Table 4.23. As can be seen, the AAD has been reduced from 10.8% to 8.5% when the density correction is considered (comparing columns 5 and 6), while it has been reduced from 19.9% to 18.1% without applying density correction term (comparing columns 7 and 8). The effect of mixture density on viscosity calculation can be realised by comparing columns 5 and 7 for original LBC and 6 and 8 for CO_2-LBC models. The table shows that applying density correction term in the original LBC model can reduce the AAD from 19.9% to 10.8% while those are reducing from 18.1% to 8.5% for the CO_2-LBC model. By comparing these two improving methods, it can be observed that

applying mixture density correction term would reduce the AAD significantly compared to adjusting the tuning parameters a_1-a_5. Figure 4.24 graphically show the effects of tuning parameters and density correction in LBC and CO_2-LBC models for MIX 2 at 0, 50 and 150 °C (273.15, 323.15 and 423.15 K).

4.5.2.2 Predictions of the models in different phases

Table 4.23 also can be used to compare the accuracy of the models prediction in different fluid phases. In the gas phase, the AADs are high for both original LBC and modified CO_2-LBC, i.e., 14.6% and 12.4%, respectively. As can be seen, the accuracy of the models have not been increased neither using tuned parameters nor applying the density correction term in the gas phase. It seems reasonable as volume correction term has mostly an effect on the density in the dense phase, i.e., liquid or supercritical phase. In the liquid or supercritical phases, the AAD reduces significantly from 28.4% to 8.6% for the LBC model and from 22.7% to 6.2% for the CO_2-LBC model by applying CO_2 volume correction term in liquid phase. Those are reducing from 16.0% to 9.2% and from 18.9% to 6.9% for LBC and CO_2-LBC models in the supercritical phase, respectively. The effect of tuning parameters in the liquid phase can be observed by comparing columns 5 and 6 or columns 7 and 8 with and without considering density correction. The AAD reduces from 8.6% to 6.2% when the density correction term is applied while it reduces from 28.4% to 22.7% without density correction. Tuning parameters also can reduce the AAD from 9.2% to 6.9% and from 18.9% to 16.0% in the supercritical phase with and without applying density correction term, respectively.

4.5.3 Discussions on the predictive models

Predictive models in this work are based on corresponding states (CS) theory with one reference fluid, Pedersen and CO_2-Pedersen models, with two reference fluids, Aasberg-Petersen (CS2) and CO_2-CS2 models, and extended corresponding states (ECS) theory, SUPERTRAP and CO_2-SUPERTRAP models. The models were described in the modelling part. The AAD for each model were summarised in Table 4.24. As can be seen, the CO_2-Pedersen model has the lowest AAD of 3.3% while it is 8.0% for the original Pedersen model. The significant reduction in the AAD can show the effect of reference fluid selection on the viscosity prediction accuracy by corresponding states theory models for different systems. In this work, instead of methane in the original Pedersen model, the CO_2 has been selected as the reference fluid in the CO_2-Pedersen model. The original Aasberg-Petersen model with two reference fluids (methane and n-

decane) has the AAD of 13.5% which is relatively high for CO_2-rich systems. However, changing the n-decane to carbon dioxide could reduce the AAD to 7.1%. As can be seen in the table, the CO_2-CS2 model has more reasonable prediction for the systems with higher amount of hydrocarbons, i.e., MIX 3 and MIX 4, which the AADs are 7.2% and 3.9%, respectively. The CO_2-SUPERTRAP model also has the AAD of 5.5% which is the best models after CO_2-Pedersen model. The effect of the mixture density correction on the viscosity modelling by this model has been described below.

4.5.3.1 The effect of mixture density on the viscosity modelling by CO_2-SUPERTRAPP

Unlike CO_2-Pedersen model which only requires the density of reference fluid to predict the mixture viscosity, viscosity prediction of SUPERTRAPP models are a function of mixture density. In modelling the viscosity using SUPERTRAPP models, the residual viscosity of any mixture is related to residual viscosity of the reference fluid at a corresponding state point of (ρ_0, T_0). According to description of the model, also can be seen on the Equation (4-42), the viscosity of reference fluid should be evaluated at temperature T_0 and density ρ_0, which density ρ_0 is a function of the mixture density. However, the mixture density has a significant effect on the mixture viscosity in SUPERTRAPP models. Table 4.24 and Figure 4.25 show this effect for all conducted tests.

As can be seen, using the modified density for the CO_2-rich systems reduces the absolute average deviation from 14.0% to 6.0% using the original SUPERTRAPP model. This amount reduces from 11.4% to 5.5% using the CO_2-SUPERTRAPP model.

4.5.3.2 Prediction of the models in different phases

As can be seen from Table 4.24, in gas phase, most of the models, except Aasberg-Petersen, have acceptable viscosity prediction for CO_2 fluids containing impurities. The lowest AAD of 2.3% in gas phase is for the CO_2-Pedersen model. In liquid and supercritical phases, CO_2-Pedersen has the lowest AAD of 3.5% and 4.1%, respectively which is an acceptable viscosity prediction in the dense phase for CO_2 with impurity systems.

4.5.4 The effect of different impurities on viscosity of pure CO_2

The presence of impurities can affect the viscosity of pure CO_2. Table 4.25 shows the viscosity reduction in the dense phase and viscosity increase in the gas phase for each

tested mixtures and binaries at different temperatures. The effect of impurities on the viscosity of pure CO_2 also can be observed in Figure 4.27 for all tested pressure ranges and Figure 4.26 at low pressures at constant temperature of 323.15 K (50 °C). In these figures, the experimental viscosity data and modelling predictions using CO_2-Pedersen model for each system are reported at 323.15 K (50 °C). As expected, the presence of the tested systems with impurities caused a decrease in the viscosity at higher pressure ranges, i.e., in liquid and supercritical phases. This reduction can be explained by a reduction in density and molecular weight of the tested mixtures. The reduction in viscosity of pure CO_2 in the presence of impurities for each system can be seen in Figure 4.27. The lowest viscosity reduction of 9.6% is for MIX 1 with 4.4% impurities, while the highest reduction of 30.9% is for those of MIX 3 with almost 30.01% impurities. Also 10.33% hydrogen in the BIN 2 reduces the viscosity significantly (23.8%). This is due to low molecular weight of hydrogen compare to that of carbon dioxide.

In gas phase, as illustrated in Figure 4.28, the presence of impurities increased viscosity (which was expected). The increase in viscosity is due to the increase in kinetic energy of the system. The lowest viscosity increase of 0.9% is for MIX 1, while that is 8.9% for MIX 3 which has the highest viscosity increase due to the presence of impurities.

The viscosity changes from pure CO_2 for MIX 1 at different temperatures were shown in Figure 4.29. The highest reduction in the viscosity of MIX 1 is happening nearby critical point, at 25 °C (298.15 K) and at pressures around 8 MPa. At high temperatures in supercritical phase, viscosity reduction from pure CO_2 would be smooth. As could be seen in Figure 4.29, the high reduction of 25% in viscosity of pure CO_2 due to the presence of MIX 1 impurities were measured at 50 °C (323.15 K) at pressures around 9 MPa.

4.6 Conclusions

Viscosities of pure CO_2, two CO_2–H_2 binary systems (with 5 and with 10 mol% H_2), and 4 multi-component mixtures (MIX 1 with 5% impurity, MIX 2 with 10% impurity, MIX 3 with 30% impurity and MIX 4 with 50% impurity) were measured at pressures ranging from 10 to 140 MPa at six different temperatures, 0, 10, 25, 50, 100, 150 °C (273.15, 283.15, 298.15, 323.15, 373.15 and 423.15 K) in gas, liquid and supercritical regions using capillary tube technique.

The measured viscosity data were employed to tune LBC and CO_2-LBC models and to evaluate the modified predictive models, i.e., corresponding states theory models. One reference fluid corresponding states models are Pedersen and CO_2-Pedersen; two reference fluid corresponding states models are Aasberg-Petersen (CS2) and CO_2-CS2 models and two other models based on extended corresponding states (ECS) theory, i.e., SUPERTRAP and CO_2-SUPERTRAP models.

New values for the LBC parameters were tuned to experimental data for CO_2-rich systems. The Absolute Average Deviation (AAD) was reduced significantly.

Three predictive models were modified by using pure CO_2 data as a reference fluid for CO_2-rich systems. CO_2-Pedersen and CO_2-CS2 predict well viscosity of CO_2-rich systems compared to the original models. The original SUPERTRAPP model over-predicts viscosity while CO_2-SUPERTRAPP model under-predicts.

The mixture density has a significant effect on the mixture viscosity, in a way that using a modified density for the CO_2-rich systems reduces the absolute average deviation.

The high reduction of the viscosity of mixtures compared to that of pure CO_2 was observed at points nearby the critical points of each tested system in the dense phase.

Table 4.8 Experimental and modelling results (LBC model) of the viscosity of pure CO_2

1	2	3	4	5	6	7	8	9	10	11	12	13	14	15
No	Phase	T	P	Viscosity / μPa.s							Deviation (%)			
		K	MPa	EXP.	$u_A(\eta)$	$u_c(\eta)$	LBC	CO_2-LBC	LBC	CO_2-LBC	LBC	CO_2-LBC	LBC	CO_2-LBC
Density Correction?		(±0.1)	(±0.02)		μPa.s	μPa.s	Yes	Yes	No	No	Yes	Yes	No	No
1	Gas	238.2	1.03	12.9	0.2	0.2	12.9	14.2	12.9	14.2	0.1	10.7	0.1	10.7
2	Liq.	238.2	10.22	191.6	0.9	0.9	159.5	171.5	195.7	202.6	-16.8	-10.5	2.1	5.7
3	Liq.	238.2	21.18	209.4	0.3	1.0	177.7	187.5	229.8	229.7	-15.2	-10.5	9.7	9.7
4	Liq.	238.2	51.70	257.4	0.6	1.2	227.9	228.2	323.4	296.1	-11.4	-11.3	25.7	15.1
5	Liq.	243.2	102.78	316.3	1.7	1.5	293.8	276.2	450.7	374.9	-7.1	-12.7	42.5	18.5
6	Liq.	243.2	126.15	349.9	1.3	1.6	328.7	299.7	518.7	413.3	-6.1	-14.4	48.3	18.1
7	Gas	253.2	1.03	13.9	0.2	0.2	12.8	14.2	12.8	14.2	-7.4	2.4	-7.4	2.4
8	Liq.	253.2	50.43	215.0	0.8	1.0	188.0	196.3	257.7	250.5	-12.6	-8.7	19.8	16.5
9	Liq.	253.2	102.56	281.7	0.6	1.3	264.4	255.4	400.7	345.2	-6.1	-9.3	42.2	22.5
10	Liq.	253.2	150.16	343.8	0.9	1.6	332.7	302.3	531.3	420.2	-3.2	-12.1	54.6	22.2
11	Gas	273.2	1.05	13.7	0.1	0.2	12.8	14.2	12.8	14.2	-6.3	3.6	-6.3	3.6
12	Gas	273.2	2.05	13.9	0.1	0.2	13.2	14.7	13.2	14.7	-5.2	5.7	-5.2	5.7
13	Liq.	273.2	10.47	114.5	0.4	0.6	99.3	111.4	103.1	115.6	-13.2	-2.7	-10.0	0.9
14	Liq.	273.2	20.13	131.7	0.3	0.6	113.0	126.3	126.3	140.0	-14.2	-4.1	-4.1	6.3
15	Liq.	273.2	52.05	174.1	1.3	0.8	152.7	165.4	199.7	206.0	-12.3	-5.0	14.8	18.3
16	Liq.	273.2	102.61	230.5	1.0	1.1	215.4	218.5	319.7	293.7	-6.5	-5.2	38.7	27.4
17	Liq.	273.2	150.44	282.2	1.1	1.3	277.3	264.6	436.8	366.8	-1.7	-6.2	54.8	30.0
18	Gas	283.2	1.09	14.3	0.1	0.2	12.8	14.2	12.8	14.2	-10.7	-1.3	-10.6	-1.3
19	Gas	283.2	2.07	14.4	0.1	0.2	13.1	14.6	13.1	14.6	-8.7	1.7	-8.6	1.8
20	Liq.	283.2	7.89	91.4	0.7	0.5	82.2	91.5	79.2	87.9	-10.1	0.1	-13.3	-3.8
21	Liq.	283.2	23.07	120.9	0.6	0.6	104.5	117.1	114.5	127.9	-13.5	-3.1	-5.2	5.8
22	Liq.	283.2	39.85	143.8	1.5	0.7	124.4	138.1	149.9	162.7	-13.5	-4.0	4.2	13.2
23	Liq.	283.2	59.01	167.4	0.4	0.8	146.0	159.1	190.4	198.3	-12.8	-5.0	13.8	18.5
24	Liq.	283.2	101.38	212.7	0.5	1.0	194.2	201.5	283.8	269.2	-8.7	-5.3	33.4	26.6
25	Liq.	283.2	151.26	260.4	1.1	1.2	254.2	248.0	398.5	343.8	-2.4	-4.8	53.0	32.0
26	Gas	293.2	1.13	14.6	0.1	0.2	12.8	14.2	12.8	14.2	-12.3	-3.1	-12.3	-3.1
27	Gas	293.2	2.05	14.7	0.1	0.2	13.1	14.6	13.1	14.6	-11.3	-1.2	-11.2	-1.2
28	Liq.	293.2	11.47	86.5	0.3	0.5	76.9	85.1	73.9	81.4	-11.1	-1.6	-14.6	-5.9
29	Liq.	293.2	20.37	103.6	0.6	0.5	90.3	101.1	93.7	105.0	-12.9	-2.5	-9.6	1.3
30	Liq.	293.2	36.79	129.5	0.9	0.6	109.6	122.6	125.7	139.4	-15.4	-5.3	-2.9	7.7
31	Liq.	293.2	68.99	165.9	0.8	0.8	143.3	156.6	188.5	196.7	-13.6	-5.6	13.7	18.6
32	Liq.	293.2	101.04	195.3	1.1	0.9	177.1	187.0	254.2	248.0	-9.3	-4.3	30.2	27.0
33	Liq.	293.2	141.60	234.7	1.2	1.1	221.8	223.6	341.2	307.9	-5.5	-4.8	45.4	31.2
34	Gas	308.2	1.20	15.3	0.0	0.2	12.8	14.2	12.8	14.2	-16.4	-7.6	-16.4	-7.6
35	Gas	308.2	2.07	15.4	0.0	0.2	13.1	14.5	13.1	14.5	-15.1	-5.6	-15.1	-5.6
36	Gas	308.2	5.09	18.4	0.1	0.2	14.6	16.5	14.7	16.6	-20.6	-10.6	-20.2	-10.1
37	Liq.	308.2	11.33	63.9	0.4	0.4	59.5	63.8	53.8	56.9	-6.9	-0.2	-15.9	-11.0
38	Liq.	308.2	22.09	88.4	0.6	0.5	78.5	87.1	78.9	87.5	-11.1	-1.4	-10.7	-1.0
39	Liq.	308.2	34.97	107.0	0.5	0.5	93.3	104.6	101.5	113.8	-12.8	-2.3	-5.2	6.3
40	Liq.	308.2	68.93	144.4	0.7	0.7	126.1	139.7	159.5	171.6	-12.7	-3.2	10.5	18.8
41	Liq.	308.2	101.20	173.6	0.3	0.8	156.3	168.6	218.1	220.7	-10.0	-2.9	25.6	27.1
42	Liq.	308.2	150.52	222.4	1.0	1.1	204.8	210.1	314.1	289.9	-7.9	-5.5	41.2	30.4
43	Gas	323.2	1.27	16.1	0.1	0.2	12.8	14.2	12.8	14.2	-20.5	-12.2	-20.5	-12.2
44	Gas	323.2	2.05	16.3	0.0	0.2	13.0	14.5	13.0	14.5	-20.2	-11.3	-20.2	-11.3
45	Gas	323.2	5.04	17.4	0.1	0.2	14.3	16.1	14.3	16.1	-17.8	-7.5	-17.5	-7.1
46	SC	323.2	11.44	39.8	0.2	0.3	38.3	39.7	34.6	35.9	-3.8	-0.3	-13.1	-9.8
47	SC	323.2	20.67	71.1	0.3	0.4	64.6	70.0	62.0	66.8	-9.1	-1.5	-12.8	-6.0
48	SC	323.2	50.82	111.9	0.6	0.6	96.6	108.3	109.3	122.4	-13.7	-3.3	-2.3	9.3
49	SC	323.2	105.53	160.6	0.3	0.8	143.1	156.4	195.8	202.7	-10.9	-2.6	21.9	26.2
50	SC	323.2	150.43	195.3	0.4	0.9	182.7	191.9	274.7	262.8	-6.4	-1.8	40.6	34.5
51	Gas	373.2	1.48	18.6	0.0	0.2	12.8	14.2	12.8	14.2	-30.9	-23.7	-30.9	-23.6

1	2	3	4	5	6	7	8	9	10	11	12	13	14	15
No	Phase	T	P	Viscosity / μPa.s							Deviation (%)			
		K	MPa	EXP.	$u_A(\eta)$	$u_c(\eta)$	LBC	CO_2-LBC	LBC	CO_2-LBC	LBC	CO_2-LBC	LBC	CO_2-LBC
Density Correction?		(±0.1)	(±0.02)		μPa.s	μPa.s	Yes	Yes	No	No	Yes	Yes	No	No
52	Gas	373.2	2.06	18.7	0.0	0.2	12.9	14.3	12.9	14.3	-30.9	-23.3	-30.8	-23.3
53	Gas	373.2	5.15	19.5	0.1	0.2	13.8	15.5	13.8	15.5	-29.1	-20.3	-29.0	-20.2
54	Gas	373.2	8.38	21.0	0.1	0.2	15.4	17.3	15.5	17.4	-26.5	-17.3	-26.2	-16.9
55	SC	373.2	21.67	40.2	0.2	0.3	36.5	37.9	34.5	35.8	-9.2	-5.9	-14.2	-10.9
56	SC	373.2	51.46	78.3	0.2	0.4	69.2	75.7	72.2	79.4	-11.6	-3.3	-7.7	1.5
57	SC	373.2	102.71	119.2	0.3	0.6	103.2	115.7	126.5	140.2	-13.5	-3.0	6.2	17.6
58	SC	373.2	149.33	150.1	0.7	0.7	133.2	146.9	183.4	192.4	-11.2	-2.1	22.2	28.2
59	Gas	423.2	1.71	20.8	0.1	0.2	12.8	14.2	12.8	14.2	-38.4	-31.9	-38.4	-31.9
60	Gas	423.2	2.06	20.8	0.1	0.2	12.9	14.3	12.9	14.3	-38.2	-31.6	-38.2	-31.6
61	Gas	423.2	5.13	21.5	0.0	0.2	13.5	15.2	13.5	15.2	-37.1	-29.5	-37.0	-29.4
62	Gas	423.2	8.12	22.3	0.1	0.2	14.5	16.3	14.5	16.3	-35.0	-26.7	-34.9	-26.6
63	SC	423.2	51.25	59.4	0.2	0.3	52.8	55.7	53.2	56.1	-11.1	-6.2	-10.6	-5.5
64	SC	423.2	102.61	95.0	0.3	0.5	81.9	91.1	93.3	104.5	-13.8	-4.1	-1.8	10.0
65	SC	423.2	148.94	121.0	0.5	0.6	105.6	118.3	133.3	146.9	-12.7	-2.2	10.2	21.4
				Average Absolute Deviation (AAD)							**13.6**	**7.7**	**20.2**	**14.9**

Table 4.9 Experimental and modelling results (LBC model) of the viscosity of MIX 1

1	2	3	4	5	6	7	8	9	10	11	12	13	14	15
No	Phase	T	P	Viscosity / μPa.s							Deviation (%)			
		K	MPa	EXP.	$u_A(\eta)$	$u_c(\eta)$	LBC	CO_2-LBC	LBC	CO_2-LBC	LBC	CO_2-LBC	LBC	CO_2-LBC
Density Correction?		(±0.1)	(±0.02)		μPa.s	μPa.s	Yes	Yes	No	No	Yes	Yes	No	No
1	Gas	243.2	1.48	12.7	0.1	0.2	15.1	16.5	15.1	16.5	18.5	29.6	18.5	29.6
2	Liq.	243.2	21.11	168.6	1.2	0.8	154.2	166.4	190.1	197.6	-8.5	-1.3	12.7	17.2
3	Liq.	243.2	52.54	217.3	1.0	1.0	204.3	209.2	279.0	265.1	-6.0	-3.7	28.4	22.0
4	Liq.	243.2	103.76	288.1	0.8	1.3	284.4	268.9	424.6	358.3	-1.3	-6.7	47.4	24.4
5	Liq.	243.2	151.14	349.8	1.4	1.6	354.3	315.3	559.0	433.5	1.3	-9.9	59.8	23.9
6	Gas	253.2	1.56	13.4	0.0	0.2	15.1	16.5	15.1	16.5	12.9	23.5	12.9	23.5
7	Gas	253.2	2.04	13.4	0.1	0.2	15.3	16.8	15.3	16.8	14.2	25.4	14.2	25.4
8	Liq.	253.2	21.53	144.0	0.8	0.7	135.7	149.0	161.6	173.1	-5.7	3.5	12.2	20.2
9	Liq.	253.2	52.04	193.9	0.8	0.9	180.4	189.5	240.7	237.4	-7.0	-2.3	24.1	22.4
10	Liq.	253.2	103.74	260.2	0.9	1.2	256.0	248.7	377.6	329.9	-1.6	-4.4	45.1	26.8
11	Liq.	253.2	151.65	314.4	0.4	1.5	325.0	296.3	506.0	404.8	3.4	-5.8	60.9	28.7
12	Gas	273.2	1.73	14.5	0.0	0.2	15.1	16.5	15.1	16.5	3.9	13.6	3.9	13.6
13	Gas	273.2	2.11	14.6	0.1	0.2	15.3	16.7	15.3	16.7	4.8	15.0	4.8	15.0
14	Gas	273.2	3.45	15.0	0.1	0.2	16.0	17.7	16.0	17.7	7.0	18.4	7.0	18.3
15	Liq.	273.2	10.46	97.6	0.6	0.5	89.4	99.7	92.0	102.7	-8.4	2.2	-5.8	5.2
16	Liq.	273.2	20.94	119.0	0.7	0.6	105.5	118.0	116.2	129.3	-11.3	-0.9	-2.4	8.7
17	Liq.	273.2	52.10	157.2	0.7	0.8	144.9	157.8	183.9	192.4	-7.8	0.4	17.0	22.4
18	Liq.	273.2	102.75	212.6	0.3	1.0	207.4	211.7	298.6	278.7	-2.5	-0.4	40.4	31.1
19	Liq.	273.2	151.29	262.5	0.9	1.2	269.9	258.7	413.8	351.9	2.8	-1.4	57.6	34.1
20	Gas	283.2	1.81	14.9	0.1	0.2	15.1	16.5	15.1	16.5	1.1	10.6	1.1	10.6
21	Gas	283.2	2.16	15.0	0.1	0.2	15.2	16.7	15.2	16.7	1.4	11.3	1.4	11.2
22	Gas	283.2	3.49	15.5	0.1	0.2	15.9	17.6	15.9	17.6	2.4	13.1	2.3	13.1
23	Liq.	283.2	10.41	78.5	0.7	0.4	77.0	84.9	76.4	84.2	-1.9	8.2	-2.7	7.2
24	Liq.	283.2	21.08	104.4	0.9	0.5	94.2	105.3	100.3	112.2	-9.8	0.8	-4.0	7.4
25	Liq.	283.2	51.67	145.1	0.7	0.7	130.7	144.1	161.2	172.7	-9.9	-0.7	11.0	19.0
26	Liq.	283.2	103.18	196.7	0.8	0.9	189.0	196.7	268.7	257.8	-3.9	0.0	36.6	31.1
27	Liq.	283.2	151.00	242.0	0.4	1.1	246.1	241.5	374.9	328.2	1.7	-0.2	54.9	35.6
28	Liq.	288.2	9.02	67.8	0.7	0.4	67.5	73.3	65.2	70.4	-0.4	8.1	-3.8	3.9
29	Liq.	288.2	16.58	88.7	0.2	0.5	82.4	91.5	84.0	93.4	-7.0	3.2	-5.2	5.3
30	Liq.	288.2	34.23	115.6	0.3	0.6	105.3	117.7	118.6	131.8	-8.9	1.9	2.6	14.1
31	Liq.	288.2	48.29	132.6	0.6	0.7	121.0	134.4	145.1	158.0	-8.7	1.4	9.5	19.2
32	Liq.	288.2	102.20	186.0	0.6	0.9	179.5	188.7	252.6	246.2	-3.5	1.5	35.8	32.4
33	Liq.	288.2	151.11	230.2	1.0	1.1	235.6	233.6	357.6	317.4	2.3	1.5	55.3	37.9
34	Gas	298.2	2.08	15.3	0.0	0.2	15.1	16.6	15.2	16.6	-0.8	8.7	-0.7	8.7
35	Gas	298.2	4.18	15.9	0.2	0.2	16.1	17.8	16.1	17.9	0.9	11.7	1.2	12.0
36	Liq.	298.2	10.59	59.8	0.3	0.4	59.2	63.1	56.2	59.5	-0.9	5.6	-5.9	-0.5
37	Liq.	298.2	20.66	81.0	0.5	0.4	79.0	87.3	80.3	88.9	-2.5	7.7	-0.9	9.8
38	Liq.	298.2	51.60	124.2	0.3	0.6	113.9	126.9	134.7	148.0	-8.3	2.2	8.4	19.2
39	Liq.	298.2	103.07	173.0	0.2	0.8	165.4	176.5	229.3	228.8	-4.4	2.0	32.5	32.2
40	Liq.	298.2	151.12	213.2	0.3	1.0	216.3	218.7	325.5	296.7	1.4	2.6	52.7	39.2
41	SC	323.2	2.22	17.0	0.1	0.2	15.1	16.6	15.1	16.6	-10.8	-2.4	-10.8	-2.3
42	SC	323.2	5.26	17.7	0.1	0.2	16.4	18.1	16.4	18.2	-7.7	2.2	-7.4	2.6
43	SC	323.2	6.97	18.7	0.1	0.2	17.7	19.6	17.8	19.7	-5.5	4.7	-4.8	5.5
44	SC	323.2	13.41	38.5	0.1	0.3	41.0	42.3	37.8	39.1	6.4	10.0	-1.8	1.7
45	SC	323.2	20.45	60.3	0.3	0.4	58.9	62.7	56.8	60.2	-2.3	4.0	-5.7	-0.1
46	SC	323.2	51.13	100.5	0.3	0.5	92.5	103.4	102.9	115.1	-8.0	2.8	2.3	14.5
47	SC	323.2	103.26	145.2	0.8	0.7	136.4	149.7	180.1	189.2	-6.0	3.1	24.0	30.3
48	SC	323.2	151.25	180.8	0.5	0.9	178.3	187.7	260.3	251.8	-1.4	3.8	44.0	39.3
49	SC	373.2	2.66	19.3	0.0	0.2	15.1	16.6	15.1	16.6	-21.4	-14.0	-21.4	-13.9
50	SC	373.2	5.22	19.9	0.1	0.2	15.8	17.5	15.9	17.5	-20.2	-11.8	-20.1	-11.7
51	SC	373.2	24.20	40.7	0.5	0.3	39.4	40.7	37.6	38.9	-3.2	0.1	-7.7	-4.5

1	2	3	4	5	6	7	8	9	10	11	12	13	14	15
No	Phase	T	P	Viscosity / μPa.s							Deviation (%)			
		K	MPa	EXP.	$u_A(\eta)$	$u_c(\eta)$	LBC	CO_2-LBC	LBC	CO_2-LBC	LBC	CO_2-LBC	LBC	CO_2-LBC
Density Correction?		(±0.1)	(±0.02)		μPa.s	μPa.s	Yes	Yes	No	No	Yes	Yes	No	No
52	SC	373.2	52.04	72.6	0.1	0.4	67.5	73.2	70.0	76.4	-7.1	0.8	-3.5	5.2
53	SC	373.2	102.98	110.8	0.4	0.6	100.6	112.5	120.7	134.0	-9.2	1.6	8.9	20.9
54	SC	373.2	145.34	137.0	0.3	0.7	127.4	140.8	169.0	179.7	-7.0	2.8	23.4	31.1
55	SC	423.2	3.08	21.0	0.1	0.2	15.1	16.6	15.1	16.6	-28.1	-21.3	-28.1	-21.3
56	SC	423.2	5.22	21.5	0.2	0.2	15.6	17.2	15.6	17.2	-27.4	-20.0	-27.4	-20.0
57	SC	423.2	10.41	23.7	0.1	0.2	17.4	19.3	17.4	19.3	-26.6	-18.6	-26.6	-18.6
58	SC	423.2	34.14	41.9	0.1	0.3	38.1	39.4	37.1	38.4	-9.0	-5.8	-11.4	-8.3
59	SC	423.2	51.08	56.0	0.2	0.3	51.8	54.3	52.1	54.6	-7.4	-3.0	-7.1	-2.6
60	SC	423.2	102.22	89.2	0.3	0.5	80.2	88.8	89.8	100.2	-10.1	-0.5	0.7	12.3
61	SC	423.2	152.00	115.9	0.4	0.6	105.1	117.5	130.4	143.8	-9.3	1.3	12.5	24.1
Average Absolute Deviation (AAD)											**7.3**	**6.7**	**18.1**	**17.6**

Table 4.10 Experimental and modelling results (LBC model) of the viscosity of MIX 2

1	2	3	4	5	6	7	8	9	10	11	12	13	14	15
No	Phase	T	P	Viscosity / μPa.s							Deviation (%)			
		K	MPa	EXP.	$u_A(\eta)$	$u_c(\eta)$	LBC	CO_2-LBC	LBC	CO_2-LBC	LBC	CO_2-LBC	LBC	CO_2-LBC
Density Correction?		(±0.1)	(±0.02)		μPa.s	μPa.s	Yes	Yes	No	No	Yes	Yes	No	No
1	Liq.	243.2	21.40	162.2	1.5	0.8	138.7	151.6	166.1	176.5	-14.5	-6.5	2.4	8.8
2	Liq.	243.2	51.95	207.5	1.4	1.0	188.7	195.7	249.4	242.6	-9.1	-5.7	20.2	16.9
3	Liq.	243.2	103.29	260.8	2.2	1.2	270.8	258.0	392.1	336.9	3.8	-1.1	50.4	29.2
4	Liq.	243.2	151.69	329.8	2.4	1.5	344.6	307.4	528.3	414.6	4.5	-6.8	60.2	25.7
5	Liq.	253.2	52.88	179.4	0.5	0.9	168.3	178.4	218.3	219.3	-6.2	-0.5	21.7	22.2
6	Liq.	253.2	104.06	239.0	1.7	1.1	244.5	239.0	350.1	310.9	2.3	0.0	46.5	30.1
7	Liq.	253.2	152.66	289.3	1.7	1.4	316.2	289.0	478.8	387.4	9.3	-0.1	65.5	33.9
8	Gas	273.2	1.79	14.5	0.1	0.2	13.7	15.1	13.7	15.1	-5.6	4.1	-5.6	4.1
9	Gas	273.2	2.26	14.0	0.2	0.2	13.8	15.3	13.8	15.3	-1.4	9.1	-1.4	9.1
10	Liq.	273.2	21.08	107.0	0.9	0.5	93.4	104.6	101.0	113.1	-12.7	-2.3	-5.6	5.7
11	Liq.	273.2	52.31	142.9	0.9	0.7	134.0	147.0	165.5	175.9	-6.2	2.9	15.8	23.1
12	Liq.	273.2	103.39	195.6	1.1	0.9	197.9	203.2	276.9	262.3	1.2	3.9	41.6	34.1
13	Liq.	273.2	151.09	241.7	1.3	1.1	260.4	250.6	387.7	334.2	7.7	3.7	60.4	38.3
14	Gas	283.2	1.74	14.6	0.1	0.2	13.6	15.0	13.6	15.0	-6.9	2.6	-6.9	2.6
15	Gas	283.2	2.28	14.7	0.2	0.2	13.8	15.3	13.8	15.3	-6.1	3.8	-6.1	3.8
16	Liq.	283.2	20.28	89.4	0.6	0.5	81.6	90.8	85.5	95.4	-8.8	1.5	-4.4	6.7
17	Liq.	283.2	52.66	125.0	1.0	0.6	121.0	134.2	145.6	158.1	-3.2	7.4	16.5	26.4
18	Liq.	283.2	103.54	187.1	0.9	0.9	179.9	188.3	248.4	241.9	-3.8	0.7	32.8	29.3
19	Liq.	283.2	151.55	230.8	0.4	1.1	238.1	234.3	352.4	312.3	3.1	1.5	52.7	35.3
20	Gas	298.2	2.08	15.3	0.1	0.2	13.7	15.1	13.7	15.1	-10.6	-1.4	-10.6	-1.4
21	Gas	298.2	3.53	15.2	0.2	0.2	14.2	15.8	14.2	15.8	-6.6	3.9	-6.5	4.1
22	Liq.	298.2	10.42	43.1	0.2	0.3	42.8	44.4	41.2	42.7	-0.7	3.0	-4.3	-0.8
23	Liq.	298.2	20.57	73.8	0.4	0.4	68.5	74.9	69.4	76.0	-7.1	1.5	-5.9	3.0
24	Liq.	298.2	51.42	114.8	0.6	0.6	104.6	117.0	121.0	134.2	-8.9	1.9	5.4	16.8
25	Liq.	298.2	104.49	167.4	0.6	0.8	157.8	169.2	213.0	215.2	-5.7	1.0	27.2	28.5
26	Liq.	298.2	150.46	206.4	0.7	1.0	207.7	211.0	303.3	280.4	0.6	2.2	47.0	35.8
27	Gas	323.2	2.57	16.7	0.2	0.2	13.8	15.2	13.8	15.2	-17.6	-9.0	-17.6	-8.9
28	Gas	323.2	3.70	17.0	0.1	0.2	14.1	15.7	14.1	15.7	-16.8	-7.6	-16.7	-7.4
29	SC	323.2	12.77	29.7	0.1	0.3	29.7	31.1	28.0	29.5	-0.1	4.7	-5.6	-0.6
30	SC	323.2	20.77	53.4	0.2	0.3	50.9	53.5	49.5	51.9	-4.7	0.2	-7.3	-2.8
31	SC	323.2	52.43	95.2	0.2	0.5	86.2	96.3	95.0	106.4	-9.5	1.1	-0.3	11.7
32	SC	323.2	103.47	138.8	1.1	0.7	129.4	142.6	166.6	176.9	-6.8	2.7	20.0	27.5
33	SC	323.2	151.25	177.1	1.0	0.8	171.4	181.1	243.4	238.2	-3.2	2.3	37.5	34.5
34	Gas	373.2	1.53	18.8	0.2	0.2	13.5	14.8	13.5	14.8	-28.5	-21.6	-28.5	-21.6
35	Gas	373.2	2.57	19.3	0.2	0.2	13.7	15.1	13.7	15.1	-29.2	-22.0	-29.2	-22.0
36	SC	373.2	20.30	32.7	0.1	0.3	28.9	30.4	27.9	29.4	-11.7	-7.3	-14.8	-10.2
37	SC	373.2	51.86	68.3	0.2	0.4	62.1	66.9	64.1	69.5	-9.2	-2.0	-6.2	1.7
38	SC	373.2	101.20	104.0	0.3	0.5	94.0	105.3	110.4	123.2	-9.6	1.3	6.1	18.5
39	SC	373.2	152.29	136.2	0.3	0.7	126.5	139.7	166.4	176.8	-7.1	2.6	22.2	29.8
40	Gas	423.2	2.42	20.9	0.2	0.2	13.6	14.9	13.6	14.9	-35.2	-28.8	-35.2	-28.7
41	Gas	423.2	3.57	21.2	0.2	0.2	13.8	15.2	13.8	15.2	-34.9	-28.0	-34.9	-28.0
42	SC	423.2	27.35	34.9	0.1	0.3	28.3	29.8	27.7	29.2	-18.8	-14.5	-20.7	-16.4
43	SC	423.2	51.81	54.1	0.1	0.3	48.3	50.6	48.6	50.8	-10.8	-6.6	-10.3	-6.1
44	SC	423.2	103.45	85.6	0.3	0.5	76.4	84.6	85.0	94.8	-10.7	-1.2	-0.8	10.8
45	SC	423.2	151.71	111.0	0.3	0.6	100.4	112.4	122.4	135.6	-9.6	1.2	10.2	22.1
Average Absolute Deviation (AAD)											**9.6**	**5.4**	**21.1**	**17.5**

Table 4.11 Experimental and modelling results (LBC model) of the viscosity of MIX 3

1	2	3	4	5	6	7	8	9	10	11	12	13	14	15
No	Phase	T	P	Viscosity / μPa.s							Deviation (%)			
		K	MPa	EXP.	$u_A(\eta)$	$u_c(\eta)$	LBC	CO_2-LBC	LBC	CO_2-LBC	LBC	CO_2-LBC	LBC	CO_2-LBC
Density Correction?		(±0.1)	(±0.02)		μPa.s	μPa.s	Yes	Yes	No	No	Yes	Yes	No	No
1	Gas	273.2	2.13	13.7	0.2	0.2	13.7	15.1	13.7	15.1	0.0	9.6	0.0	9.6
2	Liq.	273.2	12.92	64.5	0.4	0.4	65.6	72.0	66.9	73.6	1.7	11.6	3.7	14.1
3	Liq.	273.2	20.94	76.8	0.7	0.4	80.2	89.5	84.2	94.1	4.3	16.4	9.5	22.4
4	Liq.	273.2	52.31	109.7	0.5	0.6	126.1	137.5	146.4	156.1	14.9	25.3	33.4	42.3
5	Liq.	273.2	104.24	156.9	1.0	0.8	201.8	201.4	259.6	243.2	28.6	28.4	65.5	55.0
6	Liq.	273.2	124.73	167.6	0.5	0.8	233.2	224.7	307.6	274.9	39.1	34.1	83.5	64.0
7	Liq.	273.2	152.00	188.3	0.9	0.9	276.0	254.3	373.2	315.3	46.6	35.1	98.2	67.4
8	Gas	283.2	2.09	13.7	0.1	0.2	13.7	15.0	13.7	15.0	0.1	9.7	0.2	9.7
9	Gas	283.2	4.89	18.0	0.2	0.2	15.6	17.2	15.5	17.2	-13.8	-4.6	-13.9	-4.7
10	Liq.	283.2	9.47	41.4	0.4	0.3	45.8	47.9	45.5	47.7	10.4	15.7	9.8	15.0
11	Liq.	283.2	20.76	68.0	0.2	0.4	70.9	78.5	73.1	81.1	4.4	15.5	7.6	19.4
12	Liq.	283.2	52.01	110.7	0.8	0.6	113.7	125.5	129.6	140.9	2.7	13.3	17.1	27.2
13	Liq.	283.2	103.54	141.9	0.2	0.7	182.3	186.3	232.4	224.1	28.5	31.2	63.7	57.9
14	Liq.	283.2	125.84	158.6	0.6	0.8	213.8	210.5	280.8	257.5	34.8	32.7	77.0	62.3
15	Liq.	283.2	150.47	183.6	1.8	0.9	249.8	236.4	336.3	293.0	36.1	28.8	83.2	59.6
16	Gas	298.2	1.11	13.5	0.1	0.2	13.4	14.5	13.4	14.5	-1.0	7.6	-1.0	7.6
17	Gas	298.2	2.09	14.9	0.2	0.2	13.6	14.9	13.6	14.9	-8.6	0.0	-8.6	0.0
18	Gas	298.2	5.18	15.8	0.1	0.2	15.3	16.9	15.3	17.0	-3.6	6.8	-3.3	7.1
19	SC	298.2	10.96	34.8	0.3	0.3	36.1	37.3	35.4	36.6	3.8	7.3	1.8	5.3
20	SC	298.2	20.83	58.0	0.5	0.4	59.9	65.0	60.5	65.7	3.4	12.2	4.3	13.3
21	SC	298.2	51.93	92.0	0.7	0.5	99.0	110.4	110.0	121.8	7.6	19.9	19.5	32.3
22	SC	298.2	102.59	129.5	0.6	0.6	158.3	166.4	198.3	198.7	22.2	28.5	53.1	53.5
23	SC	298.2	125.57	149.3	0.7	0.7	186.9	189.9	242.7	231.5	25.2	27.2	62.5	55.0
24	Gas	323.2	2.11	16.6	0.1	0.2	13.6	14.8	13.6	14.9	-18.0	-10.3	-18.0	-10.3
25	Gas	323.2	5.23	17.1	0.2	0.2	14.8	16.4	14.8	16.4	-13.6	-4.4	-13.4	-4.1
26	SC	323.2	11.74	25.9	0.3	0.3	25.0	26.4	24.2	25.6	-3.7	1.7	-6.9	-1.3
27	SC	323.2	20.14	43.1	0.3	0.3	44.6	46.6	43.7	45.6	3.6	8.3	1.5	5.9
28	SC	323.2	49.94	76.7	0.2	0.4	79.3	88.4	84.5	94.5	3.4	15.3	10.2	23.2
29	SC	323.2	103.66	112.4	0.7	0.6	131.1	142.2	159.3	167.3	16.6	26.5	41.7	48.8
30	SC	323.2	125.00	125.6	0.4	0.6	152.8	161.7	193.3	194.9	21.7	28.8	53.9	55.2
31	Gas	373.2	2.15	18.5	0.2	0.2	13.5	14.7	13.5	14.7	-27.0	-20.3	-27.0	-20.3
32	Gas	373.2	5.24	19.2	0.2	0.2	14.3	15.8	14.3	15.8	-25.2	-17.4	-25.1	-17.3
33	Gas	373.2	10.44	20.7	0.1	0.2	17.0	18.8	17.1	18.8	-17.8	-9.4	-17.5	-9.1
34	SC	373.2	20.72	31.8	0.2	0.3	29.1	30.4	28.3	29.6	-8.4	-4.6	-10.9	-7.0
35	SC	373.2	46.22	56.4	0.4	0.3	55.5	59.5	56.2	60.4	-1.6	5.6	-0.3	7.2
36	SC	373.2	63.26	67.3	0.1	0.4	68.0	75.0	71.4	79.1	1.0	11.4	6.0	17.4
37	SC	373.2	103.20	87.8	0.3	0.5	95.9	107.1	109.4	121.2	9.2	21.9	24.5	37.9
38	SC	373.2	125.26	102.4	0.2	0.5	112.0	123.8	133.3	144.3	9.3	20.8	30.1	40.8
39	SC	373.2	151.47	119.1	1.1	0.6	132.0	143.1	164.4	171.6	10.8	20.1	38.0	44.0
40	Gas	423.2	5.22	20.7	0.1	0.2	14.1	15.5	14.1	15.5	-32.0	-25.0	-31.9	-25.0
41	Gas	423.2	10.36	22.1	0.1	0.2	15.8	17.5	15.8	17.5	-28.4	-20.8	-28.3	-20.7
42	Gas	423.2	20.96	26.7	0.2	0.3	22.8	24.3	22.5	24.1	-14.7	-8.9	-15.5	-9.7
43	SC	423.2	29.11	34.7	0.2	0.3	30.0	31.2	29.5	30.7	-13.5	-10.1	-15.2	-11.7
44	SC	423.2	49.79	48.4	0.2	0.3	46.2	48.5	46.3	48.5	-4.5	0.2	-4.4	0.3
45	SC	423.2	102.95	75.1	0.3	0.4	76.5	85.1	83.2	93.0	1.8	13.4	10.8	23.8
46	SC	423.2	124.68	84.6	0.3	0.4	88.5	99.0	99.8	111.3	4.6	17.0	18.0	31.5
47	SC	423.2	146.38	94.4	0.6	0.5	101.1	112.6	118.0	129.8	7.1	19.3	25.0	37.5
				Average Absolute Deviation (AAD)							**13.6**	**16.2**	**25.4**	**25.9**

Table 4.12 Experimental and modelling results (LBC model) of the viscosity of BIN 1

1	2	3	4	5	6	7	8	9	10	11	12	13	14	15
No	Phase	T	P	Viscosity / μPa.s							Deviation (%)			
		K	MPa	EXP.	$u_A(\eta)$	$u_c(\eta)$	LBC	CO_2-LBC	LBC	CO_2-LBC	LBC	CO_2-LBC	LBC	CO_2-LBC
Density Correction?		(±0.1)	(±0.02)		μPa.s	μPa.s	Yes	Yes	No	No	Yes	Yes	No	No
1	Gas	273.2	2.11	13.7	0.3	0.2	14.7	16.1	14.7	16.1	7.1	17.6	7.1	17.6
2	Liq.	273.2	10.76	94.3	0.6	0.5	81.6	90.7	83.8	93.3	-13.5	-3.9	-11.2	-1.1
3	Liq.	273.2	21.31	117.1	0.9	0.6	98.0	109.6	107.3	119.7	-16.3	-6.4	-8.4	2.3
4	Liq.	273.2	51.84	161.1	1.1	0.8	135.6	148.4	170.3	179.9	-15.8	-7.8	5.7	11.7
5	Liq.	273.2	103.82	210.9	1.5	1.0	197.7	202.7	283.0	266.0	-6.3	-3.9	34.2	26.1
6	Liq.	273.2	124.87	228.2	0.9	1.1	223.7	223.1	330.7	297.8	-2.0	-2.2	44.9	30.5
7	Liq.	273.2	152.64	253.2	2.1	1.2	258.6	248.9	394.6	337.7	2.1	-1.7	55.8	33.4
8	Gas	283.2	2.11	14.3	0.3	0.2	14.7	16.1	14.7	16.1	2.4	12.3	2.4	12.4
9	Gas	283.2	4.51	15.3	0.2	0.2	16.1	17.9	16.1	17.9	5.0	16.6	4.9	16.4
10	Liq.	283.2	10.36	71.9	0.4	0.4	68.8	75.2	68.3	74.5	-4.2	4.6	-4.9	3.7
11	Liq.	283.2	20.75	96.1	0.9	0.5	86.4	96.4	91.3	102.1	-10.1	0.3	-4.9	6.3
12	Liq.	283.2	51.78	134.0	1.2	0.7	122.7	135.8	150.0	161.9	-8.4	1.4	11.9	20.8
13	Liq.	283.2	105.53	183.0	1.4	0.9	181.6	189.5	257.2	247.9	-0.7	3.6	40.6	35.5
14	Liq.	283.2	125.22	201.3	1.8	1.0	204.1	207.8	298.7	276.7	1.4	3.3	48.4	37.5
15	Liq.	283.2	153.19	227.0	1.3	1.1	236.8	233.0	359.2	316.0	4.3	2.6	58.2	39.2
16	Gas	298.2	2.20	14.4	0.1	0.2	14.7	16.1	14.7	16.1	1.6	11.4	1.7	11.5
17	Gas	298.2	5.20	16.3	0.1	0.2	16.2	18.0	16.3	18.1	-0.8	10.1	-0.4	10.6
18	SC	298.2	10.08	44.3	0.4	0.3	48.4	50.6	46.2	48.1	9.4	14.2	4.4	8.6
19	SC	298.2	20.63	86.6	0.8	0.5	72.5	79.6	73.6	81.0	-16.3	-8.0	-15.0	-6.5
20	SC	298.2	51.51	120.4	1.2	0.6	106.8	119.2	125.2	138.2	-11.3	-1.0	3.9	14.8
21	SC	298.2	103.85	168.3	1.4	0.8	157.4	168.6	216.7	217.7	-6.5	0.2	28.7	29.3
22	SC	298.2	124.52	187.9	1.0	0.9	178.1	186.6	255.6	246.7	-5.2	-0.7	36.0	31.3
23	SC	298.2	152.50	205.0	1.5	1.0	207.2	210.3	310.3	284.5	1.1	2.6	51.3	38.8
24	Gas	323.2	2.04	17.0	0.3	0.2	14.6	15.9	14.6	15.9	-14.4	-6.4	-14.4	-6.3
25	Gas	323.2	5.25	17.5	0.1	0.2	15.7	17.5	15.8	17.5	-9.9	-0.1	-9.6	0.2
26	Gas	323.2	10.36	24.0	0.1	0.3	23.1	24.9	22.7	24.5	-3.8	3.7	-5.6	2.0
27	SC	323.2	20.46	54.5	0.3	0.3	53.7	56.7	51.9	54.6	-1.5	4.0	-4.6	0.3
28	SC	323.2	51.80	97.8	0.7	0.5	87.5	97.7	97.0	108.6	-10.5	-0.1	-0.8	11.0
29	SC	323.2	102.73	142.7	1.4	0.7	128.9	141.9	168.4	178.3	-9.7	-0.6	18.0	24.9
30	SC	323.2	125.38	159.9	0.5	0.8	147.5	159.6	203.5	207.4	-7.7	-0.2	27.3	29.7
31	SC	323.2	153.10	179.9	0.8	0.9	171.2	180.7	248.9	241.8	-4.8	0.5	38.4	34.4
32	Gas	373.2	2.10	19.5	0.2	0.2	14.5	15.8	14.5	15.8	-25.7	-18.9	-25.7	-18.9
33	Gas	373.2	5.20	19.9	0.1	0.2	15.3	16.9	15.3	16.9	-23.4	-15.4	-23.3	-15.2
34	Gas	373.2	10.37	22.3	0.2	0.2	17.8	19.7	17.9	19.8	-19.9	-11.4	-19.6	-11.0
35	Gas	373.2	17.54	29.8	0.2	0.3	26.1	27.7	25.5	27.1	-12.5	-7.0	-14.5	-8.9
36	SC	373.2	51.90	67.9	0.5	0.4	63.6	68.7	65.9	71.5	-6.3	1.2	-2.9	5.4
37	SC	373.2	103.05	91.7	0.6	0.5	95.7	107.0	114.0	126.9	4.3	16.7	24.3	38.3
38	SC	373.2	124.10	101.7	0.5	0.5	108.3	120.9	136.0	148.8	6.5	18.8	33.7	46.3
39	SC	373.2	151.81	122.4	0.7	0.6	125.4	138.4	167.4	177.4	2.5	13.1	36.8	45.0
40	Gas	423.2	5.22	21.6	0.2	0.2	15.0	16.6	15.1	16.6	-30.2	-23.0	-30.2	-23.0
41	Gas	423.2	10.47	25.2	0.1	0.3	16.7	18.6	16.8	18.6	-33.5	-26.2	-33.5	-26.2
42	Gas	423.2	20.81	29.8	0.1	0.3	23.4	25.2	23.1	24.9	-21.5	-15.5	-22.4	-16.4
43	SC	423.2	50.81	61.9	0.2	0.4	48.9	51.1	49.1	51.3	-20.9	-17.3	-20.6	-17.0
44	SC	423.2	104.08	89.2	0.8	0.5	77.3	85.6	86.7	96.7	-13.3	-4.0	-2.8	8.4
45	SC	423.2	124.07	101.7	0.9	0.5	86.9	96.9	101.4	113.4	-14.6	-4.7	-0.3	11.5
46	SC	423.2	151.34	111.9	0.9	0.5	100.0	111.9	123.2	136.3	-10.7	-0.1	10.1	21.8
				Average Absolute Deviation (AAD)							**10.0**	**7.5**	**19.7**	**18.9**

Table 4.13 Experimental and modelling results (LBC model) of the viscosity of BIN 2

1	2	3	4	5	6	7	8	9	10	11	12	13	14	15
No	Phase	T	P	Viscosity / μPa.s							Deviation (%)			
		K	MPa	EXP.	$u_A(\eta)$	$u_c(\eta)$	LBC	CO_2-LBC	LBC	CO_2-LBC	LBC	CO_2-LBC	LBC	CO_2-LBC
Density Correction?		(±0.1)	(±0.02)		μPa.s	μPa.s	Yes	Yes	No	No	Yes	Yes	No	No
1	Gas	273.2	1.22	14.1	0.2	0.2	14.3	15.5	14.3	15.5	1.7	10.5	1.7	10.5
2	Gas	273.2	2.09	14.3	0.1	0.2	14.6	15.9	14.6	15.9	2.1	11.6	2.1	11.6
3	Gas	273.2	3.92	15.1	0.1	0.2	15.5	17.1	15.5	17.1	2.4	13.0	2.3	13.0
4	Liq.	273.2	20.76	86.0	0.6	0.5	81.4	90.6	86.9	97.1	-5.4	5.4	1.1	12.9
5	Liq.	273.2	52.93	129.5	1.0	0.6	120.4	132.9	146.7	157.8	-7.0	2.6	13.3	21.8
6	Liq.	273.2	103.76	172.1	1.2	0.8	178.9	185.5	247.5	238.1	4.0	7.8	43.9	38.4
7	Liq.	273.2	124.90	186.3	0.5	0.9	204.1	205.7	292.1	268.9	9.6	10.5	56.8	44.3
8	Liq.	273.2	153.11	219.8	1.7	1.0	238.6	231.6	353.4	308.2	8.5	5.4	60.8	40.2
9	Gas	283.2	1.42	15.1	0.0	0.2	14.3	15.6	14.3	15.6	-5.0	3.3	-5.0	3.4
10	Gas	283.2	2.11	15.6	0.2	0.2	14.5	15.9	14.5	15.9	-6.6	2.1	-6.5	2.1
11	Gas	283.2	4.89	15.6	0.1	0.2	16.0	17.7	16.0	17.7	2.7	13.6	2.6	13.5
12	Liq.	283.2	14.51	67.8	0.3	0.4	61.7	66.7	62.5	67.7	-9.0	-1.7	-7.8	-0.2
13	Liq.	283.2	21.11	76.5	0.6	0.4	72.6	80.1	75.8	83.9	-5.0	4.7	-0.9	9.8
14	Liq.	283.2	52.88	113.9	0.8	0.6	109.1	121.4	129.7	141.9	-4.2	6.6	13.8	24.6
15	Liq.	283.2	104.03	167.2	0.6	0.8	162.9	172.1	222.4	219.7	-2.6	2.9	32.9	31.3
16	Liq.	283.2	124.60	175.8	1.4	0.8	185.5	190.9	262.5	248.7	5.5	8.6	49.3	41.4
17	Liq.	283.2	153.17	198.3	2.0	0.9	217.8	216.2	320.3	287.3	9.8	9.0	61.5	44.9
18	Gas	298.2	2.11	14.2	0.1	0.2	14.5	15.8	14.5	15.8	2.1	11.4	2.1	11.5
19	Gas	298.2	5.21	16.3	0.1	0.2	15.8	17.5	15.9	17.6	-2.6	7.7	-2.3	8.0
20	SC	298.2	13.67	40.8	0.3	0.3	45.5	47.4	44.7	46.5	11.5	16.2	9.7	14.1
21	SC	298.2	20.89	63.6	0.6	0.4	60.4	65.1	61.2	66.0	-5.1	2.3	-3.9	3.8
22	SC	298.2	52.39	114.5	1.1	0.6	95.0	106.2	108.7	121.0	-17.0	-7.2	-5.0	5.7
23	SC	298.2	103.26	154.8	0.9	0.7	142.1	153.6	188.9	193.7	-8.2	-0.8	22.0	25.1
24	SC	298.2	124.89	167.3	1.5	0.8	162.9	172.1	226.3	222.6	-2.6	2.9	35.3	33.1
25	SC	298.2	153.18	182.1	1.8	0.9	191.3	195.6	277.7	259.1	5.0	7.4	52.5	42.3
26	Gas	323.2	2.12	16.8	0.2	0.2	14.4	15.7	14.4	15.8	-14.2	-6.4	-14.2	-6.4
27	Gas	323.2	5.22	17.8	0.2	0.2	15.5	17.1	15.5	17.1	-13.1	-4.0	-12.9	-3.8
28	Gas	323.2	10.44	22.0	0.1	0.2	20.7	22.5	20.4	22.2	-6.3	1.8	-7.6	0.6
29	SC	323.2	27.26	58.7	0.5	0.4	54.2	57.5	54.2	57.6	-7.8	-2.1	-7.6	-2.0
30	SC	323.2	52.13	86.5	0.5	0.5	77.9	86.5	85.0	94.8	-9.9	0.0	-1.8	9.6
31	SC	323.2	103.96	138.7	1.0	0.7	118.0	130.5	150.1	160.8	-14.9	-5.9	8.2	15.9
32	SC	323.2	124.87	143.8	1.4	0.7	134.5	146.5	179.5	186.0	-6.5	1.8	24.8	29.4
33	SC	323.2	152.50	164.3	1.4	0.8	157.1	167.0	221.0	218.6	-4.4	1.7	34.5	33.1
34	Gas	373.2	2.24	18.7	0.1	0.2	14.4	15.7	14.4	15.7	-23.1	-16.2	-23.1	-16.2
35	Gas	373.2	5.25	20.0	0.1	0.2	15.1	16.6	15.1	16.6	-24.6	-17.0	-24.5	-16.9
36	Gas	373.2	10.39	21.9	0.0	0.2	17.3	19.1	17.3	19.1	-21.3	-13.1	-21.1	-12.8
37	Gas	373.2	18.53	28.6	0.1	0.3	24.9	26.5	24.4	26.0	-13.0	-7.5	-14.9	-9.3
38	SC	373.2	37.83	46.9	0.6	0.3	46.5	48.5	46.2	48.2	-0.9	3.4	-1.5	2.7
39	SC	373.2	51.90	58.8	0.3	0.4	57.3	61.2	59.0	63.4	-2.7	4.1	0.3	7.7
40	SC	373.2	104.86	96.9	0.6	0.5	88.6	99.0	103.8	115.8	-8.5	2.2	7.2	19.6
41	SC	373.2	124.83	109.4	0.8	0.6	100.0	111.7	122.7	135.1	-8.6	2.1	12.1	23.5
42	SC	373.2	151.14	131.0	0.7	0.6	115.4	127.8	149.6	160.4	-11.9	-2.5	14.2	22.4
43	Gas	423.2	2.10	21.0	0.1	0.2	14.3	15.6	14.3	15.6	-32.0	-26.0	-31.9	-26.0
44	Gas	423.2	5.23	22.7	0.1	0.2	14.9	16.3	14.9	16.4	-34.5	-28.0	-34.5	-28.0
45	Gas	423.2	10.39	23.6	0.1	0.2	16.3	18.1	16.4	18.1	-30.7	-23.4	-30.7	-23.3
46	Gas	423.2	20.44	28.2	0.2	0.2	21.8	23.5	21.6	23.3	-22.8	-16.6	-23.5	-17.3
47	SC	423.2	51.29	40.3	0.4	0.3	44.9	46.7	45.1	46.9	11.5	16.0	11.9	16.5
48	SC	423.2	103.72	79.3	0.7	0.4	71.3	78.4	78.7	87.5	-10.2	-1.1	-0.7	10.3
49	SC	423.2	124.07	88.0	0.9	0.4	80.4	89.5	92.3	103.1	-8.6	1.7	4.8	17.2
50	SC	423.2	151.83	97.9	1.0	0.5	93.0	104.0	112.3	124.7	-5.0	6.2	14.8	27.4
Average Absolute Deviation (AAD)											**9.8**	**7.7**	**17.6**	**18.1**

Table 4.14 Experimental and modelling results (LBC model) of the viscosity of MIX 4

1	2	3	4	5	6	7	8	9	10	11	12	13	14	15
No	Phase	T	P	Viscosity / μPa.s							Deviation (%)			
		K	MPa	EXP.	$u_A(\eta)$	$u_c(\eta)$	LBC	CO_2-LBC	LBC	CO_2-LBC	LBC	CO_2-LBC	LBC	CO_2-LBC
Density Correction?		(±0.1)	(±0.02)		μPa.s	μPa.s	Yes	Yes	No	No	Yes	Yes	No	No
1	SC	273.2	2.59	14.0	0.3	0.2	13.5	14.7	13.5	14.7	-4.1	4.5	-4.1	4.5
2	SC	273.2	5.22	15.1	0.1	0.2	15.1	16.6	15.1	16.6	-0.2	9.6	-0.2	9.6
3	SC	283.2	1.75	13.8	0.2	0.2	13.2	14.3	13.2	14.3	-4.8	3.2	-4.8	3.2
4	SC	283.2	2.09	14.0	0.1	0.2	13.3	14.4	13.3	14.4	-5.2	3.0	-5.2	3.0
5	SC	283.2	5.18	15.2	0.1	0.2	14.8	16.2	14.8	16.2	-2.5	7.1	-2.5	7.1
6	SC	298.2	2.05	14.1	0.2	0.2	13.2	14.3	13.2	14.3	-6.1	1.9	-6.0	2.0
7	SC	298.2	5.29	15.5	0.2	0.2	14.5	15.9	14.5	16.0	-6.5	2.7	-6.3	2.9
8	SC	323.2	2.00	15.0	0.1	0.2	13.2	14.3	13.2	14.3	-12.5	-5.2	-12.5	-5.2
9	SC	323.2	5.34	16.4	0.1	0.2	14.2	15.6	14.2	15.6	-13.5	-5.1	-13.4	-5.0
10	SC	323.2	10.60	19.5	0.2	0.2	18.3	19.8	18.1	19.7	-6.4	1.3	-7.1	0.6
11	SC	373.2	2.23	18.9	0.3	0.2	13.1	14.2	13.1	14.2	-30.4	-24.6	-30.4	-24.6
12	SC	373.2	5.23	18.4	0.1	0.2	13.8	15.1	13.8	15.1	-25.1	-18.1	-25.1	-18.0
13	SC	373.2	10.53	20.2	0.1	0.2	15.9	17.5	16.0	17.5	-20.9	-13.4	-20.8	-13.2
14	SC	423.2	5.23	20.0	0.1	0.2	13.6	14.9	13.6	14.9	-32.0	-25.7	-32.0	-25.7
15	SC	423.2	10.53	21.4	0.0	0.2	15.1	16.6	15.1	16.6	-29.3	-22.4	-29.3	-22.3
Average Absolute Deviation (AAD)											**13.3**	**9.9**	**13.3**	**9.8**

Table 4.15 Experimental and modelling results (predictive models) of the viscosity of pure CO_2

1	2	3	4	5	6	7	8	9	10	11	12	13	14	15	16	17	18	19	20	21	22	23
No	Phase	T	P	Viscosity / μPa.s											Deviation (%)							
		K	MPa	EXP.	$u_A(\eta)$	$u_c(\eta)$	ST	CO_2-ST	ST	CO_2-ST	CS2	CO_2-CS2	Ped.	CO_2-Ped	ST	CO_2-ST	ST	CO_2-ST	CS2	CO_2-CS2	Ped.	CO_2-Ped
Density Correction?		(±0.1)	(±0.02)		μPa.s	μPa.s	Yes	Yes	No	No	---	---	---	---	Yes	Yes	No	No	---	---	---	---
1	Gas	238.2	1.03	12.9	0.2	0.2	12.7	12.3	12.7	12.3	24.4	12.4	12.9	12.1	1.6	4.3	1.6	4.3	89.3	4.0	0.2	5.8
2	Liq.	238.2	10.22	191.6	0.9	0.9	182.0	194.0	216.6	231.9	149.7	157.6	171.7	195.2	5.0	1.2	13.1	21.0	21.9	17.8	10.4	1.8
3	Liq.	238.2	21.18	209.4	0.3	1.0	200.1	213.7	245.5	264.0	163.6	182.4	188.2	214.6	4.4	2.0	17.2	26.0	21.9	12.9	10.1	2.5
4	Liq.	238.2	51.70	257.4	0.6	1.2	244.1	262.4	313.0	340.0	196.2	230.1	228.5	263.2	5.1	2.0	21.6	32.1	23.8	10.6	11.2	2.3
5	Liq.	243.2	102.78	316.3	1.7	1.5	291.2	313.4	382.9	419.2	233.8	278.3	275.7	314.0	7.9	0.9	21.0	32.5	26.1	12.0	12.8	0.7
6	Liq.	243.2	126.15	349.9	1.3	1.6	313.8	339.3	416.2	458.1	252.8	301.9	300.5	339.9	10.3	3.0	19.0	30.9	27.7	13.7	14.1	2.9
7	Gas	253.2	1.03	13.9	0.2	0.2	13.3	13.0	13.3	13.0	24.7	13.1	13.6	12.8	3.8	6.2	3.8	6.2	78.4	5.6	1.8	7.3
8	Liq.	253.2	50.43	215.0	0.8	1.0	208.6	216.7	262.8	278.1	173.9	191.8	198.2	217.3	3.0	0.7	22.2	29.3	19.1	10.8	7.8	1.0
9	Liq.	253.2	102.56	281.7	0.6	1.3	267.3	283.4	348.6	379.3	217.7	252.9	253.5	283.9	5.1	0.6	23.7	34.6	22.7	10.2	10.0	0.8
10	Liq.	253.2	150.16	343.8	0.9	1.6	310.7	334.2	410.0	453.7	253.5	298.9	299.7	334.6	9.6	2.8	19.3	32.0	26.3	13.0	12.8	2.7
11	Gas	273.2	1.05	13.7	0.1	0.2	14.3	14.0	14.3	14.0	24.9	14.1	14.6	13.8	4.2	2.0	4.2	1.9	82.2	2.8	6.8	1.0
12	Gas	273.2	2.05	13.9	0.1	0.2	14.8	14.2	14.8	14.2	25.6	14.3	15.1	14.1	6.3	2.1	6.3	2.1	84.6	3.0	8.5	1.2
13	Liq.	273.2	10.47	114.5	0.4	0.6	117.1	114.7	121.7	119.3	106.2	97.2	116.4	115.0	2.2	0.1	6.3	4.2	7.2	15.1	1.6	0.5
14	Liq.	273.2	20.13	131.7	0.3	0.6	133.7	131.4	148.7	146.9	120.2	114.4	131.5	131.7	1.5	0.2	12.9	11.5	8.7	13.2	0.1	0.0
15	Liq.	273.2	52.05	174.1	1.3	0.8	175.2	175.4	215.0	220.3	152.8	157.0	169.8	175.5	0.7	0.8	23.5	26.5	12.2	9.8	2.5	0.8
16	Liq.	273.2	102.61	230.5	1.0	1.1	226.9	234.1	292.3	313.7	191.8	210.9	218.1	234.3	1.6	1.6	26.8	36.1	16.8	8.5	5.4	1.6
17	Liq.	273.2	150.44	282.2	1.1	1.3	268.0	283.5	349.7	387.3	223.8	255.5	258.7	283.6	5.0	0.5	23.9	37.3	20.7	9.5	8.3	0.5
18	Gas	283.2	1.09	14.3	0.1	0.2	14.7	14.4	14.7	14.4	24.4	14.6	15.1	14.3	2.6	0.5	2.7	0.5	70.3	1.5	5.3	0.2
19	Gas	283.2	2.07	14.4	0.1	0.2	15.2	14.6	15.2	14.6	25.3	14.8	15.5	14.5	5.6	1.7	5.7	1.8	75.7	2.8	8.0	1.0
20	Liq.	283.2	7.89	91.4	0.7	0.5	95.4	92.2	91.3	88.4	89.6	79.1	97.9	92.4	4.4	0.9	0.1	3.2	2.0	13.5	7.1	1.1
21	Liq.	283.2	23.07	120.9	0.6	0.6	124.2	120.2	135.8	132.0	114.1	105.9	123.5	120.3	2.7	0.5	12.4	9.3	5.6	12.3	2.2	0.5
22	Liq.	283.2	39.85	143.8	1.5	0.7	146.7	143.4	171.9	170.6	132.3	128.4	144.2	143.4	2.0	0.3	19.6	18.6	8.0	10.7	0.3	0.3
23	Liq.	283.2	59.01	167.4	0.4	0.8	168.2	166.5	206.2	209.6	149.1	150.2	164.3	166.6	0.5	0.5	23.2	25.2	10.9	10.3	1.9	0.5
24	Liq.	283.2	101.38	212.7	0.5	1.0	209.0	212.9	267.5	284.6	180.2	192.7	202.5	212.9	1.7	0.1	25.8	33.8	15.3	9.4	4.8	0.1
25	Liq.	283.2	151.26	260.4	1.1	1.2	249.9	262.5	324.9	359.7	212.0	237.5	242.6	262.5	4.0	0.8	24.7	38.1	18.6	8.8	6.8	0.8
26	Gas	293.2	1.13	14.6	0.1	0.2	15.2	14.9	15.2	14.9	12.0	15.1	15.6	14.8	4.0	1.9	4.0	1.9	17.7	3.0	6.8	1.3
27	Gas	293.2	2.05	14.7	0.1	0.2	15.6	15.1	15.6	15.1	13.8	15.2	16.0	15.0	5.8	2.2	5.8	2.2	6.3	3.3	8.4	1.5
28	Liq.	293.2	11.47	86.5	0.3	0.5	89.1	85.3	84.9	81.4	86.2	74.5	92.8	85.3	2.9	1.4	1.9	5.9	0.4	13.9	7.3	1.5
29	Liq.	293.2	20.37	103.6	0.6	0.5	107.0	102.2	111.3	106.5	101.5	90.4	108.5	102.2	3.2	1.3	7.4	2.7	2.1	12.8	4.7	1.4

1	2	3	4	5	6	7	8	9	10	11	12	13	14	15	16	17	18	19	20	21	22	23
No	Phase	T	P	Viscosity / μPa.s											Deviation (%)							
		K	MPa	EXP.	$u_A(\eta)$	$u_c(\eta)$	ST	CO_2-ST	ST	CO_2-ST	CS2	CO_2-CS2	Ped.	CO_2-Ped	ST	CO_2-ST	ST	CO_2-ST	CS2	CO_2-CS2	Ped.	CO_2-Ped
Density Correction?		(±0.1)	(±0.02)		μPa.s	μPa.s	Yes	Yes	No	No	---	---	---	---	Yes	Yes	No	No	---	---	---	---
30	Liq.	293.2	36.79	129.5	0.9	0.6	130.4	125.5	148.0	143.9	120.7	112.8	129.8	125.4	0.7	3.1	14.3	11.1	6.8	12.8	0.3	3.1
31	Liq.	293.2	68.99	165.9	0.8	0.8	165.1	162.5	202.7	205.7	148.1	147.5	162.2	162.4	0.5	2.1	22.2	24.0	10.7	11.1	2.2	2.1
32	Liq.	293.2	101.04	195.3	1.1	0.9	193.9	195.3	246.5	260.0	170.4	177.6	189.5	195.3	0.7	0.0	26.2	33.1	12.8	9.1	3.0	0.0
33	Liq.	293.2	141.60	234.7	1.2	1.1	226.1	234.3	292.3	320.7	195.4	212.8	220.7	234.2	3.7	0.2	24.5	36.6	16.8	9.3	6.0	0.2
34	Gas	308.2	1.20	15.3	0.0	0.2	15.9	15.6	15.9	15.6	12.4	15.8	16.4	15.5	3.7	1.8	3.7	1.8	18.9	2.9	6.7	1.3
35	Gas	308.2	2.07	15.4	0.0	0.2	16.3	15.8	16.3	15.8	14.1	15.9	16.7	15.7	5.7	2.4	5.7	2.5	8.6	3.6	8.6	1.9
36	Gas	308.2	5.09	18.4	0.1	0.2	18.2	17.0	18.3	17.1	19.2	17.2	18.5	17.0	1.3	7.6	0.9	7.3	4.2	6.8	0.4	8.0
37	Liq.	308.2	11.33	63.9	0.4	0.4	66.3	63.5	58.6	56.6	68.6	57.1	74.1	63.4	3.7	0.6	8.4	11.5	7.4	10.6	15.9	0.7
38	Liq.	308.2	22.09	88.4	0.6	0.5	92.4	87.4	93.0	87.8	91.3	78.5	96.1	87.3	4.6	1.2	5.2	0.6	3.3	11.1	8.7	1.2
39	Liq.	308.2	34.97	107.0	0.5	0.5	111.6	105.6	121.4	115.4	107.3	95.8	113.4	105.6	4.3	1.3	13.4	7.8	0.2	10.5	5.9	1.4
40	Liq.	308.2	68.93	144.4	0.7	0.7	147.7	143.0	177.7	176.9	136.4	130.8	147.0	142.9	2.3	1.0	23.1	22.5	5.5	9.4	1.9	1.0
41	Liq.	308.2	101.20	173.6	0.3	0.8	175.0	173.8	219.7	228.7	157.9	159.0	173.1	173.7	0.8	0.1	26.5	31.7	9.1	8.4	0.3	0.0
42	Liq.	308.2	150.52	222.4	1.0	1.1	211.0	217.6	271.9	299.5	186.3	198.8	208.2	217.5	5.1	2.2	22.2	34.7	16.2	10.6	6.4	2.2
43	Gas	323.2	1.27	16.1	0.1	0.2	16.6	16.3	16.6	16.3	12.8	16.5	17.1	16.2	2.9	1.1	3.0	1.2	20.6	2.3	6.0	0.7
44	Gas	323.2	2.05	16.3	0.0	0.2	16.9	16.4	16.9	16.4	14.3	16.6	17.4	16.4	3.6	0.8	3.7	0.8	12.6	2.0	6.6	0.4
45	Gas	323.2	5.04	17.4	0.1	0.2	18.5	17.4	18.6	17.5	18.9	17.6	18.9	17.4	6.6	0.4	7.0	0.6	8.7	1.5	9.0	0.0
46	SC	323.2	11.44	39.8	0.2	0.3	41.4	40.0	37.6	36.4	48.7	37.8	52.9	40.0	4.0	0.7	5.5	8.6	22.6	4.9	32.9	0.7
47	SC	323.2	20.67	71.1	0.3	0.4	74.3	70.2	70.8	67.0	77.3	64.1	80.3	70.1	4.6	1.3	0.4	5.8	8.7	9.8	12.9	1.4
48	SC	323.2	50.82	111.9	0.6	0.6	115.8	109.3	130.0	123.9	112.2	100.5	117.9	109.2	3.4	2.4	16.1	10.7	0.2	10.2	5.3	2.4
49	SC	323.2	105.53	160.6	0.3	0.8	162.3	159.7	201.5	208.3	149.6	147.1	162.1	159.7	1.0	0.5	25.5	29.7	6.9	8.4	0.9	0.6
50	SC	323.2	150.43	195.3	0.4	0.9	192.7	197.0	246.4	270.0	174.0	180.9	192.0	196.9	1.3	0.8	26.1	38.2	10.9	7.4	1.7	0.8
51	Gas	373.2	1.48	18.6	0.0	0.2	18.9	18.7	18.9	18.7	14.0	18.8	19.5	18.6	2.0	0.6	2.0	0.6	24.4	1.6	5.0	0.2
52	Gas	373.2	2.06	18.7	0.0	0.2	19.1	18.7	19.1	18.7	15.0	18.9	19.7	18.7	2.1	0.1	2.1	0.1	19.8	1.2	5.1	0.2
53	Gas	373.2	5.15	19.5	0.1	0.2	20.3	19.4	20.3	19.4	19.1	19.6	20.9	19.3	4.3	0.4	4.4	0.3	2.0	0.6	7.2	0.8
54	Gas	373.2	8.38	21.0	0.1	0.2	22.2	20.8	22.2	20.8	23.0	20.9	22.7	20.7	5.7	0.9	6.1	0.6	9.8	0.1	8.5	1.3
55	SC	373.2	21.67	40.2	0.2	0.3	42.7	40.6	40.6	38.6	49.6	39.1	47.9	40.5	6.1	0.9	1.0	4.0	23.4	2.6	19.1	0.8
56	SC	373.2	51.46	78.3	0.2	0.4	82.7	77.3	86.7	81.0	87.2	72.9	88.0	77.3	5.7	1.3	10.8	3.5	11.4	6.8	12.4	1.2
57	SC	373.2	102.71	119.2	0.3	0.6	122.1	117.1	143.6	142.2	120.6	109.9	125.8	117.1	2.4	1.7	20.4	19.3	1.2	7.8	5.5	1.8
58	SC	373.2	149.33	150.1	0.7	0.7	149.0	148.9	183.4	195.7	143.0	139.1	152.4	149.0	0.7	0.8	22.2	30.4	4.7	7.3	1.5	0.7
59	Gas	423.2	1.71	20.8	0.1	0.2	21.2	21.0	21.2	21.0	15.2	21.1	21.8	20.8	2.1	0.9	2.1	0.9	27.2	1.4	4.7	0.2
60	Gas	423.2	2.06	20.8	0.1	0.2	21.3	21.0	21.3	21.0	15.7	21.1	21.9	20.9	2.3	0.9	2.3	0.9	24.6	1.4	5.0	0.2

1	2	3	4	5	6	7	8	9	10	11	12	13	14	15	16	17	18	19	20	21	22	23
No	Phase	T	P	Viscosity / μPa.s											Deviation (%)							
		K	MPa	EXP.	$u_A(\eta)$	$u_c(\eta)$	ST	CO_2-ST	ST	CO_2-ST	CS2	CO_2-CS2	Ped.	CO_2-Ped	ST	CO_2-ST	ST	CO_2-ST	CS2	CO_2-CS2	Ped.	CO_2-Ped
Density Correction?		(±0.1)	(±0.02)		μPa.s	μPa.s	Yes	Yes	No	No	---	---	---	---	Yes	Yes	No	No	---	---	---	---
61	Gas	423.2	5.13	21.5	0.0	0.2	22.2	21.5	22.2	21.5	19.5	21.6	22.8	21.4	3.4	0.1	3.4	0.1	9.4	0.5	6.2	0.7
62	Gas	423.2	8.12	22.3	0.1	0.2	23.4	22.3	23.4	22.3	22.5	22.4	24.1	22.1	5.2	0.0	5.2	0.1	0.9	0.6	8.1	0.6
63	SC	423.2	51.25	59.4	0.2	0.3	63.6	60.1	64.0	60.5	70.3	57.7	68.9	60.0	6.9	1.1	7.6	1.7	18.3	2.9	15.9	0.9
64	SC	423.2	102.61	95.0	0.3	0.5	98.4	94.2	110.5	107.4	102.2	89.5	103.7	94.1	3.6	0.9	16.3	13.0	7.5	5.8	9.2	1.0
65	SC	423.2	148.94	121.0	0.5	0.6	122.1	121.1	144.4	150.2	122.5	114.4	127.2	121.0	1.0	0.1	19.3	24.2	1.3	5.4	5.1	0.1
Average Absolute Deviation (AAD)															**3.6**	**1.3**	**12.4**	**14.3**	**18.8**	**7.4**	**6.9**	**1.3**

Table 4.16 Experimental and modelling results (predictive models) of the viscosity of MIX 1

1	2	3	4	5	6	7	8	9	10	11	12	13	14	15	16	17	18	19	20	21	22	23
No	Phase	T	P	Viscosity / μPa.s											Deviation (%)							
		K	MPa	EXP.	$u_A(\eta)$	$u_c(\eta)$	ST	CO_2-ST	ST	CO_2-ST	CS2	CO_2-CS2	Ped.	CO_2-Ped	ST	CO_2-ST	ST	CO_2-ST	CS2	CO_2-CS2	Ped.	CO_2-Ped
Density Correction?		(±0.1)	(±0.02)		μPa.s	μPa.s	Yes	Yes	No	No	---	---	---	---	Yes	Yes	No	No	---	---	---	---
1	Gas	243.2	1.48	12.7	0.1	0.2	13.7	13.2	13.7	13.2	24.1	12.7	13.5	12.6	7.8	3.6	7.8	3.6	89.2	-0.2	5.8	-0.8
2	Liq.	243.2	21.11	168.6	1.2	0.8	173.9	168.2	206.2	200.2	143.0	169.7	161.0	174.2	3.1	-0.2	22.3	18.8	-15.2	0.7	-4.5	3.4
3	Liq.	243.2	52.54	217.3	1.0	1.0	219.5	213.5	273.3	268.4	175.3	217.2	200.0	221.1	1.0	-1.7	25.8	23.5	-19.3	0.0	-8.0	1.7
4	Liq.	243.2	103.76	288.1	0.8	1.3	278.2	273.5	356.6	355.8	218.4	278.0	254.2	286.1	-3.4	-5.1	23.8	23.5	-24.2	-3.5	-11.8	-0.7
5	Liq.	243.2	151.14	349.8	1.4	1.6	320.6	317.7	417.8	421.2	254.3	323.2	300.4	335.8	-8.3	-9.2	19.4	20.4	-27.3	-7.6	-14.1	-4.0
6	Gas	253.2	1.56	13.4	0.0	0.2	14.2	13.7	14.2	13.7	24.4	13.2	14.0	13.1	6.4	2.5	6.4	2.5	82.0	-1.3	4.7	-1.8
7	Gas	253.2	2.04	13.4	0.1	0.2	14.5	13.9	14.5	13.9	24.7	13.4	14.3	13.3	8.2	3.4	8.2	3.4	84.3	-0.3	6.3	-0.9
8	Liq.	253.2	21.53	144.0	0.8	0.7	155.5	147.7	180.6	172.1	131.6	149.2	146.0	152.3	8.0	2.6	25.5	19.5	-8.6	3.6	1.4	5.8
9	Liq.	253.2	52.04	193.9	0.8	0.9	198.7	190.0	244.7	237.0	162.5	193.1	182.8	195.6	2.4	-2.0	26.2	22.2	-16.2	-0.4	-5.7	0.9
10	Liq.	253.2	103.74	260.2	0.9	1.2	256.3	249.1	326.2	323.8	203.9	252.9	234.5	258.7	-1.5	-4.3	25.3	24.4	-21.6	-2.8	-9.9	-0.6
11	Liq.	253.2	151.65	314.4	0.4	1.5	299.0	294.3	385.5	389.1	237.9	298.7	277.8	308.9	-4.9	-6.4	22.6	23.7	-24.3	-5.0	-11.6	-1.8
12	Gas	273.2	1.73	14.5	0.0	0.2	15.2	14.7	15.2	14.7	24.2	14.2	15.1	14.1	4.6	1.3	4.6	1.3	66.6	-2.3	3.5	-2.7
13	Gas	273.2	2.11	14.6	0.1	0.2	15.4	14.8	15.4	14.8	24.5	14.3	15.2	14.2	5.9	1.9	5.9	1.9	68.6	-1.6	4.7	-2.1
14	Gas	273.2	3.45	15.0	0.1	0.2	16.4	15.4	16.4	15.4	25.8	15.0	16.1	14.8	9.3	3.1	9.3	3.1	72.6	0.0	7.3	-1.0
15	Liq.	273.2	10.46	97.6	0.6	0.5	101.9	94.6	105.2	97.5	94.1	96.9	102.1	97.6	4.4	-3.1	7.7	-0.1	-3.6	-0.7	4.6	-0.1
16	Liq.	273.2	20.94	119.0	0.7	0.6	122.9	113.6	135.1	124.9	110.2	115.3	119.1	116.1	3.3	-4.5	13.5	4.9	-7.4	-3.1	0.1	-2.4
17	Liq.	273.2	52.10	157.2	0.7	0.8	165.7	154.2	199.2	188.0	141.8	156.4	155.6	157.4	5.5	-1.9	26.7	19.6	-9.8	-0.5	-1.0	0.1
18	Liq.	273.2	102.75	212.6	0.3	1.0	217.9	207.6	274.4	269.4	179.5	209.9	201.6	213.2	2.5	-2.4	29.0	26.7	-15.6	-1.3	-5.2	0.2
19	Liq.	273.2	151.29	262.5	0.9	1.2	258.9	252.1	330.3	334.0	210.4	254.7	240.4	261.2	-1.4	-4.0	25.8	27.2	-19.9	-3.0	-8.4	-0.5
20	Gas	283.2	1.81	14.9	0.1	0.2	15.7	15.2	15.7	15.2	13.3	14.7	15.6	14.6	5.0	1.9	5.0	1.9	-11.3	-1.6	4.2	-2.1
21	Gas	283.2	2.16	15.0	0.1	0.2	15.9	15.3	15.9	15.3	13.9	14.8	15.7	14.7	5.7	2.0	5.7	2.0	-7.6	-1.5	4.7	-1.9
22	Gas	283.2	3.49	15.5	0.1	0.2	16.7	15.8	16.7	15.8	16.2	15.3	16.5	15.2	7.7	2.0	7.7	1.9	4.4	-1.3	6.1	-2.0
23	Liq.	283.2	10.41	78.5	0.7	0.4	85.9	79.7	85.2	79.0	82.8	84.0	89.4	81.9	9.4	1.5	8.5	0.7	5.5	7.0	13.9	4.4
24	Liq.	283.2	21.08	104.4	0.9	0.5	109.7	100.5	117.2	107.3	101.1	102.5	108.1	102.2	5.0	-3.7	12.2	2.8	-3.2	-1.8	3.5	-2.1
25	Liq.	283.2	51.67	145.1	0.7	0.7	151.7	139.7	179.6	167.5	132.7	141.5	143.8	141.9	4.5	-3.7	23.7	15.4	-8.6	-2.5	-0.9	-2.2
26	Liq.	283.2	103.18	196.7	0.8	0.9	202.6	191.5	253.9	248.0	169.9	193.2	188.9	195.8	3.0	-2.7	29.1	26.1	-13.7	-1.8	-4.0	-0.5
27	Liq.	283.2	151.00	242.0	0.4	1.1	241.4	233.8	307.1	310.5	198.9	235.8	225.1	241.2	-0.3	-3.4	26.9	28.3	-17.8	-2.6	-7.0	-0.3
28	Liq.	288.2	9.02	67.8	0.7	0.4	72.8	68.0	69.8	65.5	72.9	75.0	79.4	70.2	7.4	0.4	3.0	-3.4	7.6	10.6	17.1	3.6
29	Liq.	288.2	16.58	88.7	0.2	0.5	94.4	86.6	96.6	88.6	89.8	89.3	95.6	88.1	6.4	-2.3	8.9	-0.1	1.3	0.7	7.8	-0.6

1	2	3	4	5	6	7	8	9	10	11	12	13	14	15	16	17	18	19	20	21	22	23
No	Phase	T	P	Viscosity / μPa.s											Deviation (%)							
		K	MPa	EXP.	$u_A(\eta)$	$u_c(\eta)$	ST	CO_2-ST	ST	CO_2-ST	CS2	CO_2-CS2	Ped.	CO_2-Ped	ST	CO_2-ST	ST	CO_2-ST	CS2	CO_2-CS2	Ped.	CO_2-Ped
Density Correction?		(±0.1)	(±0.02)		μPa.s	μPa.s	Yes	Yes	No	No	---	---	---	---	Yes	Yes	No	No	---	---	---	---
30	Liq.	288.2	34.23	115.6	0.3	0.6	124.0	113.1	138.7	126.9	112.5	114.8	120.1	114.5	7.3	-2.1	20.0	9.8	-2.7	-0.6	3.9	-0.9
31	Liq.	288.2	48.29	132.6	0.6	0.7	141.7	129.8	165.1	152.7	125.7	131.3	135.3	131.4	6.9	-2.1	24.5	15.2	-5.2	-0.9	2.1	-0.8
32	Liq.	288.2	102.20	186.0	0.6	0.9	194.6	183.1	243.0	236.5	164.7	184.7	182.2	186.9	4.6	-1.5	30.6	27.1	-11.4	-0.7	-2.0	0.5
33	Liq.	288.2	151.11	230.2	1.0	1.1	233.5	225.7	296.6	300.0	193.8	227.3	218.3	232.3	1.4	-2.0	28.8	30.3	-15.8	-1.3	-5.2	0.9
34	Gas	298.2	2.08	15.3	0.0	0.2	16.5	16.0	16.5	16.0	14.0	15.5	16.4	15.4	7.9	4.9	8.0	4.9	-8.5	1.4	7.4	1.0
35	Gas	298.2	4.18	15.9	0.2	0.2	17.7	16.7	17.8	16.8	17.4	16.3	17.5	16.1	11.0	5.0	11.3	5.2	9.0	2.0	9.9	1.2
36	Liq.	298.2	10.59	59.8	0.3	0.4	62.5	58.6	58.7	55.4	65.2	66.5	70.7	60.0	4.5	-1.9	-1.7	-7.3	9.1	11.3	18.3	0.4
37	Liq.	298.2	20.66	81.0	0.5	0.4	90.7	82.8	92.6	84.5	87.7	85.3	92.3	83.7	11.9	2.3	14.3	4.3	8.3	5.4	13.9	3.3
38	Liq.	298.2	51.60	124.2	0.3	0.6	134.1	122.1	155.0	142.5	121.0	123.4	129.1	123.3	8.0	-1.7	24.8	14.7	-2.6	-0.6	3.9	-0.7
39	Liq.	298.2	103.07	173.0	0.2	0.8	182.3	170.5	226.2	219.1	156.9	171.7	171.9	173.5	5.4	-1.4	30.7	26.6	-9.3	-0.8	-0.6	0.3
40	Liq.	298.2	151.12	213.2	0.3	1.0	218.7	210.5	277.1	280.1	184.3	211.7	205.7	216.0	2.6	-1.3	30.0	31.3	-13.6	-0.7	-3.5	1.3
41	SC	323.2	2.22	17.0	0.1	0.2	17.6	17.2	17.6	17.2	14.6	16.7	17.6	16.6	3.9	1.5	4.0	1.6	-14.1	-1.7	3.9	-2.1
42	SC	323.2	5.26	17.7	0.1	0.2	19.2	18.2	19.3	18.2	19.0	17.7	19.1	17.6	8.6	2.7	9.0	2.9	6.9	-0.1	8.0	-0.8
43	SC	323.2	6.97	18.7	0.1	0.2	20.7	19.4	20.9	19.5	21.7	19.0	20.6	18.7	10.8	3.4	11.5	4.0	16.0	1.5	9.8	0.1
44	SC	323.2	13.41	38.5	0.1	0.3	42.9	40.6	39.7	37.6	47.8	46.7	49.4	39.2	11.5	5.5	3.2	-2.2	24.3	21.4	28.4	1.8
45	SC	323.2	20.45	60.3	0.3	0.4	65.1	60.1	62.5	57.9	68.2	63.3	70.1	60.1	8.0	-0.2	3.8	-3.9	13.1	5.1	16.3	-0.2
46	SC	323.2	51.13	100.5	0.3	0.5	110.1	99.4	122.2	110.6	104.5	100.3	108.8	99.5	9.5	-1.1	21.5	10.0	3.9	-0.3	8.2	-1.1
47	SC	323.2	103.26	145.2	0.8	0.7	155.7	144.0	189.4	180.9	139.4	144.4	149.5	145.5	7.3	-0.8	30.4	24.6	-4.0	-0.5	3.0	0.2
48	SC	323.2	151.25	180.8	0.5	0.9	188.5	179.9	236.3	238.0	164.6	180.3	180.0	183.3	4.3	-0.5	30.7	31.6	-9.0	-0.3	-0.4	1.4
49	SC	373.2	2.66	19.3	0.0	0.2	20.0	19.6	20.0	19.6	15.9	19.0	20.0	19.0	3.7	1.8	3.8	1.8	-17.2	-1.3	4.1	-1.5
50	SC	373.2	5.22	19.9	0.1	0.2	21.0	20.1	21.0	20.2	19.1	19.6	21.0	19.5	5.6	1.5	5.7	1.6	-4.0	-1.4	5.9	-1.7
51	SC	373.2	24.20	40.7	0.5	0.3	44.8	41.9	42.9	40.2	49.8	42.9	47.9	41.0	10.2	3.0	5.5	-1.3	22.3	5.4	17.6	0.7
52	SC	373.2	52.04	72.6	0.1	0.4	79.8	72.7	83.3	75.7	81.9	72.9	82.0	72.0	9.9	0.1	14.7	4.3	12.8	0.4	13.0	-0.9
53	SC	373.2	102.98	110.8	0.4	0.6	119.4	109.7	138.5	129.8	114.1	109.3	118.2	109.6	7.8	-1.0	25.0	17.1	2.9	-1.4	6.6	-1.1
54	SC	373.2	145.34	137.0	0.3	0.7	144.4	136.3	174.6	172.3	133.9	135.6	141.4	137.3	5.4	-0.5	27.4	25.7	-2.3	-1.0	3.2	0.2
55	SC	423.2	3.08	21.0	0.1	0.2	22.3	21.9	22.3	21.9	17.2	21.3	22.3	21.2	5.9	4.0	5.9	4.1	-18.3	1.0	6.2	0.9
56	SC	423.2	5.22	21.5	0.2	0.2	22.9	22.2	22.9	22.2	19.6	21.6	23.0	21.6	6.7	3.5	6.7	3.5	-9.0	0.6	7.1	0.4
57	SC	423.2	10.41	23.7	0.1	0.2	25.1	23.8	25.1	23.8	24.4	23.2	25.3	23.1	6.1	0.3	6.2	0.4	3.1	-1.9	6.6	-2.4
58	SC	423.2	34.14	41.9	0.1	0.3	46.0	43.1	44.9	42.1	50.6	43.1	48.3	42.2	9.8	2.9	7.3	0.5	20.8	3.0	15.3	0.8
59	SC	423.2	51.08	56.0	0.2	0.3	61.6	57.3	62.0	57.6	66.1	57.2	64.5	56.4	10.0	2.3	10.7	2.8	18.1	2.1	15.1	0.7
60	SC	423.2	102.22	89.2	0.3	0.5	96.6	89.5	107.3	100.2	96.8	88.6	97.8	88.8	8.3	0.3	20.3	12.3	8.5	-0.7	9.6	-0.5

1	2	3	4	5	6	7	8	9	10	11	12	13	14	15	16	17	18	19	20	21	22	23
No	Phase	T	P	Viscosity / μPa.s											Deviation (%)							
		K	MPa	EXP.	$u_A(\eta)$	$u_c(\eta)$	ST	CO_2-ST	ST	CO_2-ST	CS2	CO_2-CS2	Ped.	CO_2-Ped	ST	CO_2-ST	ST	CO_2-ST	CS2	CO_2-CS2	Ped.	CO_2-Ped
Density Correction?		(±0.1)	(±0.02)		μPa.s	μPa.s	Yes	Yes	No	No	---	---	---	---	Yes	Yes	No	No	---	---	---	---
61	SC	423.2	152.00	115.9	0.4	0.6	122.4	116.3	143.2	140.8	117.8	115.0	121.8	116.4	5.6	0.3	23.5	21.5	1.6	-0.7	5.1	0.4
Average Absolute Deviation (AAD)															**6.2**	**2.5**	**15.9**	**11.6**	**17.8**	**2.4**	**7.4**	**1.3**

Table 4.17 Experimental and modelling results (predictive models) of the viscosity of MIX 2

1	2	3	4	5	6	7	8	9	10	11	12	13	14	15	16	17	18	19	20	21	22	23
No	Phase	T	P	Viscosity / μPa.s											Deviation (%)							
		K	MPa	EXP.	$u_A(\eta)$	$u_c(\eta)$	ST	CO_2-ST	ST	CO_2-ST	CS2	CO_2-CS2	Ped.	CO_2-Ped	ST	CO_2-ST	ST	CO_2-ST	CS2	CO_2-CS2	Ped.	CO_2-Ped
Density Correction?		(±0.1)	(±0.02)		μPa.s	μPa.s	Yes	Yes	No	No	---	---	---	---	Yes	Yes	No	No	---	---	---	---
1	Liq.	243.2	21.40	162.2	1.5	0.8	158.6	147.3	184.6	171.7	133.4	170.2	148.5	156.3	-2.2	-9.2	13.9	5.9	-17.8	5.0	-8.4	-3.6
2	Liq.	243.2	51.95	207.5	1.4	1.0	204.1	190.3	248.8	234.1	164.4	216.4	185.7	200.3	-1.7	-8.3	19.9	12.8	-20.8	4.3	-10.5	-3.5
3	Liq.	243.2	103.29	260.8	2.2	1.2	262.9	248.0	330.2	316.5	206.3	277.5	237.9	263.9	0.8	-4.9	26.6	21.3	-20.9	6.4	-8.8	1.2
4	Liq.	243.2	151.69	329.8	2.4	1.5	305.7	291.4	390.4	379.2	241.4	323.6	282.7	314.5	-7.3	-11.7	18.4	15.0	-26.8	-1.9	-14.3	-4.6
5	Liq.	253.2	52.88	179.4	0.5	0.9	186.2	171.2	225.0	209.2	153.7	194.2	171.4	179.4	3.8	-4.6	25.5	16.6	-14.3	8.3	-4.5	0.0
6	Liq.	253.2	104.06	239.0	1.7	1.1	242.8	227.1	302.9	289.3	193.4	253.2	220.5	239.5	1.6	-5.0	26.7	21.0	-19.1	5.9	-7.7	0.2
7	Liq.	253.2	152.66	289.3	1.7	1.4	285.2	270.7	360.7	351.3	226.5	299.6	262.4	289.5	-1.4	-6.4	24.7	21.4	-21.7	3.6	-9.3	0.1
8	Gas	273.2	1.79	14.5	0.1	0.2	15.2	14.7	15.2	14.7	13.1	14.2	15.3	14.4	5.0	1.7	5.0	1.7	-9.4	-1.7	5.6	-0.8
9	Gas	273.2	2.26	14.0	0.2	0.2	15.5	14.8	15.4	14.8	13.9	14.4	15.5	14.5	10.0	5.6	10.0	5.6	-0.7	2.3	10.4	3.1
10	Liq.	273.2	21.08	107.0	0.9	0.5	109.8	98.7	119.2	106.9	102.0	115.5	109.3	103.9	2.6	-7.8	11.4	-0.1	-4.6	8.0	2.1	-2.9
11	Liq.	273.2	52.31	142.9	0.9	0.7	154.2	138.8	182.1	165.6	133.9	156.6	145.6	144.4	7.9	-2.9	27.4	15.9	-6.3	9.6	1.9	1.0
12	Liq.	273.2	103.39	195.6	1.1	0.9	206.5	190.1	255.2	241.7	170.9	210.5	190.5	198.4	5.6	-2.8	30.5	23.6	-12.6	7.6	-2.6	1.4
13	Liq.	273.2	151.09	241.7	1.3	1.1	246.0	231.6	308.0	300.8	200.2	254.5	226.9	244.0	1.8	-4.2	27.4	24.5	-17.2	5.3	-6.1	1.0
14	Gas	283.2	1.74	14.6	0.1	0.2	15.6	15.2	15.6	15.2	13.2	14.7	15.7	14.8	6.8	3.8	6.8	3.8	-9.9	0.4	7.6	1.3
15	Gas	283.2	2.28	14.7	0.2	0.2	15.9	15.3	15.9	15.3	14.1	14.8	16.0	15.0	8.0	4.1	8.0	4.1	-4.0	0.8	8.7	1.6
16	Liq.	283.2	20.28	89.4	0.6	0.5	95.5	85.6	100.6	90.0	92.1	101.2	97.5	89.9	6.8	-4.2	12.5	0.7	2.9	13.2	9.0	0.5
17	Liq.	283.2	52.66	125.0	1.0	0.6	141.9	126.7	165.4	149.1	126.0	143.2	135.5	131.4	13.5	1.4	32.3	19.3	0.8	14.6	8.4	5.1
18	Liq.	283.2	103.54	187.1	0.9	0.9	191.8	175.5	235.9	222.4	161.8	193.6	178.5	182.4	2.5	-6.2	26.1	18.9	-13.5	3.5	-4.6	-2.5
19	Liq.	283.2	151.55	230.8	0.4	1.1	229.8	215.8	287.0	280.7	189.9	236.2	213.3	226.2	-0.4	-6.5	24.3	21.6	-17.7	2.3	-7.6	-2.0
20	Gas	298.2	2.08	15.3	0.1	0.2	16.4	16.0	16.4	16.0	14.0	15.5	16.6	15.6	7.2	4.2	7.3	4.3	-8.6	1.0	8.4	1.9
21	Gas	298.2	3.53	15.2	0.2	0.2	17.2	16.4	17.2	16.4	16.3	15.9	17.3	16.0	12.7	7.4	12.9	7.5	6.8	4.6	13.6	5.2
22	Liq.	298.2	10.42	43.1	0.2	0.3	45.7	43.1	44.0	41.5	51.9	66.1	57.2	44.4	6.2	0.0	2.1	-3.7	20.6	53.4	32.7	3.2
23	Liq.	298.2	20.57	73.8	0.4	0.4	79.0	71.1	80.4	72.3	80.1	85.2	83.6	74.2	7.1	-3.6	8.9	-2.1	8.6	15.5	13.3	0.6
24	Liq.	298.2	51.42	114.8	0.6	0.6	124.0	109.9	141.1	125.8	114.1	123.3	120.7	113.4	8.0	-4.3	22.9	9.5	-0.7	7.3	5.1	-1.3
25	Liq.	298.2	104.49	167.4	0.6	0.8	173.4	157.6	211.5	198.3	150.3	173.9	163.6	163.1	3.6	-5.9	26.3	18.4	-10.3	3.9	-2.3	-2.6
26	Liq.	298.2	150.46	206.4	0.7	1.0	207.5	193.8	258.0	252.2	175.6	211.2	194.6	202.2	0.5	-6.1	25.0	22.2	-14.9	2.3	-5.7	-2.0
27	Gas	323.2	2.57	16.7	0.2	0.2	17.7	17.2	17.7	17.2	15.1	16.7	18.0	16.9	6.0	3.1	6.0	3.1	-9.4	0.1	7.5	1.1
28	Gas	323.2	3.70	17.0	0.1	0.2	18.2	17.5	18.2	17.5	16.7	17.0	18.5	17.2	7.3	3.1	7.4	3.1	-1.5	0.4	8.7	1.1
29	SC	323.2	12.77	29.7	0.1	0.3	33.7	31.6	32.1	30.0	38.2	44.2	36.6	30.2	13.7	6.3	8.3	1.2	28.9	48.8	23.3	1.9

1	2	3	4	5	6	7	8	9	10	11	12	13	14	15	16	17	18	19	20	21	22	23
No	Phase	T	P	Viscosity / μPa.s											Deviation (%)							
		K	MPa	EXP.	$u_A(\eta)$	$u_c(\eta)$	ST	CO_2-ST	ST	CO_2-ST	CS2	CO_2-CS2	Ped.	CO_2-Ped	ST	CO_2-ST	ST	CO_2-ST	CS2	CO_2-CS2	Ped.	CO_2-Ped
Density Correction?		(±0.1)	(±0.02)		μPa.s	μPa.s	Yes	Yes	No	No	---	---	---	---	Yes	Yes	No	No	---	---	---	---
30	SC	323.2	20.77	53.4	0.2	0.3	57.2	52.4	55.5	51.0	62.4	63.9	63.4	53.9	7.2	-1.7	4.0	-4.4	17.0	19.7	18.9	1.0
31	SC	323.2	52.43	95.2	0.2	0.5	103.2	91.3	113.6	100.6	99.8	101.5	103.2	93.5	8.4	-4.1	19.3	5.6	4.8	6.6	8.4	-1.9
32	SC	323.2	103.47	138.8	1.1	0.7	147.3	132.8	176.1	163.2	133.2	144.6	141.9	136.7	6.1	-4.4	26.9	17.6	-4.0	4.2	2.3	-1.5
33	SC	323.2	151.25	177.1	1.0	0.8	179.2	166.6	220.7	215.4	157.5	180.3	171.2	173.0	1.2	-5.9	24.6	21.7	-11.1	1.8	-3.3	-2.3
34	Gas	373.2	1.53	18.8	0.2	0.2	19.6	19.4	19.6	19.4	14.3	18.8	19.9	19.1	3.9	3.0	3.9	3.0	-24.0	0.1	5.8	1.2
35	Gas	373.2	2.57	19.3	0.2	0.2	19.9	19.5	19.9	19.5	15.9	19.0	20.2	19.2	3.0	1.2	3.0	1.2	-17.6	-1.6	4.9	-0.5
36	SC	373.2	20.30	32.7	0.1	0.3	35.6	33.1	34.6	32.1	40.0	36.3	37.5	32.7	8.9	1.1	5.8	-1.8	22.2	11.0	14.4	-0.2
37	SC	373.2	51.86	68.3	0.2	0.4	74.1	66.8	76.9	69.1	77.6	72.8	77.3	67.6	8.4	-2.3	12.5	1.2	13.5	6.4	13.1	-1.0
38	SC	373.2	101.20	104.0	0.3	0.5	111.7	100.7	127.6	116.7	108.4	108.1	111.7	102.8	7.4	-3.1	22.7	12.2	4.3	4.0	7.4	-1.1
39	SC	373.2	152.29	136.2	0.3	0.7	140.9	130.9	168.4	163.2	131.5	139.8	138.6	135.0	3.5	-3.9	23.7	19.9	-3.4	2.7	1.8	-0.8
40	Gas	423.2	2.42	20.9	0.2	0.2	22.0	21.7	22.0	21.7	16.4	21.2	22.4	21.4	5.1	3.7	5.1	3.8	-21.5	1.1	7.0	2.2
41	Gas	423.2	3.57	21.2	0.2	0.2	22.3	21.9	22.3	21.9	17.9	21.3	22.7	21.5	5.5	3.4	5.5	3.4	-15.6	0.9	7.5	1.9
42	SC	423.2	27.35	34.9	0.1	0.3	37.4	34.8	36.7	34.2	41.3	36.5	39.1	34.7	7.2	-0.3	5.3	-2.1	18.5	4.6	12.1	-0.7
43	SC	423.2	51.81	54.1	0.1	0.3	58.7	54.1	59.1	54.5	63.9	57.7	62.2	54.5	8.4	0.0	9.1	0.6	18.0	6.5	14.8	0.7
44	SC	423.2	103.45	85.6	0.3	0.5	92.3	84.4	101.7	93.6	93.7	89.3	94.5	85.8	7.8	-1.4	18.8	9.3	9.5	4.3	10.3	0.2
45	SC	423.2	151.71	111.0	0.3	0.6	116.3	108.8	134.3	129.2	113.5	114.9	117.0	111.7	4.8	-2.0	20.9	16.4	2.2	3.5	5.3	0.6
Average Absolute Deviation (AAD)															**5.7**	**4.1**	**15.9**	**10.1**	**12.4**	**7.1**	**8.8**	**1.7**

Table 4.18 Experimental and modelling results (predictive models) of the viscosity of MIX 3

1	2	3	4	5	6	7	8	9	10	11	12	13	14	15	16	17	18	19	20	21	22	23
No	Phase	T	P	Viscosity / μPa.s											Deviation (%)							
		K	MPa	EXP.	$u_A(\eta)$	$u_c(\eta)$	ST	CO_2-ST	ST	CO_2-ST	CS2	CO_2-CS2	Ped.	CO_2-Ped	ST	CO_2-ST	ST	CO_2-ST	CS2	CO_2-CS2	Ped.	CO_2-Ped
Density Correction?		(±0.1)	(±0.02)		μPa.s	μPa.s	Yes	Yes	No	No	---	---	---	---	Yes	Yes	No	No	---	---	---	---
1	Gas	273.2	2.13	13.7	0.2	0.2	14.3	15.6	14.3	15.6	12.7	13.5	13.8	13.0	4.3	13.5	4.3	13.5	-7.6	-1.5	0.6	-5.2
2	Liq.	273.2	12.92	64.5	0.4	0.4	68.6	58.5	70.3	59.7	77.0	73.2	81.8	76.3	6.4	-9.2	9.0	-7.4	19.3	13.4	26.8	18.2
3	Liq.	273.2	20.94	76.8	0.7	0.4	86.9	70.7	91.6	73.8	88.5	86.0	93.8	89.4	13.1	-8.0	19.2	-4.0	15.1	11.9	22.1	16.4
4	Liq.	273.2	52.31	109.7	0.5	0.6	133.2	100.7	149.7	111.3	118.1	121.9	127.0	126.9	21.4	-8.3	36.4	1.4	7.6	11.1	15.7	15.6
5	Liq.	273.2	104.24	156.9	1.0	0.8	186.5	135.1	217.3	155.4	153.0	166.1	168.1	177.5	18.9	-13.9	38.5	-1.0	-2.5	5.9	7.2	13.1
6	Liq.	273.2	124.73	167.6	0.5	0.8	204.2	146.6	239.2	169.8	165.1	181.6	182.6	196.0	21.8	-12.6	42.7	1.3	-1.5	8.3	8.9	17.0
7	Liq.	273.2	152.00	188.3	0.9	0.9	225.3	160.5	265.1	187.2	180.4	200.8	201.0	219.7	19.7	-14.8	40.8	-0.6	-4.2	6.7	6.8	16.7
8	Gas	283.2	2.09	13.7	0.1	0.2	14.7	16.1	14.7	16.1	12.8	14.0	14.2	13.4	7.6	17.6	7.6	17.6	-6.2	2.1	4.1	-1.6
9	Gas	283.2	4.89	18.0	0.2	0.2	16.7	17.3	16.6	17.3	17.3	15.7	16.2	15.0	-7.6	-4.1	-7.8	-4.2	-4.1	-12.9	-10.1	-16.6
10	Liq.	283.2	9.47	41.4	0.4	0.3	44.6	41.3	44.3	41.0	60.0	59.9	64.3	55.9	7.5	-0.5	6.8	-1.0	44.8	44.6	55.2	34.9
11	Liq.	283.2	20.76	68.0	0.2	0.4	76.2	63.6	78.9	65.5	80.8	77.0	84.9	78.7	12.2	-6.4	16.0	-3.6	18.9	13.3	24.9	15.8
12	Liq.	283.2	52.01	110.7	0.8	0.6	121.9	93.8	135.6	102.9	110.8	111.4	118.0	115.4	10.1	-15.3	22.5	-7.1	0.1	0.6	6.5	4.2
13	Liq.	283.2	103.54	141.9	0.2	0.7	172.8	127.4	200.6	146.2	144.5	153.3	157.4	163.2	21.7	-10.3	41.3	3.0	1.8	8.0	10.9	15.0
14	Liq.	283.2	125.84	158.6	0.6	0.8	191.0	139.6	223.3	161.7	157.0	169.5	172.3	182.4	20.4	-12.0	40.8	1.9	-1.0	6.8	8.6	15.0
15	Liq.	283.2	150.47	183.6	1.8	0.9	209.3	152.0	246.0	177.3	170.2	186.3	188.1	202.9	14.0	-17.2	34.0	-3.4	-7.3	1.5	2.5	10.6
16	Gas	298.2	1.11	13.5	0.1	0.2	15.0	16.6	15.0	16.6	11.6	14.4	14.5	13.9	10.7	23.1	10.7	23.1	-14.2	6.7	7.1	3.0
17	Gas	298.2	2.09	14.9	0.2	0.2	15.3	16.8	15.3	16.8	13.1	14.6	14.8	14.1	2.6	12.4	2.6	12.4	-12.4	-2.1	-0.5	-5.6
18	Gas	298.2	5.18	15.8	0.1	0.2	17.1	17.8	17.1	17.9	17.4	16.0	16.7	15.5	8.0	12.6	8.3	12.8	9.8	1.0	5.7	-2.3
19	SC	298.2	10.96	34.8	0.3	0.3	35.3	33.8	34.6	33.2	49.1	51.3	52.2	42.7	1.5	-2.8	-0.5	-4.5	41.3	47.7	50.2	22.7
20	SC	298.2	20.83	58.0	0.5	0.4	63.3	54.8	64.0	55.3	70.7	66.1	73.3	65.7	9.1	-5.5	10.3	-4.6	22.0	13.9	26.3	13.3
21	SC	298.2	51.93	92.0	0.7	0.5	107.9	85.2	118.2	92.2	101.4	98.5	106.5	101.3	17.2	-7.4	28.4	0.2	10.1	7.0	15.7	10.1
22	SC	298.2	102.59	129.5	0.6	0.6	155.0	117.3	178.8	133.9	133.3	137.1	143.5	145.2	19.7	-9.5	38.1	3.4	2.9	5.9	10.8	12.1
23	SC	298.2	125.57	149.3	0.7	0.7	172.5	129.4	201.1	149.7	145.5	152.7	157.9	163.7	15.5	-13.3	34.6	0.2	-2.6	2.3	5.7	9.6
24	Gas	323.2	2.11	16.6	0.1	0.2	16.3	17.9	16.3	17.9	13.5	15.7	15.9	15.1	-1.4	8.3	-1.4	8.3	-18.2	-5.3	-4.0	-8.5
25	Gas	323.2	5.23	17.1	0.2	0.2	17.7	18.7	17.8	18.7	17.3	16.6	17.4	16.1	3.6	9.2	3.8	9.3	0.8	-2.8	1.6	-5.8
26	SC	323.2	11.74	25.9	0.3	0.3	26.7	26.2	26.0	25.6	32.3	32.8	30.6	26.1	2.9	1.1	0.2	-1.4	24.4	26.2	18.1	0.6
27	SC	323.2	20.14	43.1	0.3	0.3	46.0	42.3	45.0	41.5	54.9	50.5	55.5	47.9	6.9	-1.8	4.5	-3.7	27.4	17.3	28.9	11.1
28	SC	323.2	49.94	76.7	0.2	0.4	87.5	72.3	93.1	76.4	87.0	80.5	89.5	81.9	14.1	-5.6	21.5	-0.4	13.4	5.0	16.7	6.9
29	SC	323.2	103.66	112.4	0.7	0.6	133.6	105.0	152.0	118.7	119.4	117.8	126.4	124.2	18.8	-6.6	35.2	5.6	6.2	4.8	12.4	10.4

1	2	3	4	5	6	7	8	9	10	11	12	13	14	15	16	17	18	19	20	21	22	23
No	Phase	T	P	Viscosity / μPa.s											Deviation (%)							
		K	MPa	EXP.	$u_A(\eta)$	$u_c(\eta)$	ST	CO_2-ST	ST	CO_2-ST	CS2	CO_2-CS2	Ped.	CO_2-Ped	ST	CO_2-ST	ST	CO_2-ST	CS2	CO_2-CS2	Ped.	CO_2-Ped
Density Correction?		(±0.1)	(±0.02)		μPa.s	μPa.s	Yes	Yes	No	No	---	---	---	---	Yes	Yes	No	No	---	---	---	---
30	SC	323.2	125.00	125.6	0.4	0.6	148.1	115.6	171.0	132.8	129.9	130.9	138.5	139.5	18.0	-7.9	36.2	5.8	3.4	4.2	10.3	11.1
31	Gas	373.2	2.15	18.5	0.2	0.2	18.4	20.2	18.4	20.2	14.5	17.8	17.9	17.2	-0.7	9.1	-0.7	9.1	-21.7	-3.9	-3.1	-6.9
32	Gas	373.2	5.24	19.2	0.2	0.2	19.4	20.7	19.4	20.7	17.7	18.4	19.1	17.8	1.1	8.0	1.2	8.0	-7.8	-3.9	-0.5	-6.9
33	Gas	373.2	10.44	20.7	0.1	0.2	22.1	22.6	22.2	22.6	22.8	20.7	22.2	20.3	6.9	9.1	7.1	9.3	10.2	0.0	7.0	-2.1
34	SC	373.2	20.72	31.8	0.2	0.3	32.8	31.7	32.1	31.1	37.8	32.6	36.0	31.6	3.1	-0.2	0.9	-2.2	18.8	2.4	13.0	-0.7
35	SC	373.2	46.22	56.4	0.4	0.3	61.0	54.6	61.8	55.3	65.7	57.4	65.3	57.8	8.2	-3.1	9.7	-1.9	16.5	1.8	15.9	2.6
36	SC	373.2	63.26	67.3	0.1	0.4	75.6	65.8	79.3	68.7	77.5	68.8	78.1	70.3	12.2	-2.3	17.7	2.0	15.2	2.2	16.0	4.4
37	SC	373.2	103.20	87.8	0.3	0.5	103.1	86.9	113.8	95.5	98.5	91.5	101.4	95.7	17.4	-1.1	29.6	8.8	12.1	4.2	15.4	9.0
38	SC	373.2	125.26	102.4	0.2	0.5	115.9	97.0	130.3	108.8	108.1	102.8	112.3	108.9	13.1	-5.3	27.2	6.2	5.5	0.4	9.6	6.3
39	SC	373.2	151.47	119.1	1.1	0.6	129.5	108.0	147.8	123.5	118.4	115.7	124.1	124.3	8.7	-9.3	24.1	3.6	-0.6	-2.9	4.2	4.3
40	Gas	423.2	5.22	20.7	0.1	0.2	21.2	22.7	21.2	22.7	18.3	20.3	20.8	19.7	2.4	9.9	2.4	9.9	-11.7	-2.0	0.6	-4.9
41	Gas	423.2	10.36	22.1	0.1	0.2	23.0	23.9	23.1	23.9	22.3	21.7	22.9	21.2	4.3	8.3	4.4	8.4	1.1	-1.8	3.8	-4.1
42	Gas	423.2	20.96	26.7	0.2	0.3	29.4	29.1	29.1	28.9	31.8	27.7	30.4	27.5	10.1	9.0	9.3	8.4	19.2	3.8	14.0	3.0
43	SC	423.2	29.11	34.7	0.2	0.3	35.8	34.7	35.2	34.3	39.9	34.2	38.2	34.1	3.0	0.0	1.5	-1.4	14.9	-1.6	10.0	-1.9
44	SC	423.2	49.79	48.4	0.2	0.3	52.0	48.6	52.0	48.7	56.8	48.9	55.6	49.5	7.5	0.4	7.6	0.6	17.5	1.1	14.9	2.3
45	SC	423.2	102.95	75.1	0.3	0.4	84.5	75.4	90.8	80.7	84.6	76.1	85.4	79.3	12.5	0.4	20.9	7.5	12.6	1.3	13.7	5.6
46	SC	423.2	124.68	84.6	0.3	0.4	95.4	84.5	104.4	92.4	93.2	85.7	95.0	90.4	12.7	-0.1	23.3	9.1	10.1	1.2	12.2	6.8
47	SC	423.2	146.38	94.4	0.6	0.5	105.2	93.1	116.9	103.4	100.9	94.9	103.7	101.3	11.5	-1.4	23.9	9.6	6.9	0.5	9.9	7.4
Average Absolute Deviation (AAD)															**10.5**	**7.8**	**17.3**	**5.8**	**11.8**	**7.2**	**12.5**	**9.1**

Table 4.19 Experimental and modelling results (predictive models) of the viscosity of BIN 1

1	2	3	4	5	6	7	8	9	10	11	12	13	14	15	16	17	18	19	20	21	22	23
No	Phase	T	P	Viscosity / μPa.s											Deviation (%)							
		K	MPa	EXP.	$u_A(\eta)$	$u_c(\eta)$	ST	CO_2-ST	ST	CO_2-ST	CS2	CO_2-CS2	Ped.	CO_2-Ped	ST	CO_2-ST	ST	CO_2-ST	CS2	CO_2-CS2	Ped.	CO_2-Ped
Density Correction?		(±0.1)	(±0.02)		μPa.s	μPa.s	Yes	Yes	No	No	---	---	---	---	Yes	Yes	No	No	---	---	---	---
1	Gas	273.2	2.11	13.7	0.3	0.2	15.1	16.1	15.0	16.1	13.6	14.3	15.3	14.4	9.6	17.3	9.6	17.3	-0.8	4.3	11.2	4.6
2	Liq.	273.2	10.76	94.3	0.6	0.5	91.2	89.2	94.1	91.9	85.9	97.5	92.5	86.6	-3.4	-5.4	-0.2	-2.6	-9.0	3.4	-2.0	-8.2
3	Liq.	273.2	21.31	117.1	0.9	0.6	111.8	107.5	122.5	117.3	102.7	115.9	109.9	105.7	-4.5	-8.2	4.6	0.2	-12.3	-1.0	-6.2	-9.7
4	Liq.	273.2	51.84	161.1	1.1	0.8	151.6	143.9	181.3	172.3	133.5	156.1	144.9	145.1	-5.9	-10.7	12.6	6.9	-17.1	-3.1	-10.0	-10.0
5	Liq.	273.2	103.82	210.9	1.5	1.0	201.5	192.0	252.9	244.3	171.0	211.0	190.1	199.9	-4.5	-9.0	19.9	15.8	-18.9	0.0	-9.8	-5.2
6	Liq.	273.2	124.87	228.2	0.9	1.1	218.8	209.2	277.0	269.1	184.2	231.0	206.4	220.4	-4.1	-8.3	21.4	17.9	-19.3	1.3	-9.5	-3.4
7	Liq.	273.2	152.64	253.2	2.1	1.2	239.7	230.4	305.2	299.3	200.8	255.9	227.0	246.4	-5.3	-9.0	20.5	18.2	-20.7	1.1	-10.4	-2.7
8	Gas	283.2	2.11	14.3	0.3	0.2	15.5	16.6	15.5	16.6	13.8	14.8	15.7	14.8	8.0	15.9	8.1	15.9	-3.9	3.2	9.9	3.5
9	Gas	283.2	4.51	15.3	0.2	0.2	17.2	17.8	17.1	17.8	17.9	16.2	17.2	15.9	11.9	16.1	11.7	16.0	16.5	5.6	12.4	3.7
10	Liq.	283.2	10.36	71.9	0.4	0.4	74.9	74.4	74.3	73.8	73.6	83.9	79.2	70.7	4.2	3.5	3.4	2.8	2.4	16.8	10.2	-1.6
11	Liq.	283.2	20.75	96.1	0.9	0.5	98.2	94.9	104.4	100.5	93.1	102.0	98.6	91.9	2.2	-1.2	8.6	4.6	-3.1	6.2	2.6	-4.3
12	Liq.	283.2	51.78	134.0	1.2	0.7	139.0	132.0	163.6	155.7	125.2	141.6	134.4	131.4	3.7	-1.5	22.1	16.2	-6.5	5.7	0.3	-1.9
13	Liq.	283.2	105.53	183.0	1.4	0.9	188.3	179.7	235.4	228.3	162.8	195.5	179.4	185.2	2.9	-1.8	28.7	24.8	-11.0	6.9	-2.0	1.2
14	Liq.	283.2	125.22	201.3	1.8	1.0	203.7	195.3	256.7	251.2	174.6	213.4	193.8	203.5	1.2	-3.0	27.6	24.8	-13.3	6.0	-3.7	1.1
15	Liq.	283.2	153.19	227.0	1.3	1.1	223.9	216.1	284.2	281.1	190.5	237.7	213.4	228.5	-1.4	-4.8	25.2	23.8	-16.1	4.7	-6.0	0.6
16	Gas	298.2	2.20	14.4	0.1	0.2	16.2	17.4	16.2	17.4	14.2	15.5	16.5	15.6	12.1	20.4	12.1	20.5	-1.8	7.5	14.4	7.9
17	Gas	298.2	5.20	16.3	0.1	0.2	18.0	18.7	18.1	18.7	18.8	17.1	18.3	16.8	10.2	14.3	10.7	14.7	15.3	4.4	11.7	2.9
18	SC	298.2	10.08	44.3	0.4	0.3	49.4	51.1	46.8	48.6	51.4	65.2	56.9	44.2	11.6	15.5	5.7	9.8	16.2	47.3	28.6	-0.2
19	SC	298.2	20.63	86.6	0.8	0.5	81.1	79.3	82.5	80.8	80.6	85.3	84.1	75.4	-6.4	-8.4	-4.7	-6.7	-6.9	-1.5	-2.9	-12.9
20	SC	298.2	51.51	120.4	1.2	0.6	122.5	116.7	140.8	134.3	114.1	123.4	120.6	114.3	1.7	-3.1	16.9	11.5	-5.3	2.5	0.1	-5.1
21	SC	298.2	103.85	168.3	1.4	0.8	168.2	161.0	208.0	202.6	149.6	172.4	162.5	163.3	-0.1	-4.4	23.6	20.4	-11.1	2.4	-3.5	-3.0
22	SC	298.2	124.52	187.9	1.0	0.9	183.3	176.5	229.3	226.1	161.4	190.0	176.7	181.1	-2.4	-6.1	22.1	20.3	-14.1	1.1	-5.9	-3.6
23	SC	298.2	152.50	205.0	1.5	1.0	202.3	196.4	255.6	255.5	176.3	212.9	195.0	204.5	-1.3	-4.2	24.7	24.6	-14.0	3.8	-4.9	-0.2
24	Gas	323.2	2.04	17.0	0.3	0.2	17.2	18.6	17.2	18.6	14.3	16.6	17.6	16.7	1.0	9.1	1.1	9.2	-15.9	-2.2	3.4	-1.7
25	Gas	323.2	5.25	17.5	0.1	0.2	18.7	19.5	18.8	19.6	18.7	17.7	19.1	17.6	7.0	11.8	7.4	12.1	7.0	1.4	9.4	1.0
26	Gas	323.2	10.36	24.0	0.1	0.3	25.8	26.6	25.4	26.1	28.8	29.3	25.9	23.3	7.3	10.6	5.7	8.6	19.7	22.1	7.9	-3.2
27	SC	323.2	20.46	54.5	0.3	0.3	57.9	58.2	55.7	56.3	62.1	63.4	63.2	54.0	6.3	6.9	2.3	3.3	14.1	16.3	16.0	-0.8
28	SC	323.2	51.80	97.8	0.7	0.5	101.2	97.5	112.0	107.7	99.2	100.9	102.5	93.5	3.5	-0.3	14.6	10.2	1.4	3.2	4.8	-4.4
29	SC	323.2	102.73	142.7	1.4	0.7	142.6	137.6	172.7	169.4	132.5	144.1	140.9	136.7	-0.1	-3.6	21.0	18.7	-7.2	0.9	-1.3	-4.3

1	2	3	4	5	6	7	8	9	10	11	12	13	14	15	16	17	18	19	20	21	22	23
No	Phase	T	P	Viscosity / μPa.s											Deviation (%)							
		K	MPa	EXP.	$u_A(\eta)$	$u_c(\eta)$	ST	CO_2-ST	ST	CO_2-ST	CS2	CO_2-CS2	Ped.	CO_2-Ped	ST	CO_2-ST	ST	CO_2-ST	CS2	CO_2-CS2	Ped.	CO_2-Ped
Density Correction?		(±0.1)	(±0.02)		μPa.s	μPa.s	Yes	Yes	No	No	---	---	---	---	Yes	Yes	No	No	---	---	---	---
30	SC	323.2	125.38	159.9	0.5	0.8	157.6	153.2	194.3	193.6	144.4	161.3	155.1	154.1	-1.4	-4.2	21.5	21.1	-9.7	0.9	-3.0	-3.6
31	SC	323.2	153.10	179.9	0.8	0.9	174.4	171.2	218.0	221.4	158.0	181.7	171.4	174.8	-3.0	-4.8	21.2	23.1	-12.2	1.0	-4.7	-2.8
32	Gas	373.2	2.10	19.5	0.2	0.2	19.4	21.0	19.4	21.0	15.2	18.9	19.9	19.0	-0.6	7.6	-0.6	7.6	-22.0	-3.0	2.0	-2.5
33	Gas	373.2	5.20	19.9	0.1	0.2	20.4	21.6	20.5	21.6	18.9	19.6	21.0	19.6	2.5	8.4	2.6	8.4	-5.0	-1.8	5.3	-1.6
34	Gas	373.2	10.37	22.3	0.2	0.2	23.3	23.9	23.4	24.0	24.5	22.2	24.0	21.9	4.7	7.5	5.0	7.8	10.3	-0.3	7.7	-1.8
35	Gas	373.2	17.54	29.8	0.2	0.3	18.9	31.7	18.9	31.2	35.0	31.4	32.5	28.9	-36.4	6.6	-36.4	4.6	17.7	5.5	9.2	-2.9
36	SC	373.2	51.90	67.9	0.5	0.4	73.0	72.5	75.9	75.3	77.4	72.8	77.2	67.9	7.5	6.8	11.8	11.0	14.1	7.3	13.7	0.1
37	SC	373.2	103.05	91.7	0.6	0.5	109.7	108.3	126.7	126.5	109.0	109.4	112.2	104.3	19.6	18.1	38.1	37.9	18.8	19.2	22.3	13.7
38	SC	373.2	124.10	101.7	0.5	0.5	121.7	120.8	143.9	145.8	119.0	122.7	123.7	117.7	19.6	18.8	41.4	43.3	16.9	20.6	21.6	15.7
39	SC	373.2	151.81	122.4	0.7	0.6	135.9	136.5	164.2	170.3	130.8	139.6	137.6	134.9	11.1	11.5	34.2	39.1	6.9	14.1	12.5	10.2
40	Gas	423.2	5.22	21.6	0.2	0.2	22.4	23.8	22.4	23.8	19.5	21.6	23.0	21.7	4.1	10.4	4.1	10.4	-9.5	0.3	6.8	0.7
41	Gas	423.2	10.47	25.2	0.1	0.3	24.4	25.3	24.5	25.3	24.2	23.2	25.2	23.2	-3.0	0.4	-2.9	0.5	-4.1	-7.7	-0.1	-8.0
42	Gas	423.2	20.81	29.8	0.1	0.3	31.0	31.6	30.7	31.4	34.0	30.2	32.4	29.2	3.9	6.0	3.0	5.1	14.0	1.1	8.5	-2.3
43	SC	423.2	50.81	61.9	0.2	0.4	56.8	57.9	57.0	58.2	62.9	57.0	61.1	53.9	-8.1	-6.4	-7.8	-6.0	1.6	-7.9	-1.2	-12.9
44	SC	423.2	104.08	89.2	0.8	0.5	90.0	91.1	99.8	101.6	93.6	89.7	94.3	86.2	0.9	2.2	11.9	14.0	5.0	0.6	5.7	-3.4
45	SC	423.2	124.07	101.7	0.9	0.5	99.9	101.7	113.5	117.0	102.3	100.5	104.0	97.0	-1.7	0.0	11.6	15.1	0.6	-1.1	2.3	-4.6
46	SC	423.2	151.34	111.9	0.9	0.5	112.2	115.4	130.6	137.5	112.9	114.8	116.1	111.5	0.3	3.1	16.7	22.8	0.8	2.5	3.7	-0.4
Average Absolute Deviation (AAD)															**5.9**	**7.8**	**14.5**	**14.7**	**10.7**	**6.1**	**7.6**	**4.4**

Table 4.20 Experimental and modelling results (predictive models) of the viscosity of BIN 2

1	2	3	4	5	6	7	8	9	10	11	12	13	14	15	16	17	18	19	20	21	22	23
No	Phase	T	P	Viscosity / μPa.s											Deviation (%)							
		K	MPa	EXP.	$u_A(\eta)$	$u_c(\eta)$	ST	CO_2-ST	ST	CO_2-ST	CS2	CO_2-CS2	Ped.	CO_2-Ped	ST	CO_2-ST	ST	CO_2-ST	CS2	CO_2-CS2	Ped.	CO_2-Ped
Density Correction?		(±0.1)	(±0.02)		μPa.s	μPa.s	Yes	Yes	No	No	---	---	---	---	Yes	Yes	No	No	---	---	---	---
1	Gas	273.2	1.22	14.1	0.2	0.2	15.0	17.1	15.0	17.1	12.1	14.1	15.1	14.5	6.4	21.6	6.4	21.6	-13.8	0.2	7.3	3.0
2	Gas	273.2	2.09	14.3	0.1	0.2	15.3	17.3	15.3	17.3	13.6	14.3	15.4	14.7	7.4	21.1	7.4	21.1	-4.9	0.3	8.3	2.8
3	Gas	273.2	3.92	15.1	0.1	0.2	16.4	18.0	16.4	18.0	16.3	15.4	16.4	15.3	8.6	19.1	8.5	19.1	8.3	2.0	8.9	1.4
4	Liq.	273.2	20.76	86.0	0.6	0.5	90.3	86.4	97.1	92.1	84.6	115.0	88.7	82.0	5.0	0.5	12.9	7.0	-1.6	33.8	3.1	-4.6
5	Liq.	273.2	52.93	129.5	1.0	0.6	132.4	121.2	154.8	140.2	117.3	157.4	124.6	121.6	2.2	-6.4	19.5	8.3	-9.4	21.5	-3.7	-6.1
6	Liq.	273.2	103.76	172.1	1.2	0.8	178.3	160.0	218.5	195.3	151.6	210.9	165.0	170.1	3.6	-7.0	27.0	13.5	-11.9	22.6	-4.1	-1.1
7	Liq.	273.2	124.90	186.3	0.5	0.9	194.3	173.9	240.0	214.6	163.8	231.1	179.7	188.9	4.3	-6.6	28.9	15.2	-12.1	24.1	-3.5	1.4
8	Liq.	273.2	153.11	219.8	1.7	1.0	213.8	191.0	265.8	238.0	179.2	256.3	198.3	213.1	-2.7	-13.1	20.9	8.3	-18.5	16.6	-9.8	-3.1
9	Gas	283.2	1.42	15.1	0.0	0.2	15.5	17.7	15.5	17.7	12.7	14.6	15.7	15.0	2.7	17.0	2.7	17.0	-16.0	-3.2	3.8	-0.5
10	Gas	283.2	2.11	15.6	0.2	0.2	15.8	17.8	15.8	17.8	13.8	14.8	15.9	15.1	1.4	14.5	1.4	14.5	-11.4	-5.0	2.4	-2.6
11	Gas	283.2	4.89	15.6	0.1	0.2	17.5	19.0	17.5	19.0	17.8	16.8	17.5	16.2	12.1	21.7	12.0	21.7	14.4	8.0	12.2	4.0
12	Liq.	283.2	14.51	67.8	0.3	0.4	65.6	69.9	66.7	71.1	69.2	91.6	72.8	64.2	-3.2	3.1	-1.6	4.8	2.1	35.1	7.3	-5.3
13	Liq.	283.2	21.11	76.5	0.6	0.4	79.9	77.7	84.0	81.2	77.2	102.6	80.1	72.3	4.6	1.6	9.9	6.1	1.0	34.2	4.8	-5.4
14	Liq.	283.2	52.88	113.9	0.8	0.6	121.5	112.4	140.2	128.5	110.1	142.9	115.9	110.8	6.6	-1.3	23.1	12.8	-3.3	25.4	1.7	-2.7
15	Liq.	283.2	104.03	167.2	0.6	0.8	165.9	150.6	202.2	183.2	143.8	194.1	155.2	157.4	-0.8	-10.0	20.9	9.6	-14.0	16.1	-7.2	-5.9
16	Liq.	283.2	124.60	175.8	1.4	0.8	180.8	163.8	222.6	201.8	155.2	212.9	168.9	174.7	2.8	-6.8	26.6	14.8	-11.7	21.1	-4.0	-0.6
17	Liq.	283.2	153.17	198.3	2.0	0.9	199.8	180.9	247.9	225.4	170.1	237.7	186.8	198.1	0.8	-8.8	25.0	13.6	-14.2	19.8	-5.8	-0.1
18	Gas	298.2	2.11	14.2	0.1	0.2	16.4	18.6	16.4	18.6	14.1	15.5	16.6	15.9	15.6	30.8	15.6	30.8	-1.0	9.0	17.2	11.8
19	Gas	298.2	5.21	16.3	0.1	0.2	18.0	19.6	18.1	19.7	18.2	17.1	18.2	16.9	10.8	20.8	11.2	21.1	12.1	5.0	12.1	4.0
20	SC	298.2	13.67	40.8	0.3	0.3	46.5	48.3	45.6	47.5	48.0	73.2	49.3	40.4	13.9	18.4	11.8	16.4	17.6	79.5	21.0	-1.0
21	SC	298.2	20.89	63.6	0.6	0.4	65.1	65.0	66.1	65.9	65.9	85.7	67.4	59.0	2.4	2.1	3.9	3.5	3.6	34.7	6.0	-7.3
22	SC	298.2	52.39	114.5	1.1	0.6	107.0	100.8	120.8	112.9	100.3	124.3	104.1	97.0	-6.5	-11.9	5.6	-1.3	-12.3	8.6	-9.0	-15.3
23	SC	298.2	103.26	154.8	0.9	0.7	149.1	137.7	180.1	166.2	133.0	171.9	141.7	140.5	-3.7	-11.1	16.3	7.3	-14.1	11.0	-8.5	-9.3
24	SC	298.2	124.89	167.3	1.5	0.8	163.8	151.0	200.4	185.4	144.4	190.3	155.3	157.4	-2.1	-9.7	19.8	10.8	-13.7	13.8	-7.2	-5.9
25	SC	298.2	153.18	182.1	1.8	0.9	181.5	167.3	224.3	208.4	158.3	213.4	171.8	179.0	-0.3	-8.1	23.2	14.5	-13.1	17.2	-5.6	-1.7
26	Gas	323.2	2.12	16.8	0.2	0.2	17.5	19.8	17.5	19.8	14.5	16.6	17.8	17.1	4.0	17.9	4.1	18.0	-13.6	-1.1	5.9	1.4
27	Gas	323.2	5.22	17.8	0.2	0.2	18.8	20.6	18.8	20.7	18.3	17.7	19.1	17.8	5.6	16.0	5.9	16.2	2.9	-0.5	7.6	0.4
28	Gas	323.2	10.44	22.0	0.1	0.2	23.9	25.3	23.6	25.0	25.6	29.9	23.7	21.6	8.3	14.8	7.1	13.5	16.1	35.6	7.6	-1.8
29	SC	323.2	27.26	58.7	0.5	0.4	58.7	59.3	58.8	59.5	61.8	73.7	61.6	53.7	0.0	1.0	0.2	1.2	5.1	25.4	4.9	-8.6

1	2	3	4	5	6	7	8	9	10	11	12	13	14	15	16	17	18	19	20	21	22	23
No	Phase	T	P	Viscosity / μPa.s											Deviation (%)							
		K	MPa	EXP.	$u_A(\eta)$	$u_c(\eta)$	ST	CO_2-ST	ST	CO_2-ST	CS2	CO_2-CS2	Ped.	CO_2-Ped	ST	CO_2-ST	ST	CO_2-ST	CS2	CO_2-CS2	Ped.	CO_2-Ped
Density Correction?		(±0.1)	(±0.02)		μPa.s	μPa.s	Yes	Yes	No	No	---	---	---	---	Yes	Yes	No	No	---	---	---	---
30	SC	323.2	52.13	86.5	0.5	0.5	88.4	85.7	96.4	92.9	87.2	101.3	88.7	80.1	2.1	-1.0	11.4	7.3	0.7	17.0	2.4	-7.4
31	SC	323.2	103.96	138.7	1.0	0.7	128.1	121.5	152.0	144.3	119.2	145.0	124.8	120.3	-7.6	-12.4	9.6	4.1	-14.0	4.6	-10.0	-13.3
32	SC	323.2	124.87	143.8	1.4	0.7	141.0	133.6	170.0	162.1	129.5	160.9	136.8	135.0	-1.9	-7.1	18.3	12.7	-10.0	11.9	-4.9	-6.1
33	SC	323.2	152.50	164.3	1.4	0.8	156.6	148.6	191.4	183.9	142.0	181.2	151.5	153.9	-4.7	-9.5	16.5	11.9	-13.6	10.3	-7.8	-6.3
34	Gas	373.2	2.24	18.7	0.1	0.2	19.7	22.4	19.7	22.4	15.6	18.9	20.2	19.4	5.5	19.5	5.5	19.5	-16.6	1.3	7.7	3.8
35	Gas	373.2	5.25	20.0	0.1	0.2	20.6	22.9	20.7	22.9	18.9	19.6	21.1	19.9	3.2	14.3	3.3	14.4	-5.8	-2.1	5.7	-0.3
36	Gas	373.2	10.39	21.9	0.0	0.2	23.0	24.8	23.1	24.8	23.7	22.2	23.7	21.8	5.1	12.9	5.4	13.1	8.0	1.2	8.0	-0.6
37	Gas	373.2	18.53	28.6	0.1	0.3	30.2	31.8	29.7	31.2	33.1	33.2	31.1	28.0	5.5	10.9	3.7	9.1	15.4	15.8	8.5	-2.2
38	SC	373.2	37.83	46.9	0.6	0.3	52.0	53.6	51.7	53.3	56.6	59.9	55.0	48.4	10.8	14.1	10.1	13.5	20.6	27.7	17.1	3.2
39	SC	373.2	51.90	58.8	0.3	0.4	64.7	65.8	66.9	67.9	68.7	72.8	67.8	60.1	10.1	11.8	13.7	15.4	16.8	23.8	15.2	2.2
40	SC	373.2	104.86	96.9	0.6	0.5	99.9	99.5	113.8	113.4	99.2	110.5	101.1	94.3	3.1	2.7	17.5	17.1	2.5	14.1	4.4	-2.6
41	SC	373.2	124.83	109.4	0.8	0.6	110.4	109.9	128.3	128.5	108.0	123.1	111.1	106.0	1.0	0.5	17.3	17.5	-1.2	12.6	1.5	-3.1
42	SC	373.2	151.14	131.0	0.7	0.6	123.0	122.7	145.8	147.4	118.5	139.2	123.1	121.0	-6.1	-6.3	11.3	12.5	-9.5	6.2	-6.1	-7.6
43	Gas	423.2	2.10	21.0	0.1	0.2	21.9	24.7	21.9	24.7	16.3	21.1	22.3	21.7	4.2	17.5	4.2	17.6	-22.7	0.4	6.1	2.9
44	Gas	423.2	5.23	22.7	0.1	0.2	22.6	25.1	22.7	25.2	19.5	21.6	23.2	22.1	-0.3	10.7	-0.3	10.7	-14.0	-4.8	2.0	-2.9
45	Gas	423.2	10.39	23.6	0.1	0.2	24.3	26.4	24.4	26.4	23.6	23.2	25.0	23.3	3.2	11.9	3.3	11.9	0.1	-1.6	6.2	-1.2
46	Gas	423.2	20.44	28.2	0.2	0.2	29.7	31.4	29.5	31.2	31.7	29.9	30.8	28.0	5.1	11.1	4.4	10.4	12.2	5.8	9.0	-0.7
47	SC	423.2	51.29	40.3	0.4	0.3	52.2	54.6	52.4	54.8	57.2	57.3	55.4	49.6	29.5	35.4	30.0	36.0	41.9	42.3	37.5	23.0
48	SC	423.2	103.72	79.3	0.7	0.4	81.9	84.7	89.7	92.9	85.1	89.5	85.1	78.5	3.2	6.8	13.0	17.1	7.3	12.9	7.3	-1.0
49	SC	423.2	124.07	88.0	0.9	0.4	91.3	94.5	102.2	106.4	93.4	100.5	94.2	88.6	3.7	7.4	16.2	20.9	6.1	14.2	7.1	0.7
50	SC	423.2	151.83	97.9	1.0	0.5	102.9	106.9	118.0	124.0	103.4	115.0	105.5	102.2	5.1	9.2	20.5	26.7	5.6	17.5	7.7	4.4
Average Absolute Deviation (AAD)															**5.4**	**11.5**	**12.3**	**14.1**	**10.8**	**15.6**	**7.9**	**4.3**

Table 4.21 Experimental and modelling results (predictive models) of the viscosity of MIX 4

1	2	3	4	5	5.1	5.2	6	7	8	9	10	11	12	13	14	15	16	17	18	19	20	21
No	Phase	T	P	Viscosity / μPa.s											Deviation (%)							
		K	MPa	EXP.	$u_A(\eta)$	$u_c(\eta)$	ST	CO_2-ST	ST	CO_2-ST	CS2	CO_2-CS2	Ped.	CO_2-Ped	ST	CO_2-ST	ST	CO_2-ST	CS2	CO_2-CS2	Ped.	CO_2-Ped
Density Correction?		(±0.1)	(±0.02)		μPa.s	μPa.s	Yes	Yes	No	No	---	---	---	---	Yes	Yes	No	No	---	---	---	---
1	Gas	273.2	2.59	14.0	0.3	0.2	14.2	14.9	14.2	14.9	12.8	13.5	13.6	12.9	1.5	6.2	1.5	6.2	-8.9	-4.0	-2.8	-8.0
2	Gas	273.2	5.22	15.1	0.1	0.2	15.9	15.6	15.9	15.6	15.9	14.7	15.3	14.1	5.1	3.3	5.1	3.3	5.0	-2.7	1.4	-7.1
3	Gas	283.2	1.75	13.8	0.2	0.2	14.3	15.3	14.3	15.3	12.1	13.7	13.7	13.2	3.6	10.4	3.6	10.4	-12.4	-1.2	-0.8	-4.7
4	Gas	283.2	2.09	14.0	0.1	0.2	14.4	15.3	14.4	15.3	12.5	13.7	13.8	13.2	3.2	9.4	3.2	9.4	-10.8	-1.8	-1.1	-5.4
5	Gas	283.2	5.18	15.2	0.1	0.2	16.0	16.0	16.0	16.0	15.8	16.1	15.5	14.3	5.9	5.3	5.8	5.3	4.0	6.3	2.3	-5.9
6	Gas	298.2	2.05	14.1	0.2	0.2	15.0	16.0	15.0	16.0	12.8	14.3	14.4	13.8	6.7	13.5	6.7	13.5	-9.2	2.0	2.6	-1.5
7	Gas	298.2	5.29	15.5	0.2	0.2	16.4	16.5	16.5	16.5	15.9	15.7	16.0	14.8	6.0	6.5	6.1	6.5	2.6	1.1	2.8	-4.9
8	Gas	323.2	2.00	15.0	0.1	0.2	16.0	17.1	16.0	17.1	13.3	15.4	15.4	14.9	6.2	13.4	6.2	13.4	-11.7	2.1	2.5	-1.1
9	Gas	323.2	5.34	16.4	0.1	0.2	17.2	17.5	17.2	17.5	16.2	16.3	16.7	15.6	4.5	6.5	4.6	6.5	-1.3	-0.5	1.9	-5.1
10	Gas	323.2	10.60	19.5	0.2	0.2	20.9	19.5	20.8	19.4	21.7	24.2	20.7	18.5	7.0	-0.3	6.4	-0.7	11.2	23.7	6.1	-5.2
11	Gas	373.2	2.23	18.9	0.3	0.2	18.0	19.2	18.0	19.2	14.6	17.4	17.4	16.9	-4.8	1.7	-4.8	1.7	-22.8	-7.9	-7.6	-10.4
12	Gas	373.2	5.23	18.4	0.1	0.2	18.7	19.5	18.8	19.5	16.9	18.0	18.3	17.3	1.6	5.5	1.7	5.5	-8.4	-2.4	-0.6	-5.9
13	Gas	373.2	10.53	20.2	0.1	0.2	20.9	20.5	20.9	20.5	20.7	20.1	20.7	19.0	3.6	1.5	3.7	1.6	2.5	-0.3	2.8	-5.9
14	Gas	423.2	5.23	20.0	0.1	0.2	20.5	21.4	20.5	21.4	17.8	19.8	20.0	19.2	2.3	7.0	2.4	7.0	-11.1	-1.3	0.1	-4.3
15	Gas	423.2	10.53	21.4	0.0	0.2	22.0	22.1	22.0	22.1	20.9	21.1	21.8	20.3	3.1	3.4	3.1	3.4	-2.0	-1.0	2.1	-5.1
Average Absolute Deviation (AAD)															**4.3**	**6.3**	**4.3**	**6.3**	**8.3**	**3.9**	**2.5**	**5.4**

Table 4. 22 Average and maximum of estimated standard uncertainties of viscosity for each material

No	Material	Phase	No of experiments	Estimated Standard Uncertainty Type A				Estimated Standard Uncertainty Type B			
				$u_A(\eta)$				$u_c(\eta)$			
				Average		Maximum		Average		Maximum	
				µPa.s	%	µPa.s	%	µPa.s	%	µPa.s	%
1	Pure CO_2	Gas	22	0.2	1.1	1.4	6.2	0.4	1.1	0.2	1.8
		Liquid	31	0.6	1.0	1.4	0.8	0.8	0.7	1.6	0.6
		SC	12	1.0	1.2	4.4	4.0	0.5	0.5	0.9	0.7
		Total	**65**	**0.6**	**1.0**	**4.4**	**6.2**	**0.6**	**0.8**	**1.6**	**1.8**
2	MIX 1	Gas	11	0.1	0.5	0.2	1.0	0.2	1.6	0.2	1.9
		Liquid	29	0.7	0.4	1.4	1.0	0.8	0.5	1.6	0.6
		SC	21	0.2	0.5	0.8	1.3	0.4	0.8	0.9	1.4
		Total	**61**	**0.4**	**0.5**	**1.4**	**1.3**	**0.6**	**0.8**	**1.6**	**1.9**
3	MIX 2	Gas	12	0.2	0.1	0.2	0.1	0.2	1.4	0.2	1.7
		Liquid	20	1.1	0.4	2.4	1.0	0.9	0.5	1.5	0.7
		SC	13	0.3	0.1	1.1	0.4	0.5	0.6	0.8	0.9
		Total	**45**	**0.6**	**0.2**	**2.4**	**1.0**	**0.6**	**0.8**	**1.5**	**1.7**
4	MIX 3	Gas	14	0.4	0.6	0.2	1.3	0.3	0.7	0.3	1.7
		Liquid	12	0.7	1.2	1.8	1.0	0.8	1.5	0.9	0.7
		SC	21	0.2	0.4	1.1	1.0	0.2	0.5	0.7	1.0
		Total	**47**	**0.4**	**0.6**	**1.8**	**1.3**	**0.4**	**0.8**	**0.9**	**1.7**
5	BIN 1 (5.18% H2)	Gas	15	0.5	0.7	0.3	1.9	0.4	0.7	0.3	1.7
		Liquid	12	1.3	1.3	2.1	0.9	1.0	1.3	1.2	0.6
		SC	19	0.4	0.4	1.5	1.1	0.3	0.4	1.0	1.2
		Total	**46**	**0.7**	**0.7**	**2.1**	**1.9**	**0.5**	**0.8**	**1.2**	**1.7**
6	BIN2 (10.33% H2)	Gas	19	0.3	0.4	0.2	1.6	0.3	0.5	0.3	1.7
		Liquid	11	1.3	1.4	2.0	1.0	0.9	1.7	1.0	0.6
		SC	20	0.3	0.4	1.8	1.2	0.3	0.5	0.9	0.7
		Total	**50**	**0.5**	**0.6**	**2.0**	**1.6**	**0.4**	**0.8**	**1.0**	**1.7**
7	MIX 4	Gas	15	0.1	0.8	0.3	1.8	0.2	1.5	0.2	1.7
		Liquid	---	---	---	---	---	---	---	---	---
		SC	---	---	---	---	---	---	---	---	---
		Total	**15**	**0.1**	**0.8**	**0.3**	**1.8**	**0.2**	**1.5**	**0.2**	**1.7**
TOTAL		Gas	108	0.3	0.6	1.4	6.2	0.3	1.0	0.3	1.9
		Liquid	115	0.8	0.8	2.4	1.0	0.8	0.9	1.6	0.7
		SC	106	0.4	0.5	4.4	4.0	0.4	0.6	1.0	1.4
		Total	**329**	**0.5**	**0.6**	**4.4**	**6.2**	**0.5**	**0.8**	**1.6**	**1.9**

Table 4.23 Absolute average deviations between experimental viscosities and predictions of all fluids investigated in this work

1	2	3	4	5	6	7	8
No	Material	Phase	Data No	Absolute Average Deviation (%)			
				LBC	CO_2-LBC	LBC	CO_2-LBC
		Density Correction?		Yes	Yes	No	No
1	**Pure CO_2**	Gas	22	19.9	13.1	19.9	13.1
		Liquid	31	10.2	5.6	23.1	16.0
		Supercritical	12	10.6	3.0	13.6	15.1
		Total	**65**	**13.6**	**7.7**	**20.2**	**14.9**
2	**MIX 1**	Gas	11	6.2	16.4	6.2	16.5
		Liquid	29	4.9	3.1	25.4	20.7
		Supercritical	21	11.2	6.4	14.3	13.8
		Total	**61**	**7.3**	**6.7**	**18.1**	**17.6**
3	**MIX 2**	Gas	12	16.6	11.8	16.6	11.8
		Liquid	20	6.0	2.7	29.3	22.5
		Supercritical	13	8.6	3.7	12.5	14.8
		Total	**45**	**9.6**	**5.4**	**21.1**	**17.5**
4	**MIX 3**	Gas	14	14.6	11.1	14.6	11.1
		Liquid	12	21.0	24.0	46.0	42.2
		Supercritical	21	8.7	15.2	20.9	26.3
		Total	**47**	**13.6**	**16.2**	**25.4**	**25.9**
5	**BIN 1 (5% H_2)**	Gas	15	14.1	13.0	14.4	13.1
		Liquid	12	7.1	3.5	27.4	20.7
		Supercritical	19	8.6	5.7	18.9	22.3
		Total	**46**	**10.0**	**7.5**	**19.7**	**18.9**
6	**BIN 2 (10% H_2)**	Gas	19	13.7	12.3	13.9	12.3
		Liquid	11	6.4	5.9	31.1	28.2
		Supercritical	20	8.0	4.4	13.7	18.1
		Total	**50**	**9.8**	**7.7**	**17.6**	**18.1**
7	**MIX 4**	Gas	15	13.3	9.9	13.3	9.8
		Liquid	---	0	0	0	0
		Supercritical	---	0	0	0	0
		Total	**15**	**13.3**	**9.9**	**13.3**	**9.8**
TOTAL		Gas	108	14.6	12.4	14.7	12.4
		Liquid	115	8.6	6.2	28.4	22.7
		Supercritical	106	9.2	6.9	16.0	18.9
		Total	**329**	**10.8**	**8.5**	**19.9**	**18.1**

Table 4.24 Absolute average deviations between experimental viscosities and predictions of all fluids investigated in this work

No	Material	Phase	Data No	Absolute Average Deviation (%)							
				ST	CO_2-ST	ST	CO_2-ST	CS2	CO_2-CS2	Ped	CO_2-Ped
Density Correction?				YES	YES	NO	NO	---	---	---	---
1	**Pure CO_2**	Gas	22	3.9	1.8	3.9	1.8	31.6	1.3	6.0	1.6
		Liquid	31	3.5	1.1	17.8	22.7	13.1	10.3	6.2	1.2
		Super Critical	12	3.4	1.0	14.3	15.8	9.8	6.3	10.2	1.0
		Total	**65**	**3.6**	**1.3**	**12.4**	**14.3**	**18.8**	**7.4**	**6.9**	**1.3**
2	**MIX 1**	Gas	11	7.2	2.9	7.3	2.9	45.8	1.2	5.9	1.6
		Liquid	29	4.8	2.8	21.1	17.2	12.0	2.8	6.7	1.5
		Super Critical	21	7.6	1.8	13.2	8.5	11.1	2.5	9.2	0.9
		Total	**61**	**6.2**	**2.5**	**15.9**	**11.6**	**17.8**	**2.4**	**7.4**	**1.3**
3	**MIX 2**	Gas	12	6.7	3.7	6.7	3.7	10.8	1.2	8.0	1.8
		Liquid	20	4.3	5.3	21.6	14.7	13.6	9.1	8.2	2.0
		Super Critical	13	7.1	2.8	15.5	8.8	12.1	9.5	10.4	1.1
		Total	**45**	**5.7**	**4.1**	**15.9**	**10.1**	**12.4**	**7.1**	**8.8**	**1.7**
4	**MIX 3**	Gas	14	5.1	11.0	5.1	11.0	10.4	3.6	4.5	5.5
		Liquid	12	15.6	10.7	29.0	3.0	10.3	11.0	16.3	16.0
		Super Critical	21	11.1	4.1	18.8	3.9	13.5	7.3	15.7	7.6
		Total	**47**	**10.5**	**7.8**	**17.3**	**5.8**	**11.8**	**7.2**	**12.5**	**9.1**
5	**BIN 1 (5% H_2)**	Gas	15	8.2	10.8	8.1	10.6	10.9	4.7	8.0	3.2
		Liquid	12	3.6	5.5	16.2	13.2	12.5	4.7	6.1	4.2
		Super Critical	19	5.6	6.7	18.5	18.9	9.3	8.1	8.4	5.4
		Total	**46**	**5.9**	**7.8**	**14.5**	**14.7**	**10.7**	**6.1**	**7.6**	**4.4**
6	**BIN 2 (10% H_2)**	Gas	19	6.1	17.1	5.9	16.9	11.0	5.4	7.7	2.5
		Liquid	11	3.3	5.9	19.7	10.4	9.1	24.6	5.0	3.3
		Super Critical	20	5.9	9.3	14.3	13.4	11.5	20.3	9.6	6.5
		Total	**50**	**5.4**	**11.5**	**12.3**	**14.1**	**10.8**	**15.6**	**7.9**	**4.3**
7	**MIX 4**	Gas	15	4.3	6.3	4.3	6.3	8.3	3.9	2.5	5.4
		Liquid	---	---	---	---	---	---	---	---	---
		Super Critical	---	---	---	---	---	---	---	---	---
		Total	**15**	**4.3**	**6.3**	**4.3**	**6.3**	**8.3**	**3.9**	**2.5**	**5.4**
TOTAL		Gas	108	5.7	7.9	5.1	6.9	17.1	2.8	5.8	2.3
		Liquid	115	5.2	4.2	20.5	15.7	12.2	9.3	7.6	3.5
		Super Critical	106	7.1	4.6	15.9	11.2	11.3	9.1	10.7	4.1
		Total	**329**	**6.0**	**5.5**	**14.0**	**11.4**	**13.5**	**7.1**	**8.0**	**3.3**

Table 4.25 Viscosity reduction of pure CO_2 in the presence of impurities for each system in the dense phase (Viscosity will increase in the gas phase)

T	T	Phase	Viscosity Reduction (%)					
°C	K		MIX 1	MIX 2	MIX 3	MIX 4	BIN 1	BIN 2
0.0	273.15	Dense	11.2	18.1	38.5	---	12.6	28.4
10.0	283.15	Dense	11.5	17.8	38.0	---	17.9	29.1
25.0	298.15	Dense	13.0	21.4	37.8	---	16.5	27.5
25.0	298.15	Dense	10.6	19.8	32.6	---	14.0	21.3
100.0	373.15	Dense	6.5	10.8	21.4	---	16.3	18.7
150.0	423.15	Dense	4.5	7.8	17.3	---	5.2	17.6
		Impurity (%)	4.4	10.2	30.01	50.07	5.18	10.33
	Total	Gas	-0.9	-2.3	-8.9	-3.3	-1.8	-3.7
		Dense	9.6	16.0	30.9	---	13.8	23.8

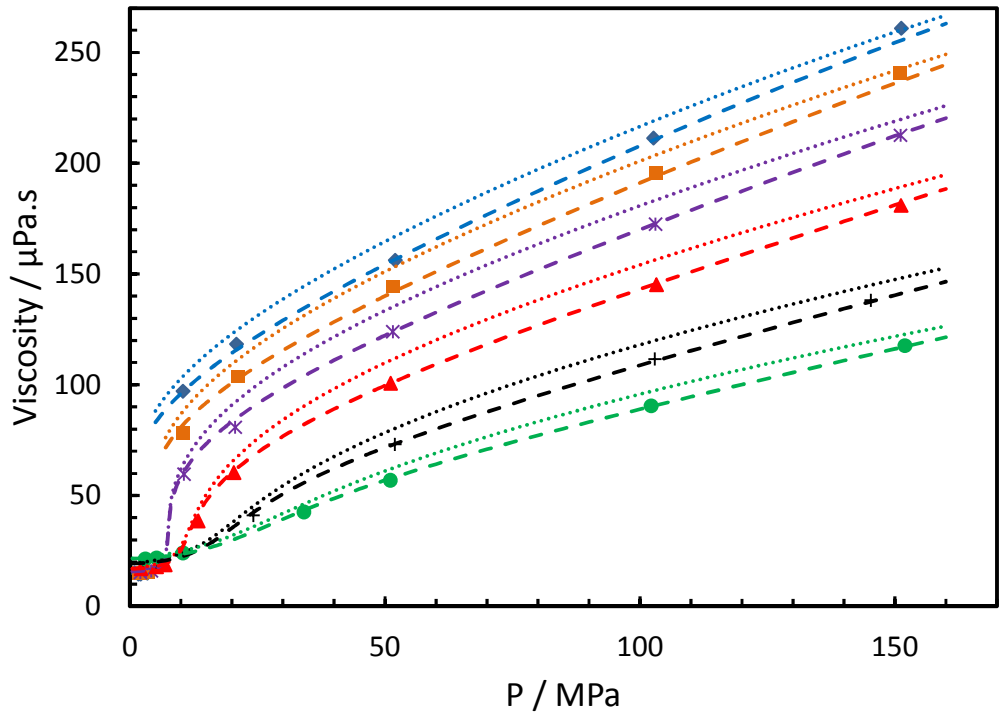

Figure 4.13 Experimental and modelling results (predictive models) of the viscosity of MIX 1 Experimental data: (♦) at 0 °C, (■) at 10 °C, (x) at 25 °C, (▲) at 50 °C, (+) at 100 °C and (●) at 150 °C Modelling results: Round dot lines (…): Original SUPERTRAP and dash lines (---) CO_2-SUPERTRAP

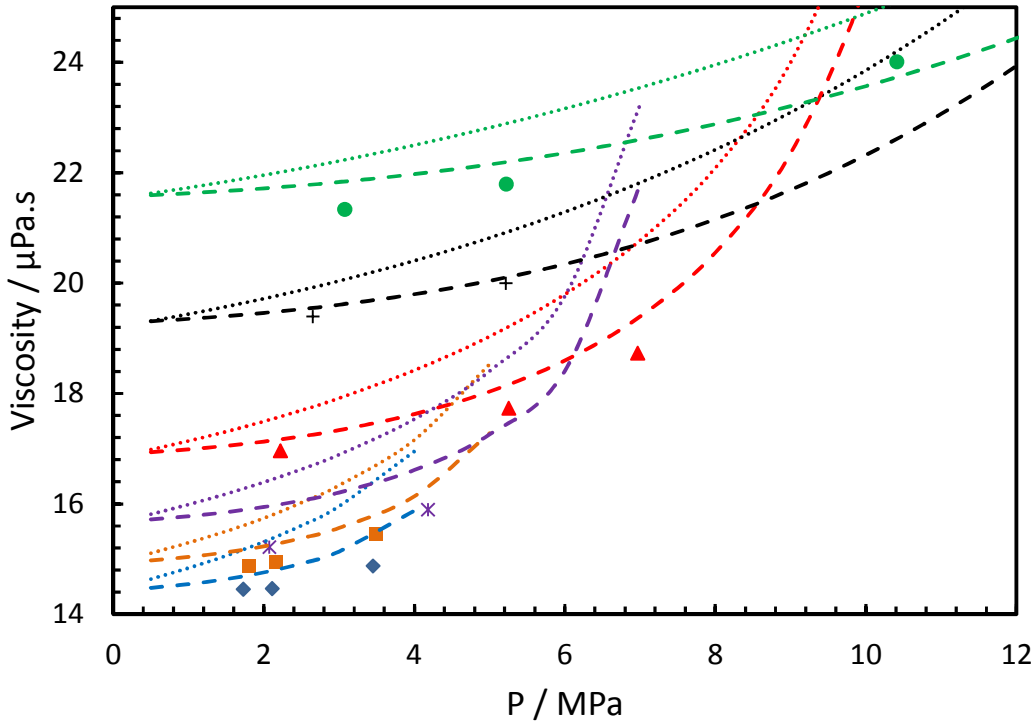

Figure 4.14 Experimental and modelling results (predictive models) of the viscosity of MIX 1 Experimental data: (♦) at 0 °C, (■) at 10 °C, (x) at 25 °C, (▲) at 50 °C, (+) at 100 °C and (●) at 150 °C Modelling results: Round dot lines (…): Original SUPERTRAP and dash lines (---) CO_2-SUPERTRAP

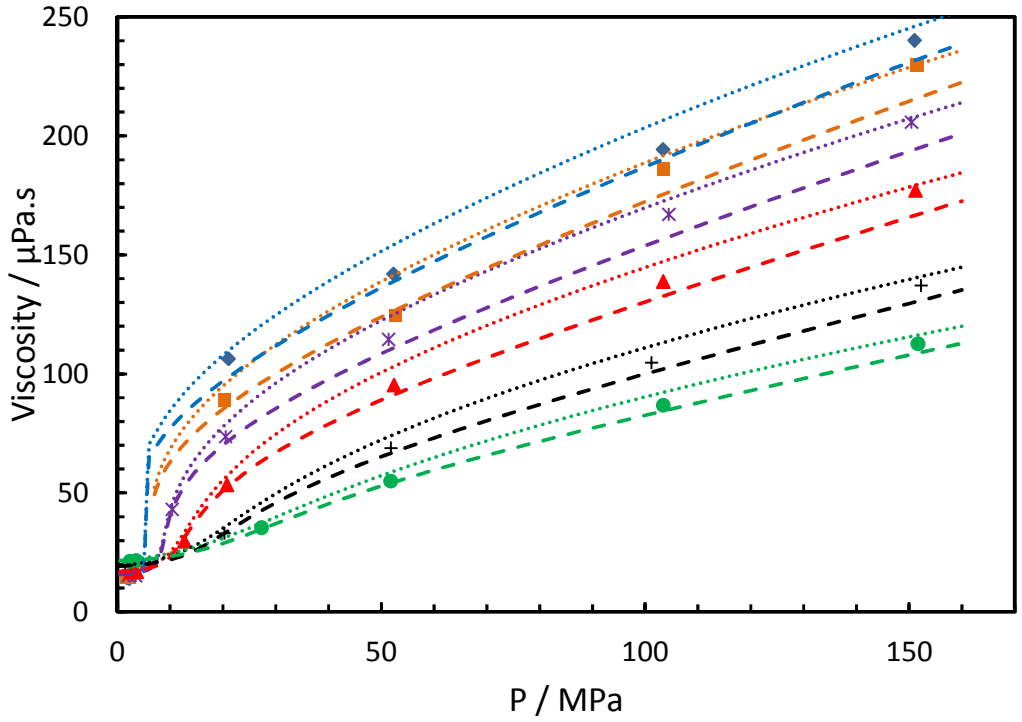

Figure 4.15 Experimental and modelling results (predictive models) of the viscosity of MIX 2 Experimental data: (♦) at 0 °C, (■) at 10 °C, (x) at 25 °C, (▲) at 50 °C, (+) at 100 °C and (●) at 150 °C Modelling results: Round dot lines (…): Original SUPERTRAP and dash lines (---) CO_2-SUPERTRAP

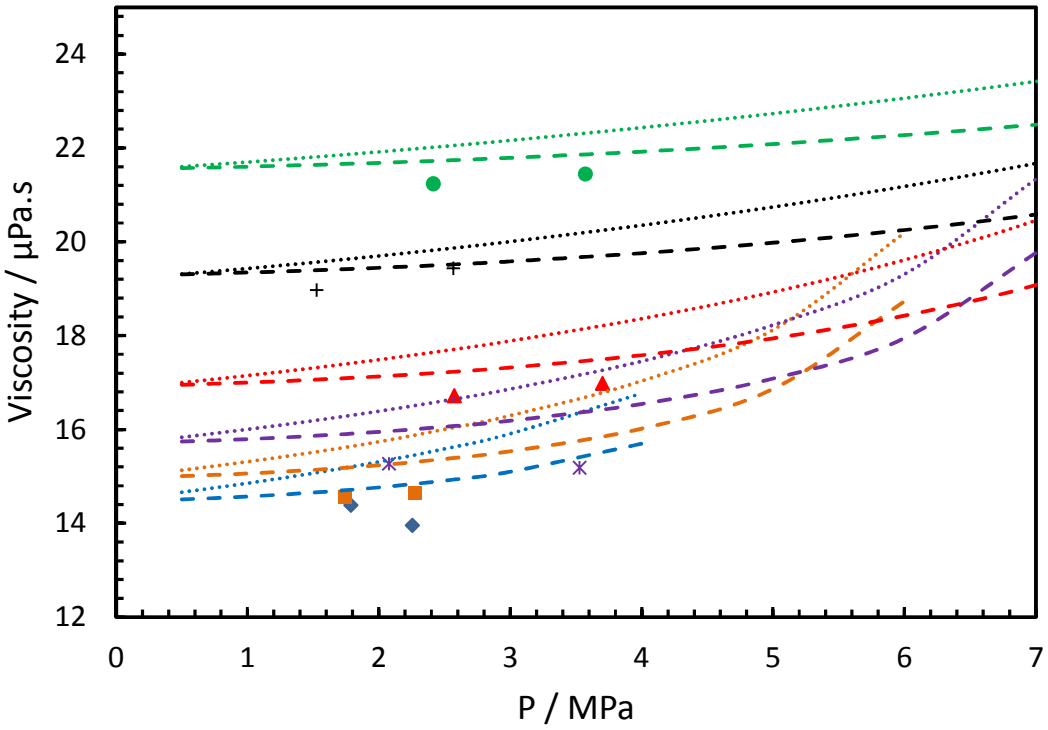

Figure 4.16 Experimental and modelling results (predictive models) of the viscosity of MIX 2 Experimental data: (♦) at 0 °C, (■) at 10 °C, (x) at 25 °C, (▲) at 50 °C, (+) at 100 °C and (●) at 150 °C Modelling results: Round dot lines (…): Original SUPERTRAP and dash lines (---) CO_2-SUPERTRAP

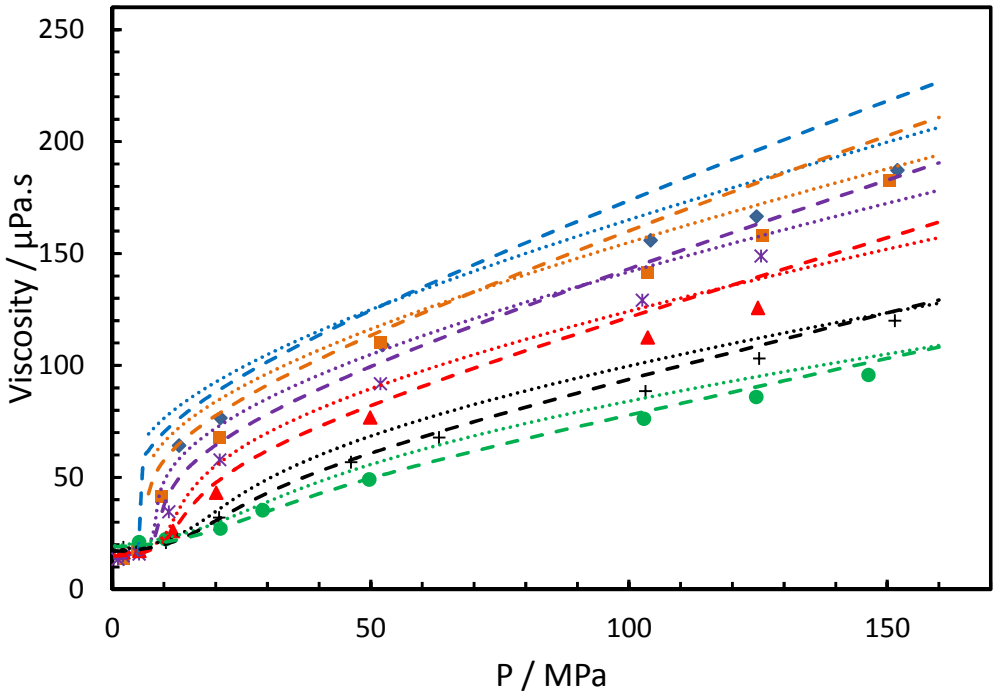

Figure 4.17 Experimental and modelling results (predictive models) of the viscosity of MIX 3 Experimental data: (♦) at 0 °C, (■) at 10 °C, (x) at 25 °C, (▲) at 50 °C, (+) at 100 °C and (●) at 150 °C Modelling results: Round dot lines (…): Original Pedersen and dash lines (---) CO_2-Pedersen

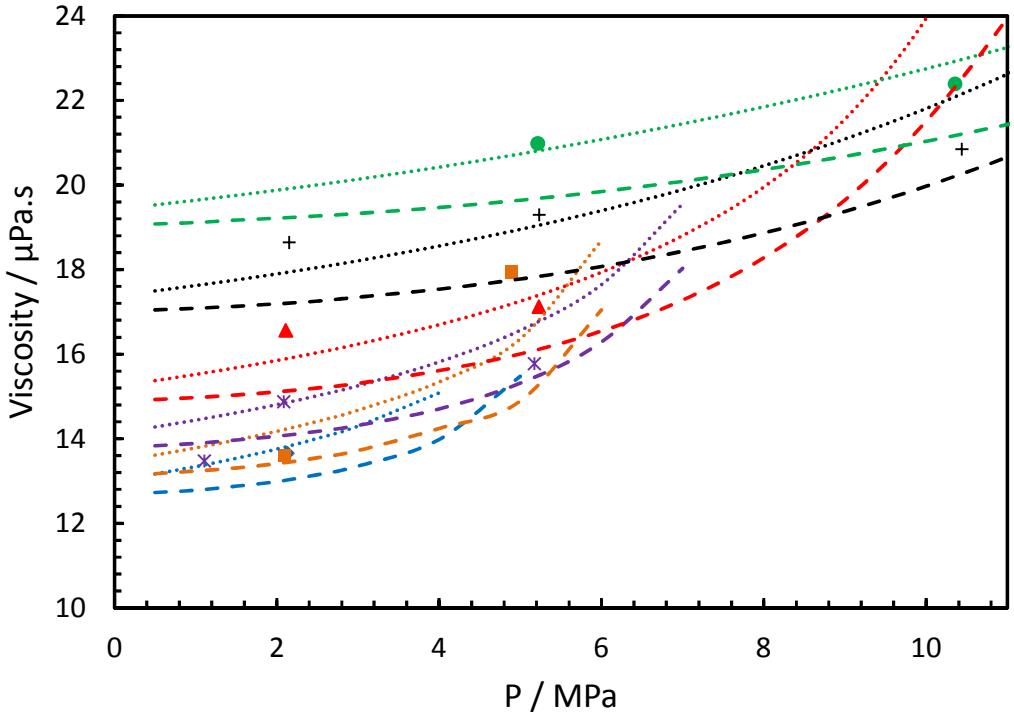

Figure 4.18 Experimental and modelling results (predictive models) of the viscosity of MIX 3 Experimental data: (♦) at 0 °C, (■) at 10 °C, (x) at 25 °C, (▲) at 50 °C, (+) at 100 °C and (●) at 150 °C Modelling results: Round dot lines (…): Original Pedersen and dash lines (---) CO_2-Pedersen

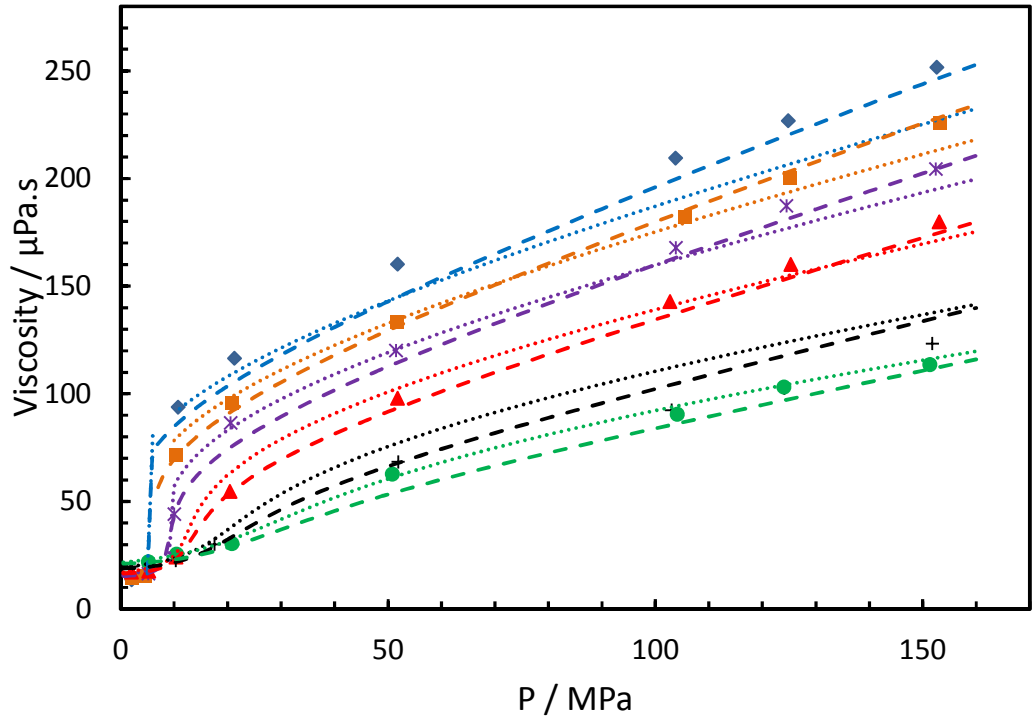

Figure 4.19 Experimental and modelling results (predictive models) of the viscosity of BIN 1 Experimental data: (♦) at 0 °C, (■) at 10 °C, (x) at 25 °C, (▲) at 50 °C, (+) at 100 °C and (●) at 150 °C Modelling results: Round dot lines (…): Original Pedersen and dash lines (---) CO_2-Pedersen

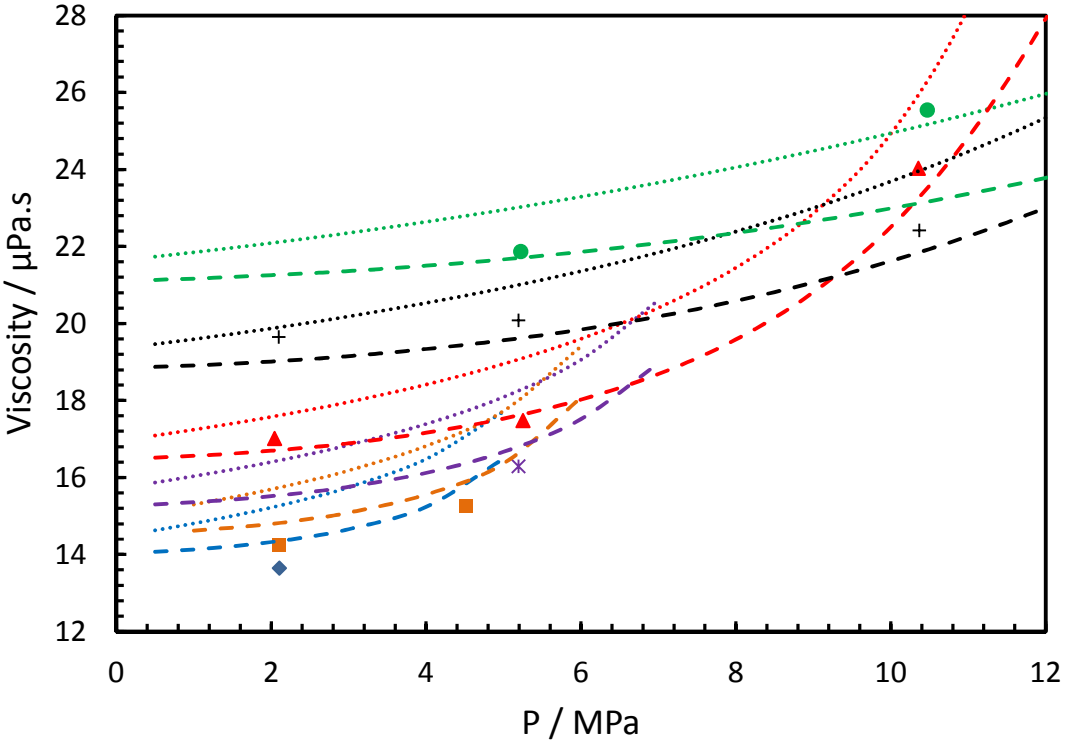

Figure 4.20 Experimental and modelling results (predictive models) of the viscosity of BIN 1 Experimental data: (♦) at 0 °C, (■) at 10 °C, (x) at 25 °C, (▲) at 50 °C, (+) at 100 °C and (●) at 150 °C Modelling results: Round dot lines (…):Original Pedersen and dash lines (---) CO_2-Pedersen

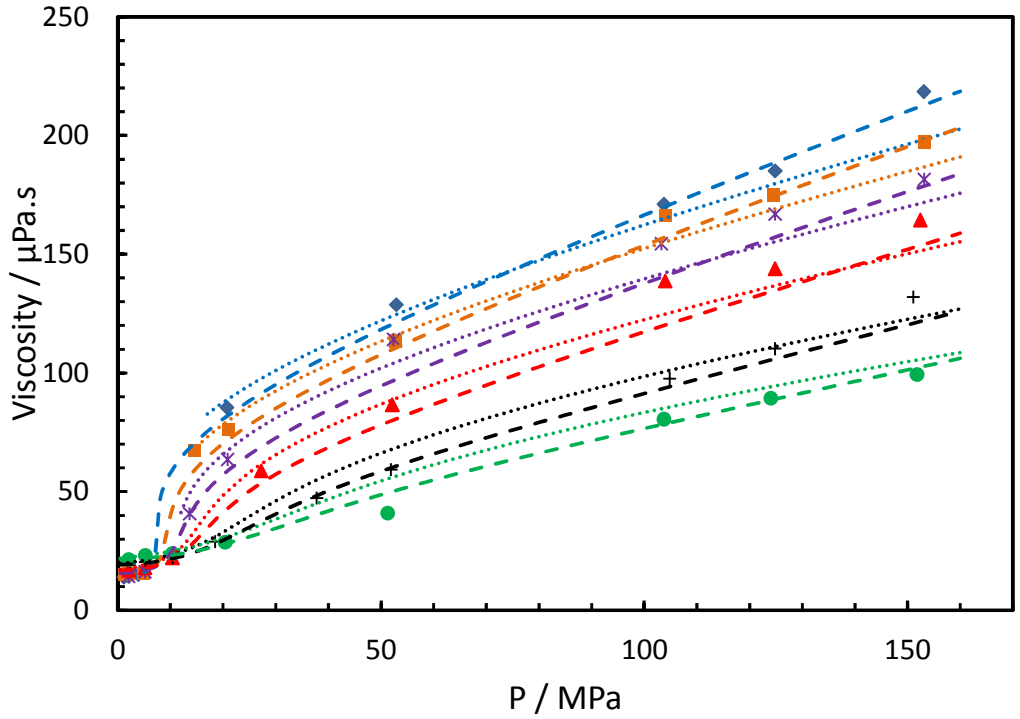

Figure 4.21 Experimental and modelling results (predictive models) of the viscosity of BIN 2 Experimental data: (♦) at 0 °C, (■) at 10 °C, (x) at 25 °C, (▲) at 50 °C, (+) at 100 °C and (●) at 150 °C Modelling results: Round dot lines (…):Original Pedersen and dash lines (---) CO_2-Pedersen

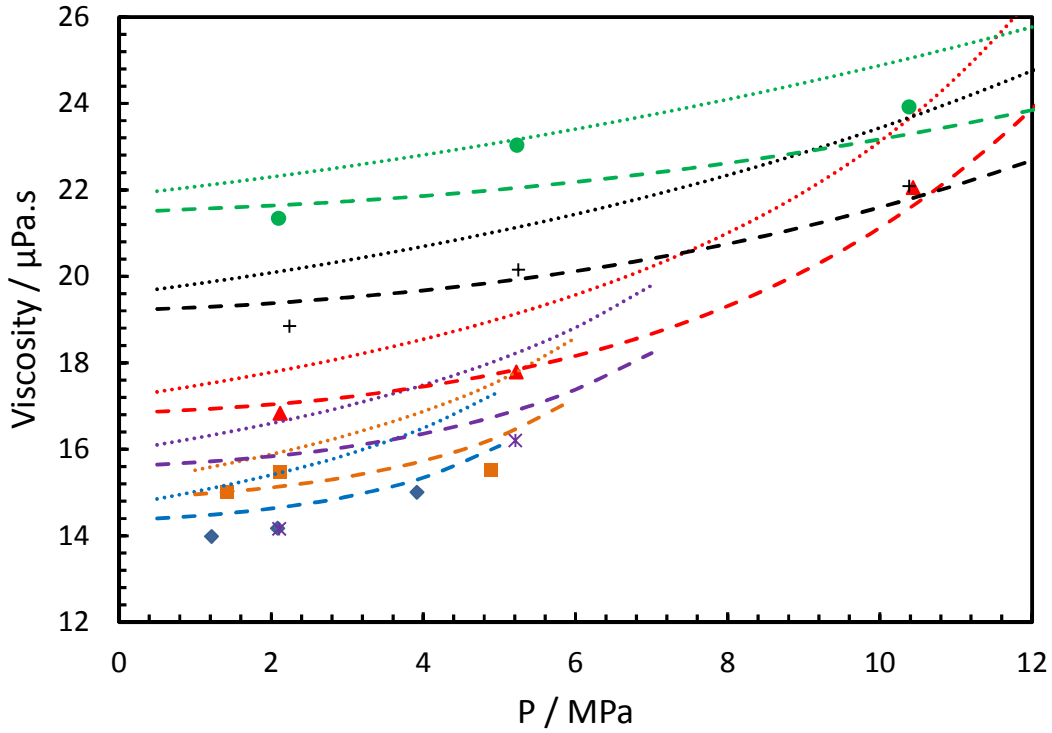

Figure 4.22 Experimental and modelling results (predictive models) of the viscosity of BIN 2 Experimental data: (♦) at 0 °C, (■) at 10 °C, (x) at 25 °C, (▲) at 50 °C, (+) at 100 °C and (●) at 150 °C Modelling results: Round dot lines (…):Original Pedersen and dash lines (---) CO_2-Pedersen

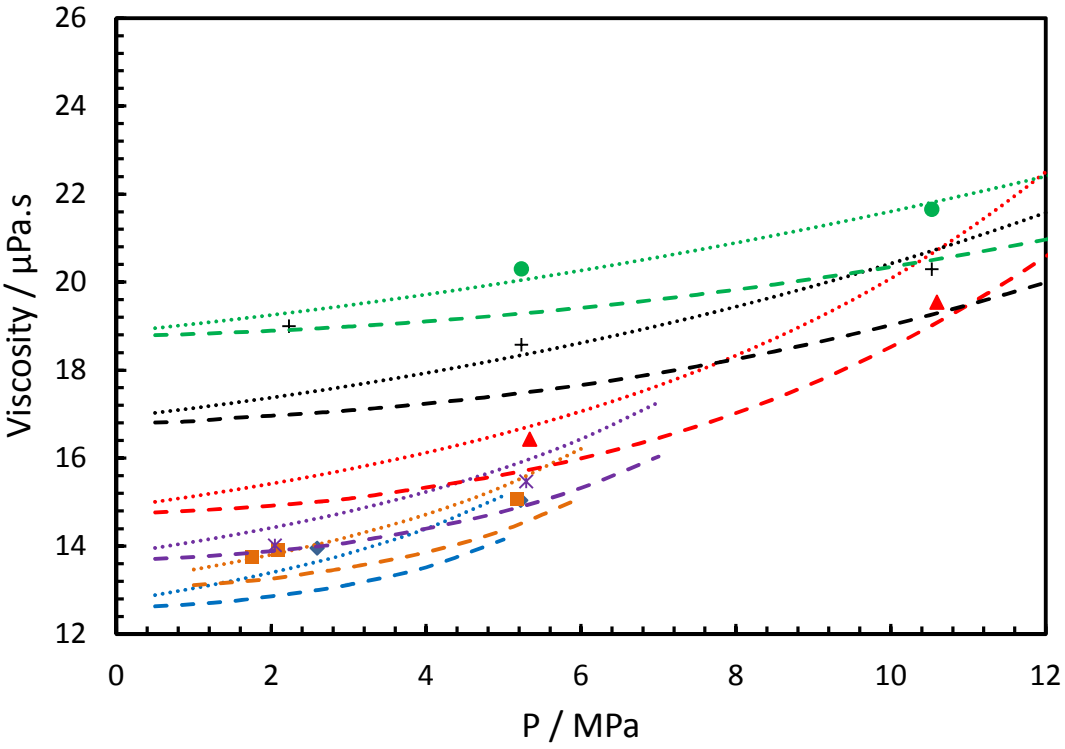

Figure 4.23 Experimental and modelling results (predictive models) of the viscosity of MIX 4 Experimental data: (♦) at 0 °C, (■) at 10 °C, (x) at 25 °C, (▲) at 50 °C, (+) at 100 °C and (●) at 150 °C Modelling results: Round dot lines (…):Original Pedersen and dash lines (---) CO_2-Pedersen

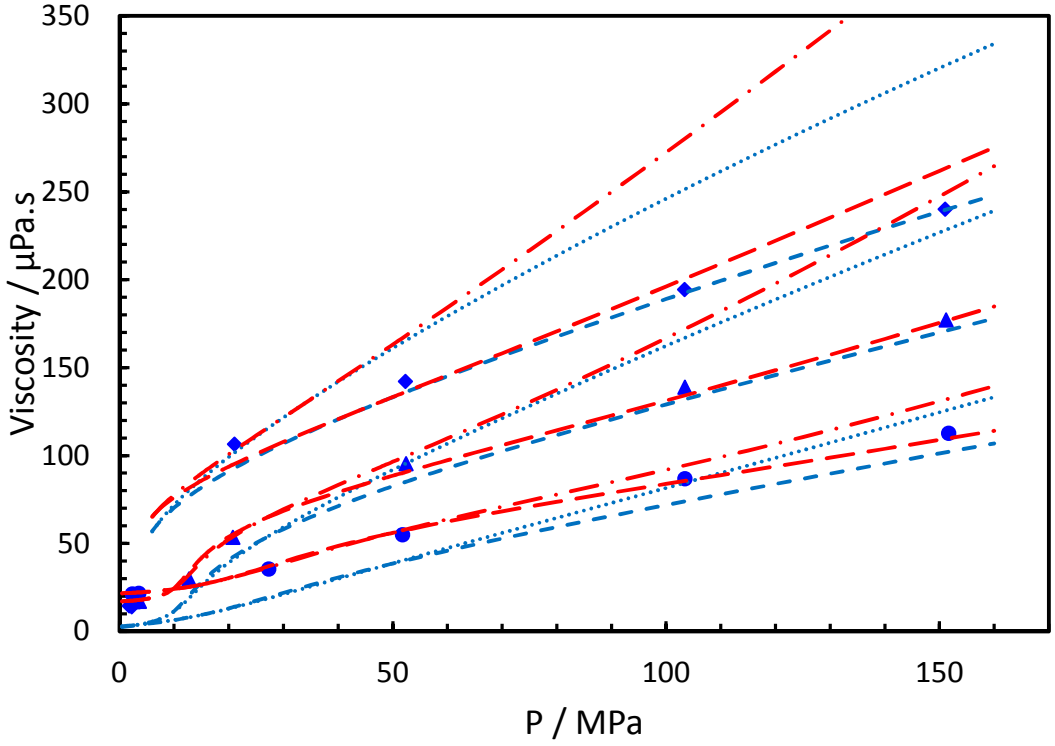

Figure 4.24 Effects of tuning parameters and density correction in LBC and CO_2-LBC models for MIX 2, Experimental data: (♦) at 0 °C, (▲) at 50 °C and (●) at 150 °C, Modelling: (___.) LBC with PR, (__ __) LBC with PR-CO_2, (…..) CO_2-LBC with PR and (----) CO_2-LBC with PR-CO_2

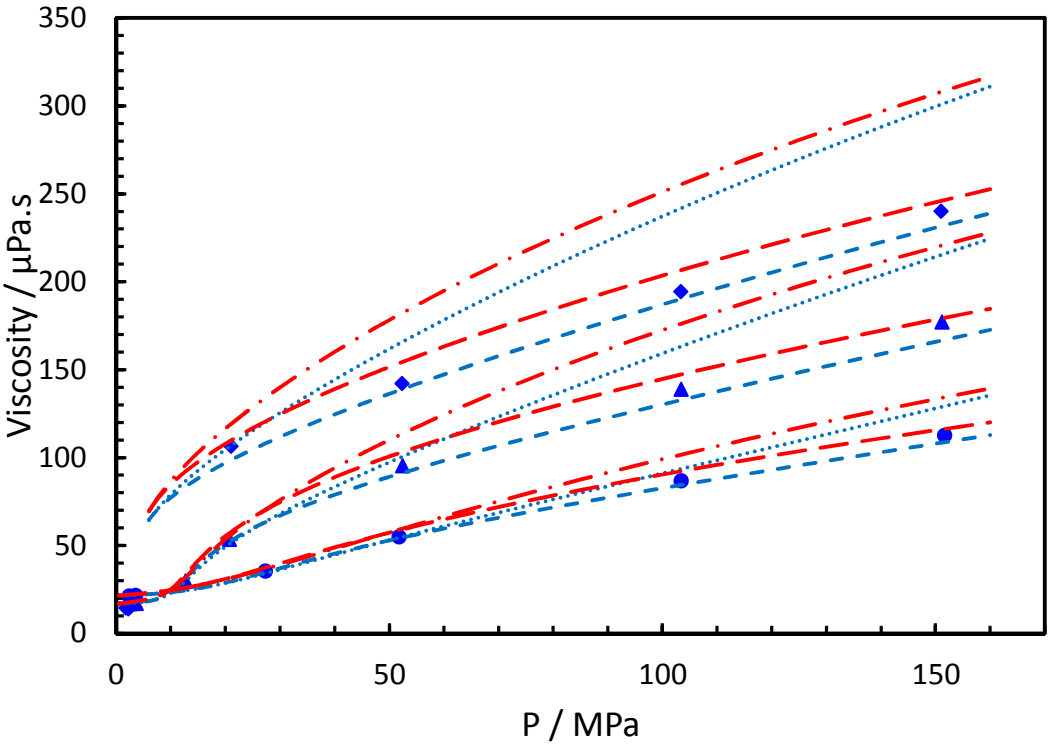

Figure 4.25 Effects of density correction in SUPERTRAP and CO_2-SUPERTRAP models for MIX 2, Experimental data: (♦) at 0 °C, (▲) at 50 °C and (●) at 150 °C, Modelling: (——.) ST with PR, (— — —) ST with PR-CO_2, (…..) CO_2-ST with PR and (----) CO_2-ST with PR-CO_2

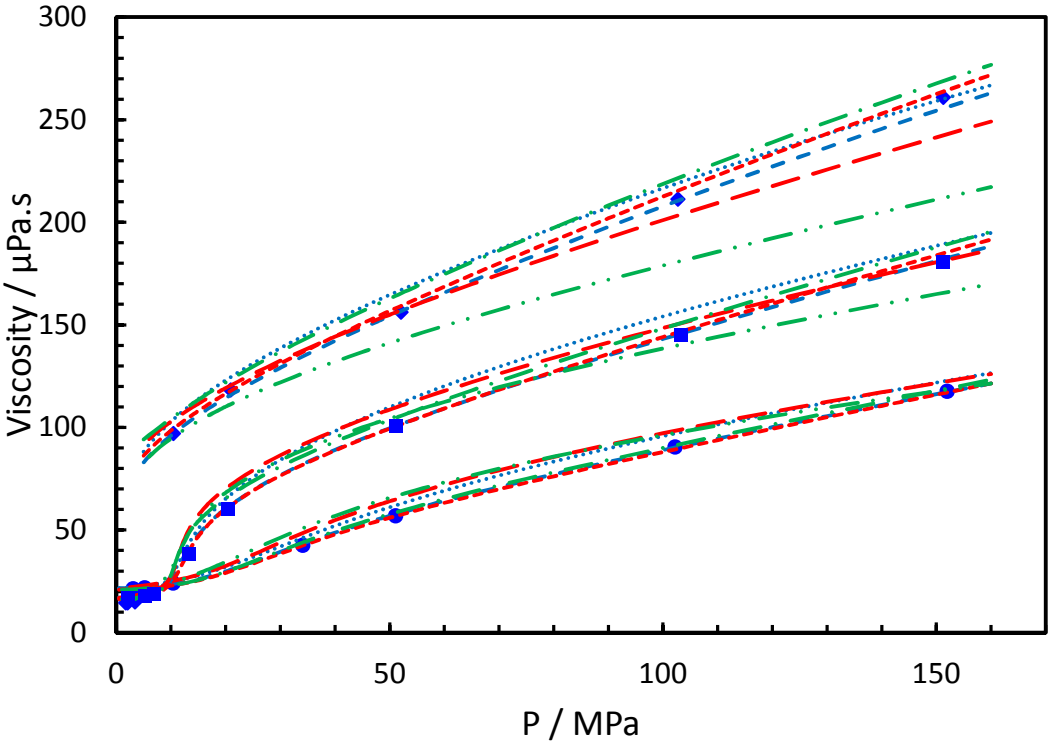

Figure 4.26 Comparison of the predictive models for MIX 1, Experimental data: (♦) at 0 °C, (■) at 50 °C and (●) at 150 °C, Modelling: (— — —) Ped, (----) CO_2-Ped, (…..) ST, (----) CO_2-ST, (——..) CS2 and (——.) CO_2-CS2

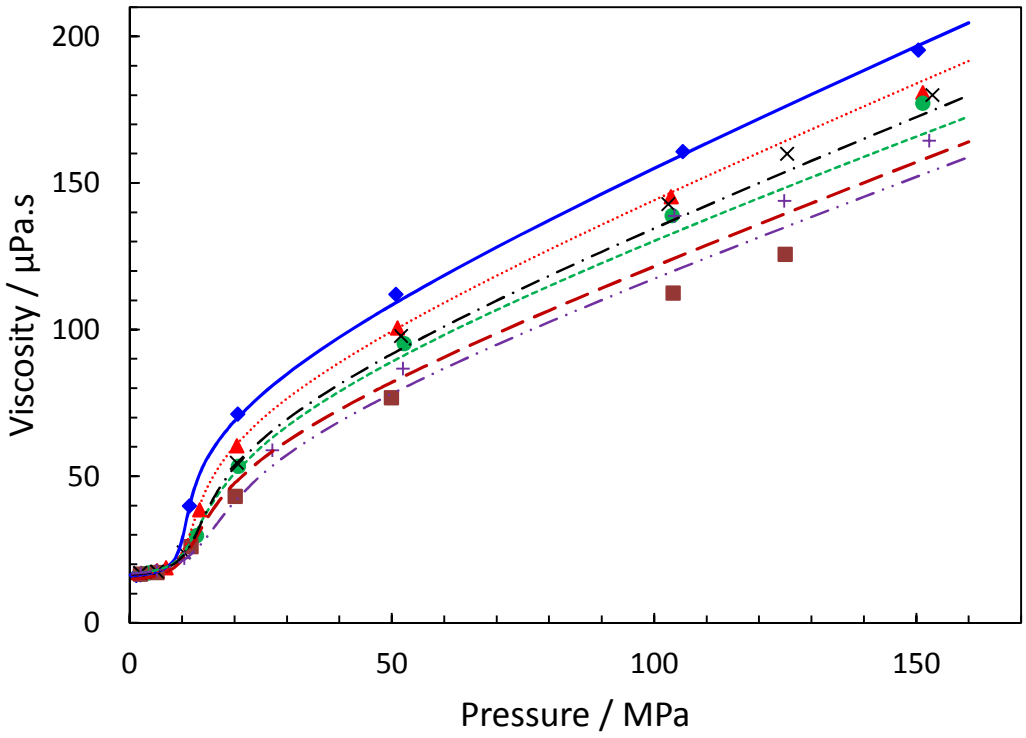

Figure 4.27 The effect of impurities on viscosity of pure CO_2 at 323.15 K (50 °C), experimental data / modelling CO_2-Pedersen: (♦/——) Pure CO_2, (▲/….) MIX 1, (●/----) MIX 2, (■/— — —) MIX 3, (x/—.) BIN 1 and (+/—..) BIN 2

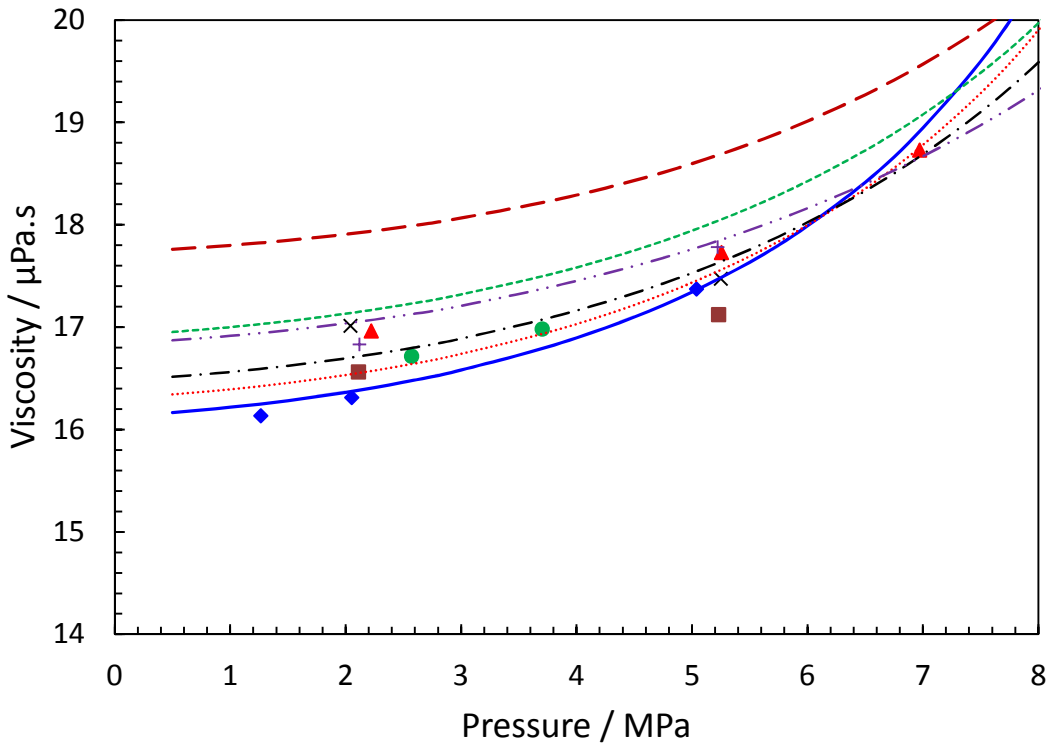

Figure 4.28 The effect of impurities on viscosity of pure CO_2 at 323.15 K (50 °C) at low pressures, experimental data / modelling CO_2-Pedersen: (♦/——) Pure CO_2, (▲/….) MIX 1, (●/----) MIX 2, (■/— — —) MIX 3, (x/—.) BIN 1 and (+/—..) BIN 2

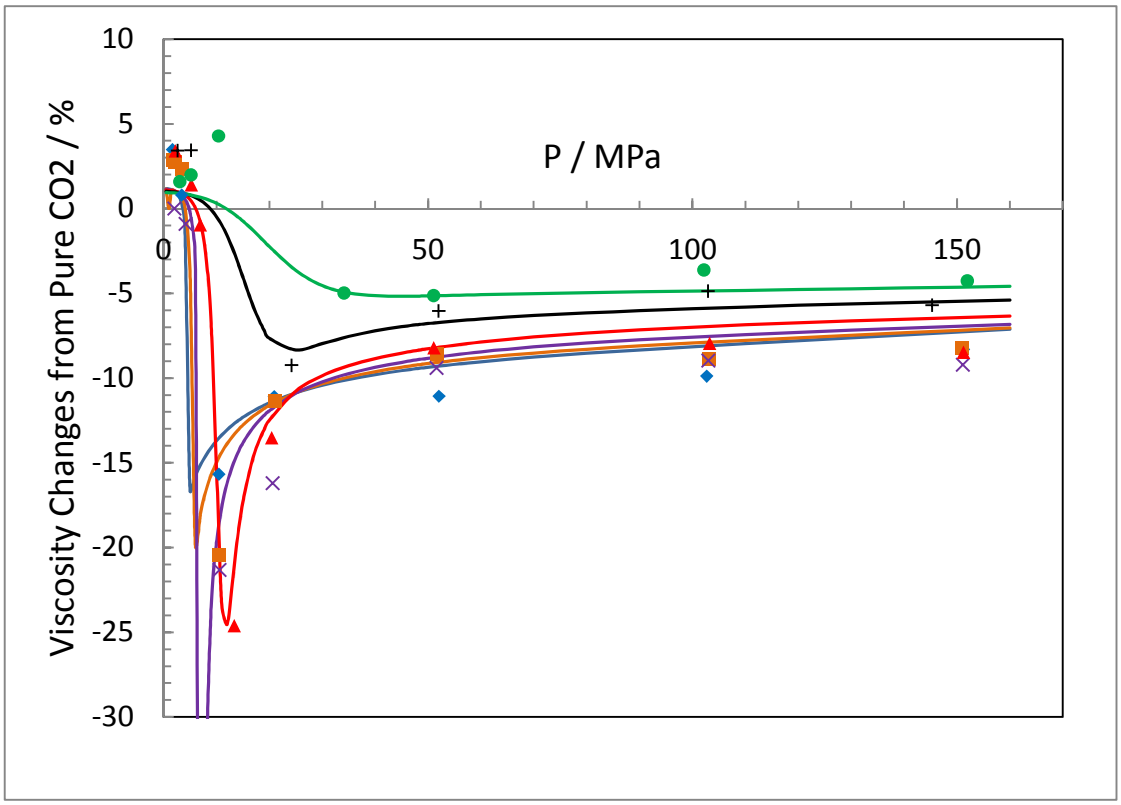

Figure 4.29 The viscosity changes from pure CO_2 for MIX 1 at different temperatures. Experimental data: (♦) at 0 °C, (■) at 10 °C, (x) at 25 °C, (▲) at 50 °C, (+) at 100 °C and (●) at 150 °C, Modelling results: lines (—) CO_2-Pedersen

REFERENCES

[1] H. Rubin, E., de Coninck, "IPCC Special Report on Carbon Dioxide Capture and Storage," *Cambridge University Press, Cambridge*, 2005.

[2] J. Koornneef, M. Spruijt, M. Molag, A. Ramirez, A. Faaij, and W. Turkenburg, "Uncertainties in risk assessment of CO2 pipelines," *Energy Procedia*, vol. 1, no. 1, pp. 1587–1594, Feb. 2009.

[3] W. Jung and J.-P. Nicot, "Impurities in CO2 - Rich Mixtures Impact CO2 Pipeline Design: Implications for Calculating CO2 Transport Capacity," in *Proceedings of SPE International Conference on CO2 Capture, Storage, and Utilization*, 2010.

[4] J. Gale, C. Hendriks, W. Turkenberg, J. Wang, D. Ryan, E. J. Anthony, N. Wildgust, and T. Aiken, "Effects of impurities on CO2 transport, injection and storage," *Energy Procedia*, vol. 4, pp. 3071–3078, 2011.

[5] C. A. Millat, J., Dymond, J.H., Nieto de Castro, *Transport Properties of Fluids, Their Correlation, Prediction and Estimation*. 2005.

[6] Z. K. S. Al-Siyabi, "The contact angle, interfacial tension and viscosity of reservoir fluids : experimental data and modelling." Petroleum Engineering, 2000.

[7] J. Kestin and W. Leidenfrost, "The effect of pressure on the viscosity of N2CO2 mixtures," *Physica*, vol. 25, no. 1–6, pp. 525–536, Jan. 1959.

[8] J. Kestin, Y. Kobayashi, and R. T. Wood, "The viscosity of four binary, gaseous mixtures at 20° and 30°C," *Physica*, vol. 32, no. 6, pp. 1065–1089, Jun. 1966.

[9] G. J. Gururaja, M. A. Tirunarayanan, and A. Ramachandran, "Dynamic viscosity of gas mixtures," *J. Chem. Eng. Data*, vol. 12, no. 4, pp. 562–567, Oct. 1967.

[10] J. Kestin and S. T. Ro, "The Viscosity of Nine Binary and Two Ternary Mixtures of Gases at Low Density," *Berichte der Bunsengesellschaft für Phys. Chemie*, vol. 78, no. 1, pp. 20–24, Jan. 1974.

[11] J. Kestin, H. E. Khalifa, S. T. Ro, and W. A. Wakeham, "The viscosity and diffusion coefficients of eighteen binary gaseous systems," *Phys. A Stat. Mech. its Appl.*, vol. 88, no. 2, pp. 242–260, Aug. 1977.

[12] J. Kestin and S. T. Ro, "The Viscosity and Diffusion Coefficients of Binary Mixtures of Nitrous Oxide with Ar, N2, and CO2," *Berichte der Bunsengesellschaft für Phys. Chemie*, vol. 86, no. 10, pp. 948–950, Oct. 1982.

[13] J. Kestin and S. T. Ro, "The Viscosity of Carbon-Monoxide Mixtures with Four Gases in the Temperature Range 25-200°C. Supplement," *Berichte der Bunsengesellschaft für Phys. Chemie*, vol. 87, no. 7, pp. 600–602, Jul. 1983.

[14] V. A. Mal'tsev, O. A. Nerushev, S. A. Novopashin, V. V. Radchenko, W. R. Licht, E. J. Miller, and V. S. Parekh, "Viscosity of H 2 −CO 2 Mixtures at (500, 800, and 1100) K," *J. Chem. Eng. Data*, vol. 49, no. 3, pp. 684–687, May 2004.

[15] L. Herning, F., Zipperer, "Calculation of the viscosity of technical gas mixtures from the viscosity of the individual gases," *das Gas- und Wasserfach*, vol. 79, pp. 49–54, 69–73, 1936.

[16] J. Kestin, J. and Yata, "Viscosity and Diffusion Coefficient of Six Binary Mixtures," *J. Chem. Phys.*, vol. 49, no. 11, p. 4780, Sep. 1968.

[17] J. Kestin, S. T. Ro, and W. A. Wakeham, "The transport properties of binary mixtures of hydrogen with CO, CO2 and CH4," *Phys. A Stat. Mech. its Appl.*, vol. 119, no. 3, pp. 615–638, May 1983.

[18] A. Hobley, G. P. Matthews, and A. Townsend, "The use of a novel capillary flow viscometer for the study of the argon/carbon dioxide system," *Int. J. Thermophys.*, vol. 10, no. 6, pp. 1165–1179, Nov. 1989.

[19] M. M. Lemmon EW, Huber ML, "NIST standard reference database 23: reference fluid thermodynamic and transport properties – REFPROP version 8.0.

Gaithersburg: National Institute of Standards and Technology, Standard Reference Data Program." 2007.

[20] K. Kashefi, A. Chapoy, K. Bell, and B. Tohidi, "Viscosity of binary and multicomponent hydrocarbon fluids at high pressure and high temperature conditions: Measurements and predictions," *J. Pet. Sci. Eng.*, vol. 112, pp. 153–160, Dec. 2013.

[21] I. Al-Siyabi, "Effect of Impurities on CO2 Stream Properties," Heriot-Watt University, 2013.

[22] A. S. Pensado, A. A. H. Pádua, M. J. P. Comuñas, and J. Fernández, "Viscosity and density measurements for carbon dioxide+pentaerythritol ester lubricant mixtures at low lubricant concentration," *J. Supercrit. Fluids*, vol. 44, no. 2, pp. 172–185, Mar. 2008.

[23] Barry N. Taylor, *Guidelines for Evaluating and Expressing the Uncertainty of NIST Measurement Results*. DIANE Publishing, 2009.

[24] S. Bell, *Measurement Good Practice Guide No. 11 (Issue 2), A Beginner's Guide to Uncertainty of Measurement*. National Physical Laboratory, 2001.

[25] B. Tohidi, R. W. Burgass, A. Danesh, and A. C. Todd, "Viscosity and Density of Methane + Methylcyclohexane from (323 to 423) K and Pressures to 140 MPa," *J. Chem. Eng. Data*, vol. 46, no. 2, pp. 385–390, Mar. 2001.

[26] J. A. Jossi, L. I. Stiel, and G. Thodos, "The viscosity of pure substances in the dense gaseous and liquid phases," *AIChE J.*, vol. 8, no. 1, pp. 59–63, Mar. 1962.

[27] J. Lohrenz, B. G. Bray, and C. R. Clark, "Calculating Viscosities of Reservoir Fluids From Their Compositions," *J. Pet. Technol.*, vol. 16, no. 10, pp. 1171–1176, Apr. 1964.

[28] L. I. Stiel and G. Thodos, "The viscosity of nonpolar gases at normal pressures," *AIChE J.*, vol. 7, no. 4, pp. 611–615, Dec. 1961.

[29] A. Y. Dandekar, "Interfacial Tension and Viscosity of Reservoir Fluids, PhD thesis," Heriot-Watt University, 1994.

[30] E. Vogel, C. Küchenmeister, E. Bich, and A. Laesecke, "Reference Correlation of the Viscosity of Propane," *J. Phys. Chem. Ref. Data*, vol. 27, no. 5, p. 947, Sep. 1998.

[31] K. S. Pedersen and A. Fredenslund, "An improved corresponding states model for the prediction of oil and gas viscosities and thermal conductivities," 1987.

[32] P. L. Christensen and A. A. Fredenslund, "A corresponding states model for the thermal conductivity of gases and liquids," *Chem. Eng. Sci.*, vol. 35, no. 4, pp. 871–875, 1980.

[33] H. J. M. Hanley, W. M. Haynes, and R. D. McCarty, "The viscosity and thermal conductivity coefficients for dense gaseous and liquid methane," *J. Phys. Chem. Ref. Data*, vol. 6, no. 2, p. 597, Apr. 1977.

[34] Fenghour; A.; Wakeham; W.A.; Vesovic;, "The Viscosity of Carbon Dioxide," *J. Phys. Chem. Ref. Data, Vol. 27, No. 1,* 1998.

[35] B. a. Younglove and J. F. Ely, "Thermophysical Properties of Fluids. II. Methane, Ethane, Propane, Isobutane, and Normal Butane," *J. Phys. Chem. Ref. Data*, vol. 16. pp. 577–798, 1987.

[36] S. Murad and K. E. Gubbins, "Corresponding states correlation for thermal conductivity of dense fluids," *Chem. Eng. Sci.*, vol. 32, no. 5, pp. 499–505, Jan. 1977.

[37] K. Aasberg-Petersen, K. Knudsen, and A. Fredenslund, "Prediction of viscosities of hydrocarbon mixtures," *Fluid Phase Equilibria*, vol. 70. pp. 293–308, 1991.

[38] A. Et-Tahir, C. Boned, B. Lagourette, and P. Xans, "Determination of the viscosity of various hydrocarbons and mixtures of hydrocarbons versus temperature and pressure," *Int. J. Thermophys.*, vol. 16, no. 6, pp. 1309–1334, Nov. 1995.

[39] H. J. M. Hanley and E. G. D. Cohen, "Analysis of the transport coefficients for simple dense fluids: The diffusion and bulk viscosity coefficients," *Phys. A Stat. Mech. its Appl.*, vol. 83, no. 2, pp. 215–232, Jan. 1976.

[40] K. C. Mo and K. E. Gubbins, "Conformal solution theory for viscosity and thermal conductivity of mixtures," *Mol. Phys.*, vol. 31, no. 3, pp. 825–847, Mar. 1976.

[41] K. C. Mo, K. E. Gubbins, G. Jacucci, and I. R. McDonald, "The radial distribution function in fluid mixtures: Conformal solution theory and molecular dynamics results," *Mol. Phys.*, vol. 27, no. 5, pp. 1173–1183, May 1974.

[42] J. F. Ely and H. J. M. Hanley, "Prediction of transport properties. 1. Viscosity of fluids and mixtures," *Ind. Eng. Chem. Fundam.*, vol. 20, no. 4, pp. 323–332, Nov. 1981.

[43] J. F. Huber, M. L. and Ely, "NIST Standard Rejerence Database 4: NIST Thermophysical Properties of Hydrocarbon Mixtures," *U.S. Department of Commerce, Washington, DC*, 1990.

[44] M. L. Huber, D. G. Friend, and J. F. Ely, "Prediction of the thermal conductivity of refrigerants and refrigerant mixtures," *Fluid Phase Equilib.*, vol. 80, pp. 249–261, Nov. 1992.

[45] I. D. Watson and J. S. Rowlinson, "The prediction of the thermodynamic properties of fluids and fluid mixtures-II Liquid-vapour equilibrium in the system argon + nitrogen + oxygen," *Chem. Eng. Sci.*, vol. 24, no. 10, pp. 1575–1580, Oct. 1969.

[46] Ivan D. Zaytsev, Georgiy G. Aseyev, "Properties of Aqueous Solutions of Electrolytes - CRC Press Book," *CRC Press*, 1992.

[47] C. R. Wilke, "A Viscosity Equation for Gas Mixtures," *J. Chem. Phys.*, vol. 18, no. 4, p. 517, Dec. 1950.

[48] K. E. Gubbins, W. R. Smith, M. K. Tham, and E. W. Tiepel, "Perturbation theory for the radial distribution function," *Mol. Phys.*, vol. 22, no. 6, pp. 1089–1105, Jan. 1971.

[49] EU Emissions Trading Scheme – established under Directive 2003/87/EC.

[50] European CCS Directive – Directive of the European Parliament and of the council on the geological Storage of Carbon Dioxide Amending Council Directives 85/337/EEC, 96/61/EC, Directives 2000/60/EC, 2001/80/EC, 2004/35/EC, 2006/12/EC and Regulation (EC) No 1013/2006 – Brussels 23.1.2008.

[51] Glen, N. F., CO_2 Fluid Properties and Flow Calculations for Operational and Measurement Purposes, TUV NEL technical report, NEL, East Kilbride, Nov 2012.

[52] Leslie, G., CCS Metering Challenges and Options, TUV NEL technical report, NEL, East Kilbride, June 2009

CHAPTER 5: DENSITY OF ACID GASES AND LIQUIDS

The aim of this chapter is to investigate the densities of acid gases and liquids. Densities of 95 mol% CO_2 - 5 mol% H_2S and 95 mol% CO_2 - 5 mol% SO_2 binary systems were measured continuously using a high temperature and pressure Vibrating Tube Densitometer (VTD), Anton Paar DMA 512 at pressures up to 40 MPa at five different temperatures, 273.15, 283.15, 298.15, 323.15 and 353.15 K (0, 10, 25, 50 and 80 °C) in gas, liquid and supercritical regions. The experimental data then were used to evaluate a new CO_2 volume correction model as well as classical cubic equation of states (PR and SRK) with and without Peneloux shift parameters. The specific heat capacity, dew point and bubble point of the systems also could be estimated using the experimental density data.

5.1 Introduction

One of the most common impurities in natural gas is carbon dioxide. Most reservoirs around the world contain carbon dioxide. For instance, one of the biggest gas resources in Prudhoe Bay Alaska with more than 20 trillion cubic feet associated gas (with the oil) contains roughly 12 mol% carbon dioxide and over 10 ppmv hydrogen sulphide. Similar acid gas content can be found in the Tangguh field in the South-East Asia, Indonesia. The In Salah gas field in Algeria also contains typically 10 mol% CO_2. In the Middle East, there are some gas fields typically containing 3 mol% H_2S and 5 mol% CO_2. A comprehensive survey by Weeks et al. [1] shows that acid gas content composition can span from a few ppm to 90 mol% for carbon dioxide and from 0 to 60 mol% for hydrogen sulphide.

CO_2 content in natural gas pipelines should not be more than a specific amount which is typically 2 - 2.5 mol%. Any extra carbon dioxide from natural gas reservoirs, therefore, should be first removed and then transported to either re-injection to oil fields for

enhanced oil recovery or should be stored in a non-oil formations (e.g., Sleipner field [2] in the Norwegian North Sea or aqueifer in In Salah gas field [3] in Algeria).

The pressure-volume-temperature behaviour, thermal properties and densities of sour gas mixtures are essential to proper design of sour natural gas systems and CO_2 transport and injections scheme.

5.2 Literature review

Despite the importance of the volumetric behaviour of acid gases and liquids, there are very few experimental data available in the literature on the density of CO_2-H_2S binary systems. The first study on the pressure-volume-temperature behaviour of the CO_2-H_2S systems has been conducted by Bierlein and Kay [4] for saturated state of eight mixtures of CO_2-H_2S from 273.15 K (0 °C) to critical temperature of hydrogen sulphide. Mole fractions of CO_2 in this study are 0.0, 0.0630, 0.1614, 0.2608, 0.3759, 0.4728, 0.6659, 0.8292, 0.9009 and 1.0. Sobocinski and Kurata [5] experimentally studied the CO_2-H_2S systems at lower temperatures, i.e., below 273.15 K, to cover the data obtained by Bierlein and Kay. They studied seven mixtures from solid-liquid-vapour region to the critical region. A research report from the Gas Processors Association about thermodynamic properties of CO_2-H_2S mixtures [6] includes the density measurements for four mixtures. The systems in this study were 93.93 mol% CO_2 + 6.07 mol% H_2S, 90.45 mol% CO_2 + 9.55 mol% H_2S, 70.67 mol% CO_2 + 29.33 mol% H_2S and 50.01 mol% CO_2 + 49.99 mol% H_2S. The performed experiments for each mixture are Burnett and Burnett-isochoric measurements at temperatures ranging from 200 K to 450 K and at pressures from 0.1 to 23 MPa. All the results of this research report were also published by Stouffer et al. [7]. The phase behaviour of CO_2-H_2S also has been studied by Chapoy et al. [8] in order to improve the design of acid gas injection in CCS scheme. The measurements included VLE tests at 258.41 K, 273.15 K, 293.47 K and 313.02 K at pressures from 1.0 to 5.5 MPa. They also have mentioned that both PR and SRK equation of states with classical mixing rules and proper binary interaction parameters can well predict the phase behaviour of CO_2-H_2S systems.

The lack of experimental data for CO_2-SO_2 systems is certainly due to toxicity of the system. The first available data for this system is reported by Caubet [9]. A comprehensive thermodynamic behaviour of CO_2-SO_2 mixture has been studied experimentally by Coquelet et al. [10], [11] for transport purposes of CO_2 mixtures in

CCS context. Only VLE data are available at 263.15 K and 333.21 K and at pressures ranging from 0.1 to 8.8 MPa.

5.3 Experimental part

5.3.1 Equipment description

Densities of CO_2-rich systems were measured using a high temperature and pressure Vibrating Tube Densitometer (VTD), Anton Paar DMA 512 and using forced path mechanical calibration (FPMC) model which is well described by Bouchot et al. [12] and Coquelet et al. [13]. A schematic view and picture of the apparatus is shown in Figure 5.1 and Figure 5.2, respectively. A detailed description of a typical vibrating-tube densitometer is given by Bouchot and Richon [14]. The main part of the set-up is the Anton Paar DMA 512 densitometer. The U-shape vibrating tube made from Hastelloy which can work up to 70 MPa pressure and temperature range of 263.15 K to 423.15 K (-10 °C to 150 °C). Temperature of the densitometer can be set by a liquid bath (model: Lauda RE206) keeping the temperature stable to ±0.01 K. The setup is fully immersed in a liquid bath (model: West P6100) to keep the temperature constant during the test. Temperature in the vibrating tube part and liquid bath is measured using four-wire 100-Ω platinum resistance probes (Pt100) which were calibrated against a 25-Ω reference thermometer of Tinsley Precision Instrument. The period of the vibration, τ, is recorded with a HP53131A data acquisition unit. The uncertainty of the vibrating period values is $\pm 10^{-8}$ seconds. Three pressure transducers (model: Druck PTX611) with different complementary ranges of 0-10 MPa, 10-30 MPa and 30-70 MPa were used to record the pressure data by connection to the HP34970A data acquisition unit. All the pressure transducers were calibrated by means of an electronic balance (model: GE Sensing PACE 5000) for pressures up to 20 MPa and a dead weight pressure balance (model: Desgranges & Huot model 5202S) for higher pressures up to 40 MPa. All the parts of the apparatus are connected together by 1/16 inch lines.

The uncertainty on the measured density data because of the uncertainties of the mechanical parameters used in the FPMC model is calculated in gas and liquid phases [13]. Total uncertainties on temperature after calibration are estimated to be ±0.02 K. Also uncertainties on pressure measurements after calibration are ±0.002, ±0.005 and ±0.005 MPa for the pressure transducers ranging from 0-10 MPa, 10-30 MPa and 30-70 MPa, respectively.

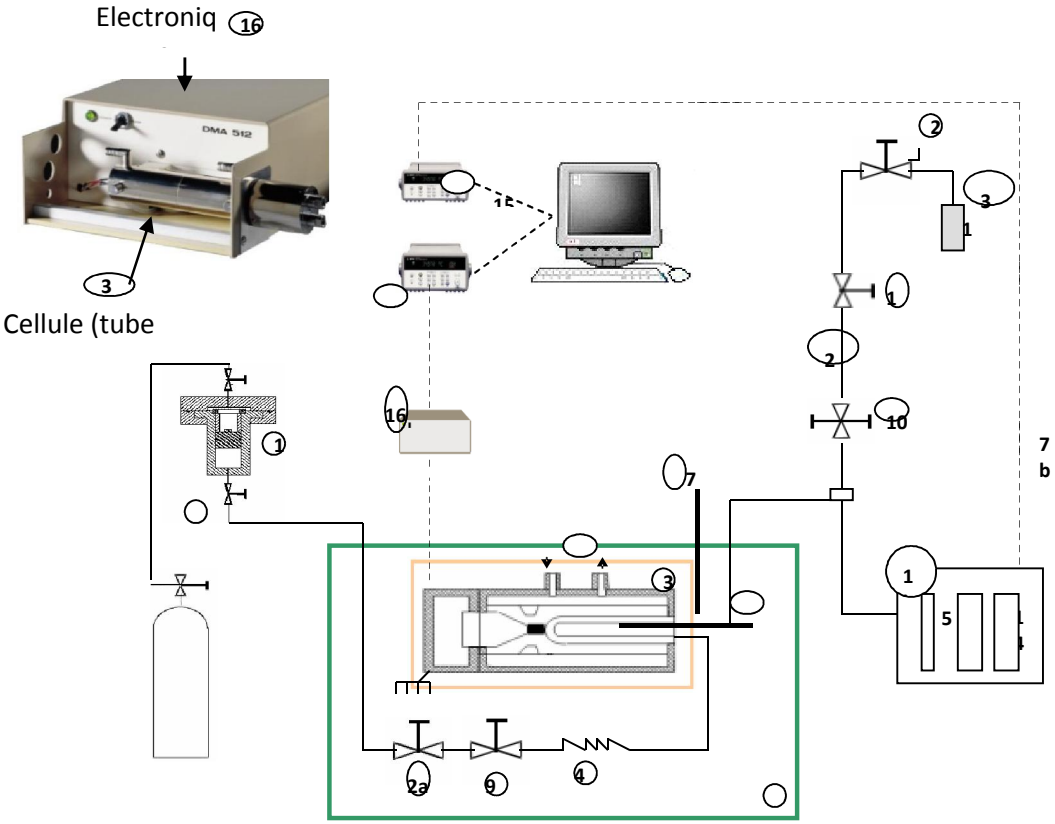

Figure 5.1 Schematic diagram of the densitometer apparatus

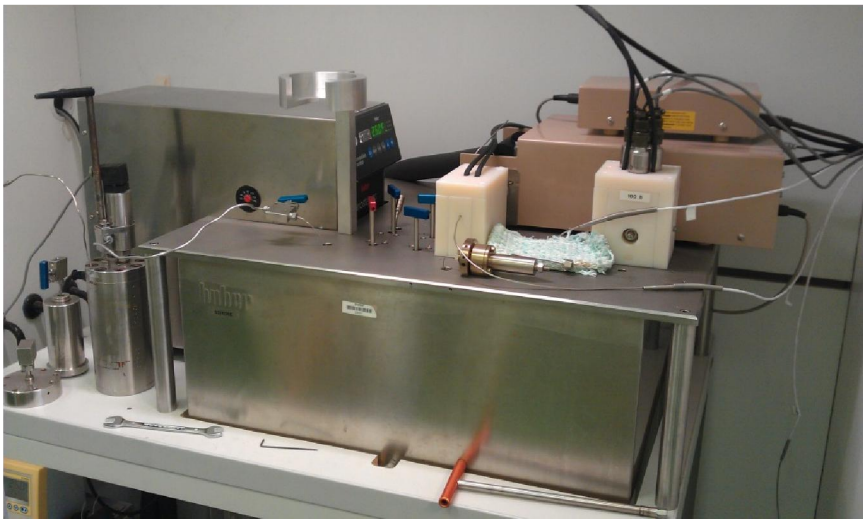

Figure 5.2 The density measurement set-up

The proposed apparatus is designed for quasi-continuous data acquisition. Near the saturation points a great number of data are recorded so subsequent graphical determination of the exact saturation point is accurate. Pressure is recorded as the output tension of the pressure transducer measured by a digital voltmeter (Schlumberger model 7081). This tension is converted into pressure values by a direct calibration described before. The vibration period measurement is made by means of a periodmeter

(Universal Counter Schlumberger model 2721; resolution, 10^{-6} ms). The voltmeter and the periodmeter are equipped with a parallel GPIB/ IEEE488 standard interface. A computer is used to communicate with them through a serial COM port via a RS232/IEEE488 interface cable (see Figure 5.3).

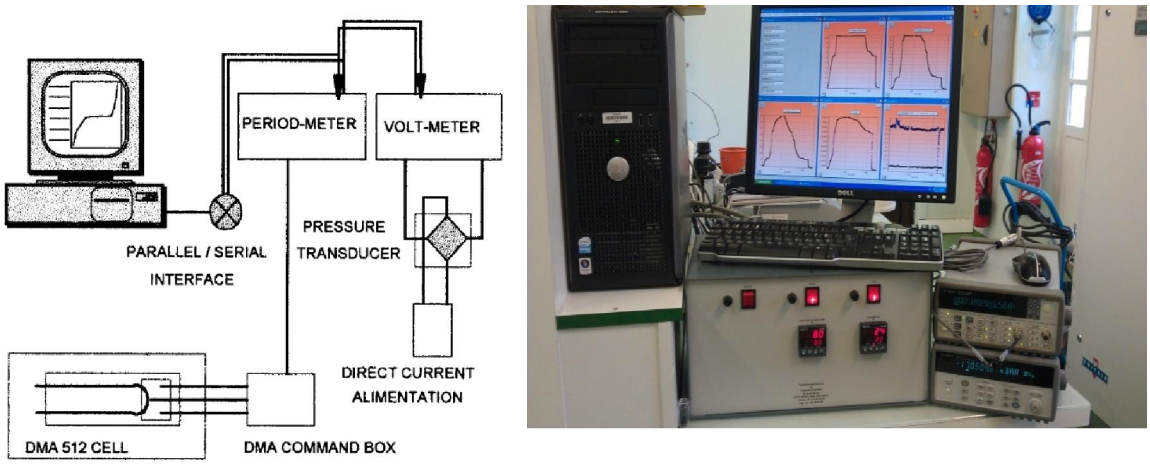

Figure 5.3 Flow diagram of the pressure vs period data acquisition

5.3.2 Mixture preparation of CO_2+H_2S and CO_2+SO_2 systems

The mixtures were prepared gravimetrically. First, the component with the lowest vapour pressure at laboratory condition was injected to the pressure vessel. At about 20 °C (293 K), vapour pressure of the H_2S, CO_2 and SO_2 are 1.78, 5.73 and 0.33 MPa, respectively. Therefore, for preparing the CO_2+H_2S mixture, first H_2S was injected while for preparing the CO_2+SO_2 mixture, first SO_2 was injected to the high pressure vessel. The exact weight of the injected pure component was measured using a four digit balance three times (see Figure 5.4). The average of the readings was calculated and accordingly the calculated amount for the second pure component was injected to the high pressure vessel. After injecting both pure components, weight percent and mole percent of the mixture were calculated. Then, the pressure of the mixtures was increased to 40 MPa by injecting nitrogen to the other side of the piston in each pressure vessel. As the components in the mixture are toxic and corrosive, proper O-rings for the pistons of the pressure vessels were selected.

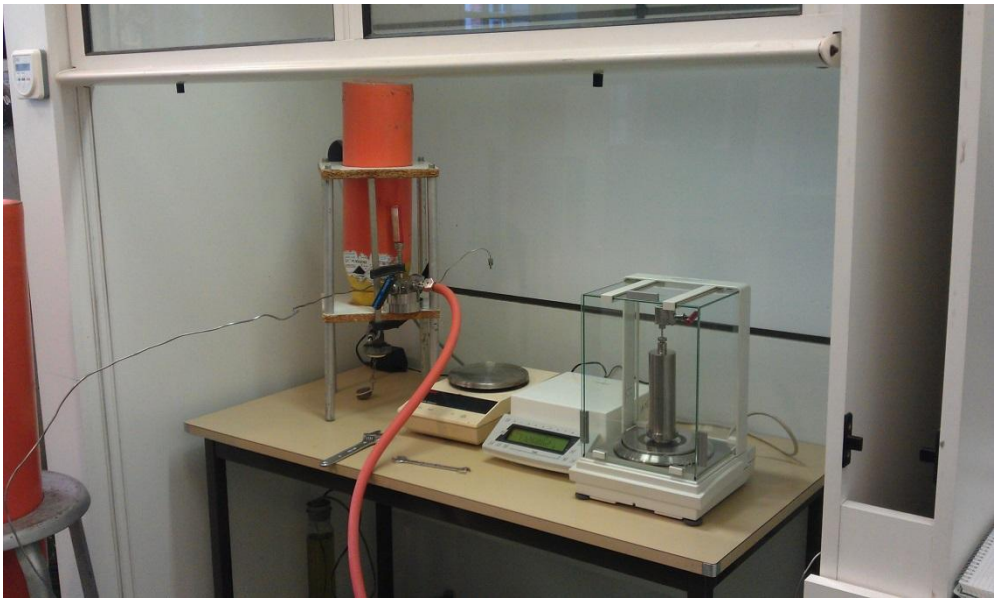

Figure 5.4 Mixture Preparation

5.3.3 Safety Consideration

Hydrogen sulphide, H_2S, is a colourless, flammable and extremely hazardous compound which can cause a wide range of health effects. The characteristic of the gas is a pungent odour of rotten egg which irritates the eyes, nose and throat even in very low concentrations. It destroys the sense of smell rapidly and can cause unconsciousness and death at higher levels of concentrations [15].

Sulphur dioxide, SO_2, is a corrosive and colourless gas and well-known air pollutant causing winter smog [16]. The inhalation of the pungent odour toxic SO_2 can irritate the nose and throat at low concentration. The higher concentrations may cause stomach pain, vomiting and corrosive damage to the lungs [17].

From health and safety perspective, the recommendations at work by INRS (Health and Safety - INRS) have been implemented in this work. Health and safety training about toxic gases has been provided. Personal Protective Equipment (PPE) i.e., safety glasses, laboratory coats, safety shoes and masks with specific filter, has been used in the laboratory to be protected against safety and health risks during the tests.

To reduce the exposure to toxic gases and inhalation in the case of leakage, all the work from preparing the mixtures to conducting the tests has been performed under properly designed and operated fume-hood. Fume-hood includes two double-glazed sashes which can move either vertically or horizontally. Vertical sashes can increase the safety of operations as a safety shield during conducting tests and the horizontal sashes can reduce the cost for energy of HVAC system [19]. During the test, the fume-hood must

not be kept in a fully open position. Vertical sashes must be kept down as much as possible and horizontal sashes, which move from side to side only, could be used to operate the valves during the tests [20]. The airflow inside the fume-hood also must be checked from control panel to have adequate flow.

Hydrogen sulphide is a colourless highly toxic gas with rotten egg odour. To detect H_2S, odour is unreliable and proper portable atmospheric gas detector has been provided. H_2S at approximately 5 ppm level has moderate odour and can be easily detected. However at 10 ppm level will irritate the eyes. To personal protection, the workplace exposure limits (WELs) for H_2S at long term (8-hour time weighted average (TWA)) are 5 ppm and 10 ppm for short term (15-minute TWA) [21]. Also, the long term exposure limit (LTEL) of sulphur dioxide, SO_2, is 2 ppm and the short term exposure limit (STEL) is 5 ppm [22].

The design pressure of the lines and valves in the set-up is 100 MPa and that of densitometer is 120 MPa. The maximum desired pressure to conduct experiments was 40 MPa. Thus, the leak test has been performed before starting the main experiments. The entire system was under pressure by nitrogen at 150% of operation pressure, i.e., 60 MPa, for 48 hours to find and resolve any possible leakage in the system with helium and a specific detector.

The vessel for the mixture preparation has 150 ml volume and the design pressure is 70 MPa. It also includes a piston to isolate the mixture from the gas injected to pressurise the system. Proper NBR O-rings have been selected around the piston to isolate the mixture from the nitrogen side. These types of O-rings are suitable for both carbon dioxide and hydrogen sulphide or sulphur dioxide. Three valves have been mounted in the connection line in order to proper control of the gas flow from pressure vessel containing the prepared mixture to the densitometer circuit.

5.3.4 Calibration procedure

First, three pressure transducers and temperature sensors were calibrated. The model of pressure transducers is Druck PTX611 with different ranges of 0-10 MPa, 10-30 MPa and 30-70 MPa. The pressure transducers were calibrated using an electronic balance GE Sensing PACE 5000 for pressures up to 20 MPa and a dead weight tester Desgranges & Huot 5202S for pressures from 20 MPa to 40 MPa. For P-302, calibration from atmospheric pressure up to 20 MPa has been conducted by Electronic device and those for pressures from 20 MPa up to 30 MPa has been calibrated using

dead weight tester. The results of both calibrations can be found below. Transducer P-303 has been calibrated against dead weight tester from pressure of 20 MPa up to 40 MPa. The calibration data for the pressure transducers are available in Table 5.1 to Table 5.4 and Figure 5.5 to Figure 5.8.

Two temperature probes in the vibrating tube part and liquid bath were calibrated against a 25-Ω reference thermometer (model: Tinsley Precision Instrument). The calibration data are available in Table 5.5 and Figure 5.9 for densimeter temperature probe and in Table 5.6 and Figure 5.10 for the bath temperature probe.

Table 5. 1 Pressure transducer P-301 for pressures from atmospheric pressure up to 10 MPa

P imposed	P imposed	P Read	P Read^2	Linear Regression		Order 2 Regression	
				Pcal	Err	Pcal	Err
MPa	bar	bar	bar	bar	MPa	bar	MPa
0.10085	1.0085	0.8098	0.6558	1.0400	-0.0031	1.0274	-0.0019
1.000	10.00	9.7293	94.6593	9.9855	0.0015	9.9800	0.0020
1.900	19.00	18.6954	349.5180	18.9777	0.0022	18.9779	0.0022
2.800	28.00	27.6721	765.7451	27.9806	0.0019	27.9849	0.0015
3.700	37.00	36.6497	1343.2005	36.9844	0.0016	36.9913	0.0009
4.600	46.00	45.6264	2081.7684	45.9872	0.0013	45.9954	0.0005
5.500	55.00	54.6004	2981.2037	54.9874	0.0013	54.9953	0.0005
6.400	64.00	63.5797	4042.3783	63.9929	0.0007	63.9989	0.0001
7.300	73.00	72.5578	5264.6343	72.9971	0.0003	72.9999	0.0000
8.200	82.00	81.5360	6648.1193	82.0015	-0.0001	81.9995	0.0000
9.100	91.00	90.5154	8193.0376	91.0071	-0.0007	90.9988	0.0001
10.000	100.00	99.4920	9898.6581	100.0098	-0.0010	99.9938	0.0006
9.100	91.00	90.5148	8192.9290	91.0065	-0.0006	90.9982	0.0002
8.200	82.00	81.5403	6648.8205	82.0058	-0.0006	82.0038	-0.0004
7.300	73.00	72.5643	5265.5776	73.0036	-0.0004	73.0064	-0.0006
6.400	64.00	63.5885	4043.4973	64.0017	-0.0002	64.0078	-0.0008
5.500	55.00	54.6125	2982.5252	54.9995	0.0000	55.0074	-0.0007
4.600	46.00	45.6400	2083.0096	46.0009	-0.0001	46.0090	-0.0009
3.700	37.00	36.6679	1344.5349	37.0026	-0.0003	37.0096	-0.0010
2.800	28.00	27.6907	766.7749	27.9992	0.0001	28.0036	-0.0004
1.900	19.00	18.7230	350.5507	19.0054	-0.0005	19.0056	-0.0006
1.000	10.00	9.7657	95.3689	10.0220	-0.0022	10.0165	-0.0017
0.10091	1.0091	0.7892	0.6228	1.0193	-0.0010	1.0067	0.0002
		Max Error / MPa			**0.0022**		**0.0022**
		Min Error / MPa			**-0.0031**		**-0.0019**
		Error / MPa					**± 0.002**

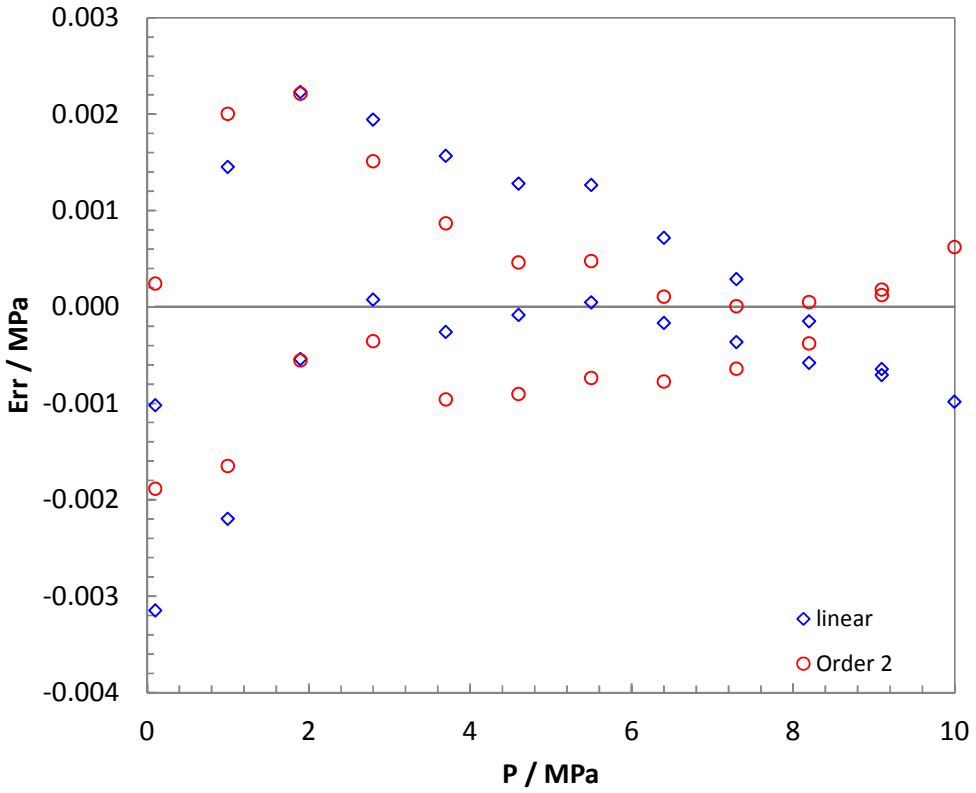

Figure 5. 5 Pressure transducer P-301 for pressures from atmospheric pressure up to 10 MPa

Table 5. 2 Pressure transducer P-302 for pressures from 10 MPa up to 30 MPa

P imposed	P imposed	P Read	P Read^2	Linear Regression		Order 2 Regression	
				Pcal	Err	Pcal	Err
MPa	bar	bar	bar	bar	MPa	bar	MPa
0.10092	1.0092	0.3464	0.1200	0.9602	0.0049	1.0046	0.0005
1.095	10.95	10.3544	107.2136	10.9159	0.0034	10.9462	0.0004
2.090	20.90	20.3678	414.8473	20.8769	0.0023	20.8947	0.0005
3.085	30.85	30.3797	922.9262	30.8364	0.0014	30.8433	0.0007
4.000	40.00	39.6222	1569.9187	40.0305	-0.0031	40.0287	-0.0029
5.000	50.00	49.6791	2468.0130	50.0348	-0.0035	50.0250	-0.0025
6.000	60.00	59.7327	3567.9954	60.0358	-0.0036	60.0196	-0.0020
7.000	70.00	69.7806	4869.3321	70.0311	-0.0031	70.0101	-0.0010
8.000	80.00	79.8300	6372.8289	80.0279	-0.0028	80.0037	-0.0004
9.000	90.00	89.8845	8079.2233	90.0298	-0.0030	90.0040	-0.0004
10.050	100.50	100.4116	10082.4894	100.5018	-0.0002	100.4759	0.0024
11.045	110.45	110.4240	12193.4598	110.4618	-0.0012	110.4375	0.0013
12.040	120.40	120.4367	14504.9987	120.4221	-0.0022	120.4009	-0.0001
13.035	130.35	130.4491	17016.9677	130.3821	-0.0032	130.3656	-0.0016
14.030	140.30	140.4473	19725.4441	140.3280	-0.0028	140.3178	-0.0018
15.025	150.25	150.4396	22632.0732	150.2680	-0.0018	150.2656	-0.0016
16.020	160.20	160.4295	25737.6245	160.2056	-0.0006	160.2126	-0.0013
17.015	170.15	170.4126	29040.4542	170.1364	0.0014	170.1543	-0.0004

18.010	180.10	180.3910	32540.9129	180.0626	0.0037	180.0930	0.0007
19.005	190.05	190.3633	36238.1860	189.9827	0.0067	190.0271	0.0023
19.005	190.05	190.3653	36238.9474	189.9847	0.0065	190.0291	0.0021
18.010	180.10	180.3955	32542.5364	180.0671	0.0033	180.0975	0.0003
17.015	170.15	170.4166	29041.8176	170.1404	0.0010	170.1583	-0.0008
16.020	160.20	160.4338	25739.0042	160.2099	-0.0010	160.2168	-0.0017
15.025	150.25	150.4460	22633.9989	150.2743	-0.0024	150.2720	-0.0022
14.030	140.30	140.4473	19725.4441	140.3280	-0.0028	140.3178	-0.0018
13.035	130.35	130.4387	17014.2545	130.3717	-0.0022	130.3553	-0.0005
12.040	120.40	120.4298	14503.3367	120.4152	-0.0015	120.3941	0.0006
11.045	110.45	110.4143	12191.3176	110.4521	-0.0002	110.4278	0.0022
10.050	100.50	100.3905	10078.2525	100.4808	0.0019	100.4549	0.0045
9.000	90.00	89.8772	8077.9111	90.0225	-0.0023	89.9967	0.0003
8.000	80.00	79.8142	6370.3065	80.0122	-0.0012	79.9880	0.0012
7.000	70.00	69.7559	4865.8856	70.0065	-0.0007	69.9856	0.0014
6.000	60.00	59.6990	3563.9706	60.0022	-0.0002	59.9861	0.0014
5.000	50.00	49.6612	2466.2348	50.0170	-0.0017	50.0072	-0.0007
4.000	40.00	39.6150	1569.3482	40.0233	-0.0023	40.0215	-0.0022
3.085	30.85	30.3467	920.9222	30.8035	0.0046	30.8105	0.0040
2.090	20.90	20.3615	414.5907	20.8706	0.0029	20.8884	0.0012
1.095	10.95	10.3528	107.1805	10.9143	0.0036	10.9446	0.0005
0.1009	1.0094	0.3783	0.1431	0.9920	0.0017	1.0363	-0.0027
		Max Error / MPa			**0.0067**		**0.0045**
		Min Error / MPa			**-0.0036**		**-0.0029**
		Error / MPa					**± 0.005**

Table 5. 3 Pressure transducer P-302 for pressures from 10 MPa up to 30 MPa

P imposed	P imposed	P Read	P Read^2	Linear Regression		Order 2 Regression	
				Pcal	Err	Pcal	Err
MPa	bar	bar	bar	bar	MPa	bar	MPa
20.101	201.01	201.4562	40584.6005	200.9583	0.0052	200.9872	0.0023
21.101	211.01	211.4733	44720.9566	210.9912	0.0019	210.9958	0.0014
23.101	231.01	231.4809	53583.4071	231.0305	-0.0021	231.0051	0.0005
25.101	251.01	251.4597	63231.9807	251.0409	-0.0031	251.0105	-0.0001
27.101	271.01	271.4143	73665.7222	271.0271	-0.0017	271.0163	-0.0006
29.101	291.01	291.3327	84874.7421	290.9771	0.0033	291.0105	-0.0001
29.101	291.01	291.3292	84872.7028	290.9736	0.0036	291.0069	0.0003
27.101	271.01	271.4071	73661.8139	271.0199	-0.0010	271.0091	0.0001
25.101	251.01	251.4567	63230.4720	251.0379	-0.0028	251.0074	0.0002
23.101	231.01	231.4823	53584.0552	231.0319	-0.0022	231.0065	0.0003
21.101	211.01	211.5132	44737.8338	211.0312	-0.0021	211.0357	-0.0026
20.101	201.01	201.4953	40600.3559	200.9975	0.0012	201.0262	-0.0017
		Max Error / MPa			**0.0052**		**0.0023**
		Min Error / MPa			**-0.0031**		**-0.0026**
		Error / MPa					**± 0.003**

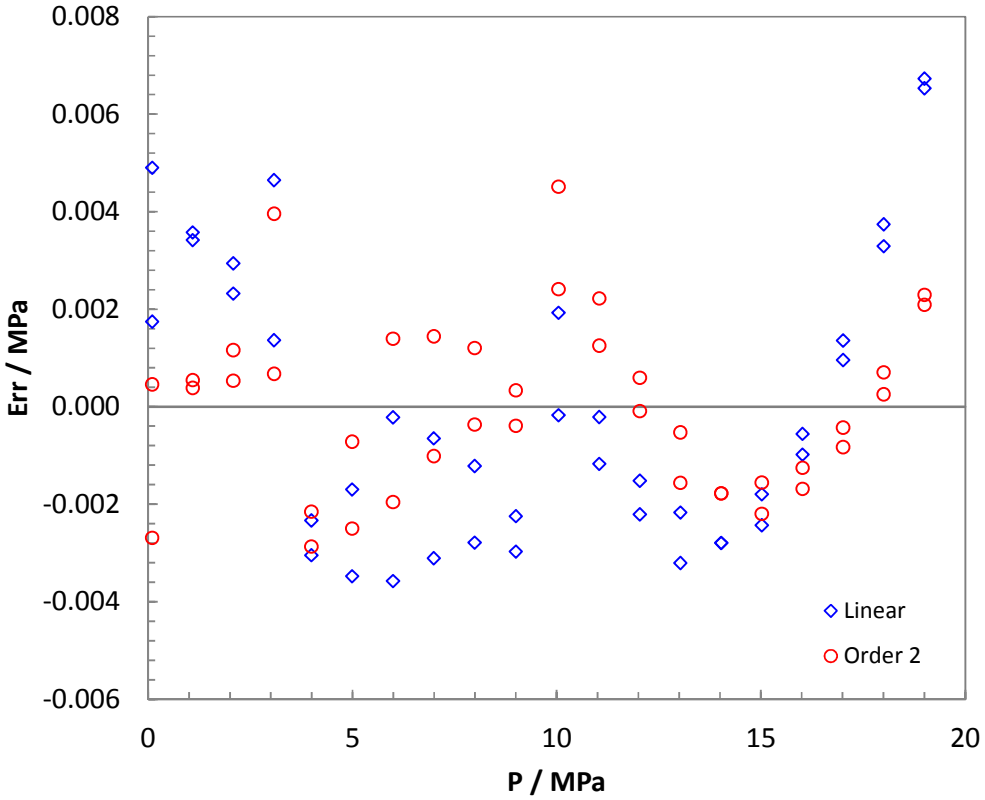

Figure 5. 6 Pressure transducer P-302 for pressures up to 20 MPa

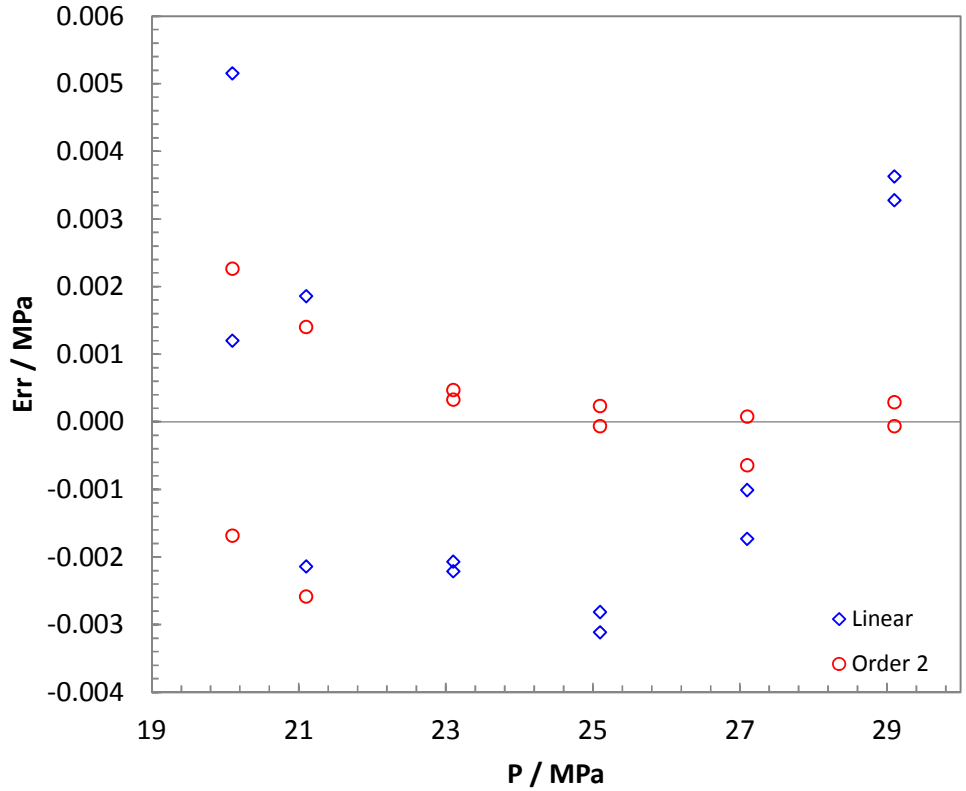

Figure 5. 7 Pressure transducer P-302 for pressures from 20 MPa to 30 MPa

Table 5. 4 Pressure transducer P-303 for pressures from 30 MPa up to 40 MPa

P imposed	P imposed	P Read	P Read^2	Linear Regression		Order 2 Regression	
				Pcal	Err	Pcal	Err
MPa	bar	bar	bar	bar	MPa	bar	MPa
20.101	201.01	198.1558	39265.7211	201.0143	-0.0005	201.0256	-0.0016
21.101	211.01	208.1310	43318.5132	211.0260	-0.0016	211.0333	-0.0024
23.101	231.01	228.0621	52012.3215	231.0300	-0.0020	231.0307	-0.0021
25.101	251.01	248.0080	61507.9681	251.0489	-0.0039	251.0447	-0.0035
27.101	271.01	267.9442	71794.0943	271.0580	-0.0048	271.0507	-0.0041
29.101	291.01	287.8691	82868.6187	291.0558	-0.0046	291.0470	-0.0037
31.101	311.01	307.7860	94732.2218	311.0456	-0.0036	311.0370	-0.0027
33.101	331.01	327.7095	107393.5164	331.0419	-0.0032	331.0354	-0.0026
35.101	351.01	347.6321	120848.0770	351.0374	-0.0028	351.0346	-0.0025
37.101	371.01	367.5440	135088.5919	371.0222	-0.0012	371.0247	-0.0015
39.101	391.01	387.4539	150120.5246	391.0049	0.0005	391.0146	-0.0005
40.101	401.01	397.4042	157930.0982	400.9916	0.0018	401.0055	0.0004
39.101	391.01	387.4370	150107.4290	390.9879	0.0022	390.9976	0.0012
37.101	371.01	367.5150	135067.2752	370.9931	0.0017	370.9956	0.0014
35.101	351.01	347.5972	120823.8134	351.0024	0.0007	350.9995	0.0010
33.101	331.01	327.6673	107365.8595	330.9996	0.0010	330.9930	0.0017
31.101	311.01	307.7302	94697.8760	310.9896	0.0020	310.9810	0.0029
29.101	291.01	287.7963	82826.7103	290.9827	0.0027	290.9739	0.0036
27.101	271.01	267.8639	71751.0689	270.9774	0.0032	270.9701	0.0040
25.101	251.01	247.9267	61467.6486	250.9673	0.0042	250.9631	0.0047
23.101	231.01	227.9951	51981.7656	230.9628	0.0047	230.9635	0.0046
21.101	211.01	208.1003	43305.7349	210.9952	0.0015	211.0025	0.0007
20.101	201.01	198.1321	39256.3291	200.9906	0.0019	201.0018	0.0008
Max Error / MPa					**0.0047**		**0.0047**
Min Error / MPa					**-0.0048**		**-0.0041**
Error / MPa							**± 0.005**

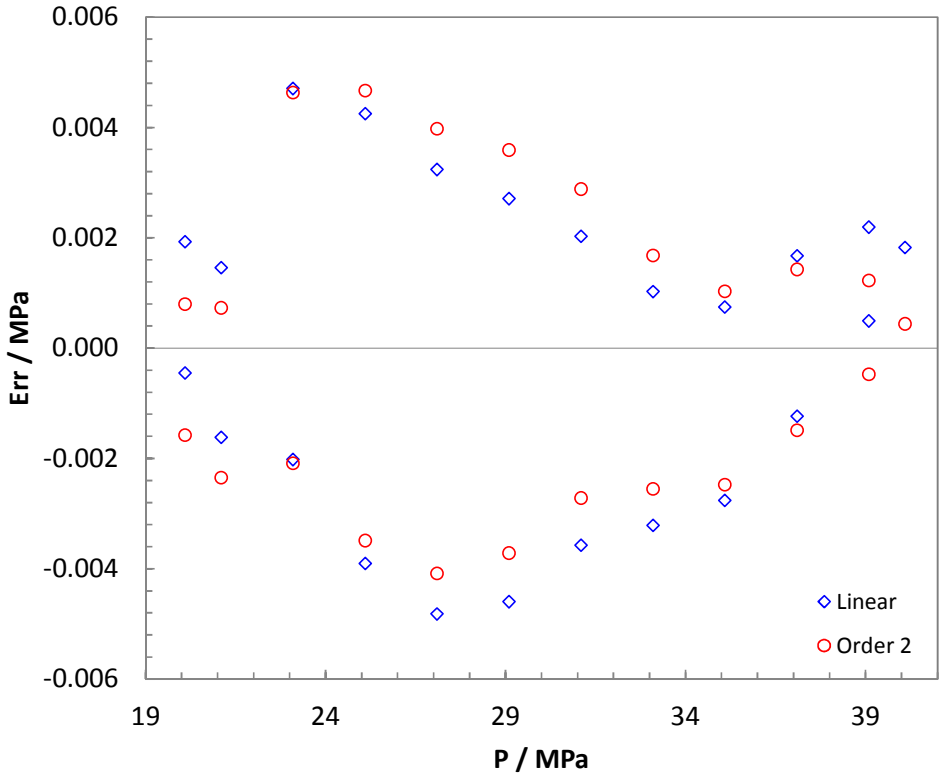

Figure 5. 8 Pressure transducer P-303 for pressures from 20 MPa to 40 MPa

Table 5. 5 Temperature probe inside densimeter

T real	T read	T^2 read	T cal	Err. Abs.	T cal	Err. Abs.
278.23	278.22	298.85	278.23	0.00	278.21	0.01
278.24	278.22	298.85	278.23	0.01	278.21	0.02
278.25	278.24	299.06	278.25	0.00	278.23	0.02
283.23	283.23	374.76	283.23	0.00	283.22	0.01
283.23	283.23	374.76	283.23	0.00	283.22	0.01
287.42	287.44	477.35	287.43	-0.01	287.43	-0.01
287.44	287.46	477.93	287.45	-0.01	287.45	-0.01
293.28	293.29	678.77	293.27	0.00	293.27	0.00
293.29	293.30	679.17	293.28	0.00	293.28	0.00
293.29	293.30	679.17	293.28	0.00	293.28	0.00
298.21	298.24	902.66	298.21	-0.01	298.22	-0.01
298.29	298.32	906.68	298.29	0.00	298.30	-0.01
298.32	298.36	908.69	298.33	-0.01	298.34	-0.02
303.20	303.22	1177.35	303.19	0.01	303.20	0.00
303.20	303.23	1177.96	303.20	0.00	303.21	-0.01
303.21	303.24	1178.56	303.21	0.00	303.22	-0.01
308.20	308.24	1504.46	308.20	0.00	308.21	-0.01
308.20	308.24	1504.46	308.20	0.00	308.21	-0.01
308.20	308.24	1504.46	308.20	0.00	308.21	-0.01
313.21	313.25	1881.16	313.21	0.00	313.22	-0.01
313.21	313.26	1881.96	313.22	0.00	313.23	-0.02
313.22	313.26	1881.96	313.22	0.00	313.23	-0.01
318.22	318.27	2308.96	318.22	0.00	318.23	-0.01
318.23	318.27	2308.96	318.22	0.00	318.23	-0.01
323.23	323.28	2786.17	323.23	0.00	323.24	-0.01
323.23	323.28	2786.17	323.23	0.00	323.24	-0.01
328.24	328.29	3313.57	328.24	0.00	328.25	-0.01
328.24	328.29	3313.57	328.24	0.00	328.25	-0.01
333.23	333.29	3889.97	333.24	0.00	333.24	-0.01
333.26	333.31	3892.38	333.26	0.01	333.26	0.00
338.25	338.31	4518.98	338.25	0.00	338.26	-0.01
338.26	338.32	4520.28	338.26	0.00	338.27	-0.01
343.27	343.33	5198.38	343.27	0.00	343.28	0.00
343.28	343.33	5198.38	343.27	0.00	343.28	0.00
348.27	348.33	5924.43	348.27	0.00	348.27	0.00
348.29	348.34	5926.69	348.28	0.01	348.28	0.01
348.30	348.35	5928.19	348.29	0.01	348.29	0.01
353.28	353.33	6701.98	353.28	0.01	353.27	0.01
353.29	353.35	6705.19	353.30	-0.01	353.29	0.00
358.27	358.32	7527.08	358.27	0.00	358.26	0.01
358.29	358.34	7530.49	358.29	0.00	358.28	0.02
363.25	363.31	8401.98	363.26	-0.01	363.24	0.01
363.28	363.34	8407.39	363.29	-0.01	363.27	0.01
363.30	363.35	8408.29	363.30	0.00	363.28	0.02

Table 5. 6 Temperature probe of the bath

T real	T read	T^2 read	T cal	Err. Abs.	T cal	Err. Abs.
273.22	273.19	273.15	273.22	0.00	273.22	0.00
278.23	278.21	298.75	278.23	-0.01	278.23	0.00
278.24	278.21	298.75	278.23	0.00	278.23	0.00
278.25	278.22	298.85	278.24	0.01	278.24	0.01
283.11	283.08	371.75	283.10	0.01	283.09	0.01
283.23	283.21	374.35	283.23	0.00	283.22	0.00
283.23	283.21	374.35	283.23	0.00	283.22	0.00
287.42	287.42	476.78	287.43	-0.01	287.43	-0.01
287.44	287.44	477.35	287.45	-0.01	287.45	-0.01
288.30	288.28	502.07	288.29	0.01	288.29	0.01
293.28	293.28	678.37	293.28	0.00	293.28	0.00
293.29	293.28	678.37	293.28	0.01	293.28	0.01
293.29	293.28	678.37	293.28	0.01	293.28	0.01
298.21	298.22	901.65	298.21	-0.01	298.21	-0.01
298.29	298.31	906.18	298.30	-0.01	298.30	-0.01
298.30	298.32	906.68	298.31	-0.01	298.31	-0.01
303.20	303.21	1176.75	303.19	0.00	303.19	0.00
303.20	303.22	1177.35	303.20	0.00	303.20	-0.01
303.21	303.23	1177.96	303.21	-0.01	303.21	-0.01
308.20	308.22	1503.05	308.20	0.00	308.20	0.00
308.20	308.22	1503.05	308.20	0.01	308.20	0.01
308.20	308.22	1503.05	308.20	0.01	308.20	0.01
313.21	313.25	1881.16	313.22	-0.01	313.22	-0.01
313.21	313.25	1881.16	313.22	-0.01	313.22	-0.01
313.22	313.25	1881.16	313.22	0.00	313.22	0.00
318.22	318.26	2308.06	318.22	0.00	318.22	0.00
318.23	318.26	2308.06	318.22	0.00	318.22	0.00
323.23	323.27	2785.16	323.22	0.00	323.22	0.00
323.23	323.28	2786.17	323.23	0.00	323.23	0.00
328.24	328.29	3313.57	328.24	0.00	328.24	0.00
328.24	328.29	3313.57	328.24	0.00	328.24	0.00
333.23	333.30	3891.17	333.24	0.00	333.24	0.00
333.26	333.32	3893.58	333.26	0.01	333.26	0.00
338.25	338.32	4520.28	338.25	0.00	338.25	0.00
338.26	338.33	4521.58	338.26	0.00	338.26	0.00
343.27	343.35	5201.19	343.27	0.00	343.27	0.00
343.28	343.35	5201.19	343.27	0.00	343.27	0.00
348.27	348.35	5928.19	348.27	0.00	348.27	0.00
348.29	348.37	5931.20	348.29	0.00	348.29	0.00
348.30	348.38	5932.70	348.30	0.01	348.30	0.01
353.28	353.37	6708.40	353.28	0.00	353.28	0.00
353.29	353.38	6710.00	353.29	0.00	353.29	0.00
358.27	358.37	7535.60	358.27	-0.01	358.27	-0.01
358.29	358.39	7539.01	358.29	0.00	358.29	0.00
363.25	363.36	8410.99	363.26	0.00	363.25	0.00
363.28	363.39	8416.41	363.29	0.00	363.28	0.00
363.30	363.40	8417.31	363.29	0.01	363.29	0.01

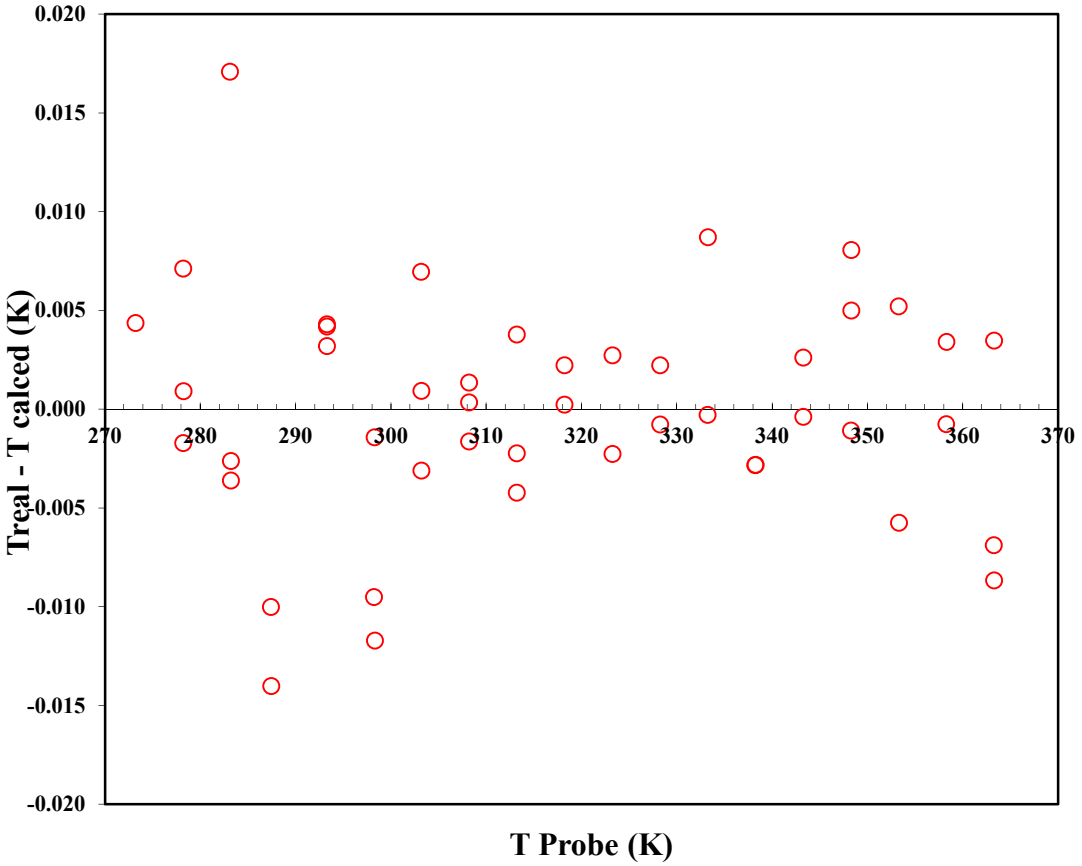

Figure 5. 9 Temperature probe inside densimeter

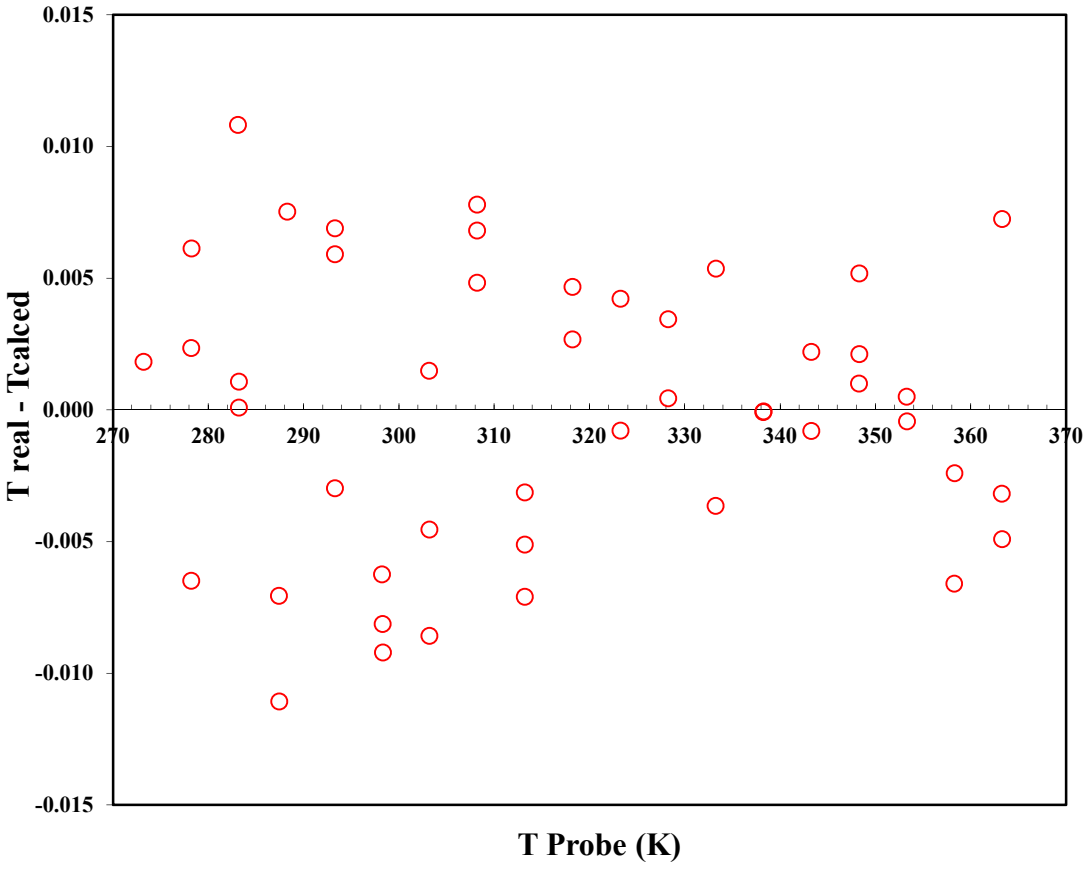

Figure 5. 10 Temperature probe of the bath

The Calibration method for the vibrating tube densitometers using a forced path mechanical calibration (FPMC) model for the Anton Parr DMA 512 densitometer were well described by Bouchot and Richon [12]. The U-tube of the DMA 512 densimeter cell can be modelled by means of a linear hollow vibrating system whose internal volume is $V_i = V_i(T,P)$ and total vibrating mass is $(M_0+\rho V_i)$. M_0 is the proper mass of the tube under vacuum and ρ the density of the inner fluid to be determined. This system has a natural transversal stiffness K = K (T, P) and is vibrating with a period (τ) in an undamped harmonic way under the effect of a mechanical excitation.

The relation between these quantities can be written in the following general form:

$$\rho = \left(\frac{M_0}{V_i}\right)\left(\left(\frac{K}{K_0}\right)\left[\frac{\tau^2}{\tau_o^2}\right]-1\right) \tag{5-1}$$

where K_0 and τ_0 are the transversal stiffness and the vibrating period of the evacuated tube, respectively.

The term K/K_0 is calculated as:

$$\frac{K}{K_0} = \frac{I}{I_0}\left(\frac{L_0}{L}\right)^3 \tag{5-2}$$

The first term in the equation above is expressed as:

$$\frac{I}{I_0} = \frac{\Delta r^4}{\Delta r_0^4} = \frac{r_e^4 - r_i^4}{r_{e0}^4 - r_{i0}^4} \tag{5-3}$$

The second term of the equation is the relative inverse cubic length change expressed by:

$$\left(\frac{L_0}{L}\right)^3 = \exp\left(-3\gamma_T P\right) \tag{5-4}$$

γ_T is one of the two unknown parameters that remain in the FPMC model.

The term (M_0/V_i) can be expressed as:

$$\frac{M_0}{V_i(T,P)} = \frac{M_0}{\pi r_i^2 L} = \frac{M_0}{L_{00}}\left(\frac{1}{\pi r_i^2 \delta L}\right) \tag{5-5}$$

where (M_0/L_{00}) is the second unknown parameter of these equations.

The complete FPMC model can be formulated as:

$$\rho(T,P) = \frac{M_0}{L_{00}}\left(\frac{1}{\pi r_i^2(T,P)\delta L(T,P)}\right)\left\{\left(\frac{\Delta r^4(T,P)}{\Delta r_0^4(T)}\right)\exp\left(-3\gamma_T P\right)\left[\frac{\tau^2(T,P)}{\tau_o^2(T)}\right]-1\right\} \tag{5-6}$$

The two unknown parameters of γ_T and (M_0/L_{00}) were optimised using the density data of pure CO_2 from REFPROP v8.0 [23] at the fully across desired pressure ranges and at each measured isotherms.

5.3.5 Measurement procedure

All the experiments were conducted using the Anton Paar DMA 512 densitometer. Before starting the main tests, the pressure transducers and the temperature probes were calibrated against a dead weight pressure balance and reference thermometer, respectively. Then, after stabilising the desired temperature the entire system was vacuumed. The vacuumed vibrating period, vacuum pressure and temperature then were recorded at desired temperatures of 273.15, 283.15, 298.15, 323.15 and 353.15 K.

In each test, after temperature stabilisation and vacuuming the entire system, the sample was injected through the pressurised vessel into the densitometer as a gas phase by opening a regulated valve in a very slow rate till reaching the dew point pressure at desired temperature. For measuring the density in the liquid phase, the pressure was increased to the maximum desired pressure, i.e., 40 MPa, then the pressure reduced slowly by opening the outlet valve till reaching the bubble point. The toxic outlet gas during the depressurisation was neutralised in the column containing the basic solution (Sodium Hydroxide, NaOH). During the injection and depressurisation, pressure, temperature and period were recorded to be able to calculate the density. Also, to find dew point of the system during the injection of the sample, as the first bubble should be produced inside the densitometer, the temperature of the bath controlling the densitometer temperature were set to be slightly lower (0.2-0.3 K) than the temperature of the liquid bath for the entire system. However, to find the bubble point, the densitometer temperature was set to be slightly higher than the entire system temperature.

5.3.6 Measurement uncertainties

The combined uncertainties of the measured densities were calculated according to the procedure explained in chapter 3.

5.4 Specific heat capacity calculations

The residual specific heat capacity can be calculated using the data from density measurements by the following procedure:

$$\left(\frac{\partial C_p}{\partial P}\right)_T = -T\left(\frac{\partial^2 \nu}{\partial T^2}\right)_P \tag{5-7}$$

The molar volume is a polynomial function of temperature at each constant pressure:

$$\nu = aT^2 + bT + c \tag{5-8}$$

Or,

$$\frac{\partial \nu}{\partial T} = 2aT + b \quad \rightarrow \quad \frac{\partial^2 \nu}{\partial T^2} = 2a \tag{5-9}$$

By replacing Eq. (5-9) in Eq. (5-7) and integrating, the specific heat capacity can be calculated from the following equation:

$$\left(\frac{\partial C_p}{\partial P}\right)_T = -T\left(\frac{\partial^2 \nu}{\partial T^2}\right)_P = -2aT \xrightarrow{\int} \int_{C_{pi}}^{C_p} dC_p = -2aT \int_{P=0}^{P} dP \tag{5-10}$$
$$C_p - C_{pi} = -2aT(P) + C$$

The constant C can be calculated from the reference fluid experiments, i.e. pure CO_2, by the following equations:

$$\left(\frac{\partial C_p}{\partial P}\right)_T = -T\left(\frac{\partial^2 \nu}{\partial T^2}\right)_P = -2aT \xrightarrow{\int} \int_{C_{pi}}^{C_p} dC_p = -2aT \int_{P=0}^{P} dP \tag{5-11}$$
$$C_p - C_{pi} = -2aT(P) + C \Rightarrow C = C_{p(REF)} - (C_{pi} + (-2aTP))$$

Where C_{pi} is the ideal gas specific heat capacity and can be calculated from the equation presented by Aly and Lee (1981) [24]:

$$C_{pi} = B + C\left[\frac{D/T}{sinh(D/T)}\right]^2 + E\left[\frac{F/T}{\cosh(F/T)}\right]^2 \tag{5-12}$$

The constants B through F in this equation can be found from Table below for the pure components CO_2, H_2S and SO_2.

Table 5.7 Constants B through F in the equation by Aly and Lee

C_{pi} constants	B	C	D	E	F	Unit
CO_2	2.94E+04	3.45E+04	-1.43E+03	2.64E+04	5.88E+02	J/Kmol.K
H_2S	3.33E+04	2.61E+04	9.13E+02	-1.80E+04	9.49E+02	J/Kmol.K

SO_2	3.34E+04	2.59E+04	9.33E+02	1.09E+04	4.24E+02	J/Kmol.K

The ideal gas heat capacity for the mixtures can be calculated using the following mixing rule:

$$C_{pi-Mix} = \sum_{i=1}^{N} y_i C_{pi} \qquad (5\text{-}13)$$

5.5 Results and discussions

The densities of CO_2-rich systems were measured continuously using a high temperature and pressure Vibrating Tube Densitometer (VTD), Anton Paar DMA 512. First, pure CO_2 were used to calibrate the densitometer. Then, the densities of two binary systems (95.05 mol% CO_2 + 4.95 mol% H_2S; and 95.03 mol% CO_2 + 4.97 mol% SO_2) were measured at pressures up to 40 MPa at five different temperatures, 273.15, 283.15, 298.15, 323.15 and 353.15 K (0, 10, 25, 50 and 80 °C) in gas, liquid and supercritical regions. The experimental data then were used to evaluate the new CO_2 volume correction model by comparing to the original PR and PR-Peneloux equations of states.

Both experimental and modelling results, using the CO_2 correction volume, Peneloux shift parameter and original equation of state (PR), are shown in Table 5.8 to Table 5.17. Also, Figure 5.11 to Figure 5.14 show the results for CO_2+H_2S and CO_2+SO_2 systems at all the measured temperatures. In each table, the measured density is shown on the corresponding pressure, temperature and phase. Also, the calculated density using CO_2 correction volume, Peneloux shift parameter and original equation of state (PR) and their deviations from experimental density for each measurement are presented in these tables. In addition the Absolute Average Deviations (AADs) for all data are listed in the tables. Table 5.18 summarises the AAD for the measured systems. As can be seen, by employing the CO_2 volume correction using the PR EoS, the AAD reduces for both the CO_2+H_2S and CO_2+SO_2 systems. Also, it can be seen that CO_2 volume correction predicts well comparing to Peneloux shift parameters for both mixtures.

The specific heat capacities were calculated using Equations (5-7) through (5-13) at different pressures of 40, 35, 30, 25, 20 and 15 MPa at five measured temperatures. Table 5.19 and Table 5.20 and Figure 5.15 and Figure 5.16 show the calculated specific heat capacity for CO_2 + H_2S and CO_2 + SO_2 systems, respectively.

The numerous data points were measured on both parts of the dew and bubble points at each temperature. Analysis of the measured data points can be used in determination of the break points, which correspond to dew and bubble point of the mixtures at measured temperatures. The importance of the large number of recorded data points is that it allows fitting the representative correlation to the experimental data in order to find the precise location of dew and bubble points. Table 5.20 and Table 5.21 show the calculated dew and bubble points for CO_2 + H_2S and CO_2 + SO_2 systems.

5.6 Conclusions

Evaluation of the new volume correction model based on EoSs using our in-house software package and the measured experimental data for CO_2+H_2S and CO_2+SO_2 show that the model predictions are in good agreement with the experimental data.

In addition the specific heat capacities of the systems were calculated from the measured density data at different pressures and temperatures using a thermodynamic equation.

Analysis of the numerous measured density data on both sides of dew and bubble points resulted in determination of the break points which correspond to dew and bubble points of the mixtures at measured temperatures. Dew and bubble points for CO_2 + H_2S and CO_2 + SO_2 systems were obtained from the measured density data for each system and then compared to the predictions from our software package. The comparison shows that the model predictions are in good agreements with the measured dew and bubble points.

Table 5.8 Experimental and modelling results for CO_2 + H_2S at 0 °C (273.15 K)

No	Phase	Temp.	Press.	Density (kg/m^3)						Abs Deviation (%)		
		K (±0.02)	MPa (±0.005)	Exp.	$u_c(\rho)$ kg/m^3	$u_c(\rho)$ %	PR-CO_2	PR	PR-Pen	PR-CO_2	PR	PR-Pen
1	Gas	272.55	0.100	1.9	0.07	3.68	1.9	1.9	1.9	2.4	2.4	2.3
2	Gas	272.55	0.151	2.8	0.10	3.62	2.9	2.9	2.9	4.3	4.2	4.2
3	Gas	272.55	0.205	4.0	0.10	2.58	4.0	4.0	4.0	0.4	0.4	0.4
4	Gas	272.55	0.301	5.9	0.10	1.76	5.9	5.9	5.9	0.3	0.4	0.4
5	Gas	272.55	0.402	8.0	0.11	1.33	8.0	8.0	8.0	0.1	0.0	0.0
6	Gas	272.55	0.501	9.9	0.11	1.09	10.0	10.0	10.0	0.7	0.7	0.6
7	Gas	272.54	0.603	12.1	0.11	0.90	12.1	12.1	12.1	0.4	0.4	0.3
8	Gas	272.54	0.892	18.5	0.12	0.62	18.4	18.4	18.3	0.5	0.6	0.7
9	Gas	272.54	1.006	20.9	0.12	0.56	20.9	20.9	20.9	0.1	0.2	0.3
10	Gas	272.56	1.104	23.0	0.12	0.52	23.1	23.1	23.1	0.5	0.5	0.4
11	Gas	272.56	1.296	27.7	0.12	0.45	27.6	27.6	27.6	0.0	0.1	0.3
12	Gas	272.56	1.499	32.4	0.13	0.40	32.6	32.6	32.5	0.5	0.4	0.2
13	Gas	272.55	1.696	37.5	0.14	0.36	37.6	37.5	37.5	0.2	0.1	0.0
14	Gas	272.56	1.905	42.8	0.14	0.34	43.1	43.1	43.0	0.7	0.6	0.4
15	Gas	272.56	2.003	45.2	0.15	0.33	45.8	45.8	45.7	1.3	1.2	1.0
16	Gas	272.56	2.205	51.1	0.16	0.31	51.6	51.5	51.4	1.0	0.8	0.6
17	Gas	272.56	2.407	56.8	0.17	0.29	57.7	57.6	57.5	1.6	1.4	1.2
18	Gas	272.56	2.502	59.8	0.17	0.29	60.7	60.6	60.4	1.4	1.3	1.0
19	Gas	272.55	2.709	66.4	0.19	0.28	67.5	67.4	67.2	1.6	1.5	1.2
20	Gas	272.56	2.906	73.0	0.20	0.28	74.4	74.3	74.0	1.9	1.7	1.4
21	Gas	272.55	2.996	76.3	0.21	0.28	77.7	77.6	77.4	1.9	1.7	1.4
22	Gas	272.55	3.196	83.9	0.24	0.28	85.6	85.5	85.1	2.0	1.9	1.5
23	Gas	272.55	3.402	92.7	0.38	0.41	94.4	94.3	93.9	1.8	1.7	1.3
24	Liquid	272.57	41.417	1058.1	0.22	0.02	1078.2	1134.2	1079.9	1.9	7.2	2.1
25	Liquid	272.58	41.400	1058.2	0.12	0.01	1078.2	1134.1	1079.8	1.9	7.2	2.0
26	Liquid	272.57	40.955	1057.0	0.22	0.02	1077.1	1132.7	1078.6	1.9	7.2	2.0
27	Liquid	272.57	40.046	1054.9	0.22	0.02	1074.9	1129.9	1076.0	1.9	7.1	2.0
28	Liquid	272.58	39.463	1053.2	0.22	0.02	1073.5	1128.0	1074.2	1.9	7.1	2.0
29	Liquid	272.57	39.008	1052.0	0.22	0.02	1072.3	1126.6	1072.9	1.9	7.1	2.0
30	Liquid	272.56	38.445	1050.7	0.22	0.02	1070.9	1124.7	1071.3	1.9	7.0	2.0
31	Liquid	272.56	38.049	1049.5	0.22	0.02	1069.9	1123.4	1070.2	1.9	7.0	2.0
32	Liquid	272.56	37.557	1048.1	0.22	0.02	1068.7	1121.8	1068.6	2.0	7.0	2.0
33	Liquid	272.56	36.988	1046.6	0.22	0.02	1067.2	1119.8	1066.9	2.0	7.0	1.9
34	Liquid	272.56	36.561	1045.5	0.22	0.02	1066.1	1118.4	1065.6	2.0	7.0	1.9
35	Liquid	272.57	36.058	1044.1	0.22	0.02	1064.8	1116.6	1064.0	2.0	7.0	1.9
36	Liquid	272.57	35.493	1042.3	0.32	0.03	1063.3	1114.7	1062.2	2.0	6.9	1.9
37	Liquid	272.56	35.060	1041.1	0.32	0.03	1062.1	1113.2	1060.8	2.0	6.9	1.9
38	Liquid	272.57	34.499	1039.5	0.22	0.02	1060.6	1111.1	1059.0	2.0	6.9	1.9
39	Liquid	272.57	33.999	1038.0	0.22	0.02	1059.3	1109.3	1057.4	2.1	6.9	1.9
40	Liquid	272.57	33.498	1036.6	0.32	0.03	1057.9	1107.5	1055.7	2.1	6.8	1.8
41	Liquid	272.58	33.011	1034.9	0.22	0.02	1056.5	1105.7	1054.0	2.1	6.8	1.8
42	Liquid	272.57	32.499	1033.1	0.22	0.02	1055.1	1103.8	1052.3	2.1	6.8	1.9
43	Liquid	272.58	31.936	1031.5	0.22	0.02	1053.5	1101.6	1050.4	2.1	6.8	1.8
44	Liquid	272.58	31.446	1030.1	0.32	0.03	1052.1	1099.7	1048.7	2.1	6.8	1.8
45	Liquid	272.57	31.002	1028.8	0.22	0.02	1050.8	1098.0	1047.1	2.1	6.7	1.8
46	Liquid	272.57	30.442	1027.2	0.22	0.02	1049.2	1095.9	1045.1	2.1	6.7	1.7
47	Liquid	272.57	30.022	1025.6	0.22	0.02	1048.0	1094.2	1043.6	2.2	6.7	1.8
48	Liquid	272.58	29.540	1023.9	0.22	0.02	1046.5	1092.2	1041.8	2.2	6.7	1.7
49	Liquid	272.58	29.015	1022.3	0.22	0.02	1044.9	1090.1	1039.9	2.2	6.6	1.7
50	Liquid	272.58	28.510	1020.5	0.22	0.02	1043.4	1088.0	1037.9	2.2	6.6	1.7
51	Liquid	272.58	28.014	1018.9	0.22	0.02	1041.9	1085.9	1036.0	2.3	6.6	1.7

No	Phase	Temp.	Press.	Density (kg/m^3)						Abs Deviation (%)		
		K (±0.02)	MPa (±0.005)	Exp.	$u_c(\rho)$ kg/m^3	$u_c(\rho)$ %	PR-CO_2	PR	PR-Pen	PR-CO_2	PR	PR-Pen
52	Liquid	272.58	27.519	1017.1	0.22	0.02	1040.3	1083.8	1034.2	2.3	6.6	1.7
53	Liquid	272.59	26.955	1015.2	0.22	0.02	1038.6	1081.3	1031.9	2.3	6.5	1.6
54	Liquid	272.59	26.517	1013.8	0.32	0.03	1037.2	1079.5	1030.2	2.3	6.5	1.6
55	Liquid	272.58	26.025	1012.1	0.27	0.03	1035.6	1077.3	1028.2	2.3	6.4	1.6
56	Liquid	272.58	25.470	1010.3	0.32	0.03	1033.8	1074.8	1025.9	2.3	6.4	1.5
57	Liquid	272.58	24.975	1008.5	0.32	0.03	1032.2	1072.5	1023.9	2.3	6.4	1.5
58	Liquid	272.58	24.527	1006.9	0.22	0.02	1030.7	1070.5	1022.0	2.4	6.3	1.5
59	Liquid	272.58	23.985	1004.9	0.22	0.02	1028.9	1067.9	1019.7	2.4	6.3	1.5
60	Liquid	272.58	23.514	1003.2	0.22	0.02	1027.2	1065.7	1017.6	2.4	6.2	1.4
61	Liquid	272.58	23.027	1001.3	0.32	0.03	1025.5	1063.4	1015.5	2.4	6.2	1.4
62	Liquid	272.58	22.532	999.5	0.32	0.03	1023.8	1060.9	1013.3	2.4	6.2	1.4
63	Liquid	272.58	22.003	997.4	0.22	0.02	1022.0	1058.3	1010.9	2.5	6.1	1.3
64	Liquid	272.58	21.490	995.3	0.32	0.03	1020.1	1055.7	1008.5	2.5	6.1	1.3
65	Liquid	272.58	20.990	993.2	0.32	0.03	1018.3	1053.1	1006.1	2.5	6.0	1.3
66	Liquid	272.58	20.515	991.4	0.32	0.03	1016.5	1050.6	1003.9	2.5	6.0	1.3
67	Liquid	272.58	20.011	989.1	0.32	0.03	1014.6	1047.9	1001.4	2.6	5.9	1.2
68	Liquid	272.58	19.576	987.6	0.32	0.03	1013.0	1045.6	999.3	2.6	5.9	1.2
69	Liquid	272.58	19.012	985.2	0.27	0.03	1010.8	1042.4	996.4	2.6	5.8	1.1
70	Liquid	272.58	18.540	983.3	0.32	0.03	1009.0	1039.8	994.0	2.6	5.7	1.1
71	Liquid	272.58	18.046	981.3	0.32	0.03	1007.0	1036.9	991.4	2.6	5.7	1.0
72	Liquid	272.57	17.556	979.1	0.27	0.03	1005.0	1034.2	988.8	2.7	5.6	1.0
73	Liquid	272.57	17.016	976.8	0.27	0.03	1002.8	1030.9	985.9	2.7	5.5	0.9
74	Liquid	272.58	16.524	974.5	0.31	0.03	1000.7	1027.9	983.1	2.7	5.5	0.9
75	Liquid	272.58	16.022	972.1	0.31	0.03	998.6	1024.8	980.2	2.7	5.4	0.8
76	Liquid	272.58	15.502	969.5	0.32	0.03	996.3	1021.5	977.2	2.8	5.4	0.8
77	Liquid	272.58	15.013	967.1	0.32	0.03	994.2	1018.3	974.3	2.8	5.3	0.7
78	Liquid	272.59	14.525	964.4	0.32	0.03	991.9	1015.0	971.3	2.8	5.2	0.7
79	Liquid	272.58	14.024	962.0	0.33	0.03	989.6	1011.7	968.3	2.9	5.2	0.7
80	Liquid	272.59	13.502	959.4	0.33	0.03	987.2	1008.1	964.9	2.9	5.1	0.6
81	Liquid	272.58	13.010	956.8	0.34	0.04	984.9	1004.6	961.8	2.9	5.0	0.5
82	Liquid	272.58	12.531	954.3	0.34	0.04	982.5	1001.1	958.6	3.0	4.9	0.4
83	Liquid	272.59	11.999	951.2	0.34	0.04	979.8	997.1	954.9	3.0	4.8	0.4
84	Liquid	272.59	11.511	948.4	0.36	0.04	977.3	993.4	951.5	3.1	4.7	0.3
85	Liquid	272.59	11.005	945.1	0.36	0.04	974.7	989.4	947.8	3.1	4.7	0.3
86	Liquid	272.59	10.504	942.3	0.37	0.04	972.0	985.3	944.1	3.1	4.6	0.2
87	Liquid	272.59	10.064	939.4	0.37	0.04	969.6	981.7	940.8	3.2	4.5	0.1
88	Liquid	272.60	9.499	936.2	0.29	0.03	966.4	976.8	936.3	3.2	4.3	0.0
89	Liquid	273.23	8.730	929.2	0.30	0.03	958.7	965.8	926.2	3.2	3.9	0.3
90	Liquid	273.29	8.504	926.7	0.30	0.03	957.0	963.3	923.8	3.3	3.9	0.3
91	Liquid	273.30	7.996	922.9	0.31	0.03	953.8	958.4	919.3	3.3	3.8	0.4
92	Liquid	273.31	7.524	919.4	0.31	0.03	950.7	953.6	914.9	3.4	3.7	0.5
93	Liquid	273.31	7.043	915.9	0.32	0.04	947.5	948.6	910.3	3.4	3.6	0.6
94	Liquid	273.31	6.504	911.6	0.33	0.04	943.8	942.8	905.0	3.5	3.4	0.7
95	Liquid	273.32	5.999	907.1	0.34	0.04	940.1	937.1	899.7	3.6	3.3	0.8
96	Liquid	273.31	5.510	902.8	0.34	0.04	936.5	931.4	894.5	3.7	3.2	0.9
97	Liquid	273.34	5.004	897.4	0.36	0.04	932.4	925.0	888.6	3.9	3.1	1.0
98	Liquid	273.33	4.504	892.6	0.37	0.04	928.5	918.6	882.7	4.0	2.9	1.1
Absolute Average Deviation (AAD)										**2.2**	**4.7**	**1.2**

Table 5.9 Experimental and modelling results for CO_2 + H_2S at 10 °C (283.15 K)

No	Phase	Temp.	Press.	Density (kg/m^3)						Abs Deviation (%)		
		K (±0.02)	MPa (±0.005)	Exp. ±0.05%	$u_c(\rho)$ kg/m^3	$u_c(\rho)$ %	PR-CO_2	PR	PR Pen	PR-CO_2	PR	PR Pen
1	Gas	282.69	0.600	11.8	0.11	0.89	11.5	11.6	11.6	2.3	2.0	2.1
2	Gas	282.70	0.820	16.6	0.11	0.65	16.0	16.1	16.0	3.7	3.3	3.4
3	Gas	282.70	1.004	20.1	0.11	0.56	19.8	19.9	19.9	1.5	1.0	1.1
4	Gas	282.70	1.194	25.0	0.12	0.46	23.9	24.0	24.0	4.5	4.0	4.1
5	Gas	282.69	1.405	29.0	0.12	0.41	28.6	28.8	28.7	1.4	0.7	0.9
6	Gas	282.70	1.631	35.0	0.13	0.36	34.0	34.0	34.0	2.8	2.7	2.9
7	Gas	282.69	1.794	39.0	0.13	0.33	37.8	38.0	37.9	3.1	2.7	2.8
8	Gas	282.70	2.040	45.1	0.14	0.30	44.4	44.1	44.0	1.8	2.3	2.5
9	Gas	282.71	2.196	49.1	0.14	0.29	48.4	48.2	48.1	1.3	1.9	2.1
10	Gas	282.70	2.423	55.3	0.15	0.27	54.6	54.3	54.2	1.1	1.7	1.9
11	Gas	282.71	2.634	61.3	0.16	0.26	60.7	60.4	60.2	0.9	1.5	1.8
12	Gas	282.71	2.835	67.2	0.17	0.25	66.8	66.4	66.2	0.6	1.2	1.5
13	Gas	282.71	3.018	72.9	0.18	0.24	72.6	72.2	71.9	0.4	1.0	1.3
14	Gas	282.71	3.243	80.2	0.19	0.24	80.2	79.7	79.4	0.1	0.7	1.0
15	Gas	282.70	3.401	85.8	0.21	0.24	85.8	85.3	85.0	0.1	0.6	0.9
16	Gas	282.71	3.592	92.8	0.22	0.24	93.1	92.5	92.1	0.3	0.3	0.7
17	Gas	282.71	3.803	101.2	0.25	0.25	101.7	101.1	100.6	0.5	0.1	0.5
18	Gas	282.72	4.012	110.3	0.28	0.26	111.1	110.4	109.9	0.7	0.1	0.4
19	Gas	282.72	4.099	114.3	0.29	0.26	115.3	114.6	114.0	0.9	0.2	0.3
20	Gas	282.71	4.201	119.4	0.32	0.27	120.5	119.7	119.1	0.9	0.2	0.3
21	Gas	282.70	4.303	125.3	0.35	0.28	126.0	125.2	124.5	0.6	0.1	0.6
22	Gas	282.73	4.361	133.9	0.45	0.34	129.3	128.4	127.7	3.4	4.1	4.6
23	Liquid	283.47	40.443	1041.5	0.22	0.02	1043.7	1094.3	1043.6	0.2	5.1	0.2
24	Liquid	283.47	40.004	1040.3	0.22	0.02	1042.5	1092.6	1042.2	0.2	5.0	0.2
25	Liquid	283.47	39.503	1038.9	0.22	0.02	1041.1	1090.8	1040.5	0.2	5.0	0.1
26	Liquid	283.46	39.000	1037.5	0.22	0.02	1039.7	1089.0	1038.8	0.2	5.0	0.1
27	Liquid	283.47	38.528	1036.2	0.22	0.02	1038.4	1087.1	1037.2	0.2	4.9	0.1
28	Liquid	283.46	38.004	1034.6	0.22	0.02	1036.9	1085.2	1035.4	0.2	4.9	0.1
29	Liquid	283.47	37.525	1033.1	0.22	0.02	1035.5	1083.3	1033.6	0.2	4.9	0.1
30	Liquid	283.47	37.000	1031.5	0.32	0.03	1033.9	1081.2	1031.8	0.2	4.8	0.0
31	Liquid	283.46	36.513	1030.0	0.22	0.02	1032.6	1079.3	1030.1	0.2	4.8	0.0
32	Liquid	283.47	36.014	1028.3	0.22	0.02	1031.0	1077.3	1028.2	0.3	4.8	0.0
33	Liquid	283.46	35.507	1026.8	0.22	0.02	1029.5	1075.3	1026.4	0.3	4.7	0.0
34	Liquid	283.46	35.004	1025.2	0.22	0.02	1028.0	1073.2	1024.5	0.3	4.7	0.1
35	Liquid	283.46	34.516	1023.7	0.22	0.02	1026.5	1071.2	1022.6	0.3	4.6	0.1
36	Liquid	283.47	34.012	1022.0	0.22	0.02	1024.9	1069.0	1020.7	0.3	4.6	0.1
37	Liquid	283.47	33.525	1020.3	0.22	0.02	1023.4	1067.0	1018.8	0.3	4.6	0.2
38	Liquid	283.47	33.004	1018.6	0.22	0.02	1021.8	1064.7	1016.7	0.3	4.5	0.2
39	Liquid	283.47	32.470	1017.0	0.22	0.02	1020.1	1062.4	1014.6	0.3	4.5	0.2
40	Liquid	283.46	32.001	1015.4	0.22	0.02	1018.5	1060.3	1012.8	0.3	4.4	0.3
41	Liquid	283.46	31.532	1013.7	0.22	0.02	1017.0	1058.2	1010.8	0.3	4.4	0.3
42	Liquid	283.46	31.005	1011.9	0.32	0.03	1015.3	1055.8	1008.6	0.3	4.3	0.3
43	Liquid	283.47	30.502	1010.1	0.22	0.02	1013.5	1053.4	1006.4	0.3	4.3	0.4
44	Liquid	283.47	30.014	1008.2	0.22	0.02	1011.9	1051.2	1004.4	0.4	4.3	0.4
45	Liquid	283.46	29.517	1006.4	0.22	0.02	1010.2	1048.8	1002.3	0.4	4.2	0.4
46	Liquid	283.47	29.025	1004.6	0.22	0.02	1008.5	1046.4	1000.0	0.4	4.2	0.5
47	Liquid	283.47	28.508	1002.7	0.22	0.02	1006.7	1043.9	997.7	0.4	4.1	0.5
48	Liquid	283.48	28.010	1000.7	0.27	0.03	1004.8	1041.4	995.4	0.4	4.1	0.5
49	Liquid	283.47	27.510	998.9	0.27	0.03	1003.0	1038.9	993.2	0.4	4.0	0.6
50	Liquid	283.47	27.006	996.9	0.27	0.03	1001.2	1036.3	990.8	0.4	4.0	0.6

No	Phase	Temp.	Press.	Density (kg/m^3)						Abs Deviation (%)		
		K (±0.02)	MPa (±0.005)	Exp. ±0.05%	$u_c(\rho)$ kg/m^3	$u_c(\rho)$ %	PR-CO_2	PR	PR Pen	PR-CO_2	PR	PR Pen
51	Liquid	283.46	26.500	994.9	0.28	0.03	999.3	1033.7	988.4	0.4	3.9	0.7
52	Liquid	283.47	26.012	993.0	0.28	0.03	997.5	1031.1	986.0	0.5	3.8	0.7
53	Liquid	283.47	25.518	991.0	0.28	0.03	995.6	1028.4	983.6	0.5	3.8	0.8
54	Liquid	283.47	25.000	988.9	0.29	0.03	993.6	1025.5	981.0	0.5	3.7	0.8
55	Liquid	283.47	24.503	986.9	0.29	0.03	991.6	1022.8	978.4	0.5	3.6	0.9
56	Liquid	283.47	24.005	984.8	0.29	0.03	989.6	1020.0	975.8	0.5	3.6	0.9
57	Liquid	283.47	23.501	982.6	0.29	0.03	987.6	1017.1	973.2	0.5	3.5	1.0
58	Liquid	283.47	23.016	980.5	0.30	0.03	985.6	1014.2	970.6	0.5	3.4	1.0
59	Liquid	283.47	22.501	978.3	0.30	0.03	983.4	1011.1	967.8	0.5	3.4	1.1
60	Liquid	283.47	22.004	976.1	0.30	0.03	981.2	1008.1	965.0	0.5	3.3	1.1
61	Liquid	283.47	21.510	973.8	0.31	0.03	979.1	1005.0	962.1	0.5	3.2	1.2
62	Liquid	283.47	21.001	971.5	0.31	0.03	976.8	1001.8	959.2	0.5	3.1	1.3
63	Liquid	283.47	20.508	969.2	0.31	0.03	974.6	998.6	956.3	0.6	3.0	1.3
64	Liquid	283.47	20.010	966.8	0.32	0.03	972.4	995.3	953.2	0.6	2.9	1.4
65	Liquid	283.47	19.503	964.5	0.32	0.03	970.0	991.9	950.1	0.6	2.8	1.5
66	Liquid	283.47	19.008	962.0	0.32	0.03	967.6	988.4	947.0	0.6	2.7	1.6
67	Liquid	283.47	18.516	959.4	0.33	0.03	965.2	985.0	943.8	0.6	2.7	1.6
68	Liquid	283.47	18.016	957.0	0.34	0.04	962.7	981.4	940.5	0.6	2.5	1.7
69	Liquid	283.47	17.517	954.5	0.34	0.04	960.2	977.7	937.1	0.6	2.4	1.8
70	Liquid	283.47	17.011	951.8	0.35	0.04	957.6	973.8	933.5	0.6	2.3	1.9
71	Liquid	283.47	16.506	949.0	0.35	0.04	955.0	969.9	929.9	0.6	2.2	2.0
72	Liquid	283.48	16.008	946.2	0.36	0.04	952.2	965.9	926.2	0.6	2.1	2.1
73	Liquid	283.47	15.509	943.3	0.36	0.04	949.5	961.9	922.6	0.7	2.0	2.2
74	Liquid	283.47	15.004	940.4	0.37	0.04	946.6	957.7	918.7	0.7	1.8	2.3
75	Liquid	283.48	14.511	937.3	0.37	0.04	943.7	953.3	914.7	0.7	1.7	2.4
76	Liquid	283.47	14.002	934.4	0.38	0.04	940.7	948.9	910.6	0.7	1.5	2.6
77	Liquid	283.47	13.504	931.2	0.39	0.04	937.6	944.3	906.4	0.7	1.4	2.7
78	Liquid	283.47	13.000	928.0	0.39	0.04	934.5	939.6	902.0	0.7	1.2	2.8
79	Liquid	283.47	12.500	924.7	0.41	0.04	931.2	934.7	897.5	0.7	1.1	2.9
80	Liquid	283.48	12.002	921.3	0.42	0.05	927.8	929.6	892.8	0.7	0.9	3.1
81	Liquid	283.48	11.502	917.6	0.43	0.05	924.4	924.4	888.0	0.7	0.7	3.2
82	Liquid	283.49	11.002	914.1	0.43	0.05	920.7	918.9	882.9	0.7	0.5	3.4
83	Liquid	283.48	10.503	910.4	0.45	0.05	917.1	913.4	877.8	0.7	0.3	3.6
84	Liquid	283.48	10.062	907.0	0.46	0.05	913.7	908.2	873.1	0.7	0.1	3.7
85	Liquid	283.49	9.506	903.0	0.47	0.05	909.2	901.4	866.7	0.7	0.2	4.0
86	Liquid	283.49	9.003	898.8	0.49	0.05	905.0	894.9	860.8	0.7	0.4	4.2
87	Liquid	283.49	8.504	894.3	0.50	0.06	900.7	888.2	854.6	0.7	0.7	4.4
88	Liquid	283.49	8.001	889.8	0.52	0.06	896.1	881.2	848.0	0.7	1.0	4.7
89	Liquid	283.49	7.466	884.7	0.54	0.06	891.0	873.2	840.7	0.7	1.3	5.0
90	Liquid	283.49	7.137	882.0	0.56	0.06	887.7	868.1	835.9	0.6	1.6	5.2
91	Liquid	283.48	6.383	875.9	0.60	0.07	879.7	855.5	824.2	0.4	2.3	5.9
92	Liquid	283.47	5.962	871.5	0.63	0.07	875.0	847.9	817.2	0.4	2.7	6.2
93	Liquid	283.47	5.586	867.8	0.66	0.08	870.4	840.7	810.5	0.3	3.1	6.6
94	Liquid	283.52	5.041	861.2	0.70	0.08	863.0	828.8	799.4	0.2	3.8	7.2
95	Liquid	283.57	4.945	859.9	0.71	0.08	861.4	826.1	796.9	0.2	3.9	7.3
96	Liquid	283.92	4.600	826.5	0.77	0.09	853.5	813.7	785.4	3.3	1.5	5.0
Absolute Average Deviation (AAD)										**0.7**	**2.7**	**1.8**

Table 5.10 Experimental and modelling results for CO_2 + H_2S at 25 °C (298.15 K)

No	Phase	Temp.	Press.	Density (kg/m^3)						Absolute Deviation (%)		
		K (±0.02)	MPa (±0.005)	Exp.	$u_c(\rho)$ kg/m^3	$u_c(\rho)$ %	PR-CO_2	PR	PR Pen	PR-CO_2	PR	PR Pen
1	Gas	297.50	0.030	0.5	0.02	4.40	0.5	0.5	0.5	3.1	3.1	3.1
2	Gas	297.51	0.320	5.7	0.10	1.69	5.7	5.7	5.7	0.1	0.3	0.3
3	Gas	297.51	0.652	11.8	0.10	0.85	11.9	11.9	11.9	0.2	0.6	0.5
4	Gas	297.50	0.710	13.0	0.10	0.78	13.0	13.0	13.0	0.6	0.2	0.3
5	Gas	297.50	0.878	16.3	0.10	0.64	16.2	16.3	16.2	0.9	0.4	0.5
6	Gas	297.50	1.019	19.5	0.11	0.54	18.9	19.0	19.0	2.9	2.4	2.5
7	Gas	297.51	1.232	23.7	0.11	0.46	23.2	23.3	23.3	2.3	1.7	1.8
8	Gas	297.51	1.419	27.5	0.11	0.40	27.0	27.2	27.2	1.9	1.2	1.3
9	Gas	297.51	1.601	31.3	0.11	0.37	30.8	31.1	31.0	1.5	0.8	0.9
10	Gas	297.51	1.810	35.8	0.12	0.33	35.3	35.6	35.6	1.3	0.4	0.5
11	Gas	297.51	2.003	40.0	0.12	0.31	39.6	40.0	39.9	1.1	0.1	0.3
12	Gas	297.51	2.203	44.6	0.13	0.28	44.1	44.6	44.5	1.1	0.0	0.2
13	Gas	297.51	2.413	49.5	0.13	0.26	49.0	49.6	49.5	0.9	0.3	0.0
14	Gas	297.50	2.616	54.4	0.14	0.25	54.0	54.7	54.6	0.8	0.5	0.2
15	Gas	297.50	2.810	59.4	0.14	0.24	58.8	59.7	59.5	0.9	0.5	0.2
16	Gas	297.50	2.998	64.3	0.15	0.23	63.7	64.7	64.5	0.9	0.6	0.3
17	Gas	297.50	3.212	70.1	0.16	0.22	69.5	70.6	70.4	0.8	0.8	0.5
18	Gas	297.51	3.399	75.3	0.16	0.22	74.7	76.0	75.8	0.8	0.9	0.6
19	Gas	297.50	3.611	81.5	0.17	0.21	80.9	82.4	82.1	0.7	1.1	0.7
20	Gas	297.50	3.810	87.7	0.18	0.21	87.0	88.7	88.4	0.7	1.2	0.8
21	Gas	297.51	4.001	93.7	0.19	0.21	93.2	95.1	94.7	0.6	1.4	1.0
22	Gas	297.50	4.206	100.8	0.21	0.21	100.1	102.2	101.8	0.6	1.5	1.0
23	Gas	297.51	4.402	107.8	0.22	0.21	107.1	109.5	109.0	0.6	1.6	1.1
24	Gas	297.50	4.609	115.8	0.25	0.21	115.1	117.7	117.1	0.7	1.6	1.1
25	Gas	297.51	4.802	123.7	0.26	0.21	122.9	125.9	125.2	0.6	1.8	1.2
26	Gas	297.50	4.999	132.4	0.29	0.22	131.7	134.9	134.1	0.6	1.9	1.3
27	Gas	297.50	5.204	142.4	0.33	0.23	141.5	145.1	144.2	0.6	1.9	1.3
28	Gas	297.50	5.404	153.1	0.38	0.25	152.2	156.2	155.1	0.6	2.0	1.3
29	Gas	297.50	5.604	165.3	0.45	0.27	164.3	168.6	167.4	0.6	2.0	1.2
30	Liquid	298.06	40.253	992.4	0.24	0.02	998.9	1041.6	995.6	0.7	5.0	0.3
31	Liquid	298.07	39.735	991.0	0.24	0.02	997.2	1039.3	993.5	0.6	4.9	0.3
32	Liquid	298.06	39.498	990.0	0.25	0.03	996.4	1038.3	992.6	0.6	4.9	0.3
33	Liquid	298.06	39.023	988.6	0.24	0.02	994.9	1036.1	990.6	0.6	4.8	0.2
34	Liquid	298.07	38.510	986.9	0.25	0.03	993.1	1033.7	988.5	0.6	4.7	0.2
35	Liquid	298.05	37.999	985.2	0.25	0.03	991.4	1031.5	986.4	0.6	4.7	0.1
36	Liquid	298.06	37.004	982.1	0.25	0.03	987.9	1026.7	982.0	0.6	4.5	0.0
37	Liquid	298.06	36.016	978.6	0.26	0.03	984.5	1021.9	977.7	0.6	4.4	0.1
38	Liquid	298.06	35.006	974.9	0.26	0.03	980.8	1016.9	973.1	0.6	4.3	0.2
39	Liquid	298.07	34.449	973.0	0.26	0.03	978.7	1014.1	970.4	0.6	4.2	0.3
40	Liquid	298.06	33.955	971.2	0.26	0.03	976.9	1011.5	968.1	0.6	4.2	0.3
41	Liquid	298.07	33.502	969.5	0.27	0.03	975.1	1009.1	965.9	0.6	4.1	0.4
42	Liquid	298.06	33.000	967.6	0.27	0.03	973.2	1006.5	963.5	0.6	4.0	0.4
43	Liquid	298.07	32.526	965.7	0.27	0.03	971.3	1003.9	961.1	0.6	4.0	0.5
44	Liquid	298.06	32.025	963.8	0.28	0.03	969.4	1001.2	958.6	0.6	3.9	0.5
45	Liquid	298.07	31.546	961.8	0.28	0.03	967.4	998.4	956.1	0.6	3.8	0.6
46	Liquid	298.06	31.090	960.2	0.28	0.03	965.6	995.9	953.8	0.6	3.7	0.7
47	Liquid	298.06	30.499	957.6	0.29	0.03	963.2	992.5	950.7	0.6	3.6	0.7
48	Liquid	298.07	29.996	955.4	0.28	0.03	961.0	989.5	948.0	0.6	3.6	0.8
49	Liquid	298.08	29.493	953.2	0.29	0.03	958.8	986.5	945.1	0.6	3.5	0.8
50	Liquid	298.07	29.029	951.1	0.29	0.03	956.9	983.7	942.6	0.6	3.4	0.9

No	Phase	Temp.	Press.	Density (kg/m^3)						Absolute Deviation (%)		
		K (±0.02)	MPa (±0.005)	Exp.	$u_c(\rho)$ kg/m^3	$u_c(\rho)$ %	PR-CO_2	PR	PR Pen	PR-CO_2	PR	PR Pen
51	Liquid	298.06	28.538	948.9	0.30	0.03	954.7	980.7	939.9	0.6	3.4	1.0
52	Liquid	298.07	28.032	946.6	0.30	0.03	952.4	977.5	936.9	0.6	3.3	1.0
53	Liquid	298.06	27.528	944.3	0.30	0.03	950.2	974.3	934.0	0.6	3.2	1.1
54	Liquid	298.06	27.004	941.7	0.31	0.03	947.7	970.9	930.9	0.6	3.1	1.2
55	Liquid	298.08	26.531	939.6	0.31	0.03	945.4	967.7	927.8	0.6	3.0	1.3
56	Liquid	298.06	26.004	937.0	0.31	0.03	943.0	964.2	924.7	0.6	2.9	1.3
57	Liquid	298.06	25.499	934.6	0.32	0.03	940.5	960.7	921.5	0.6	2.8	1.4
58	Liquid	298.07	25.023	932.1	0.32	0.03	938.1	957.3	918.3	0.6	2.7	1.5
59	Liquid	298.07	24.506	929.6	0.33	0.04	935.5	953.5	914.9	0.6	2.6	1.6
60	Liquid	298.07	24.008	926.9	0.32	0.03	932.9	949.9	911.5	0.6	2.5	1.7
61	Liquid	298.07	23.511	924.2	0.33	0.04	930.2	946.1	908.0	0.7	2.4	1.7
62	Liquid	298.07	23.013	921.5	0.33	0.04	927.6	942.3	904.5	0.7	2.3	1.8
63	Liquid	298.07	22.513	918.8	0.34	0.04	924.8	938.3	900.9	0.7	2.1	1.9
64	Liquid	298.07	22.015	915.8	0.34	0.04	922.0	934.3	897.2	0.7	2.0	2.0
65	Liquid	298.07	21.500	912.9	0.35	0.04	919.0	930.1	893.3	0.7	1.9	2.2
66	Liquid	298.06	21.003	910.0	0.36	0.04	916.1	925.9	889.4	0.7	1.7	2.3
67	Liquid	298.08	20.503	907.0	0.37	0.04	913.0	921.4	885.2	0.7	1.6	2.4
68	Liquid	298.06	19.999	903.9	0.37	0.04	910.0	917.0	881.2	0.7	1.5	2.5
69	Liquid	298.07	19.497	900.5	0.38	0.04	906.7	912.4	876.9	0.7	1.3	2.6
70	Liquid	298.06	19.001	897.3	0.38	0.04	903.5	907.7	872.6	0.7	1.2	2.7
71	Liquid	298.08	18.497	893.7	0.39	0.04	900.0	902.7	868.0	0.7	1.0	2.9
72	Liquid	298.08	18.006	890.4	0.41	0.05	896.6	897.7	863.4	0.7	0.8	3.0
73	Liquid	298.07	17.508	886.9	0.42	0.05	893.1	892.6	858.7	0.7	0.7	3.2
74	Liquid	298.08	17.005	883.1	0.42	0.05	889.3	887.2	853.6	0.7	0.5	3.3
75	Liquid	298.08	16.505	879.3	0.43	0.05	885.5	881.7	848.5	0.7	0.3	3.5
76	Liquid	298.07	16.004	875.3	0.45	0.05	881.6	876.0	843.2	0.7	0.1	3.7
77	Liquid	298.07	15.503	871.1	0.46	0.05	877.5	870.0	837.7	0.7	0.1	3.8
78	Liquid	298.07	15.005	867.0	0.47	0.05	873.3	863.8	832.0	0.7	0.4	4.0
79	Liquid	298.07	14.504	862.4	0.49	0.06	868.9	857.4	826.0	0.7	0.6	4.2
80	Liquid	298.08	14.002	857.8	0.50	0.06	864.2	850.6	819.7	0.7	0.8	4.4
81	Liquid	298.07	13.633	854.0	0.51	0.06	860.7	845.5	814.9	0.8	1.0	4.6
82	Liquid	298.07	13.024	848.3	0.54	0.06	854.7	836.5	806.6	0.7	1.4	4.9
83	Liquid	298.07	12.512	843.3	0.56	0.07	849.3	828.6	799.3	0.7	1.7	5.2
84	Liquid	298.08	11.996	837.8	0.58	0.07	843.4	820.0	791.3	0.7	2.1	5.6
85	Liquid	298.07	11.500	832.0	0.61	0.07	837.7	811.5	783.3	0.7	2.5	5.9
86	Liquid	298.08	11.013	825.9	0.64	0.08	831.5	802.3	774.8	0.7	2.9	6.2
87	Liquid	298.08	10.511	819.3	0.67	0.08	824.8	792.4	765.5	0.7	3.3	6.6
88	Liquid	298.07	9.998	812.8	0.72	0.09	817.5	781.5	755.3	0.6	3.9	7.1
89	Liquid	298.07	9.500	804.5	0.77	0.10	809.7	769.9	744.5	0.6	4.3	7.5
90	Liquid	298.08	9.001	795.9	0.84	0.11	801.1	757.0	732.4	0.7	4.9	8.0
91	Liquid	298.08	8.504	786.3	0.93	0.12	791.7	742.8	719.1	0.7	5.5	8.6
92	Liquid	298.07	8.003	775.2	1.04	0.13	781.1	726.6	703.9	0.8	6.3	9.2
93	Liquid	298.07	7.503	762.2	1.20	0.16	768.9	707.6	686.1	0.9	7.2	10.0
94	Liquid	298.08	7.001	746.0	1.48	0.20	754.3	684.1	664.0	1.1	8.3	11.0
95	Liquid	298.07	6.900	742.3	1.55	0.21	751.3	678.8	659.0	1.2	8.5	11.2
96	Liquid	298.06	6.801	738.3	1.63	0.22	748.2	673.4	653.9	1.3	8.8	11.4
97	Liquid	298.06	6.700	733.8	1.74	0.24	744.7	667.2	648.0	1.5	9.1	11.7
98	Liquid	298.08	6.600	729.1	1.87	0.26	740.9	660.1	641.3	1.6	9.5	12.0
99	Liquid	298.06	6.500	723.9	2.02	0.28	737.8	653.4	635.0	1.9	9.7	12.3
100	Liquid	298.08	6.450	720.9	2.11	0.29	735.8	649.0	630.9	2.1	10.0	12.5
101	Liquid	298.08	6.401	718.3	2.21	0.31	734.2	645.0	627.1	2.2	10.2	12.7
102	Liquid	298.10	6.354	716.1	2.34	0.33	732.5	640.5	622.7	2.3	10.6	13.0
Absolute Average Deviation (AAD)										**0.8**	**3.0**	**3.0**

Table 5.11 Experimental and modelling results for CO_2 + H_2S at 50 °C (323.15 K)

No	Phase	Temp.	Press.	Density (kg/m^3)						Abs Deviation (%)		
		K (±0.02)	MPa (±0.005)	Exp.	$u_c(\rho)$ kg/m^3	$u_c(\rho)$ %	PR-CO_2	PR	PR Pen	PR-CO_2	PR	PR Pen
1	SC	322.40	40.495	910.3	0.27	0.03	922.5	951.0	912.5	1.3	4.5	0.2
2	SC	322.40	39.992	908.1	0.27	0.03	920.3	948.0	909.8	1.3	4.4	0.2
3	SC	322.42	39.502	906.0	0.27	0.03	918.1	945.0	907.0	1.3	4.3	0.1
4	SC	322.41	39.014	903.8	0.27	0.03	916.0	942.2	904.4	1.3	4.2	0.1
5	SC	322.41	38.492	901.2	0.28	0.03	913.6	938.9	901.4	1.4	4.2	0.0
6	SC	322.42	38.008	899.1	0.28	0.03	911.4	935.9	898.6	1.4	4.1	0.0
7	SC	322.42	37.495	896.5	0.28	0.03	909.0	932.7	895.6	1.4	4.0	0.1
8	SC	322.41	37.001	894.2	0.29	0.03	906.7	929.5	892.7	1.4	4.0	0.2
9	SC	322.42	36.519	891.6	0.29	0.03	904.3	926.3	889.8	1.4	3.9	0.2
10	SC	322.42	36.000	889.0	0.29	0.03	901.8	922.9	886.6	1.4	3.8	0.3
11	SC	322.41	35.495	886.3	0.29	0.03	899.3	919.5	883.5	1.5	3.8	0.3
12	SC	322.42	35.002	883.6	0.30	0.03	896.8	916.1	880.3	1.5	3.7	0.4
13	SC	322.42	34.503	880.8	0.30	0.03	894.2	912.6	877.1	1.5	3.6	0.4
14	SC	322.42	34.004	878.0	0.31	0.04	891.6	909.0	873.8	1.6	3.5	0.5
15	SC	322.42	33.498	875.2	0.31	0.04	888.9	905.3	870.4	1.6	3.4	0.5
16	SC	322.42	33.004	872.4	0.31	0.04	886.2	901.7	867.1	1.6	3.4	0.6
17	SC	322.43	32.503	869.6	0.32	0.04	883.4	897.9	863.5	1.6	3.3	0.7
18	SC	322.43	32.002	866.5	0.32	0.04	880.6	894.0	859.9	1.6	3.2	0.8
19	SC	322.42	31.506	863.7	0.33	0.04	877.8	890.2	856.3	1.6	3.1	0.8
20	SC	322.43	31.004	860.5	0.33	0.04	874.8	886.1	852.6	1.7	3.0	0.9
21	SC	322.43	30.505	857.5	0.34	0.04	871.8	882.0	848.8	1.7	2.9	1.0
22	SC	322.43	30.006	854.1	0.34	0.04	868.7	877.8	844.9	1.7	2.8	1.1
23	SC	322.43	29.502	850.6	0.35	0.04	865.6	873.5	840.9	1.8	2.7	1.1
24	SC	322.42	29.009	847.7	0.35	0.04	862.5	869.2	837.0	1.7	2.5	1.3
25	SC	322.42	27.425	837.1	0.37	0.04	851.9	854.7	823.5	1.8	2.1	1.6
26	SC	322.43	27.003	833.6	0.37	0.04	848.9	850.6	819.7	1.8	2.0	1.7
27	SC	322.44	26.506	829.2	0.38	0.05	845.2	845.6	815.0	1.9	2.0	1.7
28	SC	322.43	26.031	824.9	0.39	0.05	841.7	840.8	810.6	2.0	1.9	1.7
29	SC	322.42	25.008	817.6	0.41	0.05	833.9	830.1	800.6	2.0	1.5	2.1
30	SC	322.43	24.503	813.0	0.41	0.05	829.8	824.4	795.4	2.1	1.4	2.2
31	SC	322.44	24.134	809.6	0.42	0.05	826.7	820.2	791.5	2.1	1.3	2.2
32	SC	322.43	20.544	780.3	0.52	0.07	792.5	773.9	748.2	1.6	0.8	4.1
33	SC	322.40	20.400	775.4	0.52	0.07	791.1	771.9	746.4	2.0	0.4	3.7
34	SC	322.43	20.014	767.7	0.53	0.07	786.5	765.9	740.8	2.4	0.2	3.5
35	SC	322.43	19.480	761.0	0.55	0.07	780.3	757.5	732.9	2.5	0.5	3.7
36	SC	322.43	19.007	754.0	0.57	0.08	774.4	749.7	725.6	2.7	0.6	3.8
37	SC	322.44	18.728	748.8	0.59	0.08	770.8	744.9	721.1	2.9	0.5	3.7
38	SC	322.42	18.005	740.8	0.62	0.08	761.2	732.1	709.1	2.7	1.2	4.3
39	SC	322.43	17.599	735.2	0.64	0.09	755.3	724.4	701.8	2.7	1.5	4.5
40	SC	322.43	17.106	726.5	0.68	0.09	747.7	714.6	692.6	2.9	1.6	4.7
41	SC	322.43	16.502	714.5	0.72	0.10	737.8	701.7	680.6	3.3	1.8	4.7
42	SC	322.44	16.031	705.9	0.77	0.11	729.3	690.9	670.4	3.3	2.1	5.0
43	SC	322.43	15.744	699.2	0.80	0.11	723.9	684.1	664.0	3.5	2.1	5.0
44	SC	322.43	15.001	682.0	0.89	0.13	708.5	665.0	645.9	3.9	2.5	5.3
45	SC	322.42	14.515	671.3	0.96	0.14	697.1	651.2	633.0	3.9	3.0	5.7
46	SC	322.44	14.019	655.5	1.06	0.16	683.9	635.7	618.2	4.3	3.0	5.7
47	SC	322.42	13.503	640.1	1.18	0.18	668.6	618.2	601.7	4.4	3.4	6.0
48	SC	322.43	12.996	620.9	1.34	0.22	650.7	598.6	583.1	4.8	3.6	6.1
49	SC	322.44	12.562	601.0	1.53	0.25	632.5	579.7	565.2	5.3	3.5	6.0
50	SC	322.44	12.023	577.0	1.85	0.32	605.0	553.0	539.8	4.9	4.2	6.4
51	SC	322.42	11.519	546.6	2.28	0.42	572.2	523.8	511.9	4.7	4.2	6.3

No	Phase	Temp.	Press.	Density (kg/m^3)						Abs Deviation (%)		
		K (±0.02)	MPa (±0.005)	Exp.	$u_c(\rho)$ kg/m^3	$u_c(\rho)$ %	PR-CO_2	PR	PR Pen	PR-CO_2	PR	PR Pen
52	SC	322.42	11.009	498.9	2.94	0.59	528.1	488.0	477.6	5.9	2.2	4.3
53	SC	322.40	10.500	448.3	3.64	0.81	472.1	444.9	436.4	5.3	0.8	2.7
54	SC	322.38	10.005	401.5	3.78	0.94	409.0	396.4	389.5	1.9	1.3	3.0
55	SC	322.39	9.505	341.5	1.19	0.35	346.5	345.3	340.1	1.5	1.1	0.4
56	SC	322.43	9.001	280.6	0.83	0.30	294.4	298.8	294.9	4.9	6.5	5.1
57	SC	322.45	8.500	247.2	0.59	0.24	254.1	260.3	257.3	2.8	5.3	4.1
58	SC	322.46	8.000	217.9	0.45	0.21	222.0	228.3	226.1	1.9	4.8	3.8
59	SC	322.46	7.503	192.7	0.36	0.19	195.6	201.4	199.6	1.5	4.5	3.6
60	SC	322.47	7.001	170.9	0.30	0.17	172.8	177.9	176.5	1.1	4.1	3.3
61	SC	322.47	6.501	151.5	0.25	0.17	153.0	157.3	156.2	0.9	3.8	3.1
62	SC	322.47	6.004	133.9	0.22	0.16	135.4	138.9	138.1	1.1	3.8	3.1
63	SC	322.47	5.503	118.8	0.19	0.16	119.3	122.2	121.6	0.5	2.9	2.4
64	SC	322.48	5.004	103.9	0.17	0.17	104.7	107.0	106.5	0.7	3.0	2.5
65	SC	322.48	4.501	90.7	0.16	0.17	91.1	92.9	92.6	0.4	2.4	2.0
66	SC	322.48	3.994	77.8	0.14	0.18	78.4	79.8	79.5	0.7	2.5	2.2
67	SC	322.48	3.544	66.6	0.13	0.20	67.8	68.8	68.6	1.8	3.4	3.1
68	SC	322.47	3.003	55.8	0.12	0.22	55.8	56.5	56.4	0.0	1.4	1.1
69	SC	322.48	2.803	51.5	0.12	0.23	51.5	52.2	52.0	0.0	1.3	1.0
70	SC	322.48	2.504	45.3	0.11	0.25	45.3	45.8	45.8	0.0	1.2	1.0
71	SC	322.48	2.249	40.2	0.11	0.27	40.2	40.6	40.6	0.1	1.1	0.9
72	SC	322.49	2.003	35.3	0.11	0.30	35.4	35.7	35.7	0.3	1.2	1.1
73	SC	322.49	1.749	30.7	0.10	0.34	30.5	30.8	30.7	0.6	0.2	0.1
74	SC	322.48	1.500	25.9	0.10	0.39	25.9	26.1	26.1	0.0	0.6	0.5
75	SC	322.49	1.306	22.1	0.10	0.45	22.4	22.5	22.5	1.1	1.8	1.7
76	SC	322.48	1.002	16.8	0.10	0.57	16.9	17.0	17.0	0.6	1.1	1.0
77	SC	322.49	0.801	13.5	0.09	0.70	13.4	13.5	13.5	0.8	0.5	0.5
78	SC	322.49	0.602	10.1	0.09	0.91	10.0	10.0	10.0	1.2	0.9	0.9
79	SC	322.49	0.498	8.0	0.09	1.14	8.2	8.3	8.3	3.0	3.2	3.2
80	SC	322.48	0.395	6.4	0.09	1.41	6.5	6.5	6.5	1.2	1.3	1.3
81	SC	322.48	0.298	4.5	0.09	2.00	4.9	4.9	4.9	8.6	8.7	8.7
82	SC	322.48	0.201	3.4	0.09	2.62	3.3	3.3	3.3	3.3	3.3	3.3
83	SC	322.48	0.109	1.7	0.07	4.11	1.8	1.8	1.8	1.7	1.7	1.7
Absolute Average Deviation (AAD)										**2.1**	**2.7**	**2.4**

Table 5.12 Experimental and modelling results for CO_2 + H_2S at 80 °C (353.15 K)

No	Phase	Temp.	Press.	Density (kg/m³)						Abs Deviation (%)		
		K (±0.02)	MPa (±0.005)	Exp.	$u_c(\rho)$ kg/m³	$u_c(\rho)$ %	PR-CO_2	PR	PR-Pen	PR-CO_2	PR	PR-Pen
1	SC	352.98	40.721	814.9	0.30	0.04	823.2	834.3	804.6	1.0	2.4	1.3
2	SC	352.99	40.702	814.4	0.30	0.04	823.1	834.2	804.4	1.1	2.4	1.2
3	SC	352.97	40.515	813.3	0.30	0.04	822.0	832.8	803.1	1.1	2.4	1.2
4	SC	352.98	40.059	810.8	0.31	0.04	819.3	829.1	799.8	1.0	2.3	1.4
5	SC	352.98	39.509	807.3	0.31	0.04	815.9	824.8	795.7	1.1	2.2	1.4
6	SC	352.98	39.054	803.9	0.31	0.04	813.0	821.1	792.2	1.1	2.1	1.5
7	SC	352.95	38.517	800.4	0.32	0.04	809.8	816.7	788.2	1.2	2.0	1.5
8	SC	352.96	38.004	797.0	0.32	0.04	806.4	812.4	784.2	1.2	1.9	1.6
9	SC	352.96	37.470	794.1	0.33	0.04	802.9	807.8	779.9	1.1	1.7	1.8
10	SC	352.96	37.004	790.2	0.33	0.04	799.8	803.7	776.1	1.2	1.7	1.8
11	SC	352.96	36.555	786.3	0.34	0.04	796.7	799.8	772.4	1.3	1.7	1.8
12	SC	352.96	35.917	782.8	0.34	0.04	792.2	793.9	767.0	1.2	1.4	2.0
13	SC	352.93	35.508	779.2	0.35	0.04	789.4	790.3	763.5	1.3	1.4	2.0
14	SC	352.96	35.000	774.5	0.35	0.05	785.5	785.4	759.0	1.4	1.4	2.0
15	SC	352.96	34.514	770.9	0.35	0.05	781.9	780.7	754.6	1.4	1.3	2.1
16	SC	352.96	33.999	767.0	0.36	0.05	778.0	775.6	749.8	1.4	1.1	2.2
17	SC	352.94	33.504	763.1	0.37	0.05	774.1	770.7	745.2	1.4	1.0	2.3
18	SC	352.96	33.000	758.5	0.38	0.05	770.0	765.4	740.3	1.5	0.9	2.4
19	SC	352.96	32.501	753.9	0.38	0.05	765.9	760.1	735.4	1.6	0.8	2.5
20	SC	352.96	32.001	749.7	0.39	0.05	761.7	754.7	730.3	1.6	0.7	2.6
21	SC	352.96	31.506	745.0	0.40	0.05	757.4	749.3	725.2	1.7	0.6	2.7
22	SC	352.96	31.043	741.1	0.41	0.06	753.3	744.0	720.3	1.6	0.4	2.8
23	SC	352.97	30.503	735.1	0.41	0.06	748.2	737.8	714.4	1.8	0.4	2.8
24	SC	352.97	30.006	730.2	0.42	0.06	743.5	731.8	708.8	1.8	0.2	2.9
25	SC	352.97	29.502	724.7	0.44	0.06	738.6	725.7	703.1	1.9	0.1	3.0
26	SC	352.98	29.007	719.7	0.44	0.06	733.6	719.4	697.2	1.9	0.0	3.1
27	SC	352.98	28.505	714.4	0.45	0.06	728.4	713.0	691.1	2.0	0.2	3.3
28	SC	352.99	28.006	708.6	0.47	0.07	723.0	706.3	684.9	2.0	0.3	3.3
29	SC	352.97	27.507	702.5	0.47	0.07	717.5	699.6	678.6	2.1	0.4	3.4
30	SC	352.98	27.002	696.2	0.49	0.07	711.7	692.5	671.9	2.2	0.5	3.5
31	SC	352.98	26.504	690.1	0.50	0.07	705.7	685.3	665.1	2.3	0.7	3.6
32	SC	352.98	25.999	683.7	0.52	0.08	699.5	677.7	658.0	2.3	0.9	3.8
33	SC	352.97	25.500	676.5	0.53	0.08	693.1	670.1	650.8	2.4	0.9	3.8
34	SC	352.97	25.005	669.8	0.54	0.08	686.4	662.3	643.4	2.5	1.1	3.9
35	SC	352.96	24.499	662.4	0.57	0.09	679.3	654.0	635.5	2.5	1.3	4.1
36	SC	352.98	24.005	654.6	0.58	0.09	671.9	645.5	627.5	2.6	1.4	4.1
37	SC	352.98	23.503	646.1	0.60	0.09	664.2	636.6	619.1	2.8	1.5	4.2
38	SC	352.98	23.002	637.9	0.63	0.10	656.0	627.4	610.4	2.8	1.6	4.3
39	SC	352.99	22.505	629.4	0.65	0.10	647.5	617.9	601.4	2.9	1.8	4.4
40	SC	352.98	22.006	619.7	0.68	0.11	638.6	608.1	592.1	3.1	1.9	4.4
41	SC	352.98	21.508	610.3	0.70	0.12	629.1	597.9	582.4	3.1	2.0	4.6
42	SC	352.96	20.999	599.7	0.74	0.12	618.9	587.0	572.1	3.2	2.1	4.6
43	SC	352.96	20.506	589.4	0.77	0.13	608.3	576.0	561.6	3.2	2.3	4.7
44	SC	352.96	19.998	577.5	0.81	0.14	596.7	564.1	550.3	3.3	2.3	4.7
45	SC	352.97	19.503	564.8	0.85	0.15	584.5	551.9	538.8	3.5	2.3	4.6
46	SC	352.96	19.005	551.2	0.89	0.16	571.6	539.3	526.7	3.7	2.2	4.5
47	SC	352.98	18.502	536.7	0.93	0.17	557.4	525.7	513.7	3.8	2.1	4.3
48	SC	352.98	18.005	522.1	0.97	0.19	542.5	511.7	500.4	3.9	2.0	4.2
49	SC	352.96	17.499	505.7	1.03	0.20	526.4	497.0	486.3	4.1	1.7	3.8
50	SC	352.97	17.001	488.9	1.07	0.22	509.2	481.6	471.5	4.2	1.5	3.6

No	Phase	Temp.	Press.	Density (kg/m^3)						Abs Deviation (%)		
		K (±0.02)	MPa (±0.005)	Exp.	$u_c(\rho)$ kg/m^3	$u_c(\rho)$ %	PR-CO_2	PR	PR-Pen	PR-CO_2	PR	PR-Pen
51	SC	352.97	16.500	471.0	1.12	0.24	490.8	465.4	456.0	4.2	1.2	3.2
52	SC	352.98	16.003	452.2	1.16	0.26	471.5	448.7	439.9	4.3	0.8	2.7
53	SC	353.00	15.503	432.9	1.20	0.28	450.9	431.0	423.0	4.2	0.4	2.3
54	SC	352.99	15.001	412.5	1.22	0.30	429.5	412.9	405.5	4.1	0.1	1.7
55	SC	352.98	14.500	391.7	1.23	0.31	407.5	394.2	387.5	4.0	0.6	1.1
56	SC	352.98	14.003	371.6	1.23	0.33	385.2	375.2	369.1	3.7	1.0	0.7
57	SC	352.98	13.497	350.2	1.20	0.34	362.4	355.5	350.0	3.5	1.5	0.1
58	SC	352.97	13.007	329.4	1.17	0.35	340.5	336.4	331.4	3.4	2.1	0.6
59	SC	353.00	12.511	308.8	1.12	0.36	318.6	316.9	312.5	3.2	2.6	1.2
60	SC	352.99	12.007	288.6	1.06	0.37	297.2	297.4	293.6	3.0	3.1	1.7
61	SC	352.98	11.500	268.9	1.00	0.37	276.6	278.3	274.9	2.9	3.5	2.2
62	SC	352.98	10.998	250.1	0.94	0.37	257.1	259.7	256.8	2.8	3.8	2.6
63	SC	352.99	10.504	232.8	0.88	0.38	238.8	242.0	239.5	2.5	4.0	2.8
64	SC	352.99	9.987	217.7	0.27	0.13	220.6	224.3	222.1	1.4	3.0	2.0
65	SC	352.99	9.504	202.4	0.25	0.12	204.6	208.3	206.4	1.1	2.9	2.0
66	SC	352.99	9.009	187.0	0.23	0.12	189.0	192.7	191.1	1.1	3.0	2.2
67	SC	352.98	8.504	172.4	0.21	0.12	173.9	177.4	176.1	0.9	2.9	2.1
68	SC	353.00	8.009	158.7	0.19	0.12	159.9	163.1	162.0	0.8	2.8	2.1
69	SC	352.99	7.526	145.7	0.18	0.13	146.9	149.8	148.9	0.8	2.9	2.2
70	SC	353.00	7.006	132.8	0.16	0.12	133.5	136.2	135.3	0.5	2.5	1.9
71	SC	352.98	6.499	120.5	0.15	0.13	121.1	123.5	122.8	0.6	2.5	1.9
72	SC	352.98	6.017	109.3	0.14	0.13	109.9	111.9	111.3	0.6	2.4	1.9
73	SC	352.98	5.511	98.1	0.14	0.14	98.6	100.3	99.8	0.5	2.2	1.8
74	SC	352.99	5.014	87.3	0.13	0.15	87.9	89.3	89.0	0.7	2.4	2.0
75	SC	352.98	4.496	77.2	0.12	0.16	77.3	78.4	78.2	0.1	1.6	1.2
76	SC	352.98	4.015	67.8	0.11	0.17	67.8	68.7	68.5	0.1	1.4	1.1
77	SC	352.98	3.498	57.6	0.11	0.19	58.0	58.7	58.5	0.6	1.9	1.6
78	SC	352.97	3.004	48.9	0.10	0.21	48.9	49.5	49.3	0.1	1.2	0.9
79	SC	352.98	2.801	44.8	0.10	0.23	45.3	45.8	45.7	1.1	2.0	1.8
80	SC	352.97	2.517	40.0	0.10	0.25	40.3	40.7	40.6	0.8	1.7	1.5
81	SC	352.97	2.253	35.5	0.10	0.27	35.8	36.1	36.0	0.7	1.5	1.4
82	SC	352.97	2.019	31.5	0.10	0.30	31.8	32.1	32.0	1.0	1.7	1.6
83	SC	352.98	1.745	27.0	0.09	0.34	27.3	27.4	27.4	1.2	1.8	1.7
84	SC	352.99	1.523	23.3	0.09	0.39	23.6	23.8	23.7	1.5	2.0	1.9
85	SC	352.98	1.267	19.0	0.09	0.47	19.5	19.6	19.6	2.5	3.0	2.9
86	SC	352.99	0.998	15.1	0.09	0.58	15.2	15.3	15.3	1.2	1.6	1.5
87	SC	352.99	0.754	11.4	0.09	0.76	11.4	11.5	11.5	0.0	0.3	0.3
88	SC	353.00	0.502	7.6	0.08	1.12	7.6	7.6	7.6	0.5	0.3	0.3
89	SC	352.99	0.399	5.9	0.08	1.42	6.0	6.0	6.0	0.7	0.9	0.9
90	SC	353.00	0.304	4.4	0.08	1.91	4.5	4.6	4.6	3.9	4.0	4.0
91	SC	353.00	0.202	3.0	0.08	2.77	3.0	3.0	3.0	0.5	0.6	0.6
Absolute Average Deviation (AAD)										**2.0**	**1.7**	**2.4**

Table 5.13 Experimental and modelling results for CO_2 + SO_2 at 0 °C (273.15 K)

No	Phase	Temp.	Press.	Density (kg/m^3)						Abs Deviation (%)		
		K (±0.02)	MPa (±0.005)	Exp.	$u_c(\rho)$ kg/m^3	$u_c(\rho)$ %	PR-CO_2	PR	PR-Pen	PR-CO_2	PR	PR-Pen
1	Gas	272.65	0.226	4.8	0.11	2.23	4.6	4.6	4.6	4.0	4.0	4.0
2	Gas	272.65	0.407	8.5	0.11	1.28	8.3	8.3	8.3	2.0	2.0	2.1
3	Gas	272.65	0.503	10.6	0.11	1.05	10.4	10.4	10.4	2.0	2.1	2.1
4	Gas	272.65	0.752	16.2	0.12	0.71	15.9	15.9	15.8	2.1	2.2	2.3
5	Gas	272.65	1.013	22.1	0.12	0.55	21.9	21.9	21.8	1.0	1.0	1.1
6	Gas	272.65	1.252	27.9	0.13	0.46	27.7	27.6	27.6	1.0	1.1	1.2
7	Gas	272.65	1.506	34.4	0.14	0.39	34.1	34.1	34.0	0.9	1.0	1.1
8	Gas	272.65	1.752	40.9	0.15	0.35	40.7	40.7	40.6	0.5	0.6	0.8
9	Gas	272.65	1.998	47.9	0.16	0.32	47.8	47.7	47.6	0.3	0.4	0.6
10	Gas	272.65	2.258	56.8	0.23	0.40	55.7	55.6	55.5	1.9	2.1	2.3
11	Gas	272.66	2.505	67.2	0.31	0.47	63.9	63.8	63.6	4.9	5.1	5.3
12	Liquid	273.54	41.723	1110.7	0.22	0.02	1110.6	1168.1	1115.0	0.0	5.2	0.4
13	Liquid	273.56	41.601	1110.4	0.22	0.02	1110.3	1167.7	1114.7	0.0	5.2	0.4
14	Liquid	273.55	41.016	1109.0	0.22	0.02	1109.0	1166.0	1113.1	0.0	5.1	0.4
15	Liquid	273.55	40.508	1107.8	0.22	0.02	1107.8	1164.4	1111.7	0.0	5.1	0.4
16	Liquid	273.55	40.023	1106.6	0.12	0.01	1106.7	1162.9	1110.3	0.0	5.1	0.3
17	Liquid	273.55	39.553	1105.7	0.22	0.02	1105.6	1161.5	1109.0	0.0	5.0	0.3
18	Liquid	273.55	38.992	1104.0	0.22	0.02	1104.2	1159.7	1107.4	0.0	5.0	0.3
19	Liquid	273.54	38.558	1103.1	0.22	0.02	1103.3	1158.3	1106.2	0.0	5.0	0.3
20	Liquid	273.54	38.033	1101.8	0.22	0.02	1102.0	1156.7	1104.7	0.0	5.0	0.3
21	Liquid	273.54	37.529	1100.5	0.22	0.02	1100.7	1155.1	1103.2	0.0	5.0	0.2
22	Liquid	273.54	37.047	1099.0	0.22	0.02	1099.6	1153.5	1101.7	0.1	5.0	0.3
23	Liquid	273.54	36.490	1097.6	0.22	0.02	1098.2	1151.6	1100.1	0.1	4.9	0.2
24	Liquid	273.54	36.045	1096.7	0.22	0.02	1097.1	1150.2	1098.7	0.0	4.9	0.2
25	Liquid	273.54	35.534	1095.1	0.22	0.02	1095.8	1148.4	1097.1	0.1	4.9	0.2
26	Liquid	273.54	35.043	1093.9	0.27	0.03	1094.6	1146.7	1095.6	0.1	4.8	0.2
27	Liquid	273.54	34.491	1092.3	0.22	0.02	1093.2	1144.8	1093.9	0.1	4.8	0.1
28	Liquid	273.54	34.032	1091.1	0.22	0.02	1092.0	1143.3	1092.4	0.1	4.8	0.1
29	Liquid	273.54	33.521	1089.7	0.22	0.02	1090.7	1141.5	1090.8	0.1	4.8	0.1
30	Liquid	273.54	33.027	1088.3	0.22	0.02	1089.4	1139.7	1089.2	0.1	4.7	0.1
31	Liquid	273.54	32.491	1086.7	0.27	0.03	1088.0	1137.8	1087.4	0.1	4.7	0.1
32	Liquid	273.54	31.975	1085.1	0.22	0.02	1086.6	1135.9	1085.7	0.1	4.7	0.1
33	Liquid	273.55	31.482	1083.6	0.22	0.02	1085.3	1134.0	1084.0	0.1	4.7	0.0
34	Liquid	273.55	30.952	1082.2	0.22	0.02	1083.8	1132.1	1082.2	0.1	4.6	0.0
35	Liquid	273.54	30.524	1080.9	0.22	0.02	1082.7	1130.5	1080.8	0.2	4.6	0.0
36	Liquid	273.55	30.026	1079.4	0.27	0.03	1081.2	1128.6	1079.0	0.2	4.6	0.0
37	Liquid	273.54	29.514	1077.7	0.22	0.02	1079.9	1126.6	1077.2	0.2	4.5	0.0
38	Liquid	273.54	29.024	1076.3	0.22	0.02	1078.5	1124.7	1075.4	0.2	4.5	0.1
39	Liquid	273.55	28.539	1074.9	0.22	0.02	1077.1	1122.7	1073.6	0.2	4.4	0.1
40	Liquid	273.55	28.041	1073.0	0.27	0.03	1075.7	1120.7	1071.8	0.2	4.4	0.1
41	Liquid	273.55	27.554	1071.7	0.22	0.02	1074.3	1118.7	1070.0	0.2	4.4	0.2
42	Liquid	273.54	26.999	1069.9	0.22	0.02	1072.7	1116.5	1068.0	0.3	4.4	0.2
43	Liquid	273.55	26.484	1068.3	0.22	0.02	1071.1	1114.3	1065.9	0.3	4.3	0.2
44	Liquid	273.55	26.016	1066.9	0.32	0.03	1069.7	1112.3	1064.1	0.3	4.3	0.3
45	Liquid	273.54	25.506	1065.1	0.22	0.02	1068.2	1110.2	1062.2	0.3	4.2	0.3
46	Liquid	273.55	25.039	1063.6	0.27	0.03	1066.8	1108.1	1060.3	0.3	4.2	0.3
47	Liquid	273.55	24.523	1061.9	0.22	0.02	1065.2	1105.8	1058.2	0.3	4.1	0.4
48	Liquid	273.55	24.032	1060.4	0.27	0.03	1063.7	1103.7	1056.2	0.3	4.1	0.4
49	Liquid	273.56	23.496	1058.4	0.32	0.03	1061.9	1101.2	1053.9	0.3	4.0	0.4
50	Liquid	273.57	23.015	1056.6	0.32	0.03	1060.4	1098.9	1051.9	0.4	4.0	0.5

No	Phase	Temp.	Press.	Density (kg/m^3)						Abs Deviation (%)		
		K (±0.02)	MPa (±0.005)	Exp.	$u_c(\rho)$ kg/m^3	$u_c(\rho)$ %	PR-CO_2	PR	PR-Pen	PR-CO_2	PR	PR-Pen
51	Liquid	273.56	22.501	1054.9	0.22	0.02	1058.8	1096.6	1049.7	0.4	4.0	0.5
52	Liquid	273.56	21.993	1053.0	0.27	0.03	1057.1	1094.1	1047.5	0.4	3.9	0.5
53	Liquid	273.56	21.519	1051.3	0.32	0.03	1055.6	1091.9	1045.4	0.4	3.9	0.6
54	Liquid	273.56	21.029	1049.7	0.27	0.03	1053.9	1089.4	1043.2	0.4	3.8	0.6
55	Liquid	273.55	20.535	1047.9	0.22	0.02	1052.3	1087.1	1041.0	0.4	3.7	0.7
56	Liquid	273.56	20.028	1046.0	0.32	0.03	1050.6	1084.4	1038.6	0.4	3.7	0.7
57	Liquid	273.56	19.509	1044.0	0.22	0.02	1048.8	1081.7	1036.1	0.5	3.6	0.8
58	Liquid	273.56	19.000	1042.1	0.32	0.03	1047.0	1079.1	1033.7	0.5	3.5	0.8
59	Liquid	273.56	18.515	1040.1	0.32	0.03	1045.3	1076.5	1031.3	0.5	3.5	0.8
60	Liquid	273.56	18.049	1038.2	0.27	0.03	1043.6	1074.0	1029.0	0.5	3.4	0.9
61	Liquid	273.56	17.514	1036.2	0.27	0.03	1041.7	1071.1	1026.3	0.5	3.4	1.0
62	Liquid	273.57	17.024	1034.2	0.32	0.03	1039.8	1068.2	1023.7	0.5	3.3	1.0
63	Liquid	273.57	16.500	1031.9	0.32	0.03	1037.9	1065.3	1021.0	0.6	3.2	1.1
64	Liquid	273.57	15.999	1029.8	0.27	0.03	1036.0	1062.3	1018.3	0.6	3.2	1.1
65	Liquid	273.58	15.602	1028.1	0.32	0.03	1034.4	1060.0	1016.1	0.6	3.1	1.2
66	Liquid	273.57	14.951	1025.4	0.32	0.03	1032.0	1056.0	1012.5	0.6	3.0	1.3
67	Liquid	273.57	14.518	1023.6	0.27	0.03	1030.3	1053.4	1010.0	0.6	2.9	1.3
49	Liquid	273.56	23.496	1058.4	0.32	0.03	1061.9	1101.2	1053.9	0.3	4.0	0.4
69	Liquid	273.56	13.506	1019.3	0.32	0.03	1026.2	1047.0	1004.2	0.7	2.7	1.5
70	Liquid	273.56	13.012	1017.2	0.32	0.03	1024.1	1043.7	1001.2	0.7	2.6	1.6
71	Liquid	273.56	12.509	1014.7	0.32	0.03	1022.1	1040.3	998.0	0.7	2.5	1.6
72	Liquid	273.57	12.005	1012.2	0.32	0.03	1019.9	1036.8	994.8	0.8	2.4	1.7
73	Liquid	273.57	11.502	1009.5	0.32	0.03	1017.7	1033.2	991.5	0.8	2.4	1.8
74	Liquid	273.57	11.003	1007.0	0.32	0.03	1015.5	1029.6	988.2	0.8	2.3	1.9
75	Liquid	273.57	10.516	1004.5	0.37	0.04	1013.3	1026.0	984.9	0.9	2.1	1.9
76	Liquid	273.57	9.944	1001.9	0.32	0.03	1010.7	1021.7	980.9	0.9	2.0	2.1
77	Liquid	273.58	9.518	999.7	0.37	0.04	1008.7	1018.3	977.7	0.9	1.9	2.2
78	Liquid	273.58	9.008	996.7	0.37	0.04	1006.3	1014.2	974.0	1.0	1.8	2.3
79	Liquid	273.58	8.503	993.8	0.37	0.04	1003.8	1010.0	970.1	1.0	1.6	2.4
80	Liquid	273.60	8.003	990.6	0.38	0.04	1001.3	1005.6	966.1	1.1	1.5	2.5
81	Liquid	273.60	7.688	987.5	0.38	0.04	999.7	1002.9	963.6	1.2	1.6	2.4
82	Liquid	273.60	7.034	984.6	0.39	0.04	996.4	997.0	958.1	1.2	1.3	2.7
83	Liquid	273.60	6.503	981.9	0.40	0.04	993.7	992.0	953.5	1.2	1.0	2.9
84	Liquid	273.60	6.005	978.7	0.41	0.04	991.1	987.2	949.1	1.3	0.9	3.0
85	Liquid	273.60	5.521	975.5	0.42	0.04	988.5	982.4	944.6	1.3	0.7	3.2
86	Liquid	273.61	5.013	972.1	0.43	0.04	985.7	977.0	939.6	1.4	0.5	3.3
87	Liquid	273.61	4.518	968.2	0.44	0.05	983.0	971.7	934.7	1.5	0.4	3.5
88	Liquid	273.60	4.001	964.9	0.45	0.05	980.1	965.9	929.3	1.6	0.1	3.7
Absolute Average Deviation (AAD)										**0.6**	**3.4**	**1.1**

Table 5.14 Experimental and modelling results for CO_2 + SO_2 at 10 °C (283.15 K)

No	Phase	Temp.	Press.	Density (kg/m^3)						Abs Deviation (%)		
		K (±0.02)	MPa (±0.005)	Exp. ±0.05%	$u_c(\rho)$ kg/m^3	$u_c(\rho)$ %	PR-CO_2	PR	PR-Pen	PR-CO_2	PR	PR Pen
1	Gas	282.66	0.120	2.5	0.10	4.13	2.3	2.3	2.3	5.5	5.5	5.5
2	Gas	282.66	0.211	4.3	0.10	2.37	4.1	4.1	4.1	5.4	5.3	5.3
3	Gas	282.66	0.301	6.1	0.10	1.69	5.9	5.9	5.9	4.2	4.1	4.1
4	Gas	282.66	0.408	8.5	0.11	1.24	8.0	8.0	8.0	5.3	5.2	5.2
5	Gas	282.66	0.511	10.6	0.11	1.01	10.1	10.1	10.1	4.3	4.0	4.1
6	Gas	282.66	0.608	12.3	0.11	0.88	12.1	12.2	12.2	1.4	1.1	1.2
7	Gas	282.65	0.800	16.5	0.11	0.68	16.2	16.2	16.2	1.9	1.5	1.6
8	Gas	282.66	1.009	21.1	0.12	0.55	20.7	20.8	20.8	1.9	1.4	1.5
9	Gas	282.65	1.249	26.3	0.12	0.46	26.1	26.3	26.2	0.6	0.0	0.1
10	Gas	282.66	1.509	32.8	0.13	0.39	32.2	32.4	32.4	1.8	1.1	1.2
11	Gas	282.66	1.705	37.5	0.13	0.35	37.2	37.3	37.3	0.7	0.4	0.5
12	Gas	282.66	1.909	42.7	0.14	0.33	42.3	42.6	42.5	0.9	0.2	0.4
13	Gas	282.66	2.010	45.2	0.14	0.32	45.5	45.3	45.2	0.7	0.2	0.0
14	Gas	282.66	2.199	50.5	0.15	0.29	50.8	50.5	50.4	0.5	0.1	0.3
15	Gas	282.66	2.508	59.6	0.16	0.27	59.8	59.5	59.4	0.3	0.2	0.5
16	Gas	282.66	2.702	65.5	0.17	0.26	65.9	65.5	65.4	0.7	0.1	0.2
17	Gas	282.66	3.008	76.0	0.19	0.26	76.3	75.8	75.6	0.3	0.3	0.6
18	Gas	282.66	3.206	84.3	0.33	0.39	83.5	83.0	82.7	1.0	1.6	1.9
19	Gas	282.66	3.305	89.3	0.38	0.43	87.3	86.8	86.5	2.2	2.8	3.1
20	Gas	282.66	3.403	94.6	0.45	0.48	91.3	90.7	90.3	3.6	4.2	4.5
21	Gas	282.66	3.503	100.0	0.56	0.56	95.4	94.8	94.5	4.5	5.1	5.5
22	Gas	282.67	3.602	104.8	0.72	0.69	99.7	99.1	98.7	4.8	5.4	5.8
23	Liquid	283.32	40.729	1080.4	0.22	0.02	1079.9	1132.4	1082.5	0.1	4.8	0.2
24	Liquid	283.33	40.700	1080.6	0.22	0.02	1079.8	1132.2	1082.4	0.1	4.8	0.2
25	Liquid	283.33	40.601	1080.3	0.22	0.02	1079.5	1131.9	1082.1	0.1	4.8	0.2
26	Liquid	283.33	40.145	1078.8	0.22	0.02	1078.3	1130.3	1080.6	0.0	4.8	0.2
27	Liquid	283.32	39.558	1077.4	0.22	0.02	1076.8	1128.3	1078.7	0.1	4.7	0.1
28	Liquid	283.32	39.056	1076.1	0.22	0.02	1075.5	1126.5	1077.1	0.0	4.7	0.1
29	Liquid	283.32	38.461	1074.6	0.22	0.02	1074.0	1124.4	1075.1	0.1	4.6	0.1
30	Liquid	283.31	38.061	1073.3	0.22	0.02	1072.9	1122.9	1073.9	0.0	4.6	0.1
31	Liquid	283.31	37.578	1072.1	0.22	0.02	1071.6	1121.2	1072.2	0.0	4.6	0.0
32	Liquid	283.32	37.026	1070.5	0.22	0.02	1070.1	1119.1	1070.3	0.0	4.5	0.0
33	Liquid	283.31	36.515	1068.6	0.22	0.02	1068.7	1117.2	1068.6	0.0	4.5	0.0
34	Liquid	283.31	36.037	1067.5	0.22	0.02	1067.4	1115.4	1066.9	0.0	4.5	0.0
35	Liquid	283.31	35.516	1065.8	0.22	0.02	1065.9	1113.4	1065.1	0.0	4.5	0.1
36	Liquid	283.32	34.989	1064.3	0.22	0.02	1064.4	1111.3	1063.2	0.0	4.4	0.1
37	Liquid	283.31	34.500	1062.8	0.22	0.02	1063.0	1109.4	1061.4	0.0	4.4	0.1
38	Liquid	283.32	33.995	1060.8	0.22	0.02	1061.5	1107.3	1059.6	0.1	4.4	0.1
39	Liquid	283.32	33.527	1059.6	0.22	0.02	1060.2	1105.4	1057.8	0.1	4.3	0.2
40	Liquid	283.32	33.032	1057.9	0.22	0.02	1058.7	1103.4	1056.0	0.1	4.3	0.2
41	Liquid	283.32	32.516	1056.2	0.22	0.02	1057.2	1101.3	1054.0	0.1	4.3	0.2
42	Liquid	283.32	32.033	1054.6	0.32	0.03	1055.8	1099.3	1052.1	0.1	4.2	0.2
43	Liquid	283.32	31.500	1052.8	0.22	0.02	1054.2	1097.0	1050.1	0.1	4.2	0.3
44	Liquid	283.32	31.007	1050.9	0.32	0.03	1052.6	1094.8	1048.1	0.2	4.2	0.3
45	Liquid	283.32	30.506	1049.6	0.32	0.03	1051.1	1092.6	1046.1	0.1	4.1	0.3
46	Liquid	283.32	30.008	1047.3	0.27	0.03	1049.5	1090.4	1044.1	0.2	4.1	0.3
47	Liquid	283.32	29.470	1045.7	0.22	0.02	1047.9	1088.0	1041.9	0.2	4.1	0.4
48	Liquid	283.32	29.081	1044.1	0.32	0.03	1046.6	1086.2	1040.2	0.2	4.0	0.4
49	Liquid	283.32	28.527	1042.4	0.22	0.02	1044.8	1083.7	1037.9	0.2	4.0	0.4
50	Liquid	283.32	28.043	1040.7	0.22	0.02	1043.2	1081.4	1035.8	0.2	3.9	0.5
51	Liquid	283.31	27.537	1038.9	0.22	0.02	1041.6	1079.1	1033.7	0.3	3.9	0.5

No	Phase	Temp.	Press.	Density (kg/m^3)						Abs Deviation (%)		
		K (±0.02)	MPa (±0.005)	Exp. ±0.05%	$u_c(\rho)$ kg/m^3	$u_c(\rho)$ %	PR-CO_2	PR	PR-Pen	PR-CO_2	PR	PR Pen
52	Liquid	283.32	27.023	1037.0	0.22	0.02	1039.8	1076.6	1031.3	0.3	3.8	0.6
53	Liquid	283.32	26.503	1034.9	0.32	0.03	1038.1	1074.0	1029.0	0.3	3.8	0.6
54	Liquid	283.32	26.038	1033.5	0.22	0.02	1036.5	1071.7	1026.9	0.3	3.7	0.6
55	Liquid	283.32	25.509	1031.3	0.27	0.03	1034.7	1069.1	1024.4	0.3	3.7	0.7
56	Liquid	283.32	25.025	1029.4	0.32	0.03	1033.0	1066.5	1022.2	0.4	3.6	0.7
57	Liquid	283.32	24.535	1027.4	0.32	0.03	1031.2	1064.0	1019.8	0.4	3.6	0.7
58	Liquid	283.33	24.074	1025.3	0.22	0.02	1029.5	1061.5	1017.6	0.4	3.5	0.8
59	Liquid	283.32	23.509	1023.3	0.22	0.02	1027.6	1058.5	1014.8	0.4	3.4	0.8
60	Liquid	283.32	23.052	1021.8	0.32	0.03	1025.8	1056.0	1012.5	0.4	3.4	0.9
61	Liquid	283.32	22.565	1019.8	0.32	0.03	1024.0	1053.3	1010.0	0.4	3.3	1.0
62	Liquid	283.32	22.046	1017.6	0.22	0.02	1022.1	1050.4	1007.3	0.4	3.2	1.0
63	Liquid	283.32	21.504	1015.3	0.27	0.03	1020.0	1047.3	1004.4	0.5	3.2	1.1
64	Liquid	283.32	21.035	1013.2	0.22	0.02	1018.1	1044.5	1001.9	0.5	3.1	1.1
65	Liquid	283.32	20.507	1011.0	0.27	0.03	1016.1	1041.3	999.0	0.5	3.0	1.2
66	Liquid	283.32	20.038	1008.7	0.32	0.03	1014.2	1038.5	996.4	0.5	2.9	1.2
67	Liquid	283.32	19.496	1006.2	0.27	0.03	1012.0	1035.1	993.3	0.6	2.9	1.3
68	Liquid	283.32	19.016	1004.1	0.27	0.03	1010.0	1032.1	990.5	0.6	2.8	1.4
69	Liquid	283.32	18.520	1001.7	0.27	0.03	1007.9	1028.9	987.5	0.6	2.7	1.4
70	Liquid	283.33	18.078	999.5	0.32	0.03	1006.0	1025.9	984.8	0.6	2.6	1.5
71	Liquid	283.32	17.551	996.8	0.33	0.03	1003.7	1022.4	981.5	0.7	2.6	1.5
72	Liquid	283.32	17.047	994.7	0.33	0.03	1001.5	1018.9	978.3	0.7	2.4	1.6
73	Liquid	283.32	16.561	992.4	0.34	0.03	999.3	1015.5	975.2	0.7	2.3	1.7
74	Liquid	283.32	16.044	989.5	0.34	0.03	997.0	1011.8	971.7	0.8	2.2	1.8
75	Liquid	283.32	15.505	986.8	0.35	0.04	994.5	1007.8	968.1	0.8	2.1	1.9
76	Liquid	283.32	15.011	984.1	0.34	0.03	992.1	1004.1	964.6	0.8	2.0	2.0
77	Liquid	283.32	14.496	980.8	0.36	0.04	989.7	1000.1	960.9	0.9	2.0	2.0
78	Liquid	283.33	14.003	978.2	0.36	0.04	987.2	996.1	957.3	0.9	1.8	2.1
79	Liquid	283.32	13.536	975.3	0.37	0.04	984.9	992.3	953.8	1.0	1.7	2.2
80	Liquid	283.32	13.000	972.6	0.37	0.04	982.1	987.8	949.6	1.0	1.6	2.4
81	Liquid	283.32	12.514	969.7	0.38	0.04	979.6	983.6	945.7	1.0	1.4	2.5
82	Liquid	283.32	12.009	966.2	0.39	0.04	976.9	979.1	941.6	1.1	1.3	2.5
83	Liquid	283.33	11.512	963.0	0.39	0.04	974.2	974.5	937.3	1.2	1.2	2.7
84	Liquid	283.32	11.007	959.9	0.40	0.04	971.4	969.8	933.0	1.2	1.0	2.8
85	Liquid	283.32	10.507	956.6	0.41	0.04	968.6	964.9	928.4	1.3	0.9	2.9
86	Liquid	283.32	9.995	953.3	0.41	0.04	965.6	959.7	923.6	1.3	0.7	3.1
87	Liquid	283.32	9.510	949.7	0.43	0.05	962.7	954.6	919.0	1.4	0.5	3.2
88	Liquid	283.33	9.019	946.2	0.44	0.05	959.8	949.2	913.9	1.4	0.3	3.4
89	Liquid	283.33	8.543	942.8	0.45	0.05	956.8	943.9	909.0	1.5	0.1	3.6
90	Liquid	283.32	8.008	938.7	0.47	0.05	953.5	937.7	903.2	1.6	0.1	3.8
91	Liquid	283.32	7.506	934.7	0.48	0.05	950.3	931.5	897.4	1.7	0.3	4.0
92	Liquid	283.32	7.000	929.5	0.49	0.05	947.0	925.0	891.4	1.9	0.5	4.1
93	Liquid	283.32	6.507	925.6	0.50	0.05	943.8	918.3	885.2	2.0	0.8	4.4
94	Liquid	283.32	6.002	920.8	0.52	0.06	940.4	911.1	878.5	2.1	1.0	4.6
95	Liquid	283.32	5.506	916.4	0.55	0.06	937.1	903.7	871.6	2.3	1.4	4.9
96	Liquid	283.32	5.005	910.4	0.57	0.06	933.9	895.7	864.1	2.6	1.6	5.1
97	Liquid	283.33	4.499	904.4	0.61	0.07	930.8	887.0	856.0	2.9	1.9	5.4
98	Liquid	283.33	4.307	902.3	0.62	0.07	929.7	883.5	852.8	3.0	2.1	5.5
Absolute Average Deviation (AAD)										**1.1**	**2.8**	**1.7**

Table 5.15 Experimental and modelling results for CO_2 + SO_2 at 25 °C (298.15 K)

No	Phase	Temp.	Press.	Density (kg/m^3)						Abs Deviation (%)		
		K (±0.02)	MPa (±0.005)	Exp.	$u_c(\rho)$ kg/m^3	$u_c(\rho)$ %	PR-CO_2	PR	PR-Pen	PR-CO_2	PR	PR Pen
1	Gas	297.42	0.051	1.0	0.04	4.40	0.9	0.9	0.9	2.8	2.8	2.8
2	Gas	297.41	0.100	1.8	0.07	3.72	1.8	1.8	1.8	2.7	2.7	2.7
3	Gas	297.41	0.200	3.6	0.10	2.69	3.7	3.7	3.7	1.0	1.1	1.1
4	Gas	297.42	0.397	7.5	0.10	1.34	7.4	7.4	7.4	1.8	1.6	1.6
5	Gas	297.42	0.502	9.4	0.10	1.08	9.4	9.4	9.4	0.3	0.0	0.1
6	Gas	297.42	1.817	37.6	0.12	0.33	37.0	37.3	37.3	1.5	0.6	0.8
7	Gas	297.41	2.012	42.1	0.13	0.30	41.5	42.0	41.9	1.3	0.3	0.4
8	Gas	297.41	2.215	47.2	0.13	0.28	46.4	46.9	46.9	1.7	0.6	0.7
9	Gas	297.42	2.421	53.0	0.14	0.26	51.5	52.2	52.1	2.8	1.6	1.8
10	Gas	297.42	2.588	57.0	0.14	0.25	55.8	56.6	56.5	1.9	0.7	0.9
11	Gas	297.42	2.854	64.1	0.15	0.24	63.0	63.9	63.7	1.7	0.3	0.6
12	Gas	297.44	3.064	70.1	0.16	0.23	68.9	70.0	69.8	1.7	0.2	0.4
13	Gas	297.43	3.223	74.6	0.17	0.23	73.5	74.7	74.5	1.4	0.2	0.1
14	Gas	297.43	3.396	79.8	0.18	0.22	78.8	80.2	79.9	1.2	0.5	0.1
15	Gas	297.42	3.638	87.4	0.19	0.22	86.5	88.2	87.8	1.0	0.8	0.5
16	Gas	297.42	3.822	93.7	0.20	0.22	92.8	94.6	94.2	0.9	1.0	0.6
17	Gas	297.42	3.996	99.9	0.22	0.22	99.0	101.0	100.6	0.9	1.1	0.7
18	Gas	297.43	4.206	107.7	0.24	0.22	106.9	109.2	108.8	0.7	1.4	1.0
19	Gas	297.42	4.401	115.6	0.26	0.23	114.9	117.5	116.9	0.6	1.7	1.2
20	Gas	297.42	4.507	120.1	0.27	0.23	119.4	122.2	121.6	0.5	1.8	1.3
21	Gas	297.42	4.600	124.4	0.29	0.24	123.6	126.5	125.9	0.6	1.8	1.2
22	Gas	297.42	4.703	129.2	0.31	0.24	128.4	131.6	130.9	0.6	1.8	1.3
23	Gas	297.40	4.803	134.4	0.55	0.41	133.4	136.7	136.0	0.7	1.8	1.2
24	Gas	297.42	4.903	140.8	0.65	0.46	138.5	142.1	141.3	1.6	0.9	0.3
25	Gas	297.42	5.001	148.3	0.77	0.52	143.9	147.7	146.8	3.0	0.4	1.0
26	Gas	297.41	5.101	155.0	0.95	0.61	149.8	153.7	152.8	3.4	0.8	1.4
27	Gas	297.41	5.200	162.9	1.21	0.74	156.0	160.2	159.1	4.2	1.7	2.3
28	Liquid	298.12	40.411	1032.1	0.22	0.02	1036.1	1080.5	1035.0	0.4	4.7	0.3
29	Liquid	298.11	40.060	1031.1	0.27	0.03	1035.0	1079.0	1033.7	0.4	4.6	0.2
30	Liquid	298.11	39.519	1029.5	0.22	0.02	1033.4	1076.7	1031.5	0.4	4.6	0.2
31	Liquid	298.11	38.913	1027.8	0.27	0.03	1031.5	1074.1	1029.1	0.4	4.5	0.1
32	Liquid	298.11	38.545	1026.6	0.27	0.03	1030.4	1072.5	1027.7	0.4	4.5	0.1
33	Liquid	298.11	37.960	1024.8	0.22	0.02	1028.5	1070.0	1025.3	0.4	4.4	0.0
34	Liquid	298.11	37.574	1023.6	0.22	0.02	1027.3	1068.3	1023.7	0.4	4.4	0.0
35	Liquid	298.10	37.078	1022.0	0.22	0.02	1025.7	1066.0	1021.7	0.4	4.3	0.0
36	Liquid	298.10	36.493	1020.2	0.32	0.03	1023.8	1063.3	1019.3	0.4	4.2	0.1
37	Liquid	298.10	35.971	1018.4	0.22	0.02	1022.1	1061.0	1017.0	0.4	4.2	0.1
38	Liquid	298.11	35.494	1016.9	0.22	0.02	1020.5	1058.7	1015.0	0.3	4.1	0.2
39	Liquid	298.10	35.077	1015.5	0.22	0.02	1019.1	1056.7	1013.2	0.4	4.1	0.2
40	Liquid	298.10	34.441	1013.3	0.32	0.03	1016.9	1053.7	1010.3	0.4	4.0	0.3
41	Liquid	298.11	33.949	1011.6	0.22	0.02	1015.2	1051.2	1008.1	0.4	3.9	0.3
42	Liquid	298.10	33.435	1009.8	0.32	0.03	1013.4	1048.7	1005.8	0.4	3.9	0.4
43	Liquid	298.10	33.068	1008.6	0.22	0.02	1012.1	1046.8	1004.1	0.4	3.8	0.4
44	Liquid	298.10	32.518	1006.5	0.22	0.02	1010.1	1044.0	1001.5	0.4	3.7	0.5
45	Liquid	298.10	32.016	1004.6	0.22	0.02	1008.3	1041.4	999.1	0.4	3.7	0.5
46	Liquid	298.11	31.516	1002.6	0.22	0.02	1006.5	1038.7	996.6	0.4	3.6	0.6
47	Liquid	298.11	30.997	1000.7	0.22	0.02	1004.5	1036.0	994.0	0.4	3.5	0.7
48	Liquid	298.11	30.505	998.9	0.28	0.03	1002.7	1033.3	991.6	0.4	3.4	0.7
49	Liquid	298.11	30.013	996.8	0.28	0.03	1000.8	1030.5	989.1	0.4	3.4	0.8
50	Liquid	298.11	29.543	994.8	0.28	0.03	999.0	1027.9	986.7	0.4	3.3	0.8
51	Liquid	298.11	28.987	993.1	0.28	0.03	996.8	1024.8	983.7	0.4	3.2	0.9

No	Phase	Temp.	Press.	Density (kg/m^3)						Abs Deviation (%)		
		K (±0.02)	MPa (±0.005)	Exp.	$u_c(\rho)$ kg/m^3	$u_c(\rho)$ %	PR-CO_2	PR	PR-Pen	PR-CO_2	PR	PR Pen
52	Liquid	298.10	28.400	990.6	0.29	0.03	994.5	1021.4	980.6	0.4	3.1	1.0
53	Liquid	298.10	27.973	988.6	0.29	0.03	992.7	1018.9	978.3	0.4	3.1	1.0
54	Liquid	298.10	27.508	986.6	0.29	0.03	990.8	1016.1	975.8	0.4	3.0	1.1
55	Liquid	298.10	27.025	984.3	0.29	0.03	988.9	1013.1	973.0	0.5	2.9	1.2
56	Liquid	298.09	26.503	982.1	0.30	0.03	986.7	1009.9	970.1	0.5	2.8	1.2
57	Liquid	298.09	26.076	980.0	0.30	0.03	984.9	1007.2	967.6	0.5	2.8	1.3
58	Liquid	298.10	25.593	977.9	0.31	0.03	982.7	1004.1	964.7	0.5	2.7	1.4
59	Liquid	298.10	25.050	975.1	0.31	0.03	980.3	1000.5	961.4	0.5	2.6	1.4
60	Liquid	298.10	24.505	972.6	0.31	0.03	977.9	996.8	958.0	0.5	2.5	1.5
61	Liquid	298.10	24.029	970.2	0.32	0.03	975.7	993.6	955.0	0.6	2.4	1.6
62	Liquid	298.10	23.522	967.7	0.32	0.03	973.3	990.0	951.7	0.6	2.3	1.6
63	Liquid	298.11	23.041	965.2	0.33	0.03	971.0	986.6	948.5	0.6	2.2	1.7
64	Liquid	298.10	22.537	962.6	0.33	0.03	968.6	983.0	945.2	0.6	2.1	1.8
65	Liquid	298.10	21.994	959.8	0.34	0.04	966.0	978.9	941.4	0.6	2.0	1.9
66	Liquid	298.11	21.501	957.0	0.34	0.04	963.5	975.1	937.9	0.7	1.9	2.0
67	Liquid	298.10	21.016	954.5	0.35	0.04	961.0	971.4	934.4	0.7	1.8	2.1
68	Liquid	298.11	20.492	951.5	0.35	0.04	958.3	967.1	930.5	0.7	1.6	2.2
69	Liquid	298.11	20.051	948.9	0.36	0.04	955.9	963.5	927.2	0.7	1.5	2.3
70	Liquid	298.11	19.477	945.6	0.36	0.04	952.8	958.7	922.8	0.8	1.4	2.4
71	Liquid	298.11	19.025	942.9	0.37	0.04	950.3	954.8	919.2	0.8	1.3	2.5
72	Liquid	298.11	18.527	939.8	0.38	0.04	947.5	950.4	915.1	0.8	1.1	2.6
73	Liquid	298.11	17.978	936.5	0.38	0.04	944.3	945.5	910.5	0.8	1.0	2.8
74	Liquid	298.11	17.492	933.3	0.39	0.04	941.5	940.9	906.2	0.9	0.8	2.9
75	Liquid	298.11	17.024	930.2	0.40	0.04	938.7	936.4	902.0	0.9	0.7	3.0
76	Liquid	298.11	16.534	926.8	0.41	0.04	935.7	931.6	897.6	1.0	0.5	3.2
77	Liquid	298.11	16.016	923.0	0.41	0.04	932.4	926.3	892.7	1.0	0.4	3.3
78	Liquid	298.11	15.500	919.1	0.42	0.05	929.0	920.8	887.6	1.1	0.2	3.4
79	Liquid	298.11	15.011	915.2	0.43	0.05	925.7	915.5	882.6	1.2	0.0	3.6
80	Liquid	298.12	14.500	910.9	0.45	0.05	922.2	909.7	877.2	1.2	0.1	3.7
81	Liquid	298.12	14.006	906.7	0.46	0.05	918.8	903.8	871.8	1.3	0.3	3.9
82	Liquid	298.11	13.500	902.3	0.47	0.05	915.2	897.7	866.1	1.4	0.5	4.0
83	Liquid	298.11	13.010	897.8	0.48	0.05	911.5	891.5	860.3	1.5	0.7	4.2
84	Liquid	298.12	12.503	892.9	0.50	0.06	907.6	884.7	854.0	1.6	0.9	4.4
85	Liquid	298.12	12.000	887.9	0.51	0.06	903.6	877.7	847.4	1.8	1.2	4.6
86	Liquid	298.12	11.504	882.9	0.53	0.06	899.7	870.5	840.7	1.9	1.4	4.8
87	Liquid	298.11	11.004	877.7	0.56	0.06	895.6	862.9	833.6	2.0	1.7	5.0
88	Liquid	298.11	10.505	872.1	0.58	0.07	891.3	854.8	826.1	2.2	2.0	5.3
89	Liquid	298.12	10.039	866.6	0.60	0.07	887.3	846.8	818.6	2.4	2.3	5.5
90	Liquid	298.12	9.508	860.5	0.64	0.07	882.6	837.1	809.5	2.6	2.7	5.9
91	Liquid	298.10	9.007	854.0	0.66	0.08	878.3	827.4	800.5	2.8	3.1	6.3
92	Liquid	298.11	8.501	846.7	0.71	0.08	874.0	816.6	790.3	3.2	3.6	6.7
93	Liquid	298.11	8.006	838.7	0.77	0.09	870.2	805.2	779.7	3.8	4.0	7.0
94	Liquid	298.11	7.503	829.8	0.83	0.10	867.3	792.5	767.7	4.5	4.5	7.5
95	Liquid	298.10	7.001	819.7	0.92	0.11	867.0	778.4	754.4	5.8	5.0	8.0
Absolute Average Deviation (AAD)										**1.2**	**2.2**	**1.9**

Table 5.16 Experimental and modelling results for CO_2 + SO_2 at 50 °C (323.15 K)

No	Phase	Temp.	Press.	Density (kg/m^3)						Abs Deviation (%)		
		K (±0.02)	MPa (±0.005)	Exp.	$u_c(\rho)$ kg/m^3	$u_c(\rho)$ %	PR-CO_2	PR	PR-Pen	PR-CO_2	PR	PR Pen
1	SC	322.47	40.947	956.3	0.26	0.03	960.1	990.5	952.1	0.4	3.6	0.4
2	SC	322.48	40.902	956.7	0.27	0.03	959.9	990.2	951.8	0.3	3.5	0.5
3	SC	322.48	40.153	953.9	0.26	0.03	956.8	986.0	947.9	0.3	3.4	0.6
4	SC	322.48	39.641	951.7	0.27	0.03	954.7	983.1	945.2	0.3	3.3	0.7
5	SC	322.47	39.200	950.0	0.27	0.03	952.9	980.6	942.9	0.3	3.2	0.7
6	SC	322.47	38.434	946.6	0.27	0.03	949.7	976.1	938.8	0.3	3.1	0.8
7	SC	322.47	38.091	945.0	0.28	0.03	948.3	974.0	936.9	0.3	3.1	0.9
8	SC	322.46	37.561	942.4	0.28	0.03	946.0	970.8	933.9	0.4	3.0	0.9
9	SC	322.46	37.005	940.1	0.28	0.03	943.5	967.4	930.8	0.4	2.9	1.0
10	SC	322.46	36.509	937.7	0.28	0.03	941.3	964.3	927.9	0.4	2.8	1.0
11	SC	322.46	36.061	935.4	0.29	0.03	939.3	961.5	925.3	0.4	2.8	1.1
12	SC	322.46	35.500	933.0	0.29	0.03	936.7	957.8	921.9	0.4	2.7	1.2
13	SC	322.46	34.988	930.2	0.29	0.03	934.3	954.5	918.8	0.4	2.6	1.2
14	SC	322.47	34.511	928.0	0.30	0.03	932.0	951.2	915.8	0.4	2.5	1.3
15	SC	322.47	34.062	925.5	0.30	0.03	929.8	948.2	912.9	0.5	2.4	1.4
16	SC	322.47	33.539	923.2	0.30	0.03	927.2	944.6	909.6	0.4	2.3	1.5
17	SC	322.47	33.070	920.6	0.31	0.03	924.8	941.2	906.5	0.5	2.2	1.5
18	SC	322.47	32.536	917.5	0.31	0.03	922.1	937.4	902.9	0.5	2.2	1.6
19	SC	322.48	32.039	914.6	0.32	0.04	919.5	933.7	899.5	0.5	2.1	1.6
20	SC	322.47	31.517	912.0	0.32	0.04	916.8	929.8	896.0	0.5	2.0	1.8
21	SC	322.47	31.027	908.9	0.33	0.04	914.2	926.1	892.5	0.6	1.9	1.8
22	SC	322.46	30.511	905.8	0.33	0.04	911.4	922.1	888.8	0.6	1.8	1.9
23	SC	322.47	29.929	902.4	0.33	0.04	908.1	917.5	884.4	0.6	1.7	2.0
24	SC	322.49	29.507	899.6	0.34	0.04	905.6	914.0	881.1	0.7	1.6	2.0
25	SC	322.49	29.025	896.4	0.34	0.04	902.8	910.0	877.5	0.7	1.5	2.1
26	SC	322.48	28.501	892.7	0.35	0.04	899.8	905.6	873.4	0.8	1.4	2.2
27	SC	322.49	28.018	889.5	0.35	0.04	896.8	901.3	869.4	0.8	1.3	2.3
28	SC	322.49	27.508	886.3	0.36	0.04	893.7	896.8	865.2	0.8	1.2	2.4
29	SC	322.48	27.026	882.9	0.37	0.04	890.6	892.5	861.2	0.9	1.1	2.5
30	SC	322.49	26.517	878.8	0.37	0.04	887.3	887.7	856.8	1.0	1.0	2.5
31	SC	322.49	26.001	875.4	0.38	0.04	883.9	882.8	852.2	1.0	0.8	2.7
32	SC	322.48	25.500	871.4	0.39	0.04	880.5	877.9	847.6	1.0	0.7	2.7
33	SC	322.50	25.003	867.7	0.39	0.05	877.0	872.8	842.8	1.1	0.6	2.9
34	SC	322.50	24.497	864.4	0.40	0.05	873.4	867.6	838.0	1.0	0.4	3.1
35	SC	322.49	24.003	860.4	0.41	0.05	869.8	862.4	833.1	1.1	0.2	3.2
36	SC	322.49	23.500	856.5	0.42	0.05	866.0	856.9	828.0	1.1	0.0	3.3
37	SC	322.48	23.049	853.3	0.43	0.05	862.5	851.9	823.3	1.1	0.2	3.5
38	SC	322.49	22.496	848.2	0.43	0.05	858.1	845.4	817.3	1.2	0.3	3.6
39	SC	322.49	22.009	843.9	0.44	0.05	854.1	839.6	811.8	1.2	0.5	3.8
40	SC	322.49	21.533	839.7	0.46	0.06	850.0	833.7	806.3	1.2	0.7	4.0
41	SC	322.49	21.007	834.7	0.47	0.06	845.4	826.9	800.0	1.3	0.9	4.2
42	SC	322.48	20.496	829.2	0.48	0.06	840.7	820.2	793.7	1.4	1.1	4.3
43	SC	322.49	20.012	824.3	0.50	0.06	836.1	813.5	787.4	1.4	1.3	4.5
44	SC	322.50	19.491	818.5	0.52	0.06	830.9	805.9	780.3	1.5	1.5	4.7
45	SC	322.49	19.008	812.8	0.53	0.07	826.0	798.7	773.6	1.6	1.7	4.8
46	SC	322.50	18.503	806.6	0.55	0.07	820.5	790.8	766.1	1.7	2.0	5.0
47	SC	322.49	18.008	800.3	0.57	0.07	815.0	782.8	758.6	1.8	2.2	5.2
48	SC	322.50	17.499	793.5	0.60	0.08	808.9	773.9	750.3	1.9	2.5	5.4
49	SC	322.51	17.005	786.2	0.62	0.08	802.7	765.0	741.9	2.1	2.7	5.6
50	SC	322.51	16.502	779.1	0.65	0.08	796.0	755.4	732.8	2.2	3.0	5.9

No	Phase	Temp.	Press.	Density (kg/m^3)						Abs Deviation (%)		
		K (±0.02)	MPa (±0.005)	Exp.	$u_c(\rho)$ kg/m^3	$u_c(\rho)$ %	PR-CO_2	PR	PR-Pen	PR-CO_2	PR	PR Pen
51	SC	322.52	16.003	770.9	0.69	0.09	788.9	745.3	723.3	2.3	3.3	6.2
52	SC	322.52	15.501	761.8	0.73	0.10	781.3	734.5	713.2	2.6	3.6	6.4
53	SC	322.52	15.012	753.2	0.77	0.10	773.3	723.3	702.6	2.7	4.0	6.7
54	SC	322.52	14.504	742.9	0.83	0.11	764.2	710.8	690.8	2.9	4.3	7.0
55	SC	322.52	14.000	731.9	0.89	0.12	754.2	697.4	678.1	3.0	4.7	7.4
56	SC	322.53	13.501	720.4	0.98	0.14	742.9	682.8	664.3	3.1	5.2	7.8
57	SC	322.54	13.000	706.7	1.08	0.15	729.7	666.6	649.0	3.3	5.7	8.2
58	SC	322.53	12.505	691.1	1.21	0.18	714.4	649.1	632.4	3.4	6.1	8.5
59	SC	322.51	12.003	672.3	1.39	0.21	695.0	629.1	613.4	3.4	6.4	8.8
60	SC	322.51	11.504	649.9	1.65	0.25	669.0	605.8	591.3	2.9	6.8	9.0
61	SC	322.49	11.003	621.1	2.05	0.33	633.2	578.3	565.0	2.0	6.9	9.0
62	SC	322.47	10.501	585.0	2.74	0.47	583.6	544.2	532.4	0.2	7.0	9.0
63	SC	322.46	9.992	538.0	1.98	0.37	517.3	498.7	488.8	3.8	7.3	9.1
64	SC	322.45	9.501	460.8	2.52	0.55	441.0	439.3	431.6	4.3	4.7	6.3
65	SC	322.41	9.006	371.0	1.85	0.50	362.2	368.6	363.1	2.4	0.7	2.1
66	SC	322.41	8.521	307.2	1.06	0.35	299.4	307.6	303.8	2.6	0.1	1.1
67	SC	322.41	8.037	254.6	0.68	0.27	253.9	261.8	259.0	0.3	2.8	1.7
68	SC	322.39	7.504	218.4	0.47	0.22	216.4	223.3	221.3	0.9	2.2	1.3
69	SC	322.39	7.009	189.5	0.37	0.19	188.7	194.6	193.0	0.4	2.7	1.9
70	SC	322.41	6.514	166.3	0.29	0.18	165.4	170.3	169.1	0.5	2.4	1.7
71	SC	322.39	6.019	145.7	0.24	0.17	145.3	149.3	148.4	0.3	2.5	1.8
72	SC	322.39	5.528	127.9	0.22	0.17	127.7	130.9	130.2	0.2	2.3	1.8
73	SC	322.39	5.017	111.5	0.19	0.17	111.1	113.7	113.2	0.3	2.0	1.5
74	SC	322.39	4.519	96.9	0.17	0.17	96.5	98.5	98.1	0.5	1.6	1.2
75	SC	322.39	4.009	82.8	0.15	0.18	82.7	84.2	83.9	0.2	1.6	1.3
76	SC	322.39	3.512	70.9	0.14	0.20	70.2	71.3	71.1	1.0	0.6	0.3
77	SC	322.40	3.008	58.8	0.13	0.22	58.3	59.1	59.0	0.7	0.6	0.4
78	SC	322.40	2.511	48.1	0.12	0.25	47.4	47.9	47.8	1.5	0.4	0.6
79	SC	322.39	2.008	37.0	0.11	0.30	36.9	37.3	37.2	0.3	0.7	0.5
80	SC	322.39	1.707	31.7	0.11	0.34	30.9	31.2	31.1	2.4	1.7	1.8
81	SC	322.40	1.509	27.5	0.11	0.38	27.1	27.3	27.2	1.4	0.8	0.9
82	SC	322.39	1.252	22.2	0.10	0.46	22.2	22.3	22.3	0.2	0.4	0.3
83	SC	322.40	1.002	17.9	0.10	0.55	17.6	17.6	17.6	1.9	1.4	1.5
84	SC	322.40	0.749	13.6	0.10	0.73	13.0	13.0	13.0	4.3	4.0	4.0
85	SC	322.39	0.392	7.0	0.10	1.42	6.7	6.7	6.7	4.0	3.9	3.9
Absolute Average Deviation (AAD)										**1.3**	**2.4**	**3.1**

Table 5.17 Experimental and modelling results for CO_2 + SO_2 at 80 °C (353.15 K)

No	Phase	Temp.	Press.	Density (kg/m^3)						Abs Deviation (%)		
		K (±0.02)	MPa (±0.005)	Exp.	$u_c(\rho)$ kg/m^3	$u_c(\rho)$ %	PR-CO_2	PR	PR-Pen	PR-CO_2	PR	PR Pen
1	SC	352.98	39.330	850.5	0.31	0.04	850.7	859.7	830.6	0.0	1.1	2.3
2	SC	352.98	39.300	850.2	0.31	0.04	850.5	859.5	830.4	0.0	1.1	2.3
3	SC	352.97	39.009	848.1	0.31	0.04	848.9	857.2	828.3	0.1	1.1	2.3
4	SC	352.97	38.520	845.7	0.32	0.04	845.9	853.3	824.6	0.0	0.9	2.5
5	SC	352.98	38.023	842.1	0.32	0.04	842.8	849.2	820.8	0.1	0.8	2.5
6	SC	352.97	37.499	838.7	0.33	0.04	839.6	844.8	816.7	0.1	0.7	2.6
7	SC	352.96	36.996	835.2	0.33	0.04	836.4	840.6	812.8	0.1	0.6	2.7
8	SC	352.97	36.496	831.8	0.34	0.04	833.1	836.2	808.7	0.2	0.5	2.8
9	SC	352.98	36.013	828.1	0.34	0.04	829.8	831.9	804.7	0.2	0.5	2.8
10	SC	352.97	35.510	824.7	0.34	0.04	826.5	827.4	800.4	0.2	0.3	2.9
11	SC	352.97	35.014	821.4	0.35	0.04	823.0	822.9	796.2	0.2	0.2	3.1
12	SC	352.98	34.563	818.1	0.35	0.04	819.8	818.6	792.2	0.2	0.1	3.2
13	SC	352.97	34.055	814.5	0.35	0.04	816.2	813.8	787.7	0.2	0.1	3.3
14	SC	352.96	33.519	809.8	0.36	0.04	812.2	808.6	782.8	0.3	0.1	3.3
15	SC	352.96	33.014	805.8	0.37	0.05	808.4	803.6	778.1	0.3	0.3	3.4
16	SC	352.97	32.552	802.4	0.38	0.05	804.8	798.8	773.6	0.3	0.5	3.6
17	SC	352.96	31.993	797.6	0.38	0.05	800.4	793.0	768.2	0.4	0.6	3.7
18	SC	352.95	31.494	793.2	0.39	0.05	796.4	787.7	763.2	0.4	0.7	3.8
19	SC	352.96	31.058	789.4	0.39	0.05	792.6	782.9	758.6	0.4	0.8	3.9
20	SC	352.97	30.512	784.7	0.40	0.05	787.9	776.7	752.9	0.4	1.0	4.1
21	SC	352.96	29.991	779.0	0.42	0.05	783.3	770.7	747.3	0.6	1.1	4.1
22	SC	352.96	29.492	773.9	0.42	0.05	778.7	764.8	741.7	0.6	1.2	4.2
23	SC	352.97	29.001	768.7	0.44	0.06	774.0	758.8	736.0	0.7	1.3	4.3
24	SC	352.96	28.507	764.2	0.45	0.06	769.3	752.7	730.3	0.7	1.5	4.4
25	SC	352.96	28.006	758.3	0.46	0.06	764.2	746.3	724.3	0.8	1.6	4.5
26	SC	352.96	27.501	752.6	0.47	0.06	759.0	739.6	718.0	0.8	1.7	4.6
27	SC	352.98	27.043	747.4	0.48	0.06	754.0	733.3	712.0	0.9	1.9	4.7
28	SC	352.97	26.597	742.8	0.49	0.07	749.0	727.1	706.2	0.8	2.1	4.9
29	SC	352.96	26.036	736.4	0.50	0.07	742.6	719.1	698.6	0.8	2.4	5.1
30	SC	352.96	25.555	731.2	0.52	0.07	736.8	711.9	691.9	0.8	2.6	5.4
31	SC	352.95	25.002	723.7	0.53	0.07	729.8	703.5	683.9	0.8	2.8	5.5
32	SC	352.95	24.538	717.4	0.55	0.08	723.7	696.1	676.9	0.9	3.0	5.6
33	SC	352.96	24.023	710.4	0.57	0.08	716.6	687.6	668.8	0.9	3.2	5.8
34	SC	352.96	23.524	703.1	0.58	0.08	709.4	679.0	660.7	0.9	3.4	6.0
35	SC	352.95	23.011	694.8	0.61	0.09	701.6	670.0	652.2	1.0	3.6	6.1
36	SC	352.95	22.493	686.4	0.63	0.09	693.2	660.4	643.2	1.0	3.8	6.3
37	SC	352.95	21.993	677.2	0.66	0.10	684.7	650.8	634.0	1.1	3.9	6.4
38	SC	352.96	21.521	668.5	0.68	0.10	676.1	641.3	625.0	1.1	4.1	6.5
39	SC	352.96	20.999	657.9	0.72	0.11	666.0	630.4	614.6	1.2	4.2	6.6
40	SC	352.96	20.490	647.4	0.75	0.12	655.5	619.3	604.0	1.3	4.3	6.7
41	SC	352.96	20.014	636.9	0.78	0.12	645.0	608.4	593.7	1.3	4.5	6.8
42	SC	352.95	19.511	624.5	0.83	0.13	633.2	596.4	582.3	1.4	4.5	6.8
43	SC	352.96	19.011	611.7	0.87	0.14	620.4	583.7	570.1	1.4	4.6	6.8
44	SC	352.97	18.500	597.8	0.92	0.15	606.3	570.1	557.2	1.4	4.6	6.8
45	SC	352.97	18.007	583.3	0.97	0.17	591.6	556.3	544.0	1.4	4.6	6.7
46	SC	352.95	17.520	569.4	1.03	0.18	576.0	542.2	530.4	1.2	4.8	6.8
47	SC	352.96	17.006	552.6	1.10	0.20	558.1	526.1	515.1	1.0	4.8	6.8
48	SC	352.95	16.515	535.1	1.16	0.22	539.7	510.1	499.7	0.9	4.7	6.6
49	SC	352.96	16.004	514.7	1.24	0.24	518.9	492.3	482.6	0.8	4.4	6.2
50	SC	352.95	15.497	493.2	1.30	0.26	497.1	473.8	464.8	0.8	3.9	5.7
51	SC	352.96	15.003	470.1	1.36	0.29	474.3	454.7	446.5	0.9	3.3	5.0

No	Phase	Temp.	Press.	Density (kg/m^3)						Abs Deviation (%)		
		K (±0.02)	MPa (±0.005)	Exp.	$u_c(\rho)$ kg/m^3	$u_c(\rho)$ %	PR-CO_2	PR	PR-Pen	PR-CO_2	PR	PR Pen
52	SC	352.95	14.502	447.3	1.41	0.31	450.3	434.6	427.1	0.7	2.8	4.5
53	SC	352.96	14.004	422.3	1.43	0.34	425.5	413.7	406.9	0.8	2.0	3.7
54	SC	352.96	13.501	397.6	1.43	0.36	400.1	392.0	385.8	0.6	1.4	3.0
55	SC	352.96	12.998	371.8	1.40	0.38	374.6	369.8	364.3	0.7	0.5	2.0
56	SC	352.95	12.505	346.8	1.35	0.39	349.9	347.9	343.1	0.9	0.3	1.1
57	SC	352.95	12.000	321.9	1.27	0.40	325.3	325.5	321.3	1.1	1.1	0.2
58	SC	352.97	11.505	298.8	1.19	0.40	302.0	303.9	300.2	1.1	1.7	0.5
59	SC	352.96	11.001	276.4	1.11	0.40	279.5	282.5	279.3	1.1	2.2	1.1
60	SC	352.97	10.506	255.3	1.03	0.40	258.5	262.2	259.4	1.2	2.7	1.6
61	SC	352.96	10.075	238.1	0.96	0.40	241.2	245.3	242.8	1.3	3.0	2.0
62	SC	352.95	9.230	209.5	0.26	0.13	209.9	214.0	212.2	0.2	2.1	1.3
63	SC	352.94	9.008	201.9	0.26	0.13	202.2	206.3	204.5	0.1	2.2	1.3
64	SC	352.96	8.507	185.5	0.23	0.13	185.5	189.3	187.9	0.0	2.1	1.3
65	SC	352.94	8.038	170.3	0.22	0.13	170.8	174.4	173.2	0.3	2.4	1.6
66	SC	352.94	7.498	154.1	0.20	0.13	154.8	158.0	157.0	0.5	2.5	1.9
67	SC	352.94	7.017	140.9	0.18	0.13	141.4	144.2	143.4	0.3	2.3	1.8
68	SC	352.94	6.516	127.7	0.16	0.13	128.1	130.6	129.9	0.3	2.2	1.7
69	SC	352.93	6.001	114.8	0.15	0.13	115.2	117.3	116.7	0.3	2.2	1.7
70	SC	352.95	5.490	102.6	0.15	0.14	102.9	104.7	104.3	0.3	2.0	1.6
71	SC	352.95	4.997	91.5	0.13	0.15	91.7	93.2	92.8	0.3	1.9	1.5
72	SC	352.94	4.493	80.5	0.13	0.16	80.7	81.9	81.7	0.3	1.8	1.4
73	SC	352.94	4.003	70.6	0.12	0.17	70.5	71.5	71.3	0.1	1.2	0.9
74	SC	352.96	3.495	60.3	0.11	0.19	60.4	61.1	60.9	0.1	1.3	1.1
75	SC	352.95	3.009	51.0	0.11	0.21	51.0	51.6	51.5	0.1	1.2	0.9
76	SC	352.95	2.800	47.2	0.11	0.23	47.1	47.6	47.5	0.1	0.9	0.7
77	SC	352.94	2.504	41.8	0.10	0.25	41.7	42.1	42.0	0.3	0.6	0.5
78	SC	352.95	2.248	37.0	0.10	0.27	37.1	37.4	37.3	0.4	1.2	1.0
79	SC	352.95	2.002	33.0	0.10	0.30	32.8	33.0	32.9	0.8	0.1	0.2
80	SC	352.94	1.742	28.6	0.10	0.34	28.2	28.4	28.4	1.2	0.6	0.7
81	SC	352.95	1.507	24.3	0.09	0.39	24.2	24.4	24.4	0.1	0.5	0.4
82	SC	352.96	1.248	19.9	0.09	0.47	19.9	20.0	20.0	0.1	0.4	0.3
83	SC	352.96	0.982	15.1	0.09	0.60	15.5	15.6	15.6	2.7	3.1	3.0
84	SC	352.95	0.740	11.4	0.09	0.77	11.6	11.6	11.6	1.5	1.8	1.7
85	SC	352.95	0.511	7.6	0.09	1.14	8.0	8.0	8.0	4.2	4.4	4.4
86	SC	352.95	0.402	6.0	0.09	1.45	6.2	6.3	6.2	4.5	4.7	4.7
87	SC	352.95	0.306	4.6	0.09	1.86	4.7	4.7	4.7	2.8	3.0	2.9
88	SC	352.93	0.202	3.0	0.09	2.87	3.1	3.1	3.1	5.1	5.2	5.2
Absolute Average Deviation (AAD)										**0.8**	**2.1**	**3.5**

Table 5.18 Summarised AADs for measured systems

Material	Temperature	AAD (%)		
	°C	PR-CO_2	PR	PR-Peneloux
CO_2+H_2S	0	2.2	4.7	1.2
	10	0.7	2.7	1.8
	25	0.8	3.0	3.0
	50	2.1	2.7	2.4
	80	2.0	1.7	2.4
	Average	1.6	3.0	2.2
CO_2+SO_2	0	0.6	3.4	1.1
	10	1.1	2.8	1.7
	25	1.2	2.2	1.9
	50	1.3	2.4	3.1
	80	0.8	2.1	3.5
	Average	1.0	2.6	2.3

Table 5.19 Specific heat capacity calculations for CO_2+H_2S system

T	P	Density	v: Molar Vol	C_{pi}: CO_2	C_{pi}: H_2S	C_{pi}: CO_2+H_2S	Calced C_p	REFPROPP	Dev.
K	MPa	kg/m^3	m^3/mol	J/mol.K	J/mol.K	J/mol.K	J/mol.K	J/mol.K	%
				40 MPa					
272.57	40.046	1054.95	4.1251E-05	35.88	33.91	35.78	73.27	78.25	6.8
283.47	40.004	1040.33	4.1831E-05	36.47	34.02	36.35	73.34	78.58	7.1
298.06	40.253	992.41	4.3851E-05	37.24	34.19	37.09	73.42	79.02	7.6
322.40	39.992	908.08	4.7923E-05	38.45	34.49	38.25	74.01	80.10	8.2
352.98	40.059	810.79	5.3674E-05	39.82	34.91	39.58	74.00	80.87	9.3
				35 MPa					
272.56	35.060	1041.12	4.1799E-05	35.88	33.91	35.78	74.86	79.50	6.2
283.46	35.004	1025.18	4.2449E-05	36.47	34.02	36.35	75.19	80.07	6.5
298.06	35.006	974.89	4.4639E-05	37.24	34.19	37.09	75.78	80.97	6.8
322.42	35.002	883.60	4.9251E-05	38.45	34.49	38.25	77.01	82.73	7.4
352.96	35.000	774.52	5.6187E-05	39.82	34.91	39.58	78.03	84.47	8.3
				30 MPa					
272.57	30.022	1025.61	4.2431E-05	35.88	33.91	35.78	77.03	81.05	5.2
283.47	30.014	1008.20	4.3164E-05	36.47	34.02	36.35	77.64	81.95	5.5
298.07	29.996	955.45	4.5547E-05	37.24	34.19	37.09	78.87	83.42	5.8
322.43	30.006	854.09	5.0953E-05	38.45	34.49	38.25	81.42	86.43	6.2
352.97	30.006	730.17	5.96E-05	39.82	34.91	39.58	84.11	89.83	6.8
				25 MPa					
272.58	24.975	1008.49	4.3152E-05	35.88	33.91	35.78	79.89	83.01	3.9
283.47	25.000	988.85	4.4009E-05	36.47	34.02	36.35	80.97	84.40	4.2
298.07	25.023	932.12	4.6687E-05	37.24	34.19	37.09	83.34	86.77	4.1
322.42	25.008	817.64	5.3224E-05	38.45	34.49	38.25	88.23	92.17	4.5
352.97	25.005	669.79	6.4973E-05	39.82	34.91	39.58	93.93	98.62	5.0
				20 MPa					
272.58	20.011	989.08	4.3998E-05	35.88	33.91	35.78	82.07	85.53	4.2
283.47	20.010	966.84	4.5011E-05	36.47	34.02	36.35	83.86	87.77	4.7
298.06	19.999	903.89	4.8145E-05	37.24	34.19	37.09	87.85	91.84	4.6
322.43	20.014	767.74	5.6683E-05	38.45	34.49	38.25	98.41	102.28	3.9
352.96	19.998	577.46	7.5361E-05	39.82	34.91	39.58	108.87	114.56	5.2
				15 MPa					
272.58	15.013	967.11	4.4998E-05	35.88	33.91	35.78	88.80	89.05	0.3
283.47	15.004	940.37	4.6277E-05	36.47	34.02	36.35	92.27	92.83	0.6
298.07	15.005	867.00	5.0194E-05	37.24	34.19	37.09	100.54	100.68	0.1
322.43	15.001	682.02	6.3807E-05	38.45	34.49	38.25	131.03	130.06	-0.7
352.99	15.001	412.49	0.0001055	39.82	34.91	39.58	126.51	130.32	3.0
								AAD	**5.1**

Table 5.20 Specific heat capacity calculations for CO_2+SO_2 system

T	P	Density	ν: Molar Vol	C_{pi}: CO_2	C_{pi}: H_2S	C_{pi}: CO_2+H_2S	Calced C_p	REFPROPP	Dev.
K	MPa	kg/m^3	m^3/mol	J/mol.K	J/mol.K	J/mol.K	J/mol.K	J/mol.K	%
				40 MPa					
273.55	40.023	1106.61	4.0671E-05	35.93	39.01	36.08	76.66	79.28	3.4
283.33	40.145	1078.76	4.1721E-05	36.46	34.02	36.34	76.54	79.51	3.9
298.11	40.060	1031.14	4.3648E-05	37.24	34.19	37.08	76.92	80.05	4.1
322.48	40.153	953.87	4.7184E-05	38.45	34.49	38.25	77.63	81.00	4.3
352.98	39.330	850.47	5.292E-05	39.82	34.91	39.58	78.39	82.41	5.1
				35 MPa					
273.54	35.043	1093.91	4.1143E-05	35.93	33.92	35.83	80.66	80.47	-0.2
283.32	34.989	1064.30	4.2288E-05	36.46	34.02	36.34	81.21	80.95	-0.3
298.10	35.077	1015.50	4.432E-05	37.24	34.19	37.08	82.07	81.79	-0.3
322.46	34.988	930.22	4.8383E-05	38.45	34.49	38.25	83.86	83.57	-0.4
352.97	35.014	821.42	5.4792E-05	39.82	34.91	39.58	85.51	85.47	-0.1
				30 MPa					
273.55	30.026	1079.37	4.1697E-05	35.93	33.92	35.83	82.95	81.93	-1.2
283.32	30.008	1047.27	4.2976E-05	36.46	34.02	36.34	83.82	82.68	-1.4
298.11	30.013	996.85	4.5149E-05	37.24	34.19	37.08	85.34	84.07	-1.5
322.47	29.929	902.37	4.9877E-05	38.45	34.49	38.25	88.50	87.09	-1.6
352.96	29.991	778.96	5.7779E-05	39.82	34.91	39.58	91.81	90.71	-1.2
				25 MPa					
273.55	25.039	1063.62	4.3152E-05	35.93	33.92	35.83	87.42	83.74	-4.2
283.32	25.025	1029.35	4.4009E-05	36.46	34.02	36.34	88.89	84.91	-4.5
298.10	25.050	975.15	4.6687E-05	37.24	34.19	37.08	91.66	87.09	-5.0
322.50	25.003	867.65	5.3224E-05	38.45	34.49	38.26	97.26	92.27	-5.1
352.95	25.002	723.72	6.4973E-05	39.82	34.91	39.58	103.82	99.40	-4.3
				20 MPa					
273.56	20.028	1046.04	4.3026E-05	35.93	33.92	35.83	91.74	86.08	-6.2
283.32	20.038	1008.74	4.4617E-05	36.46	34.02	36.34	93.99	87.89	-6.5
298.11	20.051	948.90	4.7431E-05	37.24	34.19	37.08	98.42	91.49	-7.0
322.49	20.012	824.32	5.4599E-05	38.45	34.49	38.26	109.99	101.39	-7.8
352.96	20.014	636.90	7.0666E-05	39.82	34.91	39.58	121.49	116.09	-4.4
				15 MPa					
273.57	14.951	1025.38	4.3893E-05	35.93	33.92	35.83	102.28	89.31	-12.7
283.32	15.011	984.11	4.5734E-05	36.46	34.02	36.34	106.18	92.24	-13.1
298.11	15.011	915.17	4.9179E-05	37.24	34.19	37.08	115.12	98.79	-14.2
322.52	15.012	753.20	5.9754E-05	38.45	34.49	38.26	146.76	123.24	-16.0
352.96	15.003	470.12	9.5734E-05	39.82	34.91	39.58	143.82	144.44	0.4
								AAD	**4.7**

Table 5.21 Estimated dew and bubble point results from density measurement data for CO_2+H_2S

Calculation	Experimental				Model (PR-CO_2)		Deviations	
	T	T	P	Density	P	Density	P	Density
	°C	K	MPa	kg/m^3	MPa	kg/m^3	%	%
Dew Point	-0.60	272.55	3.487	97.7	3.379	93.3	-3.1	-4.5
Dew Point	9.57	282.72	4.364	124.2	4.387	125.6	0.5	1.1
Dew Point	24.35	297.50	6.166	225.0	6.232	236.0	1.1	4.9
Bubble Point	-0.57	272.58	4.044	907.1	3.382	923.6	-16.4	1.8
Bubble Point	10.75	283.90	4.621	861.4	4.537	850.5	-1.8	-1.3
Bubble Point	24.92	298.07	6.320	714.3	6.313	731.9	-0.1	2.5
Absolute Average Deviation (AAD)							3.8	2.7

Table 5.22 Estimated dew and bubble point results from density measurement data for CO_2+SO_2

Calculation	Experimental				Model (PR-CO_2)		Deviations	
	T	T	P	Density	P	Density	P	Density
	°C	K	MPa	kg/m^3	MPa	kg/m^3	%	%
Dew Point	-0.50	272.65	3.129	106.2	3.225	89.8	3.1	-15.5
Dew Point	9.51	282.66	3.835	125.3	4.153	122.8	8.3	-2.0
Bubble Point	0.41	273.56	3.484	964.4	3.303	976.4	-5.2	1.2
Bubble Point	10.18	283.33	4.304	908.4	4.221	929.2	-1.9	2.3
Absolute Average Deviation (AAD)							4.6	5.3

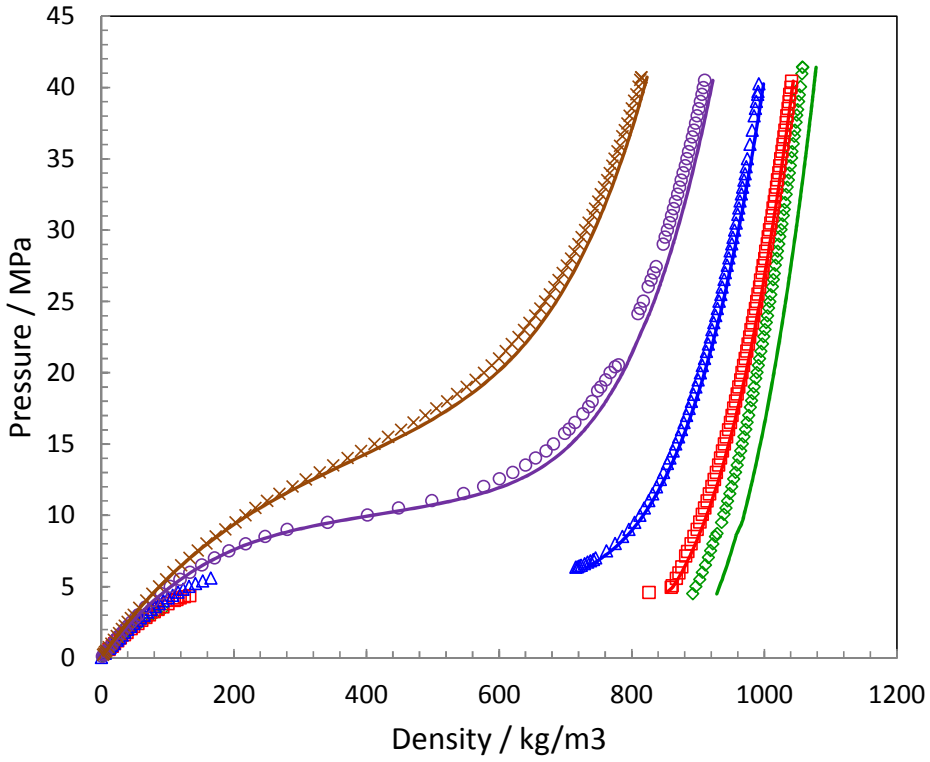

Figure 5.11 Experimental and modelling results of CO_2+H_2S at different isotherms, experimental results: (◊) 273. 15 K, (□) 283.15 K, (Δ) 298.15 K, (○) 323.15 K and (×) 353.15 K. Lines are the modelling results using PR-CO_2

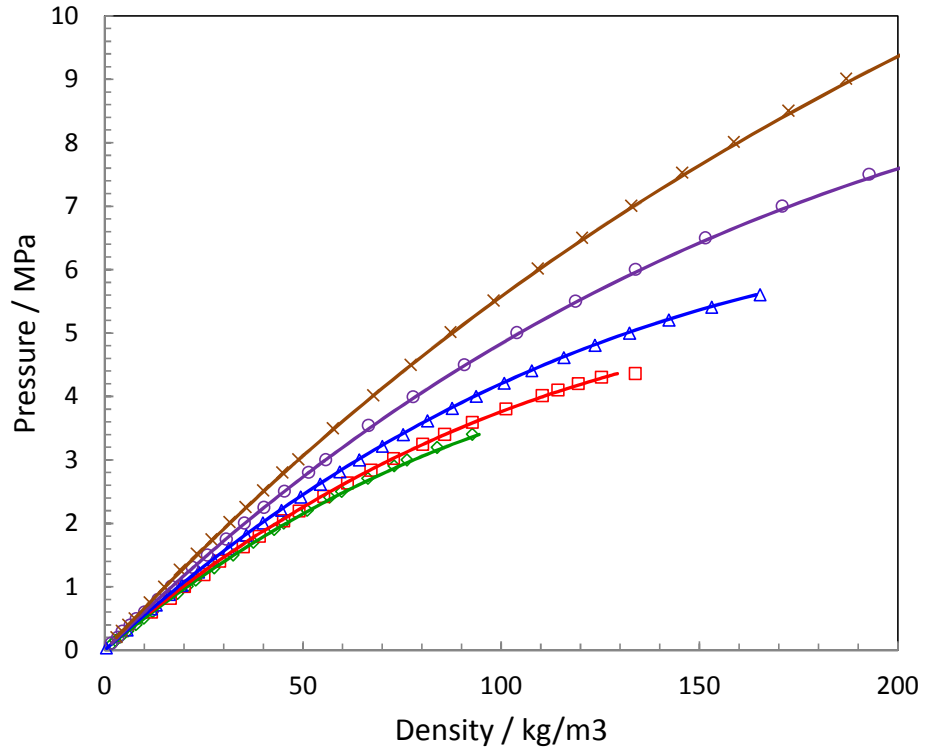

Figure 5.12 Experimental and modelling results of CO_2+H_2S at different isotherms at low pressures, experimental results: (◊) 273. 15 K, (□) 283.15 K, (Δ) 298.15 K, (○) 323.15 K and (×) 353.15 K. Lines are the modelling results using PR-CO_2

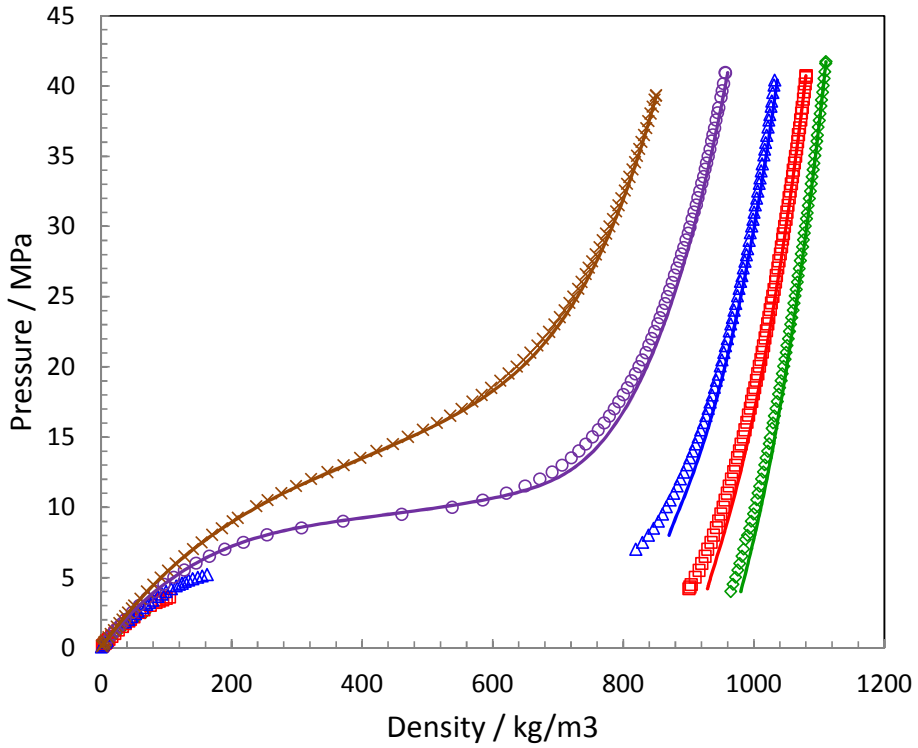

Figure 5.13 Experimental and modelling results of CO_2+SO_2 at different isotherms, experimental results: (◊) 273. 15 K, (□) 283.15 K, (Δ) 298.15 K, (○) 323.15 K and (×) 353.15 K. Lines are the modelling results using PR-CO_2

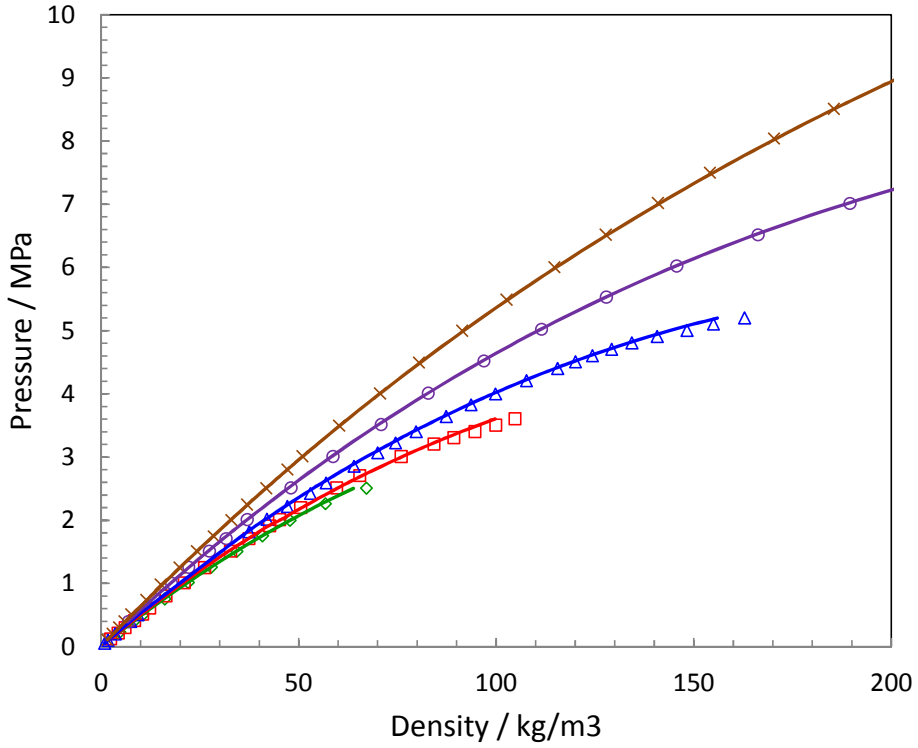

Figure 5.14 Experimental and modelling results of CO_2+ SO_2 at different isotherms at low pressures, experimental results: (◊) 273. 15 K, (□) 283.15 K, (Δ) 298.15 K, (○) 323.15 K and (×) 353.15 K. Lines are the modelling results using PR-CO_2

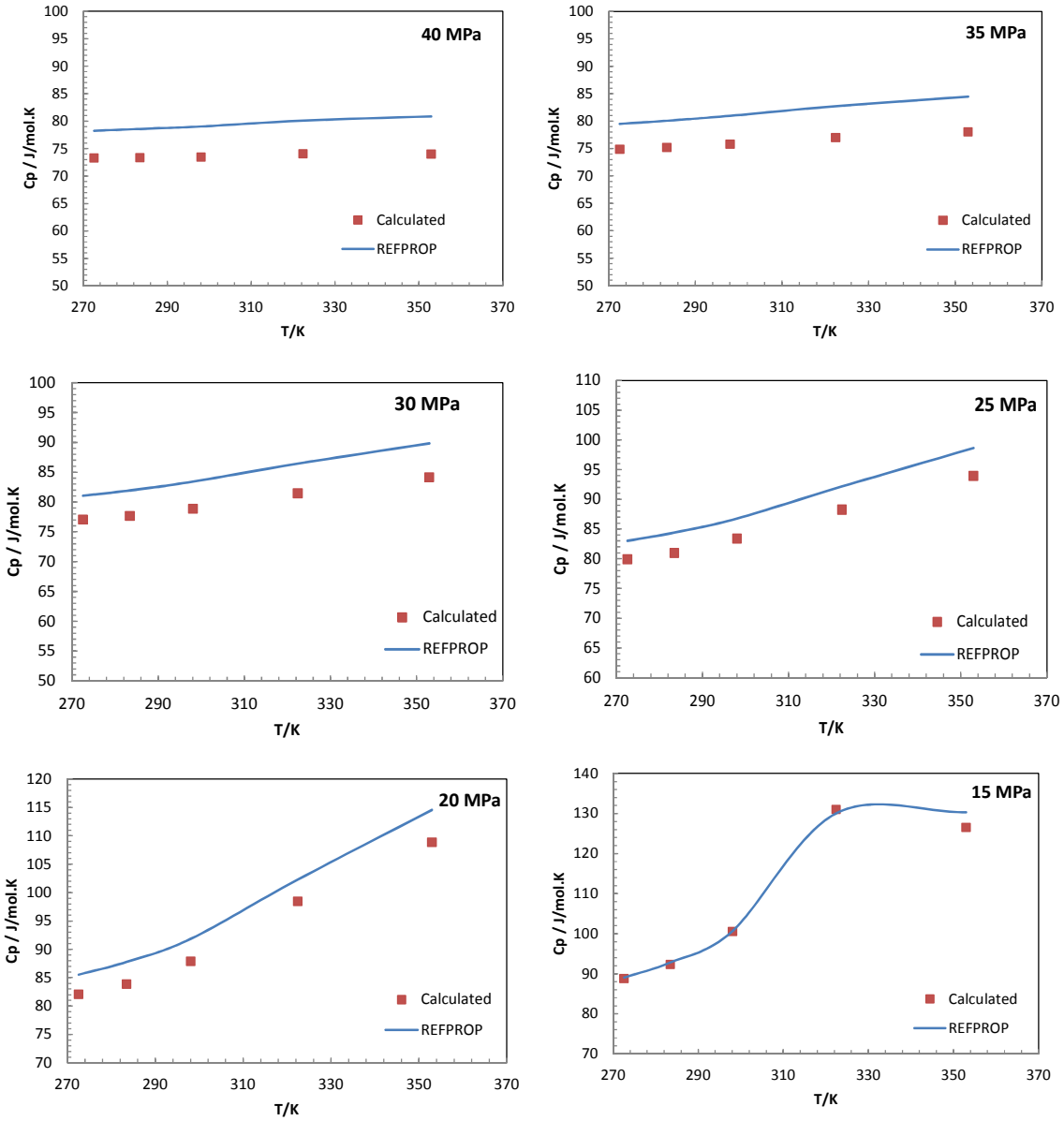

Figure 5.15 Specific heat capacity for CO_2+H_2S system

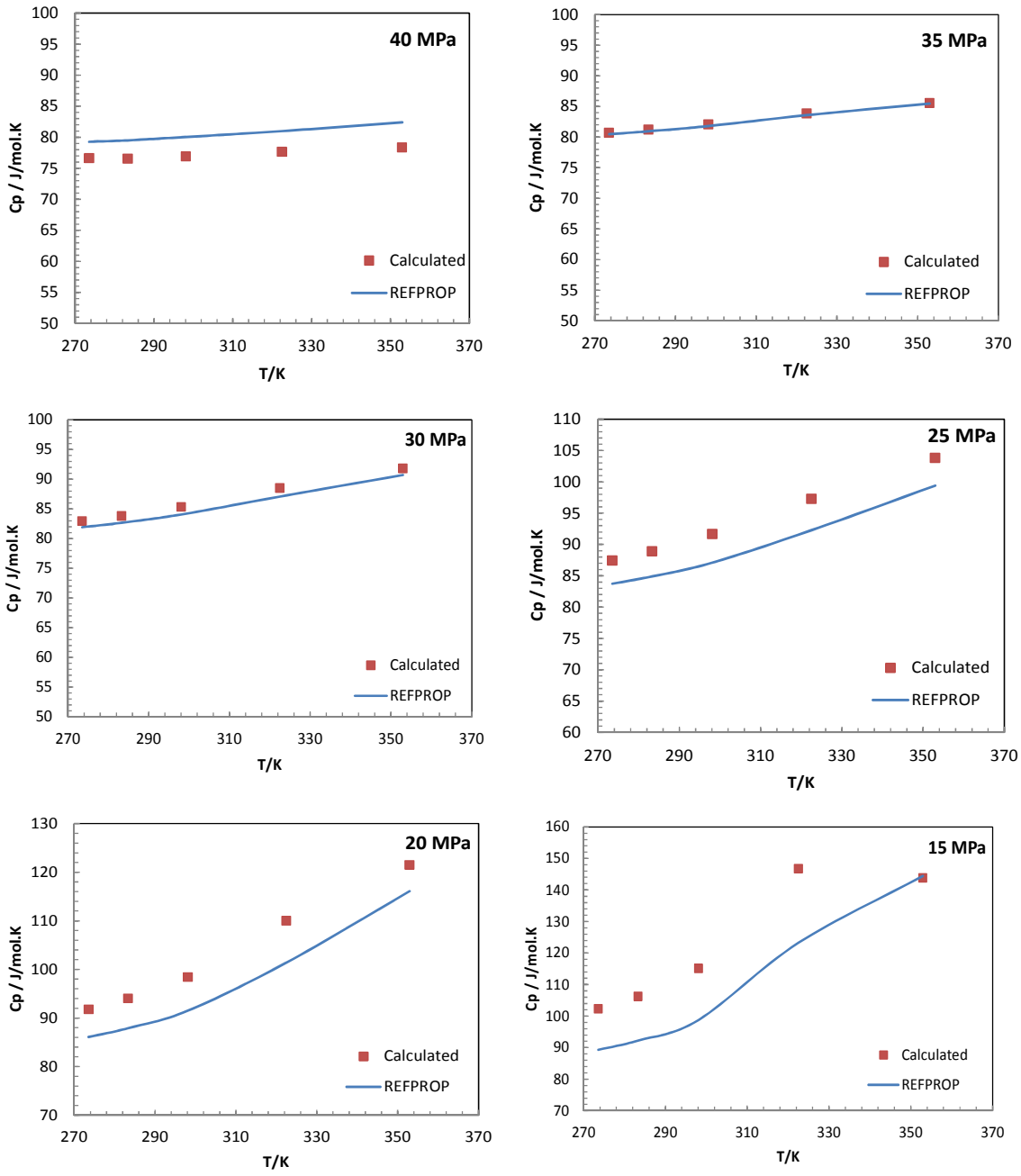

Figure 5.16 Specific heat capacity for CO_2+SO_2 system

REFERENCES

[1] D. W. and J. Driscoll, "Processing Considerations for Carbon Capture & Storage," *Kellog Pap. No. 2059*.

[2] R. A. Chadwick, *10 – Offshore CO2 storage: Sleipner natural gas field beneath the North Sea*. Elsevier, 2013.

[3] P. S. Ringrose, A. S. Mathieson, I. W. Wright, F. Selama, O. Hansen, R. Bissell, N. Saoula, and J. Midgley, "The In Salah CO2 Storage Project: Lessons Learned and Knowledge Transfer," *Energy Procedia*, vol. 37, pp. 6226–6236, 2013.

[4] J. A. Bierlein and W. B. Kay, "Phase-Equilibrium Properties of System Carbon Dioxide-Hydrogen Sulfide," *Ind. Eng. Chem.*, vol. 45, no. 3, pp. 618–624, Mar. 1953.

[5] D. P. Sobocinski and F. Kurata, "Heterogeneous phase equilibria of the hydrogen sulfide–carbon dioxide system," *AIChE J.*, vol. 5, no. 4, pp. 545–551, Dec. 1959.

[6] J. C. H. and K. R. H. S. J. Kellerman, C. E. Stouffer, P. T. Eubank, "Thermodynamic Properties of CO2 + H2S Mixtures, GPA Research Report No. 143, prepared as part of GPA Project 842," *Ga Process. Assoc.*, 1995.

[7] C. E. Stouffer, S. J. Kellerman, K. R. Hall, J. C. Holste, B. E. Gammon, and K. N. Marsh, "Densities of Carbon Dioxide + Hydrogen Sulfide Mixtures from 220 K to 450 K at Pressures up to 25 MPa," *J. Chem. Eng. Data*, vol. 46, no. 5, pp. 1309–1318, Sep. 2001.

[8] A. Chapoy, C. Coquelet, H. Liu, A. Valtz, and B. Tohidi, "Vapour–liquid equilibrium data for the hydrogen sulphide (H2S)+carbon dioxide (CO2) system at temperatures from 258 to 313K," *Fluid Phase Equilib.*, vol. 356, pp. 223–228, Oct. 2013.

[9] Z. Caubet, F., Kompr, "Fluess. Gase Pressluft-Ind." Fluess. Gase Pressluft-Ind., 1904.

[10] V. Lachet, T. de Bruin, P. Ungerer, C. Coquelet, A. Valtz, V. Hasanov, F. Lockwood, and D. Richon, "Thermodynamic behavior of the CO2+SO2 mixture: Experimental and Monte Carlo simulation studies," *Energy Procedia*, vol. 1, no. 1, pp. 1641–1647, Feb. 2009.

[11] C. Coquelet, A. Valtz, and P. Arpentinier, "Thermodynamic study of binary and ternary systems containing CO2+impurities in the context of CO2 transportation," *Fluid Phase Equilib.*, vol. 382, pp. 205–211, Nov. 2014.

[12] C. Bouchot and D. Richon, "An enhanced method to calibrate vibrating tube densimeters," *Fluid Phase Equilib.*, vol. 191, no. 1–2, pp. 189–208, Nov. 2001.

[13] C. Coquelet, D. Ramjugernath, H. Madani, A. Valtz, P. Naidoo, and A. H. Meniai, "Experimental Measurement of Vapor Pressures and Densities of Pure Hexafluoropropylene," *J. Chem. Eng. Data*, vol. 55, no. 6, pp. 2093–2099, Jun. 2010.

[14] C. Bouchot and D. Richon, "Direct Pressure−Volume−Temperature and Vapor−Liquid Equilibrium Measurements with a Single Equipment Using a Vibrating Tube Densimeter up to 393 K and 40 MPa: Description of the Original Apparatus and New Data," *Ind. Eng. Chem. Res.*, vol. 37, no. 8, pp. 3295–3304, Aug. 1998.

[15] Health and Safety Executive, "Offshore COSHH essentials OCE6 Hydrogen sulphide," 2011.

[16] F. and R. A. (Defra) webmaster@defra. gsi. gov. u. Department for Environment, "Pollutant information - Defra, UK."

[17] K. Foxall, "Sulphurdioxide - General Information, Version 1," *CRCE HQ, HPA*, 2010.

[18] "Health and Safety - INRS." [Online]. Available: http://www.inrs.fr/. [Accessed: 20-Aug-2015].

[19] G. T. Saunders, *Laboratory Fume Hoods: A User's Manual*. New York, NY: John Wiley & Sons, Inc., 1993.

[20] SEFA1, *SEFA 1-2002 Recommended Practices for Laboratory Fume Hoods*. Scientific Equipment & Furniture Association, 2002.

[21] Health and Safety Executive, *EH40/2005 Workplace exposure limits, Containing the list of workplace exposure limits for use with the Control of Substances Hazardous to Health Regulations (as amended) , Second Edition*. 2011.

[22] BOC, "Safety data sheet Sulphur dioxide, version 1.5," 2011.

[23] M. M. Lemmon EW, Huber ML, "NIST standard reference database 23: reference fluid thermodynamic and transport properties – REFPROP version 8.0. Gaithersburg: National Institute of Standards and Technology, Standard Reference Data Program." 2007.

[24] F. A. Aly and L. L. Lee, "Self-consistent equations for calculating the ideal gas heat capacity, enthalpy, and entropy," *Fluid Phase Equilib.*, vol. 6, no. 3–4, pp. 169–179, Jan. 1981.

CHAPTER 6: FROST POINT MEASUREMENTS

This chapter presents the frost point of CO_2 mixtures containing impurities. Frost points were measured for multi-component mixtures with various impurities using a SETARAM BT 2.15 calorimeter. In the modelling part, a model based on classical thermodynamics was implemented and tested with the new experimental data.

6.1 Introduction

A good understanding of vapour/liquid-solid equilibrium of CO_2 and CO_2-mixtures at low temperature is an important issue regarding the safety assessment of CO_2 pipelines and the possibility of solid or 'dry ice' discharge during an accidental release or rapid decompression. Furthermore removal of CO_2 from high carbon dioxide content natural gas fields is important to the gas industry development since some undeveloped gas fields can have high CO_2 content. One challenge in developing such gas fields is the economical separation of CO_2 from the feed gas. A technique has been suggested based on frosting CO_2 at low temperature and separating the CO_2 solid from the natural gas, hence technologies are being developed to efficiently separate CO_2 especially in high CO_2 content feed gases. Therefore better understanding of vapour-solid equilibrium at low temperature is critical in designing such separation processes.

6.2 Literature review

Existing experimental data on CO_2 frost from CO_2-rich mixtures are scarce and normally focused on low CO_2 content systems. Pikaar [1] measured frost points in CO_2-methane systems for 1 to 20 mol% CO_2 concentration range. Agrawal [2] measured frost points in the CO_2-N_2-CH_4 system for 0.12 to 10.67 mol% CO_2 concentration range. And more recently, Le [3] measured the frost points in CO_2-CH_4, CO_2-CH_4-N_2 and CO_2-CH_4-C2H_6 systems for 1 to 2.93 mol% CO_2 concentration range. No data were found for systems of interest in CCS.

A literature review on solid-fluid equilibrium for systems containing carbon dioxide has been carried out. Data are widely available for carbon dioxide with methane, however very scarce for other hydrocarbon systems and not available for many of the other systems relevant to CCS.

Table 6.1 List of Sources for Solid-Fluid Equilibrium in mixtures of Carbon Dioxide - Methane

Temperature Range / K	CO_2/ mole fraction	Reference	Ref.
195 - 215	0.4 - 0.9	Donnelly and Katz, 1954	[4]
174 - 210	0.01 - 0.2	Pikaar, 1959	[1]
166.48 -177.59	0.019 - 0.052	Sterner, 1961	[5]
129.65 - 201.26	0.0016 - 0.205	Davis et al., 1962	[6]
110 -195	0.001 - 0.126	Cheung and Zander, 1968	[7]
126 - 138	0.0007 - 0.0024	Preston et al., 1971	[8]
138 -198	0.0012 - 0.11	Agrawal and Laverman, 1974	[2]
168 - 188	0.01 - 0.03	Le and Trebble, 2007	[3]
191 - 210	0.1 - 0.54	Longman et al., 2011	[9]
112 - 169.9	0.0002 - 0.02896	Shen et al., 2012	[10]
113.15 - 169.85	0.000172 - 0.02896	Gao et al., 2012	[11]
90.92 -215.37	0 - 1	Brewer and Kuarata, 1958	[12]
111.5 -128.0	0.00027 - 0.00148	Boyle, 1987	[13]
110 - 218.30	0.00031 - 1	Streich, 1970	[14]

Table 6.2 List of Sources for Solid-Fluid Equilibrium in mixtures of Carbon Dioxide – Ethane

Temperature Range / K	CO_2/ mole fraction	Reference	Ref.
130 - 170	0.02 - 0.067	Clark and Din, 1953	[15]
164 -180	0.025 - 0.076	Cheung and Zender, 1968	[7]
105 - 213	0.0001 - 0.91	Jensen and Kurata, 1971	[16]
130 -170	0.002 - 0.031	Brewer and Kuarata, 1958	[12]

Table 6.3 List of Sources for Solid-Fluid Equilibrium in mixtures of Carbon Dioxide – Propane

Temperature Range / K	CO_2/ mole fraction	Reference	Ref.
87 - 180	0.00001 - 0.057	Cheung and Zender, 1968	[7]
108 - 212	0.00025 - 0.82	Jensen and Kurata, 1971	[16]
105.0 - 180.2	0.00009 - 0.057	Brewer and Kuarata, 1958	[12]

Table 6.4 List of Sources for Solid-Fluid Equilibrium in mixtures of Carbon Dioxide Systems

System	Temperature/ K	CO_2/ mole fraction	Reference	Ref.
CO_2 - N_2	220 - 344	---	Brown et al., 1989	[17]
CO_2 - Ar	109 - 116	0.00008 - 0.0002	Preston et al., 1971	[8]
CO_2 - O_2	90	5 ppm	McKinley and Wang, 1960	[18]
CO_2 - O_2	91 - 107	>40 ppm	Rest et al., 1990	[19]
CO_2 - O_2	90 - 110	>100 ppm	De Stefani et al., 2002	[20]
CO_2 - H_2S	180 - 215	0.11 - 0.90	Sobocinski and Kurata, 1959	[21]

6.3 Experimental part

6.3.1 Equipment description

The SETARAM BT 2.15 calorimeter comprises of a calorimetric chamber, electrical or pneumatic peripherals and a liquid nitrogen supply. The calorimeter can work at temperatures from -196 °C to 200 °C with scanning rate of 0.01 to 1 K/min and cooling rate of 1 °C/min with liquid nitrogen. The calorimetric chamber can receive different types of experimental cells depending on the experiment to carry out. The calorimetric block is located in a vacuum-tight cylindrical chamber which is 1000 mm high and 360 mm in diameter.

Figure 6.1 represents a cross-sectional view of the instrument: the core is made up of the calorimetric block in which two cylindrical cavities are located inside, each one containing a calorimetric element: socket and flux-meter. The couples are built and arranged in such a way that they have good thermal contact with both the socket and the block.

The block and its thermostat form a compact assembly, heated by a peripheral coiled heating element. The regulation temperature sensor embedded in the thermostat inner wall controls this coil. The assembly is suspended from the upper part of the calorimeter through the metal pipes providing access to the cells. A composite tank, fixed hermetically to the upper part of the apparatus defines the calorimetric chamber. This chamber is kept under controlled atmosphere.

The high pressure cells are made of Inconel 265 which has working pressure of 600 bars and working temperature of -196 °C to 200 °C. The outside diameter of each cell is 16.92 mm, the height is 17 mm and the internal volume is 3.6 ml. The access to the cells is blocked with lids fitted with gaskets to ensure the sealing of the calorimetric chamber. This sealing is cancelled when the experimental cells are introduced, the chamber being

then set to the atmospheric pressure, while an appropriate gas flow prevents the entry of ambient air. Sealing must be restored during operation of the instrument. The cells are removable: the experimental setup is therefore prepared outside, and then introduced into the set-up when measuring. It remains accessible from the outside with rods or connecting tubes that penetrate into each corresponding pit. This provides the possibility of intervening the setup during the experiment, for mechanical control (valve), introduction of gas or liquid, etc.

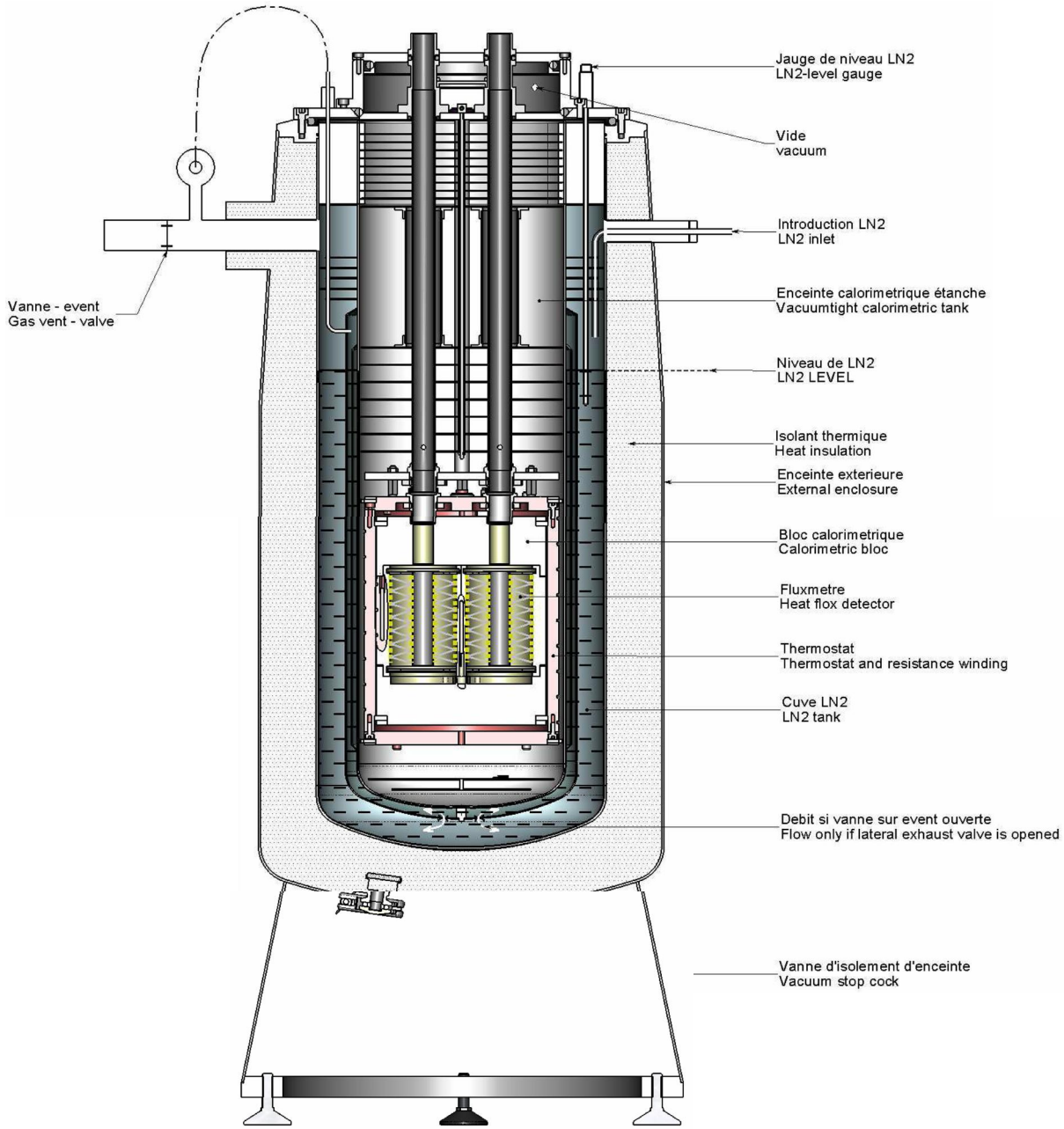

Figure 6.1 Cross-sectional view of the SETARAM BT 2.15

Pneumatic peripheral consists of vacuum pump and gas circuit. Vacuum pump is used to evacuate gas from the calorimetric chamber (air purging or gas changing). The calorimeter cannot operate satisfactorily in the presence of condensable compounds like water at temperature of liquid nitrogen. In addition, the choice of gas filling the calorimetric chamber enables the calorimeter specifications to be optimally adapted to the desired operating conditions.

6.3.2 Measurement procedure

First, the sample can be injected to the vacuumed cell by connecting the cylinder containing sample fluid through a valve on top of the calorimeter and connecting tubes inside the calorimeter. The mass of the injected sample should be measured by weighing the sample cylinder before and after injection into the cell. After reaching the desired pressure and disconnecting cylinder from the calorimeter, vacuum should be applied inside the chamber using the vacuum pump. Then, helium should be injected into the chamber up to 200 mbar. To make sure of the vacuum conditions inside the chamber, the process of vacuuming and helium injection can be repeated. Then, to cool down the chamber temperature to the desired temperature (about -70 °C to make sure that the sample is frozen), liquid nitrogen can be injected at constant flow rate from the fully insulated tank containing liquid nitrogen by opening the two valves on top of the tank. The injected liquid nitrogen then flows through the tube connected to the jacket surrounded the chamber. The Calisto data acquisition programme installed on the system can control the process of heating up. First, to reach equilibrium in both the sample and furnace, the temperature should be kept constant for 3 hours at -70 °C. The furnace then can be heated up with scanning rate of 0.05 °C/min till reaching -40 °C and after that the temperature should be kept constant at -40 °C for another 3 hours. The total time of the test would be 16 hours.

In order to find the pressure of the system at the frost point, the pressure of the cell also should be recorded. Sample and furnace temperatures versus time and heat flow can be monitored directly from the programme during the test. When the sample starts to melt, the heat flow reduces sharply due to melting of the sample. By processing the data using the programme, the onset point of the sample and the corresponding time can be obtained.

6.4 Modelling

A full description of the model can be found in Longman et al. [4]. In summary the model is based on the equality of fugacity in all phases where the fugacity of solid CO_2 is calculated from:

$$f_{CO2}^{Solid} = P_{CO2}^{Sub}\varphi_{CO2}^{Sub} e^{\frac{V_{CO2}^{Solid}}{RT}(P-P_{CO2}^{Sub})}$$

where P_{CO2}^{Sub} is the sublimation pressure of CO_2, φ_{CO2}^{Sub} is fugacity coefficient of CO_2 at the sublimation pressure at the system temperature T, V_{CO2}^{Solid} is the CO_2 solid specific volume at the triple point temperature.

6.5 Results and discussion

The measurements were carried out in the calorimeter for MIX 1, MIX 2, MIX 3 and MIX 4. The experimental data and modelling results for the measured systems are reported in Table 6.5 for MIX 1, Table 6.6 for MIX 2, Table 6.7 for MIX 3 and Table 6.8 for MIX 4 and plotted with the predicted vapour-solid, vapour-liquid, liquid-solid and vapour-liquid-solid zones in Figure 6.2 and Figure 6.3 for MIX 1, Figure 6.4 and Figure 6.5 for MIX 2, Figure 6.6 and Figure 6.7 for MIX 3 and Figure 6.8 and Figure 6.9 for MIX 4. In these graphs, the first figure for each mixture shows the measured and predicted frost point for the all pressure ranges and the second figure illustrates those at lower pressures. The absolute average deviations (AAD) of the thermodynamic model predictions from the experimental data of frost points measured in calorimeter are 0.5%, 0.4%, 0.2% and 0.6% for the MIX1, MIX 2, MIX 3 and MIX 4, respectively. The frost points of the mixture also were measured using an equilibrium set-up at lower pressures which is in good agreement with both model predictions and calorimeter experimental data. The circle points with pink colour in Figure 6.2 to Figure 6.9 show the results measured by the equilibrium set-up. Also as seen in the figures, for these systems the thermodynamic model using Peng-Robinson equation of state with k_{ij} tuned on VLE data [22] is in good agreement with the new experimental data. The blue square points and yellow diamond points show the measured bubble and dew points, respectively [22]. For this system, we have first a vapour + solid CO_2 line (P is more or less exponentially increasing with T), then a vapour +liquid + solid line (the pressure has a high temperature dependency and is

decreasing with increasing temperature) and finally a solid + liquid line where the pressure has also high temperature dependency but is increasing with increasing temperature.

6.6 Conclusions

Frost point for multi-component mixtures (MIX 1, 2, 3 and 4) were measured with the high pressure calorimeter.

The predictions of the developed model are compared against independent experimental data and the data generated in this work over a wide range of temperature, pressure and CO_2 concentration. A good agreement between predictions and experimental data is observed, demonstrating the reliability of the developed model.

Table 6.5 Experimental Frost Points of MIX 1 using the calorimeter BT 2.15

T / K	T / °C	P / psia	P / bar	P / MPa	T / K	Deviation
(±0.01)	**(±0.01)**	**(±0.1)**	**(±0.007)**	**(±0.0007)**	**PR-CO_2**	**%**
215.59	-57.56	92	6.34	0.634	216.24	0.3
215.62	-57.54	102	7.03	0.703	216.19	0.3
215.49	-57.66	126	8.69	0.869	216.08	0.3
215.65	-57.50	147	10.14	1.014	215.99	0.2
215.77	-57.38	154	10.62	1.062	215.96	0.1
215.73	-57.42	304	20.96	2.096	215.51	-0.1
213.44	-59.71	740	51.02	5.102	215.22	0.8
213.99	-59.16	809	55.78	5.578	215.31	0.6
212.86	-60.29	971	66.95	6.695	215.54	1.3
215.02	-58.13	1029	70.95	7.095	215.62	0.3
213.90	-59.25	1245	85.84	8.584	217.39	1.6
217.03	-56.12	1451	100.04	10.004	217.70	0.3
Absolute Average Deviation (AAD)						**0.5**

Table 6.6 Experimental Frost Points of MIX 2 using the calorimeter BT 2.15

T / K	T / °C	P / psia	P / bar	P / MPa	T / K	Deviation
(±0.01)	**(±0.01)**	**(±0.1)**	**(±0.007)**	**(±0.0007)**	**PR-CO_2**	**%**
215.64	-57.51	116	8.00	0.800	216.12	0.2
215.06	-58.09	268	18.48	1.848	215.39	0.2
214.67	-58.49	418	28.82	2.882	214.73	0.0
213.98	-59.17	863	59.50	5.950	213.04	-0.4
212.46	-60.69	1490	102.73	10.273	213.75	0.6
212.54	-60.61	2538	174.99	17.499	215.06	1.2
Absolute Average Deviation (AAD)						**0.4**

Table 6.7 Experimental Frost Points of MIX 3 using the calorimeter BT 2.15

T / K	T / °C	P / psia	P / bar	P / MPa	T / K	Deviation
(±0.01)	**(±0.01)**	**(±0.1)**	**(±0.007)**	**(±0.0007)**	**PR-CO_2**	**%**
212.63	-60.52	106	7.31	0.731	212.37	-0.1
211.63	-61.52	142	9.79	0.979	211.67	0.0
210.54	-62.61	190	13.10	1.310	210.84	0.1
209.20	-63.95	945	65.16	6.516	208.73	-0.2
208.89	-64.26	945	65.16	6.516	208.73	-0.1
208.16	-64.99	1160	79.98	7.998	208.95	0.4
208.52	-64.63	1230	84.81	8.481	209.02	0.2
207.88	-65.27	1430	98.60	9.860	209.22	0.6
Absolute Average Deviation (AAD)						**0.2**

Table 6.8 Experimental Frost Points of MIX 4 using the calorimeter BT 2.15

T / K	T / °C	P / psia	P / bar	P / MPa	T / K	Deviation
(±0.01)	**(±0.01)**	**(±0.1)**	**(±0.007)**	**(±0.0007)**	**PR-CO_2**	**%**
205.21	-67.94	80	5.52	0.552	206.86	0.8
211.33	-61.82	130	8.96	0.896	211.86	0.2
211.67	-61.48	142	9.79	0.979	211.83	0.1
211.22	-61.94	218	15.03	1.503	210.99	-0.1
208.87	-64.29	350	24.13	2.413	209.17	0.1
207.95	-65.20	640	44.13	4.413	205.58	-1.1
208.84	-64.32	672	46.33	4.633	205.31	-1.7
206.72	-66.43	1490	102.73	10.273	205.63	-0.5
Absolute Average Deviation (AAD)						**0.6**

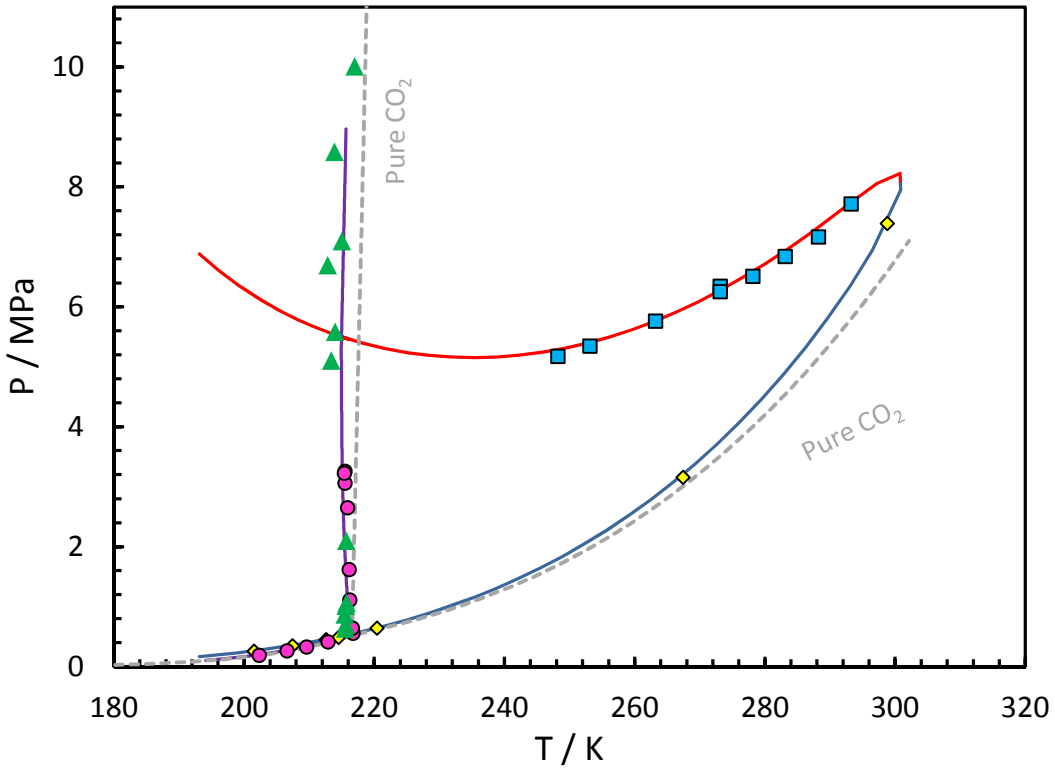

Figure 6.2 Phase behaviour and frost points of MIX 1 using calorimeter (▲) (Lines: Model predictions using the PR-EoS)

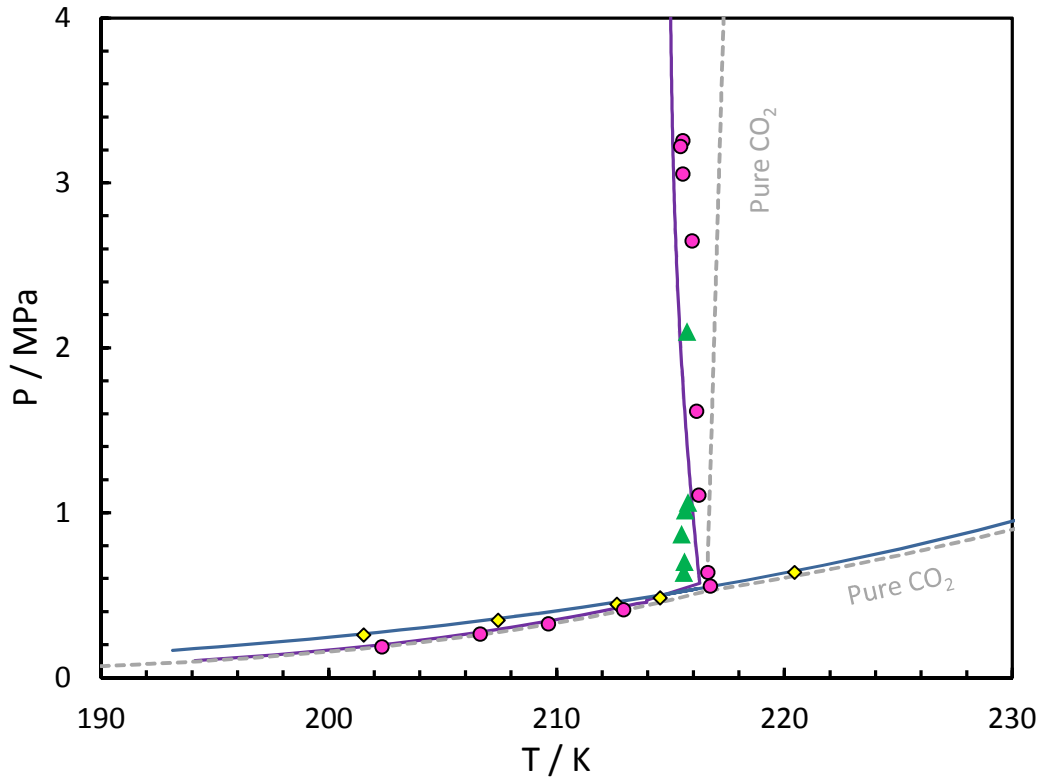

Figure 6.3 Frost points of MIX 1 using calorimeter (▲) at low pressures

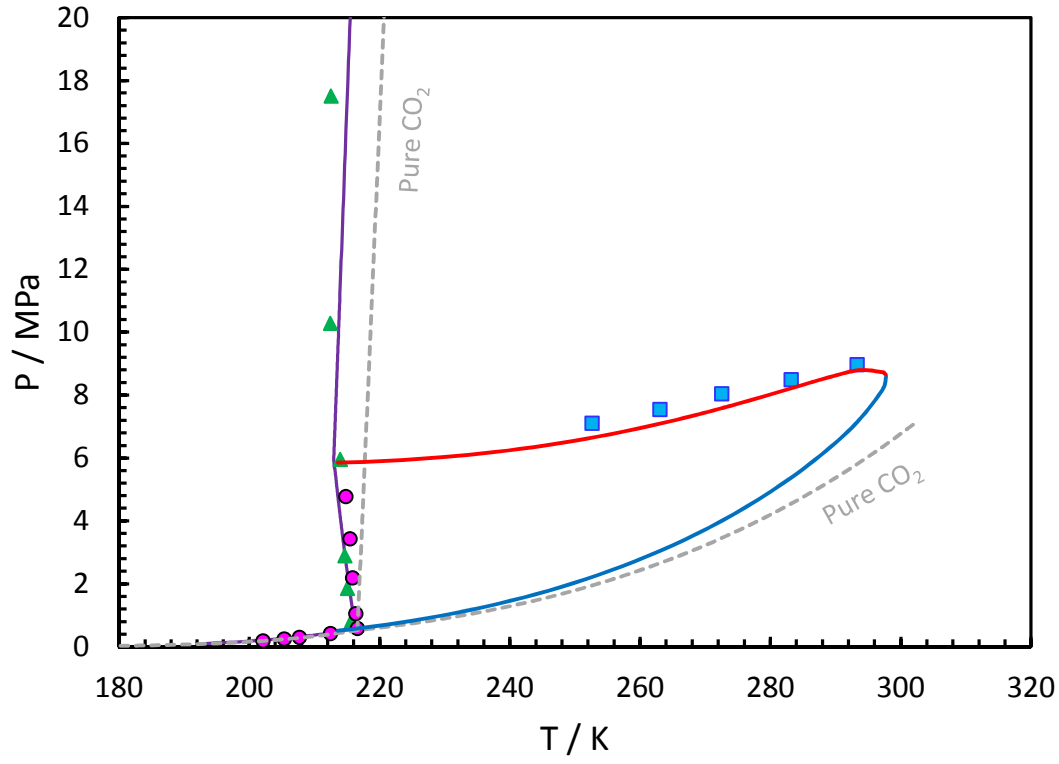

Figure 6.4 Phase behaviour and frost points of MIX 2 using calorimeter (▲) (Lines: Model predictions using the PR-EoS)

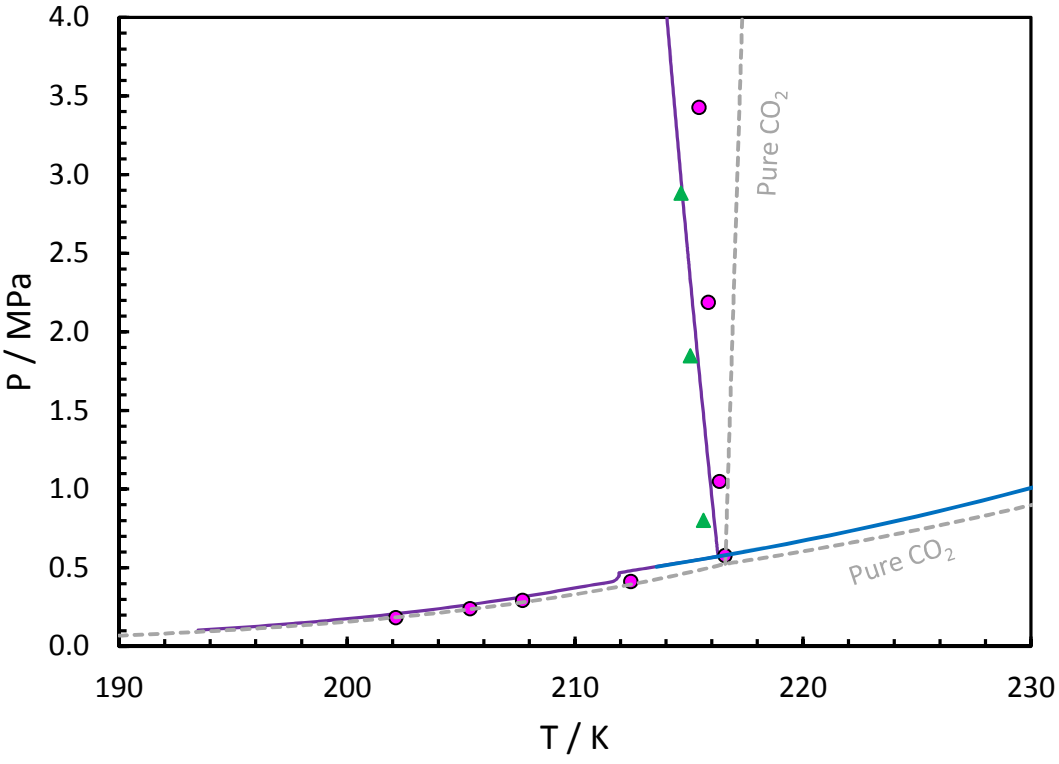

Figure 6.5 Frost points of MIX 2 using calorimeter (▲) at low pressures

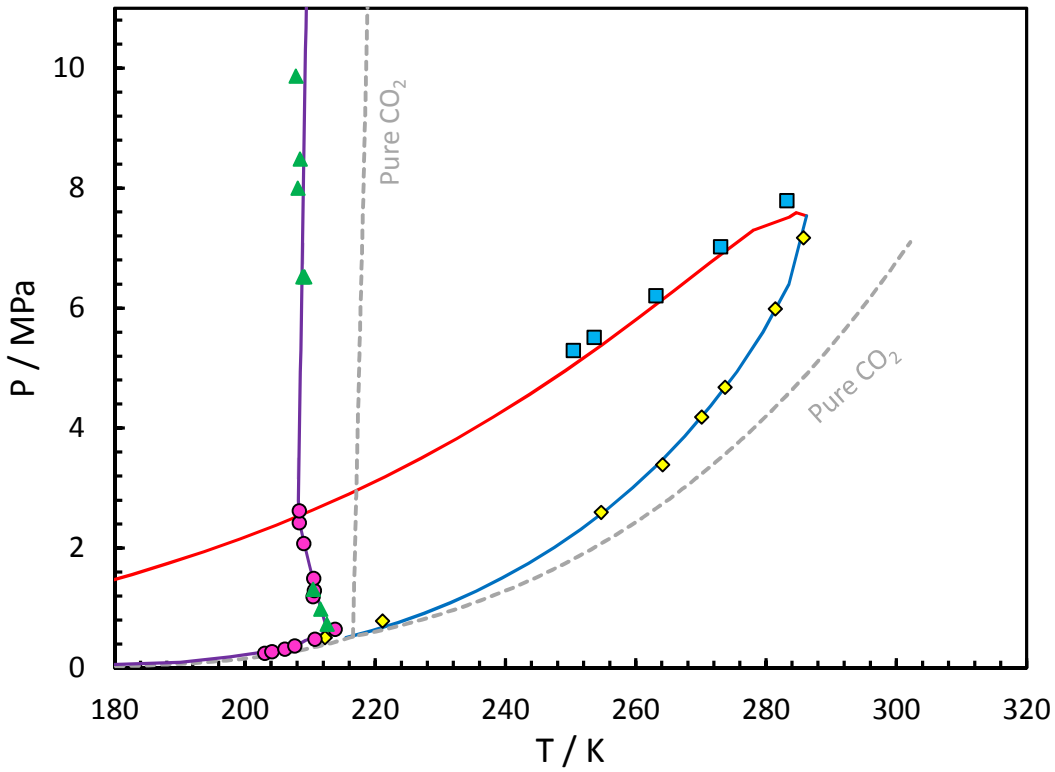

Figure 6.6 Phase behaviour and frost points of MIX 3 using calorimeter (▲) (Lines: Model predictions using the PR-EoS)

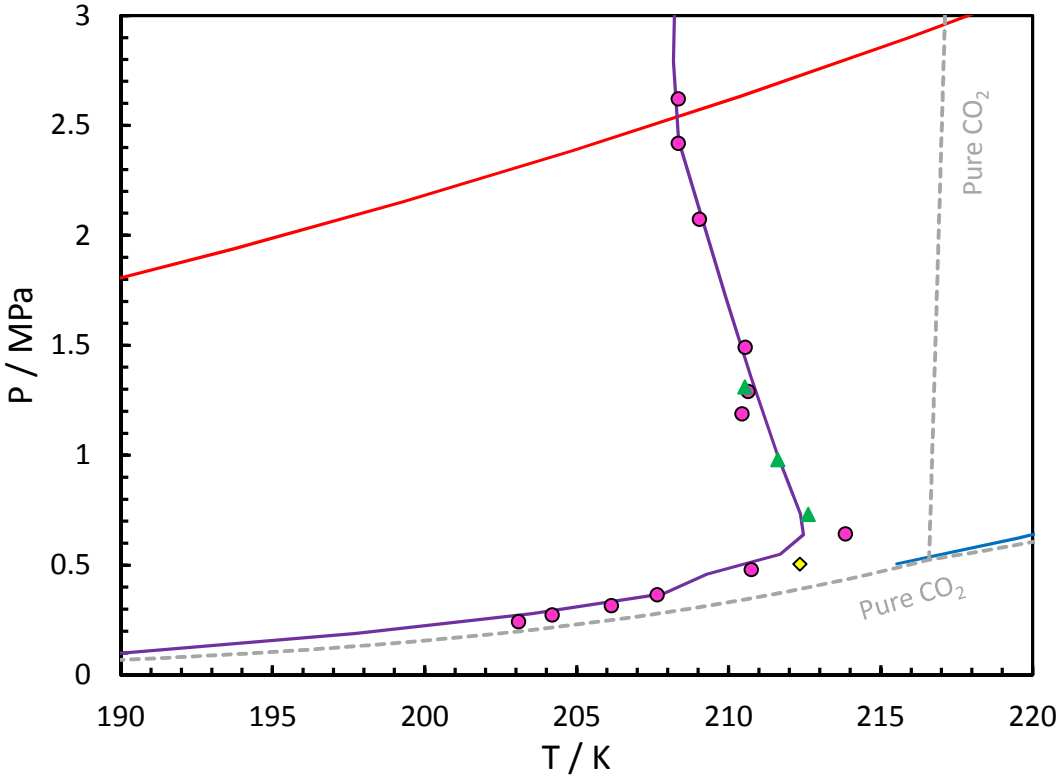

Figure 6.7 Frost points of MIX 3 at low pressures using calorimeter (▲)

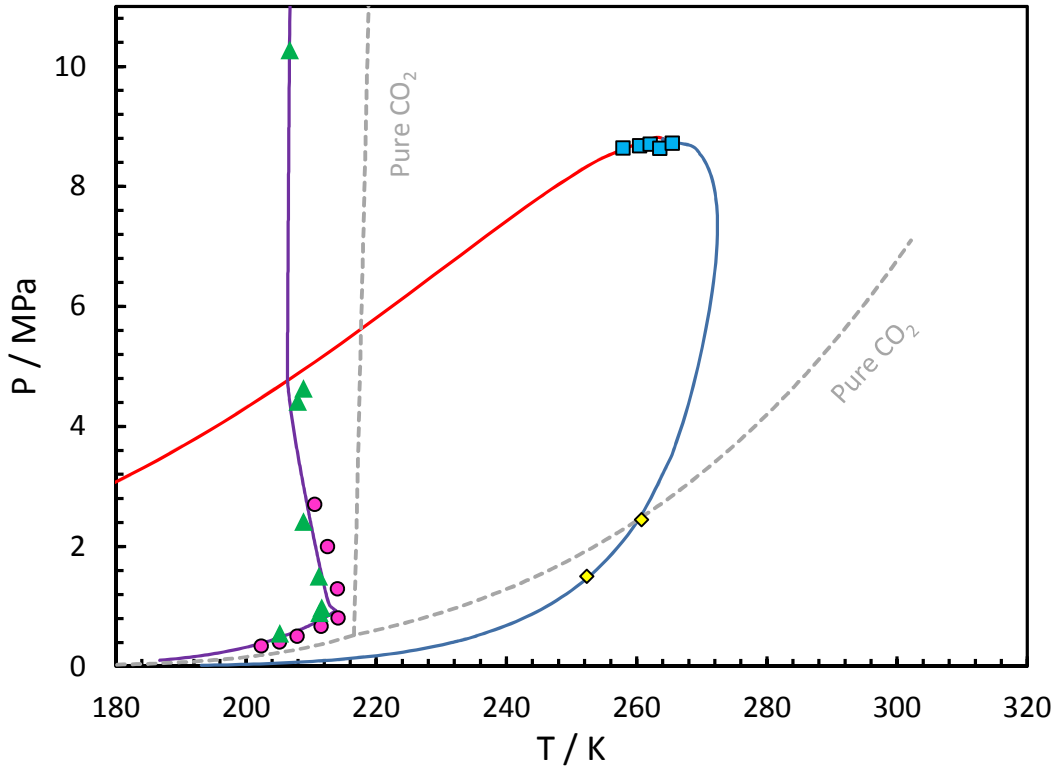

Figure 6.8 Phase behaviour and frost points of MIX 4 using calorimeter (▲) (Lines: Model predictions using the PR-EoS)

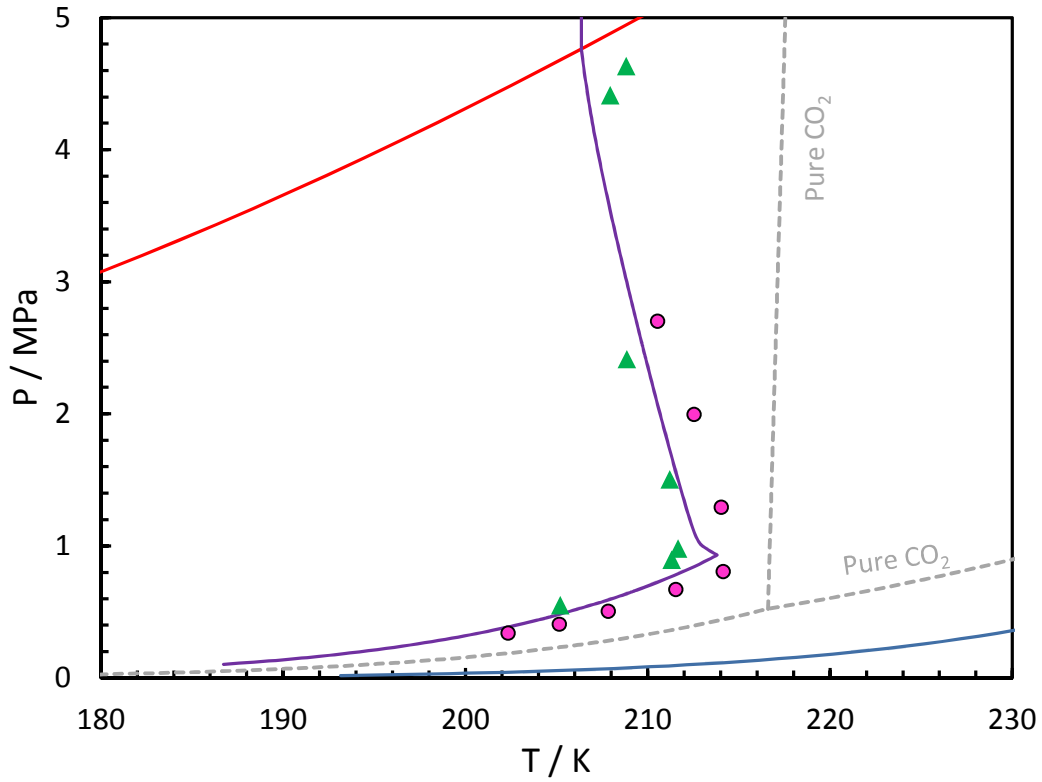

Figure 6.9 Frost points of MIX 4 using calorimeter (▲) at low pressures

REFERENCES

[1] M. J. Pikaar, "Study of phase equilibria in hydrocarbon-CO2 systems," *Thesis (doctoral)--University of London*, 1959.

[2] G. M. Agrawal, R. J. Laverman, "Phase Behavior of the Methane-Carbon Dioxide System in the Solid-Vapor Region," *Adv. Cryog. Eng.*, vol. 19, p. pp 327–338, 1995.

[3] T. Tan. Le and M. A. Trebble, "Measurement of Carbon Dioxide Freezing in Mixtures of Methane, Ethane, and Nitrogen in the Solid−Vapor Equilibrium Region," *J. Chem. Eng. Data*, vol. 52, no. 3, pp. 683–686, May 2007.

[4] H. G. Donnelly and D. L. Katz, "Phase Equilibria in the Carbon Dioxide–Methane System," *Ind. Eng. Chem.*, vol. 46, no. 3, pp. 511–517, Mar. 1954.

[5] C. J. Sterner, *Phase Equilibria in the CO2-Methane Systems*. Boston, MA: Springer US, 1961.

[6] J. A. Davis, N. Rodewald, and F. Kurata, "Solid-liquid-vapor phase behavior of the methane-carbon dioxide system," *AIChE J.*, vol. 8, no. 4, pp. 537–539, Sep. 1962.

[7] Cheung, H.E. Zender, H., "Solubility of carbon dioxide and hydrogen sulfide in liquid hydrocarbons at cryogenic temperatures," *Chem. Eng. Prog. Symp. Ser.*, vol. 64, no. 88, pp. 34–43, Jul. 1968.

[8] G. T. Preston, E. W. Funk, and J. M. Prausnitz, "Solubilities of hydrocarbons and carbon dioxide in liquid methane and in liquid argon," *J. Phys. Chem.*, vol. 75, no. 15, pp. 2345–2352, Jul. 1971.

[9] Longman. Z., Burgass, R., Chapoy, A., Tohidi, B., and Solbraa, E., "Measurement and Modeling of CO 2 Frost Points in the CO 2 –Methane Systems," *J. Chem. Eng. Data*, vol. 56, no. 6, pp. 2971–2975, Jun. 2011.

[10] T. Shen, T. Gao, W. Lin, and A. Gu, "Determination of CO 2 Solubility in Saturated Liquid CH 4 + N 2 and CH 4 + C 2 H 6 Mixtures above Atmospheric Pressure," *J. Chem. Eng. Data*, vol. 57, no. 8, pp. 2296–2303, Aug. 2012.

[11] T. Gao, T. Shen, W. Lin, A. Gu, and Y. Ju, "Experimental Determination of CO 2 Solubility in Liquid CH 4 /N 2 Mixtures at Cryogenic Temperatures," *Ind. Eng. Chem. Res.*, vol. 51, no. 27, pp. 9403–9408, Jul. 2012.

[12] J. Brewer and F. Kurata, "Freezing points of binary mixtures of methane," *AIChE J.*, vol. 4, no. 3, pp. 317–318, Sep. 1958.

[13] Boyle, T.B., Carroll, J.J., "Study determines best methods for calculating acid-gas density - Oil & Gas Journal.".

[14] M. Streich, "N2 Removal from Natural Gas," *Hyrocarbon Process.*, vol. 49, pp. 86–88, Sep. 1970.

[15] A. M. Clark and F. Din, "Equilibria between solid, liquid and gaseous phases at low temperatures. The system carbon dioxide + ethane + ethylene," *Discuss. Faraday Soc.*, vol. 15, p. 202, Jan. 1953.

[16] R. H. Jensen and F. Kurata, "Heterogeneous phase behavior of solid carbon dioxide in light hydrocarbons at cryogenic temperatures," *AIChE J.*, vol. 17, no. 2, pp. 357–364, Mar. 1971.

[17] T. S. Brown, V. G. Niesen, E. D. Sloan, and A. J. Kidnay, "Vapor-liquid equilibria for the binary systems of nitrogen, carbon dioxide, and n-butane at temperatures from 220 to 344 K.," *Fluid Phase Equilib.*, vol. 53, pp. 7–14, Dec. 1989.

[18] C. McKinley, E. S. J. Wang, "Hydrocarbon-Oxygen Systems Solubility," *Adv. Cryog. Eng.*, vol. 4, pp. 11–25, 1960.

[19] A. J. Rest, R. G. Scurlock, and M. F. Wu, "The solubilities of nitrous oxide, carbon dioxide, Aliphatic ethers and alcohols, and water in cryogenic liquids," *Chem. Eng. J.*, vol. 43, no. 1, pp. 25–31, Feb. 1990.

[20] V. De Stefani, A. Baba-Ahmed, A. Valtz, D. Meneses, and D. Richon, "Solubility measurements for carbon dioxide and nitrous oxide in liquid oxygen at temperatures down to 90 K," *Fluid Phase Equilib.*, vol. 200, no. 1, pp. 19–30, Jul. 2002.

[21] D. P. Sobocinski and F. Kurata, "Heterogeneous phase equilibria of the hydrogen sulfide–carbon dioxide system," *AIChE J.*, vol. 5, no. 4, pp. 545–551, Dec. 1959.

[22] Antonin Chapoy, Mahmoud Nazeri, Mahdi Kapateh, Rod Burgass, Bahman Tohidi, Christophe Coquelet "Impact of Common Impurities on CO2 Capture, Tr ansport and Storage 2011 – 2014 PROGRAMME FINAL REPORT," 2014.

CHAPTER 7: CONCLUSIONS AND RECOMMENDATIONS FOR FUTURE WORK

7.1 Conclusions

In order to proper design and sizing of the equipment and pipeline to transport carbon dioxide containing impurities from the captured point to storage/injection site, as mentioned in the early chapters, the availability of accurate models to predict the thermo-physical properties of high CO_2 content fluids is of crucial. The existing equations of state and transport property prediction models, available in the oil and gas industry, may not be accurate for the high CO_2 concentration fluids in the carbon capture and storage. On the other hand, evaluation of these existing models is challenging due to the lack of experimental data of CO_2 systems with impurities. Therefore, the primary aim of this work was to generate numerous experimental density and viscosity data over wide pressure and temperature ranges to be able to evaluate / modify the existing equations of states and transport property prediction models. The particular emphasis of this work was focused on the impact of impurities such as hydrocarbons, non-condensable gases and toxic gases on the thermo-physical properties of the CO_2-rich fluids. The importance of these properties is evident in the CO_2 transport pipelines because of their impact on the sizing of equipment as well as health, safety and environmental issues.

The type and concentration of the impurities in CO_2-rich fluids depends on the source and process of the capture part. Also, apart from the CCS chain, some accumulation of high CO_2 concentration fluids can be happen in geological structures. Different binary and multi component mixtures have been suggested in chapter 2 to cover the possible compositions of the streams producible from various sources and deployed capturing technologies. The impurities, which have been investigated in this work are methane, ethane, propane, iso-butane, n-butane, n-pentane, hydrogen, nitrogen, oxygen, carbon monoxide, argon, hydrogen sulphide and sulphur dioxide. The concentration of the impurities varied from as low as 4 mol% to as high as 50 mol% in multi component

mixtures. In pre-combustion capturing technology, hydrogen could be one of the impurities in the CO_2 fluid. Due to the small size of the hydrogen molecule in comparison to carbon dioxide molecule, two particular hydrogen binary systems have been investigated.

Undoubtedly, thermodynamic properties of CO_2 mixtures play an important role in the design and modelling of CO_2 infrastructures. Chapter 3 concentrated on the density measurement and modelling of the suggested binary and multi component mixtures. The densities of the mixtures were measured in the gas, liquid and supercritical regions after calibrations using pure CO_2 at each desired isotherm. It has been concluded that the uncertainty of measurements in the gas phase is much higher than dense liquid / supercritical phase. The standard uncertainty of pressure transducer in the lower pressure can result in the high expanded uncertainty of the measured density in the gas phase. Also, it is obvious that the uncertainties of the measurement at few points which are closed to the two-phase region are high due to the sharp changes of densities with pressure changes.

The importance of equations of state to predict the thermodynamic properties, particularly density, is evident. In the density modelling part of this work, two cubic equations of state, Peng-Robinson and Soave-Redlich-Kwong, have been studied. These two equations have been selected due to the popularity in the oil and gas industry and availability in commercial software packages. Also, CO_2 volume correction has been introduced to these cubic EoSs to improve the density prediction in the dense phase. It is concluded that generally both PR and SRK with CO_2 volume correction have acceptable predictions with Absolute Average Deviation (AAD) of 2.2% and 2.3%, respectively. The predictions by SRK in the gas phase are slightly more accurate than PR, while in the dense liquid / supercritical phase, predictions by PR are better than SRK. It also has been concluded that introducing the CO_2 volume correction to the original equations can improves the density predictions significantly in the dense liquid / supercritical phases. Overall, the AAD for PR has been reduced from 4.4% to 2.2% by introducing the CO_2 volume correction. That's for SRK has been reduced from 4.9% to 2.3%. The other conclusion worth noting is that the accuracy of predictions using CO_2 volume correction is higher than that of using Peneloux shift parameter.

Moreover, the reduction in density of pure CO_2 due to the presence of impurities in the supercritical phase also has been investigated for each mixture. It is concluded that a

maximum reduction of the pure CO_2 density at a given temperature of 323.15 K (50 °C) has been observed at pressures approximately 11 to 12 MPa depends on the composition of mixtures. Overall, lighter molecular weight impurities tend to reduce CO_2 density much more than those with a molecular weight close to pure CO_2.

Estimation of transport properties is imperative to analyse fluid flow behaviour and heat transfer from fluids to the environment. Viscosity is a key transport property for pipeline systems as well as sub-surface and process systems. Chapter 4 has focussed on the viscosity of CO_2-rich mixtures. Both experimental measurements and modelling practices are covered. The viscosities of proposed mixtures have been measured in the gas, liquid and supercritical phases. It has been concluded that, as expected, the uncertainty of measurements in the gas phase is higher than dense liquid / supercritical phases. Results from the measured viscosity data showed that presence of the impurities reduces the viscosity of the mixture compared to pure carbon dioxide in the dense liquid / supercritical phases. Conversely, the viscosity increases in the gas phase due to the presence of impurities. The extent of the reduction / increase depends on the type and concentration of the impurity. Generally, it concluded that the lighter the molecule, the higher the reduction in the viscosity of pure CO_2.

Extensive tuning and modifications also has been performed on the existing viscosity models available in the literature as well as in the oil and gas industry and commercial packages. The obtained viscosity data were employed to tune the Lohrenz-Bray-Clarck, (LBC) model, to match the experimental data. New parameters were calculated by optimising the parameters and the model with the specific set of parameters for CO2 fluids was renamed CO_2-LBC. The absolute average deviations (AAD) were calculated for both models and it has been concluded that the CO_2-LBC model has a lower AAD than original LBC as expected. The prediction improvement could be seen on the gas phase as well as in the dense liquid / supercritical phases. Moreover, the effect of density correction on the viscosity prediction using LBC and CO_2-LBC has been investigated. The conclusion comes from comparing the AAD of the models from experimental data. By applying the CO_2 volume correction to the Peng-Robinson equation of state, the AAD for the CO_2-LBC model were reduced from 18.1% to 8.5% while that of original LBC reduced from 19.9 to 10.8%.The conclusions drawn during the course of this study show that as the correlative LBC models are strong function of the mixture density, improving the density prediction using the CO_2 volume correction

can improve the viscosity predictions significantly. This improvement is more evident in the dense liquid / supercritical phases as the CO_2 volume correction is suitable to improve the density prediction in the dense phase. In the gas phase, as mentioned above, density predictions has been not effected by applying the CO_2 volume correction.

The predictive models investigated in this thesis were based on the corresponding states theory. The one reference fluid corresponding state model, Pedersen, has been modified by selecting pure CO_2 as a reference fluid for CO_2-rich systems. It is concluded that the modified model, CO_2-Pedersen, improved the viscosity predictions significantly. The absolute average deviation was reduced from 8.0% to 3.3%. The improvements in the viscosity predictions were in all phases. The two reference fluid corresponding state model, Aasberg-Petersen, also has been modified for CO_2-rich systems by changing the reference fluid from n-decane to carbon dioxide. The results show that the new model after modification, CO_2-CS2, predicts with greater accuracy particularly for hydrocarbon – carbon dioxide systems in the gas phase. The SUPERTRAP model, based on extended corresponding states (ECS) theory, has also been modified by changing the reference fluid from propane to carbon dioxide. It has been concluded that the new model, CO_2-SUPERTRAP, predicts well the viscosity of CO_2 systems in the liquid phase. The AAD of this model in the liquid phase is 4.2%. Totally, the original SUPERTRAP model over-predicts the viscosity while CO_2-SUPERTRAP model under-predicts the viscosity. In addition, the effect of density correction on viscosity prediction using this model has also been investigated. The SUPERTRAP model, similar to LBC, is a strong function of mixture density. The conclusion from the results is that applying the CO_2 volume correction can improve the viscosity prediction in the liquid phase significantly.

As a result, CO_2-Pedersen has been recommended to predict the viscosity of CO_2-rich systems in the gas phase as well as it is recommended for the dense liquid / supercritical phase.

Some natural gas reservoirs contains high amount of carbon dioxide and hydrogen sulphide. To transport / re-injection of these gases, as discussed in Chapter 5, the concentration of these gases should be limited. Therefore, to proper design of the facilities, access to reliable properties such as density, viscosity, specific heat capacity, etc. is imperative. Due to the toxicity of CO_2+H_2S and CO_2+SO_2 systems, there is no experimental data available in the literature. Therefore, in the experimental part, the

densities of above systems have been measured in the gas, liquid and supercritical phases. The uncertainty of the measurements also reported and concluded that it can be high in the gas phase and in area close to the phase boundary of two phase region. It also has been concluded that applying CO_2 volume correction to equations of states can improve the prediction accuracy for the acid gas and liquid systems. Moreover, by applying thermodynamic equations, the residual specific heat capacities of above systems were calculated from measured densities at different pressures and isotherms. By comparing the calculated properties to the predictions from software it has been concluded that there are a good agreement between the measured and predicted results. Numerous measurements of the density on both sides of dew and bubble point resulted in calculating the dew and bubble points for above systems. The comparison of the measured dew / bubble points to the predicted values by software shows that there is a good agreement between model data and experimental data for dew / bubble points.

Rapid release due to the leakage from CO_2 transport pipelines can make major safety problems. Due to the Joule-Thomson effect, solid CO_2 or dry ice can be formed. The frost point of the mixture has been measured using calorimeter and the results has been reported and discussed earlier in chapter 6. The results have been employed to evaluate the thermodynamic package predictions and it has been concluded that there is a good agreement between experimental data and model predictions.

7.2 Recommendations

Densities of MIXs 1, 2, 3, 4, 5 and 6 and CO_2-H_2 binaries were measured in this work. It is recommended to measure density and viscosity of CO_2+brine for storage purposes. In the modelling part, other equation of states can be studied using the generated experimental data. One of the best models to predict the density of the CO_2 mixtures can be Benedict-Webb-Rubin-Starling (BWRS) equation of state [1], which is recommended to use in oil and gas industry with satisfactory prediction of density. The other equation of state which is recommended is multi parameter equations of state, for instance, the GERG equation of state [2].

In this work, viscosities of MIXs 1, 2 and 3 and CO_2-H_2 binary systems were measured at various pressure and temperature ranges. It is recommended to measure viscosity of MIXs 4, 5 and 6 to cover a wider range and concentrations of impurities. In the modelling of viscosity both correlative and predictive models can be improved by some modifications. Viscosity in the LBC model is a strong function of reduced density of the

mixture and is not a function of temperature. The temperature dependant term, i.e., reduced temperature can be applied to consider temperature as well as the mixture density in the LBC model [3]. In SUPERTRAPP predictive model, mass shape factor can be applied to improve the model prediction [4]. Mass shape factor for the mixtures is a function of viscosity of each pure compound. In viscosity modelling using friction theory (f-theory), the friction law based on classical mechanics has been connected to the Van der Waals repulsive and attractive pressure terms. These repulsive and attractive pressure contributions may also predictable using other equations of state, e.g. SRK and PR. The friction theory already applied to predict viscosity of hydrocarbon systems [5]. This method also applied to predict viscosity of carbon dioxide + hydrocarbon systems [6]. It is recommended to evaluate this method further using the experimental data generated in this work.

During continuous density measurement using FPMC method [7], as described in chapter 5, heat capacity as well as dew and bubble points of the mixtures could be calculated and estimated from the measured density data. It is recommended that the Joule-Thomson coefficient also be calculated by equation below using the measured density data at various isotherms.

$$\mu_{JT} = \left(\frac{\partial T}{\partial P}\right)_H = -\frac{1}{C_p}\left[\nu - T\left(\frac{\partial \nu}{\partial T}\right)_P\right] \qquad (7\text{-}1)$$

The frost points of several CO_2-rich gas mixtures were measured using a SETARAM BT 2.15 calorimeter which has been discussed in chapter 6. The other property which can be measured using this calorimeter is the specific heat capacity of CO_2–rich mixtures. It is recommended to measure specific heat capacity of CO_2–rich mixtures which could provide vital information for thermal modelling

REFERENCES

[1] K. E. Starling, "Fluid Thermodynamic Properties for Light Petroleum Systems," *Gulf Publishing Company*, 1973.

[2] O. Kunz and W. Wagner, "The GERG-2008 Wide-Range Equation of State for Natural Gases and Other Mixtures: An Expansion of GERG-2004," *J. Chem. Eng. Data*, vol. 57, no. 11, pp. 3032–3091, Nov. 2012.

[3] Z. Al-Syabi, A. Danesh, B. Tohidi, A. . Todd, and D. . Tehrani, "A residual viscosity correlation for predicting the viscosity of petroleum reservoir fluids over wide ranges of pressure and temperature," *Chem. Eng. Sci.*, vol. 56, no. 24, pp. 6997–7006, 2001.

[4] Millat, J., Dymond, J.H., Nieto de Castro, C.A., "Transport Properties of Fluids Their Correlation, Prediction and Estimation | Chemical engineering | Cambridge University Press," *Cambridge University Press, IUPAC*, 2005.

[5] S. P. Tan, H. Adidharma, B. F. Towler, and M. Radosz, "Friction Theory and Free-Volume Theory Coupled with Statistical Associating Fluid Theory for Estimating the Viscosity of Pure n -Alkanes," *Ind. Eng. Chem. Res.*, vol. 44, no. 22, pp. 8409–8418, Oct. 2005.

[6] C. K. Zéberg-Mikkelsen, S. E. Quiñones-Cisneros, and E. H. Stenby, "VISCOSITY PREDICTION OF CARBON DIOXIDE + HYDROCARBON MIXTURES USING THE FRICTION THEORY," *Pet. Sci. Technol.*, Feb. 2007.

[7] C. Bouchot and D. Richon, "An enhanced method to calibrate vibrating tube densimeters," *Fluid Phase Equilib.*, vol. 191, no. 1–2, pp. 189–208, Nov. 2001.

Appendix

Table A. 1 Experimental and modelling results of BINARY 1 using SRK EoS

No	Phase	Temp.	Press.				Density (kg/m^3)			Absolute Deviation (%)		
		K (±0.1)	MPa (±0.02)	Exp.	*U(ρ)* kg/m^3	*U(ρ)* %	SRK-CO_2	SRK	SRK Pen	SRK-CO_2	SRK	SRK Pen
1	Gas	273.28	1.425	29.9	0.91	3.0	29.0	28.8	28.9	3.1	3.7	3.5
2	Gas	273.28	2.106	46.9	1.03	2.2	45.3	44.9	45.1	3.5	4.3	4.0
3	Liq.	273.28	10.730	910.1	1.14	0.1	872.2	793.8	841.2	4.2	12.8	7.6
4	Liq.	273.28	21.025	968.9	0.81	0.1	942.0	874.3	932.1	2.8	9.8	3.8
5	Liq.	273.28	51.473	1,062.2	0.61	0.1	1,044.9	993.0	1,068.3	1.6	6.5	0.6
6	Liq.	273.28	103.269	1,151.9	0.43	0.0	1,137.4	1,091.2	1,182.8	1.3	5.3	2.7
7	Liq.	273.28	124.556	1,179.3	0.33	0.0	1,164.1	1,117.6	1,213.8	1.3	5.2	2.9
8	Gas	283.35	1.438	28.9	0.85	3.0	27.8	27.7	27.8	3.9	4.0	3.8
9	Gas	283.33	2.099	41.7	0.94	2.3	42.5	42.3	42.5	2.0	1.6	1.9
10	Gas	283.32	4.515	115.9	1.75	1.5	117.3	114.4	115.4	1.2	1.3	0.5
11	Liq.	283.31	10.220	855.3	1.47	0.2	796.7	716.5	755.7	6.9	16.2	11.6
12	Liq.	283.31	20.702	934.3	0.87	0.1	896.6	827.3	880.1	4.0	11.5	5.8
13	Liq.	283.32	51.487	1,042.2	0.55	0.1	1,016.6	966.2	1,038.9	2.5	7.3	0.3
14	Liq.	283.31	105.354	1,139.5	0.33	0.0	1,119.0	1,076.3	1,167.4	1.8	5.5	2.4
15	Liq.	283.31	124.983	1,161.9	0.41	0.0	1,144.9	1,102.1	1,197.8	1.5	5.1	3.1
16	Gas	298.38	2.189	43.5	0.86	2.0	41.2	41.2	41.3	5.4	5.5	5.2
17	Gas	298.38	5.203	126.3	1.50	1.2	122.8	121.7	122.8	2.8	3.7	2.8
18	Liq.	298.37	10.096	654.1	3.05	0.5	633.1	560.3	584.8	3.2	14.3	10.6
19	Liq.	298.37	20.440	841.7	1.00	0.1	821.1	750.3	794.9	2.4	10.9	5.6
20	Liq.	298.38	51.445	986.1	0.55	0.1	973.5	924.4	993.0	1.3	6.3	0.7
21	Liq.	298.39	103.469	1,096.2	0.41	0.0	1,084.4	1,046.2	1,135.0	1.1	4.6	3.5
22	Liq.	298.38	124.467	1,127.4	0.33	0.0	1,114.7	1,077.1	1,171.5	1.1	4.5	3.9
23	Gas	323.44	2.051	36.5	0.74	2.0	34.4	34.3	34.4	5.9	6.0	5.7
24	Gas	323.47	5.251	104.1	1.02	1.0	101.7	101.1	102.0	2.3	2.8	2.0
25	Gas	323.48	10.358	298.8	2.74	0.9	300.8	278.6	284.8	0.7	6.8	4.7
26	SC	323.46	20.557	702.7	1.28	0.2	680.2	611.5	642.4	3.2	13.0	8.6
27	SC	323.44	51.982	914.3	0.57	0.1	902.4	854.9	916.5	1.3	6.5	0.2
28	SC	323.45	102.822	1,041.4	0.41	0.0	1,031.6	998.5	1,083.6	0.9	4.1	4.1
29	SC	323.45	125.382	1,078.7	0.41	0.0	1,068.3	1,037.2	1,129.3	1.0	3.8	4.7
30	Gas	373.54	1.996	27.8	0.60	2.2	28.0	28.0	28.0	0.9	0.7	0.9
31	Gas	373.54	5.210	77.6	0.70	0.9	78.6	77.9	78.5	1.3	0.5	1.1
32	Gas	373.54	10.392	178.6	0.91	0.5	177.7	173.0	175.6	0.5	3.1	1.7
33	Gas	373.55	17.543	356.2	1.20	0.3	351.0	323.7	333.0	1.4	9.1	6.5
34	SC	373.54	29.181	589.9	0.89	0.2	572.9	519.7	544.1	2.9	11.9	7.8
35	SC	373.55	52.182	777.9	0.55	0.1	762.2	717.1	764.4	2.0	7.8	1.7
36	SC	373.55	103.531	948.7	0.37	0.0	936.1	908.4	985.5	1.3	4.3	3.9
37	SC	373.55	124.391	991.2	0.34	0.0	978.5	954.1	1,039.6	1.3	3.7	4.9
38	Gas	423.45	2.065	28.0	0.51	1.8	25.2	25.1	25.2	10.0	10.3	10.1
39	Gas	423.45	5.231	67.1	0.56	0.8	66.4	65.7	66.1	1.0	2.1	1.5
40	Gas	423.45	10.475	139.6	0.64	0.5	141.6	137.9	139.7	1.4	1.3	0.0
41	Gas	423.45	20.833	302.1	0.74	0.2	306.7	286.9	294.8	1.5	5.0	2.4
42	SC	423.43	48.610	629.5	0.53	0.1	617.8	575.6	608.5	1.9	8.5	3.3
43	SC	423.45	104.123	859.4	0.34	0.0	851.2	825.1	894.2	1.0	4.0	4.1
44	SC	423.46	124.288	907.1	0.32	0.0	899.5	877.0	955.6	0.8	3.3	5.3
Absolute Average Deviation (AAD)										**2.3**	**6.1**	**3.9**

Table A. 2 Experimental and modelling results of BINARY 2

No	Phase	Temp.	Press.				Density (kg/m^3)			Absolute Deviation (%)		
		K (±0.1)	MPa (±0.02)	Exp.	$U(\rho)$ kg/m^3	$U(\rho)$ %	SRK-CO_2	SRK	SRK Pen	SRK-CO_2	SRK	SRK Pen
1	Gas	273.29	1.177	24.7	0.81	3.3	22.1	22.0	22.0	10.6	11.0	10.9
2	Gas	273.27	2.078	43.0	0.93	2.2	41.5	41.1	41.3	3.7	4.4	4.1
3	Gas	273.28	3.916	93.1	1.40	1.5	92.2	90.8	91.4	1.0	2.5	1.8
4	Liq.	273.26	20.564	829.8	0.85	0.1	852.2	795.9	842.1	2.7	4.1	1.5
5	Liq.	273.27	52.306	973.2	0.52	0.1	982.4	936.9	1,001.6	1.0	3.7	2.9
6	Liq.	273.27	103.290	1,076.7	0.33	0.0	1,081.4	1,039.6	1,119.9	0.4	3.4	4.0
7	Liq.	273.26	124.687	1,106.6	0.41	0.0	1,109.7	1,067.5	1,152.3	0.3	3.5	4.1
8	Gas	283.29	1.383	26.0	0.79	3.0	25.0	25.0	25.0	3.7	3.8	3.6
9	Gas	283.28	2.106	39.7	0.86	2.2	39.8	39.6	39.7	0.2	0.1	0.2
10	Gas	283.31	4.900	115.7	1.53	1.3	117.3	114.5	115.4	1.3	1.0	0.2
11	Liq.	283.30	14.412	794.4	1.28	0.2	734.7	677.1	711.1	7.5	14.8	10.5
12	Liq.	283.30	20.241	809.1	0.93	0.1	800.7	744.5	785.7	1.0	8.0	2.9
13	Liq.	283.32	52.629	899.0	0.52	0.1	954.9	910.9	973.5	6.2	1.3	8.3
14	Liq.	283.32	103.634	992.8	0.41	0.0	1,060.8	1,022.2	1,101.6	6.9	3.0	11.0
15	Liq.	283.32	124.467	1,022.9	0.33	0.0	1,090.0	1,051.2	1,135.3	6.6	2.8	11.0
16	Gas	298.38	2.058	39.4	0.78	2.0	36.0	35.9	36.0	8.7	8.8	8.6
17	Gas	298.37	5.210	113.8	1.22	1.1	109.9	109.0	109.8	3.4	4.2	3.4
18	Liq.	298.37	52.278	773.9	0.52	0.1	910.9	868.4	927.0	17.7	12.2	19.8
19	Liq.	298.37	102.842	936.9	0.38	0.0	1,028.1	993.7	1,071.1	9.7	6.1	14.3
20	Liq.	298.38	124.735	979.5	0.41	0.0	1,061.4	1,027.3	1,110.3	8.4	4.9	13.4
21	Gas	323.44	2.058	34.6	0.69	2.0	32.4	32.4	32.4	6.4	6.5	6.2
22	Gas	323.47	5.237	94.6	0.90	0.9	92.8	92.4	93.1	1.9	2.4	1.7
23	Gas	323.45	10.447	247.7	1.75	0.7	250.0	234.0	238.3	0.9	5.5	3.8
24	SC	323.44	26.518	531.2	0.94	0.2	667.2	616.1	646.6	25.6	16.0	21.7
25	SC	323.45	52.306	746.6	0.53	0.1	838.9	798.0	850.0	12.4	6.9	13.9
26	SC	323.46	104.136	913.2	0.37	0.0	979.6	950.1	1,024.6	7.3	4.0	12.2
27	SC	323.47	125.148	956.3	0.34	0.0	1,015.2	987.2	1,067.9	6.2	3.2	11.7
28	Gas	373.54	2.271	28.6	0.57	2.0	30.2	30.1	30.2	5.5	5.3	5.6
29	Gas	373.53	5.251	72.2	0.64	0.9	73.9	73.3	73.8	2.3	1.5	2.2
30	Gas	373.54	10.392	161.8	0.80	0.5	161.8	157.8	160.0	0.0	2.4	1.1
31	Gas	373.54	18.513	332.8	0.99	0.3	330.0	305.5	313.5	0.8	8.2	5.8
32	SC	373.53	36.462	528.3	0.68	0.1	589.8	546.6	573.0	11.7	3.5	8.5
33	SC	373.54	52.423	649.3	0.51	0.1	704.4	666.1	705.6	8.5	2.6	8.7
34	SC	373.52	104.880	861.1	0.35	0.0	887.6	863.0	930.6	3.1	0.2	8.1
35	SC	373.54	125.024	906.0	0.32	0.0	929.4	907.5	982.4	2.6	0.2	8.4
36	Gas	423.42	2.058	25.9	0.48	1.9	23.7	23.6	23.7	8.6	8.9	8.7
37	Gas	423.42	5.224	62.2	0.52	0.8	62.2	61.6	62.0	0.1	0.9	0.4
38	Gas	423.41	10.379	128.0	0.58	0.4	130.1	126.9	128.4	1.6	0.8	0.3
39	Gas	423.41	20.420	267.9	0.64	0.2	273.6	257.8	264.0	2.1	3.8	1.4
40	SC	423.41	38.906	464.4	0.55	0.1	492.3	457.0	477.0	6.0	1.6	2.7
41	SC	423.43	52.113	565.4	0.46	0.1	592.1	556.8	586.7	4.7	1.5	3.8
42	SC	423.45	103.999	783.9	0.32	0.0	802.7	779.5	839.5	2.4	0.6	7.1
43	SC	423.46	124.659	836.2	0.30	0.0	852.8	832.7	901.5	2.0	0.4	7.8
Absolute Average Deviation (AAD)										**5.2**	**4.4**	**6.7**

Table A. 3 Experimental and modelling results of MIX 1

No	Phase	Temp.	Press.				Density (kg/m^3)			Abs Deviation (%)		
		K (±0.1)	MPa (±0.02)	Exp.	*U(ρ)* kg/m^3	*U(ρ)* %	SRK-CO_2	SRK	SRK Pen	SRK-CO_2	SRK	SRK Pen
1	Gas	273.39	1.714	38.4	0.99	2.6	37.5	37.2	37.3	2.4	3.1	2.8
2	Gas	273.41	2.072	47.4	1.07	2.3	46.8	46.4	46.6	1.2	2.0	1.7
3	Gas	273.41	2.732	66.4	1.26	1.9	66.1	65.3	65.6	0.4	1.5	1.1
4	Liq.	273.40	6.710	888.0	1.40	0.2	890.2	797.0	844.5	0.2	10.2	4.9
5	Liq.	273.42	11.308	927.8	1.08	0.1	933.5	848.6	902.6	0.6	8.5	2.7
6	Liq.	273.41	21.803	983.9	0.81	0.1	994.3	922.6	986.9	1.1	6.2	0.3
7	Liq.	273.42	36.270	1,034.2	0.62	0.1	1,047.5	986.7	1,060.6	1.3	4.6	2.6
8	Liq.	273.42	51.734	1,073.6	0.52	0.0	1,088.7	1,034.5	1,115.9	1.4	3.6	3.9
9	Liq.	273.43	76.401	1,121.7	0.41	0.0	1,138.2	1,088.7	1,179.3	1.5	2.9	5.1
10	Liq.	273.41	104.377	1,164.4	0.43	0.0	1,180.9	1,132.9	1,231.3	1.4	2.7	5.7
11	Liq.	273.42	126.015	1,192.1	0.41	0.0	1,207.6	1,159.4	1,262.7	1.3	2.7	5.9
12	Gas	283.32	1.810	36.5	0.94	2.5	37.7	37.6	37.7	3.2	3.0	3.3
13	Gas	283.32	3.365	78.3	1.29	1.6	81.5	79.9	80.4	4.1	2.1	2.7
14	Liq.	283.28	6.359	810.8	1.63	0.2	795.0	698.5	735.5	1.9	13.8	9.3
15	Liq.	283.27	11.679	888.9	1.26	0.1	878.9	791.2	839.0	1.1	11.0	5.6
16	Liq.	283.28	22.567	956.3	0.84	0.1	957.5	885.1	945.3	0.1	7.4	1.1
17	Liq.	283.27	36.414	1,004.6	0.72	0.1	1,015.8	955.2	1,025.8	1.1	4.9	2.1
18	Liq.	283.28	54.129	1,052.1	0.52	0.0	1,066.9	1,014.9	1,094.9	1.4	3.5	4.1
19	Liq.	283.27	77.997	1,099.3	0.52	0.0	1,117.2	1,070.7	1,160.1	1.6	2.6	5.5
20	Liq.	283.27	105.093	1,141.3	0.43	0.0	1,160.7	1,116.2	1,213.8	1.7	2.2	6.3
21	Liq.	283.29	124.852	1,167.1	0.33	0.0	1,186.6	1,142.2	1,244.6	1.7	2.1	6.6
22	Gas	298.29	1.679	32.1	0.84	2.6	32.3	32.3	32.3	0.6	0.5	0.7
23	Gas	298.29	1.961	38.6	0.87	2.3	38.3	38.3	38.4	0.7	0.8	0.5
24	Gas	298.29	2.760	57.0	0.97	1.7	56.7	56.6	56.8	0.5	0.7	0.3
25	Gas	298.29	3.076	64.8	1.02	1.6	64.6	64.5	64.8	0.3	0.5	0.1
26	Liq.	298.33	12.553	778.4	1.68	0.2	782.2	693.3	730.9	0.5	10.9	6.1
27	Liq.	298.37	20.262	865.2	1.02	0.1	872.5	795.0	844.8	0.8	8.1	2.4
28	Liq.	298.36	50.117	999.6	0.59	0.1	1,012.8	960.5	1,034.2	1.3	3.9	3.5
29	Liq.	298.38	75.616	1,061.8	0.41	0.0	1,076.0	1,032.4	1,118.1	1.3	2.8	5.3
30	Liq.	298.38	103.393	1,111.8	0.43	0.0	1,125.8	1,086.0	1,181.1	1.3	2.3	6.2
31	Liq.	298.40	126.332	1,145.6	0.33	0.0	1,158.5	1,119.4	1,220.9	1.1	2.3	6.6
32	Gas	323.35	1.452	24.0	0.73	3.0	24.9	24.9	25.0	4.0	3.9	4.1
33	Gas	323.35	2.189	37.4	0.77	2.1	38.7	38.7	38.8	3.6	3.5	3.8
34	Gas	323.34	3.599	66.0	0.89	1.3	67.9	67.7	68.1	3.0	2.7	3.3
35	Gas	323.34	5.217	104.6	1.07	1.0	107.2	106.7	107.6	2.5	2.0	2.9
36	Gas	323.35	8.266	209.5	1.92	0.9	212.6	208.1	211.5	1.5	0.7	1.0
37	SC	323.37	15.884	642.4	2.03	0.3	644.1	565.3	591.3	0.3	12.0	7.9
38	SC	323.36	22.595	758.5	1.15	0.2	762.4	687.4	726.3	0.5	9.4	4.2
39	SC	323.36	29.518	822.1	0.88	0.1	828.5	760.9	808.8	0.8	7.4	1.6
40	SC	323.38	54.067	941.5	0.57	0.1	952.6	903.6	972.0	1.2	4.0	3.2
41	SC	323.35	77.970	1,008.7	0.52	0.1	1,021.3	981.7	1,063.0	1.2	2.7	5.4
42	SC	323.35	106.001	1,065.5	0.43	0.0	1,078.0	1,043.9	1,136.3	1.2	2.0	6.6
43	SC	323.37	126.462	1,099.1	0.33	0.0	1,110.6	1,078.3	1,177.1	1.0	1.9	7.1
44	Gas	373.53	2.120	28.0	0.62	2.1	31.3	31.2	31.3	7.6	7.4	7.7
45	Gas	373.53	2.753	38.0	0.64	1.6	41.2	41.1	41.2	2.6	2.3	2.6
46	Gas	373.53	3.517	50.3	0.66	1.3	53.6	53.4	53.6	6.5	6.0	6.5
47	Gas	373.53	5.244	79.9	0.73	0.9	83.4	82.7	83.3	4.3	3.5	4.2
48	Gas	373.53	10.613	191.4	1.00	0.5	194.6	189.0	192.1	1.7	1.2	0.4
49	SC	373.47	26.160	568.5	1.04	0.2	568.1	511.5	534.9	0.1	10.0	5.9
50	SC	373.53	53.565	805.3	0.57	0.1	808.7	761.4	814.3	0.4	5.5	1.1
51	SC	373.54	77.942	900.8	0.45	0.0	906.4	870.2	940.0	0.6	3.4	4.3
52	SC	373.55	104.584	970.6	0.38	0.0	977.1	948.3	1,031.7	0.7	2.3	6.3
53	SC	373.55	123.180	1,008.7	0.41	0.0	1,015.0	989.3	1,080.5	0.6	1.9	7.1
54	Gas	423.40	0.950	11.4	0.51	4.5	11.9	11.9	11.9	4.5	4.4	4.5

No	Phase	Temp.	Press.				Density (kg/m^3)			Abs Deviation (%)		
		K (±0.1)	MPa (±0.02)	Exp.	$U(\rho)$ kg/m^3	$U(\rho)$ %	SRK-CO_2	SRK	SRK Pen	SRK-CO_2	SRK	SRK Pen
55	Gas	423.41	2.085	25.3	0.53	2.1	26.6	26.5	26.6	5.1	4.7	5.0
56	Gas	423.41	3.593	44.5	0.55	1.2	46.8	46.5	46.7	5.2	4.5	4.9
57	Gas	423.41	5.279	66.8	0.58	0.9	70.4	69.6	70.1	5.3	4.2	4.8
58	Gas	423.41	7.743	101.7	0.62	0.6	106.7	104.8	105.8	5.0	3.1	4.1
59	SC	423.41	34.178	521.3	0.68	0.1	519.7	476.7	498.7	0.3	8.6	4.3
60	SC	423.42	53.524	682.4	0.51	0.1	684.3	640.5	680.9	0.3	6.1	0.2
61	SC	423.42	76.139	791.7	0.41	0.1	796.4	761.0	818.7	0.6	3.9	3.4
62	SC	423.42	104.164	880.1	0.36	0.0	887.5	860.2	934.5	0.8	2.3	6.2
63	SC	423.42	121.851	922.5	0.33	0.0	930.8	906.9	990.1	0.9	1.7	7.3
Absolute Average Deviation (AAD)										**1.8**	**4.3**	**4.1**

Table A. 4 Experimental and modelling results of MIX 2

No	Phase	Temp.	Press.	Density (kg/m^3)						Abs Deviation (%)		
		K (±0.1)	MPa (±0.02)	Exp.	$U(\rho)$ kg/m^3	$U(\rho)$ %	SRK-CO_2	SRK	SRK Pen	SRK-CO_2	SRK	SRK Pen
1	Gas	273.18	1.789	38.4	0.97	2.5	38.1	37.8	37.9	0.9	1.6	1.3
2	Gas	273.18	2.244	49.8	1.05	2.1	49.6	49.2	49.4	0.4	1.2	0.9
3	Liq.	273.27	8.796	841.6	1.62	0.2	828.1	756.8	798.5	1.6	10.1	5.1
4	Liq.	273.28	10.922	867.7	1.36	0.2	856.2	786.1	831.2	1.3	9.4	4.2
5	Liq.	273.28	20.998	941.0	0.89	0.1	937.5	874.9	931.1	0.4	7.0	1.1
6	Liq.	273.29	52.044	1,048.9	0.62	0.1	1,054.0	1,005.1	1,080.1	0.5	4.2	3.0
7	Liq.	273.29	104.164	1,145.6	0.41	0.0	1,152.7	1,108.6	1,200.5	0.6	3.2	4.8
8	Liq.	273.29	125.705	1,174.9	0.41	0.0	1,180.8	1,136.4	1,233.2	0.5	3.3	5.0
9	Gas	283.31	1.741	37.0	0.90	2.4	34.9	34.9	35.0	5.6	5.7	5.5
10	Gas	283.30	2.278	46.5	0.97	2.1	47.3	47.3	47.5	1.6	1.7	2.0
11	Liq.	283.31	10.674	803.7	1.85	0.2	776.9	707.0	744.0	3.3	12.0	7.4
12	Liq.	283.31	20.840	895.0	0.97	0.1	890.5	827.0	878.2	0.5	7.6	1.9
13	Liq.	283.32	52.457	1,012.6	0.62	0.1	1,026.4	979.1	1,051.7	1.4	3.3	3.9
14	Liq.	283.32	104.116	1,114.4	0.43	0.0	1,131.1	1,090.4	1,181.1	1.5	2.2	6.0
15	Liq.	283.31	125.258	1,145.3	0.41	0.0	1,160.5	1,119.7	1,215.6	1.3	2.2	6.1
16	Gas	298.38	2.078	39.2	0.85	2.2	39.6	39.5	39.6	0.9	0.8	1.1
17	Gas	298.38	3.531	75.3	1.03	1.4	73.3	73.1	73.5	2.6	2.9	2.4
18	SC	298.38	12.581	702.1	2.38	0.3	680.9	615.1	643.8	3.0	12.4	8.3
19	SC	298.39	20.805	827.0	1.12	0.1	813.9	749.7	792.9	1.6	9.3	4.1
20	SC	298.40	51.342	979.9	0.59	0.1	979.2	932.9	1,000.7	0.1	4.8	2.1
21	SC	298.40	104.102	1,097.0	0.43	0.0	1,099.0	1,062.6	1,151.4	0.2	3.1	5.0
22	SC	298.38	125.877	1,130.3	0.43	0.0	1,131.7	1,095.8	1,190.5	0.1	3.1	5.3
23	Gas	323.49	2.574	45.3	0.78	1.7	44.8	44.8	44.9	1.0	1.1	0.7
24	Gas	323.50	3.703	67.5	0.86	1.3	67.5	67.4	67.7	0.0	0.2	0.3
25	SC	323.45	12.271	409.1	2.78	0.7	401.8	360.6	370.8	1.8	11.8	9.4
26	SC	323.45	20.908	687.5	1.39	0.2	672.2	610.6	640.4	2.2	11.2	6.9
27	SC	323.48	51.555	909.3	0.60	0.1	905.7	860.9	921.2	0.4	5.3	1.3
28	SC	323.50	105.058	1,047.7	0.41	0.0	1,048.7	1,017.5	1,102.9	0.1	2.9	5.3
29	SC	323.49	125.478	1,082.4	0.43	0.0	1,083.2	1,053.4	1,145.3	0.1	2.7	5.8
30	Gas	373.57	1.528	20.7	0.59	2.9	21.7	21.6	21.7	4.5	4.4	4.5
31	Gas	373.58	2.567	34.5	0.62	1.8	37.2	37.1	37.2	7.8	7.5	7.8
32	SC	373.49	17.220	353.9	1.12	0.3	341.9	317.8	326.4	3.4	10.2	7.8
33	SC	373.50	21.005	439.7	1.12	0.3	430.2	392.7	405.9	2.2	10.7	7.7
34	SC	373.53	52.560	777.7	0.57	0.1	768.9	726.5	773.3	1.1	6.6	0.6
35	SC	373.55	103.937	951.8	0.39	0.0	949.3	923.0	999.7	0.3	3.0	5.0
36	SC	373.55	125.148	996.1	0.36	0.0	993.9	970.7	1,055.9	0.2	2.5	6.0
37	Gas	423.48	2.395	30.4	0.52	1.7	29.9	29.8	29.9	1.5	1.9	1.6
38	Gas	423.49	3.414	43.6	0.54	1.2	43.2	42.9	43.1	0.9	1.4	1.1
39	SC	423.38	18.472	283.7	0.71	0.2	271.1	256.8	262.9	4.4	9.5	7.4
40	SC	423.38	21.748	335.5	0.72	0.2	323.5	303.1	311.6	3.6	9.7	7.1
41	SC	423.41	52.787	660.6	0.51	0.1	650.9	611.9	647.6	1.5	7.4	2.0
42	SC	423.42	102.774	862.5	0.35	0.0	859.2	834.0	901.8	0.4	3.3	4.6
43	SC	423.42	124.646	915.9	0.33	0.0	913.7	892.2	970.3	0.2	2.6	5.9
Absolute Average Deviation (AAD)										**1.6**	**5.3**	**4.3**

Table A. 5 Experimental and modelling results of MIX 3

No	Phase	Temp.	Press.				Density (kg/m^3)			Abs Deviation (%)		
		K (±0.1)	MPa (±0.02)	Exp.	$U(\rho)$ kg/m^3	$U(\rho)$ %	SRK-CO_2	SRK	SRK Pen	SRK-CO_2	SRK	SRK Pen
1	Gas	273.28	1.067	20.0	0.77	3.8	18.9	18.9	18.9	5.3	5.6	5.5
2	Gas	273.26	2.127	41.6	0.91	2.2	40.9	40.6	40.7	1.7	2.3	2.0
3	Liq.	273.23	12.712	685.5	1.05	0.2	642.4	608.6	637.0	6.3	11.2	7.1
4	Liq.	273.20	20.895	740.2	0.72	0.1	710.7	678.0	713.4	4.0	8.4	3.6
5	Liq.	273.20	52.278	838.1	0.44	0.1	827.1	800.1	849.9	1.3	4.5	1.4
6	Liq.	273.18	103.765	920.2	0.33	0.0	914.3	889.4	951.3	0.6	3.3	3.4
7	Liq.	273.20	124.501	944.3	0.30	0.0	937.5	912.3	977.6	0.7	3.4	3.5
8	Gas	283.32	1.122	18.7	0.73	3.9	19.1	19.0	19.1	1.7	1.6	1.8
9	Gas	283.32	2.085	36.8	0.84	2.3	37.7	37.6	37.7	2.5	2.2	2.5
10	Gas	283.28	4.873	110.8	1.60	1.4	115.1	112.9	113.9	3.9	1.9	2.7
11	Liq.	283.31	9.518	564.7	2.41	0.4	515.9	485.8	504.0	8.7	14.0	10.8
12	Liq.	283.32	20.633	701.4	0.77	0.1	671.9	638.9	670.7	4.2	8.9	4.4
13	Liq.	283.34	51.893	814.3	0.44	0.1	804.3	778.1	825.9	1.2	4.5	1.4
14	Liq.	283.34	103.365	902.8	0.32	0.0	898.0	875.0	935.9	0.5	3.1	3.7
15	Liq.	283.32	125.368	929.6	0.30	0.0	924.0	900.9	965.6	0.6	3.1	3.9
16	Gas	298.36	1.101	18.6	0.68	3.7	17.5	17.5	17.6	5.8	5.8	5.7
17	Gas	298.36	2.085	36.0	0.76	2.1	34.9	34.9	35.0	2.9	3.0	2.7
18	Gas	298.38	5.175	108.2	1.23	1.1	106.7	106.0	106.9	1.4	2.0	1.2
19	SC	298.40	10.964	462.0	2.84	0.6	428.8	401.8	414.5	7.2	13.0	10.3
20	SC	298.29	20.833	642.9	0.86	0.1	615.3	582.0	609.1	4.3	9.5	5.3
21	SC	298.30	51.734	779.9	0.44	0.1	771.5	745.9	790.8	1.1	4.4	1.4
22	SC	298.29	102.106	873.8	0.32	0.0	873.2	852.4	911.7	0.1	2.4	4.3
23	SC	298.30	124.969	903.9	0.30	0.0	902.5	882.0	945.6	0.2	2.4	4.6
24	Gas	323.44	1.218	19.3	0.62	3.2	17.8	17.7	17.8	8.0	8.0	7.9
25	Gas	323.45	2.113	32.7	0.66	2.0	31.8	31.8	31.9	2.8	2.9	2.6
26	Gas	323.44	5.231	90.6	0.88	1.0	89.8	89.4	90.1	0.9	1.3	0.6
27	SC	323.47	11.810	316.8	1.83	0.6	299.2	277.8	284.1	5.6	12.3	10.3
28	SC	323.49	20.227	531.8	1.05	0.2	504.7	471.8	490.1	5.1	11.3	7.8
29	SC	323.41	49.821	718.0	0.45	0.1	710.1	684.4	723.8	1.1	4.7	0.8
30	SC	323.43	103.427	837.2	0.31	0.0	837.2	819.2	876.2	0.0	2.2	4.7
31	SC	323.45	124.838	868.2	0.29	0.0	867.7	850.7	912.3	0.1	2.0	5.1
32	Gas	373.54	2.099	24.5	0.54	2.2	26.5	26.5	26.5	8.2	8.0	8.2
33	Gas	373.55	5.237	68.9	0.62	0.9	70.6	70.1	70.6	2.4	1.8	2.4
34	Gas	373.55	10.427	156.3	0.77	0.5	156.3	153.3	155.3	0.0	2.0	0.7
35	SC	373.56	20.730	364.2	0.84	0.2	348.5	326.1	335.4	4.3	10.5	7.9
36	SC	373.57	46.524	601.3	0.46	0.1	588.4	562.1	590.5	2.1	6.5	1.8
37	SC	373.53	63.338	668.4	0.38	0.1	661.9	639.9	677.0	1.0	4.3	1.3
38	SC	373.54	63.159	667.7	0.38	0.1	661.2	639.2	676.2	1.0	4.3	1.3
39	SC	373.55	103.400	767.8	0.30	0.0	766.3	750.8	802.4	0.2	2.2	4.5
40	SC	373.55	122.278	800.7	0.28	0.0	799.4	785.6	842.3	0.2	1.9	5.2
41	SC	373.56	125.292	804.9	0.27	0.0	804.1	790.5	847.9	0.1	1.8	5.3
42	Gas	423.43	2.120	23.2	0.46	2.0	23.2	23.2	23.2	0.2	0.0	0.2
43	Gas	423.43	5.224	58.2	0.50	0.9	59.3	58.8	59.1	1.8	1.1	1.6
44	Gas	423.43	10.358	120.5	0.55	0.5	123.8	121.4	122.8	2.8	0.8	1.9
45	Gas	423.44	20.943	258.3	0.59	0.2	264.2	251.9	257.9	2.3	2.5	0.2
46	SC	423.45	29.078	371.6	0.54	0.1	359.0	338.6	349.5	3.4	8.9	6.0
47	SC	423.45	49.869	527.2	0.40	0.1	517.5	493.5	516.9	1.8	6.4	2.0
48	SC	423.46	103.359	704.5	0.27	0.0	702.4	687.5	733.8	0.3	2.4	4.2
49	SC	423.47	124.804	746.2	0.25	0.0	745.4	732.7	785.5	0.1	1.8	5.3
Absolute Average Deviation (AAD)										**2.4**	**4.6**	**3.9**

Table A. 6 Experimental and modelling results of MIX 4

No	Phase	Temp.	Press.				Density (kg/m^3)			Abs Deviation (%)		
		K (±0.1)	MPa (±0.02)	Exp.	$U(\rho)$ kg/m^3	$U(\rho)$ %	SRK-CO_2	SRK	SRK Pen	SRK-CO_2	SRK	SRK Pen
1	SC	273.24	1.872	30.5	0.69	2.3	29.1	29.0	29.0	4.6	5.0	4.8
2	SC	273.24	2.085	33.7	0.71	2.1	32.8	32.7	32.7	2.7	3.1	2.8
3	SC	273.24	2.767	45.9	0.78	1.7	45.4	45.1	45.3	1.2	1.7	1.4
4	SC	273.25	3.469	60.3	0.86	1.4	59.5	59.1	59.4	1.3	1.9	1.5
5	SC	273.25	5.279	104.9	1.21	1.1	104.5	103.4	104.2	0.4	1.4	0.7
6	SC	273.25	7.467	189.7	2.25	1.2	188.3	185.2	187.6	0.7	2.4	1.1
7	SC	273.25	11.404	403.0	1.96	0.5	379.0	368.4	378.0	6.0	8.6	6.2
8	SC	273.27	15.719	509.7	1.05	0.2	465.2	451.5	466.0	8.7	11.4	8.6
9	SC	273.26	20.730	560.0	0.75	0.1	521.0	506.0	524.3	7.0	9.6	6.4
10	SC	273.26	27.591	601.7	0.58	0.1	570.4	555.0	577.2	5.2	7.8	4.1
11	SC	273.28	31.094	627.0	0.53	0.1	589.6	574.1	597.9	6.0	8.4	4.6
12	SC	273.29	54.783	699.3	0.38	0.1	673.7	658.9	690.4	3.7	5.8	1.3
13	SC	273.30	78.362	744.3	0.31	0.0	723.1	708.7	745.2	2.9	4.8	0.1
14	SC	273.29	104.556	781.5	0.28	0.0	761.4	746.8	787.5	2.6	4.4	0.8
15	SC	273.26	124.102	804.3	0.26	0.0	783.4	768.6	811.8	2.6	4.4	0.9
16	SC	283.28	1.796	26.4	0.65	2.5	26.4	26.4	26.5	0.2	0.1	0.3
17	SC	283.29	2.072	30.4	0.67	2.2	30.9	30.9	30.9	1.8	1.6	1.8
18	SC	283.27	3.462	54.6	0.78	1.4	55.9	55.4	55.6	2.4	1.4	1.8
19	SC	283.27	5.217	91.9	1.00	1.1	93.9	92.7	93.3	2.1	0.9	1.5
20	SC	283.27	9.050	221.5	1.99	0.9	221.7	216.7	220.1	0.1	2.1	0.6
21	SC	283.28	14.522	434.3	1.33	0.3	398.0	385.8	396.6	8.4	11.2	8.7
22	SC	283.28	20.791	518.4	0.79	0.2	486.5	471.8	488.0	6.2	9.0	5.9
23	SC	283.29	27.908	569.2	0.60	0.1	544.2	529.0	549.4	4.4	7.1	3.5
24	SC	283.30	35.210	604.3	0.49	0.1	584.8	569.7	593.4	3.2	5.7	1.8
25	SC	283.29	41.941	629.1	0.43	0.1	613.5	598.7	625.0	2.5	4.8	0.7
26	SC	283.28	50.048	653.5	0.39	0.1	641.3	626.9	655.7	1.9	4.1	0.3
27	SC	283.32	78.169	724.8	0.32	0.0	707.3	693.8	729.3	2.4	4.3	0.6
28	SC	283.32	104.370	764.1	0.28	0.0	747.9	734.4	774.4	2.1	3.9	1.3
29	SC	283.33	122.650	786.7	0.26	0.0	769.7	756.1	798.5	2.2	3.9	1.5
30	SC	298.37	2.595	39.0	0.64	1.6	36.9	36.9	36.9	5.4	5.5	5.3
31	SC	298.37	5.403	89.5	0.83	0.9	87.0	86.5	87.1	2.8	3.3	2.7
32	SC	298.34	7.626	141.1	1.08	0.8	139.8	136.2	137.5	0.9	3.5	2.5
33	SC	298.35	10.929	251.1	1.47	0.6	234.2	227.2	230.9	6.7	9.5	8.0
34	SC	298.30	16.173	399.1	1.15	0.3	365.3	353.0	362.2	8.5	11.5	9.2
35	SC	298.33	20.908	468.6	0.83	0.2	436.2	421.9	435.1	6.9	10.0	7.2
36	SC	298.36	20.661	465.9	0.85	0.2	433.1	418.9	431.9	7.0	10.1	7.3
37	SC	298.35	36.311	583.3	0.49	0.1	554.8	539.9	561.6	4.9	7.4	3.7
38	SC	298.32	51.246	630.3	0.38	0.1	616.3	602.3	629.6	2.2	4.4	0.1
39	SC	298.36	54.288	646.5	0.37	0.1	625.9	612.2	640.3	3.2	5.3	1.0
40	SC	298.36	77.619	699.0	0.31	0.0	683.4	670.9	704.8	2.2	4.0	0.8
41	SC	298.38	99.036	734.7	0.28	0.0	720.4	708.3	746.3	1.9	3.6	1.6
42	SC	298.40	124.026	768.1	0.26	0.0	753.2	741.2	782.9	1.9	3.5	1.9
43	SC	323.40	2.443	32.3	0.56	1.7	31.1	31.0	31.1	3.8	3.9	3.7
44	SC	323.44	5.203	73.0	0.66	0.9	71.5	71.3	71.7	2.0	2.3	1.7
45	SC	323.42	9.243	146.2	0.84	0.6	144.0	141.7	143.3	1.5	3.0	2.0
46	SC	323.44	20.736	385.6	0.81	0.2	358.3	344.5	353.5	7.1	10.7	8.3
47	SC	323.45	28.224	465.3	0.60	0.1	439.6	424.6	438.5	5.5	8.7	5.8
48	SC	323.45	35.306	513.8	0.50	0.1	492.0	477.2	494.8	4.2	7.1	3.7
49	SC	323.48	53.923	599.8	0.37	0.1	579.5	566.2	591.1	3.4	5.6	1.5
50	SC	323.47	78.534	663.5	0.31	0.0	648.3	636.8	668.5	2.3	4.0	0.8
51	SC	323.48	104.652	710.6	0.27	0.0	696.8	686.4	723.3	1.9	3.4	1.8
52	SC	323.47	119.209	731.9	0.25	0.0	717.8	707.7	747.1	1.9	3.3	2.1
53	SC	373.54	2.388	24.2	0.46	1.9	25.5	25.5	25.5	5.4	5.3	5.5
54	SC	373.37	5.182	55.1	0.50	0.9	57.6	57.4	57.6	4.6	4.1	4.6

No	Phase	Temp.	Press.				Density (kg/m^3)			Abs Deviation (%)		
		K (±0.1)	MPa (±0.02)	Exp.	$U(\rho)$ kg/m^3	$U(\rho)$ %	SRK-CO_2	SRK	SRK Pen	SRK-CO_2	SRK	SRK Pen
55	SC	373.42	11.239	134.4	0.58	0.4	134.5	132.5	133.9	0.1	1.4	0.4
56	SC	373.55	19.931	266.5	0.59	0.2	250.5	240.4	245.1	6.0	9.8	8.0
57	SC	373.56	28.032	354.5	0.52	0.1	337.7	323.7	332.2	4.7	8.7	6.3
58	SC	373.57	34.563	407.9	0.45	0.1	391.2	376.6	388.3	4.1	7.7	4.8
59	SC	373.57	41.397	452.3	0.41	0.1	436.0	421.7	436.3	3.6	6.8	3.5
60	SC	373.56	56.015	525.3	0.33	0.1	507.0	494.1	514.3	3.5	5.9	2.1
61	SC	373.56	73.579	581.5	0.29	0.1	566.6	555.4	581.1	2.6	4.5	0.1
62	SC	373.47	105.754	651.5	0.25	0.0	639.9	631.1	664.4	1.8	3.1	2.0
63	SC	373.47	124.350	682.0	0.23	0.0	670.5	662.5	699.4	1.7	2.9	2.6
64	SC	423.42	2.512	25.5	0.39	1.5	23.3	23.3	23.3	8.5	8.7	8.5
65	SC	423.39	3.104	30.7	0.40	1.3	29.0	28.9	29.0	5.7	5.9	5.7
66	SC	423.41	5.217	50.4	0.41	0.8	49.4	49.2	49.4	1.9	2.5	2.1
67	SC	423.42	10.599	103.2	0.43	0.4	103.6	102.2	103.1	0.4	1.0	0.1
68	SC	423.41	20.372	216.5	0.44	0.2	202.8	196.6	200.0	6.3	9.2	7.6
69	SC	423.41	28.004	285.7	0.42	0.1	272.4	262.2	268.1	4.7	8.2	6.2
70	SC	423.42	34.618	335.8	0.38	0.1	323.5	311.2	319.7	3.7	7.3	4.8
71	SC	423.42	41.507	379.9	0.35	0.1	368.3	355.2	366.3	3.1	6.5	3.6
72	SC	423.32	46.676	413.5	0.34	0.1	397.4	384.3	397.2	3.9	7.1	3.9
73	SC	423.42	47.983	414.9	0.33	0.1	404.1	391.0	404.4	2.6	5.8	2.5
74	SC	423.37	73.971	521.1	0.27	0.1	507.7	496.7	518.5	2.6	4.7	0.5
75	SC	423.40	103.957	594.0	0.24	0.0	584.0	575.4	604.9	1.7	3.1	1.8
76	SC	423.42	124.742	659.2	0.22	0.0	622.7	615.2	649.1	5.5	6.7	1.5
	Absolute Average Deviation (AAD)									**3.6**	**5.4**	**3.2**

Table A. 7 Experimental and modelling results of MIX 5

No	Phase	Temp.	Press.	Density (kg/m³)						Abs Deviation (%)		
		K (±0.1)	MPa (±0.02)	Exp.	*U(ρ)* kg/m³	*U(ρ)* %	SRK-CO_2	SRK	SRK Pen	SRK-CO_2	SRK	SRK Pen
1	Gas	273.28	1.666	35.3	0.99	2.8	36.0	35.8	35.9	2.1	1.4	1.7
2	Gas	273.28	2.127	47.7	1.09	2.3	48.0	47.6	47.8	0.7	0.2	0.2
3	Gas	273.29	2.815	67.8	1.30	1.9	68.3	67.6	67.9	0.7	0.4	0.1
4	Gas	273.28	3.503	93.5	1.67	1.8	93.2	91.8	92.4	0.4	1.9	1.2
5	Liq.	273.28	6.084	896.7	1.47	0.2	881.3	786.5	833.3	1.7	12.3	7.1
6	Liq.	273.28	10.344	932.4	1.13	0.1	923.1	836.4	889.5	1.0	10.3	4.6
7	Liq.	273.28	20.310	986.4	0.84	0.1	982.6	909.5	972.6	0.4	7.8	1.4
8	Liq.	273.29	34.907	1,038.1	0.72	0.1	1,037.4	975.9	1,049.0	0.1	6.0	1.0
9	Liq.	273.29	52.168	1,082.1	0.52	0.0	1,083.0	1,029.0	1,110.6	0.1	4.9	2.6
10	Liq.	273.30	77.158	1,130.2	0.41	0.0	1,132.1	1,082.8	1,173.5	0.2	4.2	3.8
11	Liq.	273.30	100.984	1,166.9	0.41	0.0	1,168.3	1,120.3	1,217.8	0.1	4.0	4.4
12	Liq.	273.30	120.234	1,192.3	0.41	0.0	1,192.7	1,144.7	1,246.6	0.0	4.0	4.6
13	Liq.	273.29	123.957	1,196.8	0.43	0.0	1,197.0	1,148.9	1,251.6	0.0	4.0	4.6
14	Gas	283.27	1.094	20.7	0.85	4.1	21.5	21.5	21.5	3.9	3.8	3.9
15	Gas	283.28	1.473	29.0	0.90	3.1	29.7	29.7	29.8	2.5	2.3	2.5
16	Gas	283.29	2.085	43.0	0.99	2.3	44.1	43.9	44.1	2.6	2.2	2.5
17	Gas	283.29	2.836	63.3	1.14	1.8	62.7	63.6	63.9	1.0	0.5	1.0
18	Gas	283.29	3.544	84.9	1.37	1.6	87.0	85.3	85.8	2.6	0.5	1.1
19	Liq.	283.27	6.538	807.8	1.17	0.1	800.3	702.9	740.9	0.9	13.0	8.3
20	Liq.	283.29	10.606	877.0	1.35	0.2	864.4	774.3	820.7	1.4	11.7	6.4
21	Liq.	283.30	21.108	951.4	0.88	0.1	944.7	870.6	929.6	0.7	8.5	2.3
22	Liq.	283.32	36.559	1,013.5	0.64	0.1	1,010.0	949.6	1,020.3	0.3	6.3	0.7
23	Liq.	283.26	52.450	1,056.1	0.62	0.1	1,055.9	1,003.4	1,082.6	0.0	5.0	2.5
24	Liq.	283.29	77.915	1,106.5	0.52	0.0	1,109.4	1,063.1	1,152.3	0.3	3.9	4.1
25	Liq.	283.33	106.490	1,151.7	0.41	0.0	1,154.4	1,110.2	1,207.9	0.2	3.6	4.9
26	Liq.	283.31	126.256	1,178.1	0.43	0.0	1,179.9	1,135.6	1,238.1	0.2	3.6	5.1
27	Gas	298.31	1.211	22.7	0.80	3.5	22.5	22.5	22.5	1.0	1.1	0.9
28	Gas	298.30	1.652	31.3	0.84	2.7	31.5	31.4	31.5	0.6	0.5	0.8
29	Gas	298.30	2.106	41.0	0.89	2.2	41.2	41.2	41.3	0.6	0.5	0.8
30	Gas	298.30	3.503	75.1	1.10	1.5	75.5	75.2	75.6	0.4	0.1	0.7
31	Liq.	298.29	10.964	753.4	2.11	0.3	749.4	657.8	692.0	0.5	12.7	8.2
32	Liq.	298.31	20.268	869.1	1.03	0.1	869.1	791.5	841.5	0.0	8.9	3.2
33	Liq.	298.32	34.198	946.6	0.73	0.1	949.7	887.1	950.5	0.3	6.3	0.4
34	Liq.	298.32	52.409	1,008.9	0.62	0.1	1,013.3	962.2	1,037.1	0.4	4.6	2.8
35	Liq.	298.31	77.509	1,068.4	0.52	0.0	1,072.8	1,029.7	1,116.0	0.4	3.6	4.5
36	Liq.	298.30	105.024	1,117.2	0.43	0.0	1,120.7	1,081.0	1,176.6	0.3	3.2	5.3
37	Liq.	298.30	126.008	1,148.0	0.33	0.0	1,150.1	1,111.1	1,212.3	0.2	3.2	5.6
38	Gas	323.55	1.239	21.8	0.72	3.3	20.9	20.9	20.9	4.1	4.1	3.9
39	Gas	323.57	2.113	36.9	0.77	2.1	37.0	36.9	37.0	0.3	0.2	0.5
40	Gas	323.62	2.822	50.7	0.82	1.6	50.9	50.8	51.0	0.4	0.2	0.6
41	Gas	323.36	3.572	65.8	0.89	1.4	66.8	66.7	67.0	1.6	1.3	1.9
42	Gas	323.36	5.327	108.1	1.11	1.0	109.5	108.9	109.9	1.3	0.8	1.6
43	Gas	323.37	7.323	170.5	1.56	0.9	172.7	170.5	172.8	1.3	0.0	1.3
44	SC	323.37	15.864	647.3	2.04	0.3	643.2	563.7	589.9	0.6	12.9	8.9
45	SC	323.36	21.294	747.2	1.25	0.2	743.4	666.8	703.8	0.5	10.8	5.8
46	SC	323.38	36.910	871.5	0.74	0.1	872.2	811.5	866.9	0.1	6.9	0.5
47	SC	323.38	52.884	939.9	0.59	0.1	942.5	892.9	960.5	0.3	5.0	2.2
48	SC	323.39	77.288	1,009.5	0.52	0.1	1,012.8	973.2	1,054.0	0.3	3.6	4.4
49	SC	323.35	104.522	1,065.4	0.43	0.0	1,068.0	1,033.8	1,125.6	0.2	3.0	5.6
50	SC	323.35	124.019	1,097.9	0.33	0.0	1,099.2	1,066.9	1,164.9	0.1	2.8	6.1
51	Gas	373.53	1.363	19.0	0.60	3.2	19.6	19.6	19.6	3.0	2.9	3.1
52	Gas	373.53	2.099	29.4	0.62	2.1	30.7	30.7	30.7	4.5	4.3	4.6
53	Gas	373.53	3.496	50.9	0.67	1.3	52.9	52.6	52.9	3.9	3.5	3.9
54	Gas	373.54	5.389	81.8	0.73	0.9	85.4	84.7	85.3	4.4	3.5	4.2

No	Phase	Temp.	Press.		Density (kg/m^3)					Abs Deviation (%)		
		K (±0.1)	MPa (±0.02)	Exp.	*U(ρ)* kg/m^3	*U(ρ)* %	SRK-CO_2	SRK	SRK Pen	SRK-CO_2	SRK	SRK Pen
55	Gas	373.53	7.756	127.3	0.84	0.7	130.8	128.7	130.2	2.7	1.1	2.2
56	Gas	373.54	10.454	187.1	0.99	0.5	189.8	184.5	187.5	1.4	1.4	0.2
57	SC	373.53	27.743	595.8	1.00	0.2	589.7	531.8	557.4	1.0	10.7	6.4
58	SC	373.53	31.452	644.0	0.88	0.1	637.9	579.2	609.7	0.9	10.1	5.3
59	SC	373.54	43.544	750.3	0.67	0.1	744.8	691.7	735.5	0.7	7.8	2.0
60	SC	373.54	55.747	818.9	0.55	0.1	814.7	768.7	823.3	0.5	6.1	0.5
61	SC	373.55	76.325	898.1	0.46	0.1	895.3	858.6	927.3	0.3	4.4	3.2
62	SC	373.55	101.411	965.6	0.40	0.0	963.2	933.8	1,015.6	0.2	3.3	5.2
63	SC	373.55	116.022	996.6	0.37	0.0	994.3	967.7	1,055.8	0.2	2.9	5.9
64	SC	373.56	125.513	1,014.2	0.41	0.0	1,012.1	986.8	1,078.7	0.2	2.7	6.4
65	Gas	423.43	2.099	26.7	0.53	2.0	26.6	26.5	26.6	0.4	0.7	0.5
66	Gas	423.44	3.510	44.9	0.55	1.2	45.3	45.1	45.3	1.0	0.4	0.8
67	Gas	423.45	5.237	67.5	0.58	0.9	69.3	68.5	69.0	2.6	1.5	2.2
68	Gas	423.45	7.619	100.8	0.61	0.6	104.1	102.3	103.2	3.2	1.4	2.4
69	Gas	423.45	11.225	155.2	0.68	0.4	160.6	155.8	158.1	3.5	0.4	1.9
70	Gas	423.46	17.137	252.4	0.76	0.3	260.5	246.8	252.6	3.2	2.2	0.1
71	SC	423.39	43.778	614.5	0.59	0.1	610.4	564.6	596.1	0.7	8.1	3.0
72	SC	423.40	53.799	685.3	0.53	0.1	681.8	638.3	678.8	0.5	6.9	0.9
73	SC	423.41	78.142	800.3	0.42	0.1	799.0	764.3	823.3	0.2	4.5	2.9
74	SC	423.41	104.542	882.1	0.36	0.0	882.5	855.3	929.8	0.0	3.0	5.4
75	SC	423.41	104.845	883.1	0.36	0.0	883.3	856.1	930.8	0.0	3.1	5.4
76	SC	423.41	94.955	855.9	0.38	0.0	855.5	825.9	895.2	0.0	3.5	4.6
77	SC	423.42	126.442	933.8	0.33	0.0	934.3	911.2	996.2	0.0	2.4	6.7
Absolute Average Deviation (AAD)										**1.0**	**4.2**	**3.2**

Table A. 8 Experimental and modelling results of MIX 6

No	Phase	Temp.	Press.		Density (kg/m^3)					Abs Deviation (%)		
		K (±0.1)	MPa (±0.02)	Exp.	$U(\rho)$ kg/m^3	$U(\rho)$ %	SRK CO_2	SRK	SRK Pen	SRK-CO_2	SRK	SRK Pen
1	Gas	273.27	1.198	23.3	0.86	3.7	23.4	23.3	23.3	0.3	0.1	0.1
2	Gas	273.27	2.085	45.7	1.03	2.3	44.1	43.8	44.0	3.6	4.2	3.9
3	Liq.	273.29	10.523	714.8	1.08	0.2	662.4	626.2	657.9	7.3	12.4	7.9
4	Liq.	273.30	15.747	749.9	0.80	0.1	709.7	674.9	711.9	5.3	10.0	5.1
5	Liq.	273.30	21.610	777.8	0.66	0.1	745.9	713.0	754.4	4.1	8.3	3.0
6	Liq.	273.31	36.077	825.7	0.51	0.1	804.6	775.5	824.8	2.6	6.1	0.1
7	Liq.	273.31	53.620	866.2	0.42	0.0	850.9	824.7	880.6	1.8	4.8	1.7
8	Liq.	273.31	78.541	908.7	0.36	0.0	896.4	872.1	934.9	1.4	4.0	2.9
9	Liq.	273.31	104.852	943.8	0.33	0.0	931.4	907.5	975.7	1.3	3.8	3.4
10	Liq.	273.31	126.063	967.6	0.30	0.0	953.8	929.6	1001.3	1.4	3.9	3.5
11	Gas	283.30	1.239	22.3	0.82	3.7	23.1	23.1	23.1	3.3	3.2	3.4
12	Gas	283.32	2.072	40.3	0.94	2.3	41.2	41.0	41.1	2.0	1.7	2.0
13	Gas	283.31	3.145	68.4	1.19	1.7	67.4	68.7	69.0	1.5	0.4	0.9
14	Liq.	283.29	10.461	658.2	1.39	0.2	606.2	569.7	596.2	7.9	13.5	9.4
15	Liq.	283.30	14.467	699.3	0.96	0.1	657.7	621.7	653.4	5.9	11.1	6.6
16	Liq.	283.31	21.445	743.3	0.70	0.1	712.6	678.9	716.9	4.1	8.7	3.5
17	Liq.	283.31	35.485	797.9	0.53	0.1	778.2	749.0	795.5	2.5	6.1	0.3
18	Liq.	283.32	53.131	843.2	0.43	0.1	829.7	804.1	858.1	1.6	4.6	1.8
19	Liq.	283.32	78.052	889.1	0.36	0.0	878.9	855.8	917.2	1.1	3.7	3.2
20	Liq.	283.31	105.836	928.1	0.32	0.0	918.0	895.8	963.2	1.1	3.5	3.8
21	Liq.	283.32	126.628	952.5	0.29	0.0	940.9	918.6	989.7	1.2	3.6	3.9
22	Gas	298.32	1.342	24.1	0.76	3.2	23.5	23.5	23.6	2.2	2.2	2.0
23	Gas	298.33	2.092	39.3	0.84	2.1	38.4	38.4	38.5	2.1	2.2	1.9
24	Gas	298.34	2.732	53.5	0.93	1.7	52.4	52.3	52.5	2.0	2.2	1.8
25	Gas	298.33	3.937	84.8	1.16	1.4	83.0	82.7	83.3	2.2	2.5	1.9
26	Gas	298.32	5.279	131.3	1.65	1.3	128.0	127.0	128.3	2.5	3.2	2.2
27	Gas	298.32	6.401	191.4	2.71	1.4	171.5	181.7	184.3	10.4	5.1	3.7
28	Liq.	298.37	9.498	489.8	3.29	0.7	462.5	429.5	444.8	5.6	12.3	9.2
29	Liq.	298.37	10.723	541.8	2.20	0.4	508.2	472.7	491.2	6.2	12.8	9.4
30	Liq.	298.36	14.632	621.3	1.19	0.2	588.7	551.6	577.0	5.3	11.2	7.1
31	Liq.	298.36	21.149	683.0	0.79	0.1	658.5	623.5	656.2	3.6	8.7	3.9
32	Liq.	298.36	34.804	751.8	0.55	0.1	737.7	707.8	750.3	1.9	5.8	0.2
33	Liq.	298.36	51.707	803.5	0.44	0.1	795.6	770.2	820.7	1.0	4.1	2.1
34	Liq.	298.36	75.320	853.4	0.36	0.0	848.9	827.0	885.6	0.5	3.1	3.8
35	Liq.	298.36	105.506	900.1	0.32	0.0	895.8	875.8	941.7	0.5	2.7	4.6
36	Liq.	298.36	126.373	926.2	0.29	0.0	920.7	900.9	970.8	0.6	2.7	4.8
37	Gas	323.36	1.500	25.0	0.69	2.8	24.0	24.0	24.0	3.9	3.9	3.8
38	Gas	323.36	2.113	35.9	0.73	2.0	34.7	34.7	34.8	3.4	3.5	3.2
39	Gas	323.33	3.138	55.8	0.80	1.4	54.1	54.0	54.2	3.2	3.3	2.9
40	Gas	323.34	4.184	77.0	0.91	1.2	76.0	75.8	76.3	1.3	1.6	0.9
41	Gas	323.34	5.292	103.2	1.04	1.0	102.3	101.9	102.8	0.8	1.2	0.3
42	Gas	323.33	7.681	177.0	1.54	0.9	174.5	172.6	175.1	1.4	2.5	1.1
43	Gas	323.34	9.904	285.7	2.20	0.8	271.7	259.5	265.2	4.9	9.2	7.2
44	SC	323.44	15.967	520.4	1.38	0.3	486.4	449.2	466.6	6.5	13.7	10.3
45	SC	323.44	18.906	569.8	1.07	0.2	536.6	499.4	520.9	5.8	12.4	8.6
46	SC	323.44	23.792	623.2	0.80	0.1	593.7	558.2	585.3	4.7	10.4	6.1
47	SC	323.44	37.591	706.5	0.54	0.1	687.2	657.5	695.3	2.7	6.9	1.6
48	SC	323.45	53.159	761.8	0.43	0.1	748.9	724.1	770.3	1.7	5.0	1.1
49	SC	323.46	78.541	822.0	0.36	0.0	813.6	793.6	849.4	1.0	3.5	3.3
50	SC	323.48	105.437	867.8	0.31	0.0	860.1	842.7	905.9	0.9	2.9	4.4
51	SC	323.47	127.061	897.5	0.29	0.0	888.9	872.4	940.4	1.0	2.8	4.8
52	Gas	373.53	3.152	42.7	0.62	1.4	44.3	44.1	44.3	3.7	3.4	3.8
53	Gas	373.53	4.191	58.3	0.65	1.1	60.4	60.1	60.4	3.5	3.1	3.6
54	Gas	373.53	5.237	74.6	0.69	0.9	77.4	77.0	77.5	3.8	3.1	3.8

No	Phase	Temp.	Press.		Density (kg/m^3)					Abs Deviation (%)		
		K (±0.1)	MPa (±0.02)	Exp.	*U(ρ)* kg/m^3	*U(ρ)* %	SRK CO_2	SRK	SRK Pen	SRK-CO_2	SRK	SRK Pen
55	Gas	373.53	7.626	116.8	0.78	0.7	119.7	118.3	119.6	2.5	1.3	2.4
56	SC	373.51	20.819	410.7	0.89	0.2	389.9	363.9	376.0	5.1	11.4	8.5
57	SC	373.51	27.632	502.7	0.70	0.1	482.8	451.2	470.0	3.9	10.2	6.5
58	SC	373.53	35.465	571.5	0.56	0.1	553.1	522.5	547.8	3.2	8.6	4.1
59	SC	373.54	52.787	663.7	0.42	0.1	650.0	624.9	661.5	2.1	5.8	0.3
60	SC	373.55	76.277	738.2	0.34	0.0	729.1	709.8	757.5	1.2	3.8	2.6
61	SC	373.55	104.529	798.6	0.30	0.0	791.4	776.4	833.7	0.9	2.8	4.4
62	SC	373.55	126.256	834.4	0.27	0.0	826.9	813.7	876.9	0.9	2.5	5.1
63	Gas	423.43	1.707	19.7	0.49	2.5	20.1	20.1	20.1	2.3	2.1	2.3
64	Gas	423.42	2.175	25.2	0.50	2.0	25.8	25.7	25.8	2.4	2.2	2.4
65	Gas	423.42	3.083	36.0	0.51	1.4	37.0	36.9	37.0	2.8	2.4	2.8
66	Gas	423.43	4.219	49.7	0.53	1.1	51.4	51.1	51.4	3.4	2.8	3.3
67	Gas	423.43	5.320	63.2	0.54	0.9	65.8	65.3	65.7	4.1	3.2	3.9
68	Gas	423.43	7.598	92.9	0.57	0.6	96.7	95.4	96.3	4.1	2.7	3.7
69	SC	423.41	19.243	282.0	0.65	0.2	266.7	255.1	261.4	5.4	9.5	7.3
70	SC	423.43	28.045	395.3	0.58	0.1	379.4	357.8	370.3	4.0	9.5	6.3
71	SC	423.43	38.644	491.0	0.48	0.1	477.1	451.1	471.2	2.8	8.1	4.0
72	SC	423.44	52.202	572.4	0.39	0.1	561.2	536.6	565.2	2.0	6.3	1.3
73	SC	423.45	76.882	665.9	0.31	0.0	659.0	639.8	680.9	1.0	3.9	2.3
74	SC	423.45	104.790	734.6	0.27	0.0	730.6	715.9	767.8	0.5	2.5	4.5
75	SC	423.45	125.292	783.4	0.25	0.0	769.7	757.1	815.4	1.7	3.3	4.1
Absolute Average Deviation (AAD)										**2.9**	**5.3**	**3.8**